GA Technologies

GA-A--16953

DE84 005205

HTGR APPLICATIONS PROGRAM

SEMIANNUAL REPORT FOR THE PERIOD APRIL 1, 1982 THROUGH SEPTEMBER 24, 1982

by
PROJECT STAFF

Prepared under
Contract DE-AT03-76SF70046
for the San Francisco Operations Office
Department of Energy

GA PROJECT 6000
DATE PUBLISHED: OCTOBER 1983

ABSTRACT

This report summarizes the current progress of the GA commercial HTGR application program, which includes studies of three basic nuclear heat source categories related to core outlet temperatures of 750°C (1382°F), 850°C (1562°F), and 950°C (1747°F). These categories in turn define the supporting technical systems and the potential process applications. The heat sources are presented in the report as the HTGR-SC/C, the HTGR-PH (monolithic plant), the HTGR-MRS-PH and SC/C plants, and the HTGR-GT/C plant concept.

Emphasis is placed on the 2240-MW(t) HTGR-SC/C plant, which can provide for the cogeneration production of process steam and electric power. The status of plant performance, NSSS component and core nuclear density, plant control and instrumentation, dynamics, availability and maintainability, safety/reliability, licensing, fuel cycle cost, and economics and BOP interfacing is included.

A preconceptual design and cost estimate of a monolithic six-loop 2240-MW(t) 950°C (1742°F) core outlet temperature direct reforming HTGR-PH plant is described to assess the economic potential of scale-up from the earlier 1170-MW(t) to the 2240-MW(t) plant, and a first iteration design of an HTGR module reactor system (MRS) for HTGR-SC conditions is presented to evaluate the concept and to compare the multimodule concept and the monolithic HTGR-SC/C lead plant design. The results of a brief study of a PCRV concept applicable to the HTGR-MRS-SC/C are presented, as are safety assessment and seismic scoping study results for the current HTGR-MRS design and fuel cycle cost comparisons between a 250-MW(t) HTGR-MRS-PH and an HTGR-MRS-SC/C plant.

Status of HTGR-Gas Turbine/Cogeneration (HTGR-GT/C) design is discussed.

Application process development progress includes (1) studies of selected shale retorting processes together with comparative assessment with competing energy sources and (2) an assessment of the HTGR application for a modified in situ (MIS) process for shale retorting.

Other applications reported include a study to investigate the conceptual design of a reboiler design for heavy oil/tar sand application, a safety site suitability study for a 2240-MW(t) HTGR-SC/C plant at Port Arthur, Texas, and a summary evaluation of HTGR-PH application studies of work performed during 1980-1982 in the integration of an HTGR-PH plant into an SRC-II refinery.

A scoping type of evaluation and economic comparison is given on the application of two 2240-MW(t) HTGR SC/C plants (one a lead plant, the second an equilibrium plant) located on the St. Rosalie site. The plants would supply process steam and electric power to an Alliance (Louisiana) refinery and to new energy intensive industries in the vicinity.

A site-specific study identifies the Midway/Sunset oil field in California as a potential candidate site for an HTGR application to supply a steam flooding process for heavy oil recovery.

Preliminary cost and economic assessments are presented for the HTGR-SETS for combined base/peaking, large oil refinery repowering, indirect Paraho shale oil above-ground retorting (AGR), and Supersets (2 x 2240-MW(t) HTGR-SETS) application. Cost and economic data are developed from earlier application studies.

LIST OF ACRONYMS

AIPA	accident initiation and progresion analysis
BFP	boiler feed pump
BOP	balance of plant
CACS	core auxiliary cooling system
CACWS	core auxiliary cooling water system
CAHE	core auxiliary heat exchanger
CE	Combustion Engineering
DBA	design basis accident
DOE	Department of Energy
DV&S	design verification and support
EES	economizer-evaporator-superheater
FMEA	failure mode and effects analysis
FSV	Fort St. Vrain
GA	GA Technologies Inc.
GCR	gas-cooled reactor
GCRA	Gas Cooled Reactor Associates
GA	General Electric
HEU	high-enriched uranium
HP	high pressure
HTGR-GT	high-temperature gas-cooled reactor - gas turbine
HTGR-PH	high-temperature gas-cooled reactor - process heat
HTGR-SC/C	high-temperature gas-cooled reactor - steam cycle/cogeneration
HTGR-SETS	high-temperature gas-cooled reactor - sensible energy transmission and storage
IP	intermediate pressure
ISI	in-service inspection
LEU	low-enriched uranium
LOFC	loss of forced circulation
LP	low pressure
LWR	light water reactor

MRS	modular reactor system
MRS-SC/C	modular reactor system - steam cycle/cogeneration
NHS	nuclear heat source
NRC	Nuclear Regulatory Commission
NSSS	nuclear steam supply system
OBE	operating basis earthquake
PCRV	prestressed-concrete reactor vessel
P&I	piping and instrumentation
UE&C	United Engineers & Constructors
VHTR	very high temperature reactor

CONTENTS

FIGURES

FIGURES (Continued)

FIGURES (continued)

FIGURES (continued)

FIGURES (continued)

FIGURES (Continued)

TABLES

TABLES (Continued)

TABLES (Continued)

TABLES (Continued)

1. INTRODUCTION AND SUMMARY

This report describes the progress achieved during the second half of FY-82 in the technical design program for the GA HTGR-SC/C, monolithic HTGR-PH, HTGR-MRS-PH, and HTGR-GT plants, together with applications studies related to the HTGR-SC/C and HTGR-PH. The HTGR applications program encompasses core outlet temperatures of 750°C (1382°F), 850°C (1562°F), and 950°C (1742°F).

Summaries of the work performed under each of the principal tasks are presented in this section. More detailed information is given in Section 2 for the HTGR-SC/C, in Section 3 for the monolithic HTGR-PH, in Section 4 for the HTGR-MRS-PH, and in Section 5 for the HTGR-GT. Section 6 contains details of the HTGR applications development studies.

1.1. HTGR-SC/C

1.1.1. NSSS Performance

During this reporting period, the sixth issue of the Plant Technical Description (TED) was completed and an NSSS performance margin assessment was initiated. The assessment is aimed at providing a technical and economic basis for the location and amount of the performance margin.

1.1.2. NSSS Integration

In the previous semiannual report (Ref. 1.1-1), technical issues were identified and progress in their resolution was described. During the present reporting period, three of these issues were identified in the Development Plan as requiring special attention: (1) core thermal-hydraulic

phenomena and uncertainties, (2) fuel element graphite stress analysis uncertainties, and (3) water ingress. A program to resolve these issues was specially mentioned as part of the NSSS integration task. The remaining issues are being resolved in a routine manner within the normal integration procedure.

1.1.3. Plant Availability/Maintainability

Major accomplishments in support of this task were the issuance of the Plant Availability Specification, the completion of FEMAs for several major system elements, and the preparation of a draft plant availability status report. A draft HTGR-SC/C NSSS maintainability specification was also completed. Included in the availability specification are the results of a top-level system availability allocation.

1.1.4. Plant Dynamics

In the area of plant dynamics, a study coupling the HTGR-SC/C plant BOP models (developed during the first half of FY-82) to a reference 2240-MW(t) HTGR NSSS model was completed. Issue 2 of the Plant Transient Specification, containing definitions of representative plant transients and frequency of occurrence as a basis for the plant design, was completed. Some key plant transients were also analyzed using the MLTAP code, including reactor trip from 100% power and turbine trip cases to permit orderly plant operation phase transition. Such orderly transition would mitigate thermal stresses to major components, maximize electric power production, and provide adequate core cooling and afterheat removal using the main loops.

Meetings were held between GA, DOE, GCRA, UE&C, and GE to discuss the work scope for the reactor technology applications program. It was agreed that GA would take the lead for the PPS, UE&C for the plant control system, and GE for plant simulator development.

1.1.5. BOP Interfaces

A comprehensive review was made of the UE&C variable cogeneration plant configuration study for the 2240-MW(t) HTGR-SC/C application. As a result of continuing concerns regarding certain aspects of the proposed three-turbine-set arrangements to provide for all-electric, full process, or varying conditions, GA prepared a proposed evaluation program of the UE&C recommendation to be conducted by a major turbine-generator supplier in FY-83. This program includes a report stating concept limitations, proposed solutions, and estimates of development costs to resolve any considered issues.

1.1.6. Licensing Support

Revision 2 of "Nuclear Safety Plant Specification, HTGR-SC/C, 2240 MW(t)" was issued. Report GA-A16457, "Safety/Licensing Assessment of the 2240-MW(t) HTGR steam Cycle/Cogeneration Plant," was updated to include the latest source term data and dose calculations. Other activities included reviewing design and programmatic documents.

1.1.7. Safety/Reliability

A safety risk assessment was made of a 2240-MW(t) HTGR-SC/C plant for a Port Arthur, Texas, site. The assessment showed that the HTGR-SC/C in its present conceptual design phase can successfully meet the stringent qualitative safety targets.

The results of an assessment of a new core thermal radiation hole design with six hexagonal holes indicated that the design could lower the peak core temperature, following an LOFC accident, below 3315°C (6000°F) with greater margin than the previous fifteen 178-mm (7-in.) diameter hole design. Although the radial temperature distribution is rather uneven with the new design, optimization is possible via the number and configuration of the holes. Further studies are also recommended to incorporate the radiation holes in the new lower-power-density core.

1.1.8. PCRV Design

A study was made to establish the availability of coarse aggregates for 45-MPa (6500-psi) and 55-MPa (8000-psi) concrete for the construction of a PCRV at nine candidate HTGR sites in various parts of the U.S. The study showed that both concretes can be produced anywhere in the U.S., but where local materials are of poor or marginal quality, aggregates would need to be imported at additional cost. Good aggregate is available at Connecticut, Pennsylvania, Delaware, Arizona, South Carolina, and Colorado sites. Maginal aggregate is available near Florida, Idaho, and California sites. For the Port Arthur, Texas, site, coarse aggregate must be imported since there is none in the area.

The results of a cost optimization study of the PCRV liner cooling water system and thermal barrier showed that increasing the thickness of the thermal barrier increases the cost of the PCRV, liner, and thermal barrier while decreasing the cost of the liner cooling system. Owing to the small saving, <1% of the affected systems (neglecting engineering costs), it is recommended that the reference design thermal barrier thickness be retained.

A study to evaluate upgrading of the upper plenum cooling system was completed. Based on the study results, a cooling water tube array to accommodate the predicted peak heat load without boiling for an LOFC accident is recommended.

During this reporting period, a bottom head thermal barrier design was developed that incorporates a metallic primary support with a stack of ceramic pads that act as an insulator and a backup structure. This design is a viable replacment for the present reference all-ceramic pad design used on the 2240-MW(t) HTGR-SC/C plant. It is planned to quantify the potential benefits in FY-83 before making a final recommendation.

A preliminary list of all principal criteria for ISI, maintenance, and replacement for all primary system components, reactor internals, and core components was prepared. Final documentation is scheduled for completion by the end of CY-82.

1.1.9. Fuel Handling Equipment

Two layouts were made to amplify and document informal sketches prepared in the prior reporting period to justify plant interfaces. One layout illustrates the construction of the remotely operated bridge crane and grapple assembly in the Fuel Sealing and Inspection Facility. The other layout illustrates the construction of the fuel transfer vault with internal handling mechanisms, which is located beneath the PCRV. All fuel entering or leaving the reactor core passes through this vault.

There are now 13 design layouts of the new equipment in the fuel handling system and seven design studies that define various interfaces and clearances.

1.1.10. Reactor Service Equipment

Work performed during this reporting period resolved the remote handling interfaces between the circulator handling equipment and the auxiliary circulator and its isolation valve and also reduced the weight of the circulator handling cask.

1.1.11. Reactor Internals

During this reporting period, layout drawings of the core lateral restraint (CLR) system were updated.

A thermal-hydraulic analysis of the core support blocks identified reactor trip from 100% power as the most severe transient condition. Accordingly, this condition has been selected for more detailed analysis.

A study of the leakage through the core peripheral seal indicated a potential for the leak to exceed the intended leak rate.

1.1.12. Reactor Core Component Design

In the thermal-hyraulic area, a substantial effort to determine the operating stresses in the present core was initiated. (The present core is described in Ref. 1.1-1.) The main modifications from the earlier reference core are as follows: (1) The number of full columns has been increased by 102 to a total of 541; (2) the fuel elements have nine rather than 10 rows of holes; and (3) a sealing flange has been added at the end of each element.

The fuel element stress analysis, which uses input from the core nuclear design, is accomplished in several phases. Phase 1, a survey of the core to identify the critical elements, was completed. The critical elements were found to be located in layer 4 (measured from the top of the active core), regions 44 and 66. Phase 2, which is in progress, includes more detailed analysis of the critical elements. The thermal analysis of Phase 2 is being performed with the TEPC code and the stress analysis with the GBEAM code.

1.1.13. Core Nuclear Design

Evaluations were completed for the fuel element designs, core layout, core fuel loadings and fuel-cycle prescription and costs for the 2240-MW(t) HTGR-SC/C alternate core configuration. Revisions to the design in the current reporting period included an increase in the fuel volume fraction in the control rod blocks of the nine-row fuel element design and a reduction from four to three radial zones employed to reduce radial power peaking. A 1-1/2-yr initial cycle was retained with core-average ratios of C/Th = 375, C/U = 1124, and reload uranium (LEU) loadings (four segments, 1-yr cycles) were fixed with a C/U ratio of about 855. The C/Th ratios for equilibrium cycle reloads were found to average, as before, at about 607.

One- and two-dimensional diffusion theory calculations were performed to characterize the spatial distributions of flux and power, with and without burnup, in the reference design. Axial geometry calculations showed that the influence of fresh reloads around a given region do not adversely impact the stability of the axial power distribution in the region. Two-dimensional (hexagonal geometry) depletion calculations were carried out for the initial core plus eight reloads in the reference fuel cycle prescription.

Improved editing routines were developed to obtain clearer evaluations of fuel-volume specific power densities required to drive fuel rod temperature distributions and to calculate stresses. The region power (RPF) and inter-region peak-to-average power ratio (TILT) parameter sets derived for the 93 time points for the new element design and fuel loadings lie within a smaller envelope then previously achieved with the reference 2240-MW(t) designs using 10-row blocks. Preliminary evaluations of fuel temperature peak isotherms superimposed on the RPF/TILT data indicate that it is possible to limit fuel temperature to below 1200°C (2192°F).

Methods and models were developed for deriving flux and power distributions across a region on a much finer grid (384 triangular mesh intervals per column) to permit more detailed stress analysis.

Fuel Performance. A thermal analysis for the Ref. 0 (conceptual design) HTGR-SC/C core was performed to predict fuel and graphite temperatures under full-power steady-state conditions and to provide input for the stress analysis. The peak fuel temperature predicted for the new core design was 1207°C (2204°F), slightly lower than the 1226°C (2238°F) peak temperature of the previous design. While the full impact of the new core design cannot be evaluated until the entire fuel performance analysis has been completed, present results indicate that the reduction in the peak fuel temperature due to reduced maximum power tilts is an improvement over the previous core design.

During the present reporting period, source terms were updated for the new reference core design and accompanying flow parameters and for the new radionuclide design criteria. The source terms were calculated using the latest value for the fraction of fissions in the fissile and fertile particles and the activation product nuclide effective yields corresponding to the current core physics design.

During the previous reporting period, the criteria for circulating and plateout activities in the primary circuit of the 2240-MW(t) HTGR-SC/C were reviewed and the circulating activity criteria were revised. The new level B criterion of 14,000 Ci of Kr-88 is based on allowable site boundary dose and containment access requirements. The Level A criterion is based on an ALARA margin of four reduction (3500 Ci of Kr-88).

Fission product transport is no longer considered a priority critical issue owing to the relatively clean environment associated with the HTGR-SC/C and the fact that more than 90% of the circulating activity is expected to come from manufacturing defects.

Fuel Cycle Costs. Fuel cycle costs were evaluated for a number of HTGR design options, with emphasis on the 2240-MW(t) HTGR-SC/C plant with an LEU/Th initial cycle and various equilibrium reloading schemes using LEU and HEU fuel. The cost comparisons for the HTGR-SC/C options and process heat design, including costs for the modular core systems, were updated using 1982 costs and economic assumptions. For once-through designs, HEU/Th fuel with its higher-power-density capability affords about 10% lower fuel cycle costs than LEU/Th fuel, which is directly attributed to the lower unit-energy handling costs. Fuel costs for the LEU/Th modular designs are significantly higher (60% more) owing to the batch loading modes assumed. Further cost updating is expected with the resolution of waste repository designs and charges.

1.1.14. Primary Coolant System Design.

Primary Coolant Flow, Temperature, and Pressure Distributions. Two network flow models were developed and used to calculate flow, pressure, and temperature distributions in the primary coolant system of the 2240-MW(t) HTGR-SC/C plant.

The first model represents the current design of the system and the NSSS components as closely as possible. The most significant result from running this model at 100% reactor power, at 75%, 50%, and 25% feedwater flow, and at reduced power with two or three main loops operational was that the bypass flows calculated were considerably greater than those required to achieve expected plant performance.

The second model is the same as the current design model except for changes intended to produce the expected or design flow distributions. The pressure drops calculated by the second model are consistently lower than the design values. This may be partially due to conservatively large design values allocated for the primary loop pressure drop.

Water Ingress Design Solutions. A study was performed with the objective of developing design solutions that will assure compliance with the plant availability goal with respect to accidental water ingress. The maximum plant downtime tentatively allocated for this type of accident is 4 days/reactor-year. To achieve this goal with an adequate margin, all aspects of the moisture ingress problem were examined and cost-effective design solutions were identified.

1.1.15. Main Circulator Design

Main circulator aerodynamic design and off-design performance parameters were established as well as various trends and effects of vaned and vaneless diffusers and blade exit angles. The water ingress prevention

effect was concentrated in the areas of the circulator bearing and seal design and the circulator service system design in optimizing the pressure flow and control diagrams. Design layouts of the main loop shut-off valves were completed. The electric drive motor liaison and review effort has progressed in support of the motor conceptual design report, which has been completed by the vendor.

1.1.16. Main Circulator Drive System

The design specification for the main circulator was completed. The synchronous drive motor is required to operate continuously from 100 to 2400 rpm and provide a maximum power for 11.3 MW (15,200 hp) at 2400 rpm. The motor is a totally enclosed vertically mounted machine with internal air cooling provided via an air-to-water heat exchanger.

A conceptual design study of the main circulator drive motor was performed by GE for GA. Preliminary outline and assembly drawings have been prepared. The feasibility of the 11.3 MW (15,200-hp), four-pole, 100-to 2400-rpm, three-phase, 80-Hz synchronous motor appears promising.

1.1.17. Steam Generator

The transfer of steam generator technology to CE proceeded according to a planned program that involved (1) the transfer of analytical methods, (2) the transfer of software including developed design specifications, drawings, and criteria, and (3) the transfer of DV&S results as they became available.

1.1.18. Primary Coolant System Controls and Instrumentation

Block and P&I diagrams were prepared and updated for the main circulator service system and primary coolant system.

1.1.19. Auxiliary Systems Design

Owing to budgetary constraints, work in this area consisted solely of revisions to the helium service system description documents.

1.1.20. CACS Design

Prior design transients for the CACS were performed for the 900-MW(t) HTGR-SC/C and were expected to be applicable to the 2240-MW(t) HTGR-SC/C since both cores have the same rating. However, because of the larger core for the 2240-MW(t) plant and the recent changes in core design (flanged fuel element), updated transient data were needed for the design of CACS components. Six transients were analyzed, three of which were based on the DBA for the CACS system design. The transient curves for the HTGR-SC/C are not expected to vary appreciably from these presented in this report.

1.1.21. Auxiliary Circulator Design

During this reporting period, the general arrangement drawing, showing the auxiliary circulator and auxiliary loop shutoff valve installed within the PCRV, was updated to comply with the latest PCRV penetration configuration and to simplify installation and removal with the circulator handling equipment. The auxiliary circulator service system conceptual design was developed with emphasis on the equipment and procedures required for the maintenance and exchange of the bearing lubrication oil.

1.1.22. Core Auxiliary Heat Exchanger

A report was prepared that discussed how improvements resulting from flow distribution tests were incorporated into the CAHE design. Additional testing, computer code development, and design analysis were also recommended.

The cost data generated for the CAHE were considered to be "order of magnitude" only, since funding and time constraints precluded making an in-depth estimate.

The CAHE bayonet tube scoping tests were oriented toward determining flow characteristics (primarily pressure drop) as a function of the flow annulus geometry, quantification of tube insertion and removal forces, and collection of some limited tube vibrational characteristic data. The tests have been completed by CE, the raw data have been released to GA, data correlation has been completed, and the final test report is being prepared.

1.1.23. Controls and Instrumentation

Block diagrams of the PPS were prepared, and a study was made of the potential of plant availability based on advantages or disadvantages of two-out-of-three and two-out-of-four logic schemes for the PPS. From preliminary results of the study it is uncertain that the two-out-of-four logic will significantly increase plant availability over the two-out-of-three logic. Recommendations were made for work to be continued in FY-84.

A study was made to investigate the maximum electromagnetic inteference (EMI) generated by the main circulator motor/power supply that can be tolerated by safety-related electronic equipment. Preliminary findings showed that electric noise problems can exist in power plants and the large helium circulator drives and controls are known sources of noise. The minimization of electrical noise requires a coordinated effort between BOP and NSSS designs. A systems approach relative to electrical noise susceptibility is advocated. This study establishes a foundation for standards that will lead to consistent application of known noise-reducing techniques.

1.1.24. Plant Control System

Instrumentation diagrams were prepared showing the connection between major components in the NSSS and other plant systems.

Reference

1.1-1. "HTGR Applications Program Semiannual Report for the Period October 1, 1981, through March 31, 1982," DOE Report GA-A16831, 1983.

1.2. MONOLITHIC HTGR-PH

1.2.1. Monolithic HTGR-PH Concept Studies

Initial studies aimed at improving the economics of the 1170-MW(t) 850°C (1562°F) indirect cycle plant (from the FY-81 base) by optimizing the NHS parameters showed only modest improvement.

A decision was made part way through the program to investigate a process heat plant concept that had economic potential by virtue of (1) direct reforming at 950°C (1742°F) and (2) taking advantage of economy of scale by increasing the reactor thermal rating from 1170 to 2240-MW(t). A preconceptual design and cost estimate was completed for a six-loop 2240-MW(t) 950°C (1742°F) direct reforming plant.

1.2.2. Availability/Maintainability (Monolithic and MRS)

A preliminary availability comparison made by Bechtel showed that the modular system has slightly better [<1% for the HTGR-SC/C and equal for the HTGR-PH (reformer)] availability than the monolithic system. This comparison used multiple units (two monoliths and 10 to 12 modules) to produce system availabilities of about 95% for the HTGR-SC/C and 99% for the HTGR-PH.

1.3. HTGR-MRS DESIGN STUDIES

Studies of the HTGR-MRS-PH in FY-82 led to establishment of a preconceptual design of an MRS in sufficient detail to document a "first iteration" design, which is not yet optimized. Core physics studies were performed for both LEU/Th and HEU/Th cycles, details of a core reactivity approach were established, and a variety of control rod drives for the primary (long-term cold shutdown control) and secondary (hot shutdown) systems were investigated.

Work was performed to (1) investigate an MRS for HTGR-SC conditions and (2) permit a comparison between a multiple-module concept and the monolithic HTGR-SC/C lead plant in the areas of design features, economics, and availability. A "first iteration" design was generated for the HTGR-SC/C application with a reactor outlet temperature of 688°C (1270°F) and characterized by a prismatic core and a single in-line vessel arrangement with the steam generator positioned above the upflow core. With a reactor outlet temperature considerably lower than the process heat plant, initial endeavors involved an evaluation of increasing the module rating above 250 MW(t), consistent with the established criteria and the goal of retaining benign characteristics. Depressurized core heatup considerations limited the module rating to 300 MW(t).

A brief study was also made to explore the potential of a number of PCRV concepts for a 300-MW(t) MRS-SC/C plant. Several concept configurations were evaluated including single and podded multicavity vessel designs, with a varying number and location of steam generators. Based on this conceptual design and cost comparison, it appears that the single-cavity vessel with four steam generators arranged above the core has a small economic penalty but offers better availability features than the other concepts studied. Further study of the PCRV concept is planned as an ongoing activity in FY-83.

Safety assessments of the HTGR-MRS were made during the period, and it was shown that for the 250 MW(t) MRS-PH plant in-line modular vessel

arrangement, natural circulation for the pressurized system is feasible. Natural circulation cooling was shown to be feasible for vessel limits of 454°C (800°F) and 6.2 MPa (900 psia) established by CE.

Fuel cycle cost were generated for the 250-MW(t) HTGR-MRS-PH and HTGR-MRS-SC/C plants. It is recognized that changes to the MRS fuel cycles could improve the plant economics, particularly using a 4-yr cycle exposure with graded refueling, based on biennial refueling of one-half of the core. Effort in FY-83 are expected to concentrate on the biennial refueling approach.

The results of a seismic scoping study for the HTGR-MRS showed that the current design configuration produces an amplification of the seismic excitation by a factor of 3.5 in the horizontal and 2.6 in the vertical plane. Owing to the unsymmetrical configuration of the Reactor Containment Building, the in-structure response spectra in the "weak" Z direction shows a consistently higher amplification factor in both the rigid and elastic ranges. Because of the rigidity of the MRS process heat module, snubbers are unnecessary.

As a result of the complex configuration of the reactor vessel and the preliminary nature of the design, an improved mathematical model is required to evaluate the dynamic behavior of the various reactor internals and should include a more detailed model of the core.

1.4. HTGR-GAS TURBINE/COGENERATION (HTGR-GT/C) PLANT DESIGN

Design work on the HTGR-GT plant essentially ended in FY-81. The conclusion at that time was that the gas turbine concept required a major development effort and its introduction as a follow-on plant to FSV was not consistent with a lead plant project definition for operation of a commercial size HTGR in the mid-1990s. Accordingly, efforts were focused on the HTGR-SC/C concept for lead plant definition.

The results of the current HTGR-GT/C study showed commonality with data from the fossil-fired closed-cycle gas turbine (CCGT) plant in that the Brayton cycle exhibits attractive cogeneration characteristics at high power-to-heat ratios. The characteristics are superior to those of the Rankine cycle plant, especially if additional use is made of the precooler reject heat (e.g., district heating, which was not addressed in this study) and if the process steam conditions are in the 1.03- to 4.5-MPa (150- to 650-psia) range.

However, the systems data for the advanced HTGR-GT/C plant must be put into perspective:

1. The reactor primary system is complex since it embodies the helium turbomachine and three major heat exchangers.

2. Previous studies have shown that a formidable development effort must be expended to resolve the technical issues.

3. Operation with a reactor outlet temperature of 950°C (1747°F) requires significant technology advancements, particularly in the materials area.

Economic projections for the HTGR-GT/C will not become meaningful until the process steam and cogeneration electricity markets that will prevail in the HTGR-GT/C deployment time frame can be characterized.

1.5. HTGR-APPLICATIONS AND APPLICATION PROCESS DEVELOPMENT

1.5.1. HTGR-SC/C Application for Shale Surface Retorting Processes

Two shale surface retorting processes were investigated for HTGR-SC/C plant application: (1) a modified Paraho process and (2) the direct steam retorting process. The modified Paraho process uses recycle hot gas to pyrolyze shale, and the recycle gas is heated by the primary steam from a 1170-MW(t) HTGR-SC/C plant. In the direct steam retorting process, low-pressure, high-temperature steam is used for retorting the shale and the high-temperature heat is provided by an 1170-MW(t) HTGR-SC/C plant. The results of the study show that the HTGR-SC/C plants can be coupled to the process plants for providing process heat, process steam, and electric power and have significant economic and environmental advantages over fossil-fired power plants.

1.5.2. HTGR-SC/C Application to Modified In-Situ (MIS) Process

An assessment of the MIS process showed that this process requires only a moderate amount of steam for injection with air to control the temperature of the combustion zone. Since a considerable amount of off-gases is produced in the MIS process, process steam can be generated by burning the off-gases in the boiler and there is no need for any external energy source, including an HTGR-SC/C plant.

1.5.3. Conceptual Reboiler Design for Heavy Oil/Tar Sands Fields Use

A conceptual design was made of a reboiler to generate steam for heavy oil/tar sands recovery from user-process-produced waters as the feed. Steam was generated in the reboiler secondary side at 80% quality, and heating was provided by the HTGR primary steam. The conceptual reboiler consists of conventional TEMA counterflow U-tube heat exchangers for the economizer section and TEMA E-shells with cross counterflow for the evaporator section.

A preliminary reboiler cost estimte was made, which showed a cost of $4.39 million and $12.54 million (both in January 1982 dollars) for heavy oil and tar sands reboilers, respectively. In addition, 2-1/4 Cr-1 Mo tubing was selected for all heat exchangers.

1.5.4. Site Suitability

A preliminary siting study for a 2240-MW(t) HTGR-SC/C application at Port Arthur, Texas, was completed, and a primary location and an alternative location that satisfy population density criteria were identified. Because large quantities of flammable and combustible materials are routinely handled nearby, external explosion hazards were assessed for the primary site, and the public risk was found to meet the quantitative safety goals. The site is thus acceptable from the standpoint of public risk due to external hazards.

1.5.5. Site-Specific Study for Refinery Application

As part of the study to determine the desirability of using reboilers for supplying process steam to the Port Arthur refinery, a series of heat balance calculations was made to determine comparative performance (electrical power generated) for plants with and without reboilers. For a 2240-MW(t) reactor plant that is furnishing 377 kg/s (3,000,000 lb/hr) of steam at 4.8 MPa (700 psia) (at the reboiler outlet) to the refinery, the loss in electrical power output is about 27 MW(e) for the plant using a reboiler compared with one in which the same quantity of HTGR-generated steam at the same pressure and temperature is taken to the refinery. This differential power capability is one component of an economic evaluation of the two alternative designs. Additionally, this study led to the selection of a reboiler configuration and sizing, which can be used to estimate the cost of that equipment, and a decision to recommend nine reboilers, which will provide a margin of four modules to cover fouling and outages.

A scoping-type evaluation and economic comparison study was performed on the application of two 2240-MW(t) HTGR-SC/C plants (one a lead plant and the other an equilibrium plant) to supply process steam and electric power to a refinery located at Alliance (St. Rosalie site), Louisiana, and to new energy-intensive industries in the vicinity of Alliance. The lead plant HTGR is scheduled for commercial operation in 1995 and the equilibrium plant in 1997. Coal was selected as an alternative source of energy for comparison.

A total process steam demand of 630 kg/s (5 x 10^6 lb/hr) at 4.65 MPa/371°C (675 psia/700°F) is envisaged for the Alliance refinery and industrial complex. An electric power demand of 100 to 200 MW(e) is anticipated. Kaiser Aluminum has been identified as a potential large consumer of electric power to operate alumina smelting plants located in Louisiana. Kaiser is presently generating its own electricity using gas-fired power plants.

Preliminary results of an economic study showed that the steam cost (in January 1982 dollars) with HTGR-SC/C plants is nearly one-half of the cost with coal-fired plants [$3.45/GJ (3.64/MBtu) versus $6.30/GJ ($6.65/MBtu)] for the selected scenario and assumptions. The steam costs were computed with an allowance for electric credit at $0.035/kWh.

1.5.6. Site-Specific Study for Heavy Oil Recovery

A site-specific study to identify a large oil field for an HTGR-SC/C plant application to supply steam flooding process for heavy oil recovery provided a candidate in the Midway/Sunset heavy oil field in California. This oil field is estimated to contain some 95,000,000 m^3 (600,000,000 barrels) of recoverable heavy crude and by 1990 is estimated to reach a recovery rate of 0.22 of 0.24 m^3/s (120,000 to 130,000 barrels/day). Based on these projections, this crude oil recovery would justify process steam supply from one or possibly two 2240-MW(t) HTGR-SC/C plants in 1995. The

HTGR-SC/C has the lowest steam costs and shows substantial economic advantage over coal and oil for the same application. Existing environmental constraints with the conventional oil-fired boilers in the Midway/Sunset field enhance the potential of HTGR-SC/C applicability. However, because of seismic considerations prevailing at the Midway-Sunset field, it may not qualify as a potential site unless appropriate seismic design provisions are made for the HTGR-SC/C plant.

1.5.7. HTGR-PH Application Studies

Solvent Refined Coal (SRC-II) Process. A report was issued summarizing work performed during 1980-1982 on the integration of an HTGR-PH plant into a refinery that uses the solvent refined coal (SRC-II) liquefaction process. The SRC-II process was modified by an upgrading plant so that the final product from coal is transportation fuel. Integration was performed both with the HTGR-SC having a core outlet temperature of 700°C (1290°F) and with the HTGR-PH operating with a core outlet temperature of 850°C (1560°F) and a secondary helium loop, and a comparison was made with a coal-fed system.

These studies showed that nuclear energy can replace essentially all the fossil energy used in a representative coal liquefaction process plant, increasing the yield of the process plant by the amount of oil equivalent to the nuclear reactor used.

Based on a constant coal refinery feed of 352 kg/s (33,500 tons/day), the refinery product is increased by 8% with the HTGR-SC/C and by 13% with the HTGR-PH above the conventional coal-fed process used in this study. Product costs using the HTGR-SC/C are ~14% lower than for the coal process, while the HTGR-PH product costs are ~5% higher. If coal prices reach $4.11/GJ ($4.34/MBtu) or above, the HTGR-PH is a more economic energy source than coal. In addition, the capital cost for the HTGR-SC/C integrated into the process system is ~15% higher than that for the standard coal system studied. The HTGR-PH integrated capital cost is ~10% higher than for the coal system.

German (BF) Coal Gasification Process Review. The application of nuclear process heat (PNP) from a high-temperature reactor (HTR) to the German coal gasification process developed by Bergbau-Forschung (BF) was investigated. A comparison was made with a similar method, the Exxon catalytic coal gasification (ECCG) process. The ECCG process depends solely on its feed coal to cover its process heat and some additional outside electric power. However, it can be used in combination with HTGRs to provide the necessary process heat and electric power.

Both the BF and ECCG processes use the same catalyst but at somewhat different operating conditions. The BF process has the additional option to operate without any catalyst. With currently available information, it has not been possible to confirm the advantages claimed by the German process.

1.5.8. HTGR-SETS Application Costs and Economics

During this reporting period, capital cost and economic assessments of HTGR-SETS were completed for applications presented in the previous semi-annual report (Ref. 1.5-1). There applications included (1) an on-site base load and peaking electric power plant, (2) an oil shale AGR, and (3) three oil refinery repowering applications.

The HTGR-SETS combined base/peaking application economic assessment yielded two important results:

1. Both HTGR options are economically superior to the competing fossil alternative.

2. No economic advantage for the HTGR-SETS over the cycling HTGR-SC has been identified.

High fuel costs prevent the fossil alternatives from competing economically with the HTGR options for this application. The HTGR-SETS capital cost advantages accruing from its smaller reactor thermal capacity are overcome by its higher BOP costs attributable to the indirect helium loop, the molten salt equipment, and the thermal storage provisions.

The implications of these economic projections need to be studied further. While the HTGR-SETS can be shown to have considerably lower power-generating costs than its fossil competition, in its current form it does not appear economically more attractive than the cycling HTGR-SC plant.

The cost and economic assessments were made of the HTGR-SETS for three refinery applications: (1) a large refinery provided with process steam and electricity by an HTGR-SETS (2) a smaller refinery supplied by a remotely sited HTGR-SETS but using molten salt to assume fossil-fired heater duties, and (3) an extension of (2) that provides refinery needs and additional user services through a large-capacity multi-HTGR-SETS energy park.

During the large refinery study, it was recognized that the HTGR-SC/C was also a competitor for this application and therefore it was included in the economic evaluation. The study showed that close-in siting of a replacement energy supply plant at the refinery definitely favors the HTGR-SC/C relative to its assumed competition. The HTGR-SC/C maintains its advantage even at the 32.2-km (20-mi) separation distance assumed for this study, although its competitive margin is reduced considerably. On the other hand, the HTGR-SETS does not appear to be economically attractive at the 32.2-km (20-mi) pipeline distance owing to its unfavorable combination of higher pipeline cost, pumping penalties, and base-capital costs. The prospects for HTGR-SETS in this application could be improved if one or both of the following conditions prevailed:

1. Greater exclusion distances that also apply to coal-fired alternatives.

2. Additional refinery repowering needs that require high-grade heat [e.g., repowering of direct-fired and indirect-fired process heaters that require temperatures of 566°C (1050°F) or less].

A study of the cost and economics of the HTGR-SETs application to the indirect Paraho shale oil AGR process was also made that included the comparison of (1) the low-temperature HTGR-SETS, (2) the high-temperature HTGR-SETS, and (3) the fossil-fired plant cases. All options were to yield the same quantity of crude oil.

Direct and indirect capital cost comparisons for the three cases were developed, which contain enough detail to show how the various sections of the plant are affected by the proposed process changes. A product cost comparison for the three options was made based on the gross product, and assuming that fuel is purchased at the current market price for fuel oil. The results show that although the HTGR-SETS capital costs are approximately 70% higher than those of the fossil-fired reference case, the nuclear cases produce 43% more product oil at 90% of the cost of the oil produced by the fossil-fired case.

For the 2 x 1170-MW(t) HTGR-SETS refinery repowering concept, it was concluded that the lowest-cost energy system of those examined based on annual operating cost is the utility-owned 2 x 1170-MW(t) HTGR-SETS (refinery) operating at 70% capacity for the Middletown site at $245,000,000 per year, closely followed by the plant for the Gulf Coast site at $260,000,000 per year. However, the lowest product cost would occur with the same plant operating at 80% capacity.

For the SUPERSETS concept, the lowest-cost energy system of those examined based on annual operating cost was the utility-owned 2 x 2240-MW(t) HTGR-SETS (SUPERSETS) operating at 70% capacity for the Middletown site at $399,000,000/per year, with the Gulf Coast site close behind at $505,000,000/per year. However, the lowest product cost would occur with

the same plant operating at 80% capacity. The system with the greatest advantage over the nearest fossil-fired alternative was also the utility-owned 2240-MW(t) HTGR-SETS (SUPERSETS) operating at 80% capacity.

There is an economic penalty of some $100,000,000 per year associated with the use of the 4 x 1170-MW(t) concept as opposed to the 2 x 2240 MW(t) HTGR, although there may be availability/capacity improvements because of plant redundancy. However, for the analysis described here, a 70% (and alternatively 80%) average capacity was assumed for all concepts, and the quantitative ramifications of such improvements remain to be addressed in future studies.

Reference

1.5-1. "HTGR Applications Program Semiannual Report for the Period October 1, 1981, through March 31, 1982," DOE Report GA-A16831, 1983.

2. HTGR-SC/C

2.1. NSSS PERFORMANCE (6032010100)

2.1.1. Scope

The scope of this task is:

1. To describe the overall NSSS design and establish the steady-state performance that leads toward minimum cost of product and minimum technical risk.

2. To establish the basic design data, requirements, and criteria for the 2240-MW(t) HTGR-SC/C NSSS.

3. To define and document the steady-state performance requirements (performance envelopes) of the NSSS, including the expected (nominal) performance and off-design performance conditions that the NSSS design and its components must accommodate.

2.1.2. Discussion

Throughout the HTGR-SC/C plant design program, three major steady-state NSSS performance documents are being maintained in an updated status: (1) the "Plant Technical Description of the 2240 MW(t) SC/C Plant" (TED), which provides the NSSS design requirements, overall design basis, and major physical and performance features; (2) the "Expected NSSS Performance" plant specification, which provides the steady-state performance of the NSSS at nominal and reduced reactor power level with and without several main loops out of service and the expected NSSS performance conditions during plant

refueling (the performance presented for nominal reactor power is used in sizing all primary loop components and equipment); and (3) the "NSSS Thermal Performance Requirements" plant specification, which specifies the complete operating performance envelopes for all NSSS systems, subsystems, and components.

During this reporting period, the sixth issue of the TED was completed and an NSSS performance margin assessment was initiated. This latest issue of the TED is based on an extensive GA review that resulted in minor reorganization of the text and in additional plant definition. Table 2.1-1 gives the current NSSS heat balance, major parameters, and key features of major NSSS components. Figure 2.1-1 shows a current NSSS heat and mass balance diagram.

A performance margin has been added to the NSSS design to provide additional assurance that rated output can be achieved. The assessment is aimed at providing a technical and economic basis for the location and amount of this margin. The updating of assessment methodology (initial effort) was completed.

TABLE 2.1-1
MAJOR HTGR-SC/C PLANT/SYSTEM PERFORMANCE AND DESIGN PARAMETERS

NSSS Heat Balance

Heat generated by core, MW(t)	2240
Heat added by main circulators, MW(t)	41.3
Heat loss to CACS, MW(t)	1.43
Heat loss to PCRV liner cooling system	
From core cavity, MW(t)	2.75
From steam generator cavities, MW(t)	3.38
From CAHE cavities, MW(t)	0.58
Heat loss (miscellaneous), MW(t)	1.88
NSSS steam generator thermal power, MW(t)	2271
NSSS thermal efficiency,[a] %	99.56

Primary Coolant System Performance Parameters (see Fig. 2-1)

Reactor inlet	
Temperature, °C (°F)	319 (607)
Pressure, MPa (psia)	7.233 (1049)
Helium flow rate (total), kg/s (lb/hr)	1165 (9,245,000)
Reactor outlet	
Temperature, °C (°F)	688.9 (1272)
Reactor pressure drop[b] (plenum to plenum), kPa (psi)	93.73 (13.59)
Reactor power-to-flow ratio	
Expected kJ-s/kg (W-hr/lb)	1921 (242)
Maximum kJ-s/kg (W-hr/lb)	2222 (280)
Steam generator inlet	
Temperature, °C (°F)	685.6 (1266)
Pressure, MPa (psia)	7.129 (1034)
Helium flow rate (total, kg/s (lb/hr)	1173 (9,306,000)
Steam generator outlet	
Temperature, °C (°F)	313 (595)
Steam generator pressure drop, kPa (psi)	52.1 (7.56)
Main circulator inlet	
Temperature, °C (°F)	313 (595)
Pressure, MPa (psia)	7.081 (1027)
Helium flow rate (total), kg/s (lb/hr)	1176 (9,337,000)

[a] NSSS thermal efficiency = (NSSS steam generator thermal power - NSSS heat losses)/NSSS steam generator thermal power.

[b] Reactor pressure drop based on a equilibrium cycle RPF factor of 1.45.

TABLE 2.1-1 (Continued)

Main circulator outlet	
Temperature, °C (°F)	319 (607)
Pressure, MPa (psia)	7.24 (1050)
Main circulator pressure rise, kPa (psi)	160 (23.20)
Main circulator	
Shaft power/unit, MW	10.33
Input to motor power supply/unit, MW	12.04
Helium inventory	
Total (within PCRV), kg (lb)	14,890 (32,820)
Circulating, kg (lb)	11,400 (25,100)
Bypass, buffer, and leakage flows	
Total circulator bypass, kg/s (lb/hr)	3.9 (31,000)
Total steam generator buffer, kg/s (lb/hr)	5.86 (46,500)
Total leakage through standby CACS, kg/s (lb/hr)	1.83 (14,500)

Secondary Coolant System Performance Parameters (see Fig. 2-1)

Feedwater	
Temperature at steam generator inlet, °C (°F)	221 (430)
Pressure at steam generator inlet, MPa (psia)	21.19 (3074)
Flow rate (total), kg/s (lb/hr)	930 (7,380,000)
Steam	
Temperature at steam generator outlet, °C (°F)	540.6 (1005)
Pressure at steam generator outlet, MPa (psia)	17.34 (2515)

NSSS Component Design Parameters

Core	
Core power density, W/cm^3	5.78
Steam generators	
Type of steam generator bundle	Helical EES/straight tube superheater
Type of exhaust	Bottom
Tube plugging	
Method	Manual
Percent	1
Tube fouling - midpoint of cleaning cycle, %	~4

TABLE 2.1-1 (Continued)

Main circulators	
Type	Centrifugal flow
Drive	Variable-speed synchronous electric motor
Orientation	Vertical shaft
Motor power margin, %	9.7
Adiabatic efficiency (overall), %	79.0
Mechanical efficiency, %	97.5
Motor/controller combined efficiency, %	88.0
Auxiliary cooling system	
Type of heat exchanger bundle (CAHE)	Straight-tube bayonet
Penetration location in PCRV	Bottom
Auxiliary circulator	
Type	Axial flow
Drive	Variable-speed induction electric motor
Orientation	Vertical shaft

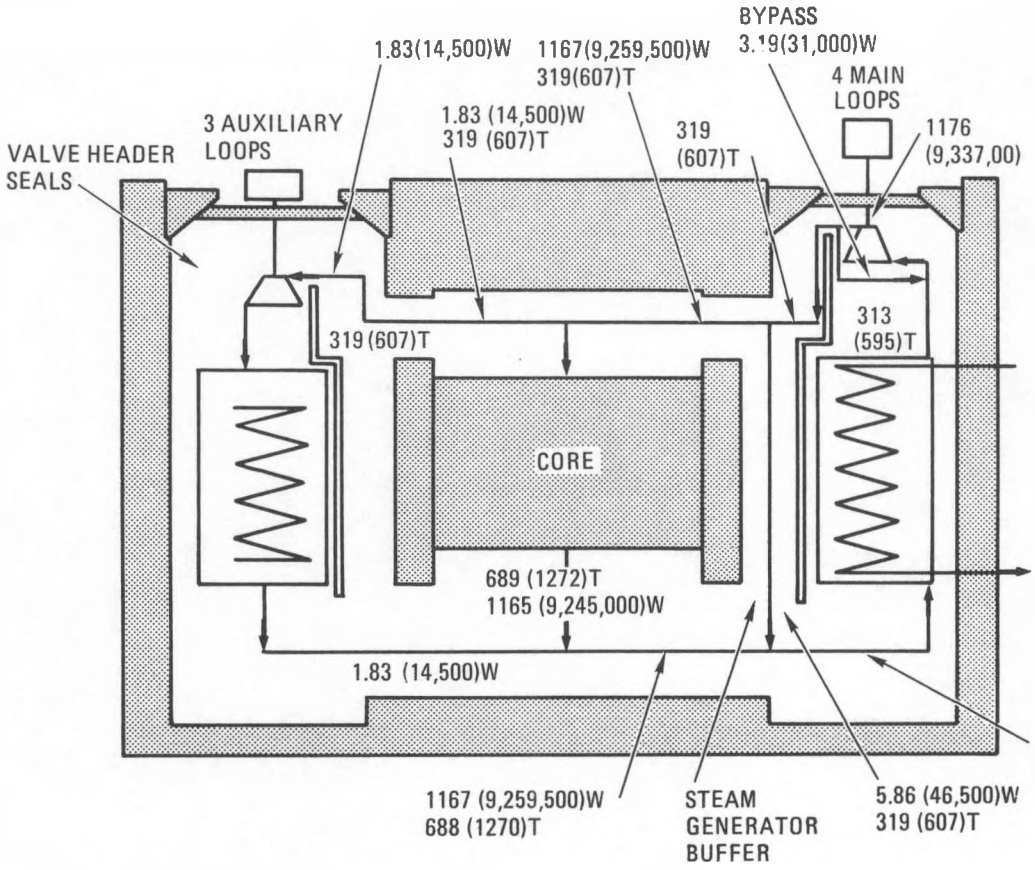

PERFORMANCE

HEAT GENERATED BY CORE	2240	MW
NSSS THERMAL POWER	2271	MW
HEAT GENERATED BY STEAM GENERATORS	2271	MW
HEAT ADDED BY CIRCULATORS	41	MW
HEAT LOSS TO CACS	1.43	MW
HEAT LOSS TO PCRV LINER COOLING SYSTEM FROM		
S.G. CAVITY	3.38	MW
CORE CAVITY	2.75	MW
CAHE CAVITY	0.58	MW
MISCELLANEOUS HEAT LOSSES	1.88	MW
HELIUM OPERATING PRESSURE	7.24 MPa (1050	PSIA)
HELIUM PRESSURE DROP	0.16 MPa (23.20	PSIA)
TOTAL CIR. HELIUM FLOW	1176 KG/S (9,337,000	LB/HR)

FEEDWATER S.G. INLET
930(7,380,000)W
221(430)T
21.20(3,074)P

MAIN STEAM
S.G. OUTLET
930(7,380,000)W
541(1,005)T
17.33(2,514)P

LEGEND
W = FLOW KG/S (LB/HR)
T = TEMPERATURE, ^{o}C (^{o}F)
P = PRESSURE, MPa (PSIA)

Fig. 2.1-1. 2240-MW(t) reference plant heat and mass balance diagram

2.2. NSSS INTEGRATION (6032010200)

2.2.1. Scope

The objective of this work is to provide assurance that the NSSS components interface with each other properly from a mechanical, thermal-hydraulic, electrical, nuclear, etc., standpoint and are consistent with the requirements of the Overall Plant Design Specification.

The workscope includes the review of NSSS technical documents to verify their technical content and applicability. It also includes the coordination of efforts to resolve outstanding technical issues.

2.2.2. Discussion

In the previous reporting period, progress was made on the resolution of technical issues. Meetings were held to assure that the technical approach was sound and that all aspects of the issue were being pursued consistent with budgetary restraints.

During this reporting period, three major issues were identified in the Development Plan as requiring special attention. Progress made on these three major issues is summarized below. The remaining issues are being resolved in a routine manner and are discussed in pertinent sections of this report.

2.2.2.1. Core Thermal-Hydraulic Phenomena and Uncertainties. Design improvements were made to the core that show a strong potential for eliminating major core thermal-hydraulic uncertainties, such as fluctuations, redistribution of core outlet temperatures, and uncontrolled region-to-region crossflow. Tests are needed to confirm the elimination of fluctuations and to quantify the improvement in crossflow.

2.2.2.2. Fuel Element Graphite Stress Analysis Uncertainty. The nominal stresses predicted using the improved seismic response model for the OBE, combined with the stresses from other sources, is 0.7 of the minimum ultimate strength, just meeting the proposed allowable stress. Programs to reduce the uncertainties in the calculations, evaluate the new nine-row reference design, apply probabilistic methods to the criteria, and develop high-strength graphite for fuel element blocks are under development.

2.2.2.3. Water Ingress. Design improvements have been proposed and are being evaluated in areas of water ingress prevention, quick detection, and fast removal and increasing tolerance to moisture by affected components. An analytical computer code has been developed to predict the behavior of moisture within the primary coolant system. Preliminary results show that significant improvements are possible and that requirements consistent with plant availability goals can be met.

2.3. PLANT AVAILABILITY/MAINTAINABILITY (6032010400)

2.3.1. Scope

The scope of this task is to develop an availability/maintainability program that will achieve the plant availability criteria. Current work is directed toward an availability assessment, unavailability allocations, the initial specification, and a plant availability status report.

2.3.2. Discussion

Publication of the plant availability specification was the culmination of efforts by GA personnel and a consultant. This document serves a top level purpose by establishing the availability nomenclature through definitions and also shows the flow of top level availability criteria down to the major subsystems.

The HTGR-SC/C plant availability criterion document establishes a criterion of 90%, which is equivalent to an allowance of 876 h per year of unavailability or nonproductive time. Although the 876-h allowance appears large, it is only a fraction of the downtime being experienced by operating LWRs. Therefore, an availability program must be performed to approach this figure. Unavailability, as defined, must allow for both scheduled and unscheduled outages. Scheduled outages include refueling, regulated inspections, preventive maintenance, and other periods of mandated plant outage. Unscheduled outages result from unanticipated events, such as component failure or system degradation. Although some component failure is inevitable, such events occur randomly and therefore cannot be scheduled. The allocation between scheduled and unscheduled outages is shown in Table 2.3-1 and design criteria for scheduled outages are shown in more detail in Table 2.3-2. Design criteria for unscheduled outages at the system level are given in Table 2.3-3. This allocation by system, which is an important

TABLE 2.3-1
HTGR-SC/C PLANT DESIGN CRITERIA FOR 90% AVAILABILITY

	Unavailability		
	Days/Year	Hours/Year	Percent of Total
Scheduled outage	18.25	438.0	50
Unscheduled outage			
NSSS	9.125	219.0	25
BOP	9.125	219.0	25
Total	36.5	876.0	100

TABLE 2.3-2
HTGR-SC/C DESIGN CRITERIA FOR SCHEDULED OUTAGES

	Unavailability	
	Hours/Year	Percent of Total
NSSS activity		
Startup and shutdown	58	13.3
Refueling	203	46.3
In-service inspection	60	13.7
Filter/adsorber maintenance	12	2.7
Contingency	105	24.0
Total	438	100.0
BOP activity		
Startup and shutdown	58	13.2
Turbine-generator inspection	380	86.8
Total	438	100.0

TABLE 2.3-3
HTGR-SC/C NSSS DESIGN CRITERIA FOR UNSCHEDULED OUTAGES

System Number	System	Unavailability	
		Hours/Year	Percent of Total
11	PCRV	13.9	6.3
12	Neutron and flow control	12.7	5.8
13	Fuel handling	(a)	--
16	Reactor service	(b)	--
17	Reactor internals	1.0	0.5
18	Reactor core	1.0	0.5
21	Primary coolant	133.7	61.0
23	Helium service	7.4	3.4
28	Core auxiliary cooling	1.0	0.4
32	Plant protection	8.0	3.7
33	Plant control	11.0	5.0
35	Data acquisition	2.0	0.9
36	Analytical instrumentation	1.0	0.5
--	Operator error	6.4	2.9
--	Allowance (10% of above)	19.9	9.1
Total		219.0	100.0

(a) Unavailability included in scheduled outage allocation.

(b) No effect on plant operation.

step in plant design, resulted from analysis of data from operating LWRs and GCRs. Current technology was considered to determine the potential of new designs as opposed to current practice. This was done so that an informed judgment could be made regarding potential improvement in availability on a system basis, considering that existing data on current systems yield a much lower availability figure.

Additional accomplishments during this reporting period included drafting FMEAs for the following systems:

System Number	System	Major Components
11	PCRV	Thermal barrier, cooling system, penetration seals, pressure relief train
12	Neutron and Flow Control	
17	Reactor Internals	
18	Reactor Core	
21	Primary Coolant	Main circulator, shaft coupling, service system, helium isolation valves, main motor and controller, core outlet thermocouples, steam generator
23	Helium Service	

An FMEA systematically identifies the failure modes of a system (or subsystem, component, or process) and evaluates their consequences on the system and plant. By performing an FMEA, the design adequacy of the system to perform its function can be determined. An FMEA results in a structured compilation of information on the causes of failure (or degraded performance).

A draft NSS maintainability specification was developed and will be reviewed and issued in FY-83 owing to lack of funding in FY-82. This draft summarizes the maintenance program for NSS systems and components and defines how maintenance considerations should be integrated into the design

process to help assure that the plant availability goals are achieved. Maintainability considerations (on-line maintenance, accessibility, replace versus repair, etc.) are discussed to minimize or ease the maintenance required. Maintenance tasks during the planned annual outage, plant operation, and unscheduled outages are outlined.

A draft plant availability status report was developed. The plant availability design criteria established in the availability specification is exceeded by the estimated availability as follows:

Outages	Downtime (h/yr)	
	Design Criteria	Estimated
Scheduled	438	294[a] - 650
Unscheduled		
NSSS	219	600[a] - 863
BOP	219	394[a]
Allowance[b]	0	0 - 629
Total	876	1288 - 2536
Plant availability, %	90	85 - 71

[a] With no allowance.

[b] 50% of unscheduled outages.

The above table shows that the design criteria availability is not obtained by the current plant design by 5% to 19%. These estimated values are comparable to the 75% to 80% availability obtained by operating LWRs.

The major systems and items that primarily contribute to exceeding the design criteria are identified on dominant unavailability contributors (DUC) lists. The scheduled outage DUCs are (1) Allowance NSS/BOP and (2) Turbine-Generator Overhaul. The unscheduled outage DUCs are (1) Primary Coolant System, (2) Allowance NSS/BOP, (3) All BOP, (4) Operator Error, (5) Reactor Core System, and (6) Neutron and Flow Control System.

2.4. PLANT DYNAMICS

2.4.1. Scope

The scope of this task is to provide plant transient analyses for component design requirements and safety evaluation and to develop functional requirements for the plant control system (PCS) and plant protection system (PPS). Specific objectives for the second half of FY-82 included:

1. Complete the MLTAP plant dynamic model for the reference HTGR-SC/C multipurpose configuration and analyze preliminary transients. Update the plant transient specification and publish Issue 2.

2. Evaluate preliminary PCS functions and analyze plant operations.

3. Evaluate PPS functions.

2.4.2. Discussion

Coupling of the HTGR-SC/C BOP models developed during the first half of of FY-82 with a reference 2240-MW(t) NSSS model was completed. This version of the MLTAP computer code (MLTAP-COGEN) also incorporates the preliminary PCS control loops and a number of PPS protective actions, as summarized in Tables 2.4-1 and 2.4-2. The control/protective system settings are tentative pending further transient analyses and design evaluation. A set of BOP-initiated transient events was identified to establish a basis for the types of events that will be modeled and analyzed in developing PPS requirements.

Issue 2 of the plant transient specification was published and incorporates more concise overall requirements for plant operation, the PCS, and the BOP as well as more detailed background and descriptive material and data. This document defines representative plant transients and their design number of occurrences as a basis for plant design.

TABLE 2.4-1
CONTROLLER SETPOINTS AND SETPOINT RANGES

Controller	Nominal Setpoint	Expected Range	
		Auto. Control	Maximum
Module/average steam temperature, °C (°F)	540 (1005)	449-549 (840-1020.5) 477-549 (890-1020.5)	426-549 (800-1020.5)
Neutron power, %	100% of nominal	10-110	0-110
Main steam temperature, °C (°F)	540 (1000)	460-538 (860-1000) 488-538 (910-1000)[a]	460-538 (800-1000)
Turbine temperature °C (°F)	357 (675)	355-357 (671.2-675.5)	355-357 (671.2-675.5)
Boiler feed pump	NA	NA	NA
Turbine speed	NA	NA	NA
Feedwater flow, kg/s (lbm/sec)	925 (2040)	208-971 (459-2142)	37-971 (82-2142)
IP turbine pressure, MPa (psia)	4.7 (687.5)	4.49-4.9 (651-713)	4.49-4.9 (651-713)
Process header pressure, MPa (psia)	4.48 (650)	NA	NA
Deaerator pressure, MPa (psia)	1.17 (170)	0.14-1.17 (20-170)	0.14-1.17 (20-170)
Deaerator valve position limiter	20, 80% of stroke	NA	NA
FW heater 3 pressure, MPa (psia)	0.758 (110)	0.83-0.75 (120.7-109.3)	0.83-0.73 (120.7-109.3)
FW heater 1 pressure, kPa (psia)	62 (9)	15.5-65 (2.24-9.45)	13.7-65 (2.0-9.45)
HP turbine throttle pressure, MPa (psia)	16.6 (2415)	NA	NA
HP turbine bypass pressure, MPa (psia)	17.6 (2550)	NA	4.13-17.6 (600-2550)
HP bypass desuperheat temperature, °C (°F)	357 (675.5)	355-357 (671.2-675.5)	149-357 (300-675.5)
HP vent pressure, MPa (psia)	18.27 (2650)	None	None

TABLE 2.4-1 (Continued)

Controller	Nominal Setpoint	Expected Range	
		Auto. Control	Maximum
IP bypass pressure, MPa (psia)	4.9 (713)	4.75-4.9 (690-713)	0.4-4.9 (60-713)
IP bypass desuperheat temperature, °C (°F)	204 (400)	246-204 (475-400)	132-246 (270-475)
IP vent pressure, MPa (psia)	5.0 (725)	None	None
LP bypass pressure, MPa (psia)	1.4 (200)	1.24-1.62 (180-235)	0.27-1.62 (40-235)
LP bypass desuperheat temperature, °C (°F)	180 (356)	NA	120-180 (248.4-356)
LP vent pressure, MPa (psia)	1.5 (225)	None	None
IP initial pressure regulator mode, kPa (psia)	IP turbine setpoint 0.103 (15)		

(a) For proportional-only IP inlet temperature control and 25% steam flow minimum load.

TABLE 2.4-2
HTGR-SC/C PLANT PROTECTION SYSTEM PARAMETERS

Parameter	Setpoint	PPS Action
High primary coolant moisture concentration	1000 ppm	Reactor trip
High circulator outlet helium temperature	362°C (684°F)	Loop trip
High core power-to-flow ratio	1.4 $\frac{\%\ \text{power}}{\%\ \text{flow}}$	Reactor trip
High steam generator inlet helium temperature	727°C (1341°F)	Reactor trip
High steam generator outlet steam temperature	582°C (1080°F)	Loop trip
High primary coolant pressure	7.96 MPa (1155 psia)	Reactor trip
Low primary coolant pressure	5.6 MPa (814 psia)	Reactor trip
High/low circulator speed-to-loop feedwater flow ratio	$\pm 0.2\ \frac{\%\ \text{speed}}{\%\ \text{flow}}$ (sched)	Loop trip
High circulator speed	110%	Loop trip
Low plant helium flow	7%	All loop trips and CACS initiation
Low main steam pressure	13.8 MPa (2000 psia)	Turbine trip[a]
Low main steam temperature	427°C (800°F)	Turbine trip
Low turbine-generator load	10% load	Turbine trip

[a] Non-PPS, but provides related protection for turbine.

Some key plant transients were analyzed using MLTAP, which yielded additional plant operational requirements and procedures. The transients included a reactor trip from 100% power and several turbine trip cases (HP unit, IP/LP unit, and both turbines). Each of these transients invoke a number of control actions that provide mitigating effects and permit an orderly transition from one phase of plant operation to another. Several trial runs were made of each event to develop the control sequencing logic for accomplishing the following objectives:

1. Maintain process steam conditions using the nuclear heat source, or for a reactor trip, provide a smooth transition to an alternate source.

2. Mitigate thermal stress to major plant components.

3. Maximize electrical power production (in conjunction with items 1 and 2).

4. Provide adequate core cooling and afterheat removal using main cooling loops.

The reactor trip transient illustrates a significant number of control actions and includes those developed for the turbine trip events. The input data for this event were chosen from the initial event studies where the sequencing and programming were being determined. When sequencing and programming for specific events have been determined, they are then programmed into the control and protective system models in the MLTAP code. The reactor trip case illustrates the flexibility using input change statements for initial event studies to establish the sequencing and programming as opposed to multiple hard code changes.

The reactor trip transient imposes a rapid cooldown of reactor and steam generator components. The PCS provides post-trip control actions that

mitigate thermal stresses experienced by major components, e.g., the core support structure, steam generator tubesheet, and main steam piping. These actions are a part of the non-safety equipment protection function of the PCS.

Most of the major actions and responses occur over the first few hundred seconds. However, floodout of the steam generator takes approximately 2000 s. The data for the reactor trip event are shown in Figs. 2.4-1 through 2.4-6.

When a reactor trip (initiated at 10 s) occurs, the feedwater flow is automatically reduced by the PCS at a rate of 1/2%/s to 15% of nominal flow. The IP/LP turbine load is reduced by decreasing the throttle valve at a rate of -1.4%/s to 50 s after reactor trip, at which point an automatic IP/LP turbine trip occurs. The ramp throttling of the IP/LP turbine diverts an increasing fraction of the total flow to the process, maximizing flow to the process. Maximizing and maintaining flow to the process as long as possible will ease the takeover of process steam supply by an alternative source. The characteristics and capacity of the alternative steam source have not yet been resolved, and no takeover of actual process supply was modeled in the run presented. A measure of the requirements that will be imposed on the alternative source can be gained by regarding the predicted HTGR-SC/C process line inlet flow as the fraction of flow that the alternative source does not need to supply.

As the feedwater flow runs back, the speed of the circulators follows and the HP turbine throttle valve starts closing to maintain throttle pressure, as shown in Fig. 2.4-1. At the IP/LP trip at 50 s, the IP bypass and LP bypass come on (Fig. 2.4-5) and act to maintain process line inlet pressure and BFP-turbine/deaerator extraction pressure.

The HP turbine trip occurs 30 s after the IP/LP turbine trip. The separation of trip time was programmed to avoid potential problems associated with a number of major transient actions occurring at once and because

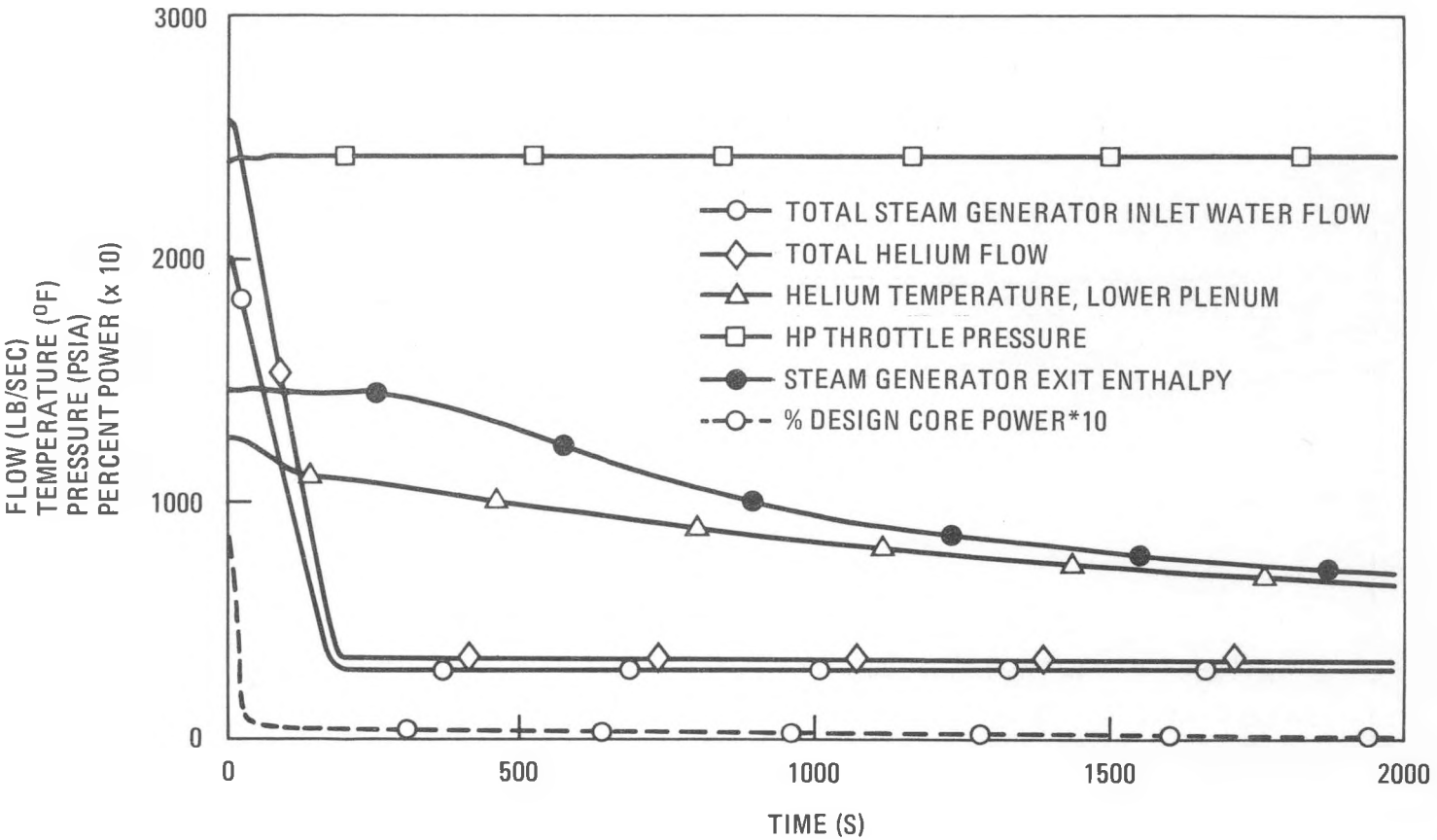

Fig. 2.4-1. Reactor trip transient: key system parameters

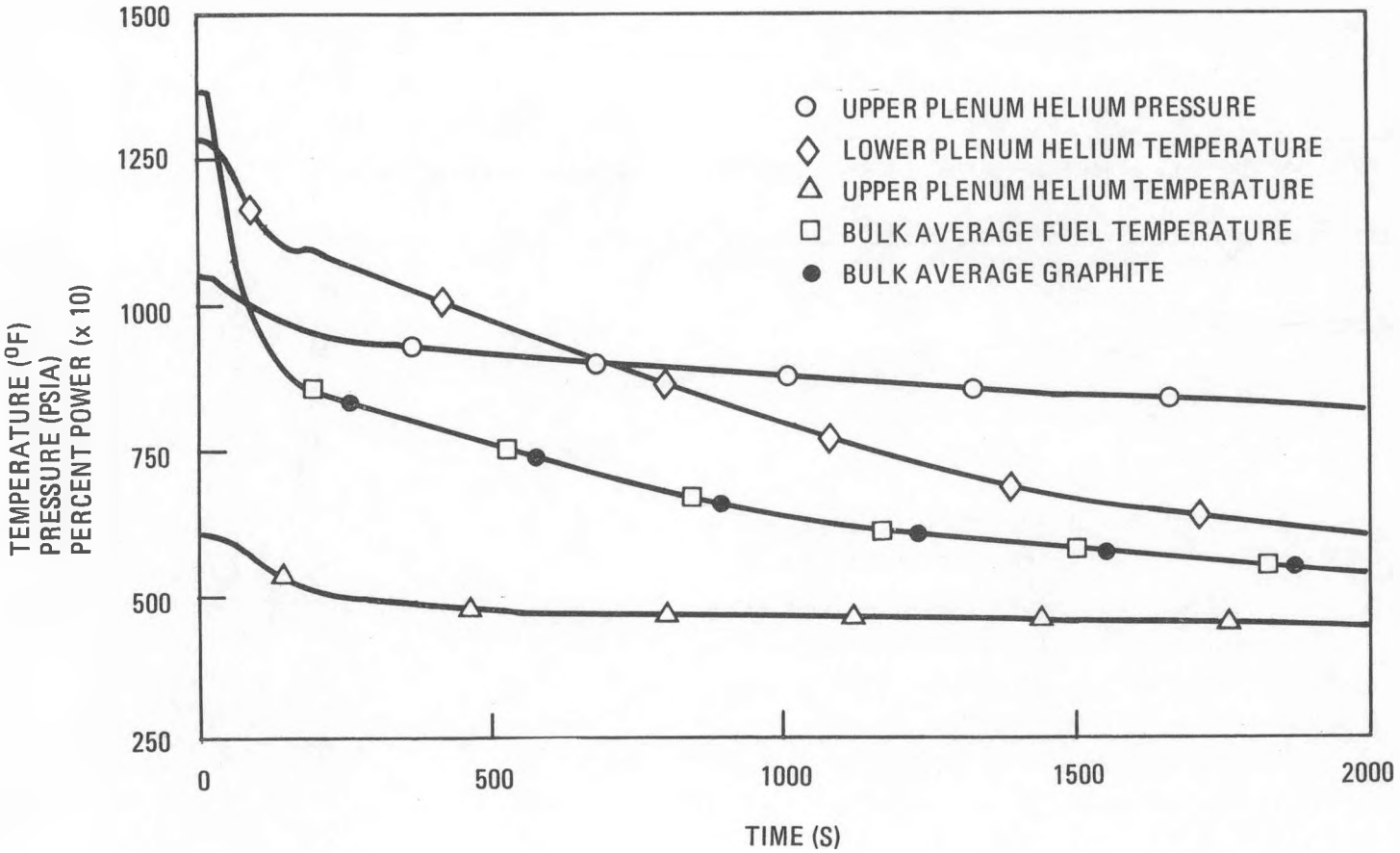

Fig. 2.4-2. Reactor trip transient: primary system parameters

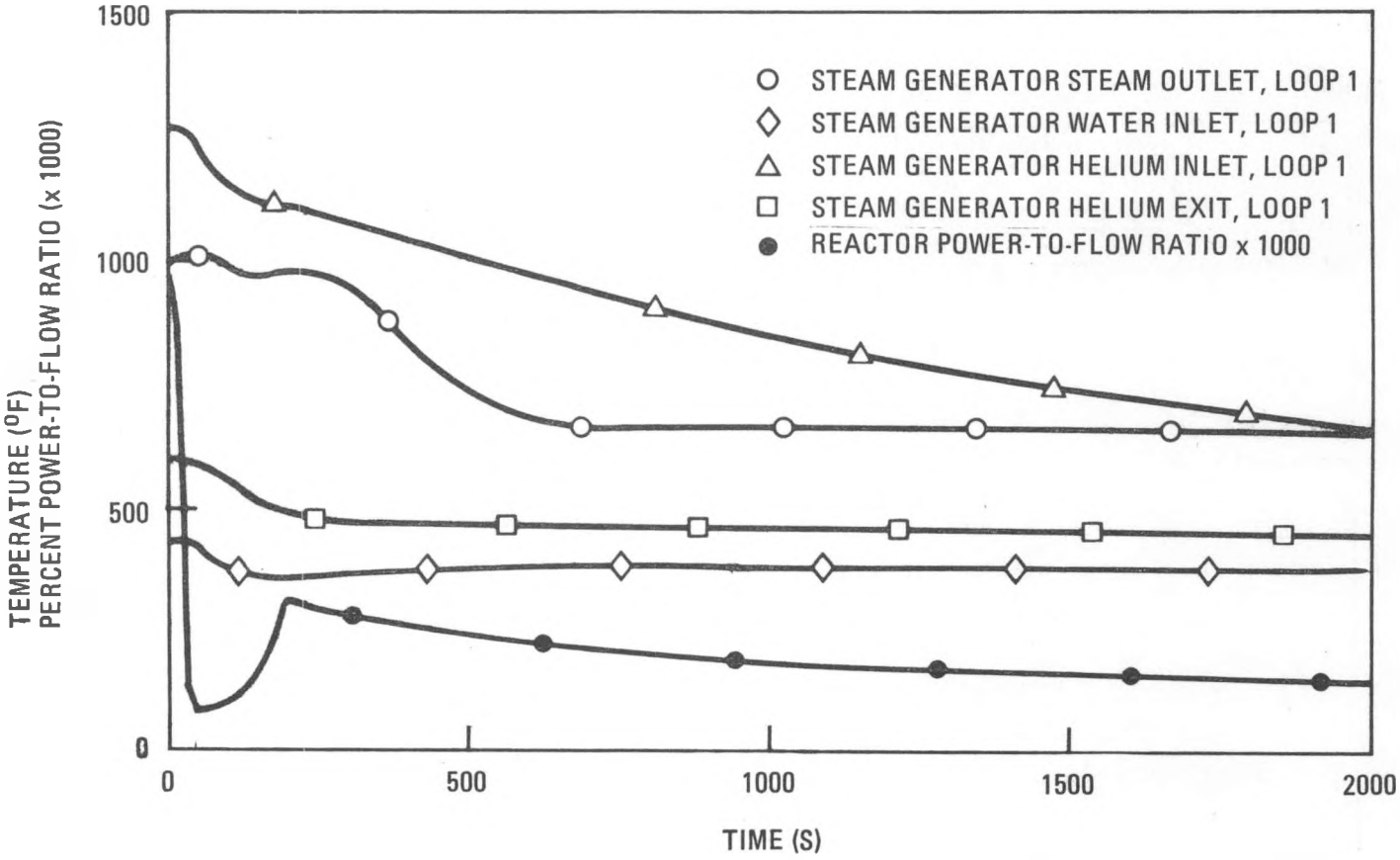

Fig. 2.4-3. Reactor trip transient: primary and secondary system temperatures

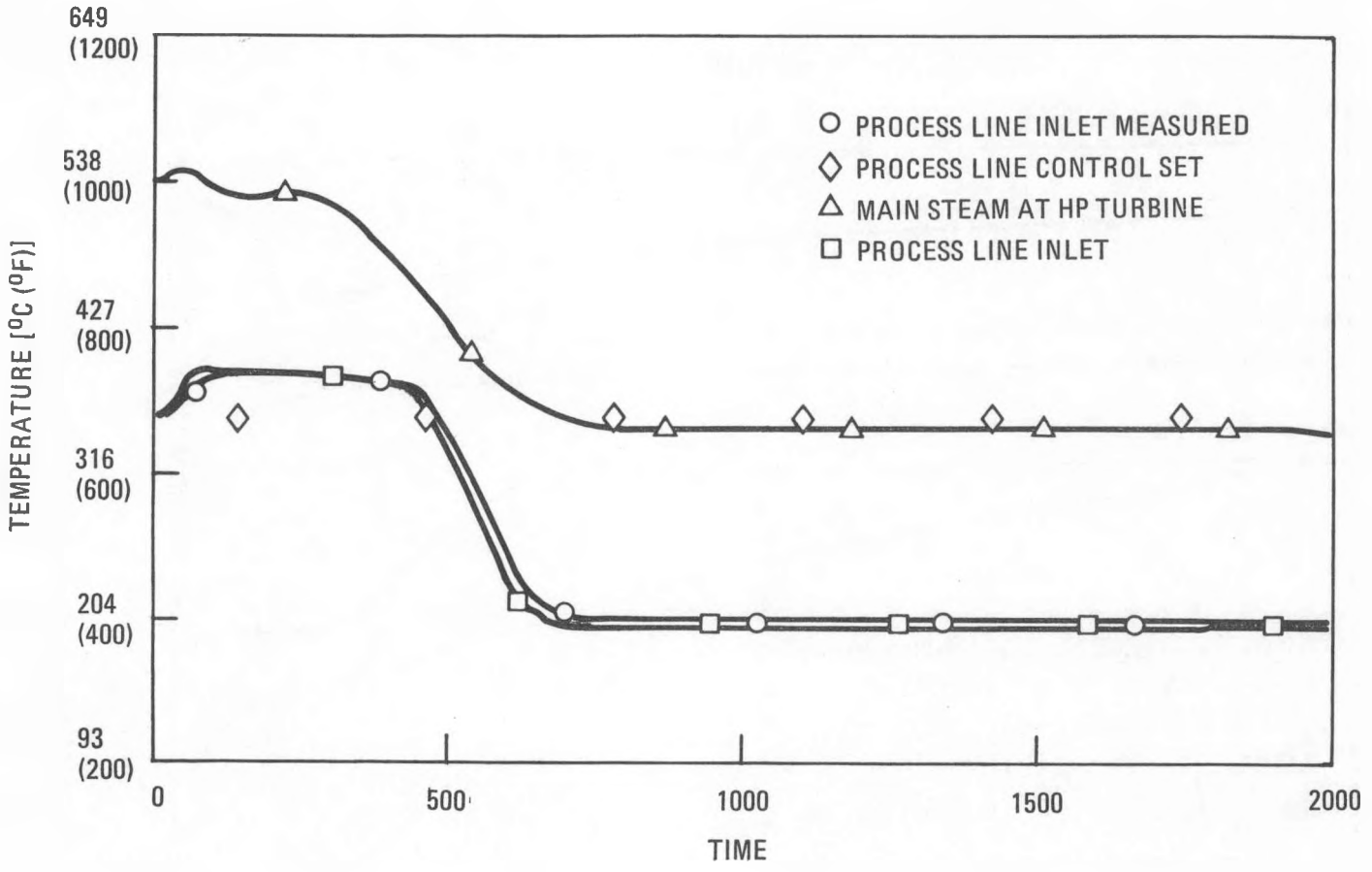

Fig. 2.4-4. Reactor trip transient: main steam and process steam temperatures

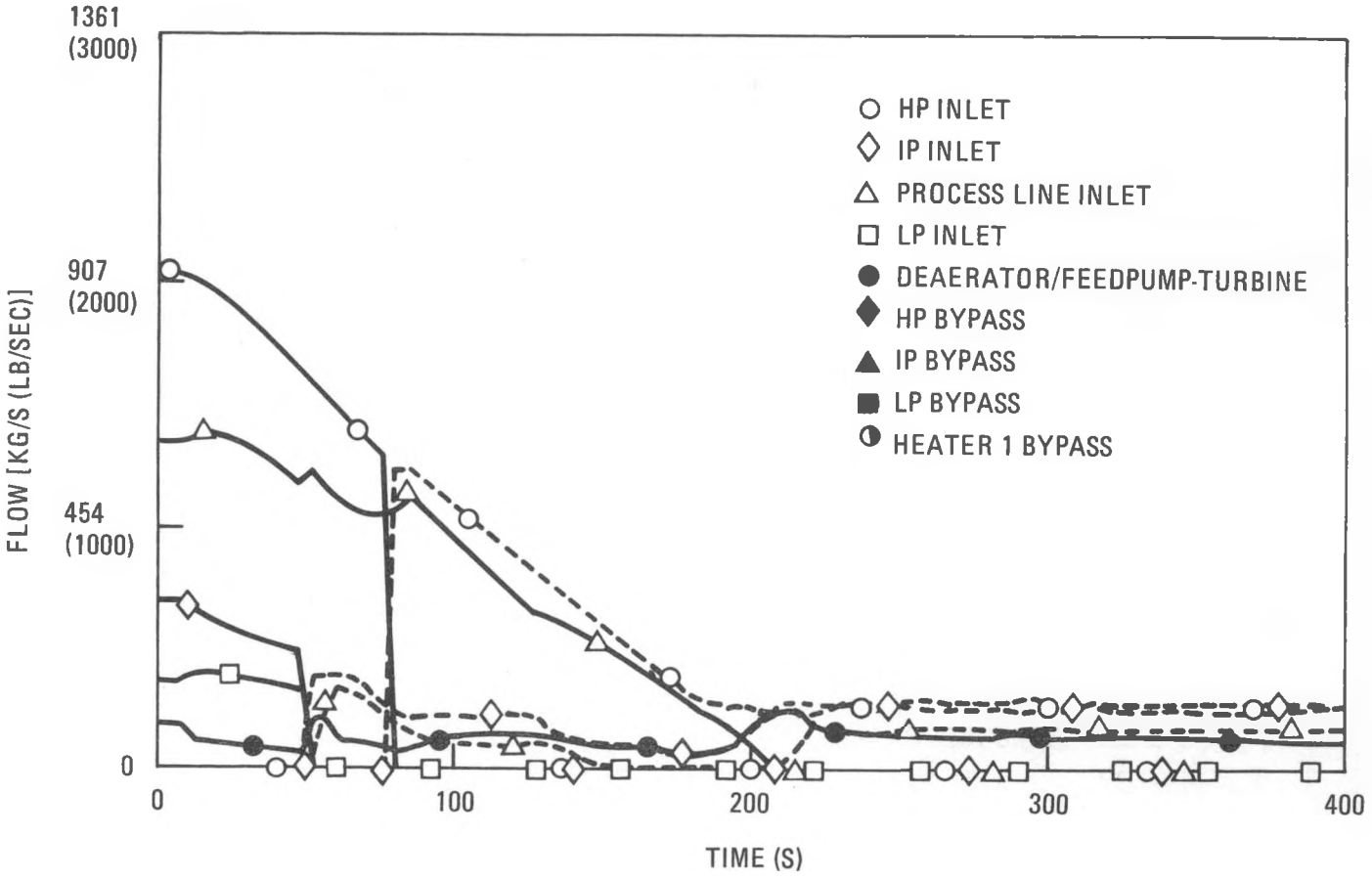

Fig. 2.4-5. Reactor trip transient: turbine inlet, extraction, and bypass flows

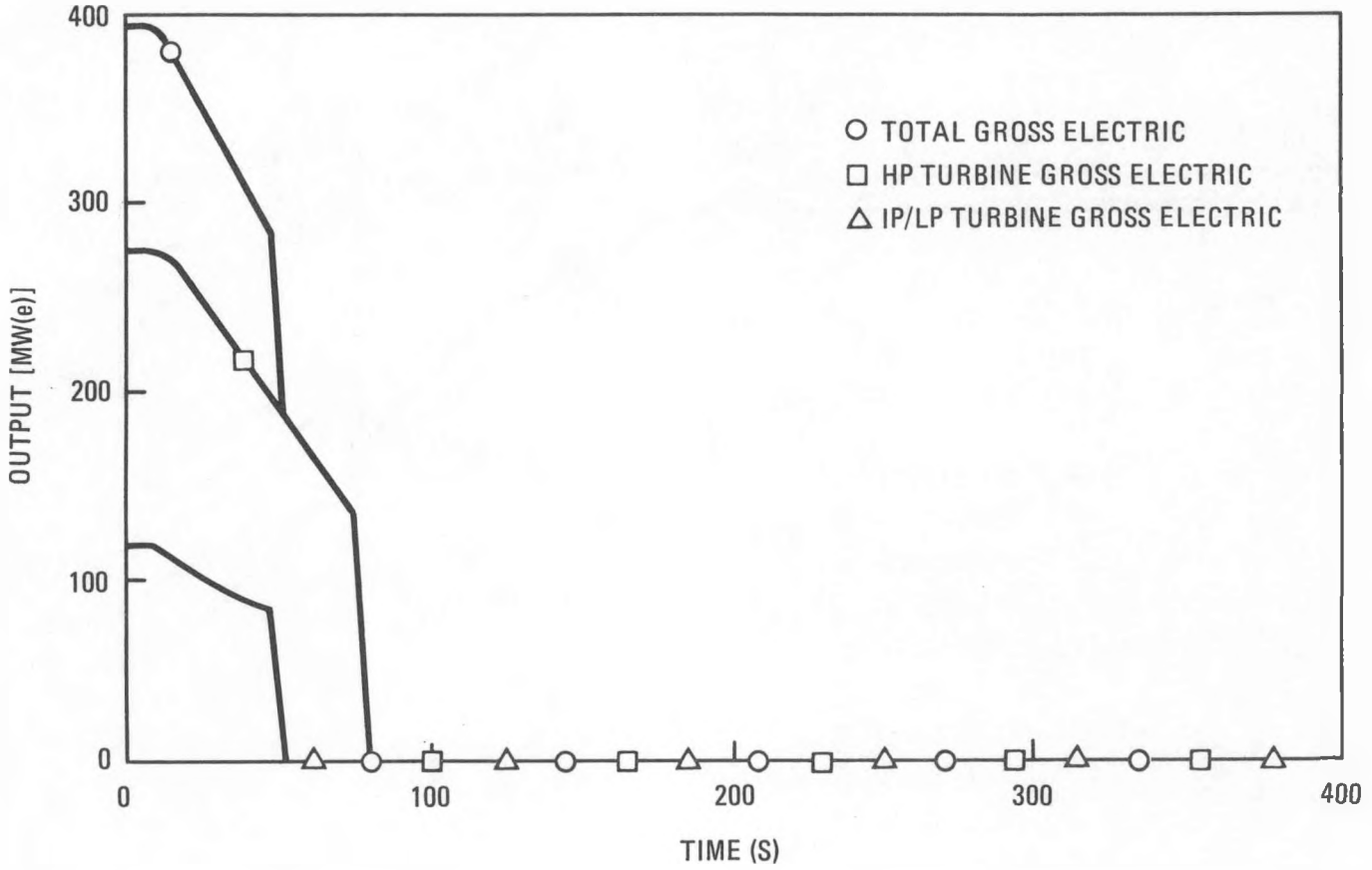

Fig. 2.4-6. Reactor trip transient: generator gross output

no significant benefit could be obtained by earlier trip. Figure 2.4-6 shows the load runback and tripping of the turbines.

As shown in Fig. 2.4-5, the process line inlet flow is thought to be a major fraction of the total flow as the turbines are run back and tripped. Process line inlet flow is then maintained as the majority of the total flow flow until the set minimum feedwater flow is reached. At the time minimum feedwater flow is reached, the process line inlet flow is down to ~15% of design. The alternative steam source should be well on-line by this time, so the HTGR-SC/C supply is continued on down to zero at ~210 s.

As shown in Fig. 2.4-4, the steam generator exit conditions reach saturation at ~700 s but floodout is not completed until over 1900 s have elapsed.

To provide continued steam supply for the BFP-turbine, the pressure in the first flash tank (downstream of the HP turbine) is lowered between 250 and 710 s from the design value of ~4.75 MPa (~690 psia) to ~1.75 MPa (~255 psia). Further reductions in the pressure of both flash tanks is scheduled later to further prolong flashing steam drive for the BFP-turbine so that any need for auxiliary steam is delayed. Additional extension of flashing time can be obtained by a feature that routes the flash tank drain flows to the LP feedwater heater system, thereby recuperating heat into the system. This option was not exercised in the run presented.

Meetings between GA, DOE, GCRA, GE, and UE&C were held to discuss the workscope for PPC, PPS, and plant simulation development tasks. It was agreed that GA would take the lead for the PPS, UE&C for the PCS, and GE for plant simulator development. It was also agreed that the GA-developed dynamic computer models would be made available to UE&C for its use in the BOP design and control system development effort. GA would retain responsibility for the overall plant dynamic analysis with input from the participants.

2.5. BOP INTERFACES (6032010800)

2.5.1. Scope

This scope of task includes:

1. Preparation of a plant specification for Balance of Plant Requirements (BOPR).

2. Preparation of a plant specification for Plant Layout Requirements (PLRs).

3. Technical coordination with the architect-engineer (A-E) on NSS/BOP interfaces.

The objective of this task is to convey NSSS requirements and information to the BOP design effort and the A-E in order to obtain an efficient integrated overall plant design. In support of the NSSS/BOP, interfacing is maintained and finally reviews of BOP designs are made to ensure compliance with interface criteria.

2.5.2. Discussion

A comprehensive review was made of the topical report prepared by UE&C presenting the results of a variable cogeneration plant configuration study for the 2240-MW(t) HTGR-SC/C application. The selection of a three-turbine-generator set arrangement to provide all-electric, full process, or varying conditions introduced some unique requirements for a large turbine-generator set and the operation of the associated feedwater system. It was suggested that a turbine-generator supplier be consulted to see if GA's concerns present problems that could impose unacceptable constraints on the concept.

As a result of these continuing concerns, GA was later requested to prepare a proposed program to be conducted by a major turbine-generator supplier for review of the proposed multi-unit turbine-generator configuration in early FY-83. The task would include:

1. Evaluating the capability of the proposed turbine-generator units to operate over the wide range of operating conditions specified for the process and electrical load generation modes.

2. Establishing whether the HP controlled-pressure extraction opening is feasible for the large volume of steam it must accommodate in the maximum process mode.

3. Evaluating the capability for removal of one or two LP units from service.

4. Assessing control valving requirements needed to support the spectrum of transient conditions.

5. Preparing a report summarizing the viability of the configuration for the application demand. The report would state limitations and present proposed solutions and recommendations with the estimated development costs and schedule required to resolve any condsidered issues.

Final draft sections of the UE&C BOP Design and Cost Report for the 2240-MW(t) HTGR-SC/C plant (Ref. 2.5-1) were reviewed. The major comments were related to a reiteration of GA's continuing concerns regarding the turbine-generator selection, corrections to the operating mode for the CACWS, and concerns related to the control and instrumentation sections of the report.

The BOPR document was the subject of a comprehensive review. Additional work is required to either resolve the issues or incorporate the review comments in a revision to the BOPR document scheduled in FY-83.

A preliminary listing of BOP input requirements needed to support the NSSS design effort during FY-83 was prepared and submitted to GCRA for review. The following topics were outlined:

1. Variable cogeneration heat balance data, for varying part-load and full-load performance.

2. Input to the Overall Plant Design Specification (OPDS).

3. Seismic model, including interface requirements.

4. Availability assessment of BOP systems that can impact outage.

5. Maintenance assessment of major component removal.

6. BOP plant dynamics data.

7. Hot loop restart evaluation, and costs to implement.

8. BOP input data to NSSS system description documents (SDDs).

Reference

2.5-1. "HTGR-SC/C Lead Plant Design and Cost Report," Vol. III, "Balance of Plant," United Engineers and Contructors Report UE&C/GCRA 82-010, to be issued.

2.6. LICENSING SUPPORT (6032020001)

2.6.1. Scope

The scope of this task consisted of revising and updating the Nuclear Safety Plant Specification, updating the report on the safety/licensing assessment of the HTGR-SC/C plant, and providing support and guidance on matters related to regulatory requirements.

2.6.2. Discussion

Revision 2 of "Nuclear Safety Plant Specification, HTGR-SC/C, 2240 MW(t)" was issued. The principal revisions consisted of updating the applicability of Division 1 regulatory guides and restructuring of the section on systems criteria to conform to the revised definitions of NSSS systems.

Report GA-A16457, "Safety/Licensing Assessment of the 2240-MW(t) HTGR Steam Cycle/Cogeneration Plant" (Ref. 2.6-1), was updated. The most recent system description and performance data were added, and the source term data and resultant dose calculation were revised.

Review comments were provided on various documents including GA design documents, GCRA's Licensing Plan and Functional Specification, and the OPDS.

Reference

2.6-1. Lewis, J. H., and R. K. Wise, "Safety/Licensing Assessment of the 2240-MW(t) HTGR Steam Cycle/Cogeneration Plant," DOE Report GA-A16457, September 1980.

2.7. SAFETY/RELIABILITY (6032070001)

2.7.1. Scope

The scope of this task was (1) to provide safety risk/reliability criteria and analysis for the 2240-MW(t) HTGR-SC/C to provide insight during the conceptual design and (2) to evaluate a six hexagonal radiation hole concept for the 2240-MW(t) HTGR-SC/C core following an LOFC accident.

2.7.2. Discussion

2.7.2.1. Safety Risk Assessment. A safety risk assessment (Ref. 2.7-1) of the 2240-MW(t) HTGR-SC/C plant was performed for a Port Arthur, Texas, site. The plant site is located in a heavily industrialized area of Port Arthur that has high-temperature steam requirements.

Core heatup events and steam generator leaks dominate the HTGR-SC/C plant risk. The dominant initiating events (Table 2.7-1) include loss of main loop cooling, which contributes to core heatup fission product release categories CH-6 and CH-7, loss of offsite power plus turbine trip contributing to CH-3, external hazards contributing to CH-0, and steam generator leaks contributing to SG-2 and SG-3. The HTGR-SC/C plant risk (Fig. 2.7-1) is defined by SG-2 and SG-3 in the low-consequence regime and by CH-3 and CH-0 in the medium-to high-consequence regimes.

The data base (Ref. 2.7-2) supporting the frequency assessment portion of the risk study was obtained from a broad range of sources. Primary sources included (1) GCR data (Ref. 2.7-3), (2) U.S. nuclear and fossil-fired plant data (Ref. 2.7-4), (3) previous risk assessment studies (Refs. 2.7-5, 2.7-6), and (4) special summarized data (Refs. 2.7-7 through 2.7-10). The common mode failure (CMF) data base was based on two analytical models: (1) the β-factor model (Ref. 2.7-6) and (2) the binominal failure rate model

TABLE 2.7-1
RELEASE CATEGORY DESCRIPTIONS[a]

SG-3	Small steam generator tube leak; detection of moisture increase in primary coolant; positive identification of leaking steam generator; operator performs orderly plant shutdown. Before PCRV pumpdown to storage is completed, steam generator dump/relief valve fails to remain closed, resulting in release of a fraction of primary coolant inventory to atmosphere. CACS operates - no core heatup.
SG-2	Large steam generator tube leak; detection and positive identification by moisture system; feedwater and superheat steam valves on leaking steam generator close; dump valves open but fail to reclose, resulting in complete PCRV depressurization through dump/relief valve to atmosphere. Total primary coolant inventory released to atmosphere. CACS operates - no core heatup.
CH-7	Loss of main loop cooling followed by successful main loop rundown; CACS operates for a period then fails with successful LCS operation. PCRV does not depressurize and containment remains intact.
CH-6	Loss of main loop cooling followed by CACS failure with successful LCS operation. PCRV pressure relief, but containment remains intact.
CH-3	Loss of offsite power followed by failure of MLCS, CACS, and LCS. PCRV pressure relief and concrete degradation with long-term containment failure due to overpressurization.
CH-0	Offsite industrial pipeline break with heavier-than-air vapor cloud drifting over plant and exploding, resulting in immediate containment failure and loss of core and liner cooling.

(a) CACS = Core auxiliary cooling system
LCS = Liner cooling system
MLCS = Main loop cooling system
PCRV = Prestressed concrete reactor vessel

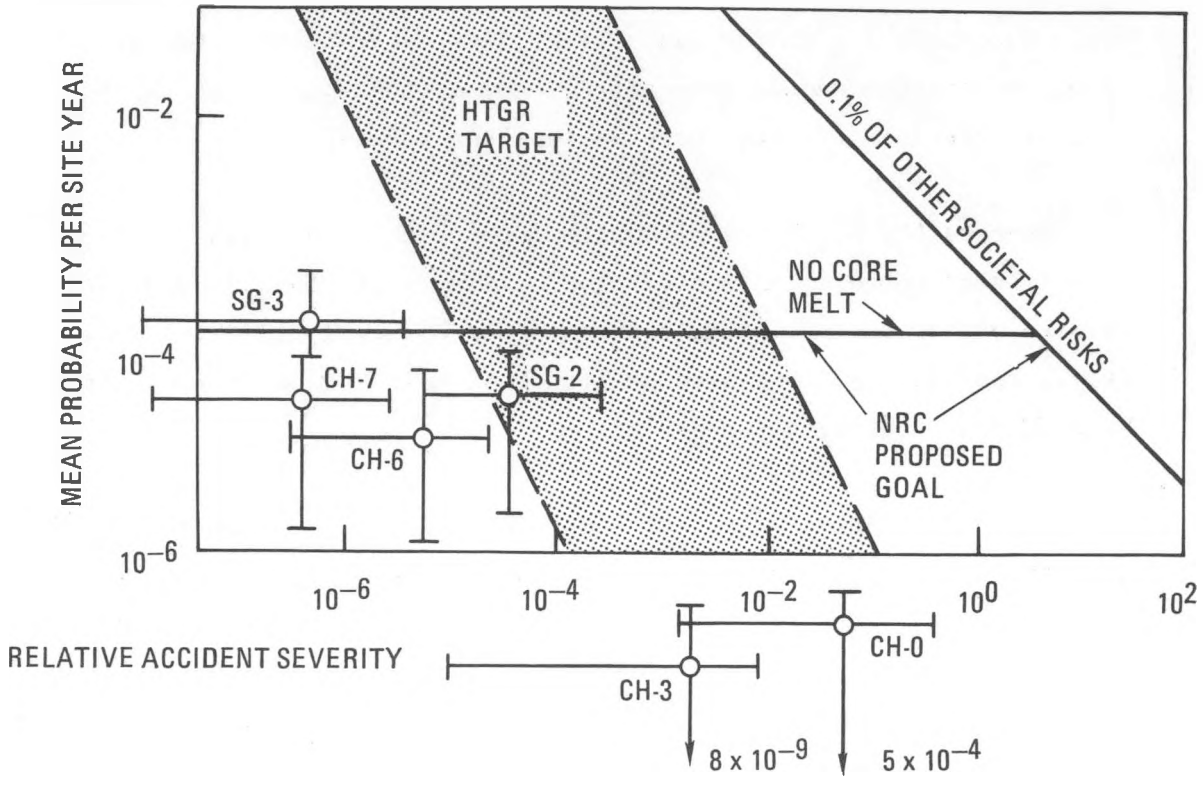

Fig. 2.7-1. Mean point risk plot

(Ref. 2.7-11). These models are important because CMFs are found to dominate the redundant HTGR safety systems. Uncertainty estimates from the data base were factored into all models predicting system success or failure. Uncertainties at the fault tree level were incorporated into the event trees to generate median branch frequency estimates, as well as upper and lower bounds for the total core heatup frequencies.

Uncertainty estimates were also made on the consequence evaluations for each fission product release category. Simplified consequence models were used to assess the effect of uncertainties on key independent variables (e.g., concrete spalling rate or containment leak rate) through the use of Monte Carlo simulation techniques.

As shown in Fig. 2.7-1, all core heatup release categories fall into the acceptable regions of the HTGR targets and far below proposed NRC national societal goals. The total mean frequency of core heatup and fission product release is 4×10^{-5} per reactor-year, which is within the 10^{-4} per reactor-year mean target core heatup frequency. The only accident category infringing upon the HTGR target goals is SG-2 (Table 2.7-1). More detailed analysis of SG-2 is expected to result in significant reduction in both frequency and consequence for accidents within this category.

A comparison of the HTGR-SC/C risk results with the Accident Initiation and Progression Analysis (AIPA) and the German PSH-1B HTGR study was made to benchmark the HTGR-SC/C risk results. All three studies were in relatively good agreement. In view of the major design and licensing differences inherent in the German PSH-1B study, the comparison of corresponding core heatup category risks to the 2240-MW(t) HTGR SC/C plant was quite reasonable. Both the AIPA and German PSH-1B studies shown higher risk than the HTGR-SC/C plant. This is due to the current use of more sophisticated analytical methods, the revised data base, and the more stringent safety targets imposed on the design of the 2240-MW(t) HTGR-SC/C plant and resulting design improvements.

In conclusion, the safety risk study showed that the 2240-MW(t) HTGR-SC/C plant meets the proposed NRC national goals and also meets the more stringent HTGR targets of no predicted fatalities over a spectrum of accidents down to the core melt probability limit of 10^{-4} per reactor-year and no identifiable fatalities in the safety margin region, which extends down to 10^{-6} per reactor-year.

2.7.2.2. Radiation Hole Evaluation. A radiation hole concept of six hexagonal holes (Fig. 2.7-2) for the 2240-MW(t) HTGR-SC/C (7.1 W/cm^3) plant was studied to determine its effect on core temperatures during a core heatup accident involving a permanent loss of forced circulation. It was found that the previously selected fifteen 178-mm (7-in) diameter hole design (Fig. 2.7-3) described in Ref. 2.7-12 would result in refueling difficulty. Therefore, a new radiation hole configuration was proposed wherein six standard fuel columns of the core would be removed to serve as radiation holes (Fig. 2.7-2). It is anticipated that this radiation hole design will minimize fuel handling and fuel block stress problems.

The version of CORCON, a two-dimensional conduction code, adapted for the fifteen 178-mm (7-in.) diameter hole design (Fig. 2.7-3) was modified to incorporate the six-hexagonal-hole design. As shown in Fig. 2.7-2 the six columns, one in each of the six refueling regions (from No. 2 to No. 7), were removed from the active core. These six radiation holes were also assumed to extend vertically 914 and 659 mm (3 and 2.25 ft) in the top and bottom reflectors, respectively. Equations for the effective conductivity and heat capacity for the active core and the top and bottom reflectors were calculated to include the radiation hole effects.

CORCON results were obtained for the six-hexagonal-hole design and compared with results for the fifteen 178-mm (7-in.) diameter hole design. Figure 2.7-4 shows the maximum and average active core temperatures as a function of time past reactor trip. With the new six hexagonal radiation

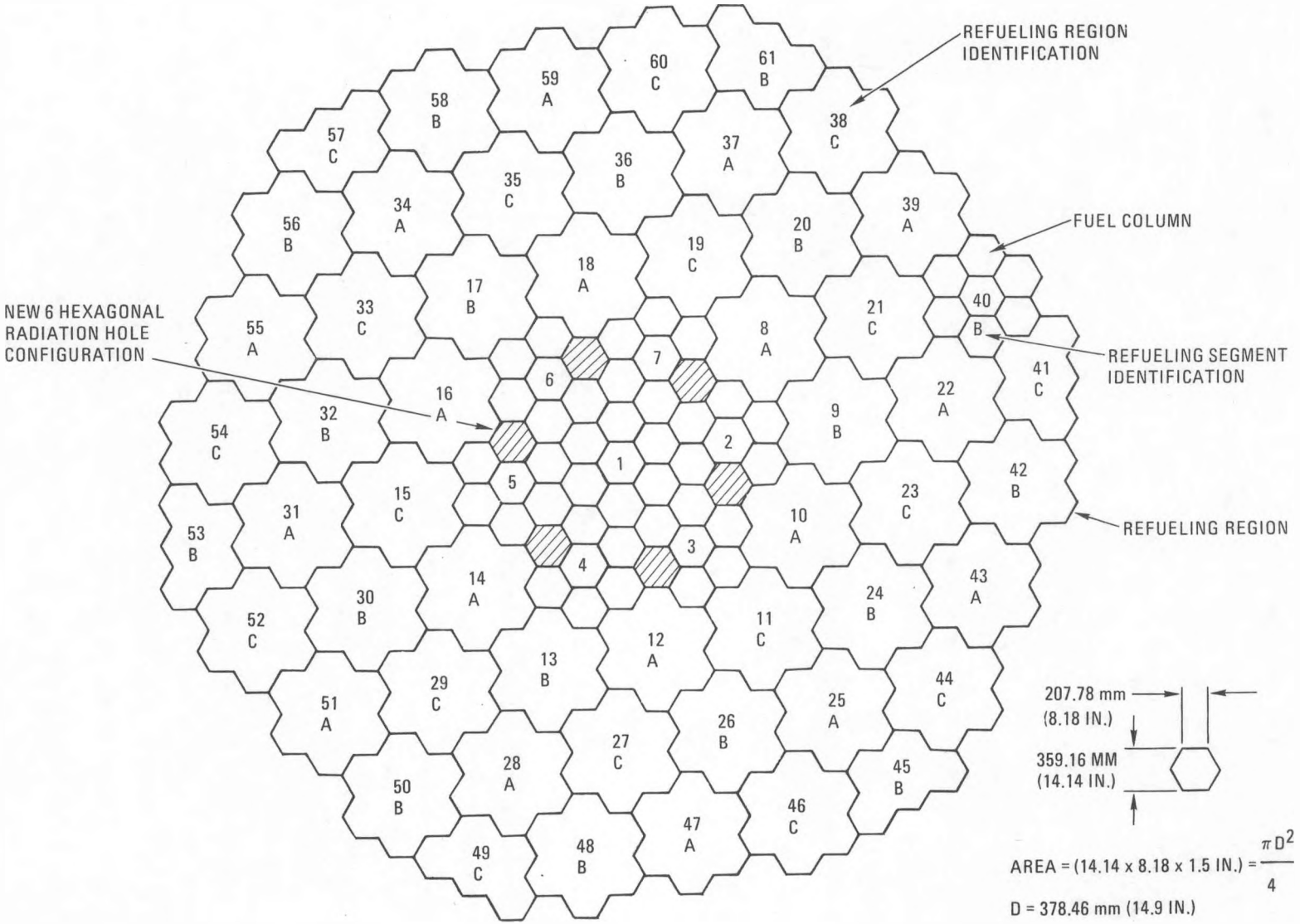

Fig. 2.7-2. HTGR core layout with hexagonal radiation hole fuel blocks in six central regiona

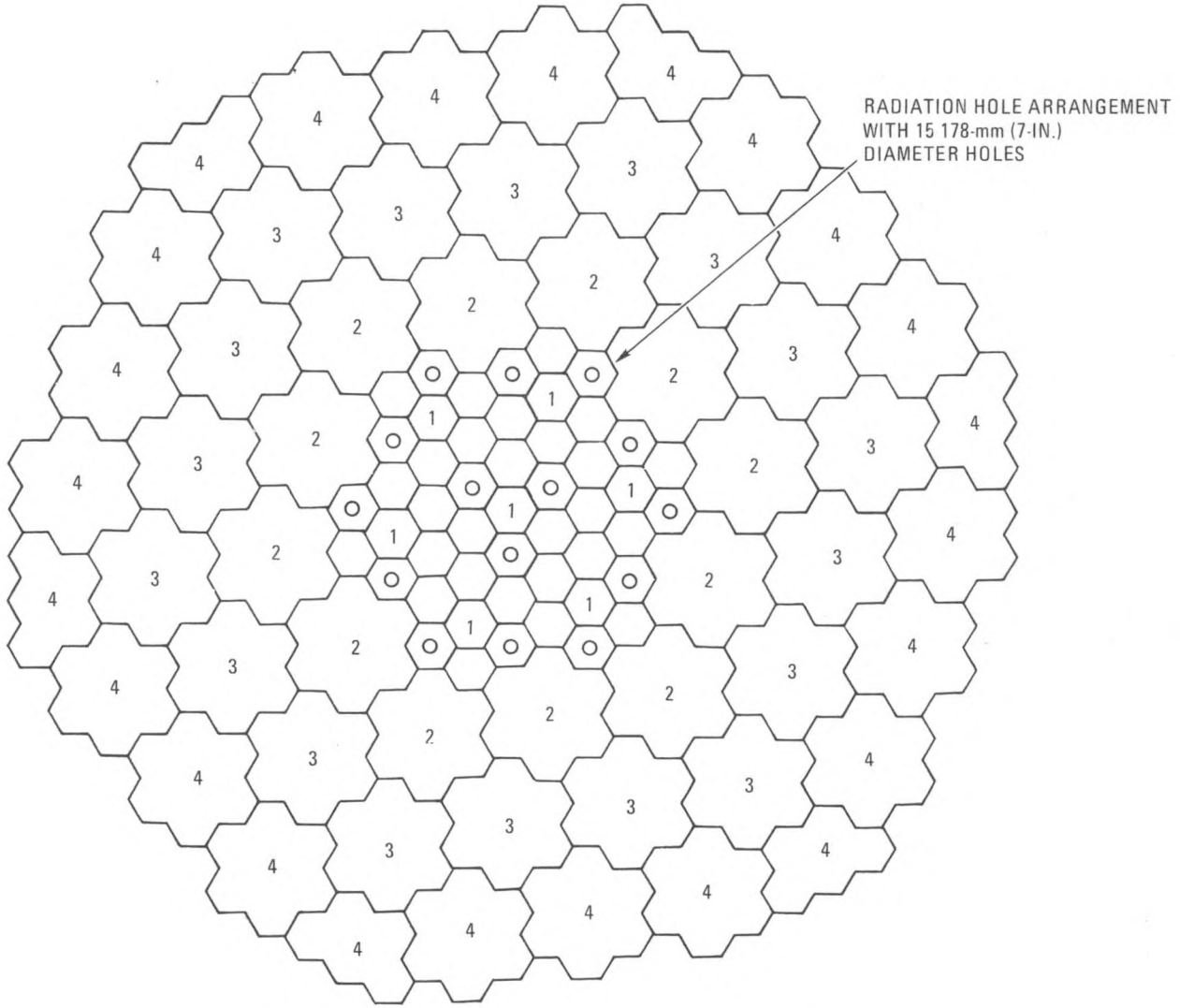

Fig. 2.7-3. HTGR core layout with fifteen 178-mm (7-in.) diameter radiation holes

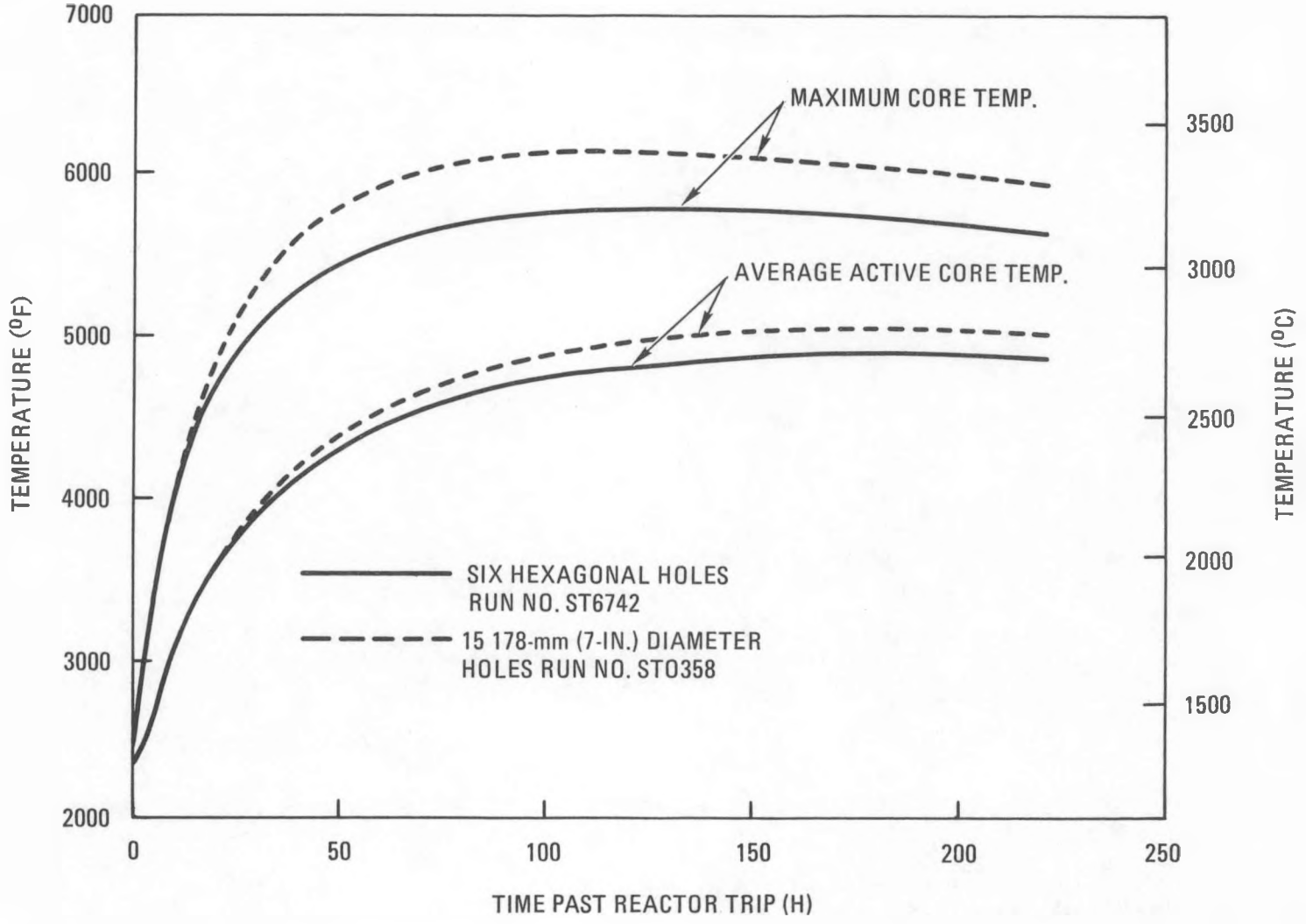

Fig. 2.7-4. Core temperature for 2240-MW(t) HTGR-SC/C core heatup accident

holes, the peak core temperature reaches only 3910°C (5774°F), which is more than 111°C (200°F) lower than that of the fifteen 178-mm (7-in.) diameter hole design. This demonstrates that the new six-hexagonal-hole design is more effective in lowering the peak core temperature than the fifteen 178-mm (7-in.) hole design.

The new radiation hole design with six hexagonal holes has been demonstrated to lower the peak core temperature to below 3315°C (6000°F) with a greater margin than the fifteen 178-mm (7-in.) diameter hole design. However, further evaluation is required to assess the effects on fuel packing fraction, power distribution, coolant pressure and flow redistribution in gaps, sealing of the hole near the top plenum, and core fluctuation.

References

2.7-1. Dunn, T. D., and D. M. Bender, "Safety Risk Assessment for the 2240-MW(t) SC/C plant," Report GA-A17000, to be published.

2.7-2. Menzel, H. F., and D. M. Bender, "Probabilistic Data Base for Probabilistic Risk Assessment," GA unpublished data.

2.7-3. Dixon, F., and H. K. Simons, "The Central Electricity Generating Board's Nuclear Power Stations: A Review of the First 10 years of MAGNOX Reactor Plant Performance and Reliability," J. Brit. Nucl. Soc. 13, No. 1, 9-38 (1974).

2.7-4. "Nuclear Power Plant Reliability Data Systems (NPPRDS) 1975 Annual Reports of System and Component Reliability," Southwest Research Institute, San Antonio, Texas, August 1976.

2.7-5. "Reactor Safety Study: An Assessment of Accident Risks in U.S. Commercial Nuclear Power Plants. Appendix III, Failure Data; Appendix IV. Common Mode Failure," U.S. Nuclear Regulatory Commission Report WASH-1400 (NUREG-75/104), October 1975.

2.7-6. "HTGR Accident Initiation and Quantitative Reliability Analysis Status Reports, Vols. II, III, and IV," DOE Report GA-A13617, October-December 1975.

2.7-7. Everline, C. J., "Safety Reliability Criteria for the 1170 MW(t) HTGR-SC/C," GA unpublished data.

2.7-8. Hannaman, G. W., "GCR Reliability Data Bank Status Report," DOE Report GA-A14839, July 1978.

2.7-9. Atwood, C. L., and J. A. Steverson, "Common Cause Fault Rates for Diesel Generators: Estimates Based on Licensee Event Reports at U.S. Commercial Nuclear Power Plants, 1976-78," Report EGG-EA-5359.1, May 1982.

2.7-10. Atwood, C. L., "Common Cause and Individual Failure and Fault Rates for Licensee Event Reports of Pumps at U.S. Commercial Nuclear Power Plant," Report EGG-EA-5289, November 1980.

2.7-11. Steverson, J. A., and C. L. Atwood, "Common Cause Failure Rate Estimates for Diesel Generators in Nuclear Power Plants," EG&G paper.

2.7-12. "HTGR Applications Program Semiannual Report for the Period October 1, 1981, through March 31, 1982," DOE Report GA-A16831, 1983.

2.8. PCRV DESIGN (6032110100, 6032110200, 6032110300)

2.8.1. Scope

The scope of this task encompassed the PCRV structure, liner, and thermal barrier. Activities during this reporting period included the following:

1. A survey was conducted to establish the availability of aggregate for high-strength concretes at selected candidate sites for future HTGR plants.

2. A cost optimization study of the PCRV liner cooling water system and thermal barrier was performed.

3. A study was performed to evaluate methods of upgrading the upper plenum liner cooling water system to ensure satisfactory performance during a postulated LOFC accident.

4. A design study of the bottom head thermal barrier was made.

5. Existing criteria for ISI maintenance and replacement of primary system components were documented.

2.8.2. Discussion

2.8.2.1. PCRV and Liner.

Aggregate Survey for High-Strength Concrete

A survey was conducted to establish the availability of coarse aggregates for 45-MPa (6500-psi) and 55-MPa (8000-psi) concretes for the

construction of a PCRV in various parts of the U.S. The nine areas investigated represent the most likely candidate sites for future HTGR plants.

The information was obtained by phone from ready-mix concrete producers at or near the vicinity of prospective construction sites and also from GA records on FSV, Philadelphia Electric/Delmarva, and Southern California Edison concrete investigations. Results are summarized in Table 2.8-1.

The investigation revealed that both 45-MPa (6500-psi) and 55-MPa (8000-psi) concretes can be produced anywhere in the U.S. In areas where local materials are of poor or marginal quality, aggregate will have to be imported and additional transportation costs will be incurred. Usually, the cost of transporting the aggregate 80 km (50 mi) is equal to the cost of the aggregate itself.

Although several vendors contacted have not produced 55-MPa (8000-psi) or even 45-MPa (6500-psi) concrete, it is safe to say that good aggregate is available near the Connecticut, Pennsylvania/Delaware, Arizona, South Carolina, and Colorado sites. Marginal aggregate is available near the Florida, Idaho, and California sites. In these areas, local materials are suitable for 45-MPa (6500-psi) concrete but will probably have to be crushed to 12.7 mm (1/2 in.) or 9.5 mm (3/8 in.) for 55-MPa (8000-psi) concrete or blended with higher-quality imported materials. For the Port Arthur, Texas, site, the coarse aggregate must be imported since there is no coarse aggregate in the area.

The cost to produce 55-MPa (8000-psi) concrete will be higher owing to concrete mix proportions requiring higher cement content and the use of special admixtures such as water-reducers/retarders, superplasticizers, and fly ash. The costs included in Table 2.8-1 are intended primarily to illustrate relative cost differences between 34-, 45-, and 55-MPa (5000-,

TABLE 2.8-1
AVAILABILITY AND PRICES OF HIGH-STRENGTH CONCRETE

Potential Customer/Site	Concrete Price[a] ($/CY) 34 MPa (5000 psi)	45 MPa (6500 psi)	55 MPa (8000 psi)	Reference/Contact	Remarks
Florida Power & Light, Florida City/Turkey Point, 48 km south of Miami	50	60	70[b] 100[c]	Rinker Materials, Miami	Marginal 38-mm (1.5-in.) limestone. For 55 MPa (8000 psi), use 9.5-mm (0.4-in.) maximum size aggregate (MSA), or import granite from Macon, Georgia.
DOE, DOD/Nat. Reactor Testing Station, 65 km west of Idaho Falls, Idaho	60	68	76[b] 106[c] (d)	Monroe Concrete, Idaho Falls; Monroe Concrete, Boise; Idaho Portland, Inkom	Marginal 25-mm (1-in.) gravel. For 55 MPa (8000 psi), use 9.5-mm (0.4-in.) MSA or import gravel from Boise.
Gulf States Utilities, Gulf/Exxon/Port Arthur, Texas	70	82	94[d]	Cowboy Concrete, Port Arthur	No local coarse aggregate. Import limestone from Austin, Texas, or flint from Louisiana.
North East Utilities/ Millstone Point, Connecticut	53	61	70	Manchester Sand & Gravel, Manchester, Connecticut	Good local traprock
Philadelphia Electric/ Delmarva, Peach Bottom, Pennsylvania/Wilmington, Delaware	56	73	80	Philadelphia Electric, Delmarva PCRV Concrete tests; ENR, Baltimore	Good local limestone
Arizona Public Service/ Palo Verde, 64 km west of Phoenix	52	60	68[d]	Union Rock, Phoenix	Good local gravel, 25-mm (1-in.) MSA
DOE/DOD Savannah River Plant, South Carolina, near Augusta, Georgia	46	53	60	Claussen Concrete, Augusta, Georgia	Good local granite and quartzite
Southern California Edison/ San Diego Gas & Electric, Blythe, California	55	62	69[d]	Southern California Edison PCRV concrete preliminary tests; ENR, Los Angeles	Good to marginal local gravel. May have to go to 12.7-mm (0.5-in.) MSA for 55 MPa (8000 psi).
Public Service Company of Colorado, Fort St. Vrain, 64 km north of Denver	57	64	72	Public Service Company of Colorado PCRV construction records; ENR, Denver	Good local andesite

[a] Commercial, non-nuclear, FOB batch plant.

[b] Local coarse aggregate.

[c] Import coarse aggregate.

[d] Test results not available.

6500-, and 8000-psi) concretes. They are based on concretes produced to commercial standards, usually by non-union labor and FOB batch plant. Actual costs per cubic yard of PCRV concrete for nuclear construction will be substantially higher.

Further investigation will include trade-off studies of the additional costs for producing 55-MPa (8000-psi) concretes and the reduced concrete volume required resulting from a smaller PCRV. The task will also update the PCRV size reduction associated with the use of 55-MPa (8000-psi) concrete in conjunction with large capacity 1361-tonne (1500-ton) tendons, taking into account the effects of thermal stress and concrete creep of 55- versus 45-MPa (8000- versus 6500-psi) concretes in addition to short-term compressive strength considerations.

Cooling Water System Optimization Studies

A cost optimization study was performed for the PCRV liner cooling water system (LCWS) and the PCRV thermal barrier. The results show that, in general, increasing the thickness of the thermal barrier increases the cost of the PCRV and liner as well as the thermal barrier cost, while decreasing the cost of the LCWS and the reactor plant cooling water system (RPCWS). The cost decreases are due to the reduced heat load to the cooling water system, which allows an increase in the cooling tube pitch.

As a result of this study, it was concluded that a 51-mm (2-in.) increase in either or both of the Class A and Class B thermal barriers results in small overall changes (less than 1%) to the total cost ($68.4 x 10^6) of the affected systems (i.e., LCWS, thermal barrier, RPCWS, PCRV, and liner). In general, increases in the Class A thermal barrier thickness result in an overall cost reduction while increases in the Class B thermal barrier thickness cause a cost increase. In view of the small overall changes in cost shown and because additional engineering costs associated with a design change were not assessed, it is recommended that the reference

design thermal barrier thicknesses be retained. Table 2.8-2 summarizes these thicknesses together with the LCWS arrangement for the 2240-MW(t) HTGR-SC/C.

In addition, the requirement for cooling tubes embedded in the PCRV concrete near the core cavity sidewall was reviewed. Based on existing analyses, this study could not establish whether or not there is a need for embedded tubes. Therefore, additional thermal analysis of the embedded cooling tubes must be performed.

Upgrading of Upper Plenum Liner Cooling for Enhanced Safety Capabilities

A study was completed to evaluate means of upgrading the upper plenum LCWS for the purpose of ensuring satisfactory performance of the LCWS during a postulated LOFC accident. During an LOFC accident, the predicted temperatures in the upper plenum would become sufficiently high that the thermal barrier would fail, exposing the liner to high-temperature helium. This scenario increases the peak heat load to the LCWS significantly. Three design options for upgrading the LCWS reliability and its adequacy to remove these peak heat loads without compromising the primary coolant boundary or damaging the PCRV were studied. The preferred option is to design the LCWS so that the mass flow rate required during the postulated accident (i.e., LOFC) always exists, even during normal operation. This is accomplished by increasing the number of tubes in the critical heat load areas while maintaining the same flow rate per tube.

Based on this study, it is recommended that 28 tubes averaging 36 m (120 ft) in length service the top head liner. Because of congestion, the tubes should be 25.4-mm (1-in.) Schedule 40 round with an average pitch of 101.6 mm (4.0 in.) and a maximum pitch of 140 mm (5.5 in.). The 28 tubes should be arranged with seven tubes in each of the four regions shown in

TABLE 2.8-2
RECOMMENDED THERMAL BARRIER AND LCWS ARRANGEMENT
FOR 2240-MW(t) HTGR-SC/C

Zone No.[a]	Thermal Barrier Class	Thermal Barrier Thickness [mm (in.)]	Liner Thickness [mm (in.)]	Cooling Tube		
				Size[b] [mm (in.)]	Pitch [mm (in.)]	Length[c] [m (ft)]
1	A	76 (3.0)	19 (0.75)	31.8 (1.25)	140 (5.5)	181 (594)
2	A	76 (3.0)	19 (0.75)	31.8 (1.25)	140 (5.5)	181 (594)
3	A	76 (3.0)	13 (0.5)	31.8 (1.25)	114 (4.5)	181 (594)
4	A	76 (3.0)	13 (0.5)	25.4 (1.0)	114 (4.5)	163 (534)
5	A	76 (3.0)	19 (0.75)	25.4 (1.0)	140 (5.5)	103 (338)
6[d]	A	76 (3.0)	19 (0.75)	25.4 (1.0)	140 (5.5)	171 (561)
6[e]	A&B	76 (3.0)	19 (0.75)	31.8 (1.25)	140 (5.5)[f]	181 (594)
7	B	127 (5.0)	19 (0.75)	25.4 (1.0)	152 (6.0)	76 (249)
8	C	356 (14.0)	19 (0.75)	31.8 (1.25)	102 (4.0)	174 (571)
9	B	152 (6.0)	13 (0.5)	25.4 (1.0)	140 (5.5)	89 (292)
10	A	76 (3.0)	13 (0.5)	25.4 (1.0)	114 (4.5)	171 (561)
10	B	127 (5.0)	19 (0.75)	25.4 (1.0)	140 (5.5)	90 (295)
11	B	127 (5.0)	19 (0.75)	25.4 (1.0)	152 (6.0)	79 (259)
12	A	76 (3.0)	13 (0.5)	25.4 (1.0)	114 (4.5)	171 (561)
13	A	76 (3.0)	13 (0.5)	31.8 (1.25)	114 (4.5)	181 (594)
14	A	76 (3.0)	13 (0.5)	25.4 (1.0)	114 (4.5)	171 (561)
15	B	127 (5.0)	13 (0.5)	25.4 (1.0)	140 (5.5)	171 (561)
16	B	127 (5.0)	13 (0.5)	25.4 (1.0)	140 (5.5)	157 (515)

[a] Zones are described in Fig. 2.8-1.

[b] Of Schedule 40 pipe.

[c] For 1.2 m/s (4 ft/sec) cooling water velocity.

[d] Zone 6 for upper sidewall.

[e] Zone 6 for center sidewall.

[f] In addition to liner cooling tubes, the zone is being designed to contain cooling tubes embedded in the concrete approximately 300 mm from the liner.

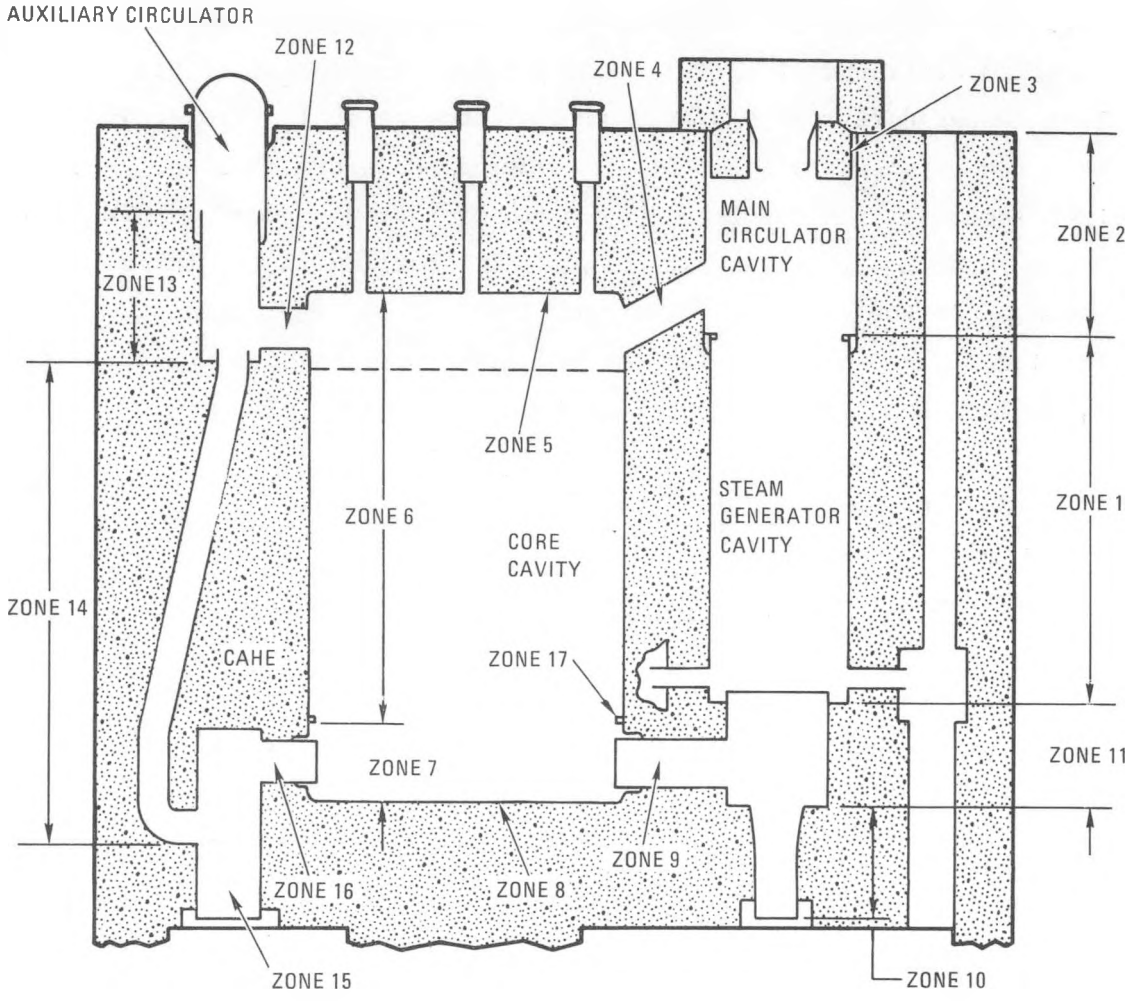

ZONE NO.	CLASS	NAME	ZONE NO.	CLASS	NAME
1	A	STEAM GENERATOR CAVITY, UPPER	11	B	STEAM GENRATOR CAVITY, LOWER
2	A	MAIN CIRCULATOR CAVITY	12	A	UPPER AUXILIARY CROSSDUCT
3	A	CLOSURE, MAIN CIRCULATOR CAVITY	13	A	AUXILIARY CIRCULATOR CAVITY
4	A	UPPER MAIN CROSSDUCT	14	A	AUXILIARY CIRCULATOR DUCT
5	A	TOP HEAD, CORE CAVITY	15	B	CAHE CAVITY
6	A & B	UPPER SIDEWALL, CORE CAVITY	16	B	LOWER AUXILIARY CROSSDUCT
7	B	LOWER SIDEWALL, CORE CAVITY	17	B	PERIPHERAL SEAL
8	C	BOTTOM HEAD, CORE CAVITY			
9	B	LOWER MAIN CROSSDUCT			
10	A & B	SUPERHEAT PENETRATION			

Fig. 2.8-1. PCRV thermal barrier zone description

Fig. 2.8-2. These modifications to the upper plenum LCWS will yield a normal operation cooling water temperature rise (ΔT_{CW}) of 8.3°C (15°F). This temperature rise can be monitored because it is significantly greater than the expected ±1°C (2±°F) accuracy of the thermocouples. Following an LOFC accident, the top head LCWS would be able to remove 1.18 W (4.04×10^5 Btu/hr) per cooling tube without inducing boiling in the tubes. This will accommodate the predicted peak heat load for an LOFC accident. The intersection of the top head with the refueling penetrations should be serviced by the top head cooling tubes, as shown in Fig. 2.8-3.

2.8.2.2. Thermal Barrier.

Bottom Head Thermal Barrier Configuration Studies

The design function of the bottom head thermal barrier is to support the core while insulating the PCRV liner and concrete from the hot primary coolant. The reference bottom head thermal barrier incorporates stacks of ceramic support pads along with fibrous insulation material sandwiched between the liner and graphite cover blocks. As shown in Fig. 2.8-4(a), the ceramic materials selected for the pads are fused silica and alumina.

This ceramic pad design is an extension of FSV technology. Ceramics were selected for the FSV design primarily because of their ability to withstand high temperatures during loss of main loop cooling conditions. For such a postulated event, the reactor would be scrammed and the core residual heat removed via the LCWS. This scenario would result in primary coolant temperatures substantially above 1093°C (2000°F) at the bottom head.

For a loss of main loop cooling, the reference HTGR-SC/C plant uses a CACS that maintains the primary coolant at substantially lower temperatures. These lower temperatures introduce the possibility of replacing the ceramic pad design with a metallic design. However, the objective remains that the

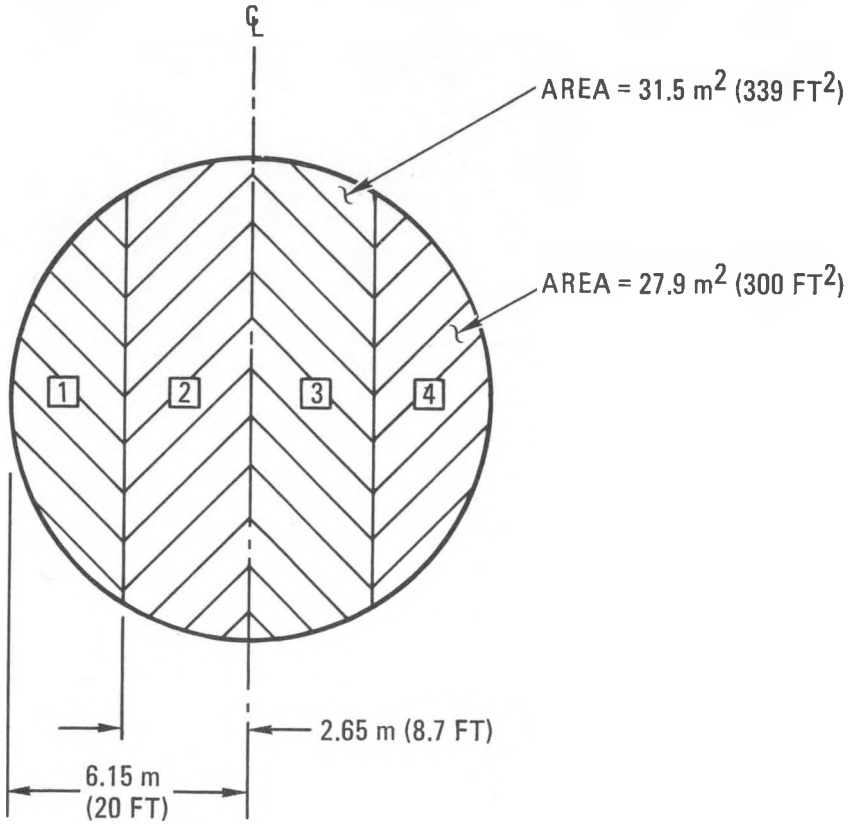

Fig. 2.8-2. Regions of the top head LCWS

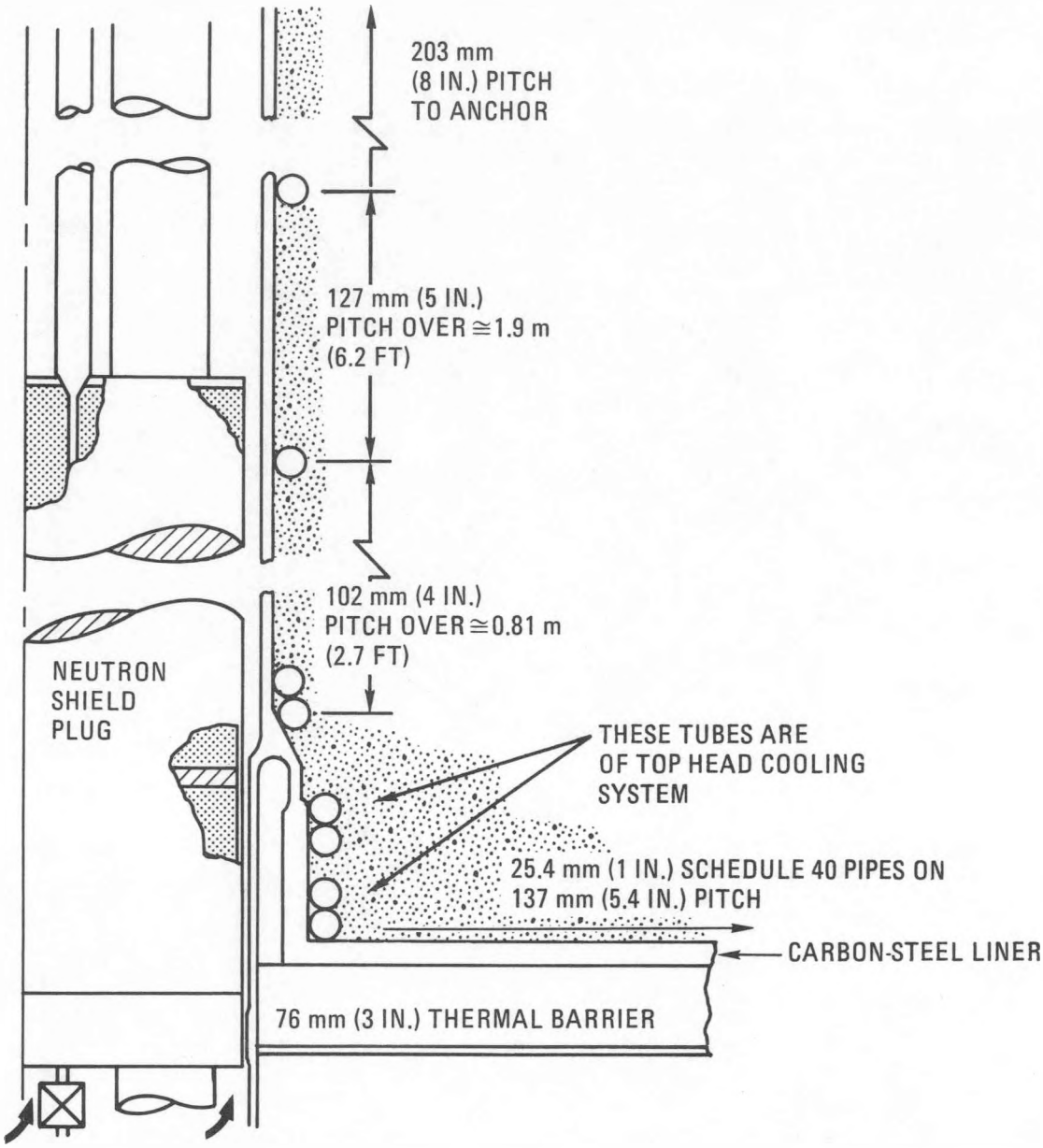

Fig. 2.8-3. Recommended cooling tube arrangement at intersection of top head liner and refueling penetration

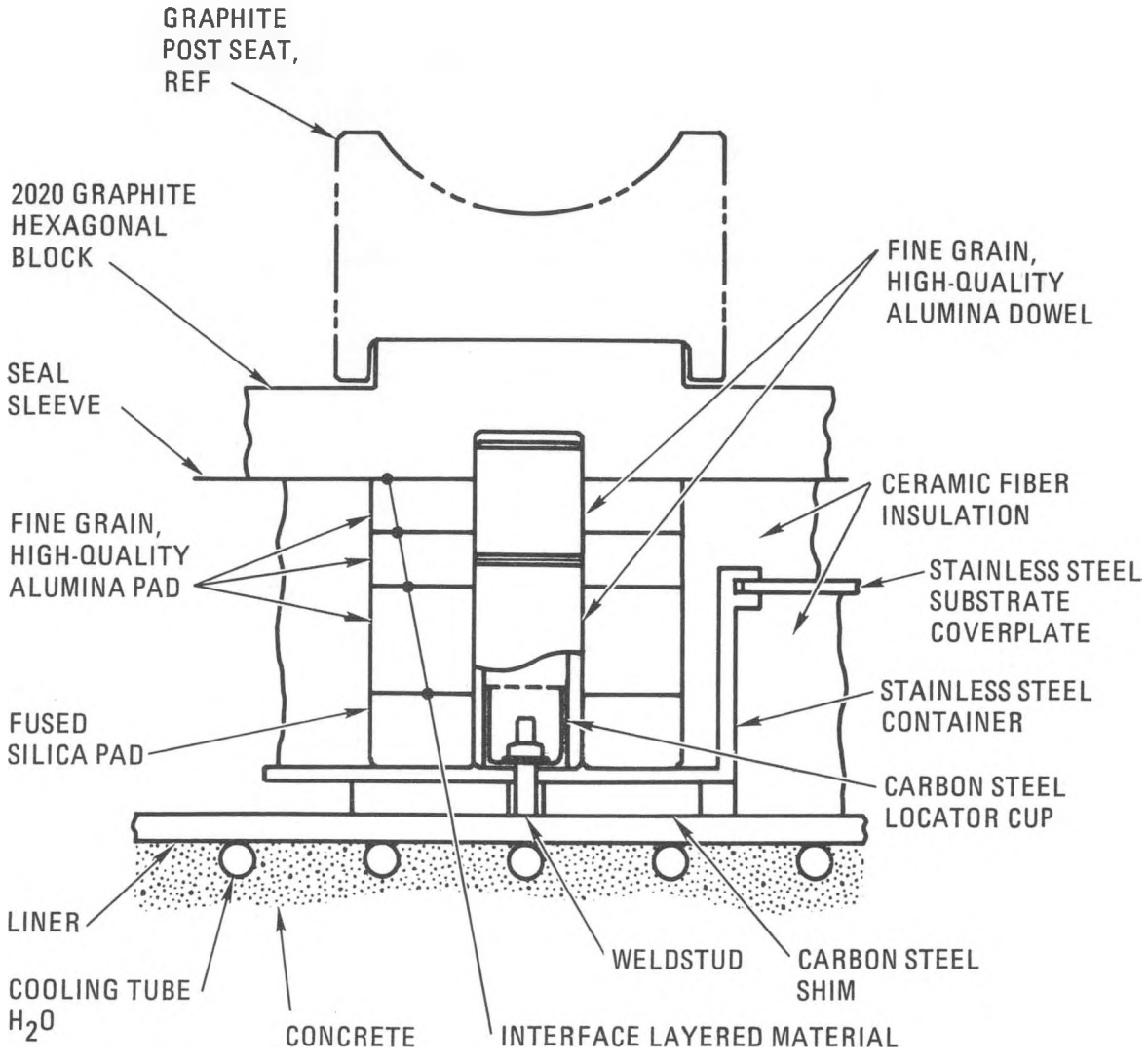

Fig. 2.8-4(a). Thermal barrier bottom head [Section A-A from Fig. 2.8-4(b)]

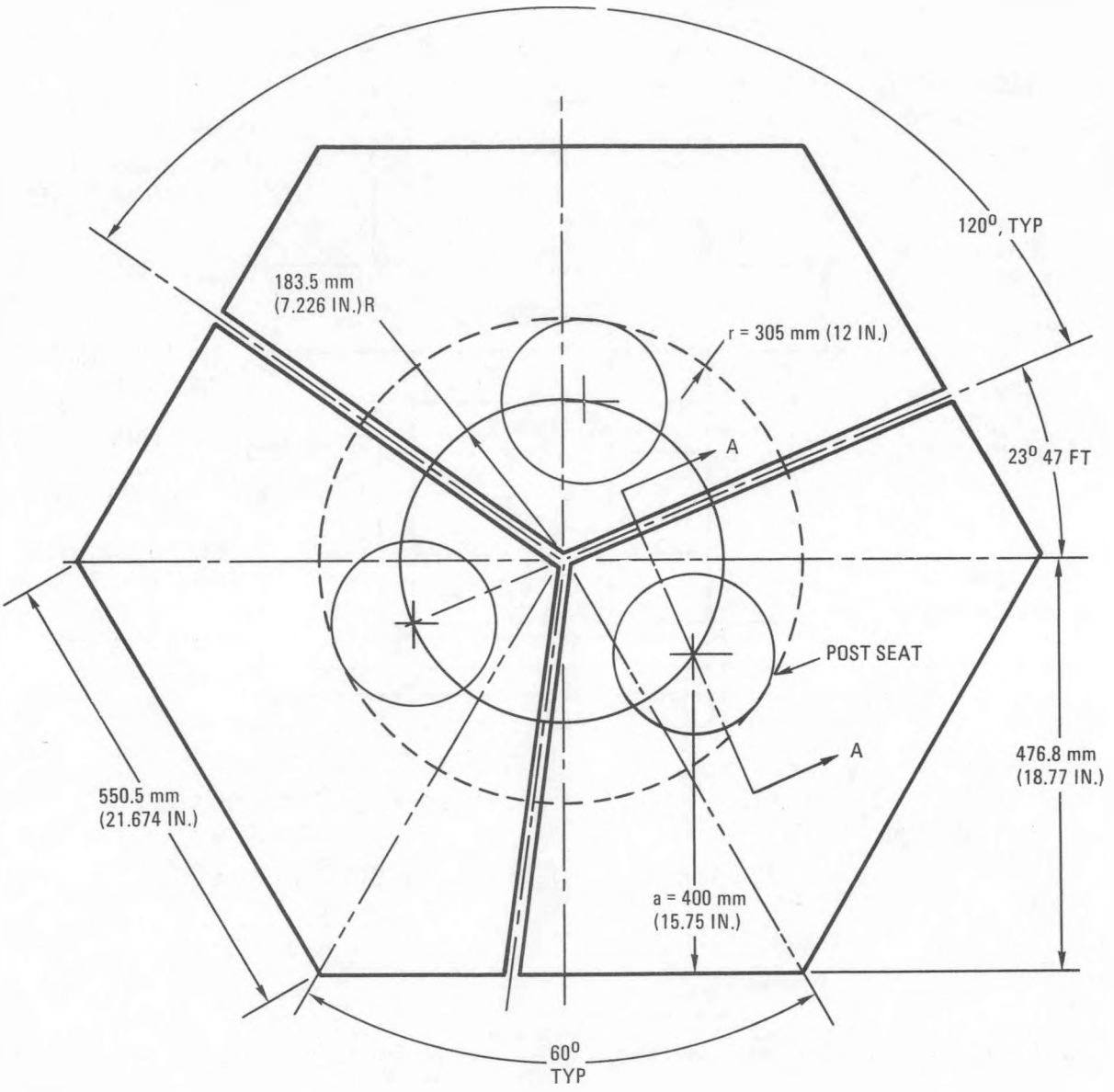

Fig. 2.8-4(b). Top view of reference Class C thermal barrier for HTGR-SC/C plant

bottom head thermal barrier be able to support the core during a non-design-basis condition that hypothetically could result from the loss of all forced circulation of the primary coolant (the loss of main loop as well as CACS cooling). During such an event, the temperatures of the hot surface of the bottom head thermal barrier are predicted to exceed 1372°C (2500°F) for almost 200 h. It therefore appears that the use of high-temperature ceramics will still be required to support the core during such a hypothetical, non-design-basis event.

During this reporting period, a bottom head thermal barrier design was introduced that incorporates a metallic primary support with a ceramic stack as a back-up structure. The proposed metallic/ceramic bottom head thermal barrier design is shown is Fig. 2.8-5. The overall thermal barrier configuration is similar to that of the current reference design (Fig. 2.8-4(a) because of the following features:

1. Each seven-fuel-column region of the core is still supported by three identical support structures positioned 120° apart as illustrated in Fig. 2.8-4(b).

2. The core load is transferred through a graphite post seal, through a graphite coverblock, to the thermal barrier support structure.

3. Shims are inserted between a metallic base and the liner to ensure that the associated graphite coverblocks are positioned correctly.

4. The region between the support structures is fitted with fibrous insulation compressed against the liner by the graphite coverblocks.

The main difference between the two designs lies in the structural support itself. The alternative design supports the core on a metallic

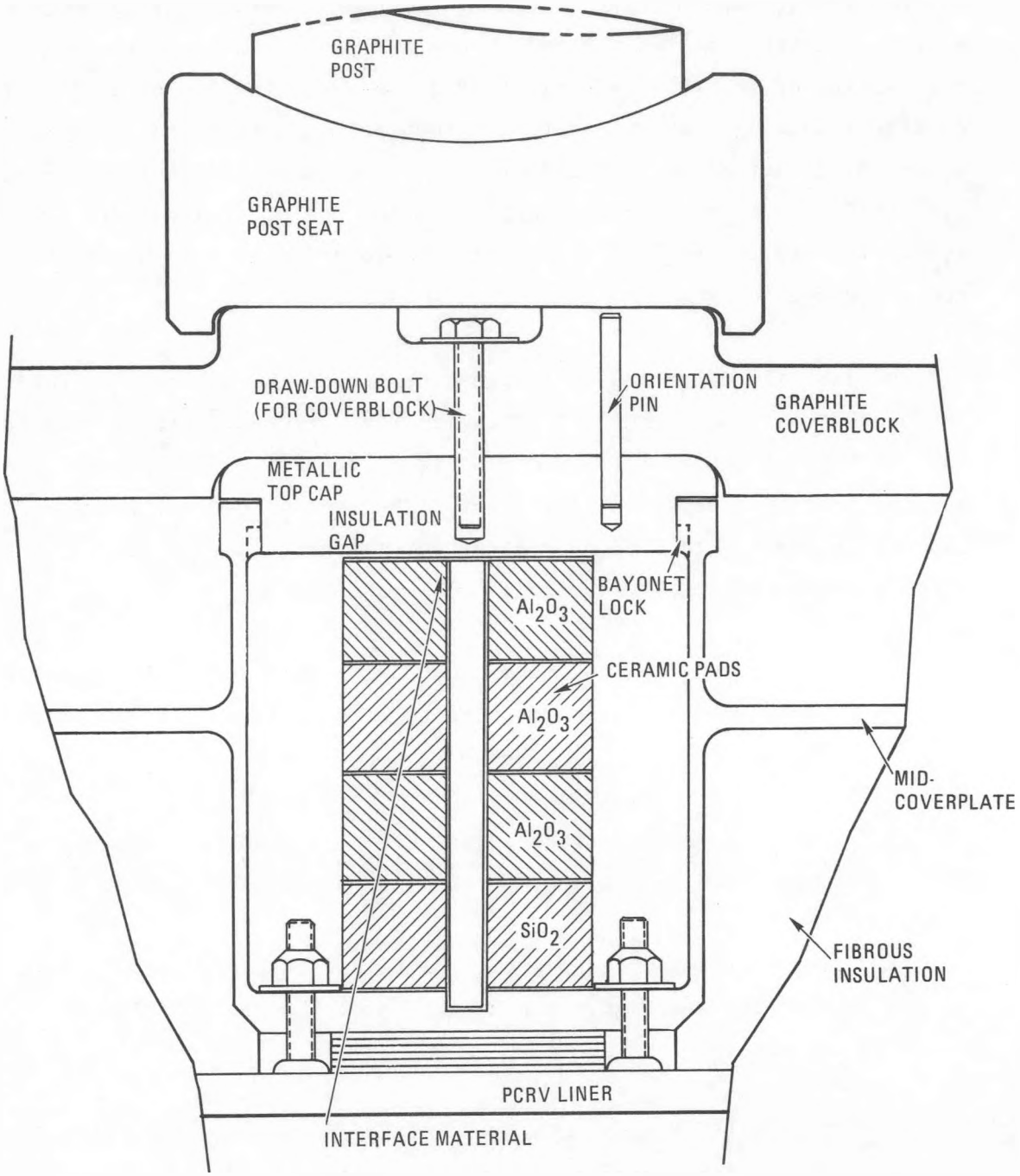

Fig. 2.8-5. Section A-A from Fig. 2.8-4(b): metallic core support with ceramic back-up

cylinder with a metallic top cap, as shown in Fig. 2.8-5. The metallic cylinder is firmly attached to the PCRV liner by bolts stud welded to the liner. The mid-coverplate is shown in Fig. 2.8-5 as being cast integrally with the cylindrical section. This was done to illustrate its position of attachment on the support structure. The coverplate will probably be made of Hastelloy X or Type 316 stainless steel and attached to the cylinder by a simpler method. Within each metallic cylinder is a stack of ceramic pads [with 114-mm (4.5-in.) outside diameter] surrounded by fibrous insulation. The pads are positioned about the centerline of the cylinder and extend from the base of the cylinder to approximately 3.2 mm (0.125 in.) from the bottom of the top cap. These pads act as an insulator and also serve as a back-up support. The fibrous insulation reduces the heat flow to the liner and minimizes radial temperature gradients in the ceramic pads. During normal operation the weight of the core is sufficient to hold the coverblock in position. However, during installation each coverblock is held in position by means of a draw-down bolt and orientation pin as shown in Fig. 2.8-5.

The metallic support is sized to handle all design basis loading conditions. The ceramic back-up structure is intended to become operative only during a postulated LOFC core heat-up event. This design is a viable replacement for the current all-ceramic pad reference design for the 2240-MW(t) HTGR-SC/C plant.

The primary incentive for pursuing the metallic/ceramic design alternative is the possibility of being able to reduce the cost and time required to qualify a design. During FY-83 more work is scheduled to quantify the potential benefits in order to justify a recommendation for the final selection of a reference design.

2.8.2.3. Criteria Documentation for ISI, Maintenance, and Replacement of Primary System Components. A study was initiated to document all principal criteria for ISI, maintenance, and replacement for all primary system

components, reactor internals, and core components. This information is being assembled in response to questions raised by the participants of Baseline Review Meetings.

The 20 components in Table 2.8-3 were identified in a preliminary listing for documentation of existing criteria. A standard format was developed for initial collection of summary level information relative to each component to ensure that all pertinent information is presented. This study is scheduled for completion in January 1983.

TABLE 2.8-3
COMPONENTS TO BE INCLUDED IN CRITERIA DOCUMENTATION

1. Main circulators
2. Auxiliary circulators
3. Steam generators
4. CAHE
5. PCRV
6. Liner
7. Thermal barrier
8. Core support structure
9. Permanent side reflector
10. Core lateral restraint
11. Core peripheral seal
12. Fuel elements
13. Hexagonal reflector elements
14. Control rods and power rods
15. Reserve shutdown system
16. Control rod drives
17. Orifice valves
18. In-vessel refueling structure
19. In-vessel refueling system
20. Instrumentation

Safety related (PPS)	System 32
Plant control system	System 33
Plant data acquisition	System 35
Analytical	System 36

2.9. FUEL HANDLING EQUIPMENT DESIGN (6032130001)

2.9.1. Scope

The scope of this task includes refinement of the conceptual design of the fuel handling system as needed to support interfacing systems, plant definition, and cost estimating. The specific subtask during this reporting period was to define the proposed construction of two equipment items in the fuel handling system to provide improved plant definition and a basis for cost estimates in these areas.

2.9.2. Discussion

A brief description of the in-vessel fuel handling system and data on the two layouts developed during this reporting period is presented below.

2.9.2.1. Reactor Refueling. The basic function of the fuel handling system is to accomplish the periodic, remote replacement of core fuel and reflector elements in a safe and efficient manner. Refueling operations are predicated on 4-yr fuel residence time, with one-quarter of the fuel elements being replaced each year with new fuel. Replaceable reflector elements adjacent to the active core are replaced at 8-yr intervals.

The basic procedure for replacing fuel or replaceable reflector elements (see Figs. 2.9-1 and 2.9-2) involves the exchange of new hexagonal elements from the Temporary Fuel Storage Facility beside the PCRV for selected spent core elements. This exchange occurs after the reactor has been shut down and depressurized.

Fuel handling machine access to the various core regions is achieved through the sequential removal of control and orifice assemblies from their penetrations in the top head of the PCRV with the auxiliary service cask. A reactor isolation valve is used to maintain the helium environment in the

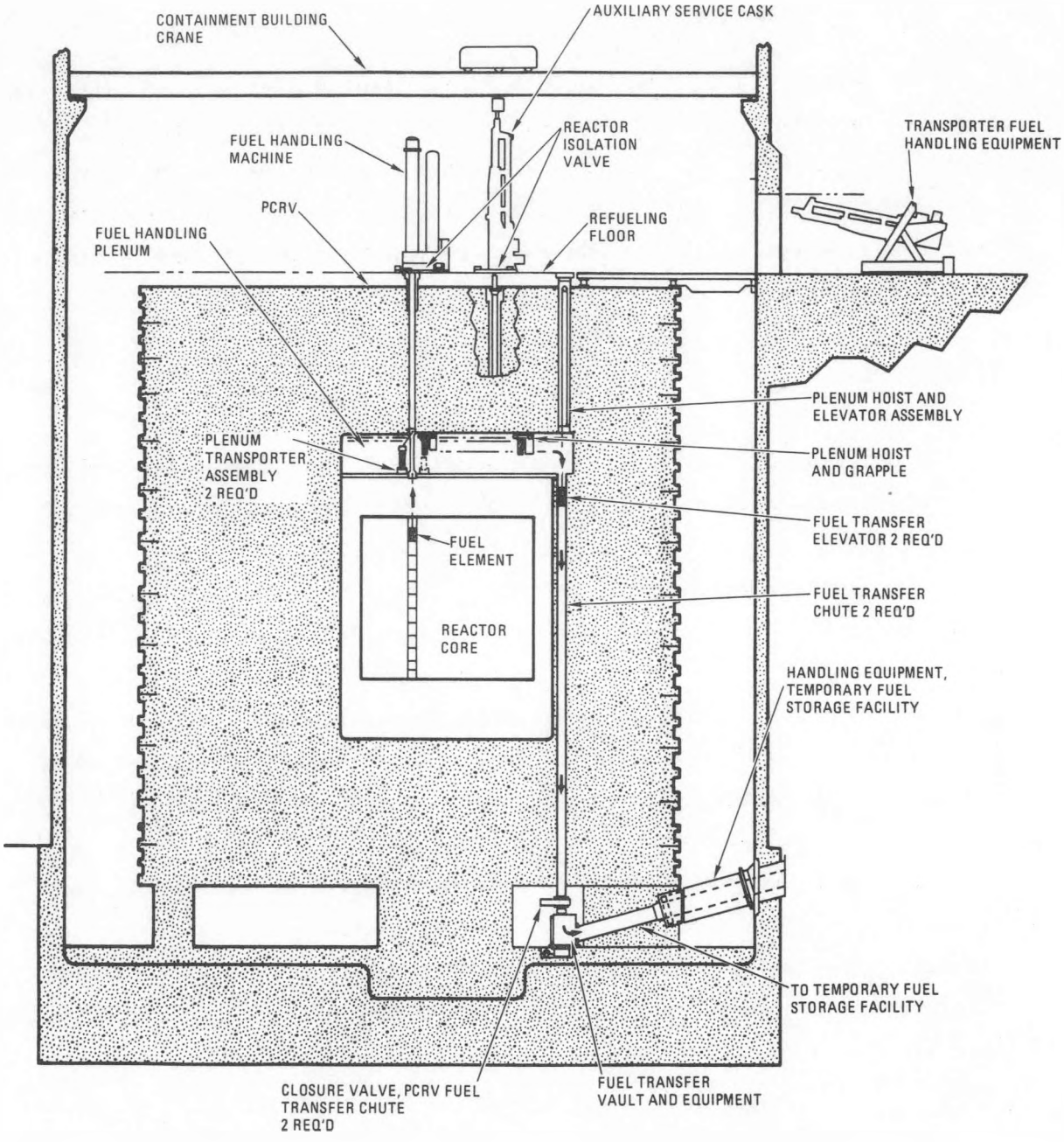

Fig. 2.9-1. In-vessel fuel handling concept

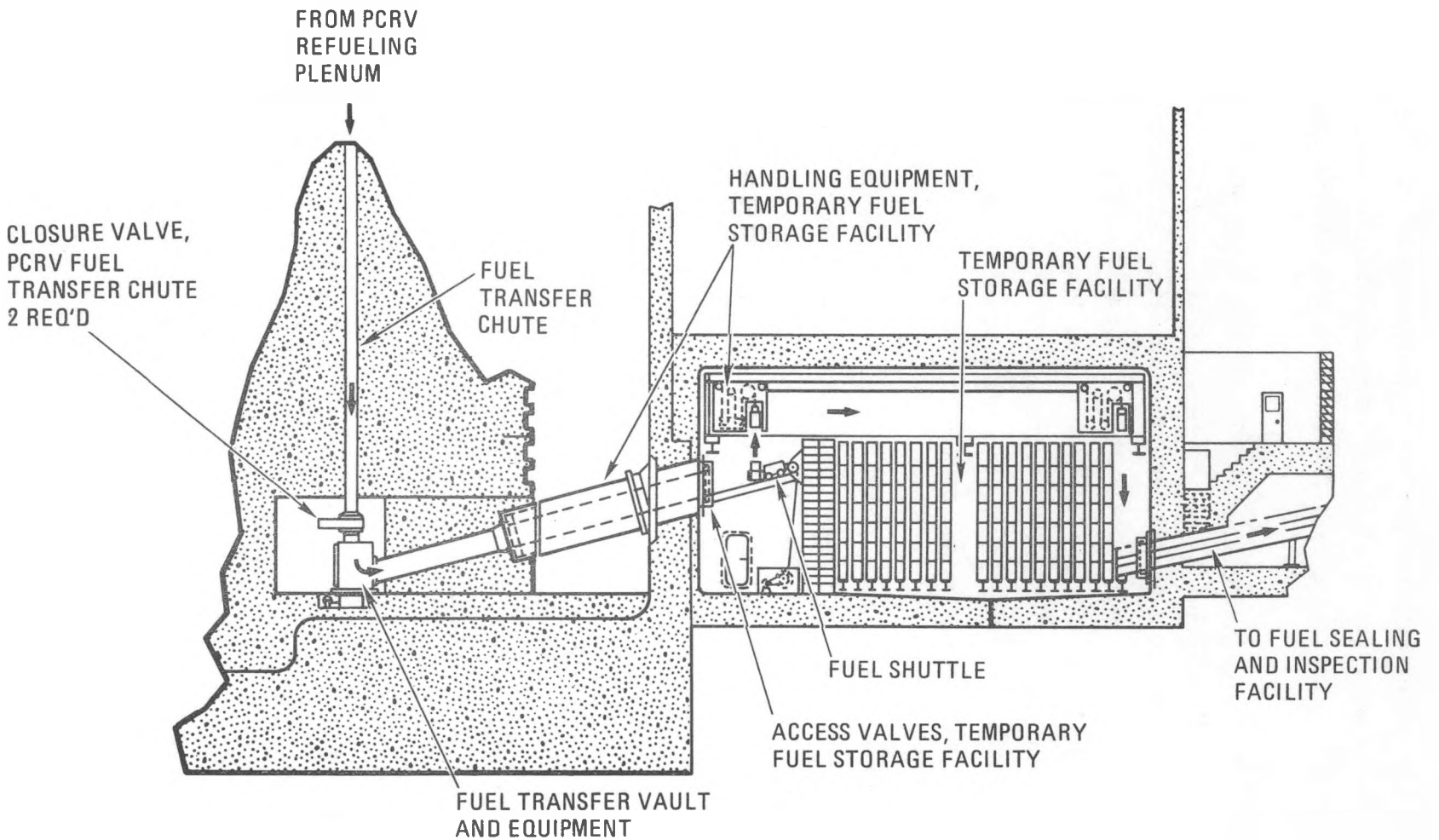

Fig. 2.9-2. Fuel transfer vault and temporary fuel storage facility

PCRV during the installation of the fuel handling machine. The plenum transportation assembly and the plenum hoist and elevator assembly are installed in their respective penetrations in a similar fashion.

The fuel handling machine lifts each spent element to the plenum at the top of the core cavity. The plenum equipment either stores the element temporarily in the upper plenum structure of translates the element horizontally to the side of the core, where it is lowered through the PCRV into the fuel transfer vault. Handling equipment in the Temporary Fuel Storage Facility receives elements from the transfer vault and places them in storage wells. New elements are moved from the Temporary Fuel Storage Facility into the empty core region by the reverse process.

The proposed construction of the transfer vault and internal handling mechanisms (see Figs 2.9-3, 2.9-4, and 2.9-5) was defined in a new layout issued during this reporting period. The construction of this equipment is significant because of the many interfaces with other plant equipment and the necessity for high component reliability for all equipment actually handling elements in the "in-vessel" refueling concept.

The transfer vault provides a pressure boundary for the primary coolant during refueling. Spent fuel enters the vault through either of the two vertical transfer chutes in the PCRV. Spent fuel leaves the vault through the single inclined tube leading to the Temporary Fuel Storage Facility.

Two handling mechanisms and a viewing device are mounted in the top surface of the vault structure. Each handling mechanism provides two movements for spent fuel elements that are deposited on the mechanism by the fuel element elevators. The elements are deposited in a support structure that is cantilevered from the end of a rotating arm. The first movement is a 180° rotation of the rotating arm, which moves the element from a point beneath the vertical transfer chute to a point near the center of the

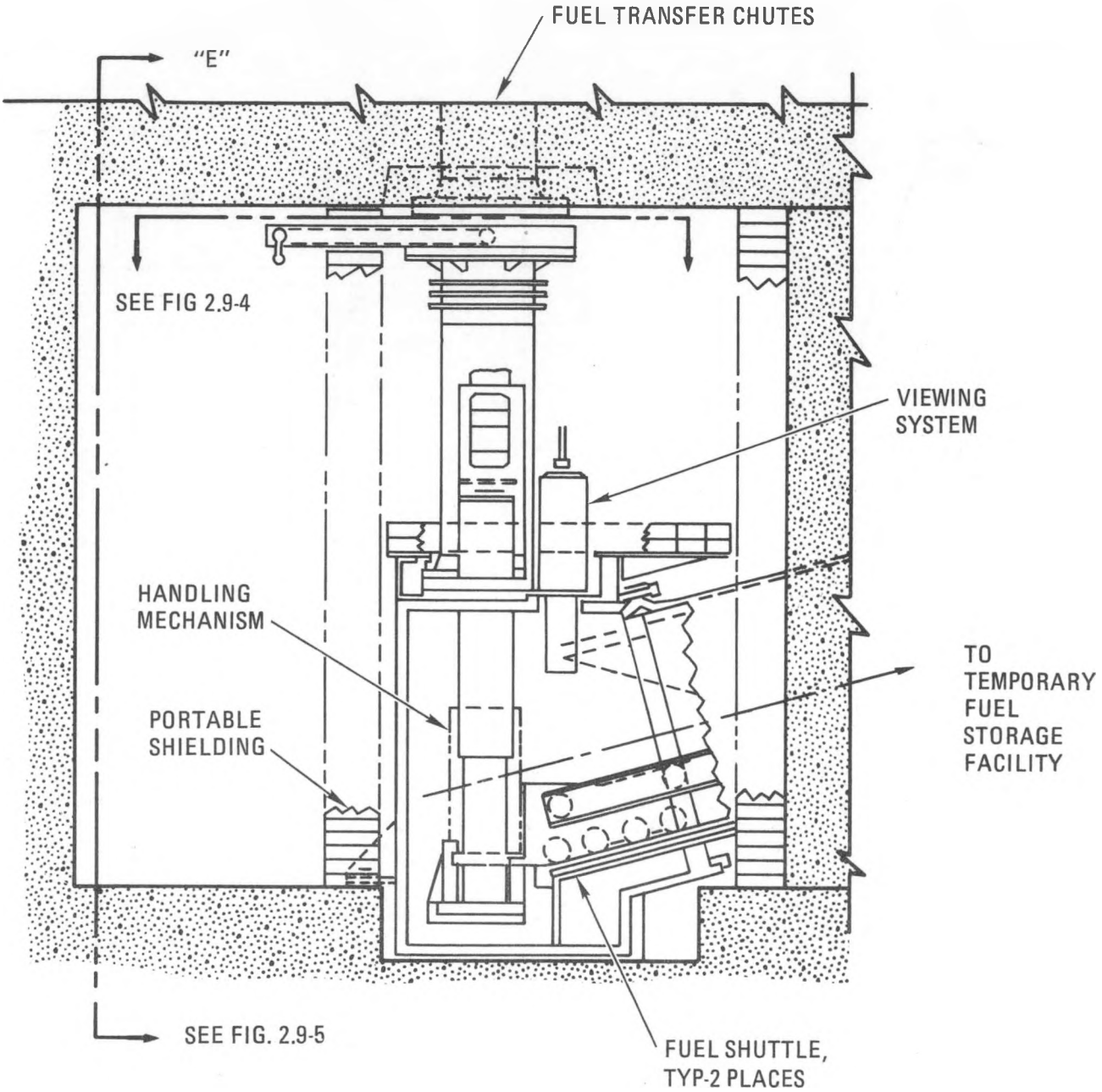

Fig. 2.9-3. Fuel transfer vault and equipment

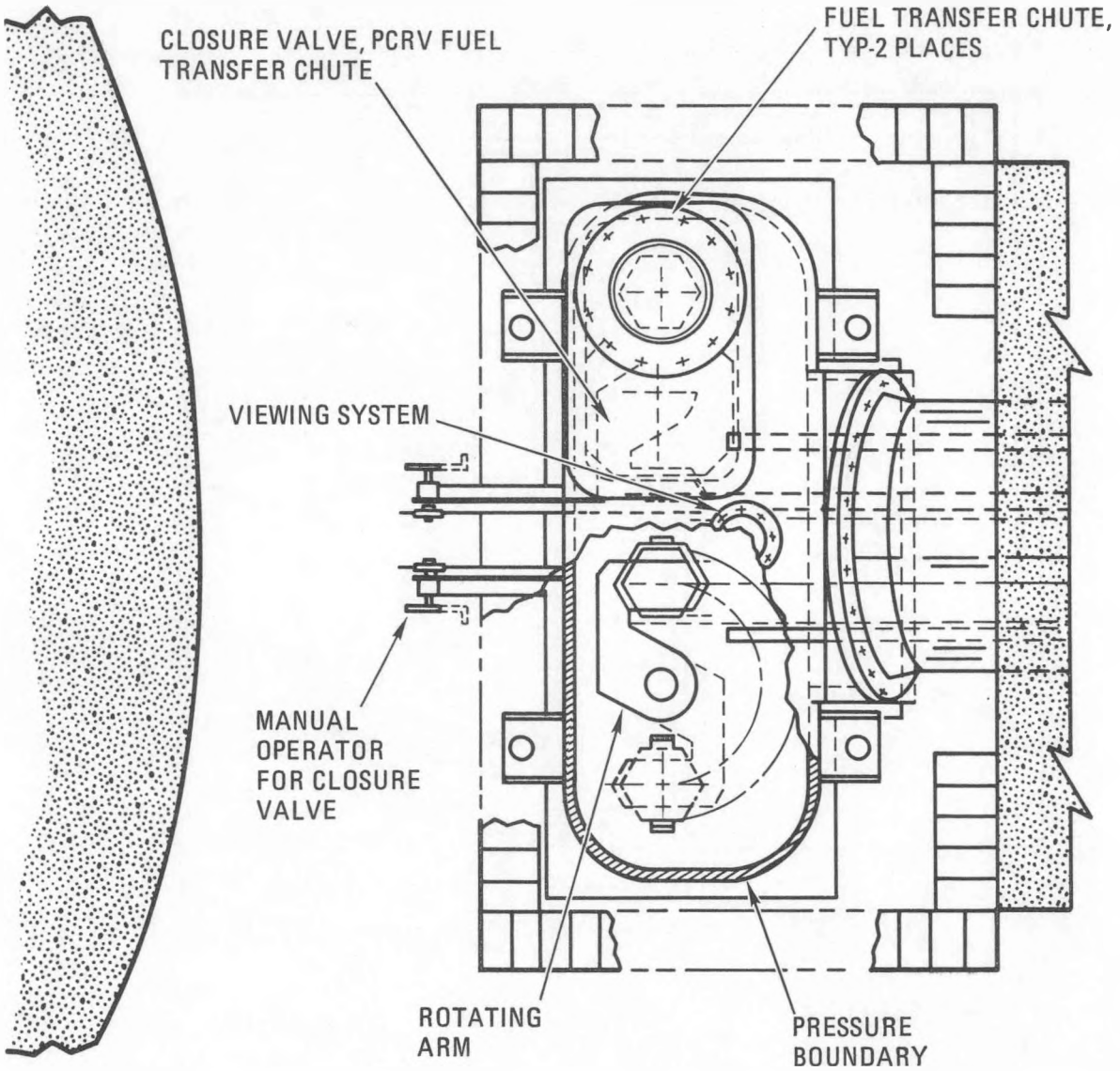

Fig. 2.9-4. Plan view of fuel transfer vault and equipment

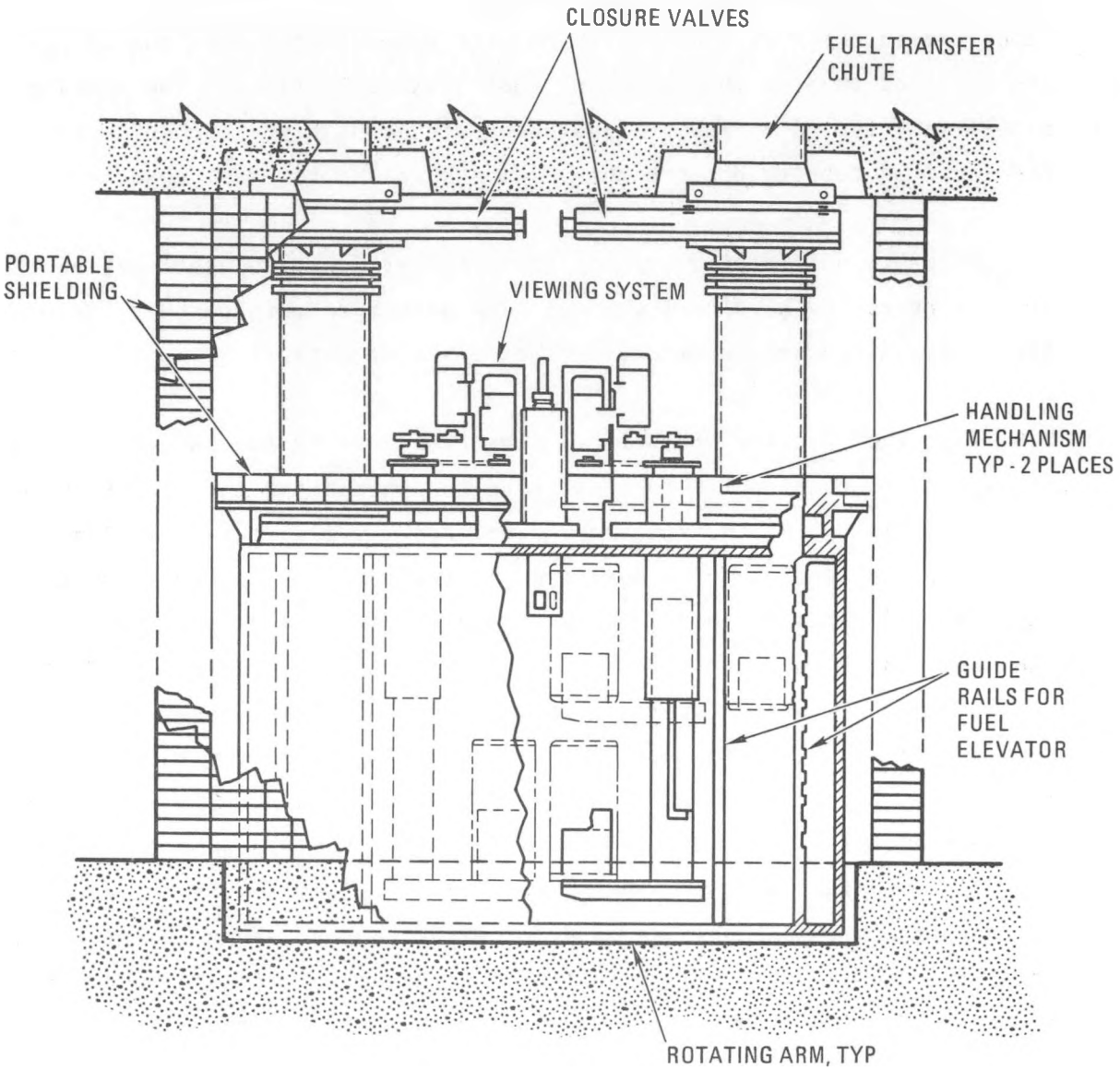

Fig. 2.9-5. Elevation view of fuel transfer vault and equipment

vault. The second movement lowers the rotating arm until the element is deposited in the fuel shuttle, which will subsequently move the element up the inclined tube to the Temporary Fuel Storage Facility. The viewing system is oriented to permit viewing of either handling mechanism or up the inclined tube to observe the movements of the two fuel shuttles.

Portable shielding surrounds the transfer vault and vertical chutes to protect operating personnel who may need access to this part of the plant for other maintenance work during the refueling outage.

2.9.2.2. Fuel Service Operations. The Fuel Sealing and Inspection Facility (FSIF) is the focal point for fuel handling operations that occur while the reactor is in operation (see Figs. 2.9-6 and 2.9-7). This facility is located in the Fuel Service Building and performs the following functions. New fuel and replaceable reflector elements enter the handling cycle at the FSIF, where they are inspected and subsequently moved remotely to the Temporary Fuel Storage Facility. Spent fuel that has decayed to acceptable heat generation rates is moved remotely from the temporary fuel storage area into the FSIF, where one of two possible events occurs. The spent elements may be placed in disposable canisters holding three elements each or placed directly into fuel shipping containers holding six elements per container. The disposable containers are used for elements that are to be placed in long-term on-site storage, while the shipping containers are used for elements to be shipped immediately to the reprocessing plant. The disposable containers may also be retrieved from long-term storage and deposited in shipping containers for shipment to reprocessing or off-site storage.

The FSIF is a shielded vault located above grade. It houses the fuel sealing and inspection equipment and has shielded windows and closed circuit television systems for viewing the operations in the facility. Access penetrations are provided in the floor for moving fuel and other components into and out of the facility.

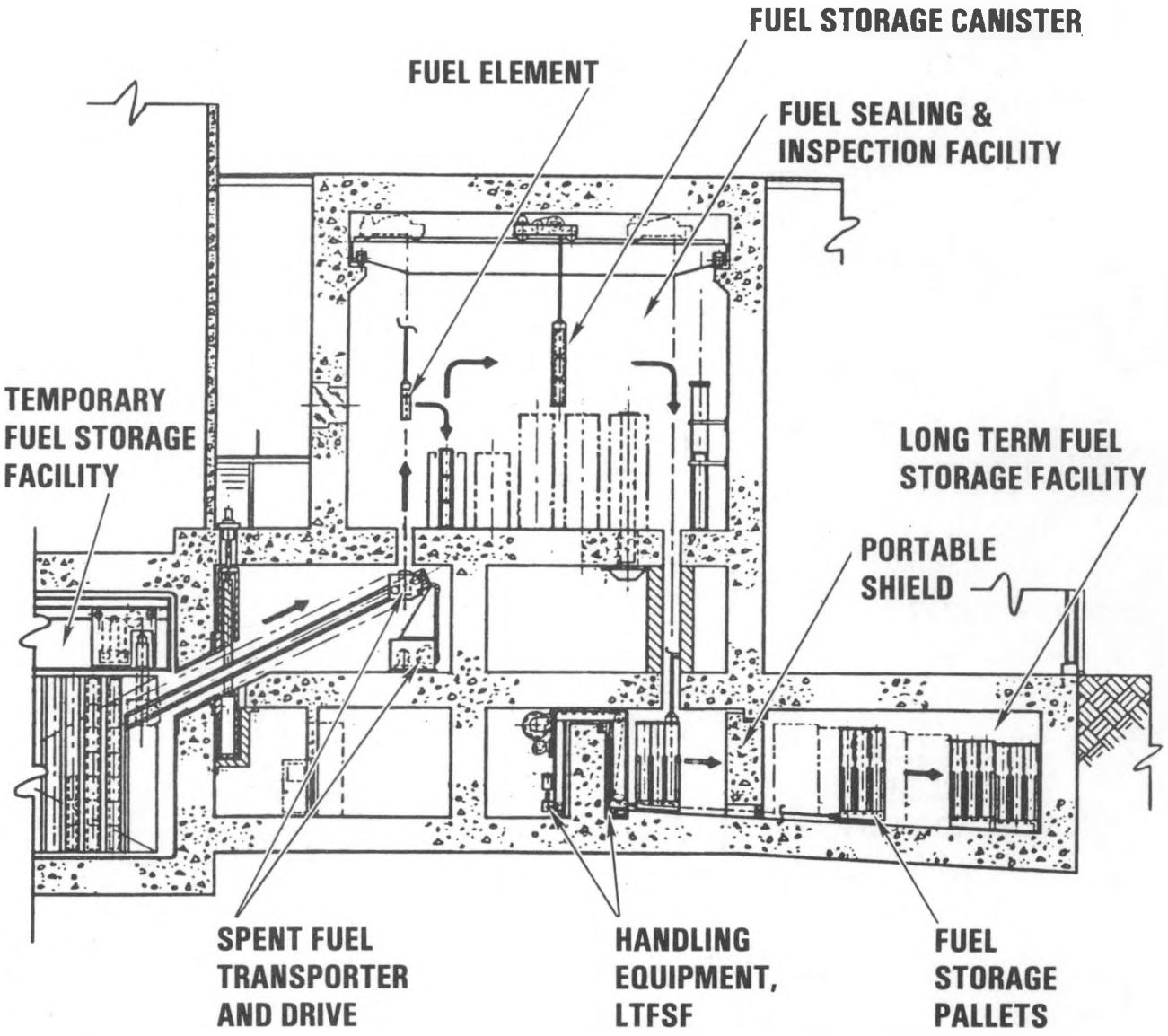

Fig. 2.9-6. Preparation of fuel elements for long-term storage

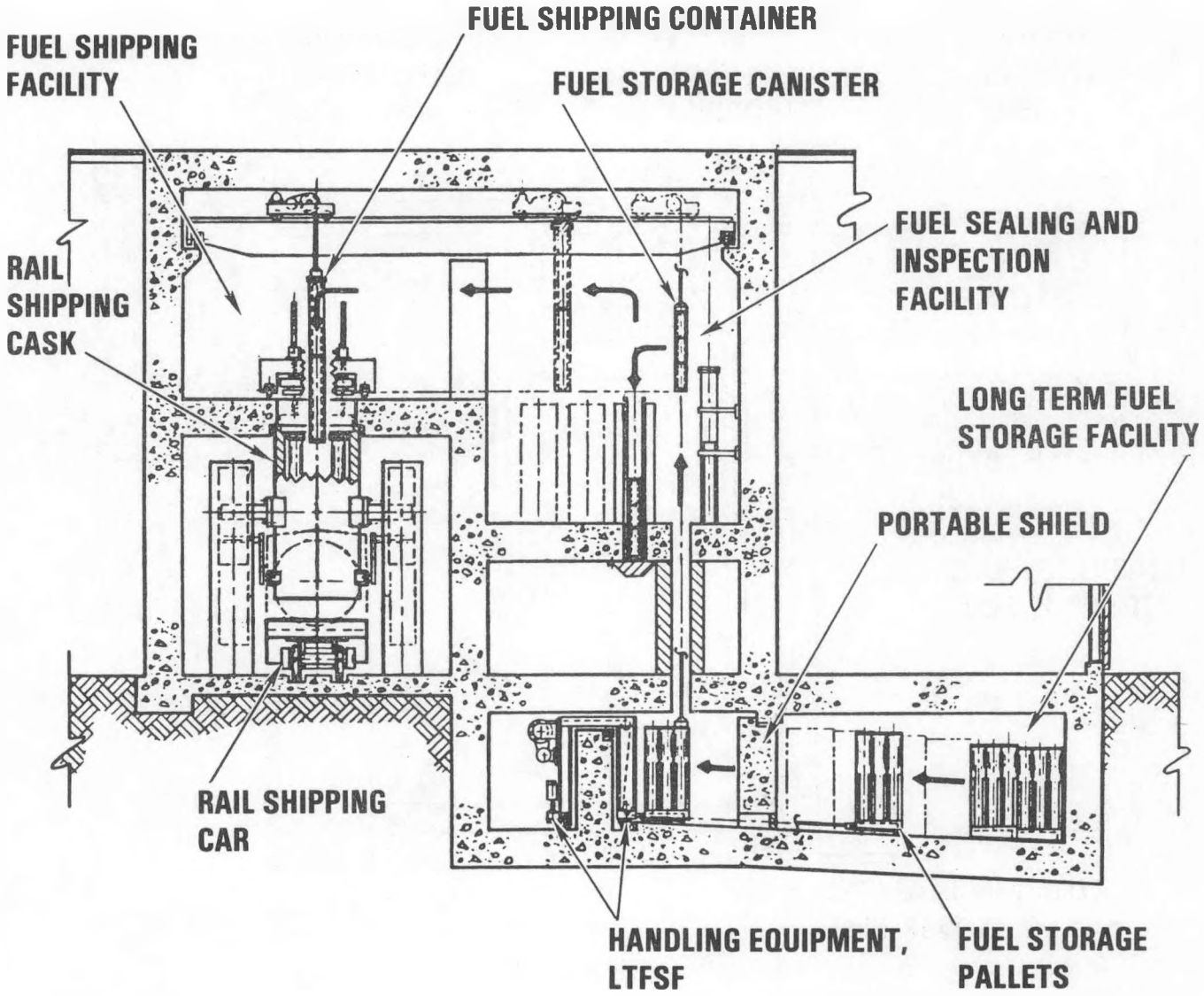

Fig. 2.9-7. Preparation of fuel elements for shipment

The handling of components is accomplished with two cable-supported grapple assemblies positioned by a common bridge crane structure. One grapple handles fuel elements and similar items by their central handling holes. The second grapple handles fuel storage canisters and fuel shipping containers.

The proposed construction of the bridge crane and grapple assembly was illustrated in a new layout issue during this reporting period. The construction of the crane is significant since it controls the size of the FSIF vault and has a major impact on the placement of other FSIF equipment within the vault. The crane also requires special features to permit remote maintenance in the event of malfunction with spent fuel in the FSIF.

2.10. REACTOR SERVICE EQUIPMENT CONCEPTUAL DESIGN (6032160001)

2.10.1. Scope

The scope of this task is (1) to refine the conceptual design of the equipment for handling the main and auxiliary circulators and (2) to update the plant system description document for the plant definition Baseline 0.

2.10.2. Discussion

The reactor service equipment system encompasses a group of subsystems and components, each comprising equipment and tools to facilitate in-vessel and ex-vessel service and maintenance operations, as well as handling and storage of a number of reactor components.

Design evolution of the main and auxiliary circulator components over the past few years has necessitated additional design work on the circulator handling equipment, first to assure that all required remote maintenance can be performed and second to minimize the effects of the design changes on plant costs.

The initial circulator handling equipment specified for large HTGRs was designed to handle the main circulators only, and the cask geometry and integral shielding were designed for this single purpose. Subsequent design reviews have shown a potential need to replace auxiliary circulators and the isolation valves beneath each type of circulator. In addition, the diameter of the main circulator assembly increased by approximately one-third (i.e., from 1651 to 2235 mm (65 to 88 in.) with the change to an electric drive system.

The initial appraisal of all of these changes indicated that the weight of the circulator handling cask would be doubled to approximately 126.9 tonnes (140 tons), and that detailed interfaces would need to be identified

on the isolation valves to accommodate the remote installation of handling adapters. The increased weight for the cask is very undesirable since it requires larger crane capacity for both the Containment Building and Service Building cranes. Therefore, design studies were performed to reduce the size of the packages to be handled and to refine the construction of the cask in order to reduce its weight. As a result of these preconceptual studies, the gross weight of a loaded cask is now estimated to be 77.1 tonnes kg (85 tons). This is still 13.6 tonnes (15 tons) greater than the weight of the auxiliary service cask, which is the next largest item to be moved with the cranes, but provides a substantial reduction from the initital 126.9-tonne (140-ton) estimate. Additional weight reductions may be possible if new shielding studies scheduled for FY-83 show that cask surface dose rates caused by plateout on the valves and circulator blades are sufficiently low to permit a reduction in the 228-mm (9.0-in.) steel wall currently specified for the cask.

A design layout illustrating the proposed sequence for remote replacement of the auxiliary circulator and its loop isolation valve has been prepared. This layout identifies the general handling procedure, the handling features required for each component, and the special handling adapters.

2.11. REACTOR INTERNALS DESIGN (6032170201, 6032170202, 6032170203)

2.11.1. Scope.

The scope of this task included the preparation of arrangement and layout drawings for the reactor internals system and the performance of supporting structural and thermal-hydraulic analyses.

2.11.2. Discussion

The reactor internals system consists of two graphite structures comprising (1) the core support structure and the permanent side reflector and (2) three metallic structures, the core lateral restraint, the core peripheral seal, and the upper plenum refueling structure.

During this reporting period, drawings of the core lateral restraint system (CLR) were updated, and owing to funding emphasis being transferred to other primary issues, the main effort was directed to the analytical studies described below.

2.11.2.1. Graphite Components. Criteria were developed for identifying the most severe thermal/flow transients with respect to the lower core support block (LCSB) design. The two parameters having the greatest effect on heat transfer rates in the block are the rate of change of coolant bulk temperature with time and the magnitude of the surface convective heat transfer coefficient. In the turbulent flow regime, the latter parameter is strongly dependent on the local coolant mass flow rate. The four transients determined to have the largest coolant temperature reduction together with the least flow rate decrease are shown in Table 2.11-1.

To determine which of these transients represents the worst lower core support block operating condition, a detailed transient thermal flow analysis of the block was performed. A description of the analytical procedure and model and the results for the reactor trip transient are given in

TABLE 2.11-1
TRANSIENTS SELECTED FOR DETAILED THERMAL-HYDRAULIC ANALYSIS

Description	Class	Occurrences
Reactor trip from 100% load	Upset	73
Rod bank insertion	Upset	5
Rod bank withdrawal at 100% load with trip on high steam generator inlet temperature	Faulted	1
41 kg/s (90 lb/sec) steam leak to primary with trip on high moisture level	Faulted	1

Ref. 2.11-1. As a means of comparing thermal stress levels within the block, differentials between the mean block cross-sectional temperature and the minimum modal temperature were calculated as a function of time. By comparing the analysis results and the parameters associated with each transient, it was concluded that the reactor trip transient provides the most severe thermal operating environment for the LCSB for the following reasons:

1. This transient generates the largest temperature differences in the graphite, which tend to remain for the longest period of time.

2. This transient has a much higher frequency of occurrence than either the rod insertion event or the two faulted events.

3. Allowable graphite stress levels are considerably lower during an upset event than during faulted events.

2.11.2.2. Core Peripheral Seal. A study was conducted to estimate the bypass flow through the potential leak paths of the present design of the core peripheral seal (CPS). These analyses showed that at least 72% of the total flow through the CPS is attributable to leakage through interfaces of the graphite logs. About 15% is through the insulated portions of the support structure, and the remaining 13% is through the uninsulated support structure. However, justification for the assumed maximum gaps around the seal logs is needed. The present seal support structure permits small adjustments that should make more precise alignment possible when the logs are first installed. Such adjustment was not possible with the previous reference design when the magnitude of these seal log misalignments was first established.

The criterion for leakage through the CPS was that the bypass flow rate should not exceed 1.5% or be less than 0.5% of the total primary coolant flow at the rated power condition, as stated in the CPS Design Specification. It was agreed that for the present, CPS leakage should be expressed as 1.5% ± 1% of the total core cavity coolant flow, under 100%-power

steady-state operating conditions as a more realistic objective than the narrower range previously defined. Leakage and the effects thereof at other reactor conditions have not yet been investigated and need to be established. The nominal 1.5% leakage would be the maximum expected based on nominal gap dimensions and expected core pressure drop (ΔP). The 2.5% maximum leakage would represent a design limit for a highly improbable event where maximum gap dimensions and maximum ΔP are assumed. It was also noted that the effects of possible waviness or bowing of sealing surfaces (owing to localized temperature differentials), the extent of which is difficult to predict, have never been included in leak calculation.

2.11.2.3. Core Lateral Restraint. A preliminary structural assessment of the redesigned core lateral restraint (CLR) was begun. The assessment consists of determining the CLR stiffness, preload, and seismic capacity followed by reviews of the magnitude of the seismic load on the CLR and stresses in the coil springs. Owing to budgetary constraints, the analysis could not be completed in FY-82 and is now scheduled for completion during the fourth quarter of FY-83.

An updated version of the CLR layout drawings (Fig. 2.11-1) was released which incorporated a slot in the faceplate that had been omitted on the layout drawings included in the previous semiannual report.

Reference

2.11-1. "HTGR Applications Program Semiannual Report for the Period October 1, 1981, through March 31, 1982," DOE Report GA-A16831, 1983.

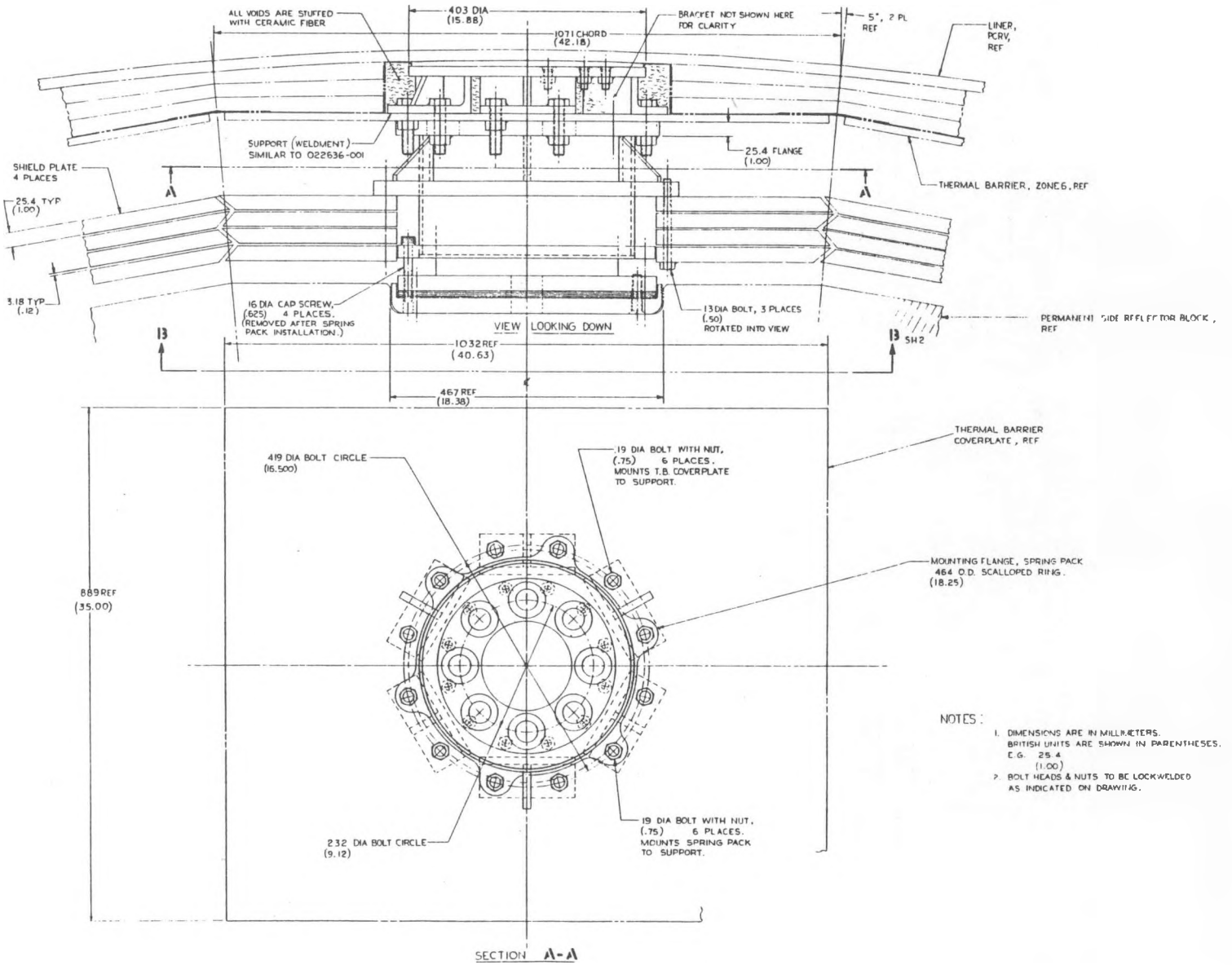

Fig. 2.11-1 (sheet 1). Core lateral restraint layout.

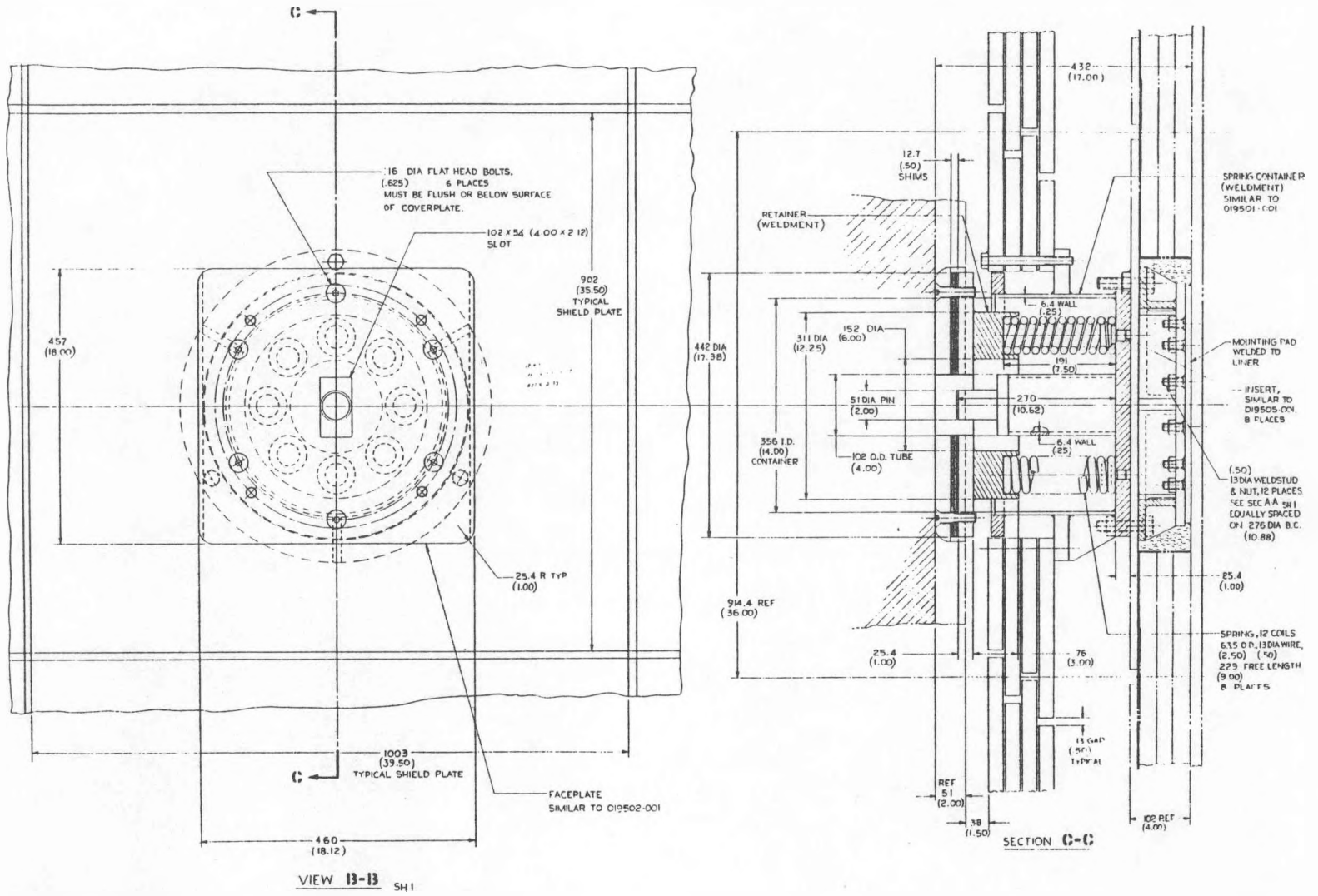

Fig. 2.11-1 (sheet 2). Core lateral restraint layout.

2.12. CORE COMPONENT DESIGN (6032180101, 6032180103)

2.12.1. Scope

The scope of this task consists of design and analysis studies and documentation to verify the major features of the core required for the Baseline 1 design and cost package.

2.12.2. Discussion. During this reporting period, preliminary stress calculations were preformed on the current fuel element design for the 2240-MW(t) HTGR-SC/C core. The entire 541-column active core was examined using the one-dimensional viscoelastic SURVEY/STRESS code (Ref. 2.12-1) to isolate the highest-stress elements for more detailed analyses. In addition, the current nine-row fuel element was compared with the 10-row (FSV) design on the basis of axial thermoelectric stress under spatially uniform power generation. These analyses were performed using the one-dimensional GBEAM code.

The SURVEY/STRESS analysis was done for a symmetrical third of the active core for all eight layers. A core average power density of 5.8 W/cc was used. Peak axial stress/strength ratios of 0.13 and 0.19 were found for the standard and control elements, respectively. The control element was in refueling region 44, layer 4. The standard element was in column 7, region 66, layer 4. The fourth layer is just above the core midplane, where the axial power factors are maximal. For the buffer fuel elements the peak stress/strength ratio was 0.17. This occurred in the seventh layer of both column 3, region 38, and column 4, region 42. All of these values are slightly lower than those obtained for comparable elements in previous SURVEY analyses of the 10-row, 7.1 W/cm^3 2240-MW(t) design.

The distribution of the maximum stress/strength ratios revealed that:

1. Maximum values are in layer 4. The top two layers have values typically only one-half of those in the fourth layer.

2. In the upper section of the core (layers 1 through 5), the highly stressed elements were all control elements, while in the lower part of the core the buffer elements experienced the highest stresses.

3. The standard elements (excluding buffer elements) usually have lower stress/strength ratios than the control and buffer elements.

4. The probability density distributions of the standard and buffer fuel elements are skewed to lower values. Thus, only a few standard and buffer elements are highly stressed. However, the distribution for the control elements is more symmetrical. Thus, a greater percentage of the control elements is subjected to high stresses.

The GBEAM analyses of the nine- and 10-row elements under flat power profiles revealed comparable thermoelastic stresses. For similar core power densities of 7.1 W/cm^3, the nine-row design had stresses 26% higher than those of the 10-row design. With a power density of 5.8 W/cm^3, however, the nine-row design thermal stresses were nearly the same as those of the 10-row design at 7.1 W/cm^3, even though the cross-element temperature differential (the driving force for thermal stress) of the nine-row design was only 60% of that of the 10-row design. This result is attributed to the fact that the maximum tensile stress depends on the difference between the element mean and the cooler temperature of the maximum stress point rather than the cross-element temperature differential. As a consequence, the maximum axial tensile stress is higher in the nine-row design owing to the presence of the cooler thick rim surrounding the hotter inner portions of the element. The condition may be alleviated by minor changes in the element geometry.

The foregoing stress analysis was accompanied by thermal-hydraulic analysis for the purpose of establishing temperature distributions for use in the GBEAM code (Ref. 2.12-2.). The computer code used for the thermal

analysis is a modified version of the TEPC code (Ref. 2.12-3). The major modifications incorporated in the TEPC code were:

1. The flow in various coolant channels and gaps is calculated using a one-dimensional momentum equation and an input pressure drop for each channel.

2. The thermal conductivity of the graphite can be calculated at each nodal point as a function of fluence and temperature using reference correlations for graphite.

The finite element mesh used for the TEPC analysis of the control rod element is shown in Fig. 2.12-1. A similar mesh is used for the standard fuel element analysis. The following core elements were analyzed during this initial phase of the analysis:

	Region	Column	Layer
Standard fuel element	66	7	4
Control rod element	44	1	4

A typical temperature distribution obtained for the control rod element is shown in Fig. 2.12-2.

The results for a complete 4-yr cycle (36 time points) for both the standard and control rod elements were written on a catalog file for stress analysis by the GBEAM code.

References

2.12-1. Smith, P. D., "SURVEY/STRESS, A Model to Calculate Irradiation Induced Stresses, Strains, and Deformations in an HTGR Fuel Block Using Viscoelastic Beam Theory," GA Report GA-A13712, October 20, 1975.

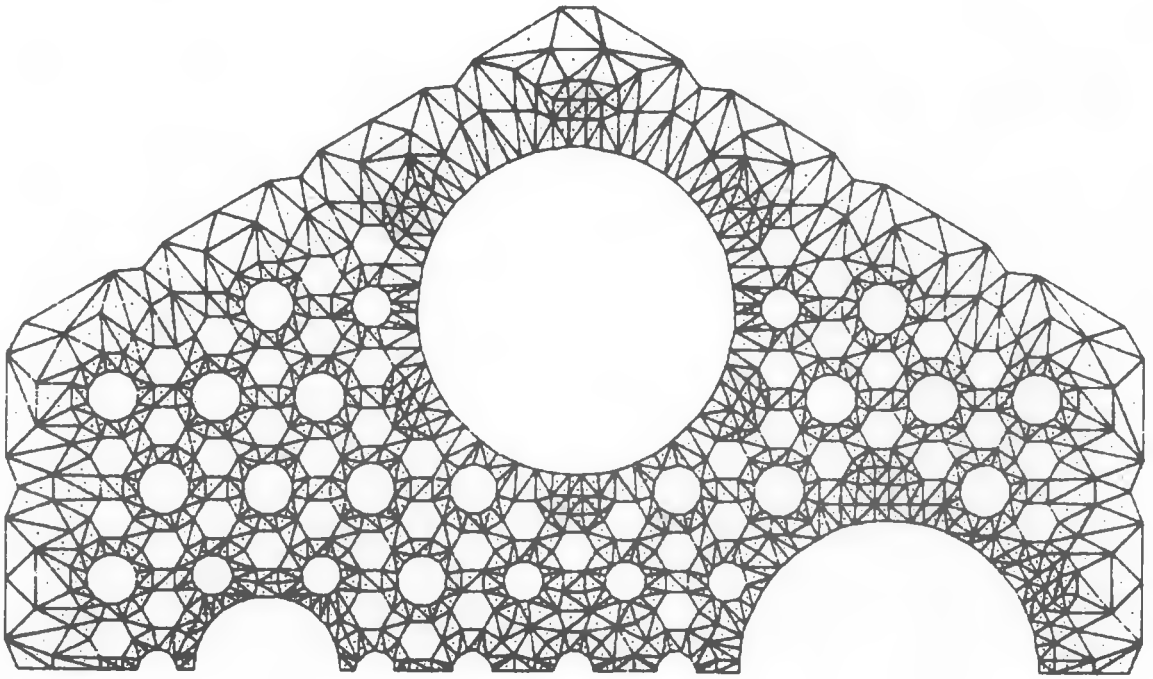

Fig. 2.12-1. Finite element mesh used for the TEPC analysis of control rod element

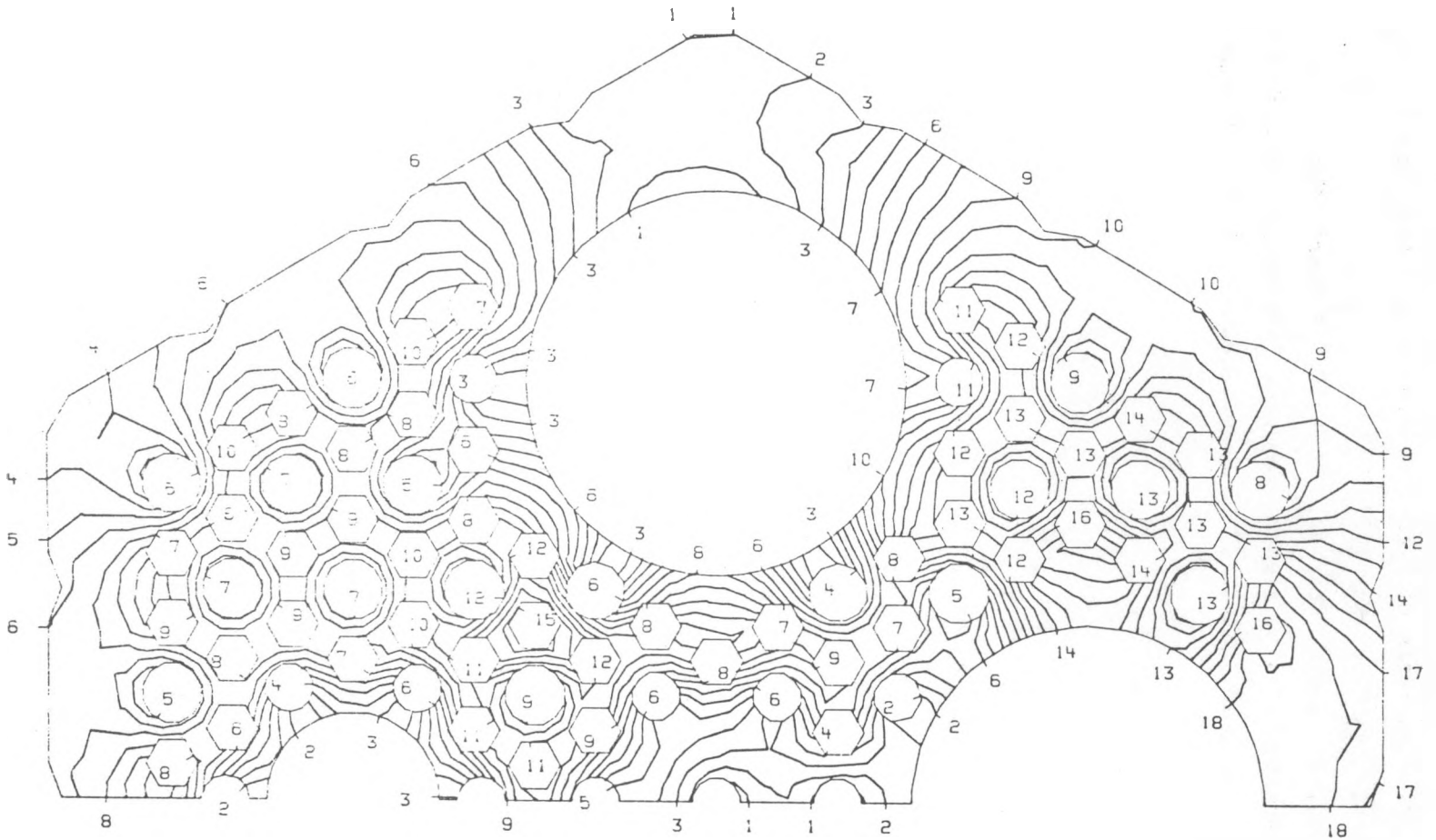

Fig. 2.12-2. Typical temperature distribution in the control rod element

2.12-2. Smith, P. D., "GBEAM4, A Computer Program for the Viscoelastic/ Cracking Analysis of Graphite Structures Using Beam Theory," GA Report GA-A14432, May 1977.

2.12-3. Tzung, F., and C. Charman, "TEPC-2D," A User's Manual for the Two-Dimensional Finite Element Computer Program for Thermal-Elastic-Plastic Creep Analysis," GA Report GULF-GA-A12753, November 7, 1973.

2.13. REACTOR CORE NUCLEAR DESIGN (6032180102, 6032180201, 6032180203)

2.13.1. Scope

This task encompasses the evaluation of fuel element designs, core layouts, core fuel loadings, and fuel cycle prescriptions for the purpose of providing a 2240-MW(t) power core design for HTGR-SC/C applications with acceptable fuel performance and with economically viable fuel cycle costs. During this reporting period, emphasis was on retaining the design and fuel cycle for the alternative core configuration, evaluating the nuclear characteristics of the adopted design, and determining comparative fuel cycle costs. This work included fuel depletion calculations to provide flux and power distributions as a function of burnup to be utilized in fuel element stress analyses and in fuel performance studies. Methods were also developed for deriving within-region power distributions on a fine-mesh basis to enable more detail in block stress analysis. Some studies were initiated on NSSS shielding analysis and on developing a higher-performance fuel element.

2.13.2. Discussion

2.13.2.1. Core Description Updating. Revisions were made to some of the core design parameters for the 2240-MW(t) HTGR-SC/C using data reported in the previous semiannual report (Ref. 2.13-1). Changes included were a refined block design for control rod fuel columns, rezoning of the core radially, and recalculation of the fuel cycle. The current reference design parameters are detailed below.

Revised Control Block Design. In the initial alternative core studies, a nine-row fuel block design with an outer flange for sealing the block ends was adopted as the reference fuel element. The flanged concept and nine-row fuel hole array were retained except for an increase in the

number of fuel holes in the control column from 88 to 96 with a commensurate addition of coolant holes. Table 2.13-1 lists the updated parameters for all the block types. With these new fuel pin loadings and the 541-column core, the average pin power for a 2240-MW(t) core output is 272.2 W per fuel rod, still about 28 W higher than in the previous 439-column core using ten-row blocks.

Radial Rezoning

In the process of optimizing the radial fuel distribution to minimize region power factors, it was found that an adequately flat radial power distribution is attainable using only three zones. Thus, the innermost two zones of the previous four-zone radial scheme, composed of 19 and 18 seven-column regions, were combined into a 37-region zone. Details on the resulting column distributions are given in Table 2.13-2. Figure 2.13-1 is a diagram of a one-third sector layout [2 rad (120°) symmetry] of the core showing the radial zoning and also the segmentation for reloading stages. The outermost zone consists of a one-column thickness of fuel next to the radial reflector.

Fuel Cycle Study

Fuel cycle calculations for defining optimum reloading parameters were redone using the zero-dimensional code GARGOYLE with the higher fuel column fraction achieved with the revised block designs. As before, a constant fissile concentration (segment average) was specified for all reloads to give a C/U ratio of about 854, and loading searches were conducted on the thorium loading to minimize age peaking factors. The equilibrium C/Th ratio appears to be on the order of 620 as in the previous calculations. Table 2.13-3 list some of the GARGOYLE results and results at radial and axial zoning calculations using the reload compositions.

TABLE 2.13-1
REFERENCE 9-ROW FUEL ELEMENT DESIGN FOR 2240-MW(t) HTGR-SC/C CORE

	Standard Block	Control Block	Short Control Block
No. of holes			
Fuel, 12.7 mm (0.5 in.)	174	96	96
Coolant, 15.875 mm (0.625 in.)	84	30	30
Coolant, 12.7 mm (0.5 in.)	7	23	23
Control rod, 101.6 mm (4 in.)	--	2	2
Reserve shutdown, 95.25 mm (3.75 in.)	--	1	1
Power rod, 43.28 mm (1.70 in.)	--	1	1
No. of fuel rods	2052	1126	864
Block height, mm (in.)	792.99 (31.22)	792.99 (31.22)	594.74 (23.41)
Fuel volume fraction[a]	0.17495	0.09600	0.09822
Coolant area fraction [a]	0.15606	0.07888	0.07888
Block unfueled weight, kg (lb)	99.09 (218.46)	89.85 (198.09)	67.14 (148.02)

[a]For hexagonal side dimension (including gap) of 208.7 mm (8.2 in).

TABLE 2.13-2
RADIAL ZONING SCHEME FOR 2240-MW(t) HTGR-SC/C CORE

	Radial Zone 1	Radial Zone 2	Radial Zone 3	Core Total
No. of Columns				
Standard	222	174	60	456
Control	37	24	24	85
No. of Blocks				
Standard	1776	1392	480	3648
Control	259	168	168	595
Short Control	37	24	24	85
No. of fuel rods	3,967,954	3,066,288	1,194,864	8,229,106
Volume, m^3 (ft^3)	185.12 (6536.6)	141.61 (5000.2)	59.77 (2110.5)	386.50 (13647.3)
Fuel volume fraction	0.16400	0.16567	0.15296	0.16291
Zone fraction of core	0.4787	0.3660	0.1553	1.000
Zone average outer radius [mm (in.)]	3054.5 (120.3)	4057.4 (159.7)	4414.6 (173.8)	4414.6 (173.8)

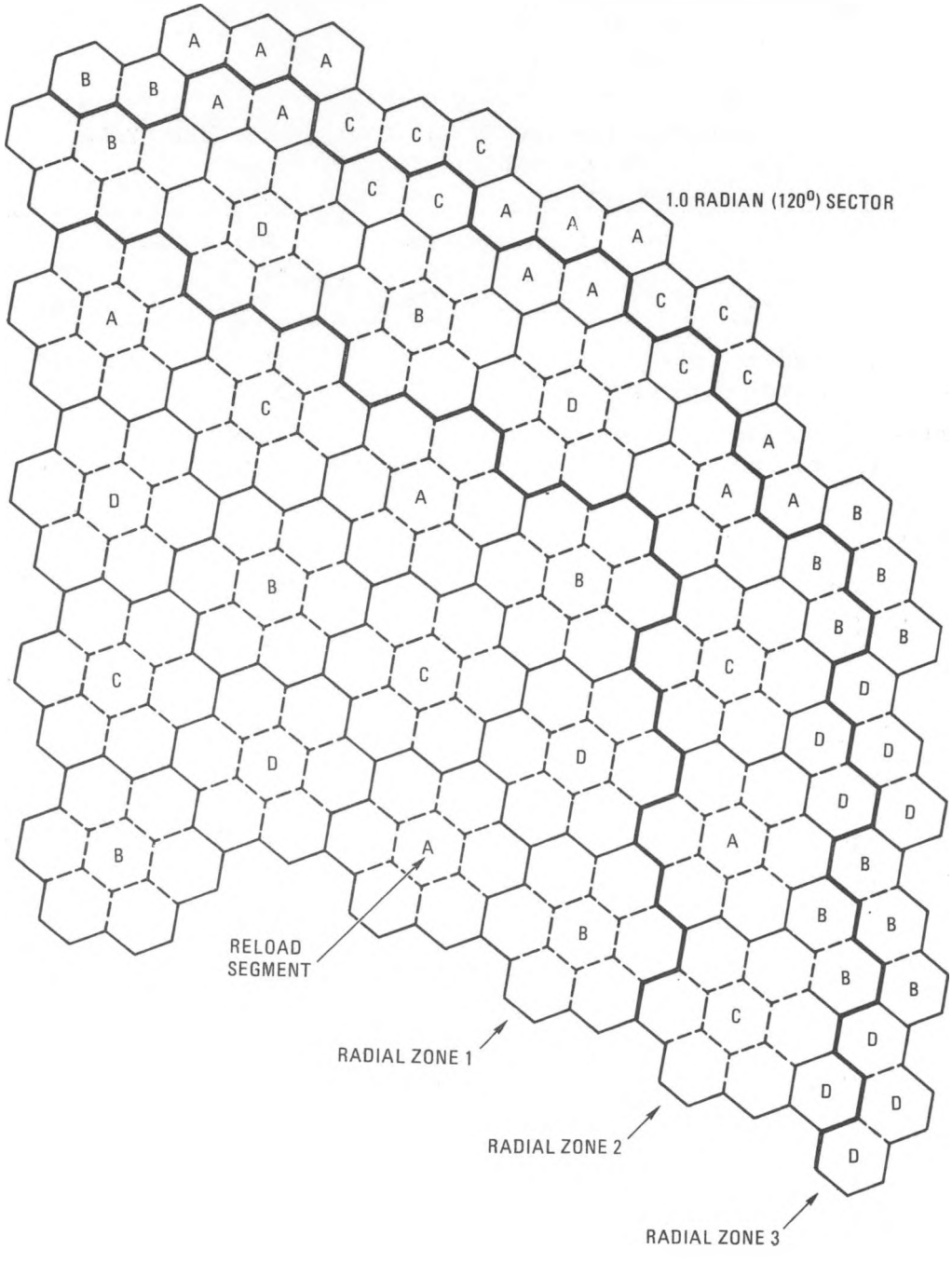

Fig. 2.13.1. Zone and segment layout for 2240-MW(t) HTGR-SC/C core

TABLE 2.13-3
TYPICAL FUEL LOADING SPECIFICATIONS IN FUEL CYCLE
OF 2240-MW(t) HTGR-SC/C CORE

Segment	Initial Core (A+B+C+D)	First Reload (A)	Equilibrium Average[a]
No. of standard columns	456	114	114
No. of control columns	85	21	21.25
Volume fraction of core	1.0000	0.2496	0.2500
No. of fuel rods	8,229,106	2,055,090	2,057,277
Average C/th ratio	375	887	619
Average C/U ratio	1124	856	854
Total loading U (20%), kg (lb)	8647.0 (19066.6)	2852.2 (6298.0)	2857.4 (6300.5)
Total loading Th, kg (lb)	25317.2 (55824.4)	2696.9 (5946.6)	3857.1 (8505)
Radial zoning factors[b]			
Fissile			
Zone 1	0.9567	1.0119	1.0102
Zone 2	1.0547	1.0302	1.0397
Zone 3	1.0046	0.8916	0.8751
Fertile			
Zone 1	1.0322	1.1177	1.0767
Zone 2	0.9840	0.9078	0.9384
Zone 3	0.9381	0.8541	0.9086
Axial zoning factor[c]			
Fissile			
Zone 1	1.2441		1.2963
Zone 2	0.7559		0.7036
Fertile			
Zone 1	1.0850		1.0011
Zone 2	0.9150		0.9989

[a] Average for reloads 21 through 24.

[b] For minimized radial power peaking in GASP (wt % burnup), equalized P/A in all zones.

[c] For 60%/40% power split: top four blocks/bottom four blocks.

2.13.2.2. Flux and Power Distribution Analyses. One- and two-dimensional diffusion theory calculations were carried out to characterize the flux and power spatial distributions for the fresh loads and reloads and as a function of burnup. Output power data from these studies are used for stress analysis, fuel heatup, and fuel failure calculations, and the flux data are used for radiation damage studies. As part of this task, some efforts were made to improve the output edits of the two-dimensional code GAUGE to make it easier to relate the power peaking parameters to fuel rod power densities.

Radial Power Profile

The radial power profile attained for the initial core loading using the new three-zone radial loading scheme is compared in Fig. 2.13-2 with the profile using the previous four-zone scheme. As shown, for the unburned condition the reduced number of zones results in at most about 2% higher power peak-to-average values. The curves shown are for loadings optimized to minimize the peaking by equalizing the peaks in all radial zones; this would be the desired condition in the initial core and early reloads (the zoning calculation, using GASP, is done assuming a whole core loaded uniformly with the composition of the reload segment in question). For later reloads, it is found that an iterative search for the optimum radial power split and peaking may be required to reduce RPF/TILT parameters in subsequent GAUGE calculations.

Axial Power Zoning

Efforts continued to define and achieve optimum axial power splits and examine methods for deriving the required distributions of fuel materials. Included were analyses of power split changes with burnup and studies of sensitivity to representations of radial leakage. Typical fuel axial loading parameters (ratios of zone-average to core-average concentrations) are included in Table 2.13-3. All of the zoning analysis described here was done with the one-dimensional codes GASP and FEVER using seven-group cross sections.

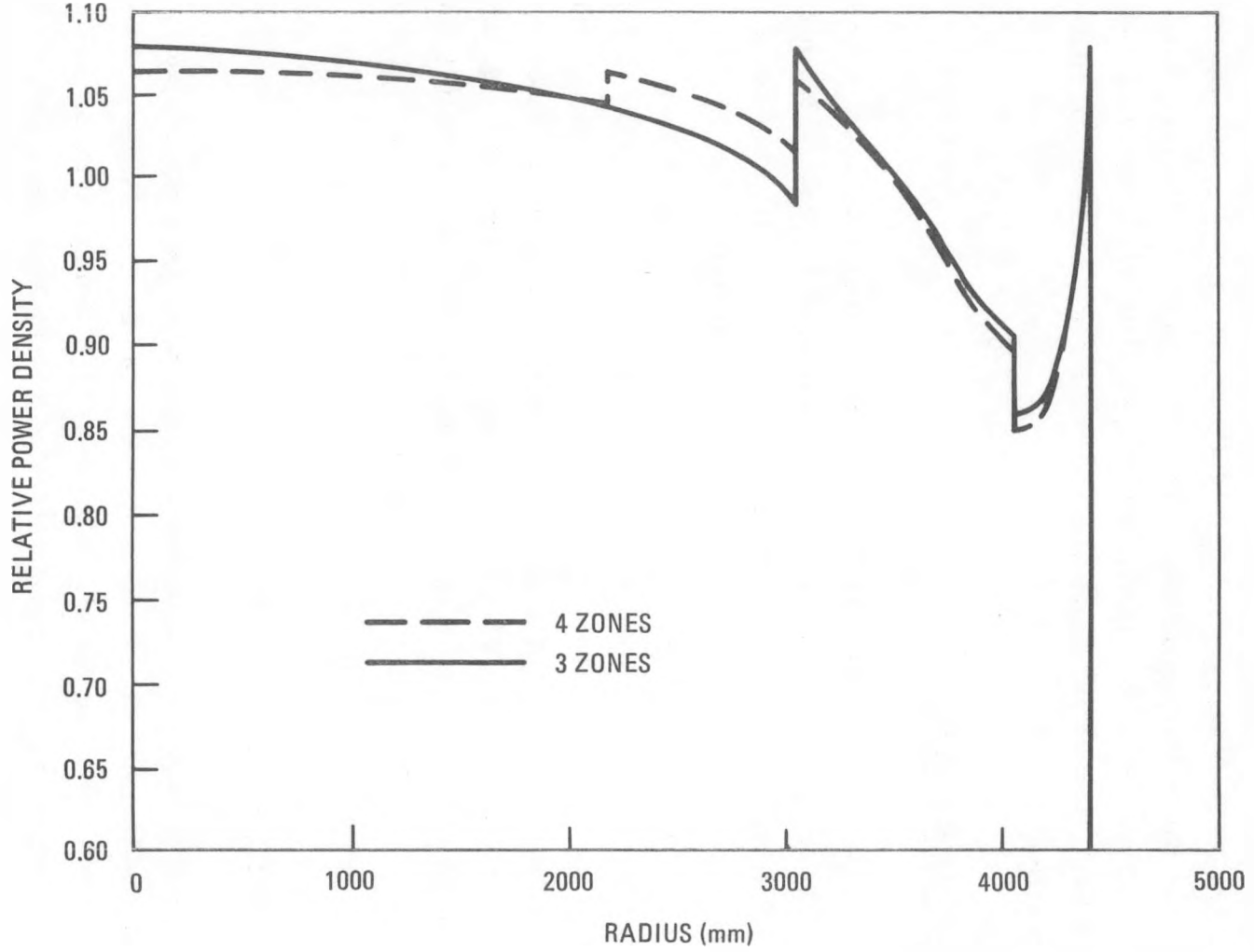

Fig. 2.13-2. 2240-MW(t) HTGR SC/C core radial power profiles (initial loading, C/Th = 375, C/U = 1124)

Results of calculations for differing top zone/bottom zone power splits are shown in Figs. 2-13-3 through 2.13-6. Figure 2.13-3 illustrates fuel rod packing fractions in the top zone as a function of the top zone power fraction. For the equilibrium reload, steeper axial power shapes, up to 66% in zone 1, are allowable without exceeding a packing limit of about 56% (to also include effects of radial zoning). Variations of unpoisoned reactivity parameters with power split are shown in Fig. 2.13-4. These data all assume the same axial average fuel composition. Figure 2.13-4 thus suggests that a reactivity decrement as introduced by the axial zoning of fuel (relative to the reactivity values from the zero-dimension GARGOYLE calculation from which the axial-averge composition is derived), with increasing decrement for sleeper zoning.

In Fig. 2.13-5, peak centerline fuel temperatures, derived using the various axial power profiles calculated for the zonal power splits, are plotted for the bottom of the two axial zones and for different radial power parameters. The 1.00/1.00 PPF/TILT combination represents the core-average-power fuel rod column with core average coolant flow. The 1.10/1.50 RPF/TILT combination represents a typical vertex of RPF/TILT envelopes as obtained in analyses at past HTGR designs. On this basis, minimizing the temperature over the full height, at the crossover points, reconfirms that the optimum power split is about 60% in the top zone and 40% in the bottom.

Results of burnup calculations in axial geometry, obtained using the FEVER code, are shown in Figs. 2.13-6 and 2.13-7, where the axial power profiles are plotted at successive time points. For both cases a given composition is burned for its designated lifetime, without reloading or mixing of new age segments. In Fig. 2.13-6, the axial average power density and the radial leakage parameters are kept constant, and reasonable stability of the axial power shape is obtained. To determine the real-life influence of fuel age, the Fig. 2.13-7 case was run with decreasing power density by year (to match the decreasing fuel density) and with adjustment by year of radial leakage parameters to represent the effects of newer fuel in surrounding

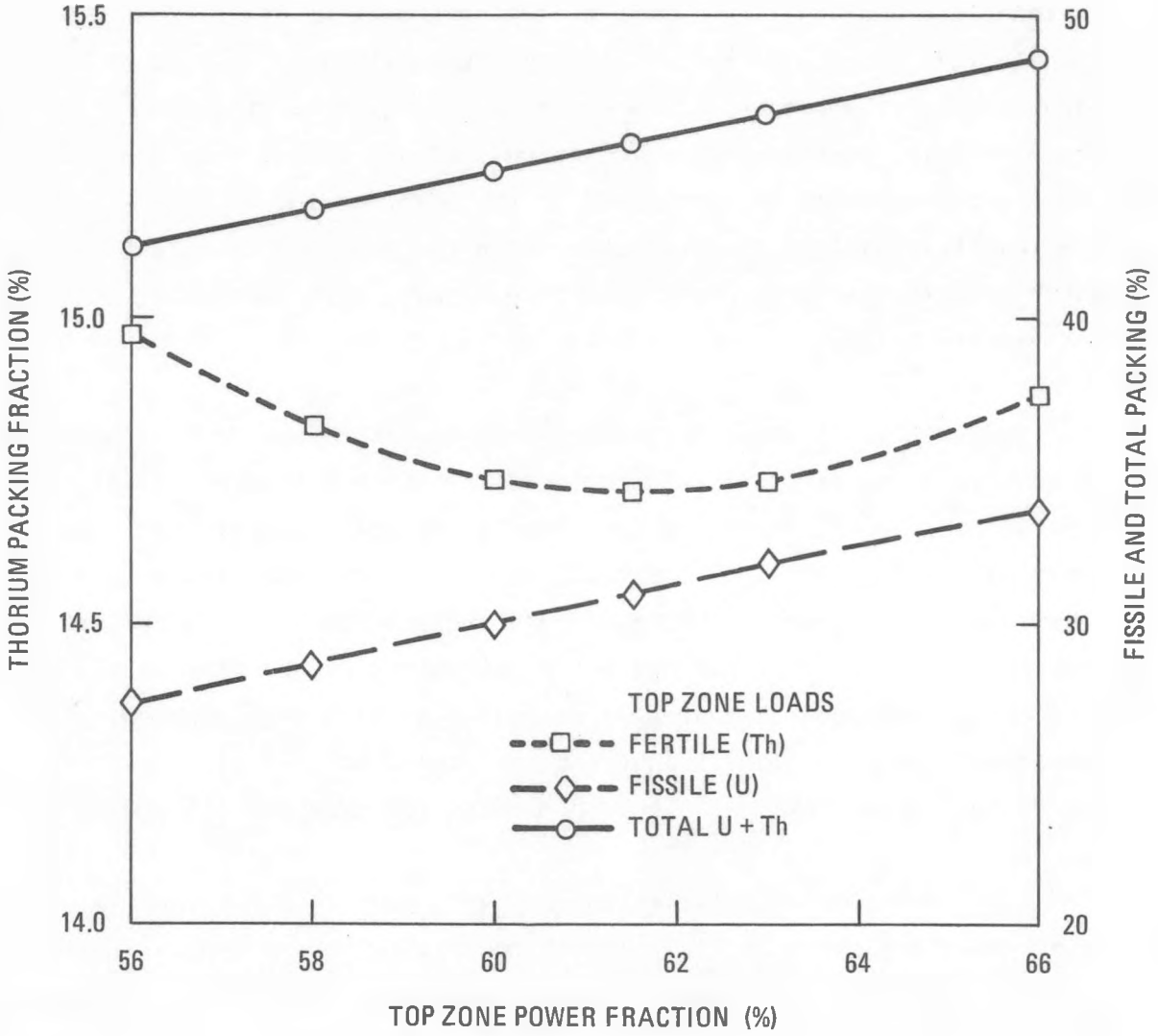

Fig. 2.13-3. Fuel rod loading versus power split for HTGR-SC/C core with nine-row elements (without radial zoning factors; equilibrium reload, C/Th = 607, C/U = 855)

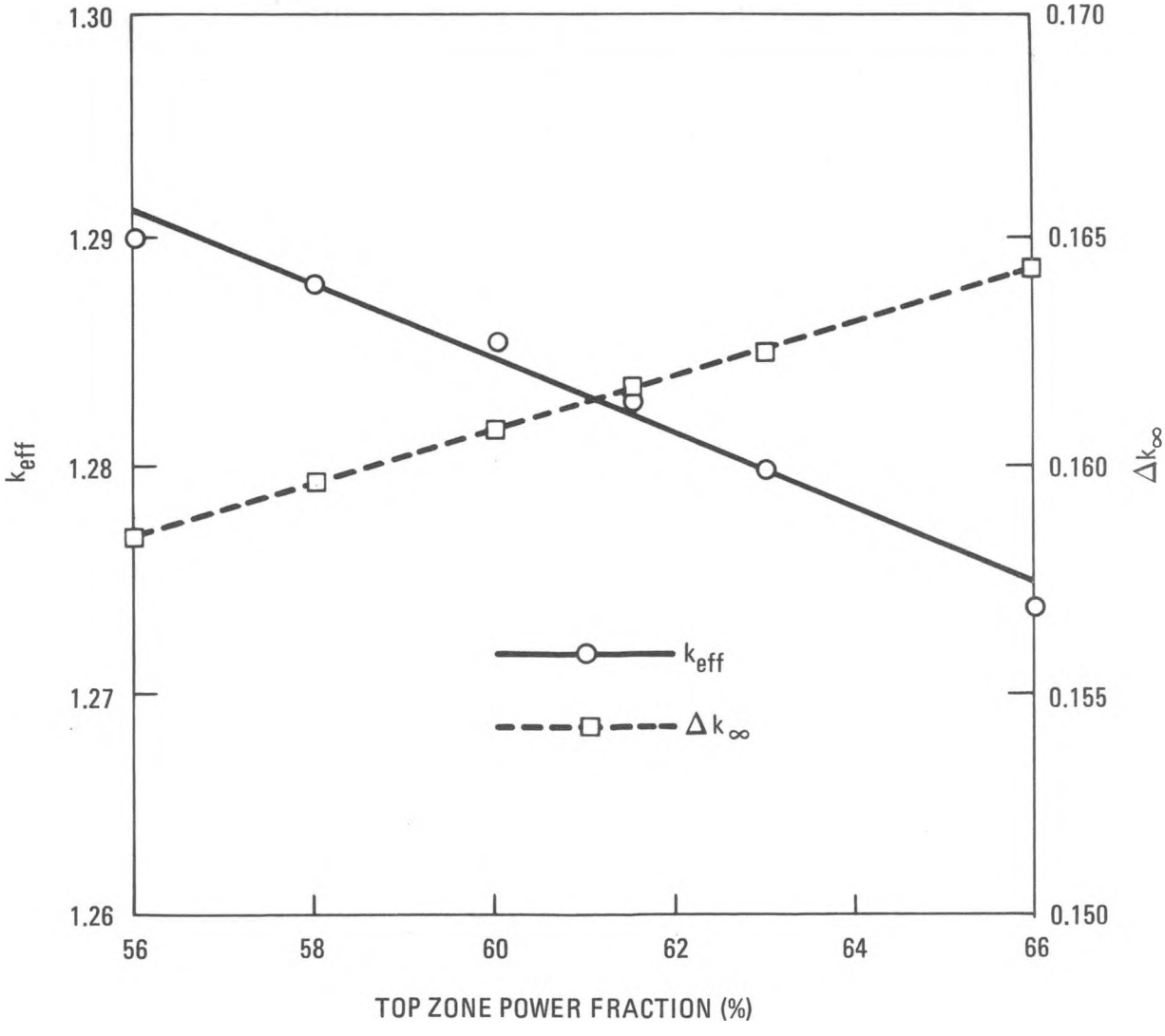

Fig. 2.13-4. HTGR-SC/C reactivity variations per axial zoning (equilibrium reload)

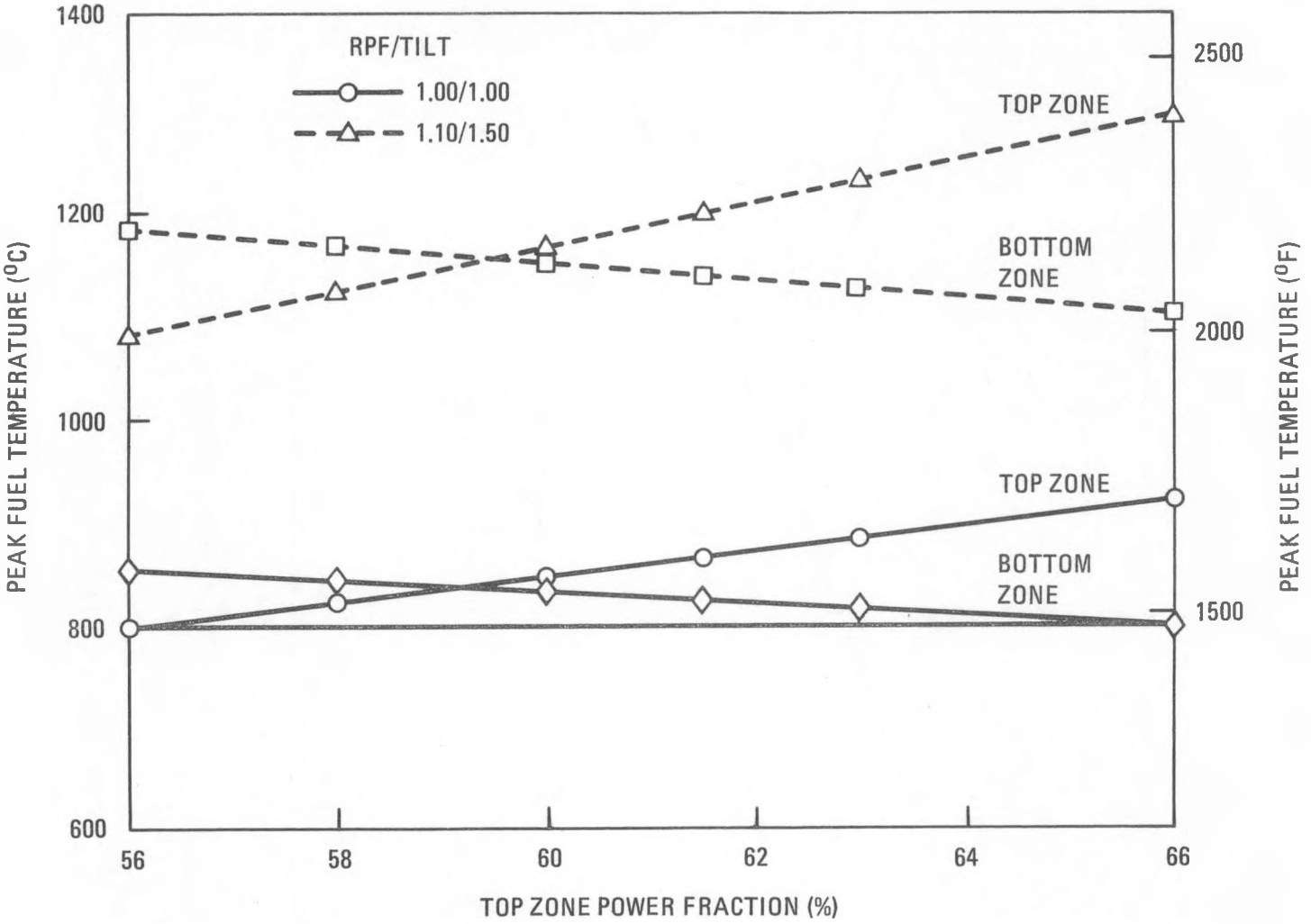

Fig. 2.13-5. Variations of fuel maximum temperature with axial power split

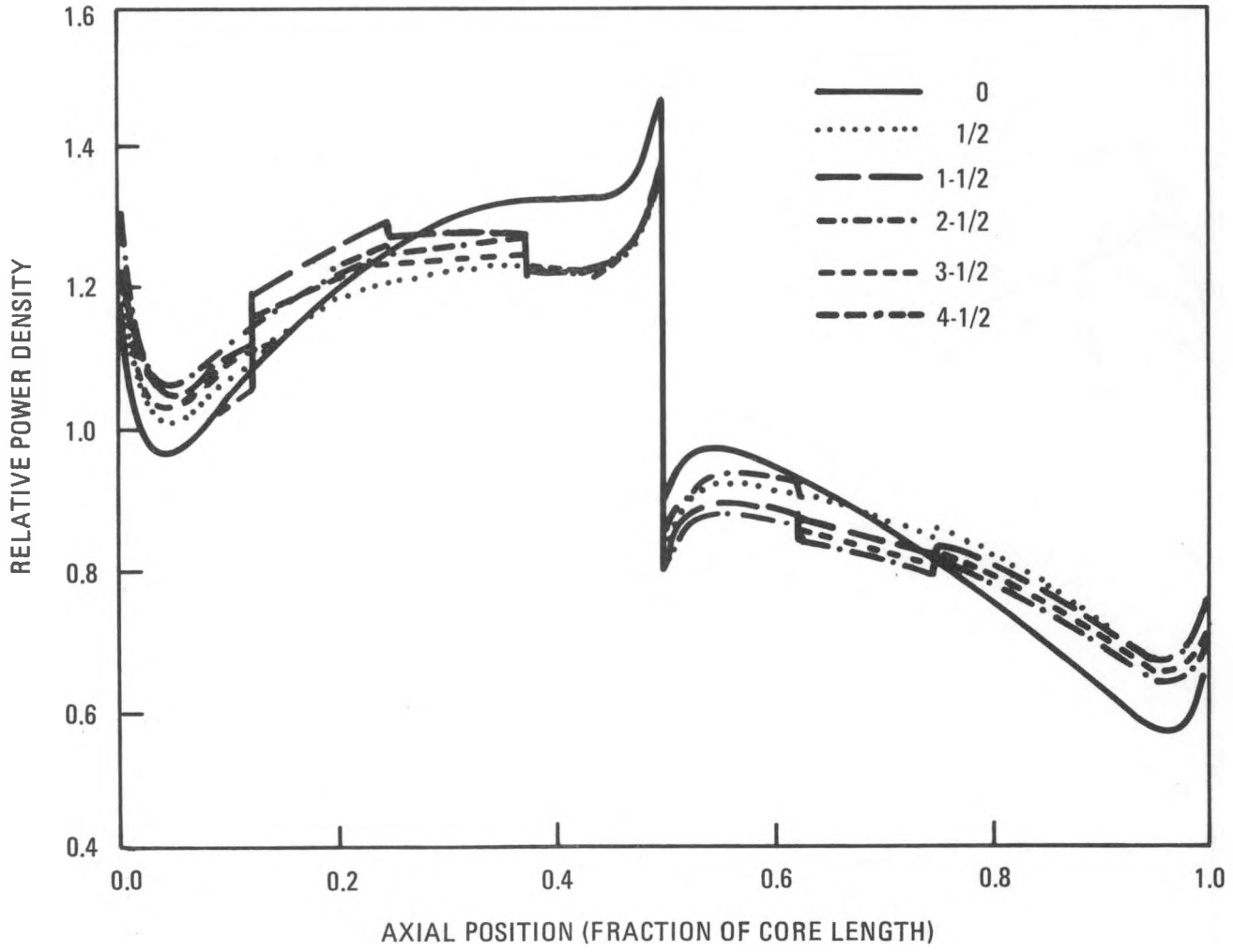

Fig. 2.13-6. 2240-MW(t) HTGR-SC/C core axial power profiles (initial load, without burnable poison)

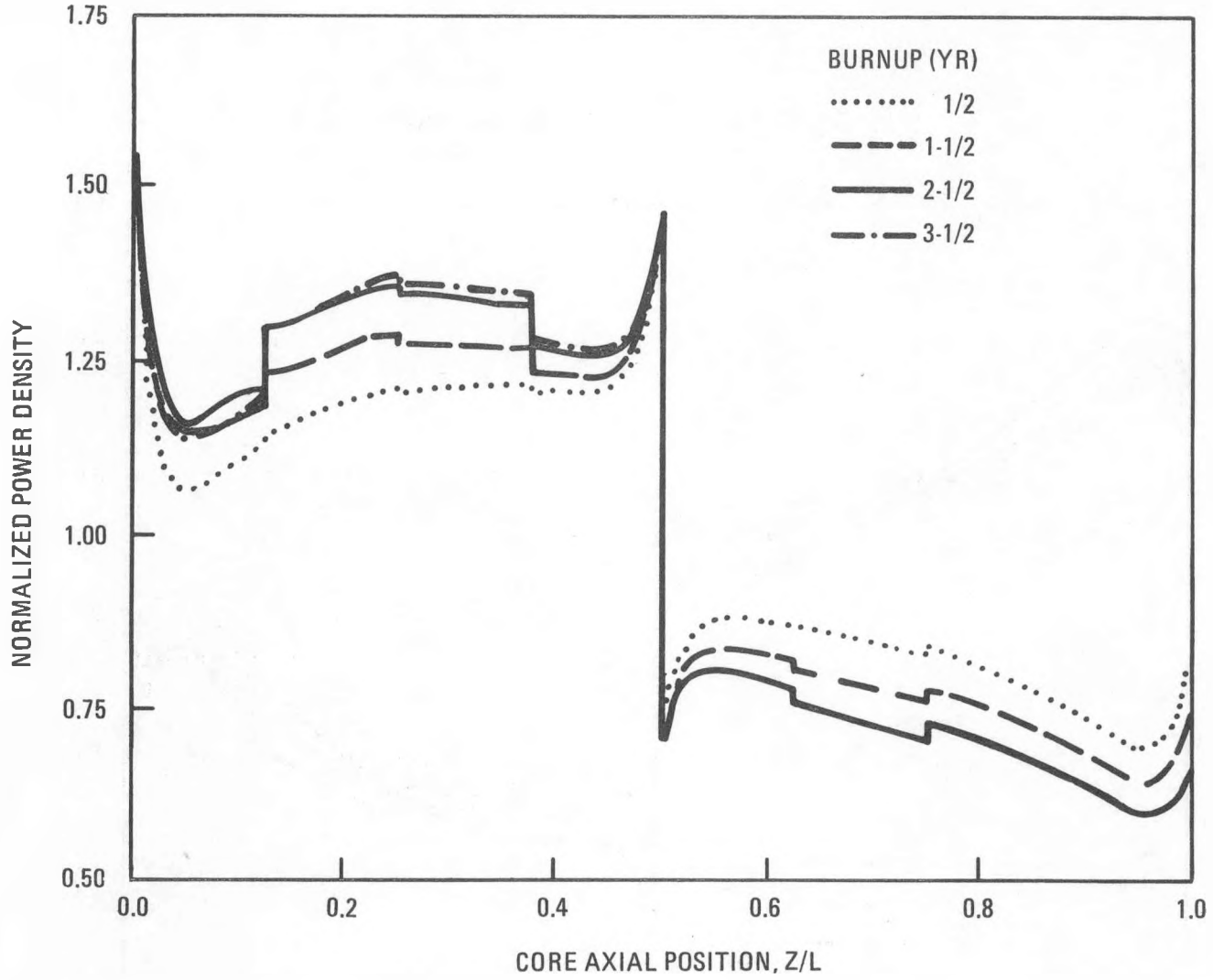

Fig. 2.13-7. 2240-MW(t) HTGR-SC/C burnup using age-dependent radial leakage (equilibrium reload)

reload segments. The power and leakage data were derived from GAUGE hexagonal geometry analyses. The plots in Fig. 2.13-7 reveal no detrimental impact on axial power stability due to the more rigorous power and leakage accounting.

Two-Dimensional Depletion Analysis

Calculations of flux and power distributions across the core as a function of burnup were carried out to provide data for stress analyses of the nine-row block in the 541-column layout. The two-dimensional, hexagonal geometry computer code GAUGE was employed for depletion of the initial core (time points 1 through 13, covering a 1.5-yr burnup plus a 14-day shutdown) and eight reloads (10 time points covering a 1.0-yr burnup plus a 14-day shutdown for each). Figure 2.13-1 shows the basic core mapping used to track the various reloadings of fuel columns, including the radial zoning where fuel concentrations are tailored to minimize radial power peaking. The depletions of fuel isotopes in the various columns were evaluated on a much finer grid than the segment/zone detail shown, with the 541 columns of the full core divided into 298 separate burnup regions, giving 102 burnup regions for the 2-rad (120°) sector of the calculational model.

The depletion calculations were carried out with nine separate GAUGE calculations, generating nine output tapes containing region power peaking values, point powers, neutron fluxes (four-group), compositions, and other details at each time point. The nine data tapes were then coalesced into one tape containing data for all 93 time points to be used as input to subsequent stress analysis and fuel performance calculations. An intermediate data processing code (TSORT) is used to combine the two-dimensional region power and flux histories with axial distributions of power and flux to synthesize three-dimensional mappings of power and flux. Since the power rod design and designated axial power split have not changed for the new nine-row block design, the axial power and flux profiles (normalized axial distributions) utilized were adopted from the TSORT prescription for the previous 2240-MW(t) core design using ten-row blocks.

Edits of GAUGE Results

Various editing codes are available to process the GAUGE-output power/flux tapes to provide tabulations and displays of performance parameters. From the GAUGE code, point powers (seven per hexagon), column powers, and region peaking factors (region power density/core power density) are provided, as well as peak tilts (maximum point power/region average and maximum column power/region average) at each time point.

Figure 2.13-8 shows a typical mapping of GAUGE core power distributions, in this case at near 1-yr burnup of the initial core (300 full-power days), indicating also the extent of power rod insertions at that point. The RPF value is the region-average to core-average power density ratio on a volumetric basis, and the TILT expresses the maximum-to-average power density ratio within the region (again on a volumetric, or "physics," basis).

Figure 2.13-9 displays the RPF/TILT combinations (on a physics basis) derived from editing the ouput power tape for all 93 time points. The solid line plotted in Fig. 2.13-9 is the RPF/TILT envelope with vertices at the maximum RPF or TILT values. Compared with envelopes from previous analysis for the 439-column HTGR-SC/C core using ten-row blocks, the current core design plus fuel cycle prescription yields a closer-in TILT boundary to give more favorable fuel temperature peaking.

The stress analysis for a block in the 2240-MW(t) HTGR-SC/C requires, as a first step, identifying likely candidates for maximum stresses. The criteria for determining worst cases are not well developed. As a result, some of the data are not provided in standard edits. To aid in these analyses, a new program was written that takes the GAUGE point powers for each time point and manipulates them to provide more information. The GAUGE code provides tilts and powers in physics terms (relative to column volume). For some of these calculations, engineering powers (relative to fuel volume) are more appropriate. A variety of edit options are available depending on the detail of point or TILT powers desired, up through maximum RPFs by region (four-, five-, or seven-column).

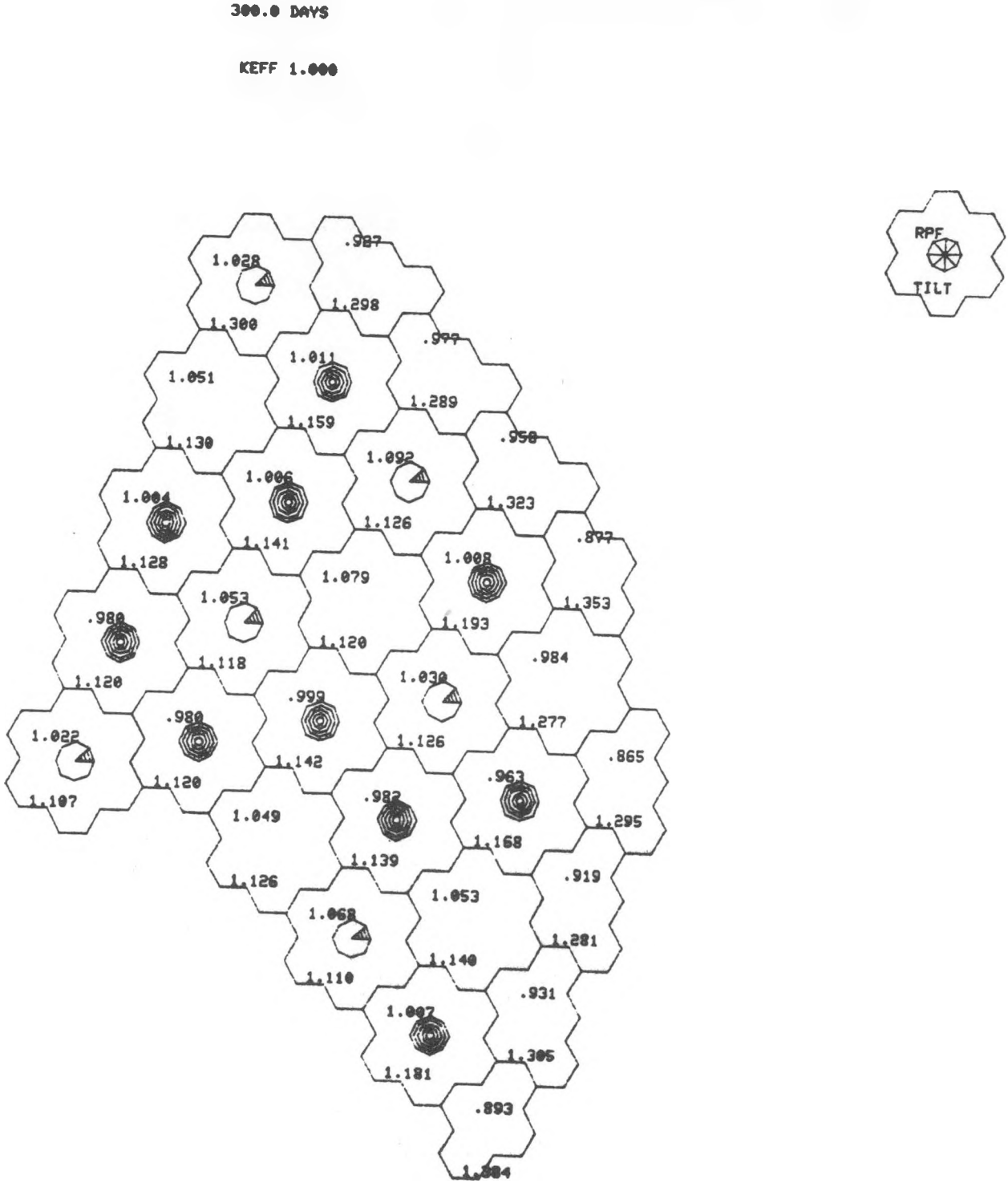

Fig. 2.13-8. Mapping of GAUGE power distribution for 2240-MW(t) HTGR-SC/C core

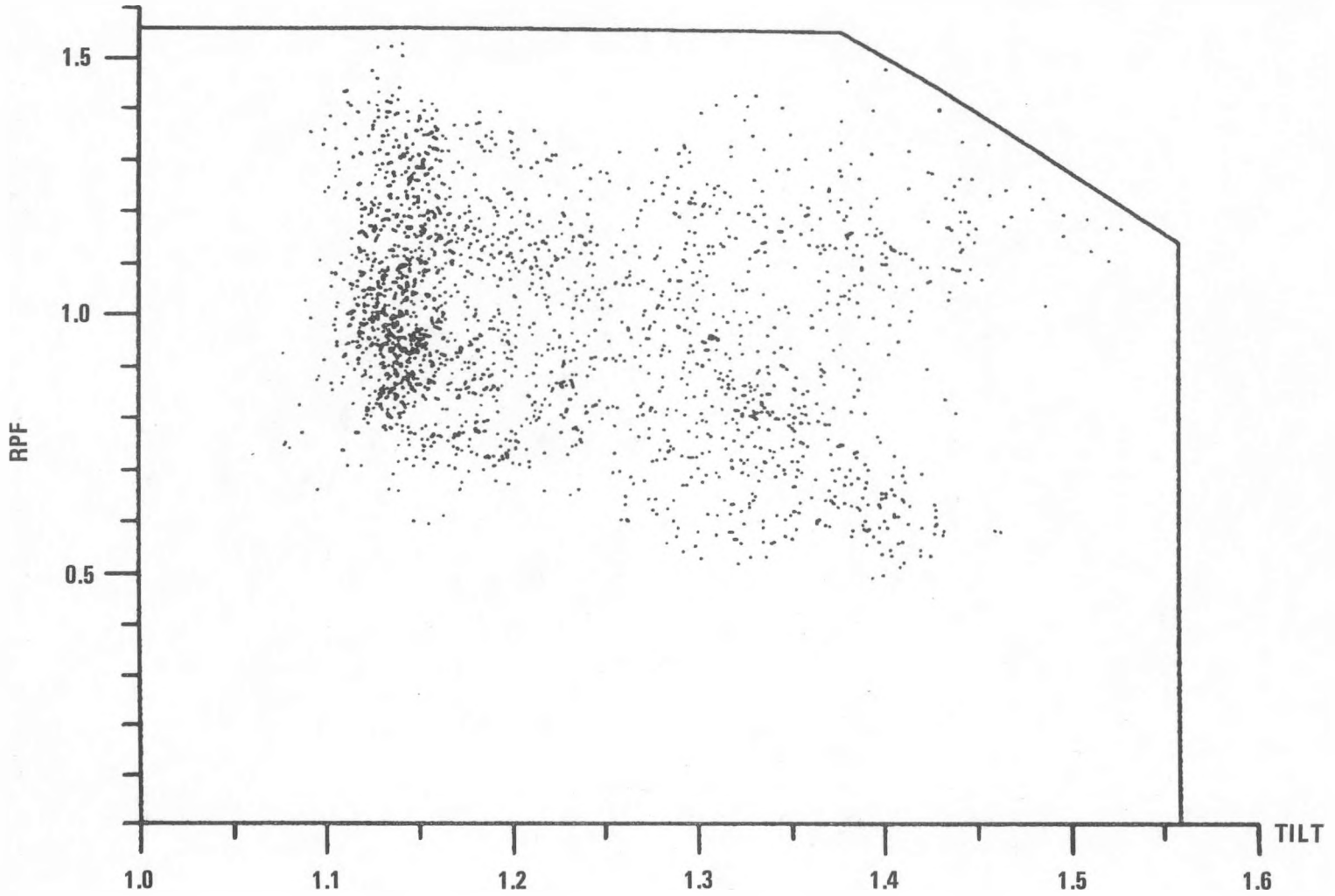

Fig. 2.13-9. RPF/TILT combinations (on a physics basis) derived from editing output power tape for all 93 time points

An example of the improved editing capabilities is shown in Fig. 2.13-10, where the RPF/TILT data for the initial core plus eight reloads are expressed on an "engineering" basis relating the power factors to the fuel volume. Thus, the figure gives the relative region-to-core average ratios of fuel rod power densities and within-region peak-to-average ratios of fuel rod powers (for the axially averaged assumptions).

Fuel Temperature Isotherms

A representative axial power distribution, with a 60%/40% top/bottom zone power split, was used in the thermal/flow code BACH to generate fuel axial temperature distributions for a variety of RPF/TILT combinations. The input data to BACH prescribed the fuel and coolant hole details and quantities in the 541 columns of nine-row blocks and total coolant flow to yield 717°C (1322°F) core outlet helium for a 318°C (604°F) inlet temperature and 2240-MW(t) power generation. Isotherms for the maximum axial temperatures were derived from the BACH edits, giving RPF/TILT combinations for specific peak temperature values. Figure 2.13-11 shows the isotherm plots for peak fuel centerline temperatures of 1100°, 1150°, 1200°, 1250°, and 1300°C (2012°, 2102°, 2192°, 2282°, and 2372°F). Included in this graph is the engineering RPF/TILT envelope generated by the above-cited GAUGE analysis; the sections of the envelope cut off by the various isotherms indicate the extent of fuel temperature peaking above the isotherm temperatures, as the envelope relates to true axial-average fuel rod power ratings (RPF x TILT) for specific coolant flow rates (proportional to RPF). Comparison of the plots in Fig. 2.13-11 with the RPF/point data in Fig. 2.13-10 indicates that fuel temperatures do not exceed 1200°C (2192°F) except for one isolated instance at the RPF/TILT vertex of 1.58/1.41.

The isotherm curves in Fig. 2.13-11 appear to be disjointed. This is because for each temperature value there are actually two intersecting curves, the upper curve representing peak fuel temperatures at the bottom of the top axial zone and the bottom curve the fuel temperatures at the bottom

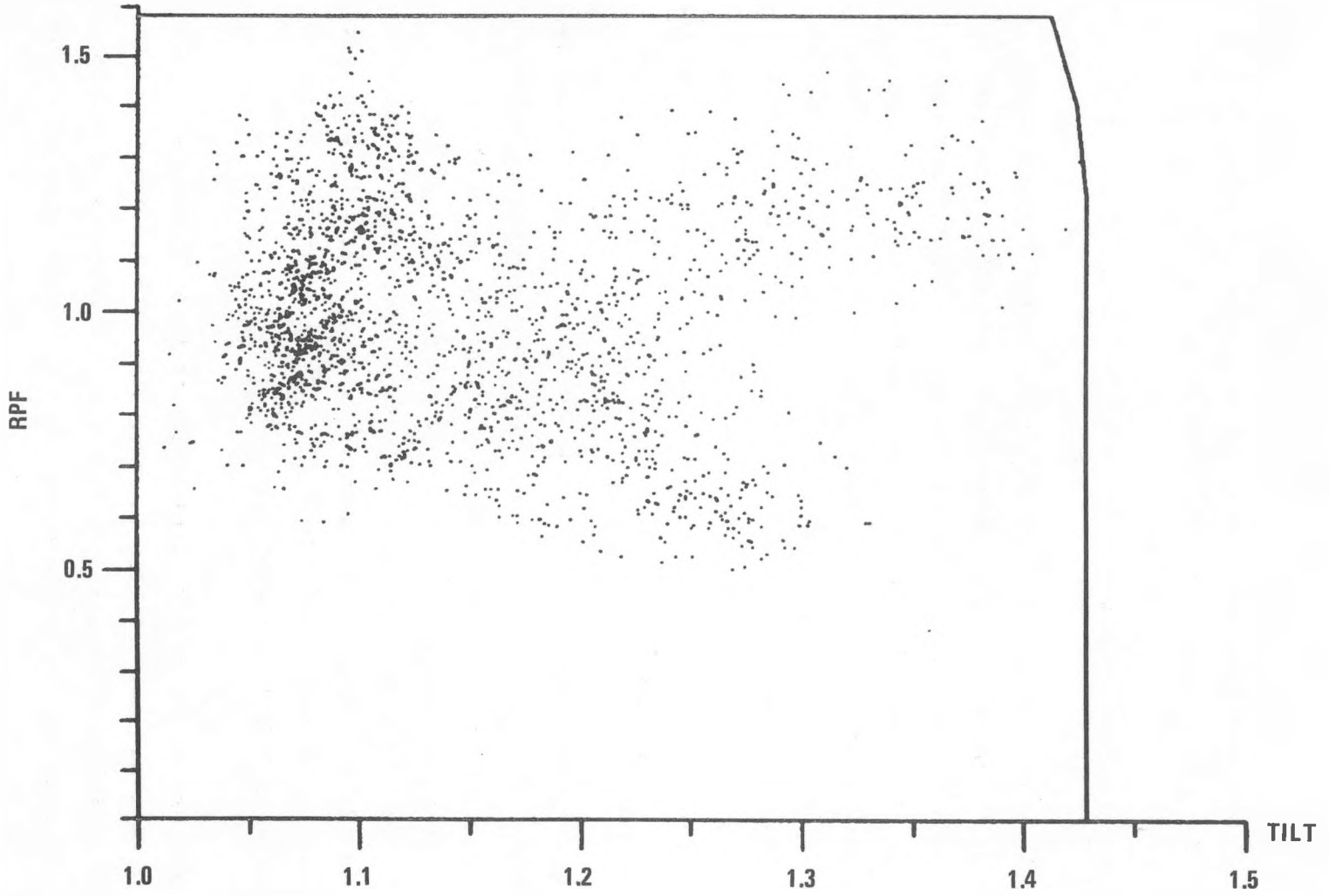

Fig. 2.13-10. RPF/TILT data for initial core plus eight reloads expressed on an engineering basis

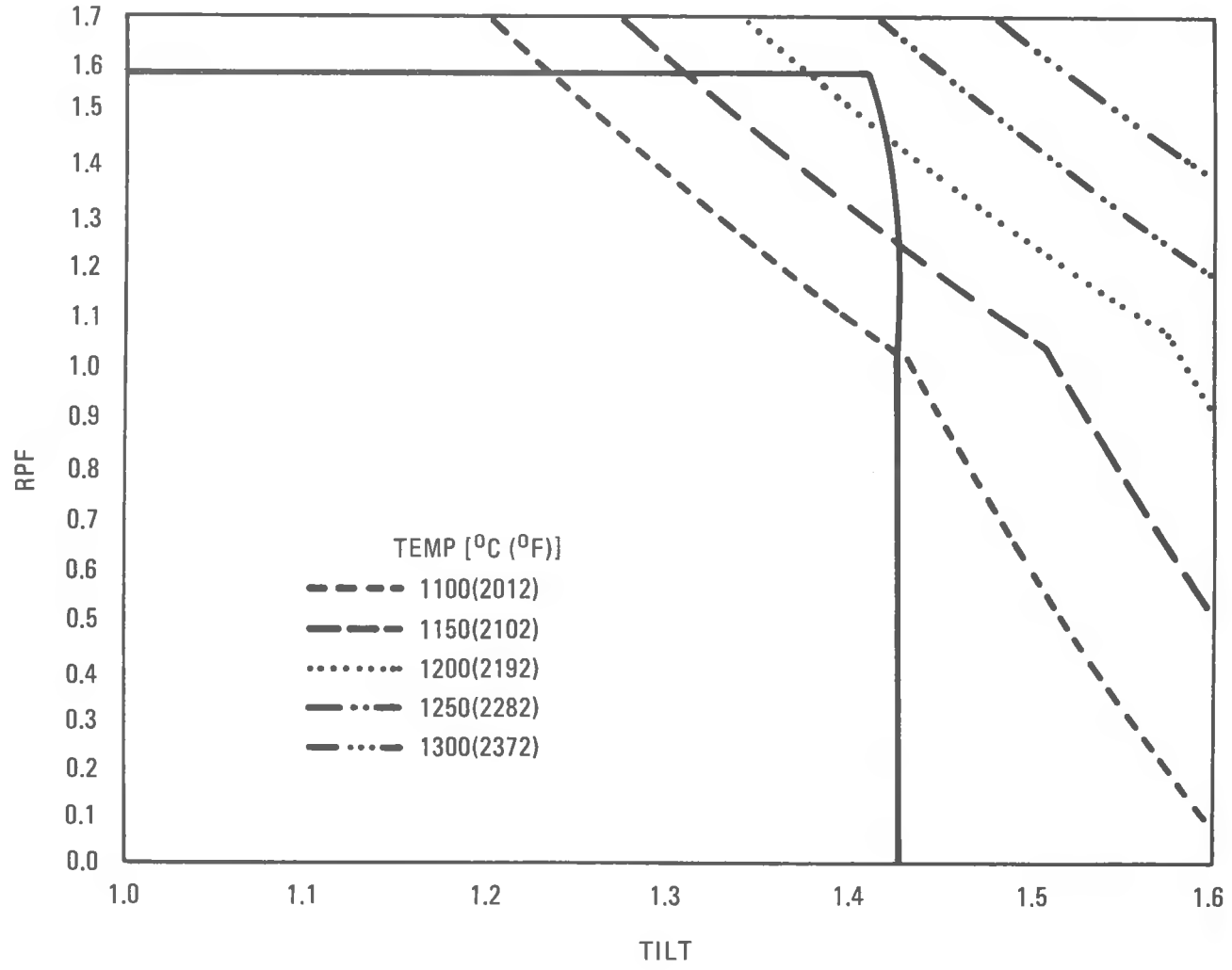

Fig. 2.13-11. Fuel isotherms for 2240-MW(t) HTGR-SC/C core for 60/40% axial power split (per-pin power flow basis), engineering RPF/TILT envelope

of the core. Decreasing the top zone power fraction would move the upper sections to the right while pulling the bottom sections into lower TILT values.

This BACH-generated analysis is a preliminary assessment of expected fuel temperature performance in the new 2240-MW(t) core design, and the more extensive fuel performance calculations will include the effects of control rod insertions on axial power shapes. Also, the BACH code has not yet been revised to account for coolant crossflow effects in the block-end plenums of the flanged-block design, and the bypass flow/bypass heat fractions for the envisioned flow stabilization schemes are not known.

2.13.2.3. 2DB Model for Calculating Fine-Mesh Region Power Distributions. Specifications were developed for a 2DB (Ref. 2.13-2) for obtaining time histories of the flux and power distributions in individual fuel columns on a much finer mesh than is available from the GAUGE code. The flux and power distributions can be used to compute temperatures and fluences for stress analysis. Using 384 mesh triangles per hexagonal column provides sufficient detail to represent explicitly the graphite sealing flange of the new block design and to represent inserted power rods. The model is general and can be adapted to study any hexagonal column of interest in the core.

Several test problems were run based on the reference GAUGE calculations for the 2240-MW(t) HTGR-SC/C with the new nine-row block design (541-column core).

Geometrical Model

The 2DB model of a single seven-column region is shown in Fig. 2.13-12. It consists of 48 rows of 79 mesh triangles each, giving 15 mesh triangles per hexagonal block side and 3792 total mesh points. The length of a mesh triangle side is 26.089 mm (1.02 in.) and 2DB calculates fluxes for the center points of the triangles. This mesh scheme permits a good representation of the graphite flange around the edge of the blocks and also allows a

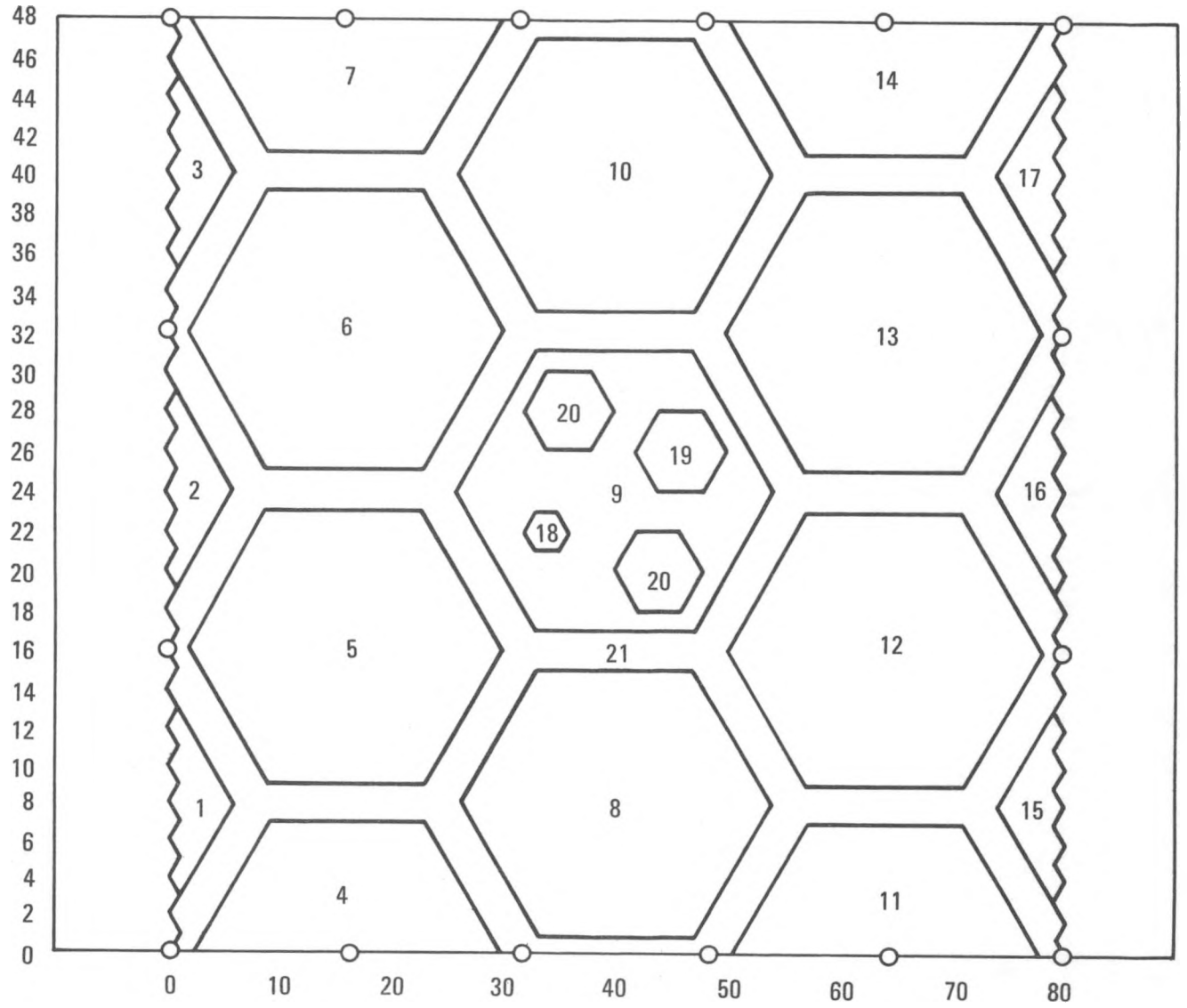

Fig. 2.13-12. Mesh and region layout for 2DB model

reasonable description of the various control rod holes. The actual areas and the areas in the 2DB model are as follows:

Hole	Actual Area (mm^2)	2DB Area (mm^2)	Percent Difference
Control rod	8107.313	7073.168	14.6
Reserve shutdown system (RSS)	7125.568	7073.168	0.7
Power Rod	1696.911	1768.2	4.2

Explicit representation of fuel rods could be done if a smaller total area were used in the models. However, diffusion theory does not adequately represent the variations in flux between fuel rods and graphite, so nothing would be gained from this level of detail. Also, one mesh point in the graphite flange will not adequately represent the flux peaking there, but this peaking has been studied (Ref. 2.13-2) and shown not to be substantial. The main objective in representing the flanges and various holes explicitly is to locate the power generation in the block areas where it is concentrated.

Although Fig. 2.13-1 shows the central column as the control column, it is relatively simple to shift the control rod holes to any other column to place a standard block at the center of the model. For maximum flexibility, each column and partial column in the model constitutes a separate load zone with its own atom density specification. This facilitates making any column a fuel or reflector element as desired.

Boundary Conditions

The 2DB calculation is run as a boundary source problem with boundary fluxes taken from GAUGE. The boundary points in the 2DB picture at which GAUGE fluxes are available are circled in Fig. 2.13-12. Boundary fluxes for other boundary points, obtained by interpolation between the nearest GAUGE

values, are somewhat approximate. Thus, boundaries should not be located too close to the column of interest, and the block to be studied should be located in the central position of the model.

Representation of Control Rods and Channels

Throughout an operating cycle, the control rods will be withdrawn and the power rods will be present for perhaps one year out of four. The zones that represent the control rods and the RSS hole will therefore be voids, while the zone representing the power rod may be void or control poison. Since neither voids nor black absorbers are treated accurately by diffusion theory and 2DB does not allow internal boundary conditions, some approximate representations are required.

For voids, the effect of axial leakage can be represented by using a fictitious diffusion coefficient in the void region given by

$$D_{void} = 2\left(D_o + \frac{r}{3} - \frac{\pi B r^2}{8}\right) \quad , \tag{2.13-1}$$

where D_o is the diffusion coefficient in the surrounding region and

$$B = \frac{\pi}{H + 2\lambda} \quad ,$$

where H is the core height, λ is the extrapolation height (= 2.13 D_o), and r is the radius of the void.

For an inserted power rod modeled by six mesh triangles, a fictitious diffusion coefficient can be adapted as given by

$$D_{rod} = \frac{\frac{1}{12\sqrt{3}} \frac{D_o J}{\phi_o}}{\left(D_o - \frac{1}{12\sqrt{3}} \frac{J}{\phi_o}\right)} \quad , \tag{2.13-2}$$

where the current-to-flux ratio, J/ϕ, is derived from transport theory cell calculations modeling the rod environment. If this formula leads to negative D_{rod} values, an alternative, less accurate approximation can be used:

$$D_{rod} = \frac{1}{12\sqrt{3}} \frac{J}{\phi_B} \quad . \tag{2.13-3}$$

Here the current-to-flux ratio is evaluated on the rod boundary in the cell calculation.

Partially inserted rods present a 2DB modeling problem. In GAUGE, partial tial insertions are simulated using a fraction of the atom density for fully inserted rods; boundary fluxes from GAUGE corresponds to this axially averaged composition. In 2DB, however, it will generally be desired to represent the rod, if present, explicitly since this is one of the justifications for the fine mesh calculation. If a particular block in the column is selected for study, it is no problem to represent the exact time history of control rod insertion and withdrawal by the appropriate fictitious diffusion coefficients for the rod or void. However, a particular block will, in general, have a fuel loading that is different from the axially homogenized GAUGE values, and hence the GAUGE boundary fluxes will not be accurate for that composition.

There is thus no completely consistent way to represent partially rodded columns. However, if the duration of partial insertion is relatively short, these inconsistencies may be acceptable. The sensitivity of stress results to approximations in the representation of flux levels, flux gradients, and fluences should be studied to resolve this question.

Region Compositions for 2DB Model

The atom densities for fuel regions of the columns in 2DB are taken from the corresponding columns in the GAUGE problem, but are densified to

account for explicitly representing the graphite flange and the control holes. The fueled volume fractions in the 2DB columns are 0.7656 for standard columns and 0.5628 for control columns, and the GAUGE densities divided by these fractions yield the 2DB fuel region densities for heavy metals and fission products. For graphite, the flange area density is 0.08217, and the carbon density in the fuel region varies with fuel loadings.

Cross Sections and Burnup Data

The four-group cross section library, burnup chain data, and shielding factor data were taken directly from the GAUGE run for the reference 2240-MW(t) HTGR-SC/C design. Since 2DB does not handle two-dimensional shielding factor tables, the GAUGE table for Pu-240 was simply deleted in 2DB. Also, the tables for U-238 were replaced by a polynomial function of the U-238 atom density, determined by running a series of MICROX calculations for various U-238 concentrations in the fuel rod.

For the purpose of this study, it was not necessary to include concentration-dependent cross-section shielding functions for all of the heavy nuclides as was done in GAUGE; use of appropriate resonance-shielded data for U-238 and thorium only, plus shielding functions for burnable poison, would have sufficed. However, full sets of shielding functions were used in the 2DB test cases to facilitate comparisons with GAUGE and verify proper operation of 2DB.

Test Problem 1

Two initial problems were simply cases to test the 2DB model, without input GAUGE fluxes. In Problem 1, a uniform fuel composition corresponding to the initial core of the reference design was assumed in all columns and the representation of control rod holes was omitted. An eigenvalue calculation was done with flat flux boundary conditions. The result would be

expected to agree reasonably well with the zero-dimensional GARGOYLE calculation done for the reference core, except for the effects of the following differences:

1. GARGOYLE used a nine-group cross-section library of different origin than the four-group GAUGE library used in 2DB.

2. The graphite/fuel ratio is not conserved in the 2DB model for this case since the boundary hexagonal columns (zones 1, 2, 3, 15, 16, and 17) have a disproportionate amount of the graphite flange represented in the model.

3. The differences in shielding functions referred to above for U-238 and Pu-240 result in different cross sections for these nuclides.

Figure 2.13-13 compares the reactivity behavior with burnup from 2DB Problem 1 with that of the GARGOYLE calculation. Considering the differences cited above, satisfactory agreement is seen.

Test Problem 2

In the second test problem, the control rod, RSS, and power rod holes in the central column were represented with a fictitious diffusion coefficient. Since the formula in Eq. 2.13-1 refers to a single hole at the center of a cell, all four holes in the control column were combined into a single hole of equivalent area. The values of D computed for this hole were then used in the actual holes in the 2DB model. It should be noted that this approximation for D was intended to reproduce axial leakage in an R-Z geometry calculation; in the present case, axial leakage is not accounted for. The results for Problem 2 showed only small increases in calculated k_{eff}, relative to Problem 1, owing to the fictitious diffusion coefficients.

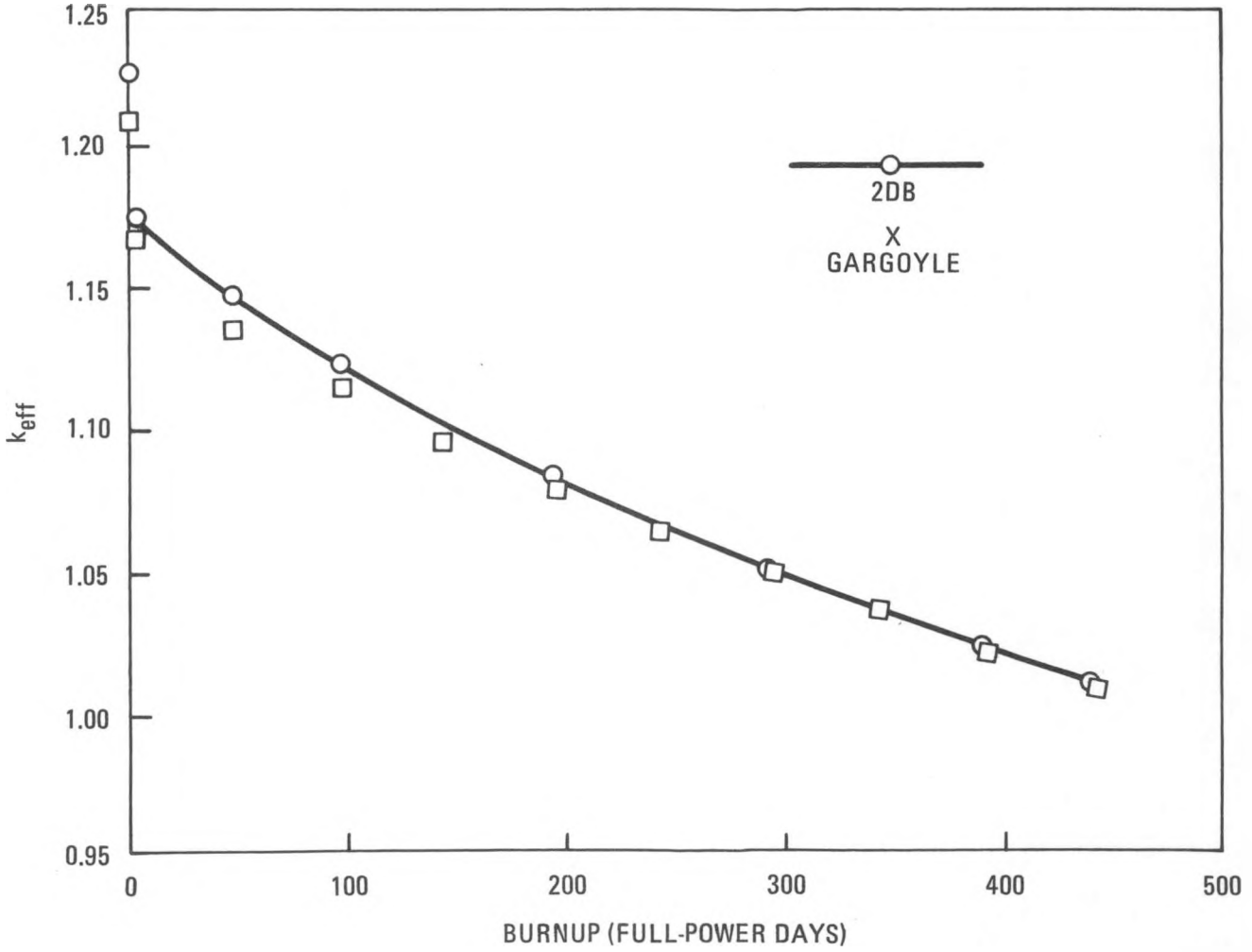

Fig. 2.13-13. Comparison of four-group 2DB and nine-group GARGOYLE burnup histories for 2240-MW(t) HTGR-SC/C initial core

GAUGE-Region Simulation Cases

Subsequent 2DB problems used the actual compositions of a selected region of the GAUGE calculation. The selected region, shown in Fig. 2.13-14, is number 25 on a partial core numbering basis or number 64 on a whole core numbering basis.

A boundary flux file was made containing data from all 93 time points of the GAUGE calculation. The initial core atom densities for region 25 and for the surrounding columns in the 2DB model were input to the 2DB calculation. The 2DB core was then run as a burnup problem for several time steps corresponding to GAUGE time steps, and at each step a new set of boundary fluxes was input from the GAUGE-output flux file. The 2DB power and flux results were saved on tape for subsequent thermal stress calculations or for use as a restart tape to continue the 2DB calculations.

Figures 2.13-15 and 2.13-16 compare the GAUGE and 2DB fluxes for groups 1 and 4, respectively, of the four-group energy structure. The boundary fluxes are the same for both codes, confirming the correct operation of the EDIT/GAUGE and 2DB codes. At internal points, two 2DB mesh triangles are adjacent to each GAUGE mesh point, and flux values are given above and below the corresponding GAUGE flux. Perfect agreement is not expected here, of course, since the 2DB model is more detailed and represents the graphite sealing flange explicitly. Except at the hexagonal block centers, all internal points are in the graphite flange region.

Figures 2.13-17 and 2.13-18 show the group-1 and group-4 fluxes along a traverse of the 2DB map (row 25). The closest GAUGE flux values are also plotted. The uneven nature of the 2DB fluxes is a consequence of the 2DB methodology, where the center of adjacent triangles do not lie on the same horizontal line (the center of a downward-pointing triangle is higher than that of an upward-pointing triangle). This aspect of the model must be considered in any subsequent codes that use the 2DB flux results for temperature or stress calculations.

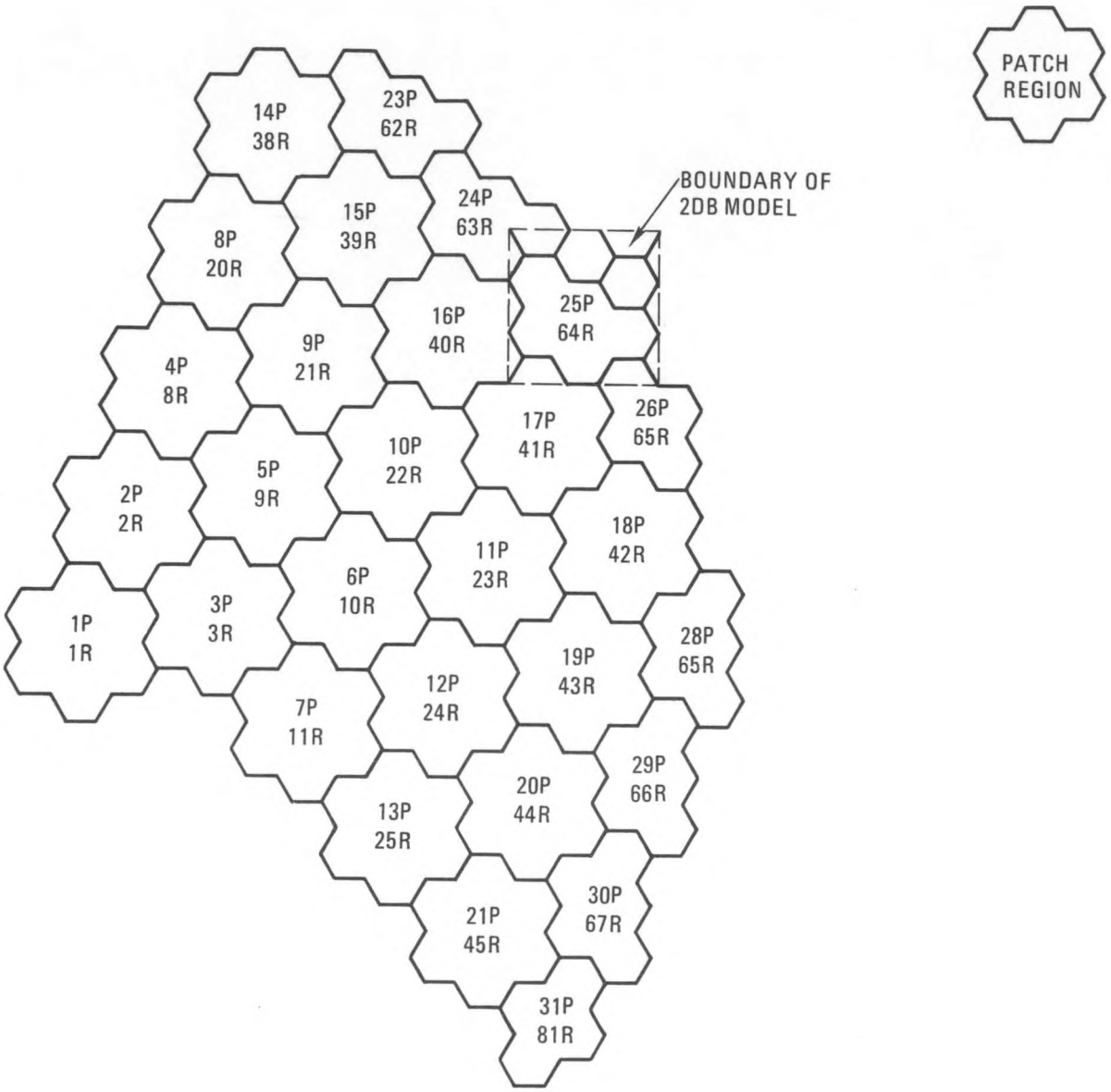

Fig. 2.13-14. Region of GAUGE calculation used for 2DB tests

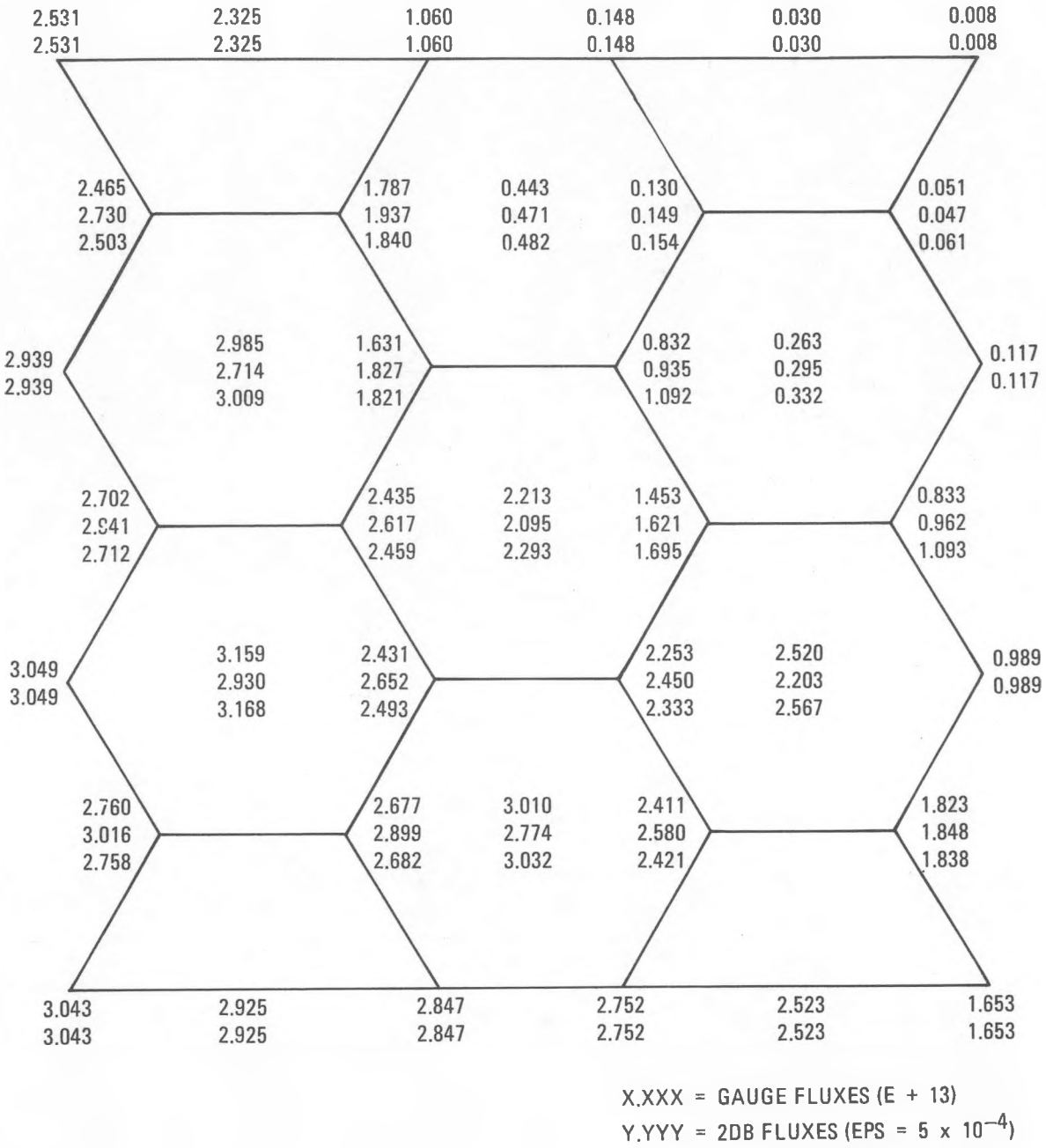

Fig. 2.13-15. Comparison of 2DB and GAUGE group-1 flux distributions

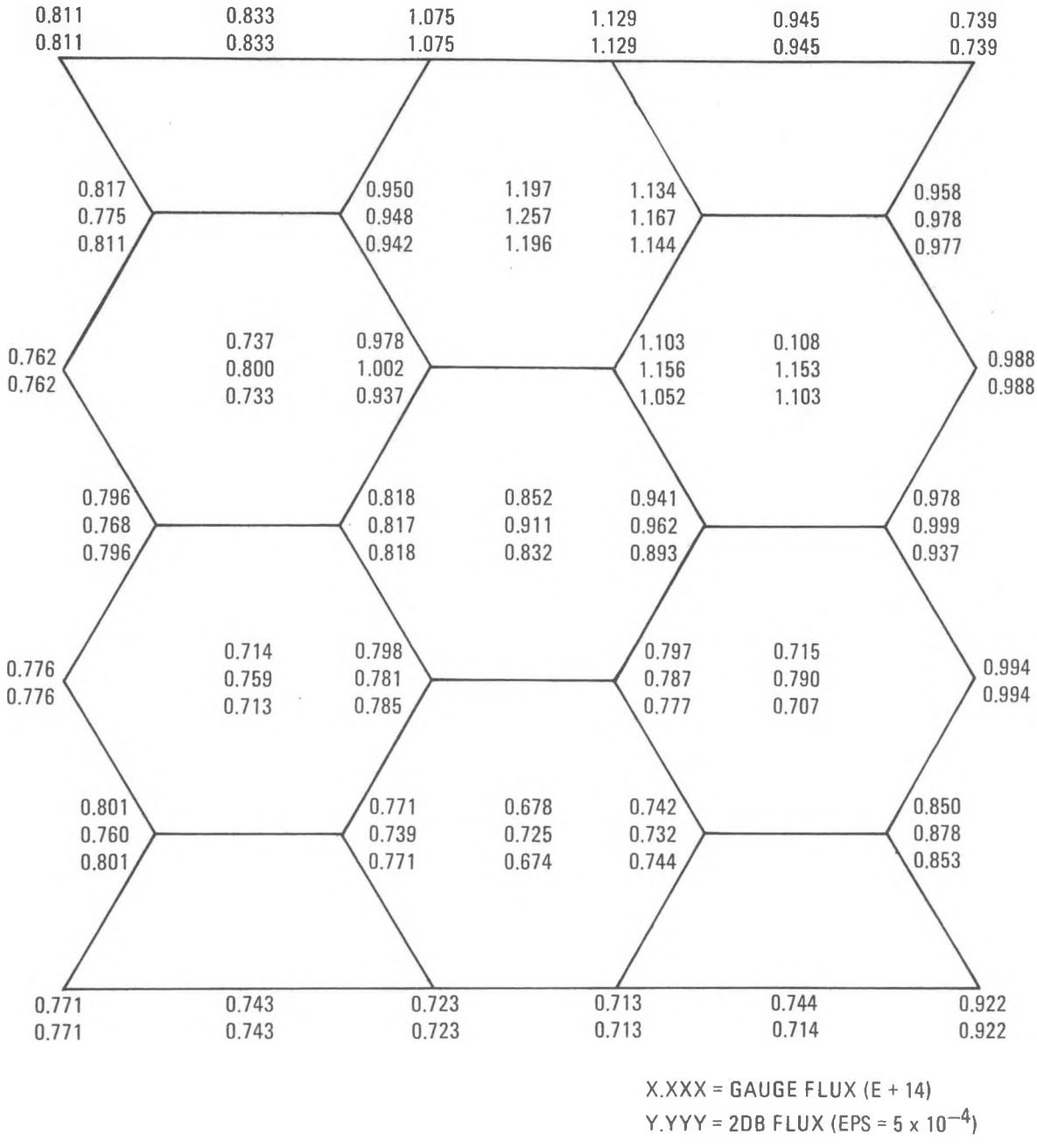

Fig. 2.13-16. Comparison of 2DB and GAUGE group-4 flux distributions

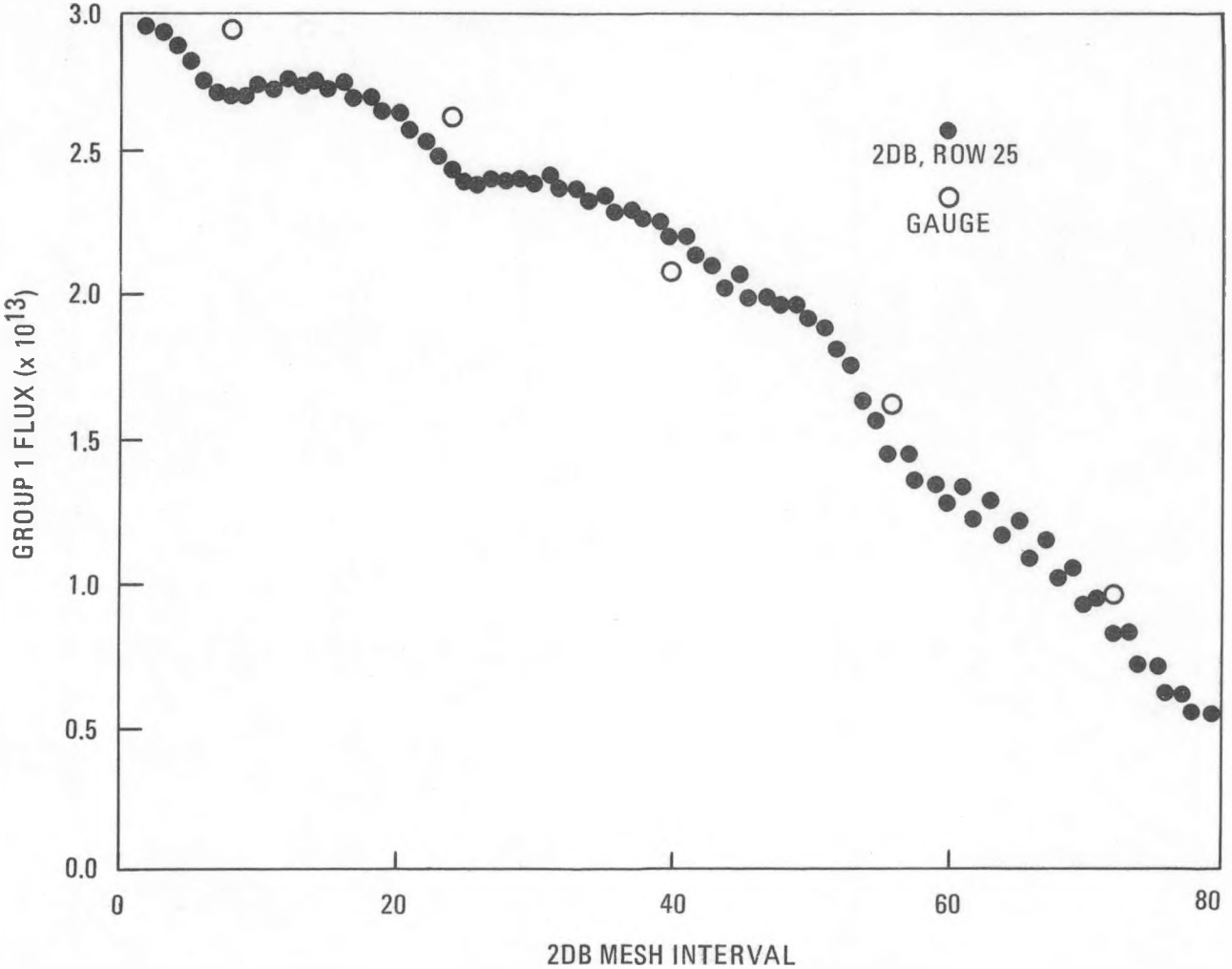

Fig. 2.13-17. Comparison of 2DB and GAUGE group 1 fluxes along traverse of 2DB map

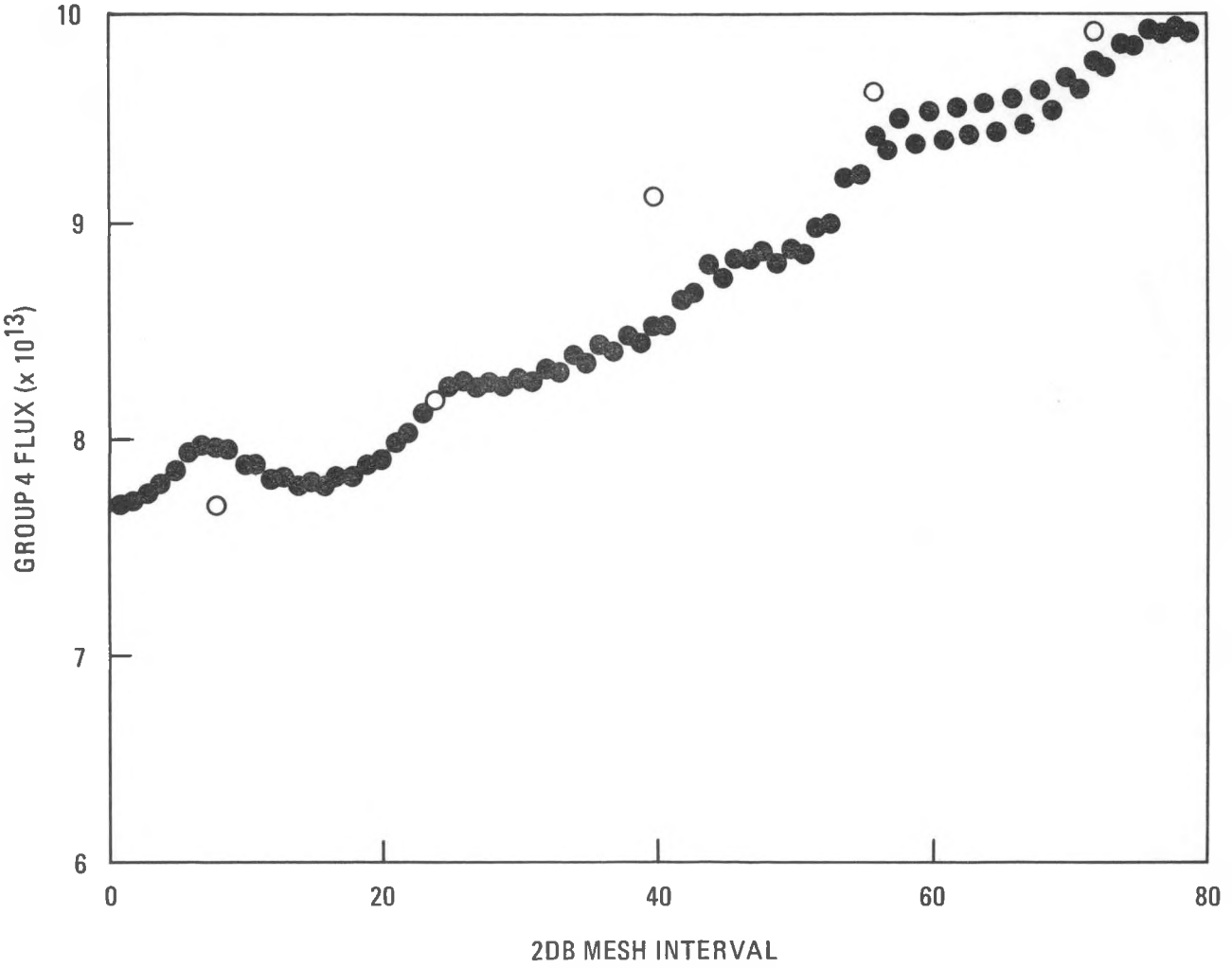

Fig. 2.13-18. Comparison of 2DB and GAUGE group 4 fluxes along traverse of 2DB map

The results in Fig. 2.13-15 through 2.13-18 were obtained by running the 2DB case with a convergence criterion (EPS) of 5×10^{-4}. Since the code running time is significant, a second run was made with EPS = 5×10^{-3}. The difference in fluxes with the two convergence criteria was on the order of 1% to 4%. It appears that the lower degree of convergence may be satisfactory, but this tentative conclusion should be reviewed if a problem with an inserted power rod is considered.

An additional test problem was then performed to confirm the feasibility of restarting 2DB from the flux tape. The test problem described above was restarted successfully at time point 3, taking boundary fluxes from the EDIT/GAUGE file and interior fluxes and atom densities from the 2DB output tape. A minor problem is encountered wherein unnecessary reiterations are carried out with the input, already converged flux solutions.

A satisfactory test was also made of the capability to change atom densities at any time point to simulate reloading of fuel. Although a calculation will normally consider the burnup behavior of one region over its time in the reactor, parts of adjacent regions are included in the model which may be reloaded with fresh fuel during the life of the region under study. The reload option can also be used to simulate the insertion or removal of control poison.

It is concluded that the 2DB options needed for the projected detailed stress studies are in reasonable working order.

2.13.2.4. Fuel Performance Analysis.

HTGR -SC/C Reference 0 Core Thermal Analysis

The original purpose of this task was to evaluate the thermal and fuel performance (including fuel particle failure and fission product release) for the new reference core design for the 2240-MW(t) HTGR-SC/C. This new design incorporates 541 columns with the new nine-row flanged fuel blocks

having graphite sleeves at the top and bottom of the blocks to reduce coolant crossflow. The power density for this design is lower (5.8 versus 7.1 W/cm^3) than that for the previous 2240-MW(t) HTGR-SC/C design with 439 columns utilizing the FSV-type 10-row fuel blocks. The scope of this task was reduced following a decision to transfer funds from this task to the new graphite block stress analysis and it was agreed to perform only the thermal analysis required as input for the stress analysis and to postpone the remaining tasks until FY-83. While this task has been reduced essentially to providing support for the stress analysis, it was still possible to make a brief evaluation of the new core design by comparing the peak fuel temperatures with those predicted for the previous design.

Thermal analysis for the Reference 0 (conceptual design) HTGR-SC/C core was performed to predict fuel and graphite temperatures under the full-power steady-state conditions and to provide input for the stress analysis. The peak fuel temperature predicted for the new core design was 1207°C (2204°F), which is slightly lower than the 1226°C (2239°F) peak temperature of the previous design. This reduction is not due to lower power density, since the average power per fuel pin is essentially the same for the two designs, but instead is a result of a reduction of approximately 10% in maximum power tilts. The reduction in fuel temperatures would have been greater had the two analyses been performed on the same basis. This analysis was performed for the most severe thermal condition (as recently defined in the system performance envelope), whereas the previous analysis assumed nominal conditions. While the full impact of the new core design cannot be evaluated until the entire fuel performance analysis is complete, the present results indicate that the reduction in the peak fuel temperature due to reduced maximum power tilts represents an improvement over the previous core design.

Source Terms for the SC/C HTGR-SC/C.

Preliminary estimates of fission products and neutron activation products in the primary circuit of the 2240-MW(t) HTGR-SC/C were made during

the previous reporting period. Those calculations were based on the previous reference core design, which consisted of 439 columns of the FSV-type 10-row fuel elements with a core power density of 7.1 W/cm^3. Those source terms were also based on the Level A/B radionuclide design criteria as defined at that time.

During this reporting period, the source terms were updated for the new reference core design and accompanying flow parameters and for the new radionuclide design criteria. The source terms were calculated using the latest value for the fraction of fissions in the fissile and fertile particles and the activation product nuclide effective yields corresponding to the current core physics design. The new design Level B circulating gaseous activity criterion, based on site boundary and containment access doses, is defined as 14,000 Ci of Kr-88 in the primary circuit, while the Level A criterion is based on an ALARA margin of four lower (3500 Ci of Kr-88). The new Level B criterion is approximately 60% larger than the value used in the previous source terms calculations. The source terms were calculated using nominal operating conditions, except that the core thermal power was taken to be 102% of nominal power per NRC Regulatory Guide 1.49 to account for uncertainties in power measurements. The calculated inventories of the significant fission products and neutron activation products in the primary coolant circuit are preliminary and suitable for use in conceptual design. Level A values are used for environmental impact reports, planning component removal and maintenance procedures, and the design of containment ventilation and exhaust equipment. The source terms based on the Level B criteria are shown in Table 2.13-4. The Level B values are used for safety analyses, sizing of the helium purification and radwaste systems, and design of associated plant equipment and shielding.

Resolution of Priority Issue: Fission Product Transport Uncertainty

During the previous reporting period, the criteria for circulating and plateout activities in the primary circuit of the 2240-MW(t) HTGR-SC/C were

TABLE 2.13-4

2285 MW(t)[a] LEVEL B CIRCUIT ACTIVITY (Ci)

NUCLIDE	HALF-LIFE	GAS BORNE WITH PURIFICATION SYSTEM		PLATEOUT AFTER 40 YR OPERATION		
		OPERATIVE	INOPERATIVE	INITIAL	1-DAY DECAY	10-DAY DECAY
H3	12.3-Y	4.68+00	5.02+03	0.00	0.00	0.00
C14	5730-Y	0.00	0.00	0.00	0.00	0.00
AR37	34.4-D	7.04-01	8.04+01	0.00	0.00	0.00
GE79	43.0-S	1.05+00	1.05+00	1.12+00	0.00	0.00
AS79	9.0-M	1.24+00	1.26+00	2.34+00	0.00	0.00
SE79M	3.89-M	4.47+01	4.46+01	6.11+01	0.00	0.00
*SE79	STABLE	1.17-04	1.20-04	1.25+02	1.25+02	1.25+02
SE80	STABLE	2.65-04	2.72-04	2.83+02	2.83+02	2.83+02
SE81	18.5-M	1.51+02	1.53+02	4.06+02	0.00	0.00
BR81	STABLE	3.82-04	3.92-04	4.09+02	4.09+02	4.09+02
SE82	STABLE	6.42-04	6.60-04	6.86+02	6.86+02	6.86+02
SE83M	70.-S	1.25+02	1.25+02	1.38+02	0.00	0.00
SE83	22.5-M	1.98+02	2.02+02	6.07+02	0.00	0.00
BR83	2.4-H	2.42+02	2.49+02	3.86+03	3.88+00	0.00
KR83M	1.86-H	5.17+03	6.61+03	0.00	0.00	0.00
KR83	STABLE	4.10-02	3.01+01	0.00	0.00	0.00
SE84	3.3-M	6.09+02	6.13+02	7.94+02	0.00	0.00
BR84	31.8-M	8.03+02	8.20+02	3.33+03	0.00	0.00
KR84	STABLE	7.24-02	5.28+01	0.00	0.00	0.00
BR85	2.87-M	8.06+02	8.10+02	1.02+03	0.00	0.00
KR85M	4.48-H	6.33+03	1.06+04	0.00	0.00	0.00
KR85	10.73Y	8.29+00	5.92+03	0.00	0.00	0.00
RB85	STABLE	2.22-04	2.75-04	2.37+02	2.37+02	2.37+02
KR86	STABLE	1.36-01	9.90+01	0.00	0.00	0.00
KR87	76.-M	8.21+03	9.77+03	0.00	0.00	0.00
RB87	STABLE	5.18-04	5.41-04	5.54+02	5.54+02	5.54+02
KR88	2.8-H	1.40+04	1.99+04	0.00	0.00	0.00
RB88	17.7-M	5.36+03	7.73+03	1.41+04	0.00	0.00
SR88	STABLE	6.79-05	8.22-05	1.20+02	1.20+02	1.20+02
KR89	3.16-M	3.31+03	3.34+03	0.00	0.00	0.00

[a]102% of nominal HTGR-SC/C power.

TABLE 2.13-4 (Continued)

NUCLIDE	HALF-LIFE	GAS BORNE WITH PURIFICATION SYSTEM		PLATEOUT AFTER 40 YR OPERATION		
		OPERATIVE	INOPERATIVE	INITIAL	1-DAY DECAY	10-DAY DECAY
RB89	15.2-M	1.42+03	1.45+03	3.40+03	0.00	0.00
SR89	50.5-D	1.73+00	1.79+00	1.35+04	1.33+04	1.18+04
Y89	STABLE	4.42-07	4.55-07	7.51+01	7.51+01	7.52+01
KR90	32.3-S	1.41+03	1.41+03	0.00	0.00	0.00
RB90M	4.28-M	1.29+02	1.30+02	1.80+02	0.00	0.00
RB90	2.7-M	1.07+03	1.08+03	1.34+03	0.00	0.00
SR90	29.-Y	9.08-03	9.34-03	6.95+03	6.95+03	6.95+03
Y90	64.-H	1.32-02	1.36-02	6.96+03	6.96+03	6.95+03
ZR90	STABLE	2.43-08	2.50-08	3.89+01	3.89+01	3.89+01
KR91	9.0-S	4.70+02	4.70+02	0.00	0.00	0.00
RB91	58.5-S	5.17+02	5.18+02	5.63+02	0.00	0.00
SR91	9.48-H	1.16+01	1.20+01	6.63+02	1.15+02	1.59-05
Y91	58.6-D	1.45-02	1.50-02	7.64+02	7.58+02	6.83+02
ZR91	STABLE	5.27-07	5.41-07	4.87+00	4.87+00	4.88+00
SR92	2.71-H	6.46+00	6.62+00	1.03+02	2.21-01	0.00
Y92	3.53-H	5.39+00	5.54+00	2.06+02	4.17+00	0.00
ZR92	STABLE	5.82-07	5.99-07	1.77+00	1.77+00	1.77+00
SR93	7.5-M	6.55+01	6.62+01	1.10+02	0.00	0.00
Y93	10.2-H	3.14+00	3.24+00	2.24+02	4.41+01	1.86-05
ZR93	STABLE	6.30-07	6.48-07	1.95+00	1.95+00	1.95+00
SR94	1.29-M	9.48+01	9.50+01	1.06+02	0.00	0.00
Y94	19.0-M	7.67+01	7.81+01	2.21+02	0.00	0.00
ZR94	STABLE	1.05-06	1.09-06	1.97+00	1.97+00	1.97+00
Y95	10.5-M	5.84+01	5.92+01	1.15+02	0.00	0.00
ZR95	65.5-D	2.02-02	2.09-02	2.31+02	2.29+02	2.08+02
NB95M	3.61-D	2.32-03	2.39-03	3.42+00	3.22+00	2.34+00
NB95	35.1-D	2.49-02	2.56-02	3.48+02	3.45+02	3.24+02
MO95	STABLE	6.35-07	6.53-07	2.73+00	2.73+00	2.73+00
Y96	6.0-S	1.05+02	1.05+02	1.06+02	0.00	0.00
ZR96	STABLE	1.22-06	1.25-06	1.31+00	1.31+00	1.31+00

TABLE 2.13-4 (Continued)

NUCLIDE	HALF-LIFE	GAS BORNE WITH PURIFICATION SYSTEM		PLATEOUT AFTER 40 YR OPERATION		
		OPERATIVE	INOPERATIVE	INITIAL	1-DAY DECAY	10-DAY DECAY
ZR97	16.8-H	1.18+00	1.21+00	1.10+02	4.08+01	5.51-03
NB97	73.6-M	1.44+01	1.48+01	2.20+02	4.41+01	5.94-03
MO97	STABLE	7.03-07	7.25-07	1.99+00	1.99+00	1.99+00
NB98	51.0-M	1.59-01	1.62-01	9.00-01	2.85-09	0.00
MO98	STABLE	6.24-07	6.41-07	6.71-01	6.71-01	6.71-01
NB99M	2.5-M	3.26+01	3.28+01	4.01+01	0.00	0.00
NB99	14.0-S	7.22+01	7.22+01	7.37+01	0.00	0.00
MO99	66.02H	6.03-01	6.21-01	2.29+02	1.78+02	1.84+01
TC99M	6.02-H	2.98+00	3.06+00	3.02+02	1.77+02	1.78+01
TC99	STABLE	6.77-07	6.96-07	2.73+00	2.73+00	2.73+00
NB100M	7.0-S	5.68+01	5.68+01	5.74+01	0.00	0.00
NB100	2.9-M	4.54+01	4.56+01	5.74+01	0.00	0.00
MO100	STABLE	9.38-07	9.66-07	1.08+00	1.08+00	1.08+00
MO101	14.6-M	4.11+01	4.17+01	9.61+01	0.00	0.00
TC101	14.2-M	5.96+01	6.08+01	1.92+02	0.00	0.00
RU101	STABLE	9.13-07	9.45-07	1.81+00	1.81+00	1.81+00
MO102	11.1-M	4.19+01	4.25+01	8.45+01	0.00	0.00
TC102M	4.3-M	9.07+01	9.19+01	1.69+02	0.00	0.00
RU102	STABLE	1.04-06	1.07-06	1.61+00	1.61+00	1.61+00
MO103	60.-S	6.44+01	6.45+01	7.03+01	0.00	0.00
RU103	39.6-D	2.60-02	2.68-02	1.42+02	1.40+02	1.19+02
RH103M	56.-M	1.16+01	1.18+01	2.12+02	1.38+02	1.18+02
RH103	STABLE	4.97-07	5.13-07	1.82+00	1.82+00	1.82+00
MO104	1.6-M	4.42+01	4.43+01	5.06+01	0.00	0.00
TC104	18.-M	3.67+01	3.74+01	1.04+02	0.00	0.00
RU104	STABLE	5.42-07	5.61-07	1.01+00	1.01+00	1.01+00
TC105	8.0-M	2.22+01	2.24+01	3.85+01	0.00	0.00
RU105	4.44-H	2.39+00	2.47+00	7.71+01	1.85+00	0.00
RH105	35.5-H	2.09-01	2.16-01	1.16+02	7.91+01	1.17+00
PD105	STABLE	2.37-07	2.44-07	1.01+00	1.01+00	1.01+00

TABLE 2.13-4 (Continued)

NUCLIDE	HALF-LIFE	GAS BORNE WITH PURIFICATION SYSTEM		PLATEOUT AFTER 40 YR OPERATION		
		OPERATIVE	INOPERATIVE	INITIAL	1-DAY DECAY	10-DAY DECAY
RU106	369.-D	5.70-04	5.86-04	2.78+01	2.77+01	2.73+01
PD106	STABLE	1.19-07	1.22-07	3.10-01	3.10-01	3.10-01
RU107	4.2-M	1.43+01	1.45+01	1.99+01	0.00	0.00
RH107	21.7-M	1.15+01	1.17+01	3.98+01	0.00	0.00
PD107	STABLE	1.95-07	2.02-07	3.96-01	3.96-01	3.96-01
RU108	4.5-M	9.07+00	9.14+00	1.28+01	0.00	0.00
PD108	STABLE	8.27-08	8.50-08	8.84-02	8.84-02	8.84-02
RH109	1.5-M	8.59+00	8.61+00	9.77+00	0.00	0.00
PD109M	4.69-M	6.43+00	6.50+00	9.79+00	0.00	0.00
PD109	13.46H	2.74-01	2.82-01	2.45+01	7.13+00	1.06-04
AG109	STABLE	9.42-03	9.68-03	1.01+04	1.01+04	1.01+04
PD110	STABLE	2.49-08	2.56-08	2.66-02	2.66-02	2.66-02
AG110M	252.-D	4.76-01	4.90-01	1.58+04	1.58+04	1.54+04
RH111	63.-S	1.73+00	1.74+00	1.90+00	0.00	0.00
PD111	22.-M	1.24+00	1.26+00	3.90+00	0.00	0.00
AG111M	74.-S	2.90+00	2.93+00	5.87+00	0.00	0.00
AG111	7.47-D	3.11+02	3.20+02	3.07+05	2.80+05	1.21+05
CD111	STABLE	2.01-06	2.13-06	2.11+03	2.11+03	2.11+03
PD112	20.1-H	8.67-03	8.91-03	9.67-01	4.23-01	2.46-04
AG112	3.13-H	5.37-02	5.51-02	1.94+00	5.04-01	2.91-04
PD113	1.5-M	5.47-01	5.49-01	6.23-01	0.00	0.00
AG113	5.3-H	3.50-02	3.60-02	1.12+00	4.87-02	0.00
CD113	STABLE	3.66-09	3.76-09	1.04-02	1.04-02	1.04-02
SN119M	245.-D	1.62-07	1.66-07	5.23-03	5.22-03	5.09-03
SN119	STABLE	2.39-09	2.46-09	2.59-03	2.59-03	2.59-03
SN123	129.-D	4.27-06	4.39-06	7.27-02	7.23-02	6.89-02
SB123	STABLE	3.66-07	3.76-07	3.92-01	3.92-01	3.92-01
SN125	9.65-D	3.38-04	3.47-04	4.30-01	4.01-01	2.10-01
SB125	2.73-Y	1.07-03	1.10-03	1.41+02	1.41+02	1.40+02
TE125M	58.-D	2.38-02	2.45-02	2.14+02	2.12+02	1.93+02

TABLE 2.13-4 (Continued)

NUCLIDE	HALF-LIFE	GAS BORNE WITH PURIFICATION SYSTEM		PLATEOUT AFTER 40 YR OPERATION		
		OPERATIVE	INOPERATIVE	INITIAL	1-DAY DECAY	10-DAY DECAY
TE125	STABLE	6.75-05	6.94-05	7.46+01	7.46+01	7.46+01
SN126	STABLE	1.83-08	1.89-08	1.96-02	1.96-02	1.96-02
SB126M	19.0-M	9.10-01	9.34-01	2.52+00	2.53-04	2.53-04
SN127M	4.4-M	6.80-01	6.86-01	9.55-01	0.00	0.00
SN127	2.12-H	3.25-01	3.33-01	4.11+00	1.61-03	0.00
SB127	3.8-D	1.27-02	1.31-02	1.05+01	8.79+00	1.70+00
TE127M	109.-D	1.36-01	1.40-01	1.95+03	1.94+03	1.83+03
TE127	9.4-H	1.85+01	1.90+01	2.89+03	2.08+03	1.80+03
I 127	STABLE	7.49-04	7.68-04	9.00+02	9.00+02	9.00+02
SN128	59.-M	1.33+00	1.36+00	8.52+00	3.83-07	0.00
SB128M	10.4-M	5.13+00	5.21+00	1.72+01	4.64-07	0.00
SB128	9.0-H	1.23-02	1.27-02	6.37-01	1.01-01	6.02-09
TE128	STABLE	1.49-03	1.54-03	1.60+03	1.60+03	1.60+03
SN129M	2.5-M	6.90+00	6.93+00	8.48+00	0.00	0.00
SN129	7.5-M	3.77+00	3.82+00	6.37+00	0.00	0.00
SB129	4.34-H	1.08+00	1.12+00	3.11+01	6.79-01	0.00
TE129M	33.4-D	1.18+00	1.21+00	5.19+03	5.09+03	4.22+03
TE129	70.-M	1.66+02	1.70+02	4.56+03	3.24+03	2.69+03
I 129	STABLE	2.87-03	2.94-03	3.41+03	3.41+03	3.41+03
SN130	3.7-M	1.52+01	1.54+01	2.04+01	0.00	0.00
SB130M	6.6-M	2.41+01	2.44+01	4.33+01	0.00	0.00
SB130	37.-M	2.28+00	2.33+00	1.05+01	0.00	0.00
TE130	STABLE	5.89-03	6.06-03	6.30+03	6.30+03	6.30+03
SN131	63.-S	1.63+01	1.64+01	1.79+01	0.00	0.00
SB131	23.-M	2.07+01	2.11+01	6.59+01	0.00	0.00
TE131M	30.-M	2.46+01	2.53+01	4.09+03	2.35+03	1.60+01
TE131	25.-M	5.87+02	5.99+02	2.71+03	4.29+02	2.92+00
I 131	8.041D	4.21+01	4.32+01	5.44+04	5.01+04	2.32+04
XE131M	11.99D	3.57+01	1.57+03	0.00	0.00	0.00
XE131	STABLE	3.75-01	2.74+02	0.00	0.00	0.00

TABLE 2.13-4 (Continued)

NUCLIDE	HALF-LIFE	GAS BORNE WITH PURIFICATION SYSTEM		PLATEOUT AFTER 40 YR OPERATION		
		OPERATIVE	INOPERATIVE	INITIAL	1-DAY DECAY	10-DAY DECAY
SN132	40.0-S	9.06+00	9.07+00	9.61+00	0.00	0.00
SB132M	4.1-M	1.72+01	1.73+01	2.40+01	0.00	0.00
SB132	2.1-M	2.99+01	3.00+01	3.59+01	0.00	0.00
TE132	78.-H	1.04+02	1.07+02	4.48+04	3.62+04	5.31+03
I 132	2.285H	5.59+02	5.73+02	5.29+04	3.73+04	5.47+03
XE132	STABLE	5.39-01	3.93+02	0.00	0.00	0.00
SB133	2.4-M	3.04+01	3.06+01	3.71+01	0.00	0.00
TE133M	55.4-M	6.72+02	6.87+02	4.09+03	6.14-05	0.00
TE133	12.5-M	7.59+02	7.71+02	2.08+03	1.03-05	0.00
I 133	20.8-H	2.85+02	2.93+02	4.03+04	1.82+04	1.36+01
XE133M	2.23-D	3.11+02	2.80+03	0.00	0.00	0.00
XE133	5.29-D	6.11+03	1.25+05	0.00	0.00	0.00
CS133	STABLE	2.03-03	3.03-03	2.18+03	2.18+03	2.18+03
TE134	42.-M	1.18+03	1.21+03	5.73+03	0.00	0.00
I 134M	3.6-M	1.28+02	1.29+02	1.74+02	0.00	0.00
I 134	52.6-M	1.48+03	1.52+03	1.39+04	2.10-04	0.00
XE134	STABLE	8.67-01	6.33+02	0.00	0.00	0.00
CS134	2.06-Y	3.09-01	3.17-01	3.06+04	3.06+04	3.03+04
I 135	6.585H	4.49+02	4.60+02	1.83+04	1.46+03	0.00
XE135M	15.3-M	3.33+03	3.45+03	0.00	0.00	0.00
XE135	9.17-H	9.56+03	1.85+04	0.00	0.00	0.00
CS135	STABLE	2.12-03	2.25-03	2.27+03	2.27+03	2.27+03
I 136	85.-S	4.46+02	4.48+02	5.10+02	0.00	0.00
XE136	STABLE	7.64-01	5.58+02	0.00	0.00	0.00
CS136	13.0-D	1.83+00	1.88+00	3.14+03	2.98+03	1.84+03
XE137	3.84-M	1.80+03	1.82+03	0.00	0.00	0.00
CS137	30.1-Y	1.78-01	1.83-01	1.34+05	1.34+05	1.34+05
BA137M	2.55-M	4.48+00	4.50+00	1.27+05	1.27+05	1.27+05
BA137	STABLE	5.45-06	5.61-06	1.15+03	1.15+03	1.15+03
XE138	14.2-M	3.24+03	3.35+03	0.00	0.00	0.00

TABLE 2.13-4 (Continued)

NUCLIDE	HALF-LIFE	GAS BORNE WITH PURIFICATION SYSTEM		PLATEOUT AFTER 40 YR OPERATION		
		OPERATIVE	INOPERATIVE	INITIAL	1-DAY DECAY	10-DAY DECAY
CS138M	2.9-M	4.44+00	4.47+00	5.63+00	0.00	0.00
CS138	32.2-M	8.51+02	8.99+02	3.36+03	0.00	0.00
BA138	STABLE	1.28-04	1.32-04	1.58+02	1.58+02	1.58+02
XE139	39.7-S	5.39+02	5.40+02	0.00	0.00	0.00
CS139	9.3-M	3.54+02	3.59+02	6.56+02	0.00	0.00
BA139	83.3M	5.50+01	5.69+01	7.77+02	5.37-03	0.00
LA139	STABLE	1.42-06	1.47-06	7.74+00	7.74+00	7.74+00
XE140	13.6-S	2.29+02	2.30+02	0.00	0.00	0.00
CS140	63.8-S	3.03+02	3.03+02	3.32+02	0.00	0.00
BA140	12.79D	8.69+00	8.94+00	1.47+04	1.39+04	8.55+03
LA140	40.23H	5.79-01	5.96-01	1.48+04	1.46+04	9.81+03
CE140	STABLE	9.79-07	1.01-06	1.30+02	1.30+02	1.30+02
BA141	18.3M	4.15+01	4.23+01	1.11+02	0.00	0.00
LA141	3.87-H	6.91+00	7.12+00	2.24+02	3.17+00	0.00
CE141	32.53D	2.78-02	2.86-02	3.36+02	3.30+02	2.72+02
PR141	STABLE	9.19-07	9.44-07	3.92+00	3.92+00	3.92+00
BA142	10.7-M	5.48+01	5.55+01	1.08+02	0.00	0.00
LA142	92.4-M	1.77+01	1.82+01	2.21+02	4.80-03	0.00
CE142	STABLE	1.07-06	1.11-06	2.94+00	2.94+00	2.94+00
LA143	14.-M	4.72+01	4.79+01	1.08+02	0.00	0.00
CE143	33.0-H	8.53-01	8.80-01	2.16+02	1.31+02	1.40+00
PR143	13.58D	6.09-02	6.27-02	3.24+02	3.17+02	2.09+02
ND143	STABLE	8.99-07	9.24-07	3.84+00	3.84+00	3.84+00
CE144	284.4D	2.56-03	2.63-03	9.59+01	9.57+01	9.36+01
PR144	17.28M	2.87+01	2.92+01	1.70+02	9.57+01	9.36+01
ND144	STABLE	8.60-07	8.88-07	2.18+00	2.18+00	2.18+00
CE145	3.3-M	5.39+01	5.43+01	7.02+01	0.00	0.00
PR145	5.98-H	3.67+00	3.78+00	1.41+02	8.74+00	0.00
ND145	STABLE	6.22-07	6.41-07	1.90+00	1.90+00	1.90+00
CE146	14.2-M	2.34+01	2.38+01	5.38+01	0.00	0.00

TABLE 2.13-4 (Continued)

NUCLIDE	HALF-LIFE	GAS BORNE WITH PURIFICATION SYSTEM		PLATEOUT AFTER 40 YR OPERATION		
		OPERATIVE	INOPERATIVE	INITIAL	1-DAY DECAY	10-DAY DECAY
PR146	24.2-M	2.41+01	2.47+01	1.08+02	0.00	0.00
ND146	STABLE	6.64-07	6.88-07	1.47+00	1.47+00	1.47+00
CE147	70.-S	3.54+01	3.55+01	3.92+01	0.00	0.00
PR147	12.-M	3.66+01	3.71+01	8.05+01	0.00	0.00
ND147	10.99D	5.37-02	5.56-02	1.22+02	1.15+02	6.49+01
PM147	2.623Y	3.28-04	3.37-04	1.63+02	1.63+02	1.63+02
SM147	STABLE	4.12-05	4.24-05	4.56+01	4.56+01	4.56+01
PR148	2.0-M	2.62+01	2.64+01	3.10+01	0.00	0.00
ND148	STABLE	4.94-07	5.09-07	5.72-01	5.72-01	5.72-01
PM148M	41.3-D	3.22-04	3.31-04	1.75+00	1.72+00	1.48+00
PM148	5.37-D	1.96-02	2.02-02	1.39+01	1.22+01	3.83+00
PR149	2.3-M	1.65+01	1.66+01	2.00+01	0.00	0.00
ND149	1.73-H	3.55+00	3.65+00	4.08+01	2.75-03	0.00
PM149	53.1-H	8.32-02	8.59-02	6.17+01	4.61+01	2.75+00
SM149	STABLE	1.23-05	1.26-05	1.35+01	1.35+01	1.35+01
ND150	STABLE	1.21-07	1.24-07	1.29-01	1.29-01	1.29-01
ND151	12.4-M	4.44+00	4.50+00	9.48+00	0.00	0.00
PM151	28.4-H	8.94-02	9.23-02	1.91+01	1.07+01	5.48-02
SM151	93.-Y	2.58-04	2.65-04	2.49+02	2.49+02	2.49+02
EU151	STABLE	1.01-05	1.03-05	1.31+01	1.31+01	1.31+01
ND152	11.5-M	3.07+00	3.11+00	6.30+00	0.00	0.00
PM152	4.1-M	6.95+00	7.04+00	1.28+01	0.00	0.00
SM152	STABLE	7.14-06	7.34-06	7.68+00	7.68+00	7.68+00
EU152	13.-Y	2.29-07	2.35-07	1.17-01	1.17-01	1.17-01
ND153	67.5-S	3.05+00	3.06+00	3.37+00	0.00	0.00
PM153	5.4-M	4.76+00	4.81+00	7.43+00	0.00	0.00
SM153	45.5-H	3.45-02	3.57-02	1.15+01	8.07+00	3.22-01
EU153	STABLE	4.36-06	4.48-06	4.77+00	4.77+00	4.77+00
ND154	7.73-D	1.48-03	1.53-03	1.52+00	1.39+00	6.18-01
PM154	2.8-M	1.55+00	1.56+00	3.46+00	1.39+00	6.18-01

TABLE 2.13-4 (Continued)

NUCLIDE	HALF-LIFE	GAS BORNE WITH PURIFICATION SYSTEM		PLATEOUT AFTER 40 YR OPERATION		
		OPERATIVE	INOPERATIVE	INITIAL	1-DAY DECAY	10-DAY DECAY
SM154	STABLE	2.59-06	2.67-06	2.79+00	2.79+00	2.79+00
EU154	8.6-Y	4.64-04	4.77-04	1.78+02	1.78+02	1.77+02
SM155	22.2-M	4.28-01	4.36-01	1.30+00	0.00	0.00
EU155	4.8-Y	1.86-04	1.91-04	4.34+01	4.34+01	4.32+01
GD155	STABLE	9.25-09	9.51-09	4.25-01	4.25-01	4.25-01
SM156	9.4-H	1.52-02	1.56-02	8.03-01	1.37-01	1.66-08
EU156	15.2-D	4.84-02	4.98-02	9.80+01	9.37+01	6.21+01
GD156	STABLE	7.77-09	8.00-09	9.56-01	9.56-01	9.57-01
SM157	83.-S	4.37-01	4.38-01	4.92-01	0.00	0.00
EU157	15.2-H	1.12-02	1.15-02	1.00+00	3.36-01	1.77-05
GD157	STABLE	2.71-09	2.78-09	8.38-03	8.38-03	8.38-03
	TOTALS	8.61+04	2.45+05	9.78+05	8.09+05	5.22+05

* - STABLE NUCLIDES ARE GIVEN IN GRAMS

EXPONENTIAL NOTATION IS EMPLOYED (1.23+01 REPRESENTS 12.3)

reviewed and the circulating activity criteria were revised. The new Level B criterion of 14,000 Ci of Kr-88 is based on allowable site boundary dose and containment access requirements. The Level A criterion is based on an ALARA margin of four reduction (3500 Ci fo Kr-88).

As a result of Baseline Review Meetings, fission product transport is no longer considered a priority critical issue owing to the relatively clean environment associated with the HTGR-SC/C and since more than 90% of the circulating activity is expected to come from manufacturing defects.

2.13.2.5. High-Performance Block Study. A scoping study was carried out on the use of a modified, flanged fuel element, with fuel and coolant holes in the flanged region, to reduce fuel cycle costs and permit operation at higher power densities than the present 5.8 W/cm^3 level. The results show that this modified block would increase the fuel rod volume to 96.7% of the original unflanged block design as compared with about 80% for the current flanged block (nine-row) design. The corresponding modified block coolant hole frontal area is 95.3% of the original design. A transition cycle from LEU/Th in a 2240-MW(t) HTGR-SC/C core using this modified block and a power density increase from 5.8 to 7.1 W/cm^3 over several cycles gave costs 6% lower than those for an equivalent 4-yr transition cycle at 5.8 W/cm^3 using the nine-row block design. Table 2.13-5 compares the three fuel element designs.

2.13.2.6. NSSS Shielding. Work was initiated on shielding analysis for reactor internals components. As part of this effort, a study was carried out to determine the feasibility of eliminating the side thermal shield. Preliminary results indicate that the thermal shield could be removed if the outer ring of the permanent side reflector were boronated to reduce neutron streaming to acceptable levels. The cost trade-off of this design change needs to be evaluated.

TABLE 2.13-5
FUEL BLOCK DESCRIPTIONS

Standard Block	10-Row	9-Row	10-Row HP
Fuel rods[a]	2568	2052	2448
Holes[b]			
Fuel type 1	192	138	138
Fuel type 2	24	36	72
Coolant type 1	102	84	84
Coolant type 2	6	7	25
Volume fraction fuel	0.2185	0.1750	0.2087
Area fraction coolant	0.1867	0.1561	0.1764
Unfueled weight, kg (lb)	87.5 (193)	99.1 (218.5)	89.9 (198)
Fuel weight; initial core, kg (lb)	123.8 (273)	129.1 (284.6)	124.8 (275)
Control Block			
Fuel Rods[a]	1344	1126	1522
Holes			
Fuel type 1	90	70	70
Fuel type 2	24	26	62
Coolant type 1	45	30	30
Coolant type 2	15	23	41
Control rod	2	2	2
Reserve shutdown	1	1	1
Power rod	1	1	1
Volume fraction fuel	0.1143	0.0960	0.1298
Area fraction coolant	0.0963	0.0789	0.0992
Unfueled weight, kg (lb)	85.1 (1876)	89.8 (198)	80.7 (178)
Fueled weight; initial core, kg (lb)	104.1 (229.5)	106.3 (234.4)	102.4 (225.7)

[a] Fuel rods are 62.89 mm in length, 12.446 mm in diameter.

[b] Fuel holes, type 1: fuel rods stacked 12 high, 12.7 mm hole. Fuel holes, type 2: fuel rods stacked 11 high, 12.7 mm hole. Coolant holes, type 1: 15.8 mm. Coolant holes, type 2: 12.7 mm.

2.13.2.7. Fuel Cycle Cost Evaluation. During the second half of FY-82, fuel cycle costs were estimated for a number of HTGR design options. The emphasis of this work was on evaluating the costs of various 2240-MW(t) HTGR-SC/C cycles, including both the LEU/Th lead plant design and various "equilibrium" follow-on design cycles. Under other Applications Program tasks, costs were also estimated for several gas turbine and process heat cycles, including the small Modular Reactor System (MRS) design. These estimates are presented here for purposes of comparison with the 2240-MW(t) HTGR-SC/C design costs.

Economic Resources, and Unit Cost Assumptions

The economic, resource, and unit handling cost assumptions used in these evaluations were data needs prepared under the HTGR Technology Program in the first half of FY-82 (Ref. 2.13-1). Those assumptions are summarized below.

Resource Costs. Resource costs, or the cost components of enriched uranium were provided by GCRA. The costs are in 1982 dollars for delivery in 1995 and thereafter.

The resource cost assumptions to be used are as follows:

U_3O_8 $/kg ($/lb)	88.2 ($40) (1995 delivery)
U_3O_8 real escalation, $/yr	2.5% after 1995
Conversion cost, $/kg ($/lb)	6.0 (2.72)
Enrichment cost, $/kg ($/lb)	140.0 (63.5)
Tails assay, %	0.2%

The $140/kg ($63.5/lb) enrichment cost is expected to be a conservatively high cost in the event that centrifuge or Advanced Isotope Separation (AIS) technologies are introduced, but realistic if diffusion remains the only fuel enrichment process available.

Economic Assumptions. The economic assumptions and economic parameters used for obtaining the 30-yr levelized fuel cycle costs for the various HTGR cycle designs are summarized in Table 2.13-6. The data were specified by GCRA for these evaluations.

Unit Handling Costs. The unit handling costs for both the lead plant and N^{th} plant cost evaluations are summarized in Table 2.13-7. All costs except the lead plant fresh fabrication unit cost are based on the equilibrium, or N^{th}, plant condition corresponding to a fully commercialized HTGR. The lead plant fabrication cost estimate was based on fabricating fuel in GA's Sorrento Valley facility. The N^{th} plant unit handling costs were based on escalating 1980-dollar handling costs to January 1982 dollars. The HTGR storage and waste costs will be reevaluated in FY-83 based on new storage and repository criteria being developed by DOE and NRC for LWR disposal costs.

Fuel Cycle Cost Results

The 30-yr levelized fuel cycle costs in constant dollars (0% inflation) are summarized in Tables 2.13-8, 2.13-9, and 2.13-10 for 1995 startup, for 2005 startup, and for sensitivity cases, respectively. The 2005 startup cases differ only in the fuel depletion (Depl) cost component due to the assumed 2.5%/yr U_3O_8 real escalation. The lead plant costs differ from the N^{th} plant costs in fuel depletion (longer preirradiation times) and in fuel fabrication. This results in the lead plant costs being about 15% higher than the N^{th} plant costs for the 2240-MW(t) HTGR-SC/C design.

Costs are given for both 7.1- and 5.8-W/cm^3 power densities for the LEU/Th design. The HEU/Th once-through or recycle designs are based on the higher power density. The costs for the HEU/Th once-through design are about 9% lower than those for the LEU/Th N^{th} plant design. The saving is entirely due to the higher power density, which reduces the handling costs.

TABLE 2.13-6
ECONOMIC ASSUMPTIONS FOR HTGR-SC/C COSTS

Plant basis	2240-MW(t) lead plant and Nth plant
Unit capacity factor	70%
Base date for all costs	January 1982
Date of operation	January 1995 and January 2005
Levelizing period	30 yr

	Economic Parameters	
	Constant Dollar	Inflated Dollar
Inflation rate	0.0%	8.0%
Gross weighted cost of capital (discount rate for fuel cycle)	5.50%	14.0%
Preirradiation working capital rate	4.3%	10.6%
In-core, postirradiation working capital rate	8.5%	21.2%

TABLE 2.13-7
HTGR-SC/C UNIT HANDLING COST SUMMARY (JANUARY 1982 DOLLARS/BLOCK)

Fresh fabrication, Nth plant	8880 (LEU/Th) 7900 (HEU/Th)
Fresh fabrication, lead plant fuel in Sorrento Valley	15130 (LEU/Th)
Refabrication	16470 (HEU/Th)
Reprocessing	8470 (HEU/Th)
Shipping	3650 (HEU/Th and LEU/Th)
Processed waste (recycle)	1910 (HEU/Th)
AFR + disposal (once-through)	9350 (LEU/Th)

TABLE 2.13-8
HTGR FUEL CYCLE COSTS FOR 1995 STARTUP
(0% Inflection, 0- to 30-yr Levelized)

Reactor/Fuel Cycle	Costs [mills/kW-h(e)]						$/GJ ($/MBtu)
	Depl.	Fab.	Ship.	Waste	Reproc.	Total	
1. 2240-MW(t) HTGR-SC/C (lead plant)							
LEU/Th once-through							
5.8 W/cm^3	6.87	3.58	0.56	1.42	0.00	12.44	1.33 (1.40)
7.1 W/cm^3 (HP)	7.71	3.05	0.46	1.15	0.00	12.37	1.32 (1.39)
2. 2240-MW(t) HTGR-SC/C (Nth plant)							
LEU/Th once-through							
5.8 W/cm^3	6.75	2.05	0.56	1.42	0.00	10.79	1.15 (1.21)
7.1 W/cm^3 (HP)	7.56	1.75	0.46	1.15	0.00	10.92	1.17 (1.23)
HEU/Th once-through							
7.1 W/cm^3 (HP)	6.79	1.48	0.46	1.15	0.00	9.87	1.05 (1.11)
HEU/Th recycle							
7.1 W/cm^3 (HP)	3.73	3.08	0.46	0.23	1.04	8.54	0.91 (0.96)
3. 1170-MW(t) HTGR-SC/C							
LEU/Th once-through	6.88	2.18	0.60	1.51	0.00	11.18	1.19 (1.26)
4. 1170-MW(t) HTGR-GT [850°C (1562°F)]							
LEU/Th once-through	6.69	2.12	0.58	1.47	0.00	10.86	1.19 (1.26)
5. 1170-MW(t) HTGR-PH [950°C (1742°F)]							
LEU/Th once-through	6.95	2.62	0.79	1.97	0.00	12.33	1.36 (1.43)
6. 2240-MW(t) HTGR-PH [950°C (1742°F)]							
LEU/Th once-through	7.02	2.74	0.82	2.08	0.00	12.66	1.39 (1.47)
7. 250-MW(t) HTGR-SC/C modular							
LEU/Th once-through	14.0	2.88	0.74	1.85	0.00	19.47	2.08 (2.19)
HEU/Th recycle	7.15	2.05	0.56	0.29	1.28	11.33	1.20 (1.27)
8. 250-MW(t) HTGR-ref. modular							
LEU/Th once-through	13.60	2.79	0.71	1.80	0.00	18.9	2.08 (2.19)
HEU/Th recycle	6.95	1.99	0.54	0.28	1.24	11.00	1.20 (1.27)
9. 300-MW(t) HTGR SC/C modular							
LEU/Th once-through	14.1	2.39	0.61	1.54	0.00	18.64	1.99 (2.10)
HEU/Th recycle	7.74	1.66	0.45	0.23	1.04	11.12	1.18 (1.25)

TABLE 2.13-9
HTGR FUEL CYCLE COSTS FOR 2005 STARTUP
(0% Inflection, 0- to 30-yr Levelized)

Reactor/Fuel Cycle	Costs [mills/kW-h(e)]						$/GJ ($/MBtu)
	Depl.	Fab.	Ship.	Waste	Reproc.	Total	
1. 2240-MW(t) HTGR-SC/C (lead plant)							
LEU/Th once-through							
5.8 W/cm^3	7.67	3.58	0.56	1.42	0.00	13.23	1.41 (1.49)
7.1 W/cm^3 (HP)	8.61	3.05	0.46	1.15	0.00	13.27	1.44 (1.52)
2. 2240-MW(t) HTGR-SC/C (Nth plant)							
LEU/Th once-through							
5.8 W/cm^3	7.56	2.05	0.56	1.42	0.00	11.59	1.24 (1.31)
7.1 W/cm^3 (HP)	8.49	1.75	0.46	1.15	0.00	11.85	1.26 (1.33)
HEU/Th once-through							
7.1 W/cm^3 (HP)	7.56	1.48	0.46	1.15	0.00	10.65	1.14 (1.20)
HEU/Th recycle							
7.1 W/cm^3 (HP)	4.14	3.08	0.46	0.23	1.04	8.95	0.96 (1.01)
3. 1170-MW(t) HTGR-SC/C							
LEU/Th once-through	7.72	2.18	0.60	1.51	0.00	12.01	1.28 (1.35)
4. 1170-MW(t) HTGR-GT [850°C (1562°F)]							
LEU/Th once-through	7.47	2.12	0.58	1.47	0.00	11.64	1.28 (1.35)
5. 1170-MW(t) HTGR-PH [950°C (1742°F)]							
LEU/Th once-through	7.79	2.62	0.79	1.97	0.00	13.17	1.45 (1.53)
6. 2240-MW(t) HTGR-PH [950°C (1742°F)]							
LEU/Th once-through	7.75	2.74	0.82	2.08	0.00	13.39	1.47 (1.55)
7. 250-MW(t) HTGR-SC/C modular							
LEU/Th once-through	15.6	2.88	0.74	1.85	0.00	21.07	2.24 (2.37)
HEU/Th recycle	8.03	2.05	0.56	0.29	1.28	12.31	1.3 (1.38)
8. 250-MW(t) HTGR-ref. modular							
LEU/Th once-through	15.2	2.79	0.71	1.80	0.00	20.5	2.24 (2.37)
HEU/Th recycle	7.81	1.99	0.54	0.28	1.24	11.86	1.3 (1.38)
9. 300-MW(t) HTGR SC/C modular							
LEU/Th once-through	15.81	2.39	0.61	1.54	0.00	20.35	2.16 (2.28)
HEU/Th recycle	8.70	1.66	0.45	0.23	1.04	12.10	1.29 (1.37)

TABLE 2.13-10
HTGR FUEL CYCLE COST SENSITIVITIES (0- to 30-YR LEVELIZED)

Reactor/Fuel Cycle	Costs [mills/kW-h(e)]					Total	$/GJ ($/MBtu)
	Depl.	Fab.	Ship.	Waste	Reproc.		
0% U_3O_8 Real Escalation, 1995 or 2005 startup							
2240-MW(t) HTGR-SC/C							
LEU/Th once-through, 5.8 W/cm^3	6.15	2.05	0.56	1.42	0.00	10.19	1.09 (1.15)
$132/kg ($60/lb) - 3% real escalation, 1995 startup							
2240-MW(t) HTGR-SC/C (lead plant)							
LEU/Th once-through, 5.8 W/cm^3	8.59	3.58	0.56	1.42	0.00	14.15	1.507 (1.59)
2240-MW(t) HTGR-SC/C							
LEU/Th once-through, 5.8 W/cm^3	8.46	2.05	0.56	1.42	0.00	12.49	1.34 (1.41)
$132/kg ($60/lb) - 3% real escalation, 2005 startup							
2240-MW(t) HTGR-SC/C							
HEU/Th once-through, 5.8 W/cm^3	10.02	2.05	0.56	1.42	0.00	14.06	1.51 (1.59)
HEU/Th recycle, 7.1 W/cm^3	5.59	3.08	0.46	0.23	1.04	10.40	1.11 (1.17)

It should be noted that the small MRS costs are appreciably higher than costs for the larger sizes. This is primarily due to the lower power density (4.1 to 4.9 W/cm^3) and batch refueling used for the MRS. Fiscal year 1983 evaluations for the MRS will consider graded refueling for that design, which will reduce fuel cycle costs by ~25% from the values for batch refueling.

References

2.13-1. "HTGR Applications Program Semiannual Report for the Period October 1, 1981, through march 31, 1982," DOE Report GA-A16831, 1983, Section 2.

2.13-2. Little, W. W., Jr., and R. W. Hardie, "2DB Users Manual - Revision 1," Pacific Northwest Laboratory Report BNWL-831, Rev. 1, 1969.

2.14. PRIMARY COOLANT SYSTEM DESIGN (6032210101)

2.14.1. Scope

1. To establish preliminary criteria for flow, temperature, and pressure distributions throughout the primary coolant loop. These criteria will include characterization of local bypass flows during normal plant operations at 100% power, at 75%, 50%, and 25% feedwater flow, at refueling conditions, and at reduced core power with one or two main loops shut down.

2. To determine cost-effective solutions for solving the water ingress technical issue. This work encompasses all those components and systems that affect or are affected by water ingress into the PCRV cavities and by its removal process. The objective of this subtask is to develop cost-effective design features specific to the solution of the water ingress problem during plant operation or during shutdowns. These solutions may be compatible with the plant performance, availability, and safety goals.

2.14.2. Discussion

2.14.2.1. Primary Coolant Flow, Temperature, and Pressure Distribution. A single-phase nonisothermal network flow model has been developed for the purpose of calculating the flow distribution throughout the primary coolant system of the 2240-MW(t) HTGR-SC/C plant at various reactor operating conditions. Of special interest is the characterization of bypass flows, such as the steam generator buffer flow, the main circulator leak flow, the CACS back-flow, and various core bypass flows. This flow model is both a means of identifying areas in which design changes may be necessary and a means of analyzing the effects of a design change on the primary coolant system. The model should be kept up to date so that it reflects the latest design of the system and the NSSS components.

Two separate models were used. The first is based on the current design of the plant. This model represents the configuration of the plant as designed; where design data were not available approximations were made. As might be expected, the flow distributions calculated with this model do not agree in all areas with the predicted plant performance. The second, or design basis, model is the same as the current design model except for selected changes that are intended to produce the expected or design flow distribution. The primary purpose of the design basis model is to identify design changes that might be necessary to achieve expected performance.

Two runs were made for each of the two above cases, one with crossflow to and from the core fuel blocks coolant channels and one without crossflow. This was necessary because there is currently no experimentally derived crossflow correlation for the new reference core design. Instead of trying to develop a correlation, these two extreme bounding cases were made. The crossflow runs used experimental correlations from the previous core design, whereas the other runs had no crossflow. It is recommended that the no-crossflow runs be used as the reference cases and that the crossflow runs be used as indicators of how the flow, pressure, and temperature distributions may be affected by the crossflow.

Figure 2.14-1 shows a schematic of the network flow model used. Each flow segment is identified. Two main circulator loops were modeled as shown in Fig. 2.14-1. Since there are four such loops in the plant, each loop in the model has the equivalent flow area of two plant loops. The resistances input for the two circulator loops in the model are identical. For the isothermal case, identical pressure rises were specified for the two loops [160 kPa (23.2 psia) for 100% power] so that there would be equal flow in each loop. The model has one CACS loop, which represents all three CACS loops and thus has a flow area three times that of an individual CACS loop.

The model represents the entire 2240-MW(t) core, which is the most detailed part of the model and is shown in Fig. 2.14-2. The refueling

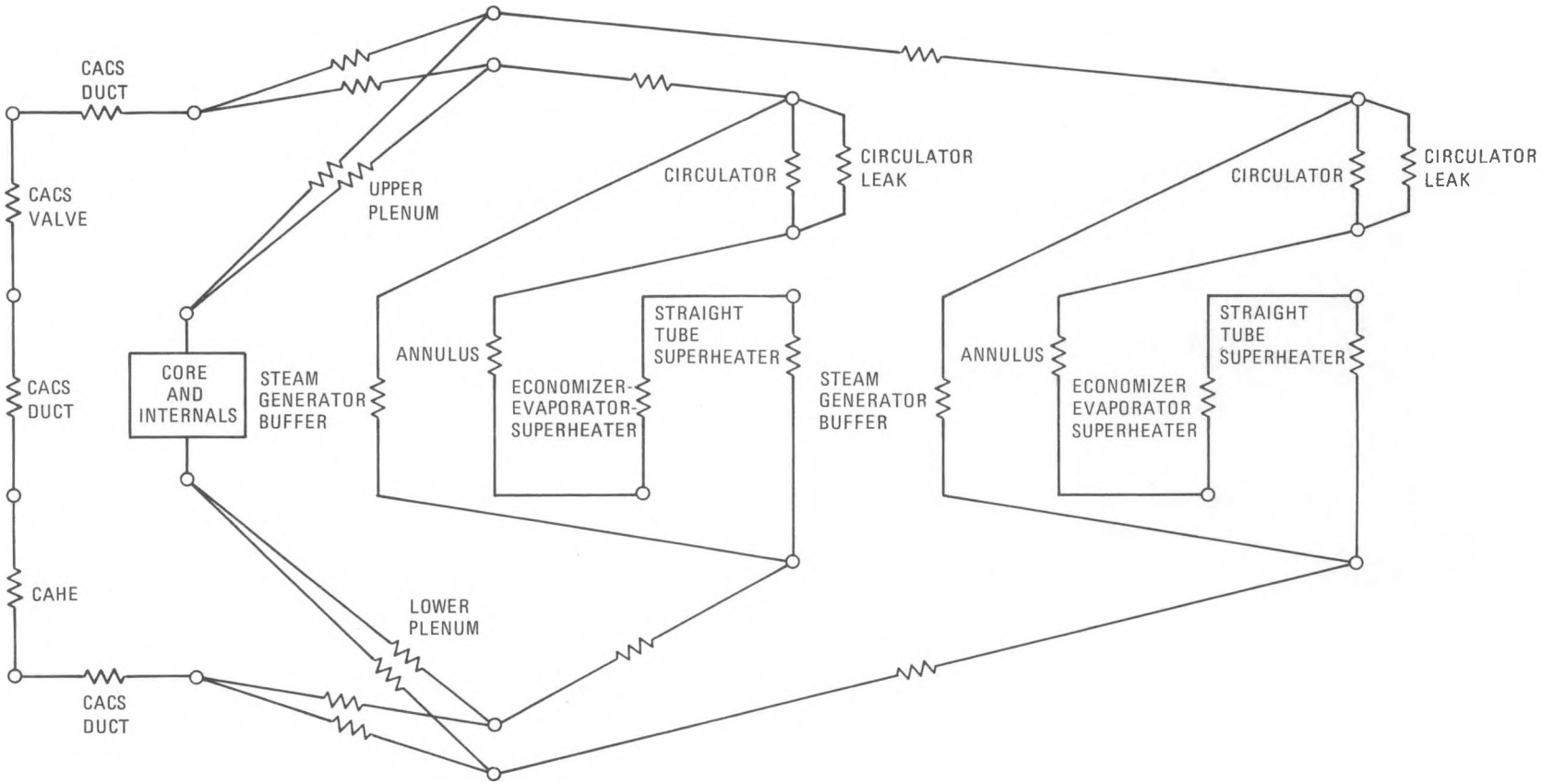

Fig. 2.14-1. Network flow model for 2240-MW(t) HTGR-SC/C primary coolant system

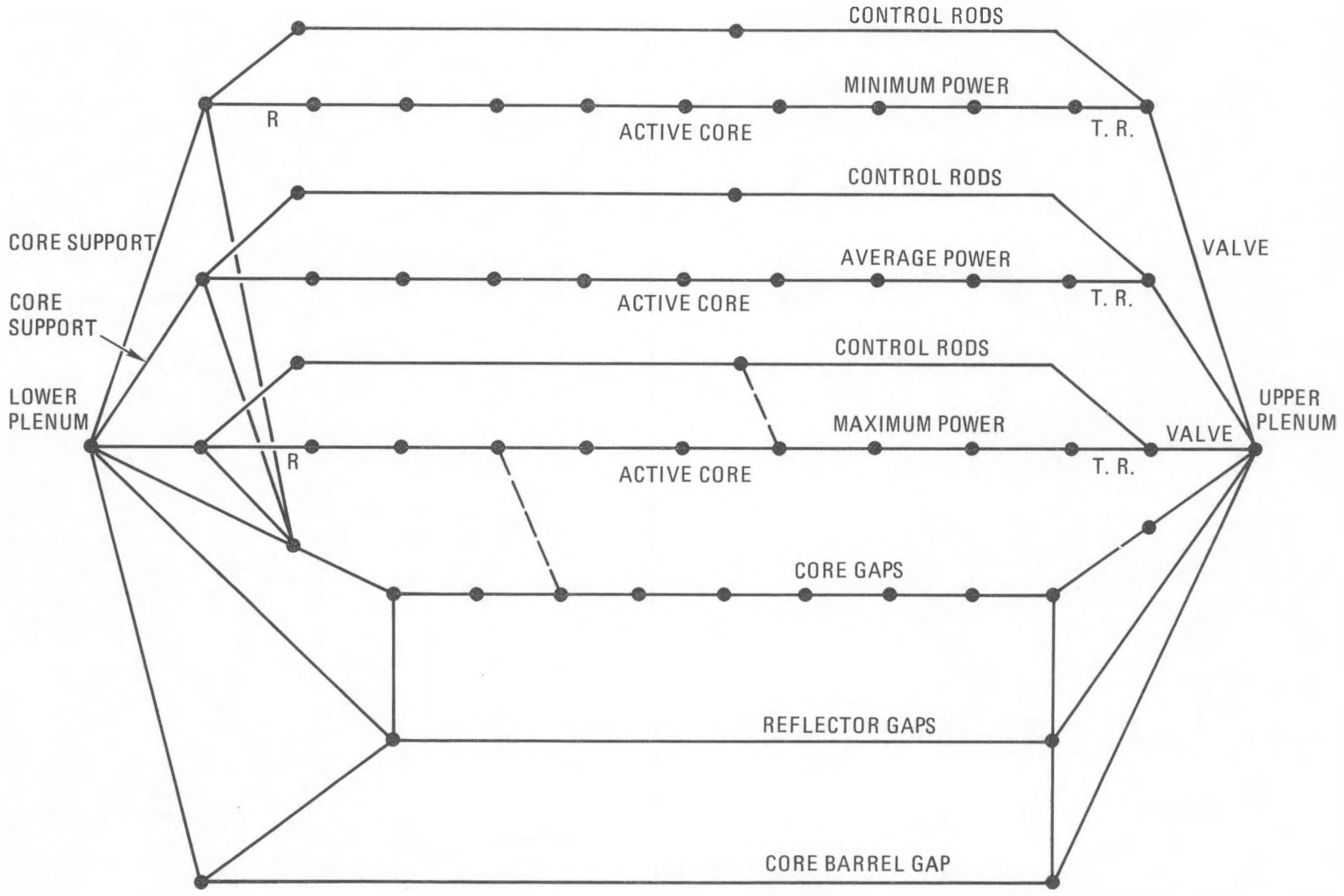

Fig. 2.14-2. Core network model

regions are divided into three groups: the maximum power region, the minimum power region, and the remaining 83 regions, which are labeled average power. The flow through each of these three groups is further divided into a branch for coolant channel flow and a branch for control rod flow.

A constant unform heat flux per unit length was input for each segment of the model. A heat flux of 0.0 was input for adiabatic segments. A positive heat flux signifies heat added to the fluid, whereas a negative value indicates heat taken from the fluid. Heat is added to the fluid in the core by the circulators. Heat is removed from the fluid primarily by the steam generators and local losses around the loops.

In general, the flow, pressure, and temperature distributions calculated with the current design model agree fairly well with expected values. The model calculates a larger bypass flow than expected. Based on the 100%-power no-crossflow results, the design basis model suggests that the following design changes would result in a flow distribution close to that required to achieve expected performance:

1. The gaps between permanent side reflector blocks should be held to approximately 0.18 mm (0.007 in.) instead of 0.76 mm (0.03 in.) as previously estimated.

2. The gaps between hexagonal reflector columns should be approximately 0.91 mm (0.036 in.) instead of 3.3 mm (0.13 in.).

3. The gap between hexagonal reflectors at the plenum element level must be held to approximately 0.2 mm (0.008 in.) instead of the current design value of 0.5 mm (0.02 in.).

4. The gap between fuel columns at the plenum element level should be held to 0.23 mm (0.009 in.) instead of 0.51 mm (0.02 in.).

5. Some type of flow restrictors should be designed for the control rod and power rod channels to keep the flow rate there down to 3.5% of the core flow.

The flow distributions calculated for the reduced-power cases (75%, 50%, 25%) as well as for the partial loop cases (three loops operating, two loops operating) are very close to that of the 100%-power cases. The percent of total circulator flow in a given branch is basically independent of the power level.

The pressure drops calculated by the model are consistently lower than the values required to achieve expected performance. For the 100%-power design basis case, the system pressure drop calculated is 143 kPa (20.8 psia) compared with 160 kPa (23.2 psia). If the calculated value is corrected for an equilibrium region peaking factor, the pressure drop decreases to 128 kPa (18.6 psia). Again, the trends in pressure drop are nearly the same for the reduced-power and partial loop cases.

The model should be refined and, most important, should evolve with the design of the primary coolant system and affected NSSS components. From a systems viewpoint, the model can be used to test the effect of component design changes on the overall system performance. The model cannot take the place of detailed component analysis, but it can be the basis for an exchange of information between the designers and the system analysts.

2.14.2.2. Water Ingress Design Solutions. The HTGR contains primary coolant within a PCRV that is protected from exposure to high-temperature gas by thermal barriers containing fibrous insulation material. If moisture accidentally enters the primary coolant from one of several potential water sources and if it reaches the fibrous insulation, its removal can be time-consuming. The plant downtime required for moisture removal can have significant impact on plant availability, since the plant cannot operate with oxidants above a certain level.

The overall objective of this subtask is to develop design solutions that will assure compliance with the plant availability goal. The maximum plant downtime tentatively allocated for moisture ingress accidents is 4 days/reactor-year. To achieve this goal with an adequate margin, all aspects of the moisture ingress problems have been examined and cost-effective design solutions have been identified.

Moisture Ingress Prevention

The three major potential sources of moisture in the HTGR primary coolant system are the steam generators, the main circulator service system, and the CAHEs.

Steam generator integrity is an industry-wide problem, and the potential for a steam generator leak cannot be fully eliminated. However, design features that limit the quantity of leakage in case of a tube failure will be incorporated. The steam generator tubesheets will have inlet orifices designed to limit the leak rate in case of a tube failure, and the leaking steam generator will be automatically isolated and dumped as soon as the moisutre detectors identify the leaking loop.

The present design of the main circulator service system appears to have a high resistance to water inleakage. The highest amount of water ingress for a malfunction of the service system with the circulator operating is about 0.095 ℓ/s (1.5 gal/min). The leaked water in this case is atomized so finely, owing to the high velocity of the helium flow, that the water is vaporized immediately. The mositure removal time in this case is short and the contribution to the overall plant unavailability is negligible.

Larger water ingresses are nevertheless possible when the circulator is shut down. In this case, the leaked water flows down along the structural surfaces, seeping through the thermal barriers, and could eventually accumulate on the flat bottom of the steam generator cavity and flood the fibrous

insulation beneath the thermal barrier coverplate. Removal of moisture from these thermal barriers by means of vaporization, draining, or purging is time-consuming and requires incorporation of specific design provisions.

The CAHEs are expected to be in one of the two operating modes: (1) standby or (2) active operation at full pressure and flow for removing the reactor residual heat. During standby operation, the circulating water is maintained at a pressure lower than the primary coolant pressure. Therefore, a tube failure in this mode of operation would not be expected to result in moisture ingress. During the active operation mode, which is rare and brief, the CAHE is pressurized in excess of the primary coolant pressure and any tube failure would cause moisture ingress into the PCRV.

The failure rate of the CAHE tube bundle is expected to be 14×10^{-6}/hr of operation with one CAHE. Based on the expected CAHE use frequencies and durations, the frequency of moisture ingress accidents from the three CAHEs is estimated to be approximately 4.3×10^{-3}/reactor-year, which is lower than that due to the steam generator leaks by a factor of at least 2000. Therefore, even assuming the same consequence in terms of cleanup time as for a steam generator leak, the contribution of moisture ingress due to the CAHE tube failure is negligible.

Moisture Detection

A delay in moisture detection adversely affects moisture removal and plant downtime by resulting in (1) more total moisture leakage and (2) a longer period of forced permeation into the fibrous thermal barrier along with the bypass primary coolant flow. The impact of moisture detection delay depends on plant conditions, leak sizes, and leak locations.

For leaks from either the circulator service system or the steam generator, the affected loop must be first identified and then isolated. The potential optimum location for the loop moisture monitor is downstream of the circulator. The current moisture monitor has an active sampling

system with its own pump and does not depend on the primary coolant pressure drop, which means that it can detect moisture in a stagnant coolant after the loop or reactor is shut down.

Moisture Removal

Moisture removal rate following a water ingress accident depends on a number of parameters, including the amount of dry helium that can permeate beneath the thermal barrier coverplates in the wetted regions, the PCRV liner temperature, the PCRV minimum obtainable pressure as a function of core fuel temperature, the capacity of the helium purification system, and the time required to pump down and replace the PCRV helium inventory. A sensitivity analysis has been performed to determine the impact of each of these parameters, and cost-effective design improvements have been identified as discussed below.

Tolerance. The maximum content of moisture in the primary coolant is determined by the acceptable amount of oxidation for components like the fuel elements and the core support blocks. The sensitivity analysis showed that an increase of the tolerance from 2 to 40 ppm results in a reduction of plant downtime by about 1 day.

Potential improvements identified as a result of this analysis are listed in Table 2.14-1. All the items in this table could improve the HTGR system by reducing potential unavailability caused by moisture ingress accidents. The moisture prevention area has the most potential for reducing the plant availability loss. Design improvements have already been made in the new main circulator service system design to prevent bearing water inleakage. Substantial progress can also be made in the reduction of the plant downtime rate if an alternative steam generator tube design with a lower rate of pinhole-type failures is developed.

Several design solutions are available for improving moisture removal from the PCRV. However, no one design feature is adequate or free of added

TABLE 2.14-1
POTENTIAL IMPROVEMENTS IDENTIFIED IN MOISTURE SENSITIVITY ANALYSIS

Prevention Area

1. Provide steam generator and CAHE tube design features for reducing the likelihood of pinhole failures.
2. Test the circulator service system to determine common mode and common cause failures of components affecting the water leak under all conditions.
3. Improve instrumentation and control for rapid isolation and leak termination.

Detection Area

1. Increase the sensitivity and accuracy of moisture monitors and reduce the detection time of a slow leak such as pinhole leaks.
2. Develop and incorporate a puddle detector.
3. Develop and test moisture detection and loop shutdown logic.
4. Develop a CAHE water leak detection system.
5. Use a separate moisture monitoring system for each loop.

Removal Area

1. Incorporate water catch basins.
2. Install dry helium purge lines beneath the catch basins and the thermal barrier regions with stagnant coolant.
3. Incorporate water shedding thermal barrier designs.
4. Increase the helium purification system dryer capacity.
5. Design a provision for vacuuming the PCRV.
6. Design a means of heating liner cooling water.

Moisture Tolerance Area

1. Use oxidation resistant graphite for the affected components.

complexity. Although the probability may be low, the possibility of water ingress during the main loop or plant shutdown cannot be completely eliminated. Water spilled without the normal helium flow tends to flow down and accumulate at the low end of the PCRV cavities and soak the thermal barriers. To prevent this situation, installation of water catch basins is recommended for these areas. In order for the water collection to be effective, a water shedding thermal barrier design should be adopted. Use of the catch basin requires installation of drain lines and puddle-detecting instruments.

Vacuuming the PCRV is another method of removing moisture from the stagnant thermal barrier areas. Moisture removal by vacuuming must proceed with heating of the liner cooling water in order to supply heat of evaporation. Vacuuming is generally time-consuming because adequate core cooling must precede depressurization, which alone takes 18 hr.

Installation of dry helium injection lines to purge the thermal barriers in the stagnant cavity bottoms appears to be an expedient method.

Among the potential improvements listed in the Table 2.14-1, the following four design changes appear to be the most cost-effective, and further study of their design impacts is therefore recommended:

1. Steam generator tube redesign to reduce pinhole failure rate.

2. Development of automatic moisture detection and loop shutdown logics for slow moisture ingress accidents such as small pinhole leaks.

3. Installation of dry helium injection lines to purge stagnant thermal barrier areas.

4. Increasing moisture tolerance by employing oxidation-resistant graphite for critical components.

2.15. MAIN CIRCULATOR DESIGN (6032210201)

2.15.1. Scope

The scope of this task includes the design and analysis effort required (1) to establish the detailed aerodynamic performance of the helium compressor, (2) to summarize the improvements made in the helium/water shaft seal system features and the detailed design layout of the main loop shut-off valve, including its override actuation and position indication systems, and (3) to continue liaison with the electric motor manufacturer to assure mechanical integration of the electric motor drive with the circulator.

2.15.2. Discussion

2.15.2.1. Main Circulator Performance. The aerodynamic performance of the main circulator was calculated for design conditions to satisfy the latest NSSS thermal performance envelope. A detailed aerodynamic analysis was also conducted for the design and off-design conditions utilizing the PREDM computer program for centrifugal compressor performance evaluation (Ref. 2.15-1). An evaluation was made of the effects of the impeller blade exit angle change on the compressor adiabatic efficiency utilizing the constant impeller blade trim shown in Fig. 2.15-1. The effect of blade exit angle is shown in Fig. 2.15-2, which indicates the change in efficiency and the required compressor speed. In addition, an evaluation was made of compressor efficiency change over the wide flow range for vaned and vaneless diffusers. As shown in Fig. 2.15-3, the peak efficiency is higher for the vaned diffuser over the narrow flow range, while the vaneless diffuser exhibits more uniform efficiency over the wide flow range. The vaned diffuser design is the most likely candidate in view of the decrease in the degree of uncertainty in core and steam generator pressure drop predictions as well as the substantial gain in overall compressor efficiency with this design.

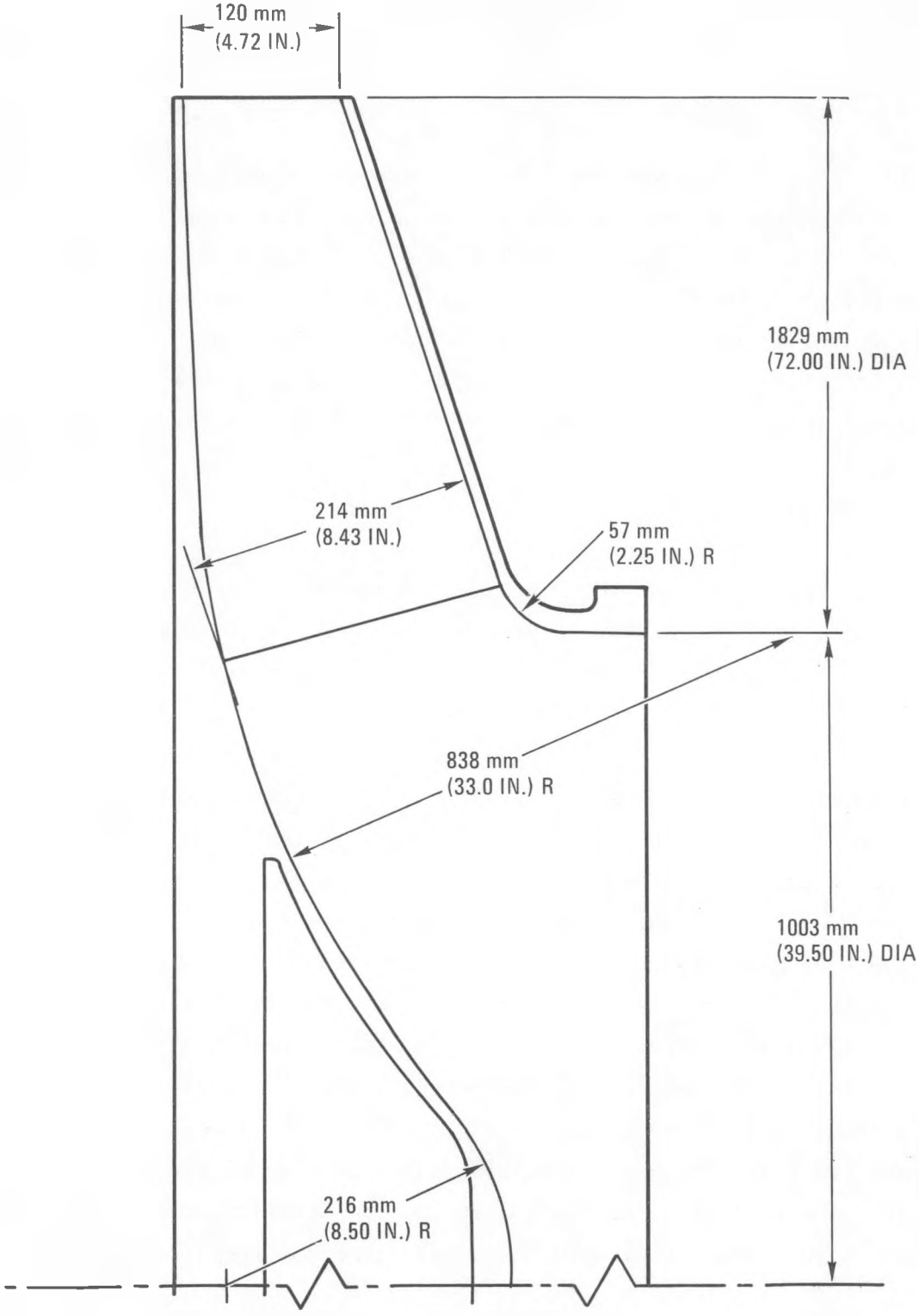

Fig. 2.15-1. Impeller design with constant blade trim

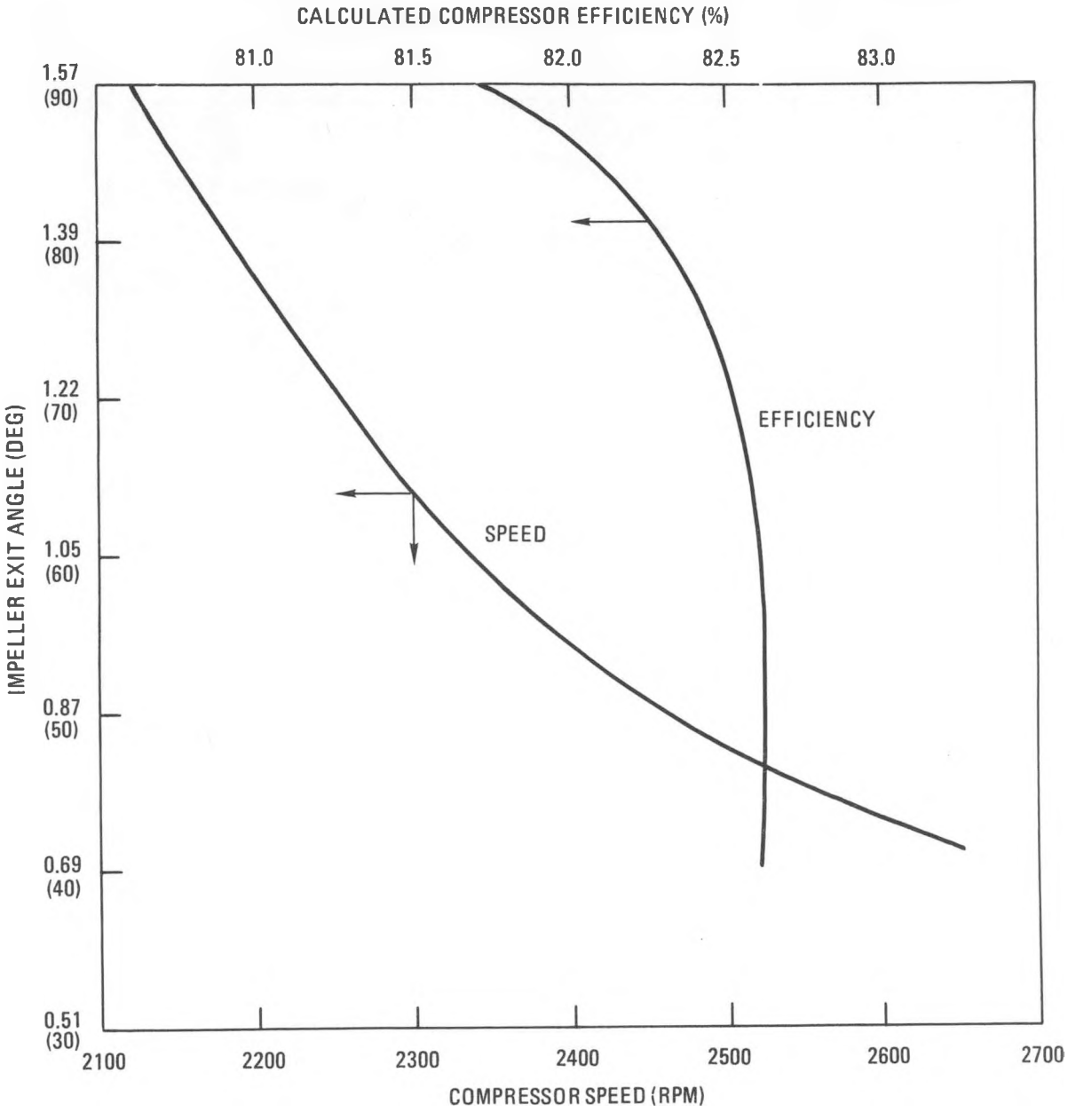

Fig. 2.15-2. Compressor efficiency versus blade exit angle

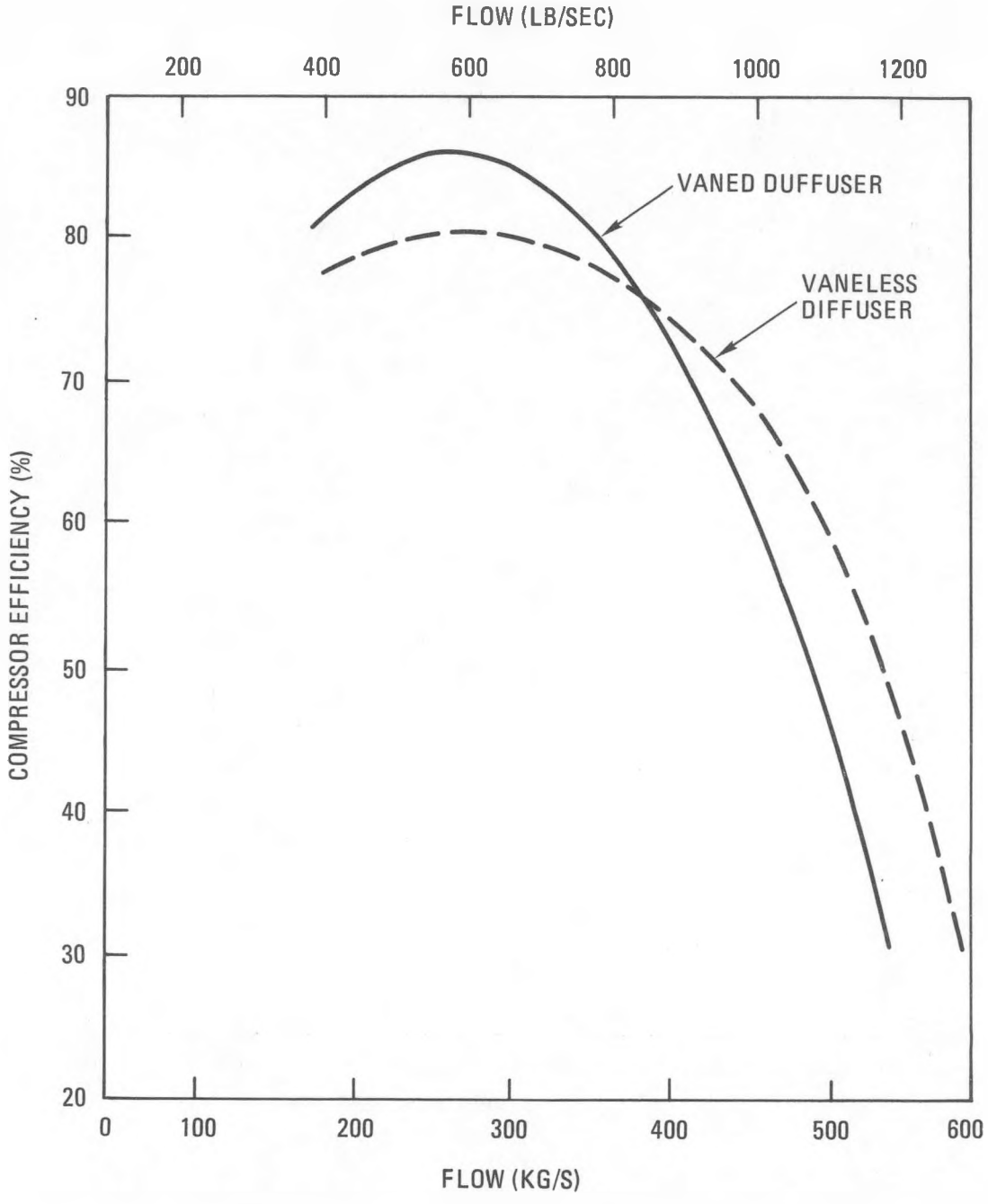

Fig. 2.15-3. Effect of vaned and vaneless diffusers on compressor efficiency

The compressor pressure ratio flow map is shown in Fig. 2.15-4. The design point was selected to satisfy the highest pressure ratio based on margins established for the core and steam generator pressure losses. The compressor surge margin at the design point is equal to 27% of the full flow at 2354 rpm.

2.15.2.2. Water Ingress Prevention. A study was made to describe and summarize progress made in solving the problem of water ingress into the reactor primary coolant flow. The study was concentrated on the problem of water egress from the main helium circulators and the solutions that will minimize the potential for water egress in terms of frequency of occurrences and the quantity of water injected into the primary coolant.

The circulators for the HTGR-SC/C plant use water bearings and are electric-motor-driven. Operating experience at FSV and in test loops has proven the reliability of the water bearing concept. However, operational upsets in the water bearing and seal system have resulted in the introduction of water into the FSV reactor environment. An improved water bearing and seal system has been designed and will undergo testing. This system will be used in the HTGR-SC/C circulator and will significantly minimize the water ingress problem associated with the FSV design.

Design work to "harden" the circulator seal design against water egress has progresses in two areas:

1. Circulator machine design in the area of bearings and seals.

2. A circulator service system that provides water lubrication and and buffer helium flows to the circulator bearings and seals.

Each of the four circulators for the 2240-MW(t) HTGR-SC/C plant has its own separate bearing and seal system.

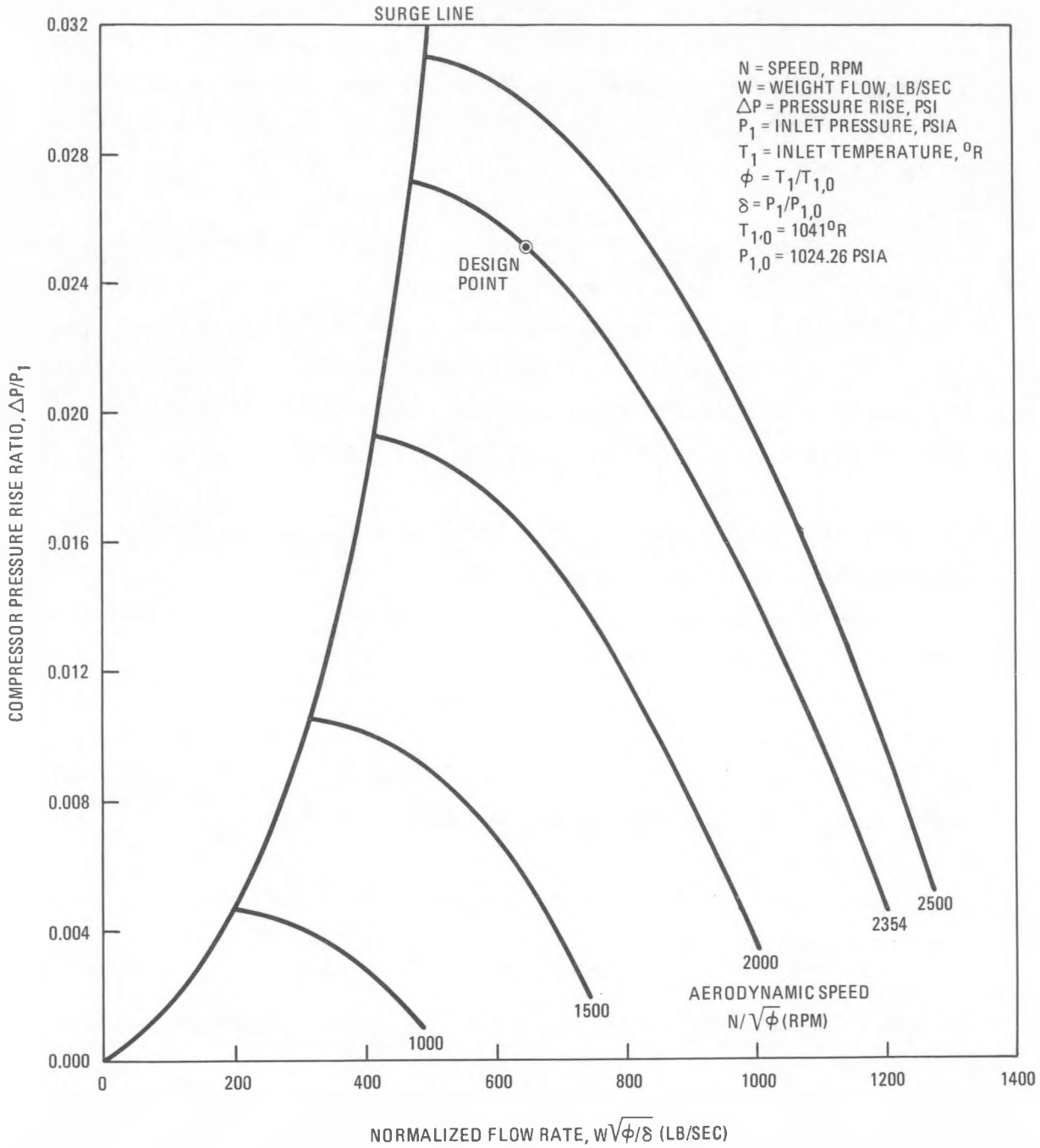

Fig. 2.15-4. Main compressor calculated performance

The study included one complete circulator and the accompanying service system. Interaction between individual circulators and associated systems is minimal in terms of their bearing and seal functions. Therefore, the results of this study apply equally to each independent circulator/service system loop.

Figure 2.15-5 shows the latest circulator helium/water seal configuration. Figure 2.15-6 is a pressure and flow diagram of the circulator service system that incorporates the seal shown in Fig. 2.15-5. Results of a service system functional analysis indicate that the current design is highly resistant to water ingress into the reactor helium. With the exception of catastrophic failure of the circulator, water ingress is possible only through multiple failures or malfunctions of system components.

The new design is less complex than the FSV circulator service system, having few active controls, and is much more effective in preventing water ingress. This improvement is achieved by using an integral shaft-mounted bearing water pump and slinger seal, the redundant drain cavity scavenging pumps, and separate service systems for each circulator and by eliminating the need for high-pressure water accumulators and the back-up bearing water system.

2.15.2.3. Main Loop Shut-Off Valve. Important details of the valve design had previously been developed. Figure 2.15-7 shows the overall valve layout and integration with the circulator. This design also includes provisions for the remote handling and reinstallaton of the valve into the reactor cavity. Figure 2.15-8 shows the detailed layout of the light-actuated valve position indicator system. Figure 2.15-9 shows the details of the remote disconnect of the pneumatic lines used for the override valve actuation and the light transmission fiber optical lines. Layout details of the valve plate hinges and the location of fiber optics lines and secondary indicator lines have been completed.

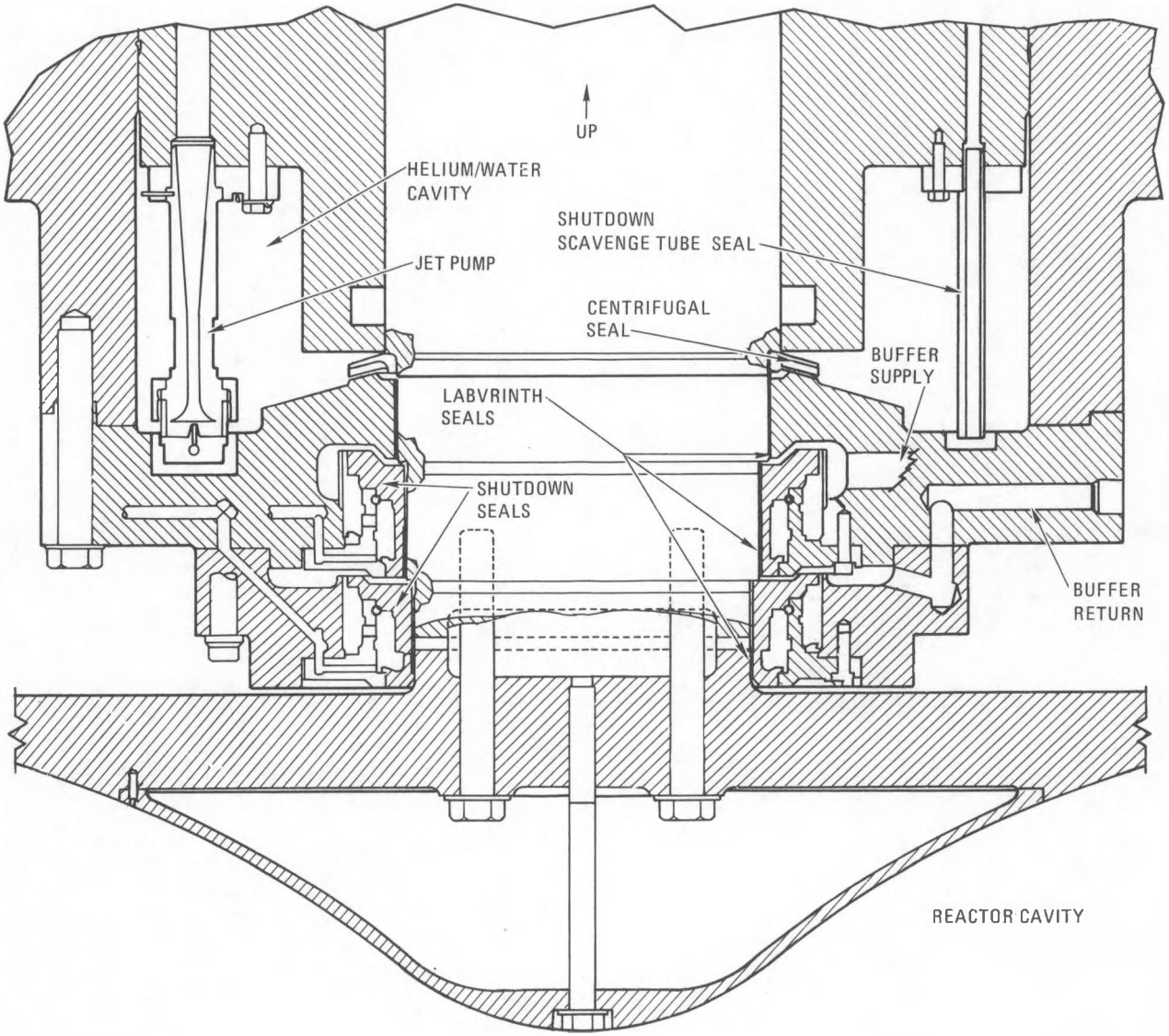

Fig. 2.15-5. Main circulator shutdown seal configuration

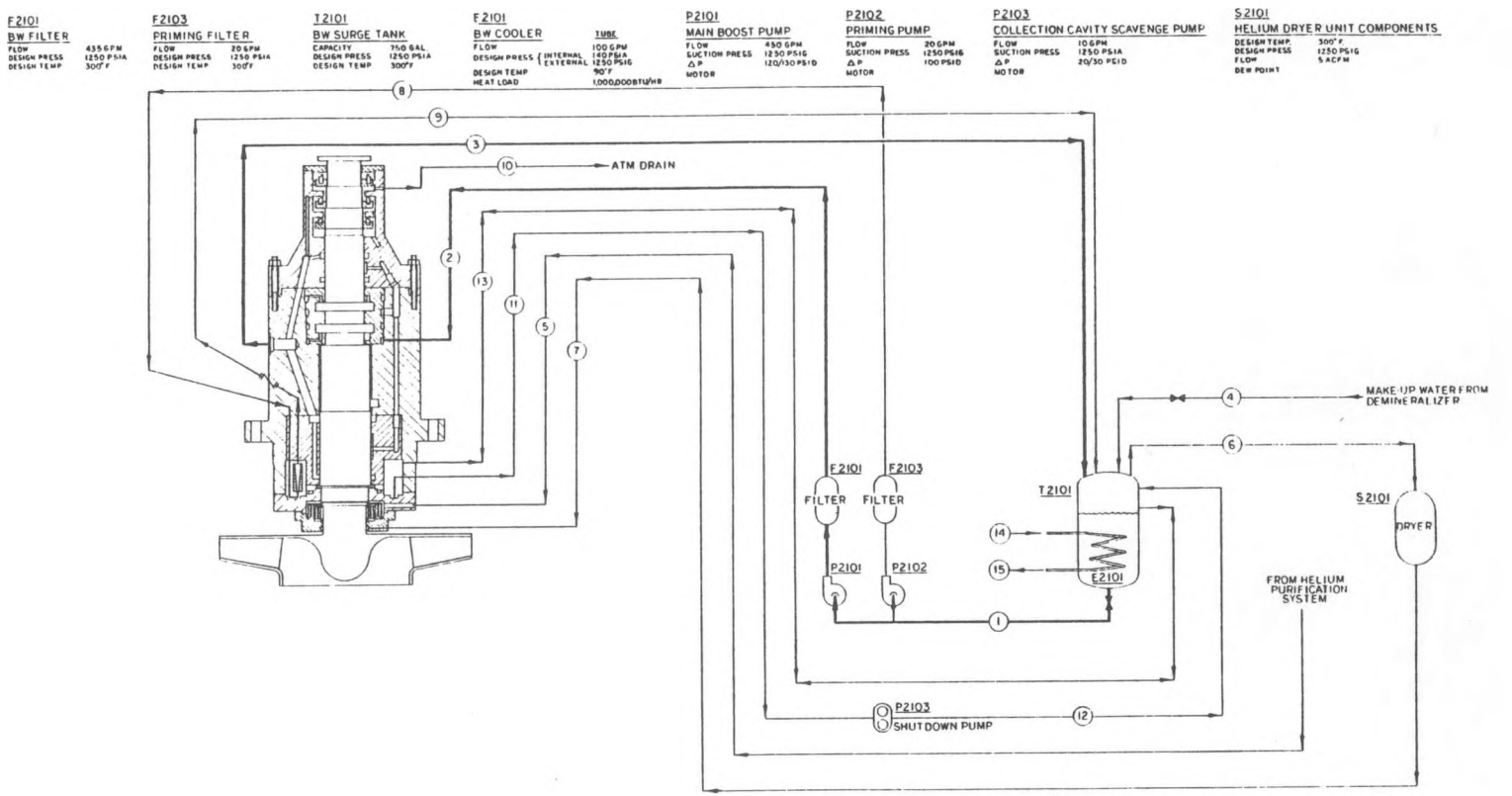

CASE	STREAM Nº	1	2	3	4	5	6	7	8	9	10	11	12	13	14	15
NORMAL	FLOW LB/HR (GPM)	(450) WATER	(450) WATER	(438) WATER	(2) WATER	200 HELIUM	80 HELIUM	80 HELIUM	(15) WATER	(25) WATER	(2) WATER	(10) WATER	(10) WATER	120 HELIUM	(135) WATER	(135) WATER
	ACFM	58.55	58.55	58.55	.26	5	2	2	2	3.34	.26	1.34	1.34	3	18.05	18.05
	PRESSURE PSIA	1050	1170	1050	1050	1051.5	1050	1050	1150	1050	14.7	1050	1055	1050	100	95
	TEMP °F	125°	125°	130°	130°	130°	130°	130°	125°	130°	140°	130°	130°	130°	105°	120°

Fig. 2.15-6. Pressure and flow diagram of circulator service system with seal configuration shown in Fig. 2.15-5

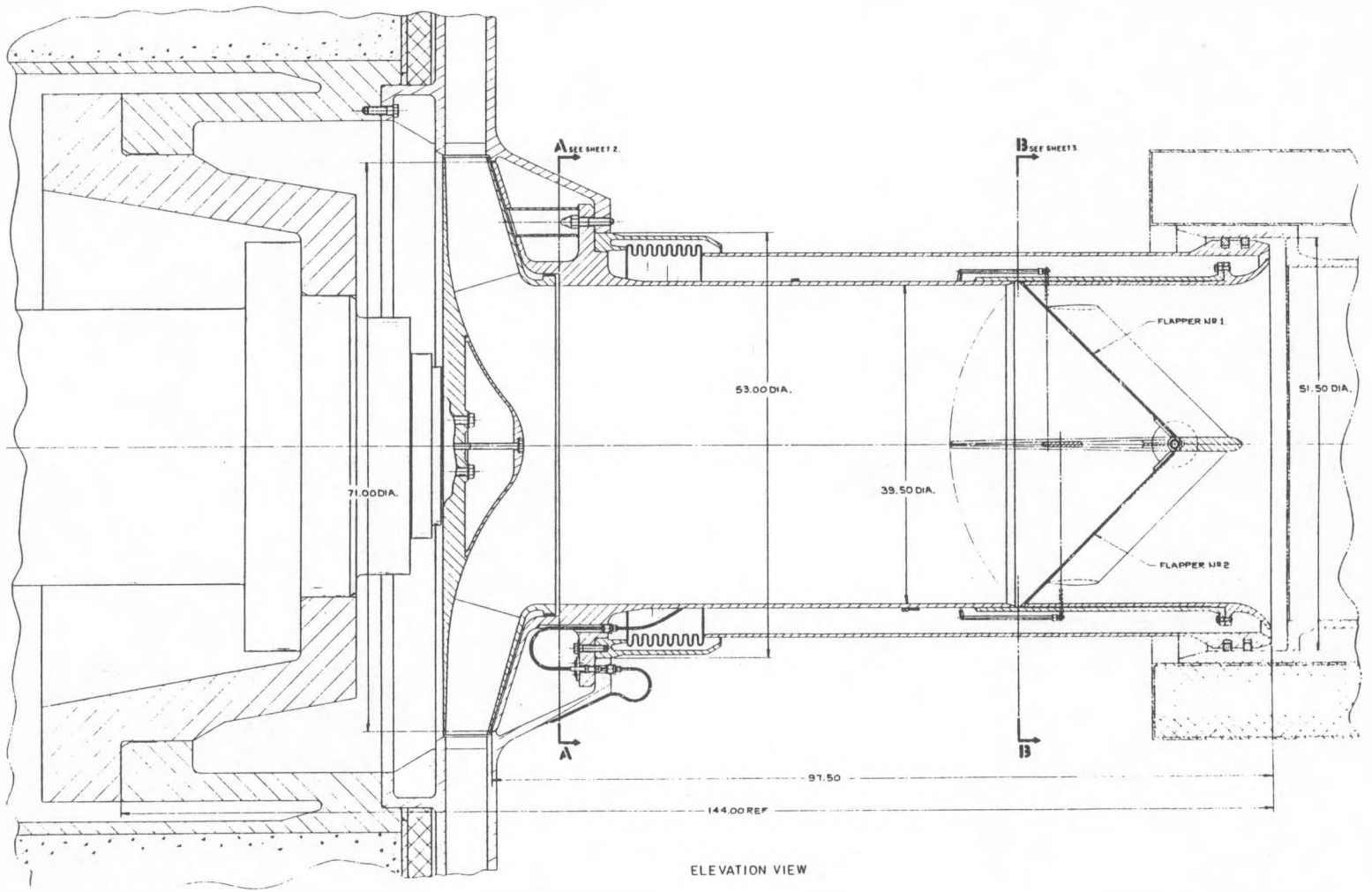

Fig. 2.15-7. Main loop shut-off valve layout

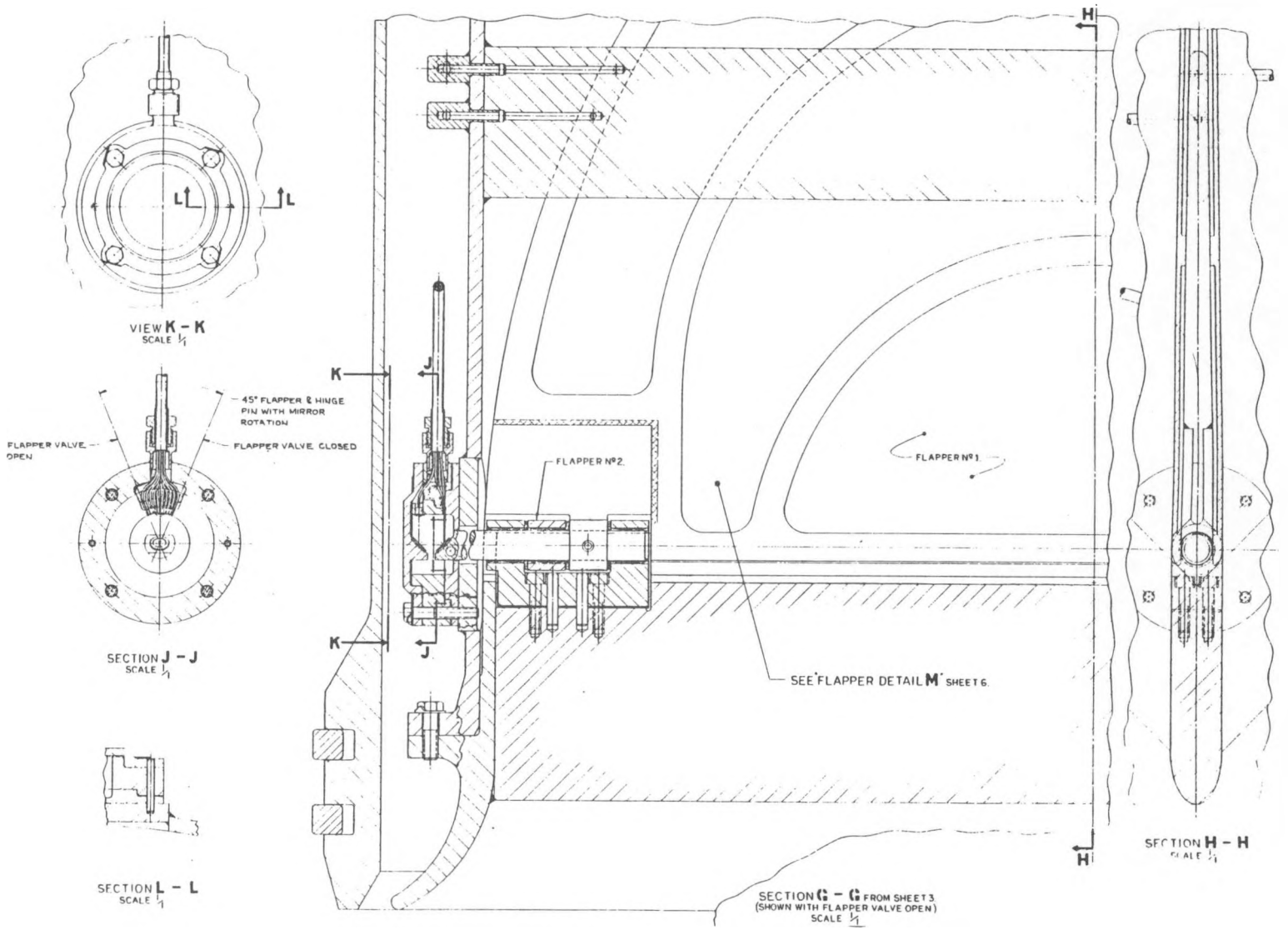

Fig. 2.15-8. Layout of position indicator system for main loop shut-off valve

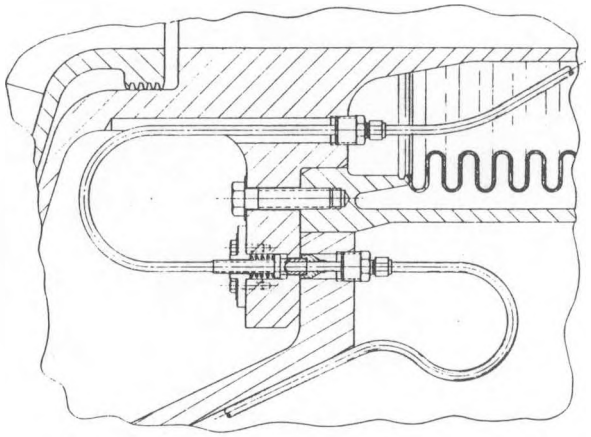

SECTION C – C FROM SHEET 2.
(VIEW ROTATED)

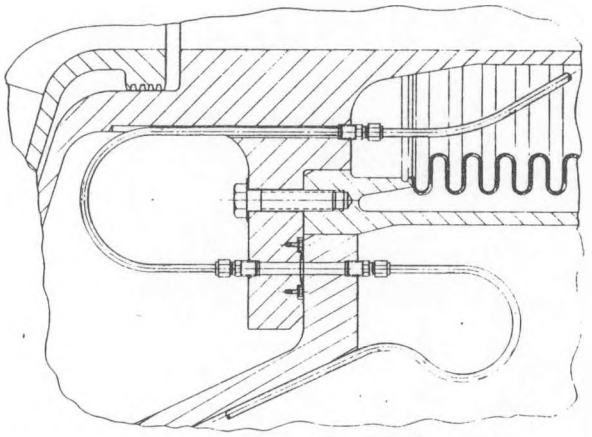

SECTION D – D FROM SHEET 2.
(VIEW ROTATED)

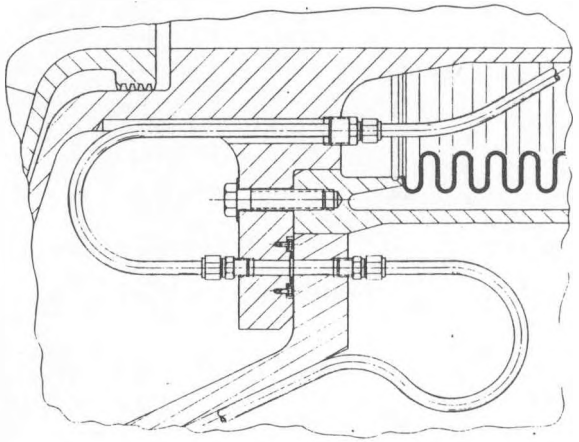

SECTION E – E FROM SHEET 2.
(VIEW ROTATED)

Fig. 2.15-9. Layout of remote disconnect of pneumatic lines for override valve actuation and light transmission fiber optical lines

A layout drawing of the valve flapper blade has been prepared using the CAD/CAM drafting technique. This design information will be used for the valve dynamic analysis methods development task planned in the FY-83 HTGR Technology Program. Figure 2.15-10 shows the single flapper blade configuration.

2.15.2.3. Electric Motor Liaison. Integration of the electric drive motor with the circulator has progressed in the mechanical area by addressing the motor critical speed and the axial shaft growth problem and its effect on the location of the motor thrust bearing. The motor conceptual design study (Section 2-16.2.2) has established the motor configuration as a four-pole, 2400-rpm, 11.3-MW (15,200-hp), three-phase, synchronous variable speed motor proposed by GE. The thrust bearing is currently located at the top of the motor. Further work planned for FY-83 in the areas of the circulator bearings and seals will firm up the acceptable thermal growth values that may affect the thrust bearing location.

Reference

2.15-1. Northern Research and Engineering Corporation Report No. 908AXA-1.

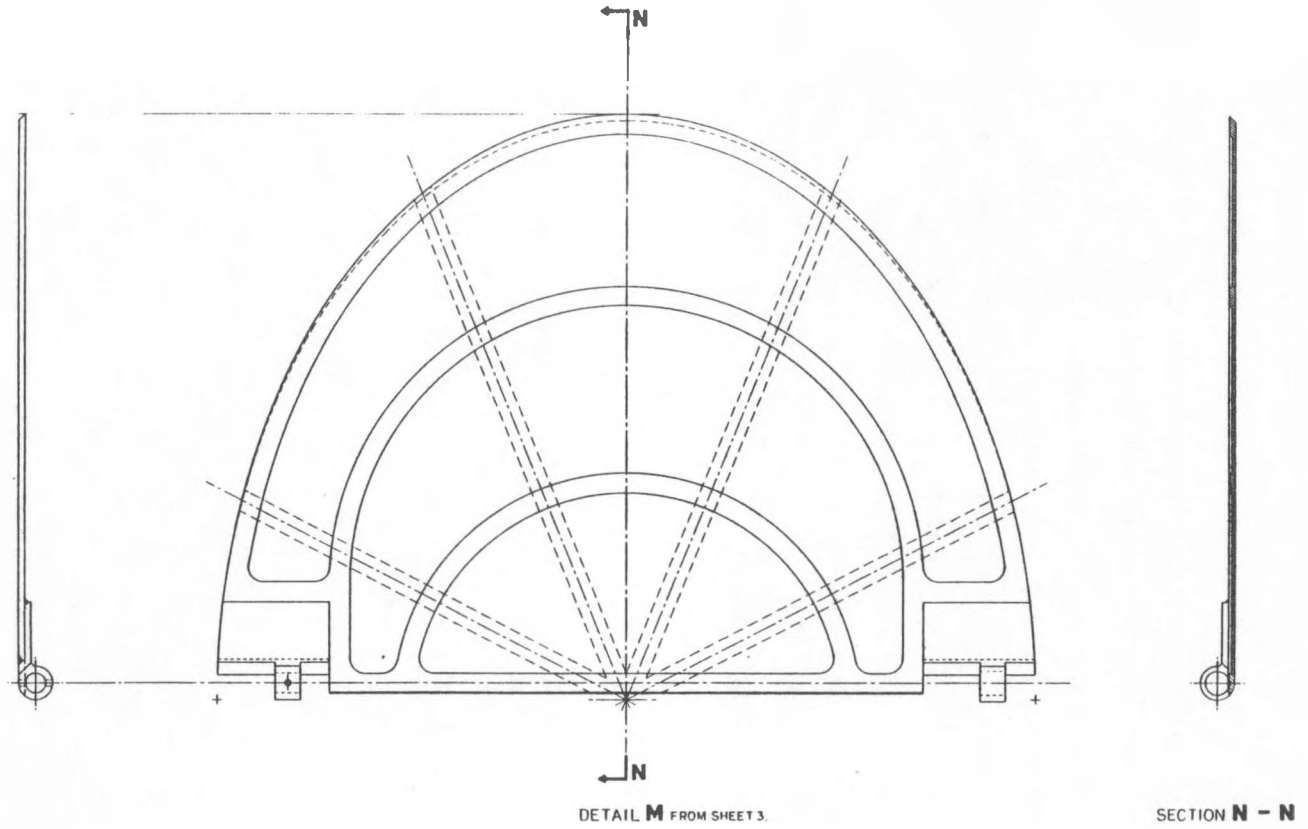

Fig. 2.15-10. Single flapper blade configuration for main loop shut-off valve

2.16. MAIN CIRCULATOR DRIVE SYSTEM (6032210202, 6032210203)

2.16.1. Scope

The scope of work for these tasks consisted of (1) developing and documenting the design specification for the main circulator drive motor and (2) reforming a conceptual design study for the main circulator drive motor.

2.16.2. Discussion

2.16.2.1. Circulator Motor Design Specification. The specification for the main helium circulator electric motor was completed, and the major requirements are summarized below.

A 2240-MW(t) HTGR plant has four main helium loops, each supplied with a main helium circulator. Drive power for these circulators will be provided by vertically mounted, variable speed electric motors. The helium circulators are located within the PCRV and the motors are external to the PCRV. A rotating shaft seal system isolates the containment environment from the reactor atmosphere.

The electric motor will be a synchronous type, equipped with a shaft-mounted brushless-type exciter. This motor will be capable of starting from zero speed synchronously to operate continuously at any speed from 100 to 2400 rpm. The maximum drive power occurs at 2400 rpm, at which point the circulator will require 11.3-MW (15,200 hp) from the motor.

Electric power for the motor will be provided from a variable frequency solid-state power supply on a constant-volts-per-cycle basis.

Operating conditions for the motor will include a temperature range of 18° to 65°C (65° to 150°F) and a relative humidity range of 2% to 80%.

The motor will be a totally enclosed machine, and the internal circulating cooling air will exchange its heat to an air-to-water heat exchanger. Cooling water to this heat exchanger will be provided at a maximum temperature of 35°C (95°F) and a maximum pressure of 0.86 MPa (125 psi).

Motor insulation for the described conditions of load and cooling will be designed for a minimum of 40 yr. Design requirements demand that adverse effects of electromagnetic interference and harmonic heating be minimized. In addition, the motor shaft design must minimize vibration response at any critical speeds within 0% to 115% of the speed range.

Mechanical brakes will be provided with the capability of stopping the rotating assembly from 10% of rated speed in 10 s. This brake system is required to perform 200 cycles of stopping from these conditions without maintenance.

Instrumentation and protective devices are required to ensure that proper operating, monitoring, and protection functions are provided during all modes of motor operation. These components will be compatible within the environmental conditions in which they are applied.

The main circulator motor with its associated components and interfacing systems is classified as non-Class 1E and non-seismic Category I. Since this motor is important from a plant availability standpoint, it will have to meet certain QA requirements.

2.16.2.2. Circulator Motor Design. A conceptual design study of the main circulator motor was performed by GE for GA. The principal findings are summarized below.

The feasibility of building an 11.3-MW (15,2000-hp), four-pole, 100-to 2400-rpm, three-phase, 80-Hz, synchronous-type drive motor for the 2240-MW(t) HTGR main helium circulator appears promising. This motor would

be vertically mounted and equipped with an induction generator type of exciter coupled to the top end of the motor drive shaft.

Electric power for the motor is expected to be provided from a 12-pulse, inverting, solid-state, variable frequency, constant-volts-per-cycle supply.

Preliminary outline and assembly drawings of the conceptual motor design have been prepared.

Field poles for the motor will be salient poles of the solid pole type that are bolted onto the shaft. Several types of pole designs were analyzed, and for the conceptual design the bolted pole design appears best from a manufacturing and mechanical integrity standpoint.

The shaft assembly was analyzed with the major components mounted in the following order from the top: exciter, thrust bearing, motor, and mechanical brake. For four different conditions of assumed structural stiffness and mass along with bearing stiffness and damping, it was determined that two critical speeds existed for each case within the operating range of 100 to 2400 rpm. Three of the four cases show feasibility because of the attenuation in vibration due to damping at the critical speeds. The first shaft bending mode was determined to be fairly constant at about 3350 rpm for the different cases examined. This critical speed point is considered to be far enough above the maximum speed of 2400 rpm not to cause any vibration problems.

Excitation will make use of a specially designed induction generator as the exciter. The induction machine acts as a transformer at zero speed and hence provides excitation to the motor field down to and including zero speed.

Motor insulation is proposed to be Class F insulation, which has an allowable hot spot temperature of 155°C (311°F). By designing the motor to operate within Class B insulation conditions, which include an allowable hot spot of 130°C (266°F), sufficient margin is provided to assure attainment of more than the 40 yr insulation life.

2.17. STEAM GENERATOR (6032210301, 6032210302)

2.17.1. Scope

The GA work scope for this reporting period primarily involved (1) the transfer of the steam generator design technology to CE, including familiarization and training of CE technical personnel, and (2) completion of certain technical aspects of the component design that had been initiated by GA.

The CE work scope for the reporting period (performed under WBS-6032210302) included (1) continuation of design justification analyses, (2) preparation of assembly, subassembly, and reference drawings, (3) generation of cost data, (4) review of GA's past studies related to the superheater tubesheet, and (5) transfer of related technology.

2.17.2. Discussion

During this period, the transfer of analytical methods entailed the training of CE technical personnel at GA in the use of several applicable computer codes and the tansmittal of users' manuals and code tapes to CE. The transferred codes were C-STRES (helical bundle structural analysis), NUSIZE (heat exchanger sizing), and SUPERHEAT (thermal performance and static stability).

Software transfer involved the revised steam generator design specification (Issue 2) and the revised general arrangement drawing.

Technical progress by GA consisted of a thermal resizing of the Mark IV-A steam generator to incorporate tube bundle design changes and performance specification revisions and a reanalysis of the thermal stresses in the tube support structure. These tasks were performed jointly with CE. A

slight height increase was required as a result of the sizing study. A tube support structure design with eight support plates was found to be necessary owing to stress considerations. A new steam generator envelope drawing was prepared to incorporate these changes.

The SUPERHEAT code for analyzing detailed thermal-fluid performance and static boiling stability was modified to include a detailed model of the straight tube superheater (STSH). The model represents multitube, multi-channel heat transfer and fluid flow including two-dimensional shell-site flow. The code was used to examine the effectiveness of the Mark IV-A STSH, and it was shown that the bundle was undersurfaced by about 8% owing to inlet and outlet flow maldistributions. This effect was accounted for in bundle resizing.

The areas selected by CE for concentration of efforts relate to design justification analyses, which were determined by the time and funding available and by the priority of need to resolve interface questions. Areas addressed included: thermal sizing using the prescribed baseline zero design conditions; assessment of heat loss between the STSH and the EES and the steam generator outlet/gas return flow annulus; thermal stresses in the EES and STSH tube support components; and seismic load carrying capability of the structural elements (shrouds).

Drawings were completed for the baseline zero general arrangement, the EES subassembly (Figs. 2.17-1a and 2.17-1b), the STSH subassembly (Figs. 2.17-2a and 2.17-2b); the steam outlet subassembly (Fig. 2.17-3), the feedwater inlet subassembly (Fig. 2.17-4), and the transition/closure subassembly (Fig. 2.17-5). These drawings reflect the baseline zero configuration and represent the first of CE's efforts to supply data base drawings. A tubing schematic (Fig. 2.17-6) was also prepared and released to GA for inclusion in the baseline zero data base.

CE also completed a tentative review of past studies which GA performed on the Alloy 800H tubesheet forging, prepared "draft" material purchase specifications, and identified a number of potential tubesheet forging

NOTES

1. THESE SURFACES SHALL BE COATED PER GA SPEC 90599 WITH CHROME CARBIDE PER GA SPEC 901546 COATING SHALL BE .002 - .004 THICK DIMENSIONS AND TOLERANCES APPLY AFTER COATING SURFACE FINISH TO BE 32

REVISIONS			
SYM	DESCRIPTION	DATE	APPROVED

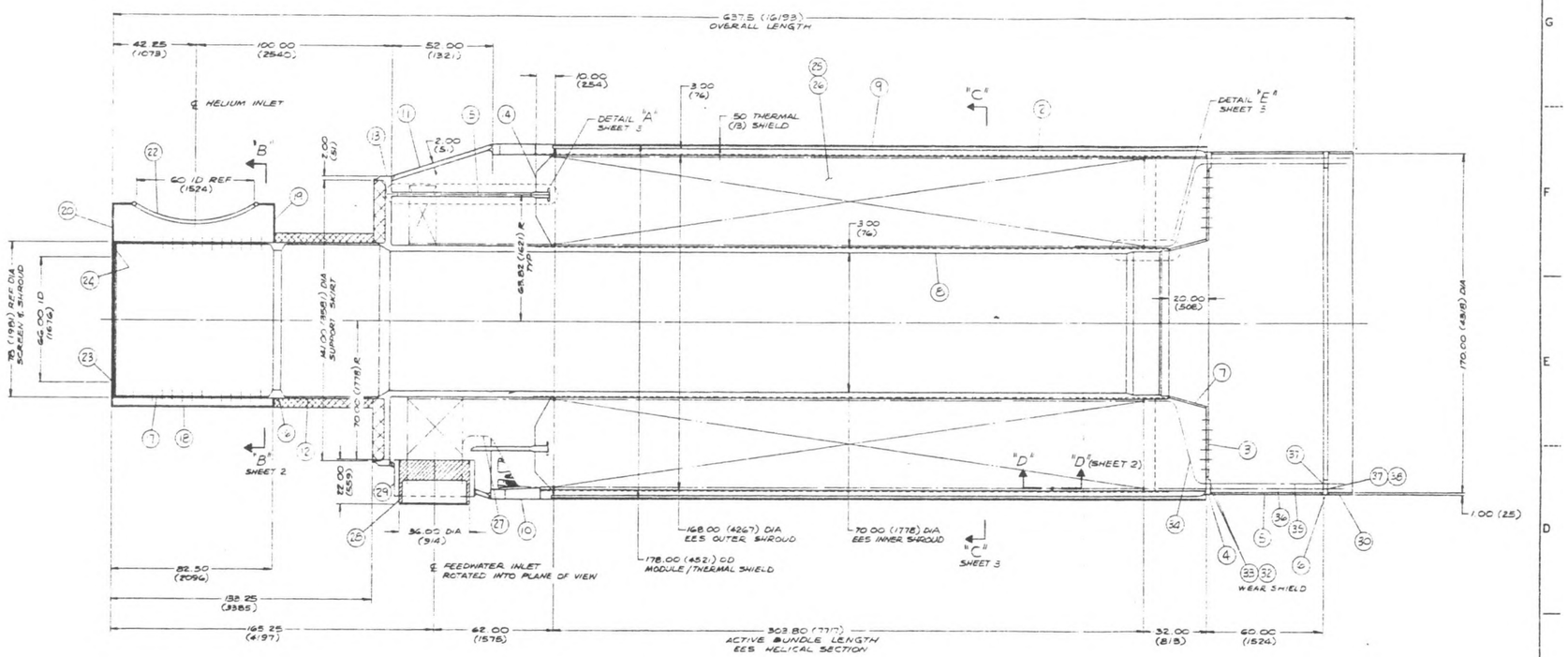

64.001 EES SUB-ASSEMBLY
SCALE 1/20

APPROX DRY WEIGHT; 579,000 LB

WELD TABLE

UNLESS OTHERWISE SPECIFIED

1. DIMENSIONS & TOLERANCES TO USAS-Y14.5 - 1966
2. ALL DIMENSIONS APPLY AT REFERENCE TEMP OF 68°F
3. REF DIMENSIONS ARE FOR INFORMATION ONLY - DO NOT USE FOR FABRICATION
4. MARKING SYMBOLS & STAMPING TOOL LOCATION & INDENT STAMP .03 MAX DEPTH
5. BREAK ALL SHARP EDGES WITH APPROX .03 RADIUS OR CHAMFER
6. MACHINED SURFACES INTERNAL - 250AA OR BETTER EXTERNAL - 500AA OR BETTER
7. SIZES IN L/M ARE FINISHED SIZES - NO ALLOWANCE MADE FOR FABRICATION OR WELD SHRINKAGE
8. TOLERANCE FOR X ± .1 X.X ± .01 X.XX ± .005 ANGLES ± 0.5°
9. SEE REF DWG NO ____ FOR NOT ITEM NO IN WELD TABLE & NOT CALL OUT ON DWG
10. SEE DWG ____ FOR APPLICABLE EQUIPMENT SPECIFICATIONS
11. DOUBLE ARROW INDICATES DIMENSION TO GIVEN REFERENCE LINE
12. DEVELOPED LENGTH IN L/M IS GIVEN ON MEAN CENTERLINE
13. DIMENSIONS SHOWN IN ( ) PARENTHESES ARE IN MILLIMETERS

WELD NUMBER	D W G NUMBER A	NO REQ	NO REQ	NO REQ	NO REQ	NO REQ	NO REQ	UT	CHEM

LIST OF MATERIAL - QUANTITIES FOR

ITEM	ASS'Y NO	PC NO	NO REQ'D	NOMENCLATURE	MATERIAL	MATERIAL SPEC	MATERIAL NOTES

GEOMETRIC TOLERANCES FOR MACHINED SURFACES UNLESS SPECIFIED ON DRAWING

SYM	GEOMETRIC CHARACTERISTIC	TOL
—	FLATNESS	.001" IN
—	STRAIGHTNESS	.001" IN
○	ROUNDNESS	SEE DWG
⌭	CYLINDRICITY	SEE DWG
⌒	PROFILE OF LINE	SEE DWG
⌓	PROFILE OF SURFACE	SEE DWG
∥	PARALLELISM	SEE DWG
⊥	PERPENDICULARITY	SEE DWG
∠	ANGULARITY	SEE DWG
⌖	POSITION	SEE DWG
◎	CONCENTRICITY	SEE DWG
⌯	SYMMETRY	SEE DWG

APPROVALS

ANAL ENGR ____ DATE ____
PROJ ENGR ____ DATE ____

POWER SYSTEMS

EES SUBASSEMBLY

STEAM GENERATOR
2 EA MW, NTGR SCIC STUDY
GENERAL ATOMIC COMPANY

DRN BY DODSON DATE 6-18-82
CHK BY [illegible] DATE 6-21-82

E-PHT-823012-82064-01

SCALE AS NOTED SHEET 1 OF 3

Fig. 2.17-1a. EES subassembly

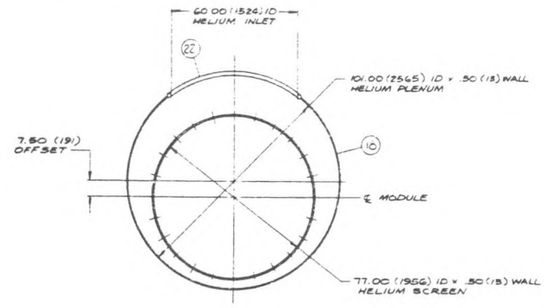

SECTION "B-B"
SCALE: 1/20

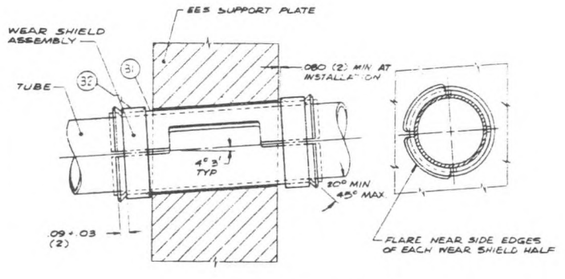

SECTION "D-D"
SCALE: 2/1

DETAIL "A"
SCALE 1/4

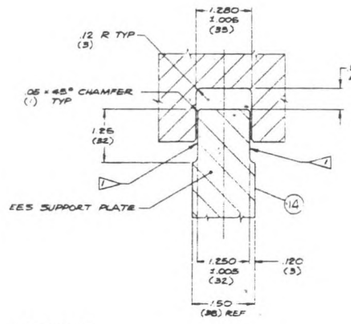

DETAIL "E" (H-3)
SCALE FULL

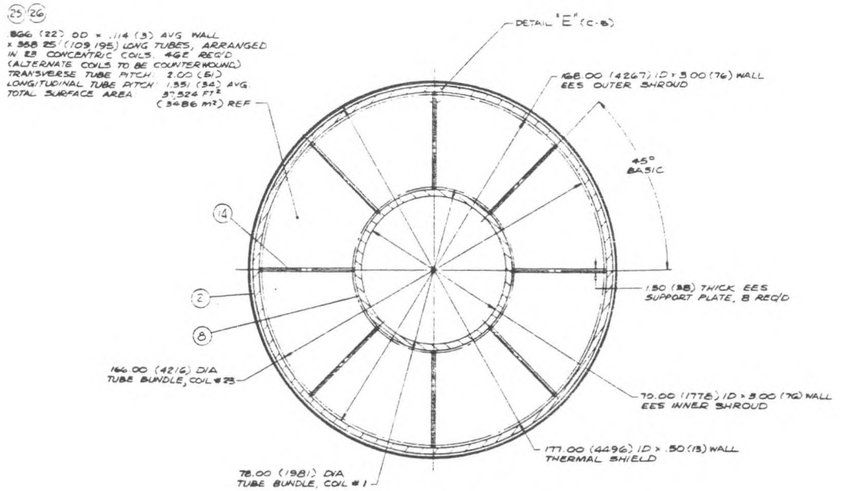

SECTION "C-C"
SCALE 1/20

REVISIONS			
BTM ZONE	DESCRIPTION	DATE	APPROVED

WELD TABLE

WELD NUMBER	D W P NUMBER	NO	PREQ	NO	PREQ	NO	PREQ	NO	PREQ	+P/- CHEM
		PT		MT		RT		UT		

UNLESS OTHERWISE SPECIFIED

1. DIMENSIONS & TOLERANCES TO USAS Y14.5 - 1966
2. ALL DIMENSIONS APPLY AT REFERENCE TEMP OF 68°F
3. REF DIMENSIONS ARE FOR INFORMATION ONLY - DO NOT USE FOR FABRICATION
4. MARKING SYMBOLS, VIBRATING TOOL, LOW STRESS STAMP AS MAX DEPTH
5. BREAK ALL SHARP EDGES WITH RADIUS, STRAIGHT OR CHAMFER
6. MACHINED SURFACES INTERNAL - 250µin OR BETTER EXTERNAL - 500µin OR BETTER
7. SIZES IN L/M ARE FINISHED SIZES - NO ALLOWANCE MADE FOR FABRICATION OR WELD SHRINKAGE
8. TOLERANCE ON X = ± [illegible] INCH; ON X.XX = ± 0.01 UNLESS OTHERWISE
9. SEE PLT DWG NO. _____ FOR HOT ITEM NO. IN WELD TABLE & WELD CALL-OUT ON DWG
10. SEE DWG _____ FOR APPLICABLE EQUIPMENT SPECIFICATIONS
11. DOUBLE ARROW INDICATES DIMENSION TO DRIVEN REFERENCE LINE
12. ON CYCLIC LENGTH IN L/M IS GIVEN ON MEAN CENTERLINE

ZONE	ASS'Y NO	PL NO	NO REQ'D	NOMENCLATURE	MATERIAL	MATERIAL SPEC	MATERIAL NOTES

LIST OF MATERIAL - QUANTITIES FOR

GEOMETRIC TOLERANCES FOR MACHINED SURFACES UNLESS SPECIFIED ON DRAWING

SYM	GEOMETRY	TOL
—	FLATNESS	.001/in
—	ROUNDNESS	.001/in
—	SQUARENESS	.003 DWG
—	PARALLELISM	.003 DWG
—	PERPENDICULARITY	.003 DWG
—	PROFILE OF SURFACE	.003 DWG
—	PROFILE OF LINE	.001/in
—	CONCENTRICITY	.001/in
—	RUNOUT	.003 DWG
—	CIRCULARITY	.003 DWG
—	CYLINDRICITY	.003 DWG
—	TRUE POSITION	.003 DWG
—	TOTAL RUNOUT	.003 DWG
—	SYMMETRY	.003 DWG

APPROVALS

ANAL ENGR	
DATE	
PROJ ENGR	
DATE	

POWER SYSTEMS

EES SUBASSEMBLY
STEAM GENERATOR
240 MWt HTGR SC/C STUDY
GENERAL ATOMIC COMPANY

DWN BY	[illegible]	CHD BY	[illegible]
DATE	6-16-82	DATE	[illegible]

E-PHT-823012-8206A-01

SHEET 2 OF 3

Fig. 2.17-1b. EES subassembly

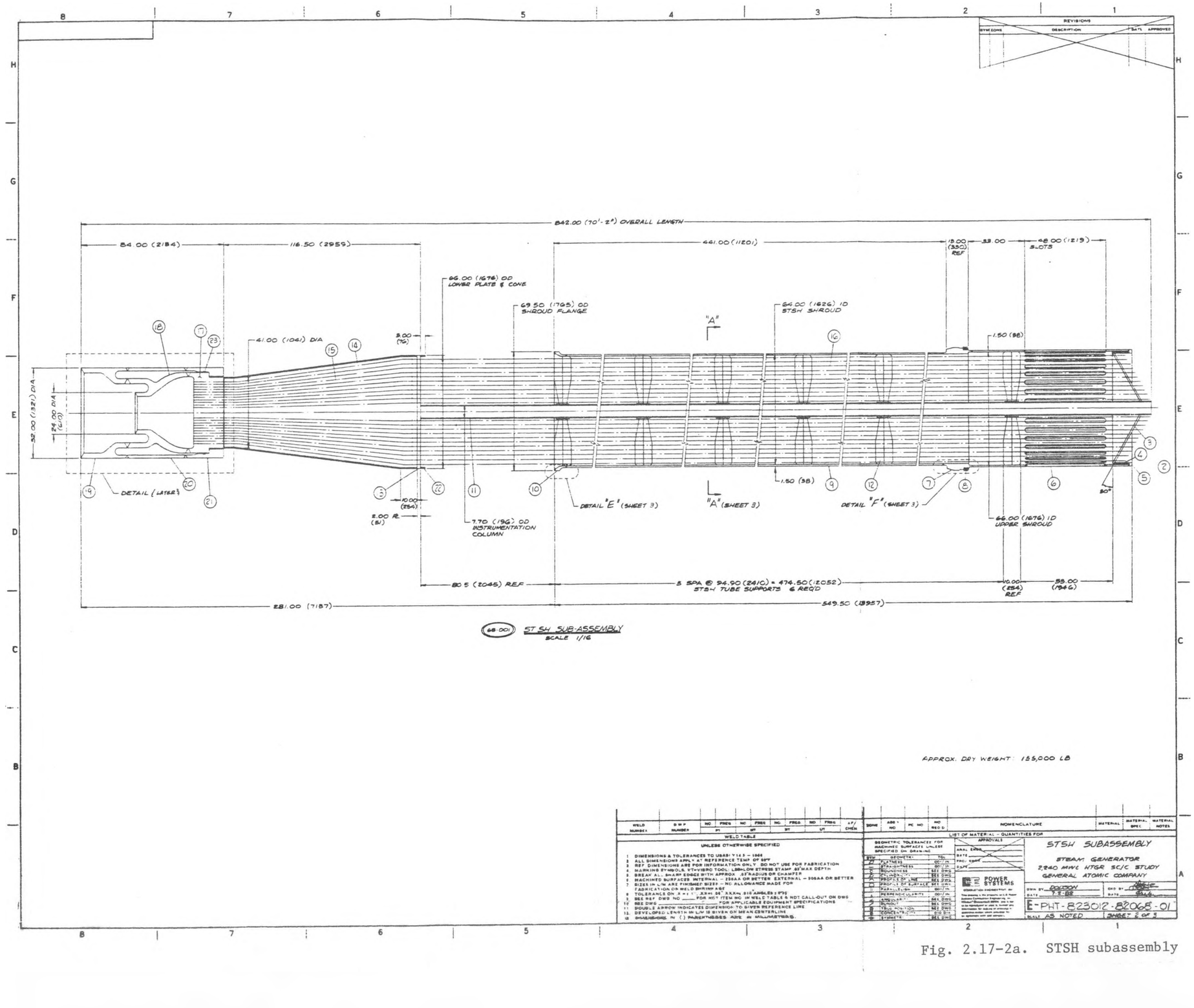

Fig. 2.17-2a. STSH subassembly

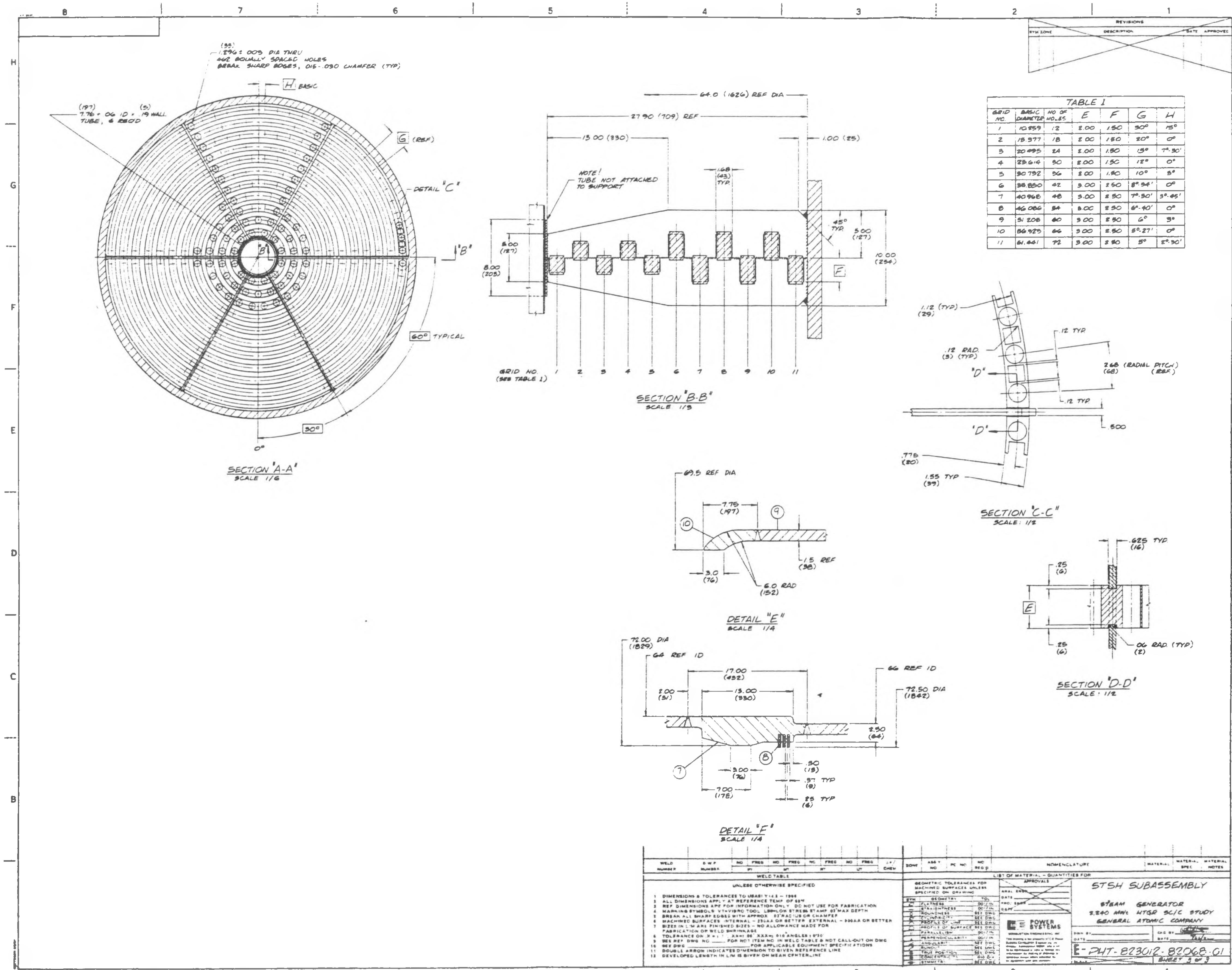

TABLE 1						
GRID NO.	BASIC DIAMETER	NO OF HOLES	E	F	G	H
1	10.859	12	2.00	1.50	30°	15°
2	15.977	18	2.00	1.50	20°	0°
3	20.495	24	2.00	1.50	15°	7°-30'
4	25.614	30	2.00	1.50	12°	0°
5	30.732	36	2.00	1.50	10°	5°
6	35.850	42	3.00	2.50	8°-34'	0°
7	40.968	48	3.00	2.50	7°-30'	3°-45'
8	46.086	54	3.00	2.50	6°-40'	0°
9	51.208	60	3.00	2.50	6°	3°
10	56.325	66	3.00	2.50	5°-27'	0°
11	61.441	72	3.00	2.50	5°	2°-30'

Fig. 2.17-2b. STSH subassembly

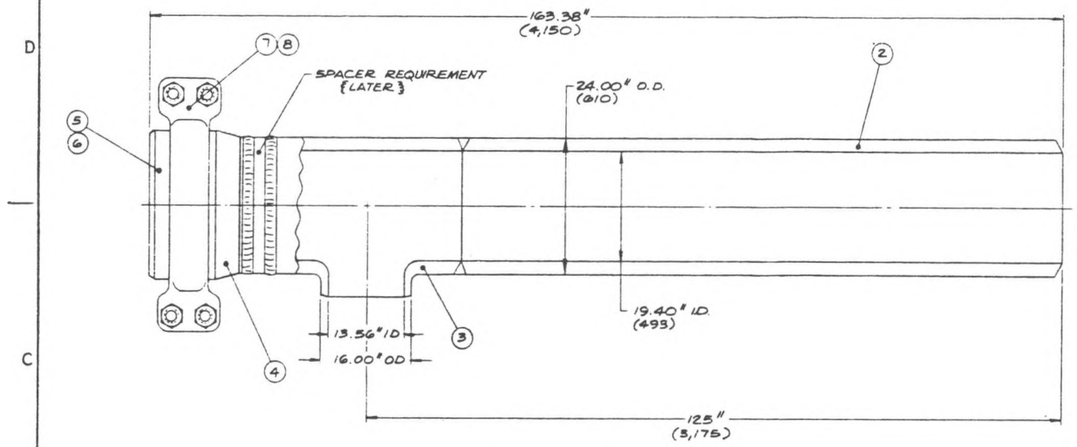

(82-001) STEAM OUTLET SUBASSEMBLY

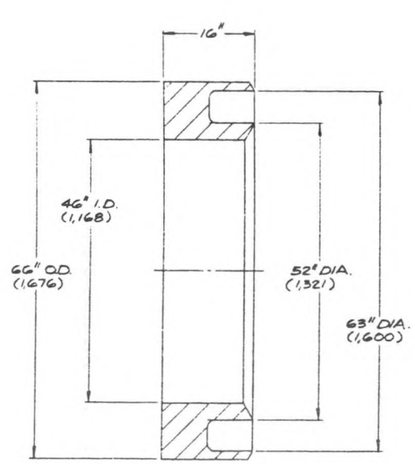

(82-009) TORUS

APPROX. DRY WEIGHT; 17,000 LP

		82-009	1	TORUS, 66" OD x 46" ID x 16" LONG	ALLOY B00H	SB-564		
		008	1	BOLTING, GRAYLOC, 2¼ - BUN	SS			
		007	1	CLAMP, GRAYLOC, 24"	316SS			
		006	1	RING, SEAL, GRAYLOC, 20"	6305S	A151		
✓		005	1	HUB, BLIND, GRAYLOC, 24"				
		004	1	HUB, BUTT WELD, GRAYLOC, 24"				
		003	1	TEE, 24" x 24" x 16"	316 S.S.	SA-403	WP316	
		002	1	PIPE, 24.00" OD x 19.40" ID x 108" LONG	ALLOY B00H	SB-409	GR. 1	
		82-001	1	STEAM OUTLET SUBASSY CONSISTING OF:				
ZONE	ASSY NO	PC. NO	NO REQ'D	NOMENCLATURE	MATERIAL	MATERIAL SPEC	MATERIAL NOTES	

LIST OF MATERIAL - QUANTITIES FOR

WELD NUMBER	D W P NUMBER	NO	FREQ	NO	FREQ	NO	FREQ	NO	FREQ	L/F/ CHEM
			PT		MT		RT		UT	

WELD TABLE

UNLESS OTHERWISE SPECIFIED

1. DIMENSIONS & TOLERANCES TO USASI Y14.5 - 1966
2. ALL DIMENSIONS APPLY AT REFERENCE TEMP. OF 68° F.
3. REF. DIMENSIONS ARE FOR INFORMATION ONLY. DO NOT USE FOR FABRICATION.
4. MARKING SYMBOLS VT=VIBRO TOOL LSS=LOW STRESS STAMP 1/32 MAX. DEPTH
5. BREAK ALL SHARP EDGES WITH APPROX. 1/32 RADIUS OR CHAMFER
6. MACHINED SURFACES INTERNAL - 250AA OR BETTER. EXTERNAL-500AA OR BETTER
7. SIZES IN L/M ARE FINISHED SIZES - NO ALLOWANCE MADE FOR FABRICATION OR WELD SHRINKAGE
8. TOLERANCE ON .X"=±.1", .XX"=±.06", .XXX"=.010" ANGLES ± 0°30'
9. SEE REF. DWG. NO.____FOR NDT ITEM NO. IN WELD TABLE & NDT CALL-OUT ON DWG.
10. SEE DWG. _____ FOR APPLICABLE EQUIPMENT SPECIFICATIONS.
11. DOUBLE ARROW INDICATES DIMENSION TO GIVEN REFERENCE LINE.
12. DEVELOPED LENGTH IN L/M IS GIVEN ON MEAN CENTERLINE.

GEOMETRIC TOLERANCES FOR MACHINED SURFACES UNLESS SPECIFIED ON DRAWING

SYM	GEOMETRY	TOL
⏥	FLATNESS	.001" IN
—	STRAIGHTNESS	.001" IN
○	ROUNDNESS	SEE DWG
⌭	CYLINDRICITY	SEE DWG
⌒	PROFILE OF LINE	SEE DWG
⌓	PROFILE OF SURFACE	SEE DWG
//	PARALLELISM	.001" IN
⊥	PERPENDICULARITY	.001" IN
∠	ANGULARITY	SEE DWG
↗	RUNOUT	SEE DWG
⌖	TRUE POSITION	SEE DWG
◎	CONCENTRICITY	.010 DIA
⌯	SYMMETRY	SEE DWG

DWN. BY DODSON
DATE 5-15-82
CKD. BY
DATE
ANAL. ENGR.
DATE
PROJ. ENGR
DATE 5/11/82

This Drawing is the Property of COMBUSTION ENGINEERING, INC., WINDSOR, CONN. and is not to be reproduced, or used to furnish any information for making of drawings or apparatus except where provided for by agreement with said Company

STEAM OUTLET SUBASSEMBLY
STEAM GENERATOR
2240 MWt HTGR SC/C STUDY
GENERAL ATOMIC COMPANY

CHATTANOOGA | SIZE D | PHT-823012-82082 | REV 00 | SCALE 1/10 | CONT | SHEET 1 OF 1

NEXT ASSEMBLY DRAWINGS	
GENERAL ARRANGEMENT	E-PHT 823301-82061

Fig. 2.17-3. Steam outlet subassembly

REVISIONS				
SYM	ZONE	DESCRIPTION	DATE	APPROVED

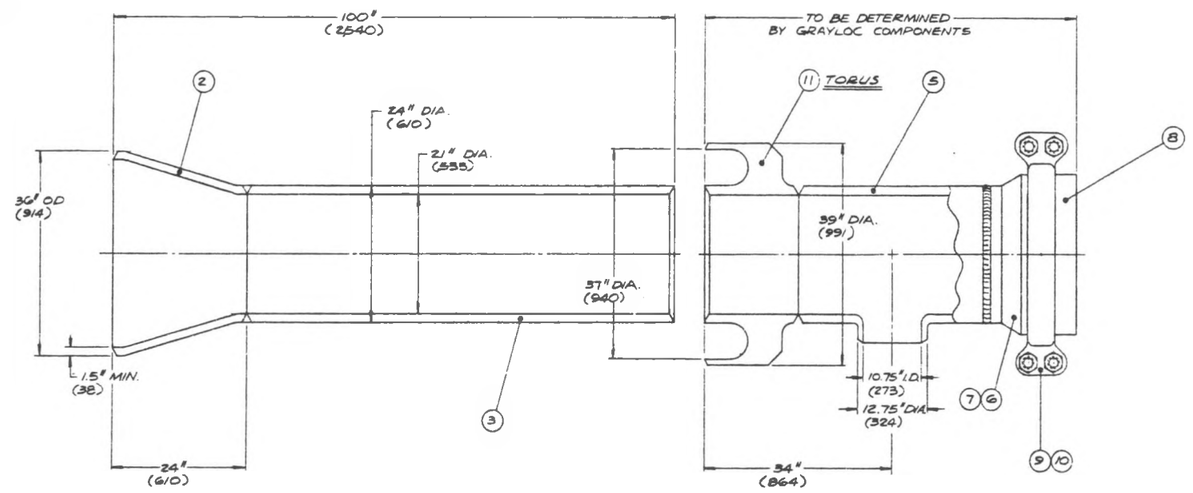

B3-001 FEEDWATER INLET INNER SUBASS'Y

B3-004 FEEDWATER INLET OUTER SUBASS'Y

APPROX; DRY WEIGHT: 9,000 LB

ZONE	ASS'Y NO	PC NO	NO REQ'D	NOMENCLATURE	MATERIAL	MATERIAL SPEC	MATERIAL NOTES
		011	1	TORUS, FW - 39" OD x 21" I.D. x 17" LONG		SA-508A	CL. 1
		010	1	BOLTING - GRAYLOC 24"			
		009	1	CLAMP - GRAYLOC 24"		SA-487	
		008	1	HUB, BLIND - GRAYLOC 24"		SA-105	
		007	1	RING, SEAL - GRAYLOC			
		006	1	HUB, BUTT WELD - GRAYLOC 24"		SA-105	
		005	1	TEE, REDUCING - 24" x 24" x 12"		SA-106	
	004		1	FEEDWATER INLET OUTER SUBASS'Y			
		003	1	PIPE, - 24" OD x 1.5" WALL x 76" LONG			
		002	1	REDUCER, CONC., 36" OD x 24" OD x 1.5" x 24" LG	C.S.	SA-106	
	001		1	FEEDWATER INLET INNER SUBASS'Y			

WELD NUMBER	D W P NUMBER	NO	FREQ PT	NO.	FREQ MT	NO.	FREQ RT	NO.	FREQ UT	OFI CHEM.

WELD TABLE

UNLESS OTHERWISE SPECIFIED

1. DIMENSIONS & TOLERANCES TO USASI Y14.5 – 1966
2. ALL DIMENSIONS APPLY AT REFERENCE TEMP OF 68° F.
3. REF DIMENSIONS ARE FOR INFORMATION ONLY. DO NOT USE FOR FABRICATION.
4. MARKING SYMBOLS VTH VIBRO TOOL LBS = LOW STRESS STAMP 1/32 MAX. DEPTH
5. BREAK ALL SHARP EDGES WITH APPROX 1/32 RADIUS OR CHAMFER
6. MACHINED SURFACES INTERNAL – 250AA OR BETTER EXTERNAL-500AA OR BETTER
7. SIZES IN L/M ARE FINISHED SIZES – NO ALLOWANCE MADE FOR FABRICATION OR WELD SHRINKAGE
8. TOLERANCE ON .X" ± .1, .XX" ± .06 .XXX" ± .010. ANGLES ± 0°30'
9. SEE REF. DWG. NO.___ FOR NOT ITEM NO. IN WELD TABLE & NOT CALL-OUT ON DWG.
10. SEE DWG ___ FOR APPLICABLE EQUIPMENT SPECIFICATIONS.
11. DOUBLE ARROW INDICATES DIMENSION TO GIVEN REFERENCE LINE.
12. DEVELOPED LENGTH IN L/M IS GIVEN ON MEAN CENTERLINE.

GEOMETRIC TOLERANCES FOR MACHINED SURFACES UNLESS SPECIFIED ON DRAWING

SYM	GEOMETRY	TOL
▱	FLATNESS	.001/IN
—	STRAIGHTNESS	.001/IN
○	ROUNDNESS	SEE DWG
⌭	CYLINDRICITY	SEE DWG
⌒	PROFILE OF LINE	SEE DWG
⌓	PROFILE OF SURFACE	SEE DWG
//	PARALLELISM	.001/IN
⊥	PERPENDICULARITY	.001/IN
∠	ANGULARITY	SEE DWG
↗	RUNOUT	SEE DWG
⌖	TRUE POSITION	SEE DWG
◎	CONCENTRICITY	0.8 Dia
⌯	SYMMETRY	SEE DWG

LIST OF MATERIAL – QUANTITIES FOR

DWN BY DODSON
DATE 5-16-82
CKD. BY
DATE
ANAL. ENGR
DATE
PROJ. ENGR
DATE 5/24/82

FEEDWATER INLET SUBASSEMBLY
STEAM GENERATOR
2,240 MWt HTGR SC/C STUDY
GENERAL ATOMIC COMPANY

CHATTANOOGA | SIZE D | PHT823012-82083 | REV 00 | SCALE 1/10 | CONT | SHEET 1 OF 1

NEXT ASSEMBLY DRAWINGS	
GENERAL ARRANGEMENT	E-PHT-L 3012-82061

Fig. 2.17-4. Feedwater inlet subassembly

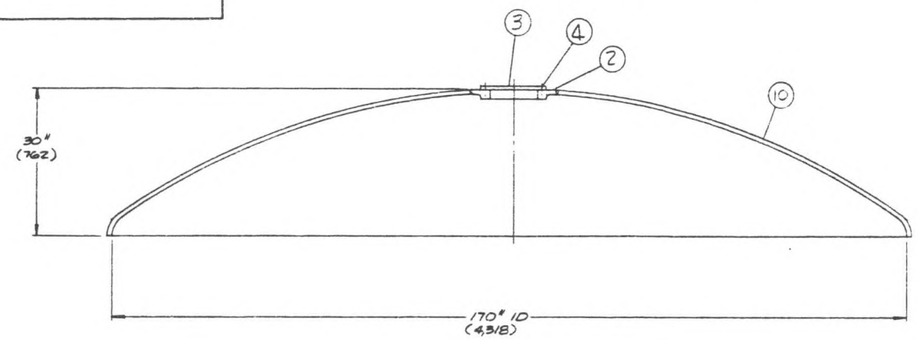

SCALE: 1/12

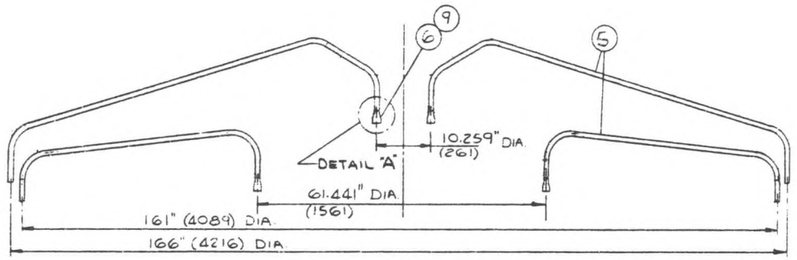

SCALE: 1/12

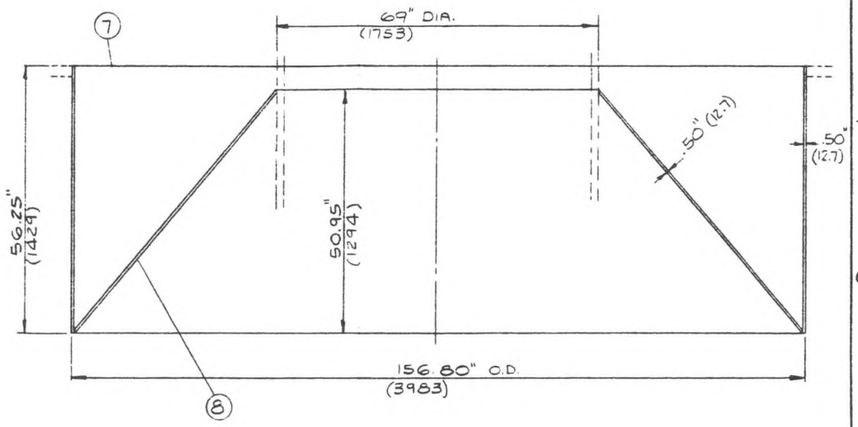

SCALE: 1/12

84-001 TRANS./CLO. SUBASSEMBLY

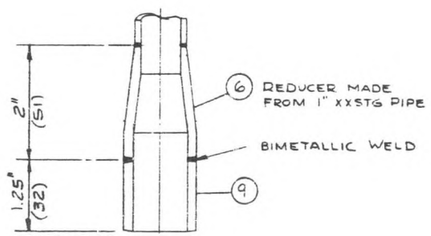

DETAIL "A"
SCALE 1/1

APPROX. DRY WEIGHT; 19,000 LB.

ITEM	ABS'Y NO	PC NO	NO REQ'D	NOMENCLATURE	MATERIAL	MATERIAL SPEC	MATERIAL NOTES
		010	1	TOP HEAD (DISHED) 1" THK.	2¼CR-1MO	SA-387 GR.22	
		009	462	TUBES 1.26" O.D. x .173" WALL x 1.25"	ALLOY 800H	SB-163 GR.	SEE DTL-"A"
		008	1	CONE BAFFLE 155.80" L.D. x 69.76" S.D. x .5" x 50.95"	↑	↑	
		007	1	CYLINDER BAFFLE 156.80" O.D. x .5" TH. x 56.25"		SA-387 GR.22	
		006	462	REDUCERS 1.26" O.D. x .866 O.D. x .173" W. x 2"		SA-355 P22	SEE DTL-"A"
		005	462	CONNECTING TUBES .866" O.D. x .130" W. x 91.42" AVG L	2¼CR-1MO	SA-213 T22	
		004	12	ACCESS BOLTS ⅝-11UNC-2A x .75"			
		003	1	ACCESS COVER 11.75" DIA. x .5" TH.	↑	↑	
		002	1	ACCESS RING 18" O.D. x 10" I.D. x 2" TH.	2¼CR-1MO	SA-387 GR.22	
	84-001		1	TRANS./CLO SUBASSEMBLY PARTS			

LIST OF MATERIAL – QUANTITIES FOR

WELD NUMBER	D W P NUMBER	NO PT	FREQ PT	NO MT	FREQ MT	NO RT	FREQ RT	NO UT	FREQ UT	∠F/ CHEM.

WELD TABLE

UNLESS OTHERWISE SPECIFIED
1. DIMENSIONS & TOLERANCES TO USAS Y14.5 – 1966
2. ALL DIMENSIONS APPLY AT REFERENCE TEMP. OF 68° F.
3. REF. DIMENSIONS ARE FOR INFORMATION ONLY. DO NOT USE FOR FABRICATION
4. MARKING SYMBOLS VT=VIBRO TOOL. LSS=LOW STRESS STAMP 1/32 MAX. DEPTH
5. BREAK ALL SHARP EDGES WITH APPROX. 1/32 RADIUS OR CHAMFER
6. MACHINED SURFACES INTERNAL – 250AA OR BETTER EXTERNAL-300AA OR BETTER
7. SIZES IN L/M ARE FINISHED SIZES – NO ALLOWANCE MADE FOR FABRICATION OR WELD SHRINKAGE.
8. TOLERANCE ON FRACTIONS . DECIMALS . ANGLES
9. SEE REF. DWG. NO.___FOR NDT ITEM NO. IN WELD TABLE & NDT CALL-OUT ON DWG.
10. SEE DWG. _____ FOR APPLICABLE EQUIPMENT SPECIFICATIONS.
11. DOUBLE ARROW INDICATES DIMENSION TO GIVEN REFERENCE LINE.
12. DEVELOPED LENGTH IN L/M IS GIVEN ON MEAN CENTERLINE.

GEOMETRIC TOLERANCES FOR MACHINED SURFACES UNLESS SPECIFIED ON DRAWING

SYM	GEOMETRY	TOL
▱	FLATNESS	.001/IN
—	STRAIGHTNESS	.001/IN
○	ROUNDNESS	SEE DWG
⌭	CYLINDRICITY	SEE DWG
⌒	PROFILE OF LINE	SEE DWG
⌓	PROFILE OF SURFACE	SEE DWG
//	PARALLELISM	.001/IN
⊥	PERPENDICULARITY	.001/IN
∠	ANGULARITY	SEE DWG
↗	RUNOUT	SEE DWG
⌖	TRUE POSITION	SEE DWG
◎	CONCENTRICITY	.010 DIA
⌯	SYMMETRY	SEE DWG

NEXT ASSEMBLY DRAWINGS	
GENERAL ARRANGEMENT	E-PHT-823012-82061

DWN. BY BULLEN 9-20-82
CKD. BY
ANAL. ENGR.
PROJ. ENGR
DATE 9/22/82

TRANSITION/CLOSURE SUBASSEMBLY
STEAM GENERATOR
2240 MWt HTGR SC/C STUDY
GENERAL ATOMIC COMPANY

CHATTANOOGA | SIZE D | PHT-823012-82084 | REV 00 | SCALE AS NOTED | CONT | SHEET 1 OF 1

REVISIONS				
SYM	ZONE	DESCRIPTION	DATE	APPROVED

Fig. 2.17-5. Transition closure subassembly

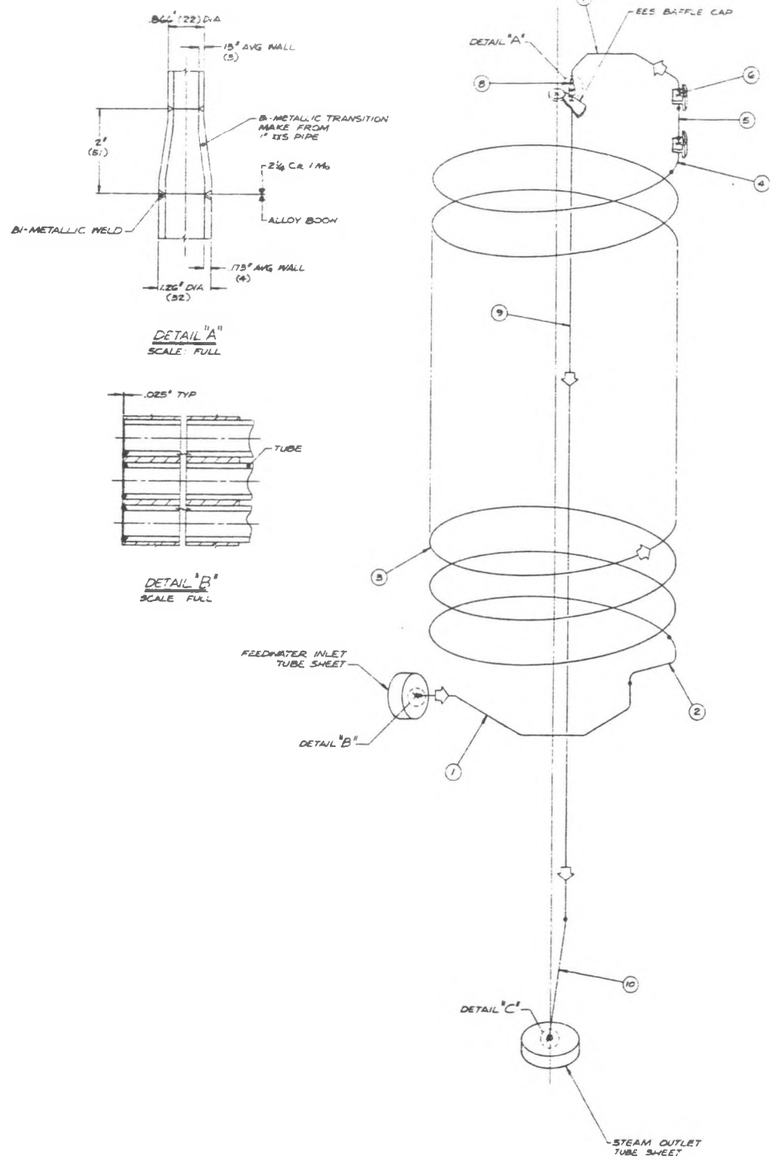

NOTES

1. ALL MATERIALS, DESIGN, FABRICATION, EXAMINATION AND TESTING SHALL BE IN ACCORDANCE WITH APPROPRIATE REFERENCE DRAWINGS
2. REFERENCE DRAWINGS
   - E-PHT823012-B20GB - ST SH SUB-ASSEMBLY
   - E-PHT823012-B20G4 - EES SUB-ASSEMBLY
   - E-PHT823012-B20G6 - TRANSITION CLOSURE SUB ASSEMBLY
3. TUBE LENGTHS SHOWN DEFINE MAX AND MIN LIMITS FOR EACH ITEM NUMBER. ACTUAL LENGTHS FOR EACH TUBE WILL VARY DEPENDING UPON FABRICATION BUT MUST FALL WITHIN LIMITS SHOWN.
4. ORDERING DIMENSIONS AND TOLERANCES TO BE DETERMINED
5. THIS DRAWING IS FOR REFERENCE AND INFORMATION ONLY. ALL DIMENSIONS ARE CONSIDERED TO BE REFERENCE DIMENSIONS.
6. TOLERANCES SHOWN ON THIS DRAWING APPLY TO A FINAL AS INSTALLED STEAM GENERATOR.
7. MAXIMUM TUBE OVALITY AFTER BENDING SHALL NOT EXCEED 6% AS DETERMINED BY $100 \times \frac{(D_{MAX} - D_{MIN})}{D}$

REVISIONS			
REVISIONS	DESCRIPTION	DATE	APPROVED

TUBE DATA - REFERENCE

ITEM NO.	DESCRIPTION	TUBE LENGTH	TUBE O.D.	WALL THICKNESS
1	FEEDWATER EXP LOCK TUBES	INFO NOT AVAILABLE	.866"	.15"
2	EES LEAD-IN TUBES			
3	HELICAL EES TUBES			
4	EES LEAD OUT TUBES			
5	EES ANCHOR MAKE-UP TUBES			
6	EES ANCHOR TUBE ASSEMBLY			
7	EES/ST SH EXP LOCK TUBES		↓	↓
8	BI METALLIC TRANSITION		.866"/1.26"	—
9	STRAIGHT SUPERHEATER TUBES		1.26"	.173"
10	CONICAL SUPERHEATER TUBES		↓	↓
	TOTAL LENGTH			

WELD TABLE

UNLESS OTHERWISE SPECIFIED

1. DIMENSIONS & TOLERANCES TO USAS B Y14.5 — 1966
2. ALL DIMENSIONS APPLY AT REFERENCE TEMP OF 68°F
3. REF DIMENSIONS ARE FOR INFORMATION ONLY. DO NOT USE FOR FABRICATION
4. MARKING SYMBOLS TO VIBRO TOOL, LOW STRESS STAMP .03 MAX DEPTH
5. BREAK ALL SHARP EDGES WITH APPROX .12 RADIUS OR CHAMFER
6. MACHINED SURFACES INTERNAL — 250AA OR BETTER, EXTERNAL — 500AA OR BETTER
7. SIZES IN ( ) ARE FINISHED SIZES — NO ALLOWANCE MADE FOR FABRICATION OR WELD SHRINKAGE
8. TOLERANCE ON X = ± .XX = ± .XXX = ± .XXXX; ANGLES ± 1°
9. REF DWG NO ____ FOR NOT-TO-BE MC IN SPECIFIED EQUIPMENT SPECIFICATIONS
10. SEE DWG ____ FOR APPLICABLE EQUIPMENT SPECIFICATIONS
11. DOUBLE ARROW INDICATES DIMENSION TO BE GIVEN REFERENCE LINE
12. DEVELOPED LENGTH IN (.) IS GIVEN ON MEAN CENTERLINE

NEXT ASSEMBLY

NAME

GEOMETRIC TOLERANCES FOR MACHINED SURFACES UNLESS SPECIFIED ON DRAWING

APPROVALS

POWER SYSTEMS

TUBING SCHEMATIC
STEAM GENERATOR
2,240 MWt HTGR SC/C STUDY
GENERAL ATOMIC COMPANY

DRAWN BY DODSON 9-28-82
DES ENGR
DATE
CHECKED
DATE

E-PHT823012-B20B5-00

SIZE A3 NOTED SHEET 1 OF 1

Fig. 2.17-6. Tubing schematic

vendors. This is considered as being the introductory step to bring CE's metallurgical expertise to bear on the HTGR steam generator design.

The CE-generated cost data tended to confirm the magnitude of the previous GA data since the values agreed within approximately 10%. The CE data was based on updates of manhour estimates generated for similar predecessor GA steam generator designs and over 85% of the material estimates confirmed by recent material vendor quotations.

Technology transfer was confirmed as several computer codes were received and made operational on CE's computer system. These codes included the basic thermal sizing code NUSIZE. A summary report of the FY-82 HTGR steam generator and CAHE studies for GA was issued (Ref. 2.1B-1).

Reference

2.17-1. Summary Report of FY-82 HTGR Steam Generator and CAHE Studies Performed for General Atomic Company, Combustion Engineering, Inc. Report CENC 1554, September 1982.

2.18. PRIMARY COOLANT SYSTEM CONTROLS/INSTRUMENTATION (6032210400)

2.18.1. Scope

The scope of this task involved the preparation of block diagrams and P&I diagrams for the main circulator service system and primary coolant system.

2.18.2. Discussion

During this reporting period, the first issue of the main circulator service system instrument block diagram was prepared and the second issue of the primary coolant system P&I diagrams was completed.

The instrumentation design presented in the main circulator service system instrument block diagram includes:

1. Flow monitoring and display required to determine that circulator seal, bearing lubrication, and bearing cooling functions are performed satisfactorily.

2. Temperature monitoring and display needed to observe that bearing cooling is effective.

3. Pressure and pressure differential monitoring and display necessary to demonstrate proper bearing lubrication or allow diagnosis of component malfunction in the bearing water supply.

4. Moisture monitoring and indication to detect the unwanted ingress of bearing water into circulator seal gas.

5. Radiation monitoring and indication to show unwanted egress of primary coolant from the reactor into the bearing water or circulator seal gas.

The second issue of the primary coolant P&I diagrams includes:

1. Identification of the interfaces between the primary coolant system and instruments in other NSSS systems.

2. Delineation of safety, seismic, and electrical class changes in primary coolant instrument systems.

3. Definition of the primary coolant pressure boundary for circulator service system instrument lines.

4. Layout of the controls and interlocks required for circulator service system operation.

2.19. AUXILIARY SYSTEMS DESIGN (6032230001)

2.19.1. Scope

The scope of this task, which was initiated at the beginning of FY-82, was (1) to prepare and issue a system description document for the helium services system, (2) to prepare similar information on the PCRV pressure relief subsystem as input for the PCRV SDD, and (3) to prepare and issue process flow diagrams (PFs) for both the helium services system and the PCRV pressure relief subsystem for the 2240-MW(t) HTGR-SC/C plant.

2.19.2. Discussion

The scope of this task was significantly reduced (to ~34%) owing to project redirection. Work performed in the second half of FY-82 was minimal, consisting solely of two revisions to the system description for the helium services system.

2.20. CACS DESIGN (6032280100)

2.20.1. Scope

The scope of this task is to provide systems input to the conceptual design of components and the control system of the CACS for the 2240-MW(t) HTGR-SC/C plant. The specific objective during this reporting period was to analyze the CACS design basis transients.

2.20.2. Discussion

Most recent design transient analyses for the CACS were performed for the previously developed 900-MW(e) HTGR-SC plant. The CACS sized for the 900-MW(e) plant might be expected to be applicable to the 2240-MW(t) plant since both have cores rated at 2240 MW(t). However, the 2240-MW(t) plant has a larger core (541 versus 439 fuel element columns), and the CACS design for the 900 MW(e) plant was developed when that core had eight-row fuel elemnts. The 2240-MW(t) plant fuel elements have pitch and hole diameters corresponding to a 10-row fuel element (although the mated lip design actually results in nine rows). The change from eight-to 10-row fuel elements appears to change the nature of depressurized core cooldown transients, displacing the time of peak core and primary coolant temperatures by an hour or more. The exact reasons for this difference in performance are unclear, and this effect requires further examination.

For these reasons alone, core performance in CACS analyses must be expected to be different for the new plant. In addition, the specific data presented for the 900-MW(e) plant were based on the long bayonet CAHE and not the more recently designed compact bayonet CAHE. Therefore, a need was recognized for publication of specifically applicable representative transients for use in the conceptual design of the CAHE, auxiliary circulator, auxiliary cooling control subsystem, and CACWS of the 2240-MW(t) HTGR-SC/C plant.

In a parallel effort during FY-82 on the HTGR Technology Program, a revised version of the RECA code was prepared and documented and a new computer code, ECSTRAN, was developed and documented. The former code is used in the design basis transient analysis of the core and primary coolant circuit for CACS cooling, and the latter code is used for analysis of the primary and secondary CACS circuit flow and heat transfer transients. The analytical results reported below were obtained by applying the newly available computer codes to the Baseline 0 design defined for the 2240-MW(t) HTGR-SC/C plant.

Six transients comprise the results of this analysis. Three of these are the design basis accident for CACS system design and are defined in the system description as follows:

1. Loss of main loop cooling with primary coolant pressurized and core cooldown on one CACS loop.

2. Depressurized cooldown on two CACS loops with pure helium.

3. Depressurized cooldown on two CACS loops with air ingress.

In each of these transients, the safety analysis requirements dictate that a number of restrictive ground rules be applied. The most significant of these requirements is the single failure criterion, which requires assumption of a coincidental safety system active component failure independent of the initiating event. Thus, one of the three CACS loop fails to start subsequent to a depressurization accident and two fail to start in the worst pressurized event. This is based on the worst case scenario, i.e., that rupture of a pipe in the CACWS circuit of one CACS loop is the initiating event, and so failure of one loop is dependent on the accident sequence and failure of the other loop is the independent failure. Other significant requirements are (1) no allowance for heat removed through the steam generators by the main loops after reactor trip, (2) no allowance for heat

removed by CACS until it reaches full rated capacity in its startup sequence, (3) reactor shutdown time delayed by control rod "holdup" due to a coincident earthquake at the time of trip, (4) the worst initial core region orifice settings permitted by the technical specification, (5) the most extreme region power factors expected in the fuel cycle, and (6) added uncertainties to all parameters affecting core heat removal, such as reactor decay heat, core flow resistance, CAHE heat transfer, etc.

The fourth transient in this analysis is a case that does not result in extreme conditions for the plant and is therefore not a system design basis event, but does represent the design point for the auxiliary circulator:

4. Depressurized cooldown on two CACS loops with pure helium but with pressure drop factors at lowest values. (The design basis depressurization with pure helium, above, yields highest primary coolant temperatures, but this scenario yields highest circulator volumetric flows.)

The remaining two transients examined are not design bases but rather expected sequences without the above extreme requirements on analysis:

5. Main loop spindown and pressurized CACS cooldown on all three loops. This is the opposite extreme to the pressurized design basis transient.

6. Main loop operation into a depressurization accident followed by CACS cooldown on all three loops. This is the opposite extreme to the depressed design basis transient. It picks up at the end of what is given in the main loop performance document for the "rapid primary system depressurization" transient.

Key system variables are provided for four of the above transients in Figs. 2.20-1 through 2.20-4. The transients shown include the following:

Fig. 2.20-1(a-d)	Expected sequence, pressurized cooldown (three CACS loops)
Fig. 2.20-2(a-d)	Design basis, pressurized cooldown (one CACS loop)
Fig. 2.20-3(a-d)	Expected sequence, depressurized cooldown with pure helium in PCRV (three CACS loops)
Fig. 2.20-4(a-b)	Design basis, depressurized cooldown with air ingress (two CACS loops)

Comparison of Figs. 2.20-1 and 2.20-2 with Figs. 2.20-3 and 2.20-4 shows the difference in CACS operation in pressurized and depressurized core cooling modes. Comparison of Fig. 2.20-1 with Fig. 2.20-2 and Fig. 2.20-3 with Fig. 2.20-4 demonstrates the conservatism incorporated in the design basis sequences with respect to expected sequences.

Transient data such as the results presented here will be used for component design. All elements of the CACS, particularly the CAHE, which is sensitive to stress and deformation due to thermal gas growth and sensitive to cycle loading, will have to consider the extreme limits of service that are represented by these transient analysis results.

The required CACS performance envelope is also significant in the design of the auxiliary circulator compressor. Figure 2.20-5 is a summary of auxiliary circulator operating points at times of peak reactor core region outlet temperature in each of the six transients. The scales of the plot are the dimensionless head coefficient, ψ, and flow coefficient, ϕ, along with a cross-plot of dimensionless speed, where n_o is the circulator design speed, 3600 rpm. Figure 2.20-5 illustrates one aspect of the service requirements that make the CACS design process somewhat complex, namely that the circulator output varies over more than two orders of magnitude in output load.

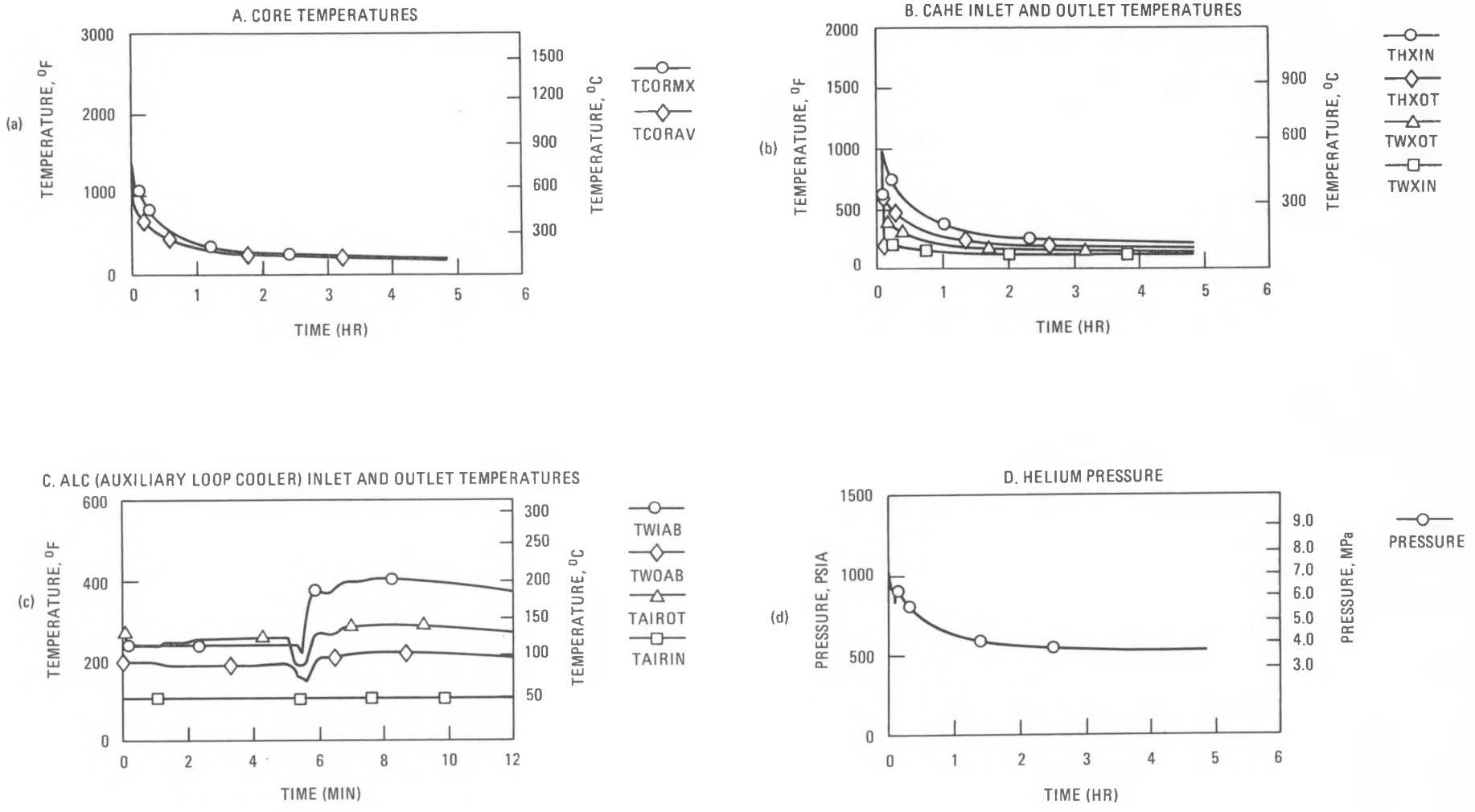

Fig. 2.20-1. Pressurized, three-loop, expected case: (a) maximum (TCORM) and average (TCORAV) core temperatures; (b) inlet (THXIN) and outlet (TXHOUT) CAHE primary coolant and inlet (TWXIN) and outlet (TWXOT) CAHE water temperatures; (c) inlet (TWIAB) and outlet (TWOAB) ALC water and inlet (TAIROT) and outlet (TAIRIN) ALC air temperatures with expanded time scale; (d) primary coolant pressure

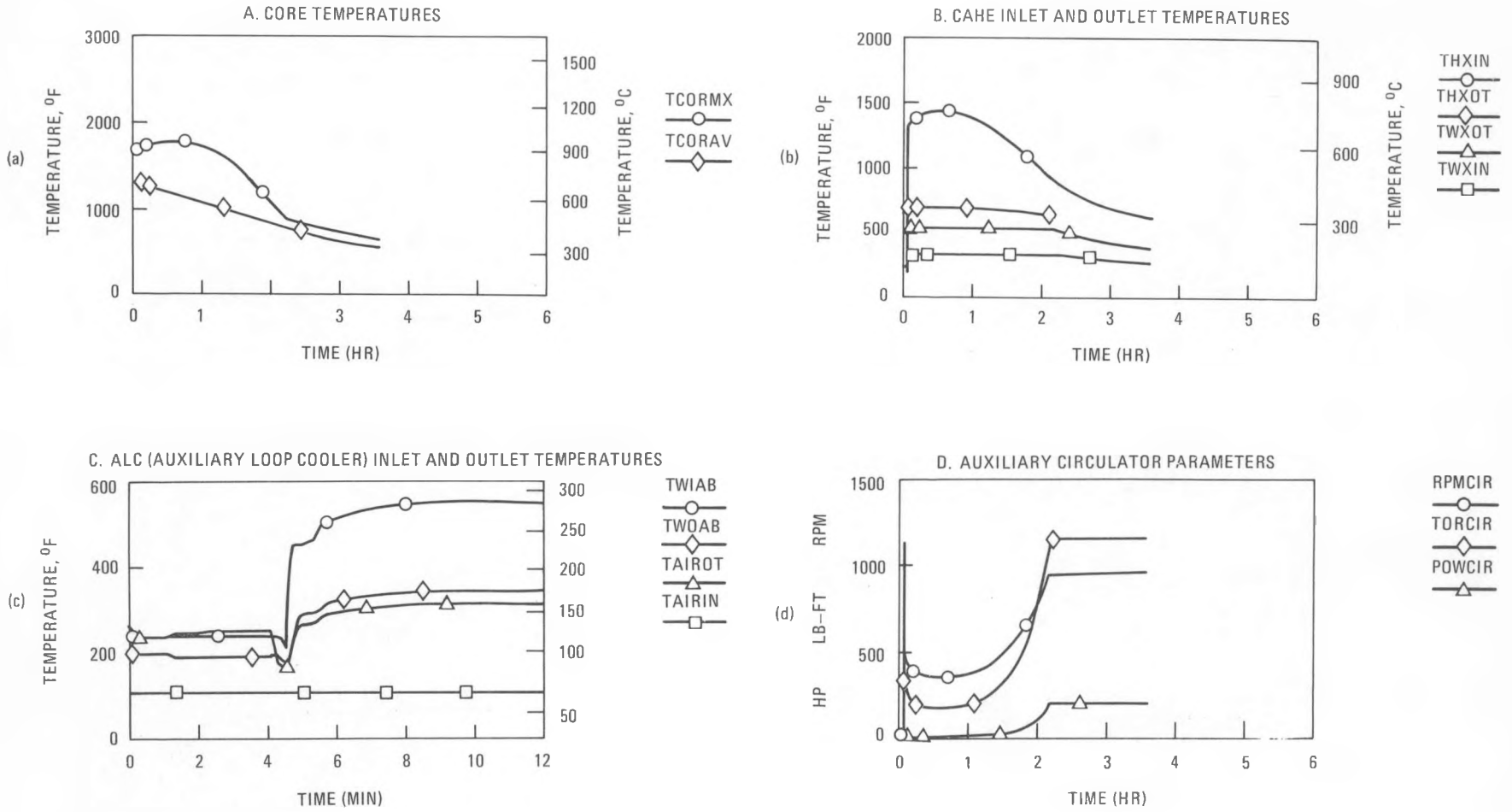

Fig. 2.20-2. Pressurized, one-loop, extreme case: (a) maximum (TCORMX) and average (TCORAV) core temperatures; (b) inlet (THXIN) and outlet (TWXOUT) CAHE primary coolant and inlet (TWXIN) and outlet (TWXOT) CAHE water temperatures; (c) inlet (TWIAB) and outlet (TWOAB) ALC water and inlet (TAIROT) and outlet (TAIRIN) ALC air temperature with expanded time scale; (d) auxiliary circulator speed (RPMCIR), torque (TORCIR), and power (POWCIR)

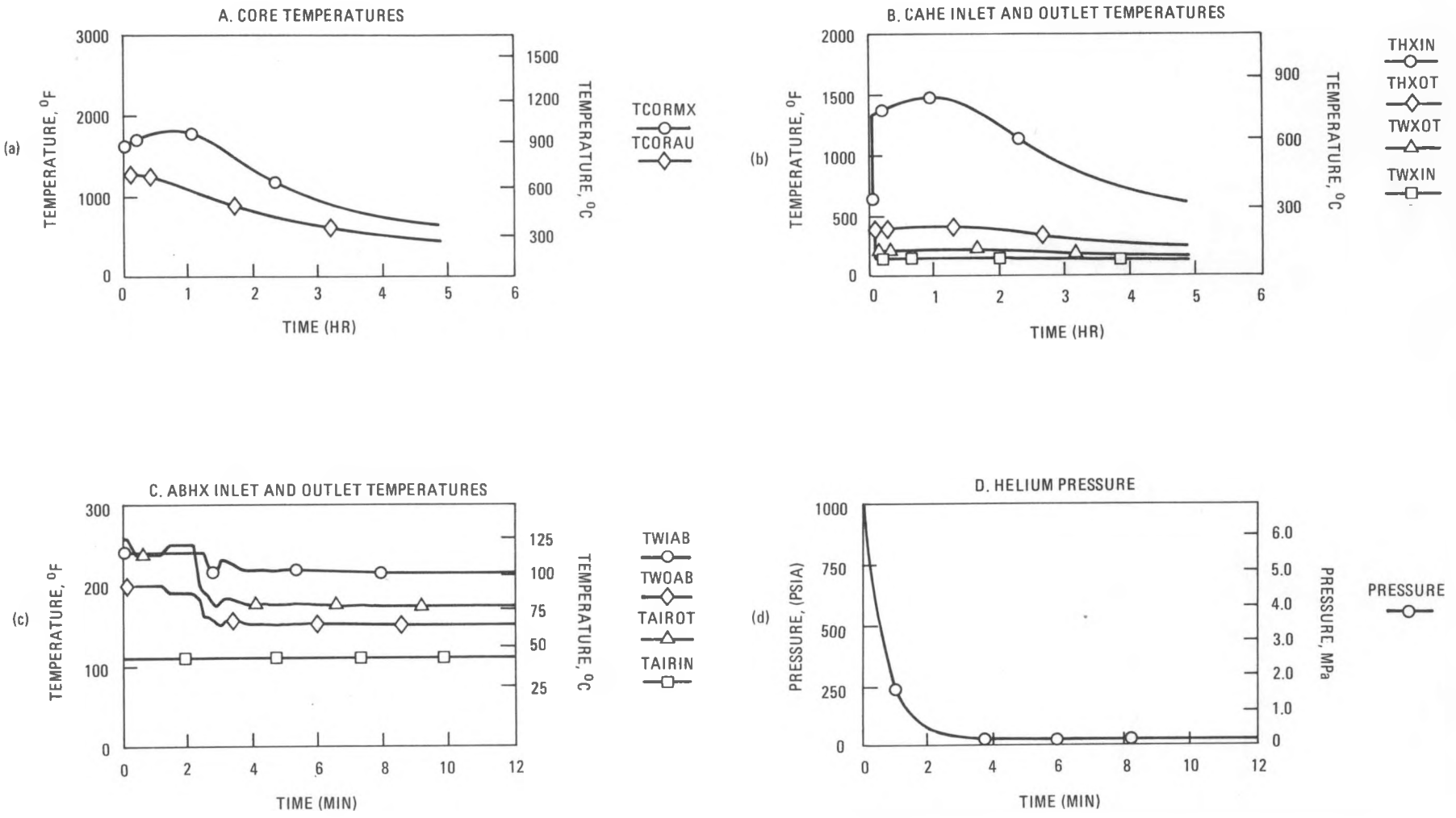

Fig. 2.20-3. Depressurized, three-loop, expected case: (a) maximum (TCORMX) and average (TCORAV) core temperatures; (b) inlet (THXIN) and outlet (THXOUT) CAHE primary coolant and inlet (TWXIN) and outlet (TWXOT) CAHE water temperatures; (c) inlet (TWIAB) and outlet (TWOAB) ALC water and inlet (TAIROT) and outlet (TAIRIN) ALC air temperatures with expanded time scale; (d) primary coolant pressure with expanded time scale

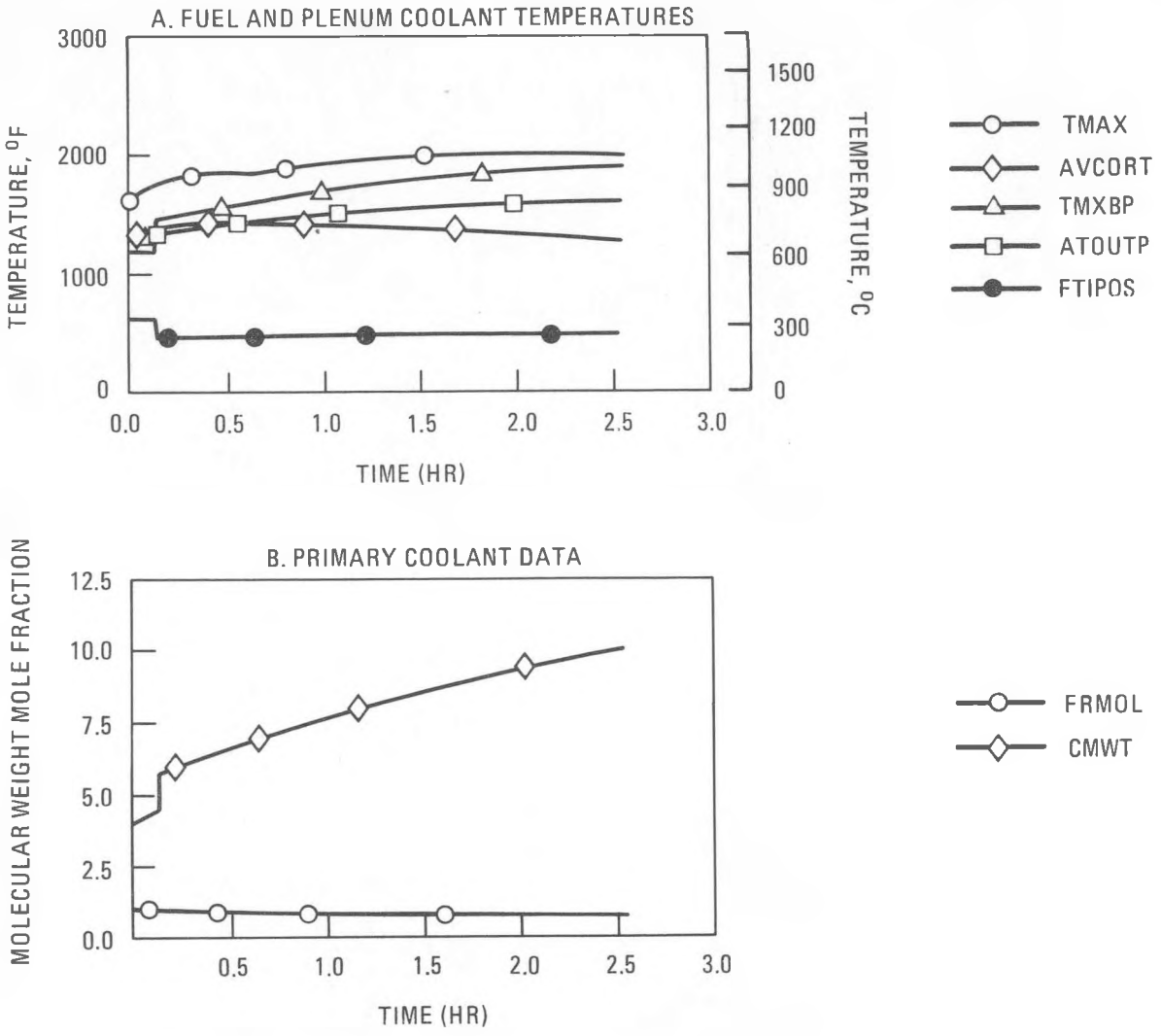

Fig. 2.20-4. Design basis depressurized cooldown with air ingress: (a) maximum (TMAX) and average (AVCORT) core and maximum (TMXBP) and average (ATOUTP) lower plenum and average (FTIPOS) upper plenum coolant temperatures; (b) He mole fraction (FRMOL) and molecular weight (CMWT) of primary coolant

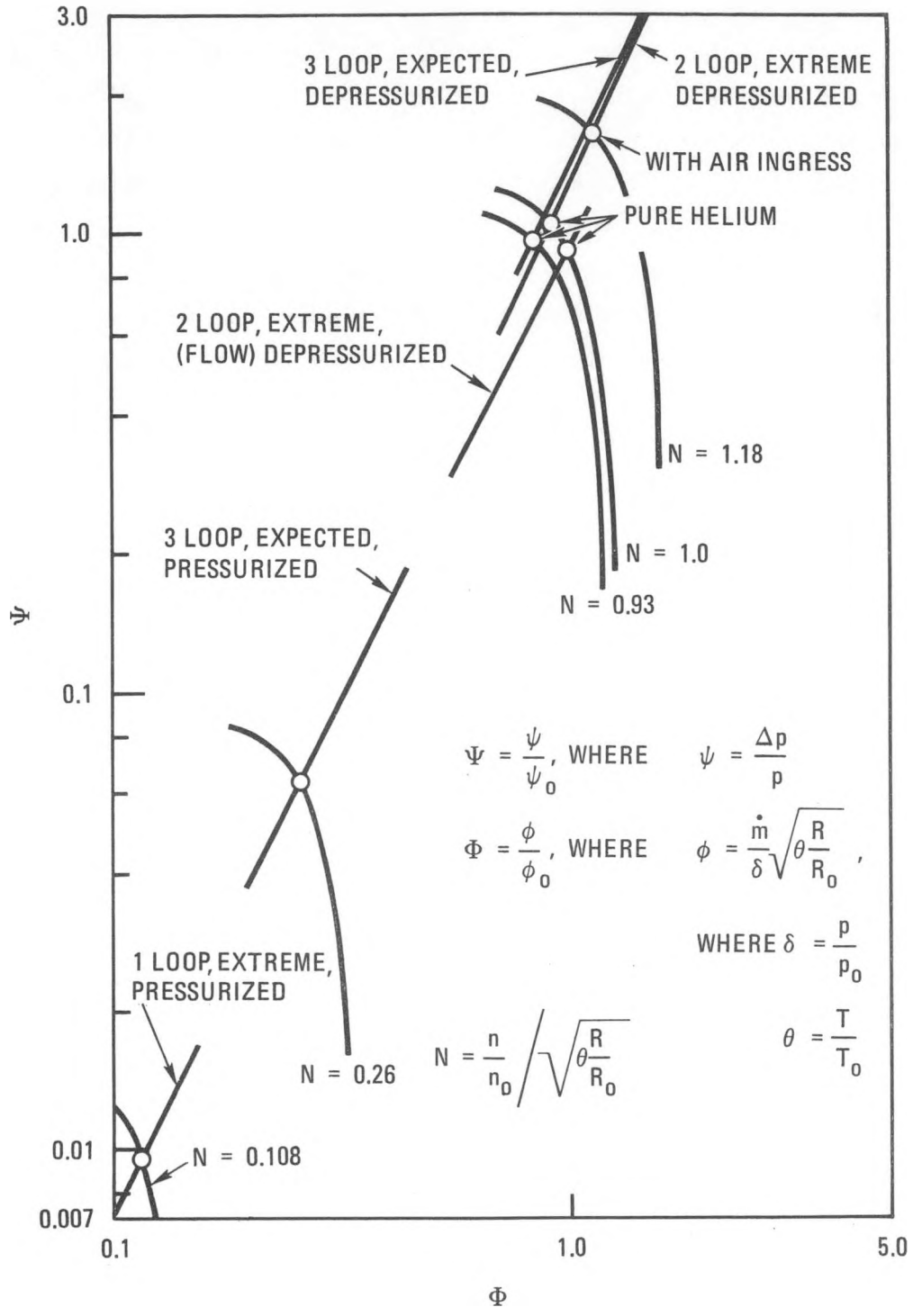

Fig. 2.20-5. Auxiliary circulator operating points at time of peak region outlet temperature in various transients, ψ versus ϕ (showing system lines and compressor characteristic curves)

The work scope for the FY-84 calls for definition of a Baseline 1 conceptual 2240-MW(t) HTGR-SC/C plant design, which is expected to include a CACS design optimized with respect to system design criteria and system cost. Therefore, the transient results reported for the Baseline 0 design are to be replaced with results for the revised and optimized design. However, the transient curves should not be expected to vary appreciably from those presented here unless some significant changes occur in CACS design criteria or in the conceptual approach to reactor core or CACS component design.

2.21. AUXILIARY CIRCULATOR DESIGN (6032280200)

2.21.1. Scope

This task covers the initial conceptual design of the auxiliary circulator, the auxiliary circulator service system, and the auxiliary loop shutoff valves, all of which are components of the CACS. The work scope during this reporting period relates primarily to the service system conceptual design and integration of the shutoff valve and circulator layout with installation interfaces and handling equipment designs.

2.21.2. Discussion

The auxiliary circulator subsystem comprises (1) the circulator assembly with compressor, motor, and housing, (2) the auxiliary loop isolation valve, and (3) the auxiliary circulator services.

2.21.2.1. Auxiliary Circulator. The auxiliary circulator is a vertically oriented compressor driven by an integral electric motor. The circulator drive motor is a 671-kW (900-hp), 3600-rpm, four-pole squirrel-cage induction motor. In order to meet the wide range of required operating conditions, the electric motor is driven by a variable frequency speed controller to a maximum frequency of 120 Hz. The motor stator and rotor are typical standard vertical motor construction. The motor operates in a cool helium environment at the same pressure as the primary coolant system.

The motor and compressor assembly along with the loop shutoff valve are installed in a penetration within the upper section of the PCRV. During this reporting period, the auxiliary circulator general arrangement drawing (Fig. 2.21-1) was updated to comply with the latest PCRV configuration and to simplify installation and removal with the circulator handling equipment as described in Section 2.10 of this report.

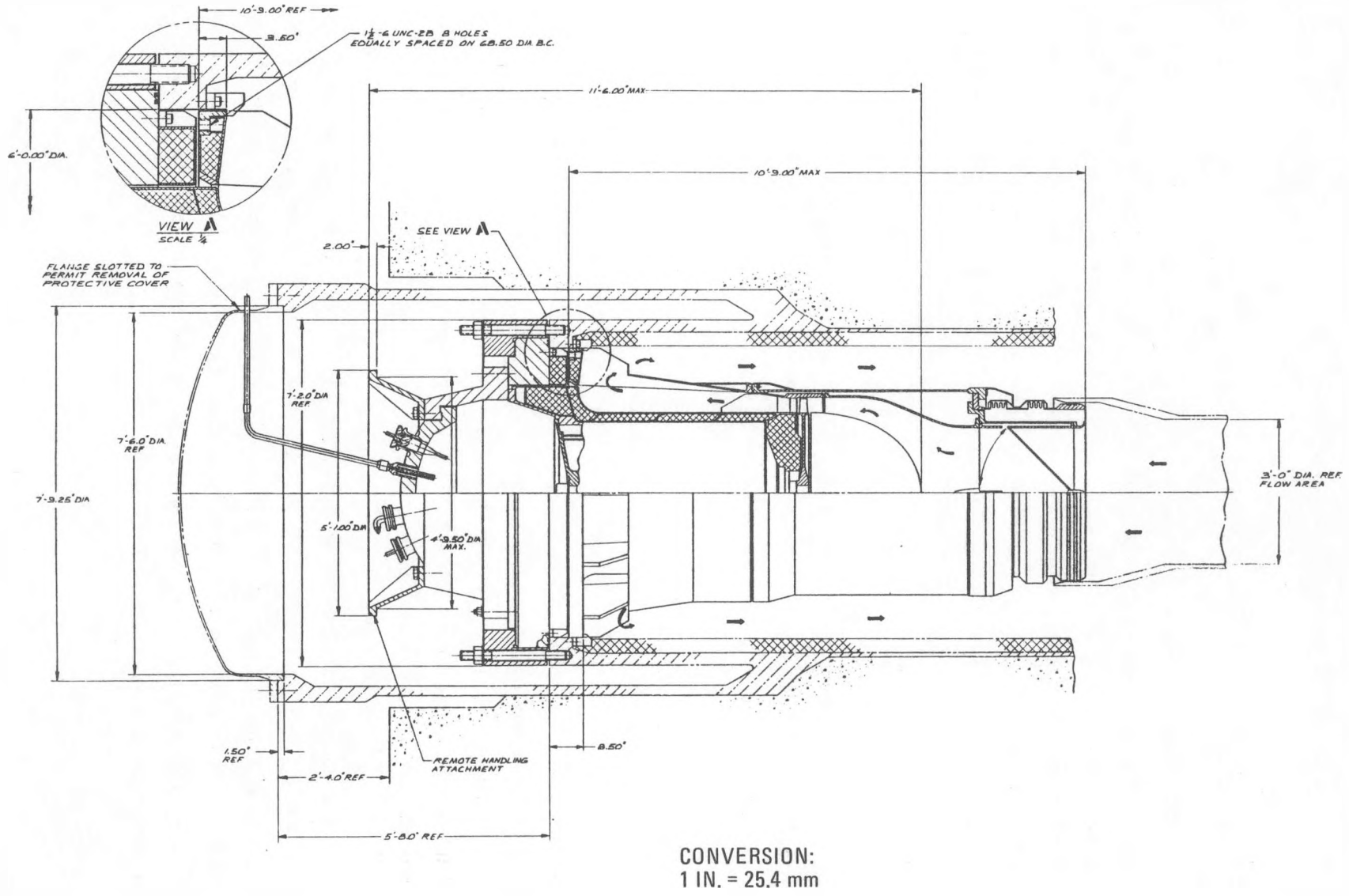

Fig. 2.21.1. Auxiliary circulator general arrangement

The rotor is supported on oil-lubricated rolling element bearings that carry the axial and radial loads and are located on each side of the motor rotor, and the compressor is overhung. Each bearing is mounted on the shaft through an inverted U-shaped extension, and the oil is prevented from escaping down the shaft by a stationary dam. A cross-sectional drawing of the auxiliary circulator motor is shown in Fig. 2.21-2. Oil vapor is prevented from entering the primary coolant loop by means of a labyrinth seal buffered by purified helium flow. Purified helium is introduced into the center of the labyrinth and flows out each end. The helium that flows down the shaft enters the primary coolant system. The helium that flows up the shaft mixes with oil vapor in the motor compartment and then is routed to external oil separation equipment.

2.21.2.2. Auxiliary Circulator Service System. The auxiliary circulator services provide the following:

1. A supply of purified buffer helium for preventing inleakage of motor bearing lubricant to the primary coolant system or leakage of primary coolant into the motor casing.

2. Removal of oil vapor carried over in purge helium for the auxiliary circulators.

3. Removal and replacement of motor bearing lubricant when an auxiliary circulator is shut down.

During reactor plant operation, buffer helium is supplied to the motor cavity of each circulator at a flow rate of about 2.8 ℓ/s (6 acfm). The flow rate will be controlled at this value regardless of fluctuations in the primary coolant system pressure. The helium purge is withdrawn from the two bearing-oil cavities in each motor and purged at a controlled flow rate of 2.1 ℓ/s (4.5 acfm) (at approximately reactor pressure). The control system thus adjusts the helium flow to effect a split so that approximately one-quarter of the flow leaks into the primary coolant system and the remainder

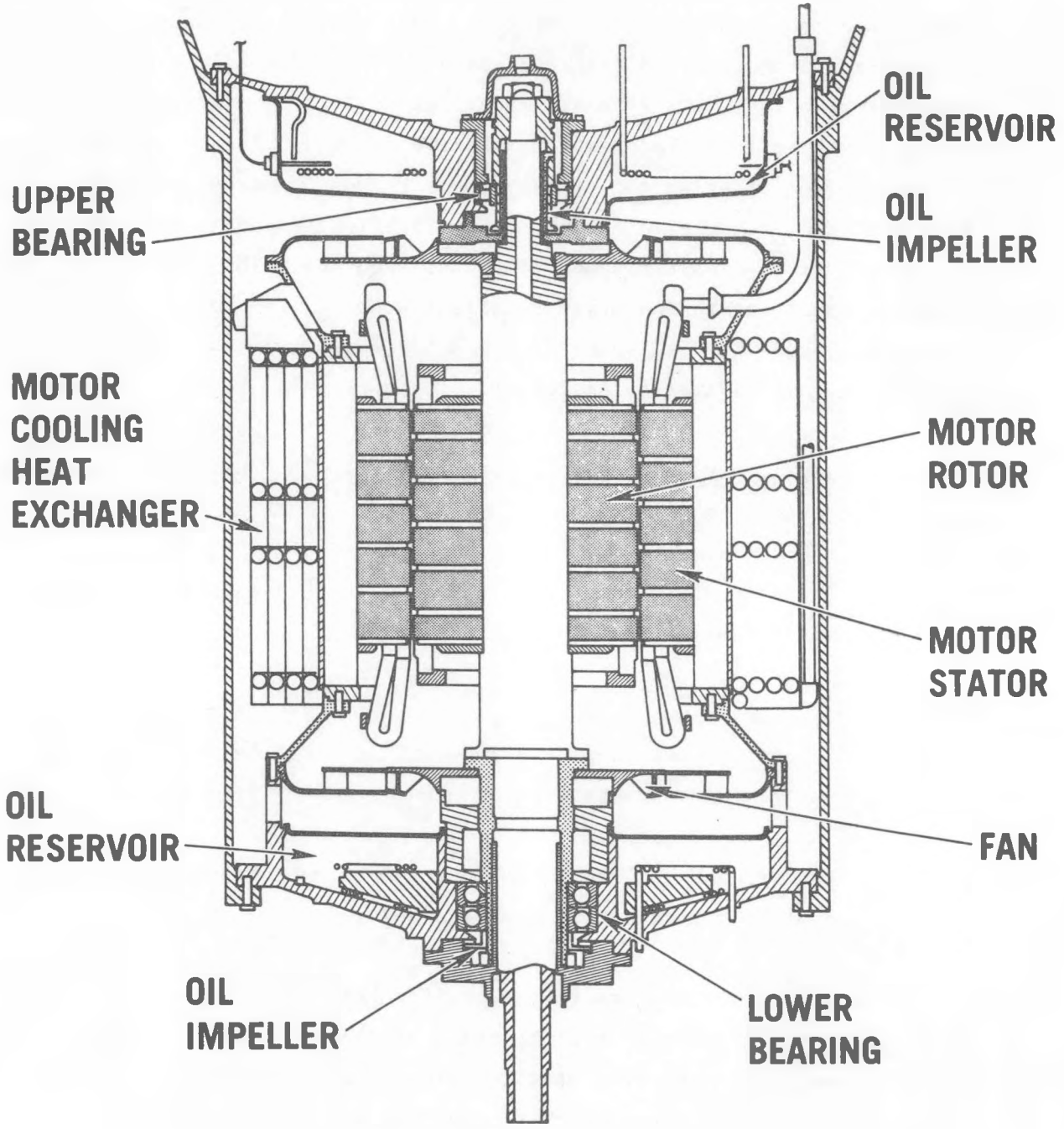

Fig. 2.21-2. Auxiliary circulator drive motor

leaks out through the vents of the motor bearing-oil cavities. This controlled leakge of buffer helium also presents leakage of lubricating oil vapor into the primary coolant system.

Helium purging from the motor bearing-oil cavities is piped first to the oil adsorber and from there to the helium purification system. The module incorporates two adsorber columns, each of which contains a non-regenerable bed of adsorbent. Each column is rated to pass the combined helium purge from the auxiliary circulators and is designed to permit adsorbent removal and replacement over the complete range of system operating pressures during auxiliary circulator standby or operating modes. The purge helium is supplemented by makeup at the helium compressor section; following recompression, it is piped to the auxiliary circulator buffer helium inlet cavity for reuse. Auxiliary circulator functional capability is not affected by the failure or unavailability of the oil adsorber.

The bearing-oil reservoirs within the circulator assembly are normally isolated from the oil service system. Oil is maintained within the reservoirs except during removal and replacement operations. Removal and replacement are achieved by helium pressure displacement. A pressure differential of 68 kPa (10 psi) is required to overcome line friction losses for removal or replacement of the oil. Since the reactor primary coolant is the pressure source for oil removal, this operation must be performed at reactor primary coolant pressures of 68 kPa (10 psig) or greater. Bearing-oil replacement can be accomplished at any pressure within the reactor operating range. The bearing-oil replacement and removal tanks have a capacity of 37.8 ℓ (10 gal) and are designed for a pressure of 3.16 MPa (1200 psig) at 150°C (300°F). A predetermined quantity of oil is supplied for each bearing cavity. The replacement interval is expected to be 2 yr, based on the amount of oil removed by the continual helium purge within the motor cavity and the radiation tolerance capability of the oil.

The circulator oil reservoir capacity is designed to hold 22.7 ℓ (6 gal) of oil in each upper and lower reservoir of the auxiliary circulator drive assembly. An oil level indicator is provided in each reservoir to monitor the oil level and also to act as an interlock to allow or prevent the oil fill or drain process. A single fill/drain line is connected to each reservoir of a circulator. The fill line is sized so that any fill or drain operation can be accomplished in less than 3 hr with a pressure differential head of 68 kPa (10 psi). Outside the circulator the line is split into two separate fill and drain lines, each connected to its respective fill and drain tanks. A shutoff and check valve is provided in each section of the fill/drain line to control the fill/drain operation.

Oil Drain Operation

During an oil drain operation, an oil level indicator (two of three) in the oil reservoir of the circulator is used as an interlock to allow or prevent oil fill and drain. The interlock also prevents the potential draining of more than one reservoir at a time. Three-way valve F (see Fig. 2.21-3) is initially positioned to connect to either the drain or fill line. Opening valve C (see Fig. 2.21-3) automatically closes valves B and D to assure that new oil is not introduced into the line during the drain operation. Draining of the reservoir continues until a high gas flow is noted in the vent flow indicator of the drain tank and a high level is noted by the drain tank level indicator. At this point, all the oil in the reservoir should be drained into the drain tank and valves A, C, and E are closed.

The drain tank is a portable tank sized to receive a premeasured amount of oil. Checking on the amount of oil collected in the drain tank provides a method of verifying that the reservoir has completely drained. The drain tank is disconnected from the drain line and transported by a portable cart or a handling cradle out of the containment building. The drain tank is sent to a Tank Service Facility outside the containment for processing of spent oil. Two tanks are handled at a time (change-out of oil from one

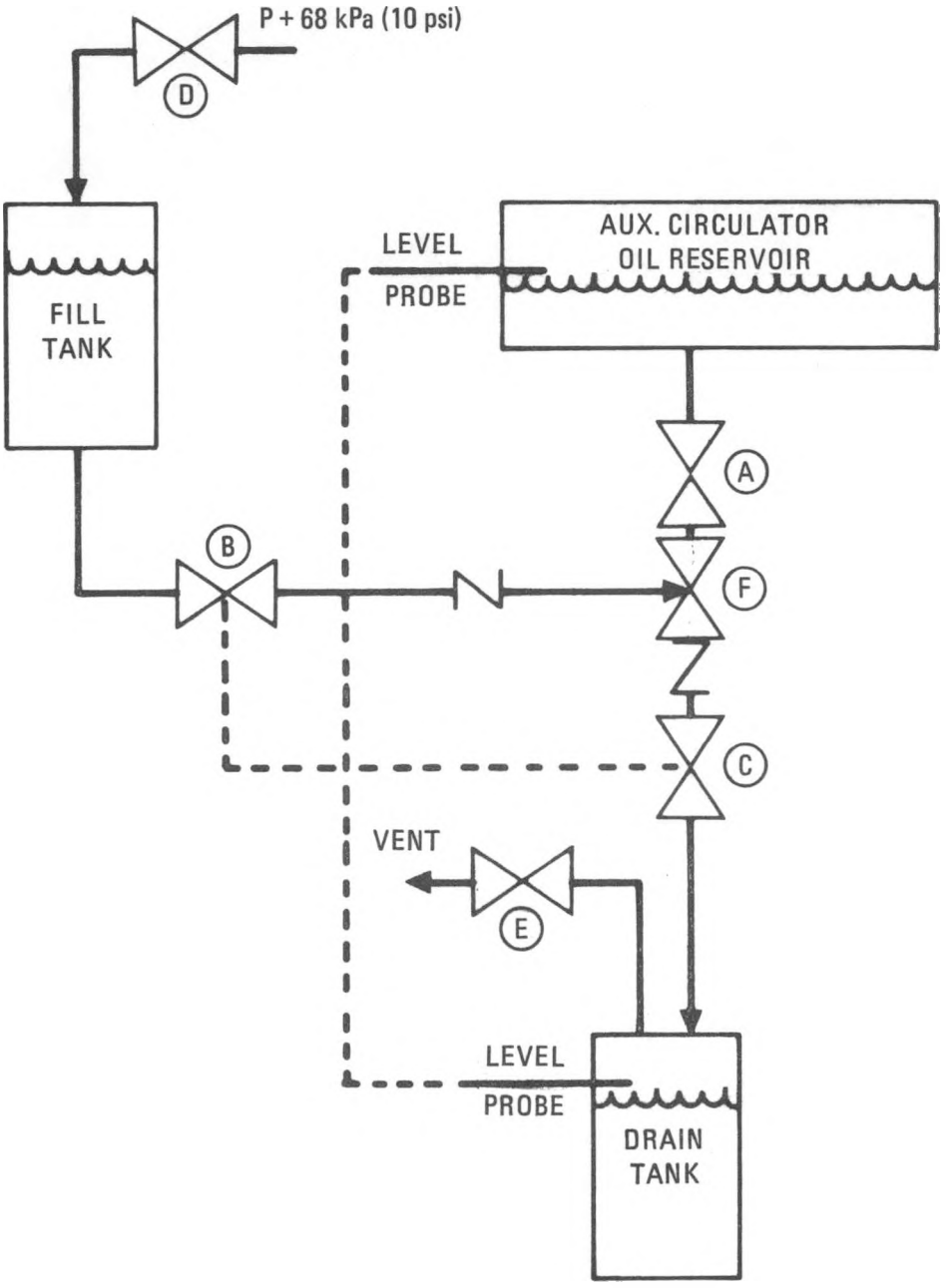

Fig. 2.21-3. Oil change service system

circulator) to minimize the time for shutdown of a circulator. The tanks have different line connection sizes or arrangements to prevent draining two reservoirs into one tank and to allow positive identification of where the oil originated for later analysis and radiation level measurements.

Oil Fill Operation

During an oil fill operation (performed during a plant shutdown), a predetermined quantity of new oil [about 26.5 ℓ (7 gal)] is initially stored in the fill tanks (see Fig. 2.21-3). Again the oil level indicator in the reservoir will provide a means to monitor the charging process when the oil level reaches the proper level and will serve as an interlock to prevent opening of the fill line unless a proper level indication is obtained from the drain tank. Valve D must be opened first to pressurize the fill tank above the reactor pressure level in order to flow the oil into the reservoir. Valve A is opened to connect the fill and drain line. Opening valve B automatically closes valves C and E. Valve F must be moved to the fill position. When the proper oil level indication in the reservoir is reached, the filling operation is stopped (valves A, B, and D are closed). Since part of the drain line is connected to the fill line (up to drain isolation valve F), a gas pocket will occur in the drain line between isolation valve A and the tee connection (valve F) to the fill line. This trapped gas will be isolated by closing valve A, which is the purpose for installing valve A in the line.

Two fill tanks are installed at a time so that filling operations can be performed for one circulator. However, separation of the lines and tanks is maintained to prevent inadvertent filling of the wrong reservoir. This is accomplished by having different size connections or arrangements so that only one can be connected to a particular fill line. This approach also allows positive identification of which reservoir the fill tank was used to fill.

Equipment

The following equipment requirements are defined for the auxiliary circulator oil change process (these requirements are based on the system as shown in Fig. 2.21-3):

1. Two fill oil tanks, each 37.8 ℓ (10 gal) in size, for filling each of the upper and lower reservoirs.

2. Two drain tanks, each 37.8 ℓ (10 gal) in size, for draining the upper and lower oil reservoir "dirty" oil.

3. A "clean" oil tank to hold only enough oil to fill one reservoir.

4. A valve with an interlock for switching from the "dirty" tank to the "clean" tank after oil is removed from the reservoir and isolated in the tank.

5. An interlock for changing one reservoir at a time.

6. A drain tank containing a level indicator to monitor the oil drain process and provide an indication of complete oil drain from the reservoir.

2.22. CORE AUXILIARY HEAT EXCHANGER (CAHE) DESIGN (6032280301)

2.22.1. Scope

The GA work scope consisted of preparing a report on the impact of the CAHE airflow test on the CAHE design. The CE work scope was limited to providing order-of-magnitude cost data and accumulating some limited scoping for bayonet tubes of the type envisioned for use in the CAHE design.

2.22.2. Discussion

As a result of the flow distribution test, several design modifications were initiated and additional recommended testing and analysis work was identified. The design modifications include:

1. A flow distribution device that is an extension of the outer shroud. Its function is to redirect the inlet gas flow.

2. Definition of the shroud exit configuration in terms of void fraction and height of the perforated section.

3. Addition of a splitter plate on the downstream side of the inlet flow distribution shroud extension to suppress acoustic oscillations.

The additional analysis work identified includes verification of the COMIX computer code, development of a computer code for detailed CAHE performance, and optimization of the outlet screen design using flow test results. The additional testing identified includes further evaluation of acoustic oscillations and modification of the test system for inlet hot streak tests.

As a result of a review of the CAHE design as required to develop the cost data, a number of design points were raised by CE which merit further consideration. These included the following:

1. The large-diameter Grayloc closure used at the lower end of the CAHE water plenum is considerably larger than hardware typically produced by Gray Tool Company. Redesign of this area (to a welded head, for example) might prove cost effective and make the design more feasible.

2. Other bayonet tube heat exchangers that CE has studied in the past indicate some extreme degradation of performance due to convective heat transfer in the annulus between the two inner tubes. It was suggested that this aspect be evaluated by testing.

3. The hexagonal tube bundle shroud will present manufacturing difficulties that could be alleviated by using a round shroud. Possibly a circular pitch should be considered in lieu of the triangular pitch now employed.

The primary data generated by the CAHE flow test task was related to the relationship between pressure drop and the configuration of the "spacer" used to maintain the flow annulus. The basic spacer was defined by GA as being a continuous strip, of appropriate thickness, helically wound around the outer diameter of the bayonet tube. In order to obtain the desired data, a test matrix was established consisting of three different sizes of bayonet tubes, each wound with more than one different configuration of helical spacer (the pitch of the helical spacer winding was varied). All spacer thicknesses were such that the finished diameters of bayonet tubes (measured over the spacer) were essentially constant at the correct diameter to fit snugly within the sheath tube. The test data are summarized in Table 2.22-1.

TABLE 2.22-1
DATA SUMMARY OF FLOW RATE VERSUS PRESSURE DROP

Bayonet Tube Diam [mm (in.)]	Spacer Type	Pitch of Wire [mm (in.)]	Average Pressure Drop at 12.5 ℓ/min (3.3 gal/min) kPa^2 (psi)
25.4 (1)	Ribbon	76.2 (3)	574 (83.3)
25.4 (1)	Ribbon	304.8 (12)	173.7 (25.2)
22.4 (0.88)	Ribbon	304.8 (12)	18.6 (2.7)
25.4 (1)	Wire	76.2 (3)	463 (67.2)
25.4 (1)	Wire	304.8 (12)	145.5 (21.1)
25.4 (1)	Wire	914.4 (36)	144 (20.9)
23.9 (0.94)	Wire	76.2 (3)	146 (21.2)
23.9 (0.94)	Wire	304.8 (12)	48.3 (7.0)
23.9 (0.94)	Wire	914.4 (36)	33 (4.8)
23.9 (0.94)	None	--	35 (5.1)

2.23. SAFETY-RELATED CONTROL AND INSTRUMENTATION (6032320100, 6032320101)

2.23.1. Scope

The scope of this task during this reporting period included preparation of PPS instrument block diagrams, initiation of a study of the potential plant availability advantages or disadvantages of 2-out-of-3 and 2-out-of-4 logic schemes, and a study of the maximum electromagnetic interference (EMI) generated by the main circulator motor/power supply that can be tolerated by safety-related electronic equipment.

2.23.2. Discussion

The PPS instrument block diagrams include six PPS subsystems: reactor trip, steam generator isolation and dump, main loop shutdown, CACS initiation, CAHE isolation, and containment isolation. The overall conceptual PPS logic scheme uses a 2-out-of-3 logic design. If the current study and analysis show that a significant increase in plant availability can be achieved cost effectively using a 2-out-of-4 logic scheme, changes in the conceptual PPS logic design will be considered.

The reactor trip system uses general 2-out-of-3 hindrance logic. Trip inputs include loop helium temperature high, reactor power high, reactor power to helium mass flow ratio high, primary coolant pressure low, primary coolant moisture high, primary coolant pressure high, containment pressure high, and a temporary initial startup reactor flux high (used only during initial fuel loading).

The steam generator dump and isolation system uses general 2-out-of-3 transmission logic. Trip input includes loop primary coolant concentration high. Detection of moisture in any other main or auxiliary loop inhibits automatic initiation of this trip.

The main loop shutdown system uses specific 2-out-of-3 transmission logic and 1-out-of-2 actuation logic. Trip inputs include circulator outlet temperature high, superheat steam temperature high, feedwater flow to circulator speed mismatch, and circulator buffer seal malfunction.

The CACS initiation system uses specific 2-out-of-3 transmission logic. Trip inputs include plant feewater flow low, plant helium flow low, and containment pressure high/primary coolant pressure low.

The CAHE isolation system uses specific 2-out-of-3 transmission logic and 1-out-of-2 actuation logic. Trip input includes CAHE leak detection. Detection of moisture in any other main or auxiliary loop inhibits automatic initiation of this trip.

The containment isolation system uses specific 2-out-of-3 transmission logic and 1-out-of-2 actuation logic. Trip inputs include containment pressure high and containment radiation level high.

The preliminary results of the PPS 2-out-of-3 versus 2-out-of-4 logic study were compiled, and recommendations for continuing work to be performed in FY-83, were made. The major purpose of this study to determine whether a significant potential increase in plant availability could be attained by using a 2-out-of-4 PPS logic scheme as opposed to the presently proposed 2-out-of-3 logic scheme.

Investigation has shown the following qualitative results in comparing the 2-out-of-3 and 2-out-of-4 logic schemes:

1. The 2-out-of-4 logic scheme clearly has a greater capital expense and is more complicated to build.

2. In general, the 2-out-of-4 logic scheme provides greater reliability to perform the safety function.

3. In general, the 2-out-of-4 logic scheme has a greater probability of causing spurious trips during normal operation.

4. In general, the 2-out-of-4 logic scheme offers more flexibility during testing and maintenance, which should result in a lower probability of spurious PPS trips during maintenance.

Since plant availability is determined for all operating conditions, it is not clear from the results of the Preliminary Study that the 2-out-of-4 logic scheme is certain to significantly increase plant availability as compared with the 2-out-of-3 logic scheme. A quantitative assessment of the effect on plant availability is required before this judgment can be made. Such a plant availability assessment could also allow a cost/benefit assessment of the 2-out-of-4 logic scheme.

The purpose of the EMI study is to establish current practices relative to electrical noise reduction. This study thus forms the basis for taking a system approach in the design of the control and electrical systems, including safety-related electronic systems, for the HTGR project and also acts as a basis for preparation of the main and CACS circulator motor/drive specifications.

The preliminary findings of this study are:

1. The large circulator motor drive control itself involves solid-state electronics and is potentially as susceptible to extraneous electrical noise pickup as other plant control and instrumentation equipment.

2. A considerable industry interest and standards development effort exists relative to electrical noise.

3. Electric noise problems can exist in power plants, and the large helium circulator drives and controls are known sources of noise. Newer plants are potentially more vulnerable to noise than older plants owing to the wider use of solid-state electronic control equipment.

4. The minimization of electrical noise problems requires a coordinated effort between the BOP and NSSS designs. In the case of the motor drive controllers, the manufacturer (GE) needs to be involved.

5. It is not appropriate to establish firm realistic design numbers for tolerable levels of electrical noise inasmuch as the details of the electrical system, physical plant, and equipment designs have not yet been completely defined. Noise susceptibility of equipment is generally determined by actual testing of equipment.

6. The military encourages (and probably mandates) a strong overall project approach to electrical noise beginning at the conceptual design. Both electrical emission and susceptibility are reflected throughout the design. Considerable testing is employed. The overall process is an iterative one.

2.24. PLANT CONTROL SYSTEM (6032330100)

2.24.1. Scope

The scope of this task is to prepare instrument diagrams for the NSSS portion of the variable HTGR-SC/C plant controls.

2.24.2. Discussion

Instrument diagrams were prepared that included a top sheet showing the connection between major components in the NSSS controls system and other plant systems. Five subsystems detailed in the balance of the diagram are as follows:

1. The NSSS loop main steam temperature/circulator speed control system.

2. The NSSS feedwater flow control system.

3. The NSSS main steam pressure control system.

4. The NSSS average main steam temperature control system.

5. The NSSS non-safety-related loop trip logic.

Each of the diagrams shows the individual control system components required to accomplish the subsystem function. The components are identified by instrument tag number and by the operation performed on control signals. For the loop main steam temperature/circulator speed controls, the operations and logic to hold each loop's steam temperature to the average of four loops are presented. The design includes provision for loop trip, changes in plant load, and modification of circulator speed setpoint by feedwater flow. The feedwater controls provide the measurement,

conditioning, and logic required to supply feedwater flow signals to loop trip logic, the loop steam temperature controls, and the flow controllers in main steam pressure control system. Main steam pressure controls include the controllers and modifiers required to maintain NSSS output steam pressure at required levels by forming the setpoints for the BOP feedpump turbine speed controls. The main steam pressure controls also include the modifier required to combine turbine throttle pressure, turbine first-stage pressure, and process steam flow into a plant load signal. Average main steam temperature controls include the measurements, modifiers, logic, and controller needed to hold NSSS output steam temperature at desired levels by forming the setpoint for the neutron flux controller. Loop trip logic includes the compactors, switches, and logic gates necessary to protect NSSS equipment against primary to secondary coolant flow mismatches and low main steam pressure. The logic also shares interlocks with the circulator service system, provides runback signals to the plant, and switches functions in other NSSS control subsystems.

3. HTGR-PH MONOLITHIC PLANT

3.1. HTGR-PH MONOLITHIC PLANT; NHS DESIGN (6042131001, 6042131100, 6042131801, 6042132001, and 6042132100)

3.1.1. Scope

The scope of work reported here was to perform design studies of the HTGR-PH monolithic plant.

3.1.2. Discussion

This period's specific task was to design the NHS for a 2240-MW(t) monolithic plant concept based on direct reforming, using a reactor with a core outlet temperature of 950°C (1742°F). The resulting data are to be used for cost estimating purposes, and the concept features will be compared with the modular variant.

3.1.2.1. NHS Design for 950° DC, 2240-MW(t) Plant

NHS Parameters and Performance

A limited scope study was conducted to establish a preconceptual design for the NHS of a 2240-MW(t) direct-cycle process heat plant with a reactor outlet temperature of 950°C (1742°F). The NHS parameters were generated in conjunction with GE to establish the overall heat balance. The NHS of the monolithic process heat plant is characterized by a helium-cooled, graphite-moderated thermal reactor core, which is installed in a multicavity PCRV.

The plant features a direct cycle configuration, i.e., there is no intermediate heat transfer system separating the NHS from the process steam and electricity-generating elements of the process plant. The main mechanical interface of the NHS with the process plant is at the NHS primary heat exchangers (reformer and steam generator). Features specific to the NHS are given below:

- Direct cycle
- Multicavity PCRV
- Six parallel primary system loops, each consisting of a reformer, a steam generator, and a main helium circulator shutoff valve connected in series
- Three parallel auxiliary cooling loops, each consisting of a core auxiliary heat exchanger and circulator connected in series

The NHS is designed to suppy 2336 MW(t) of thermal energy for sustaining a steam-methane reforming process, for generating electricity to meet in-house needs, and for export from the nuclear complex. The reactor power and the reactor outlet helium temperature associated with this output are 2240-MW(t) and 950°C (1742°F) respectively. The major design parameters and NHS heat balance are given in Table 3.1-1. Several iterations between the requirements of the NHS and the process plant were necessary, and these resulted in the generation of NHS parameters as given in Table 3.1-2.

PCRV Design (6042131100)

The multicavity PCRV is a thick-walled, cylindrically shaped prestressed concrete structure. Prestressing is provided longitudinally by vertical tendons and circumferentially by strand cables wound in channels located on the outer wall of the vessel. A plan view of the PCRV for the

TABLE 3.1-1
NHS DESIGN PARAMETERS AND HEAT BALANCE

NHS design parameters	
Reactor power	2240 MW(t)
Primary system pressure	4.80 MPa (696 psia)
Reactor outlet temperature	950°C (1742°F)
Reactor inlet temperature	500°C (932°F)
Process gas inlet temperature	538°C (1000°F)
Process gas inlet pressure	4.95 MPa (718 psia)
Process gas outlet temperature	632°C (1170°F)
Process gas outlet pressure	4.45 MPa (645 psia)
Process side steam generator inlet pressure	260°C (500°F)
Process side steam generator inlet temperature	19.99 MPa (2900 psia)
Process side steam generator outlet temperature	566°C (1050°F)
Process side steam generator outlet pressure	16.55 MPa (2400 psia)
NHS heat balance	
Reactor power, MW(t)	2240
NHS heat losses, MW(t)	12
Circulator return power, MW(t)	108
Net NHS power, MW(t)	2336
Net power to reformers, MW(t)	1254
Net power to steam generators, MW(t)	1082
NHS thermal efficiency, %	99.5

TABLE 3.1-2
NHS PERFORMANCE PARAMETERS

Reactor power, MW(t)	2240
Reactor core	
Flow rate, kg/s (lb/h)	957.5 (7,598,900)
Inlet temperature, °C (°F)	500 (932)
Inlet pressure, MPa (psia)	4.80 (695.6)
Outlet temperature, °C (°F)	950 (1742)
Outlet pressure, MPa (psia)	5.69 (680.7)
Reformers (per loop)	
Primary system side	
Flow rate, kg/s (lb/hr)	159.8 (1,268,200)
Inlet temperature, °C (°F)	948 (1739)
Inlet pressure, MPa (psia)	4.69 (680.1)
Outlet temperature, °C (°F)	697 (1286)
Outlet pressure, MPa (psia)	4.61 (669.1)
Process side	
Flow rate, kg/s (lb/hr)	89.67 (711,700)
Inlet temperature, °C (°F)	538 (1000)
Inlet pressure, MPa (psia)	4.95 (718)
Outlet temperature, °C (°F)	632 (1170)
Outlet pressure, MPa (psia)	4.45 (645)
Steam generators (per loop)	
Primary system side	
Flow rate, kg/s (lb/hr)	161.4 (1,280,900)
Inlet temperature, °C (°F)	694 (1282)
Inlet pressure, MPa (psia)	4.61 (668.9)
Outlet temperature, °C (°F)	479 (894)
Outlet pressure, MPa (psia)	4.54 (658.9)
Process side	
Flow rate, kg/s (lb/hr)	77.78 (613,300)
Inlet temperature, °C (°F)	260 (500)
Inlet pressure, MPa (psia)	19.99 (2900
Outlet temperature, °C (°F)	566 (1050)
Outlet pressure, MPa (psia)	16.55 (2400)
Helium circulators (per loop)	
Flow rate, kg/s (lb/hr)	161.4 (1,280,900)
Inlet temperature, °C (°F)	479 (894)
Inlet pressure, MPa (psia)	4.54 (658.7)
Outlet temperature, °C (°F)	501 (933)
Outlet pressure, MPa (psia)	4.80 (696.0)

6-loop 2240-MW(t) monolithic process heat plant is shown in Fig. 3.1-1. A vertical section through the PCRV showing the major cavities is presented in Fig. 3.1-2. The elevation view shown in Fig. 3.1-3 gives details of the liners and cooling tubes. Interface data between the NHS and BOP are provided on these three figures.

The PCRV layout features a central core cavity and several major and minor peripheral cavities. The 12 major cavities (six reformer and six steam generator) are grouped on one side of the central core cavity, while the three CACS cavities are grouped on the other side as indicated in Fig. 3.1-1. The main helium circulator-loop shutoff valve assemblies are housed in the upper portion of their respective steam generator cavities, and each CACS cavity houses a core auxiliary heat exchanger and an auxiliary circulator-loop shutoff valve assembly. Pipe chases, which extend vertically through the PCRV, are provided to service the reformer and steam generator cavities. In addition, the reactor plant cooling water system's header pits and two pressure relief system pits are included. The PCRV diameter is governed by the layout of the major peripheral cavities, and the height is determined by the reformer component height. The reformer envelope was provided by GE. The design of the PCRV is based on the use of 44.82 MPa (6500 psi) concrete and 11.1 MN (24,788 kip) tendon capacity. A summary of the PCRV parameters is given in Table 3.1-3.

Reactor Core (6042132801)

The reactor core assembly consists of nuclear fuel, hexagonal-shaped graphite fuel elements, replaceable reflector elements, and top layer plenum elements. Based on a minimal effort, a core layout was established for the 2240-MW(t) plant with a 950°C (1742°F) reactor outlet temperature. The core has 583 columns, eight blocks high, and uses an 11-row fuel block design modified to incorporate a pheripheral sealing lip to prevent cross flow. (This latter feature provides design similarity with the steam cycle/ cogeneration lead plant.) The power density is 5.35 W/cm^3. The design

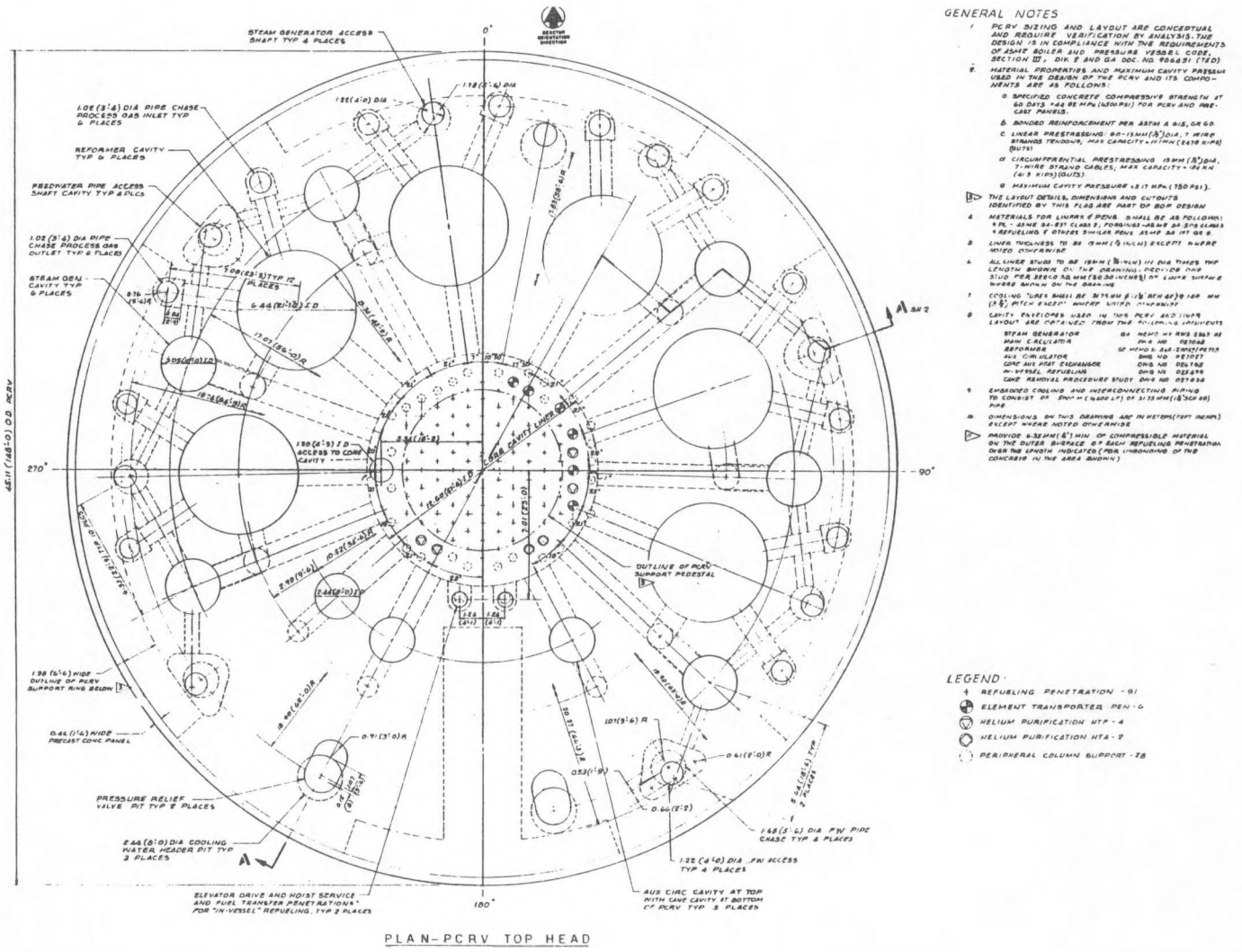

Fig. 3.1-1. PCRV layout for 950°C (1742°F) direct-cycle plant, plan view

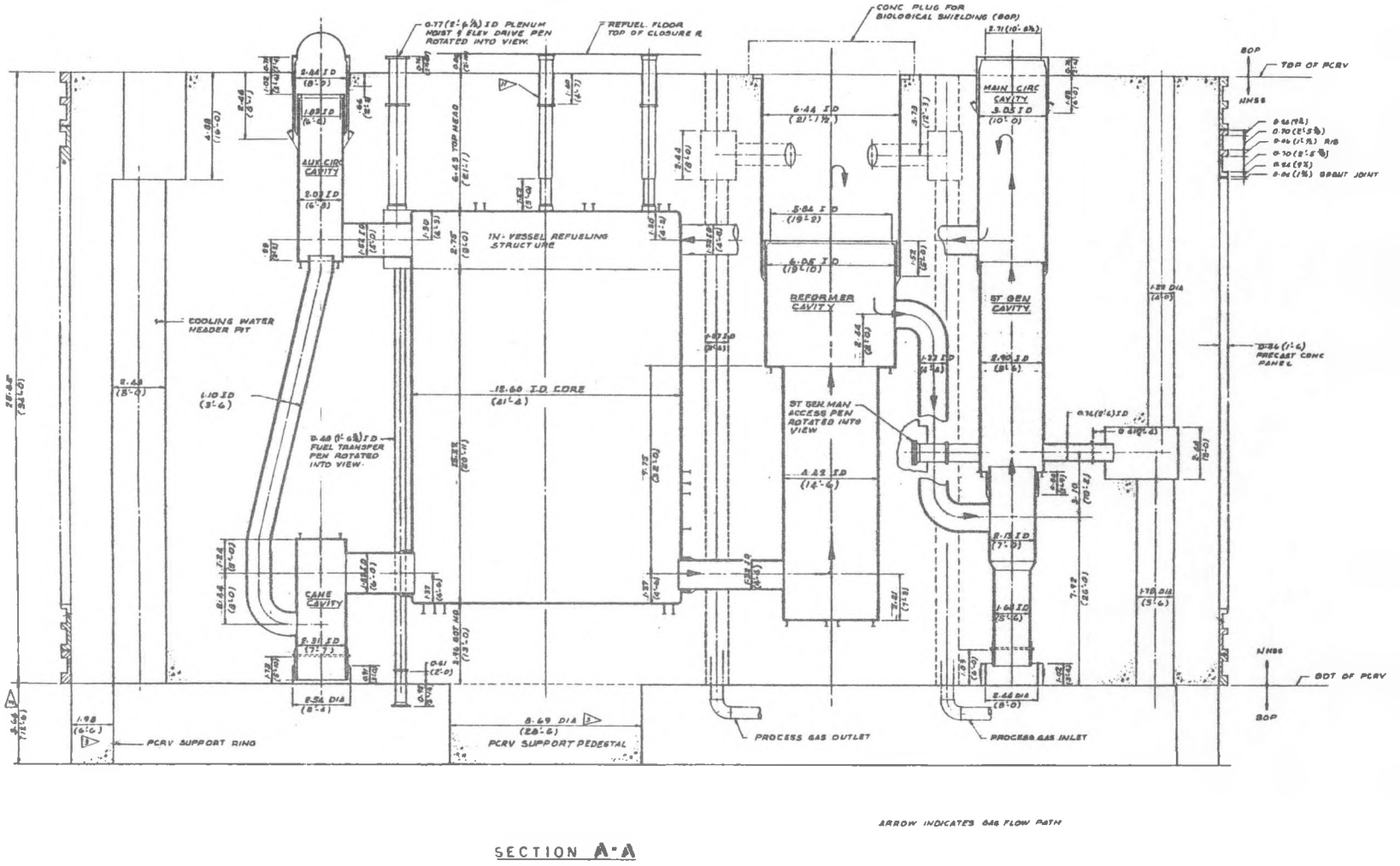

SECTION A-A

Fig. 3.1-2. PCRV layout for 950°C (1742°F) direct-cycle plant, vertical section

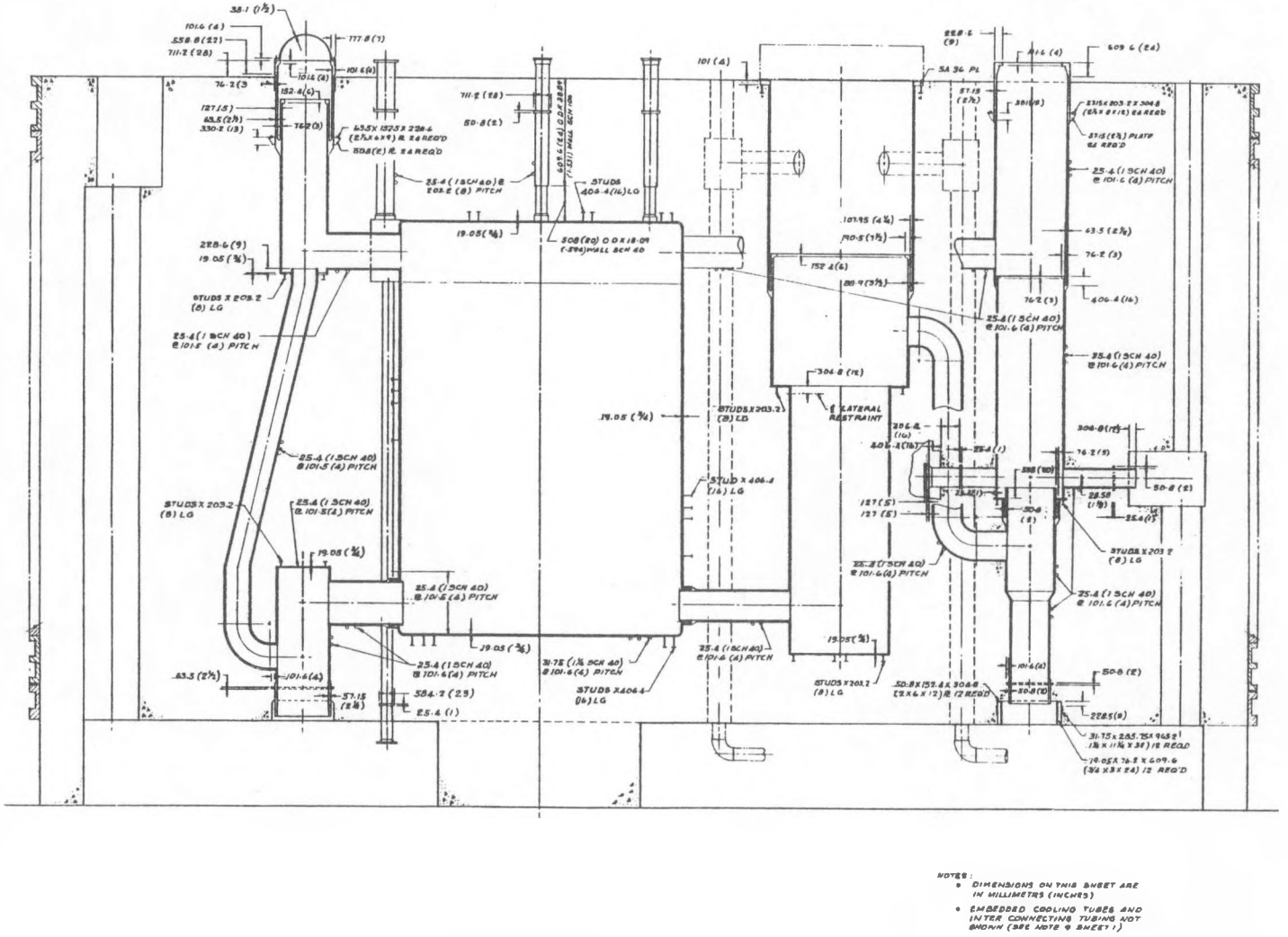

Fig. 3.1-3. PCRV layout for 950°C (1742°F) direct-cycle plant, elevation view showing cooling tubes and liner details

TABLE 3.1-3
SALIENT FEATURES OF PCRV

Type	Multicavity PCRV
Overall dimensions, m (ft-in.)	
Diameter	45.11 (148-0)
Height	28.65 (94-0)
Core cavity, m (ft-in.)	
Diameter (inside)	12.60 (41-4)
Height (inside includes in-vessel refueling)	18.26 (59-11)
Reformer, quantity	6
Diameter (inside), m (ft-in.)	
At mid-height	4.42 (14-6)
At top head	6.44 (21-1 1/2)
Height (centerline of hot duct to top of PCRV), m (ft-in.)	23.32 (76-6)
Type of primary closure	Steel
Steam generator main circulator cavity, quantity	6
Diameter (inside), m (ft-in.)	
At mid-height (at steam generator)	2.90 (9-6)
At top head (at main circulators)	3.05 (10-0)
Height (centerline of hot duct to top of PCRV), m (ft-in.)	20.73 (68.0)
Type of primary closure	Steel
Auxiliary circulator cavity, quantity	3
Diameter (inside), m (ft-in.)	
At mid-height	2.03 (6-8)
At top head	2.44 (8-0)
Type of primary closure	Steel
Core auxiliary heat exchanger cavity, quantity	3
Diameter (inside) m (ft-in.)	
At mid-height	2.31 (7-7)
At top head	2.31 (7-7)
Type of closure	Steel

has a three-year annual fuel cycle, as established for earlier 950°C (1742°F) core designs. The major core parameters are given on Table 3.1-4. These parameters are based on (1) scaling from a previous design with similar requirements, (2) power distribution calculations, and (3) radial axial zoning evaluations, all aimed at a core design with a satisfactory layout and performance.

Main Helium Circulator (6042132001)

The design of the circulator took advantage of (1) technology base from the HTGR lead plant and (2) previous units designed for the direct reforming variant. The circulator is a vertically oriented three-stage axial compressor that is directly driven by a variable-speed synchronous electric motor. The multistage axial machine is the optimum configuration for this application, where the adiabatic head rise is relatively high compared with that of other HTGR applications. The circulator is rigidly mounted to an extension of the PCRV closure liner. The overall component installation, including the motor, bearing cartridge, and loop shutoff valve, is shown in Fig. 3.1-4. The technologies for the water bearing system and for the loop shutoff valve are similar to those of other HTGR applications. Table 3.1-5 provides circulator performance and design data.

Steam Generator (6042132100)

The steam generators [six are required for a six-loop 2240-MW(t) plant] are once-through units with uphill boiling on the tube side and with cross counter-current helium flow on the shell side. Figure 3.1-5 shows the general arrangement of a single unit. The heat transfer section of a steam generator consists of two main helical coiled tube bundles. The lower bundle is an economizer-evaporator-superheater (EES), and the upper bundle is a finishing superheater. The bundles are separated by a material transition zone where bimetallic welds join the EES tube material to the

TABLE 3.1-4
MAJOR REACTOR CORE PARAMETERS FOR 2240-MW(t) 950°C (1742°F) PLANT

Thermal	
Power, MW(t)	2240
Power density, W/cm^3	5.35
Outlet temperature, °C (°F)	950 (1742)
Core ΔT, °C (°F)	450 (810)
Core inlet pressure, MPa (psia)	4.80 (696)
Core helium flow rate, kg/s (lb/hr)	958 (7.599×10^6)
Fuel cycle	
Fuel	LEU/Th
Refueling mode	3 year-patch
C/Th ratio (equilibrium)	560
Layout	
Active core layout	498 standard and 85 control columns; 8 blocks high
Active core dimensions, m (ft)	
Height	6.3 (20.8)
Diameter	9.2 (30.1)
Block configuration	11-row block with a peripheral sealing lip to restrict crossflow
Core assembly dimensions (active core, reflectors, top reflector, and top reflector elements), m (ft)	
Overall height (including top plenum elements)	10.1 (33.2)
Overall diameter	10.6 (34.7)

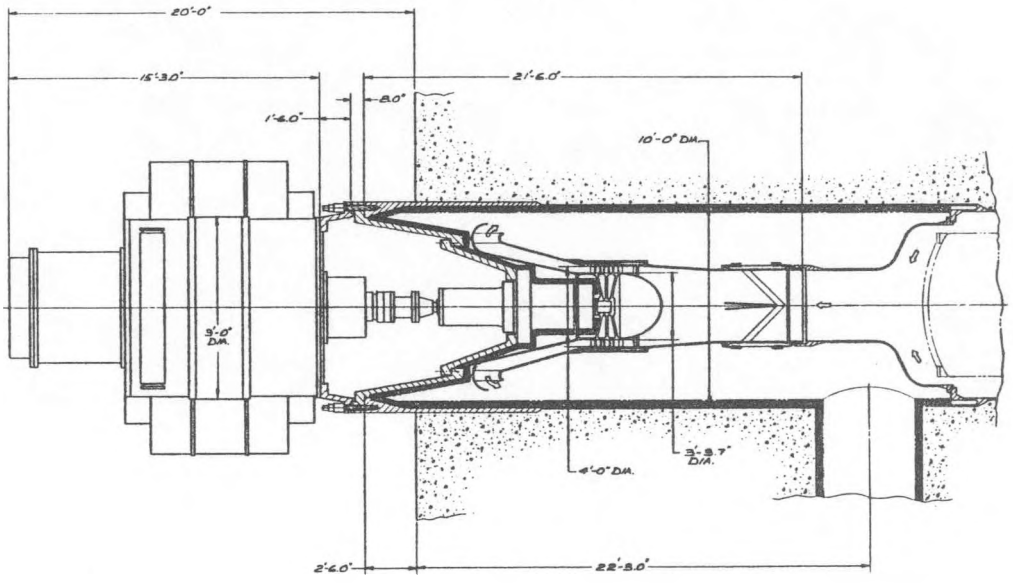

CONVERSION: 1 IN. = 25.4 mm

Fig. 3.1-4. Main circulator overall component installation

TABLE 3.1-5
HELIUM CIRCULATOR PERFORMANCE AND DESIGN DATA

Number of loops	6
Flow per loop, ks/s (lb/hr)	161.4 (1,280,900)
Inlet pressure, MPa (psia)	4.54 (658.7)
Pressure rise, kPa (psi)	257 (37.3)
Inlet temperature, °C (°F)	479 (894.0)
Compressor type	Axial flow, 3 stage
Rotating speed, rpm	4500
Adiabatic efficiency	0.82
Compressor aerodynamic power, MW (hp)	17.2 (23,000)
Bearings, seal friction, MW (hp)	0.4 (500)
Stage specific speed	163.0
Tip diameter, m (ft)	1.2 (4.0)
Hub diameter, m (ft)	1.0 (3.3)

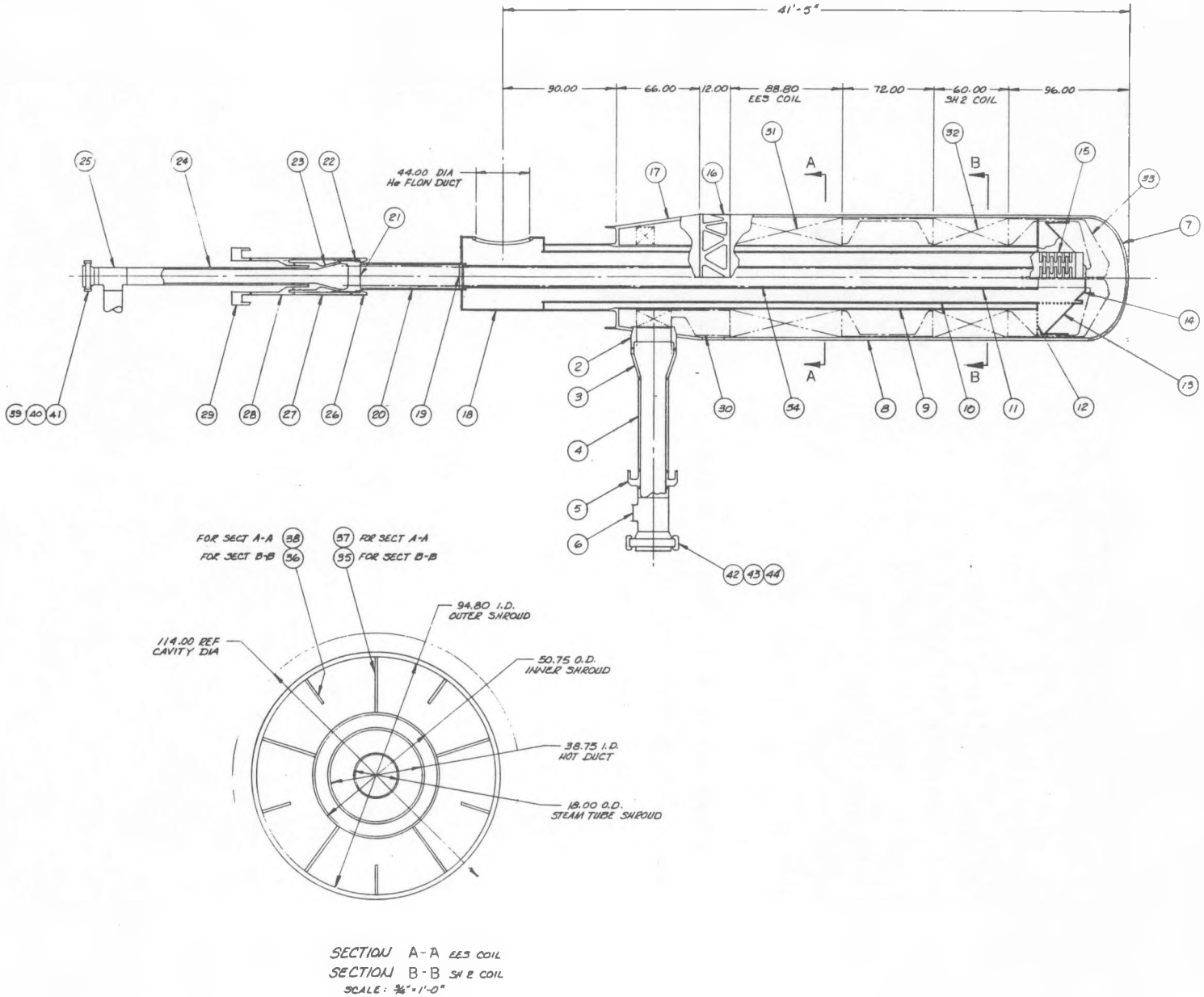

Fig. 3.1-5. 950°C (1742°F) HTGR-PH steam generator general arrangement

finishing superheater tube material. The welds are shielded from the hot helium to limit their temperatures to acceptable values. The bundles are supported by full support plates that extend between the outer and inner shrouds and by partial support plates that extend from the outer shroud only (see Fig. 3.1-5).

Feedwater is supplied to each steam generator unit through a vertically oriented tubesheet located on the side of the unit just below the EES bundle. Individual feedwater tube lead-ins, which extend between the feedwater tubesheet and the helical EES bundle, are attached to the tubesheet by front face fillet welds. A vertical hot duct shroud shields the lead-ins from the hot helium. Access to the shell side of the tubesheet and its associated welds can be gained from the annular access region around the main support joint. Access to the tube side of the tubesheet for tube leak detection and plugging can be obtained through a bolted blind flange in the horizontal portion of the feedwater duct.

Superheat leadout tubes, which extend between the finishing superheater outlet and the superheater tubesheet, are routed through thermal expansion loops to the unit center, where they are clustered into a tight hexagonal pattern. The leadout tubes are then routed verically downward to the superheater tubesheet. Appropriate baffeling shields the leadouts from the hot helium in the expansion zone, and a steam tube shroud shields the vertical tube cluster that is routed to the tubesheet.

The steam generator main support is a welded design. The diameter of the outer shroud tapers as it extends downward from below the EES bundle. The lower end of this tapered section is welded to the thermal sleeve that extends from the steam generator cavity liner. The hot helium flow from the associated reformer cavity enters the steam generator cavity at its bottom end; from there the flow is turned upward through a central annular duct to the unit top end. The flow is turned 3.14 rad (180 deg) and proceeds downward through the helical bundles, giving up its heat to form steam from

feedwater. The cooled helium exits the unit through triangular-shaped windows located in the outer shroud just below the EES bundle. Table 3.1-6 lists the sizing parameters and the design details for a single steam generator unit.

TABLE 3.1-6
STEAM GENERATOR PARAMETERS AND DESIGN DETAILS (PER STEAM GENERATOR)

Sizing parameters	
Helium flow rate kg/s (lb/hr)	161.4 (1.2809×10^6)
Helium inlet temperature, °C (°F)	694 (1282)
Helium discharge temperature, °C (°F)	479 (894)
Helium inlet pressure, MPa (psi)	4.6 (669)
Helium total pressure loss, kPa (psi)	69 (10)
Steam/water flow rate, kg/s (lb/hr)	77.27 (6.133×10^5)
Feedwater temperature, °C (°F)	260 (500)
Steam outlet temperature, °C (°F)	565 (1050)
Steam outlet pressure, MPa (psi)	16.5 (2400)
Feedwater pressure, MPa (psi)	20 (2900)
Net power transferred, MW	181
Design details	
Superheater 2	
Number of tubes	200
Geometry	Helical coil
Tube OD, mm (in.)	22 (0.866)
Wall thickness, mm (in.)	3.3 (0.13)
Transverse pitch, mm (in.)	50.8 (2.0)
Longitudinal pitch, mm (in.)	38.1 (1.5)
Length of tubes, m (ft)	12.95 (42.5)
Length of bundle, m (ft)	1.52 (5.0)
Bundle ID, m (in.)	1.29 (50.75)
Bundle OD, m (in.)	2.41 (94.8)
Tube material	Inconel 800H
Number of support plates	5 full, 5 half
Plate thickness, mm (in.)	19.0 (0.75)
Plate material	Inconel 800H
Economizer-evaporator-superheater 1	
Number of tubes	200
Geometry	Helical coil
Tube OD, mm (in.)	19.05 (0.75)
Wall thickness, mm (in.)	2.8 (0.11)
Transverse pitch, mm (in.)	38.1 (1.5)
Longitudinal pitch, mm (in.)	33.0 (1.3)
Length of tubes, m (ft)	2.26 (7.4)
Bundle ID, m (in.)	1.29 (50.75)
Bundle OD, m (in.)	2.41 (94.8)
Tube material	2 1/4 Cr-1 Mo
Number of support plates	5 full, 5 half
Plate material	2 1/4 Cr-1 Mo
Plate thickness, mm (in.)	19.0 (0.75)

3.2. AVAILABILITY/MAINTAINABILITY (6003050200, 6053010100, and 6053010101)

3.2.1. Scope

The purpose of these tasks (related to availability) was to develop monolithic HTGR-SC/C and HTGR-PH 950°C (1742°F) availability and compare that with the availability of the modular reactor.

3.2.2. Discussion

To compare the modular plant availability with monolithic plant availability, the scheduled and unscheduled downtime values had to be developed. The scheduled outages were based on best estimates of times required for refueling and reformer catalyst replacement and on allowances for extensions of refueling and scheduled maintenance. The unscheduled outages were based on best estimates modified to be consistent with LWR operating experience. After a series of meetings, the NSSS values were developed by GA and GE, and the BOP values were developed by Bechtel.

The first preliminary availability and economic comparisons were made by Bechtel, with the results summarized below.

The availability comparison for the SC/C assumed two 2240-MW monoliths and eight 250-MW MRS's. The monolith availability was about 3% better than the MRS in producing design output. The economic results showed the monolith to produce steam at 1.42 to 5.68 $/GJ (1.50 to 6.00 $/MBtu). (The lower value assumes electricity sales at 38 mills/kWh and the higher at 3.8 mills/kWh.) The MRS produces steam at 3.6 to 5.49 $/GJ (3.80 to 5.80 $/MBtu).

The availability comparison for the HTGR-PH was made assuming two 2240-MW monoliths and twelve 250-MW MRS's. The availabilities to produce design output were equal. The economic results showed the monolith to produce process heat at 13.27 to 14.21 $/GJ (14.00 to 15.00 $/MBtu) and the MRS to produce heat at 14.69 to 15.73 $/GJ (15.50 to 16.60 $/MBtu), using the

same electricity sales figures as were used in the preceding paragraph. These results were based on Bechtel cost estimates.

A preliminary forecast of the 2240-MW HTGR-SC/C, 1170-MW HTGR-PH, and 2240-MW(t) HTGR-PH NSSS availability was prepared to make a comparison with the modular reactor system and SC/C estimates.

A comparison of these calculated values with those used in the MRS versus monolithic study is shown in the table below. In all cases, the scheduled outage values used in the study are much larger than the calculated values. The study values were derived by adding the expected refueling time plus a refueling overage allowance of one week per year to a two-week-per-year allowance for maintenance outages. These values were selected by evaluating LWR operating experience.

The calculated unscheduled outages are greater than those used in the study (except for the 1170-MW HTGR-PH). The primary reason for this is that the study values were selected prior to completion of the calculations. Some items were revised (e.g., the steam generator and reformer leak rates and restore times), which also changed the values. The study values could be revised to reflect these new calculated values. In all cases, the study NSSS availability values are lower than the calculated values, which is conservative.

COMPARISON OF NSSS AVAILABILITY - CALCULATED VERSUS STUDY VALUES

	Scheduled Outages (%/Yr)		Unscheduled Outages (%/Yr)		Availability (%/Yr)	
NSSS	Calculated	Study	Calculated	Study	Calculated	Study
2240-MW HTGR-SC/C	4.0	9.6	6.8	6.0	89.1	84.4
1170-MW HTGR-PH	4.2	8.7	4.3	8.0	91.5	83.3
2240-MW HTGR-PH	5.2	9.6[a]	9.3	8.0[b]	85.5	82.4

[a] Assumed to be the same as for the 2240-MW HTGR-SC/C.

[b] Assumed to be the same as for the 1170-MW HTGR-PH

A review of Bechtel and GE availability results for the modular systems was carried out. This review showed that comparing availability and capacity factor results developed with different methods and outage data is difficult and probably not valid. The methods used were the multinominal by Bechtel and the Markov models by GE. The Bechtel outage data, based on operating reactor experience and estimates, are conservative. The GE data, based on generic failure rates and repair times and estimated refueling time, are optimistic. The Bechtel outage time data are two to five times as great as GE's for forced outages and four times as great as GE's for scheduled outages. Considering these facts, an overall comparison of the modular systems is shown below:

Modular System	Availability		Capacity Factor	
	Bechtel	GE	Bechtel	GE
8/10 300-MW HTGR-SC/C	0.95	0.98	0.86	0.94
8/12 250-MW HTGR-PH	0.99	0.99	0.84	0.95

The modular versus monolithic system comparison done by Bechtel shows that the HTGR-SC/C modular system has slightly better (~1%) availability than the monolith.

4. HTGR-MODULAR REACTOR SYSTEM (MRS)

4.1. MRS-PH; CORE NUCLEAR DESIGN (6053030100)

4.1.1. Scope

The scope of work reported here is to perform nuclear core performance studies on a 250-MW(t) core for 950°C (1742°F) operation, to establish core parameters and document design, and to provide design cost and design report input.

4.1.2. Discussion

4.1.2.1. Core Nuclear Design. Extensive core physics studies were performed for the 950°C (1742°F) MRS-PH plant for both LEU/Th and HEU/Th fuel cycles. The reference design was established for the LEU/Th case with 4-yr batch loading. The core was designed within the 3.5 m (11.5 ft) diameter limitation dictated by steel pressure vessel fabrication considerations. A layout of the MRS prismatic core is shown in Fig. 4.1-1. With the aforementioned envelope restraint for the module rating of 250 MW(t), a core power density of 4.1 W/cc was established. Details of the salient core parameters and features are given in Table 4.1-1.

4.1.2.2. Reactivity Control. Design studies of the control rod were not performed in FY-82, it being assumed that the geometries would be similar to those in the Peach Bottom 1 HTGR plant. A reactivity control approach was established that was viewed as being in accord with the general criteria for control systems (i.e., 10CFR50, Appendix A). Details of the proposed control system are given in Table 4.1-2. The outer six in-core rods

TABLE 4.1-1
BASIC CORE PARAMETERS FOR MODULAR REACTOR SYSTEM PLANTS

	MRS/PH	MRS-SC/C
Thermal		
Helium flow	Upflow configuration	Upflow configuration
Core thermal rating, MW(t)	250	300
Power density, W/cm^3	4.1	4.9
Core outlet temperature, °C (°F)	950 (1742)	688 (1270)
Core inlet temperature, °C (°F)	425 (797)	283 (541)
Inlet pressure, MPa (psia)	5.0 (725)	5.0 (725)
Core pressure loss, kPa (psi) (non-orificed core)	13.8 (2)	20.7 (3)
Fuel cycle		
Fuel	LEU/Th or HEU/Th	
Loading	Batch loaded	
Refueling interval	4-yr (LEU), 5-yr (HEU)	
Fuel element		
Fuel element type	Prismatic element	
Core layout	85 columns, 8 blocks high	
Element design	66 columns of 10-row blocks 19 columns of modified 10-row blocks to accommodate control rods	
Core layout		
Active core diameter, m (ft)	3.5 (11.5)	
Active core height, m (ft)	6.34 (20.8)	
Reflector dimensions, m (ft)	1 (3.28) side 1.2 (3.94) top and bottom	
Core status		
Core design status	Preconceptual	
Technology status	Advanced technology	
Technology bases	Fort St. Vrain experience and HTGR technology program	

TABLE 4.1-2
MRS CORE REACTIVITY CONTROL SYSTEM

Primary System	Secondary System	Comments
Primary system used for long-term cold shutdown control	Secondary system used for hot shutdown only	Different control rod drives for diversity
19 In-core rods	12 Reflector rods	Outer 6 in-core rods combined with reflector rods for immediate scram function
		Inner rods (in high temperature region of core) used only for cold shutdown
		Avoid reserve shutdown system hoppers if possible

NOTE: Proposed approach viewed as being in accord with general criteria for control systems (10CFR50, Appendix A).

combined with the 12 reflector rods are inserted for immediate scram function (see Fig. 4.1-1). The inner rods (in the high-temperature region of the core) are inserted only for cold shutdown. For diversity, different control rod drives for the primary (long-term cold shutdown control) and secondary (hot shutdown) systems are to be adopted (e.g., electrical, hydraulic, pneumatic, etc.). While a reserve shutdown system consisting of boronated spheres in a hopper embodied in the top reflectors was studied, it was not included in the reference design.

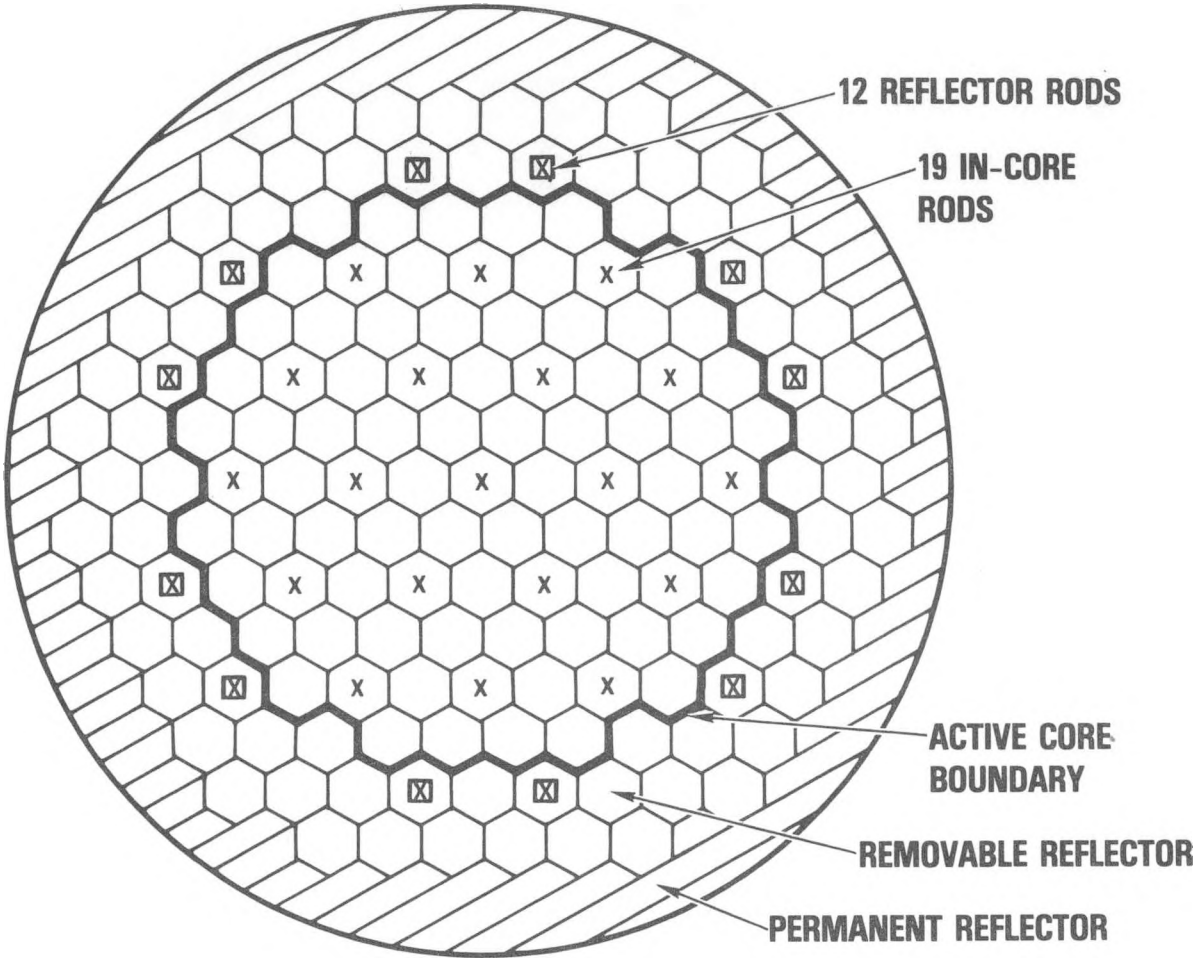

Fig. 4.1-1. Core layout for modular reactor systems

4.2. MRS-PH REACTOR INTERNALS DESIGN (6053030200)

4.2.1. Scope

The scope of work reported here is to identify the preferred concept, to issue layout drawings and interface information, and to provide a costing data package.

4.2.2. Discussion

Work on the reactor internals provided the interface details between the reactor core and the steel vessel. The major elements of the reactor internals are shown in Table 4.2-1. A forged stainless steel core support plate was selected, this in turn being supported on a cylindrical structure mounted from the lower head of the reactor vessel. Lateral restraint between the core assembly and the core barrel was provided by a radial key arrangement. Layout details of the reactor internals for the MRS-PH plant are given in Fig. 4.2-1.

TABLE 4.2-1
REACTOR INTERNALS DESIGN DETAILS FOR MRS/PH PLANT

Core support plate

- Stainless steel forging (304)
- Diameter: 5.7 m (18.6 ft)
- Thickness: 457 mm (18 in.)
- 163 holes: 203-mm (8-in.) diameter for helium flow
- Structurally mounted on core support cylinder

Core support cylinder

- Ferritic alloy (for compatibility with reactor vessel)
- Structurally mounted from lower head of reactor vessel
- Diameter: 5.08 m (16.67 ft)
- Thickness: 50 mm (2.0 in.)

Core barrel

- Stainless steel cylinder (304)
- Diameter: 5.6 m (18.3 ft)
- Height: 11.2 m (36.7 ft)
- Thickness: 38 mm (1.5 in.)
- Cylindrical structure keyed to reactor vessel

Lateral Restraint

- Radial key arrangement
- Seismic loads assumed equivalent of a 1.5-g static lateral load

Reactor internals are designed for 40-yr plant life but are removable and replaceable

Reactor internals status

- Preconceptual design status
- State-of-the-art technology

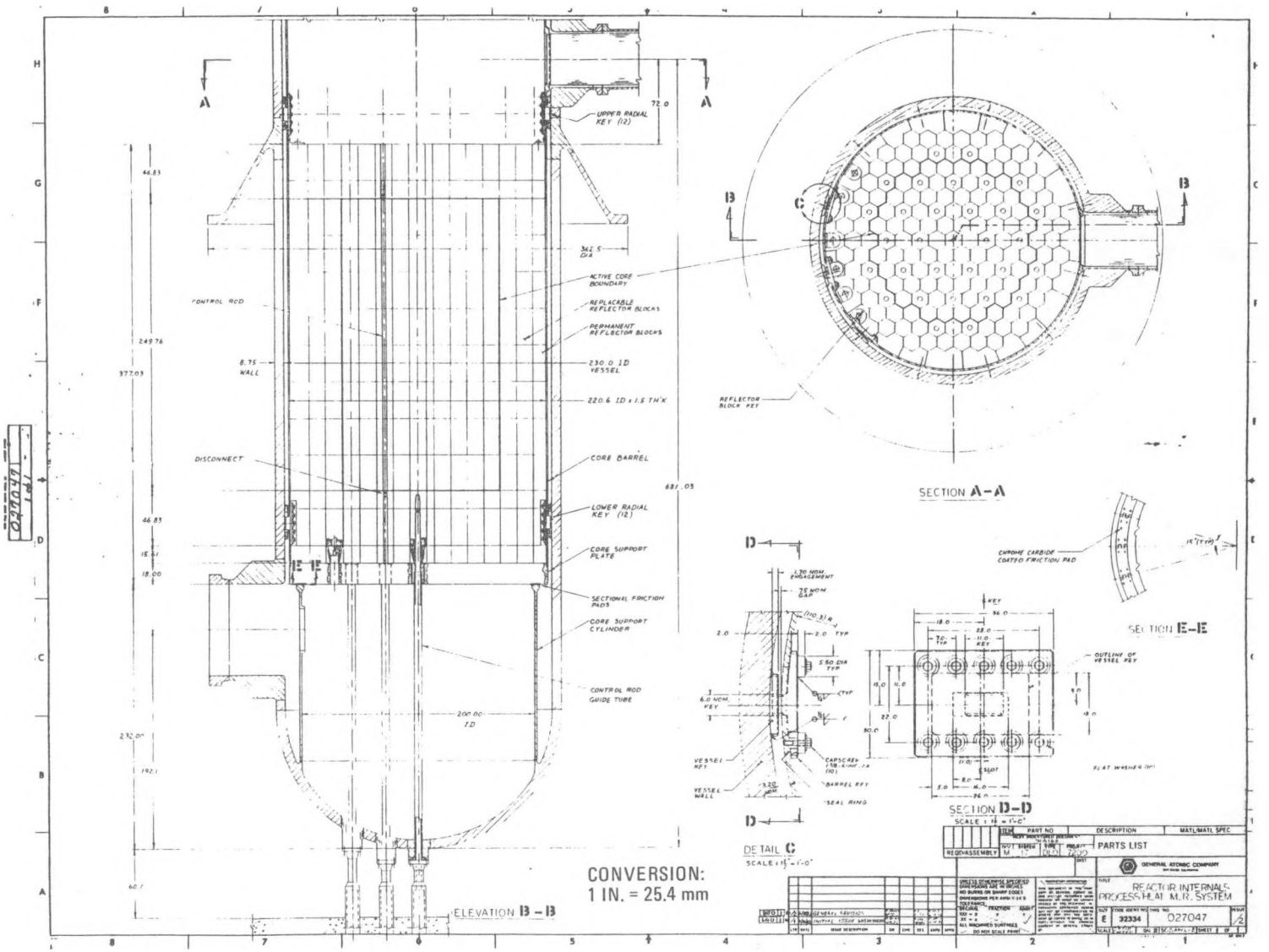

Fig. 4.2-1. Reactor internals design layout for MRS-PH plant

4.3. MRS-PH COMPONENTS DESIGN (6053050100 and 6053050200)

4.3.1. Scope

The tasks under this heading involved providing conceptual design information on the helium circulator, control rod drive (CRD), and fuel handling equipment to support scoping and cost studies for the modular reactor concept.

4.3.2. Discussion

4.3.2.1. Circulator Design. Early in the program a decision was made to utilize a single circulator, and a horizontal arrangement mounted near the bottom of the lower vessel was selected. The circulator consists of an electric-motor-driven helium axial flow compressor with a power requirement of 4103kW (5500 hp). The aerodynamic analysis indicated the requirement for two axial stages for optimum performance. The major circulator parameters and features are given in Table 4.3-1. The major design features of the circulator (i.e., impeller, rotor design, water-lubricated bearings, etc.) are based on established technology. Layout details of the MRS-PH plant circulator are given in Fig. 4.3-1.

4.3.2.2. Control Rod Drive Design. The CRDs in the HTGR-MRS are located below the reactor vessel. In an attempt to minimize the vertical height of the access area below the shielding, an offset drive arrangement was selected. Gravity assist rod insertion was provided for by incorporating a counterbalance arrangement. Capability for differing CRDs for diversity would necessitate evaluation of electric, hydraulic, and pneumatic systems. Details of the CRDs are summarized in Table 4.3-2, and layout features are shown in Fig. 4.3-2. The technology base for the CRD design is the Peach Bottom 1 Plant.

TABLE 4.3-1
CIRCULATOR DESIGN DETAILS FOR HTGR-MRS PLANTS

Number of circulators	1 per module
Circulator type	Electric-motor-driven helium axial flow compressor
Compressor type	Axial flow machine
Circulator orientation	Horizontal
Bearing type	Water lubricated
Design status	Preconceptual
Technology base	Fort St. Vrain circulator operation and HTGR technology program in support of lead plant circulator design

	MRS-PH	MRS-SC/C
Number of compressor stages	Two	One
Helium flow, kg/s (lb/hr)	92 (7.3×10^5)	143 (1.13×10^6)
Inlet temperature, °C (°F)	419 (786)	282 (540)
Inlet pressure, MPa (psia)	4.53 (657)	4.95 (718)
Pressure rise, kPa (psi)	110 (16.0)	48 (7.0)
Specific speed	216	257
Adiabatic efficiency, %	82	81
Impeller tip diameter, mm (in.)	900 (35.4)	988 (38.9)
Motor shaft power, kW (hp)	4103 (5500)	2131 (2857)
Full load drive speed, rpm	4500	3600
Pony motor power, kW (hp)	600 (804)	336 (450)

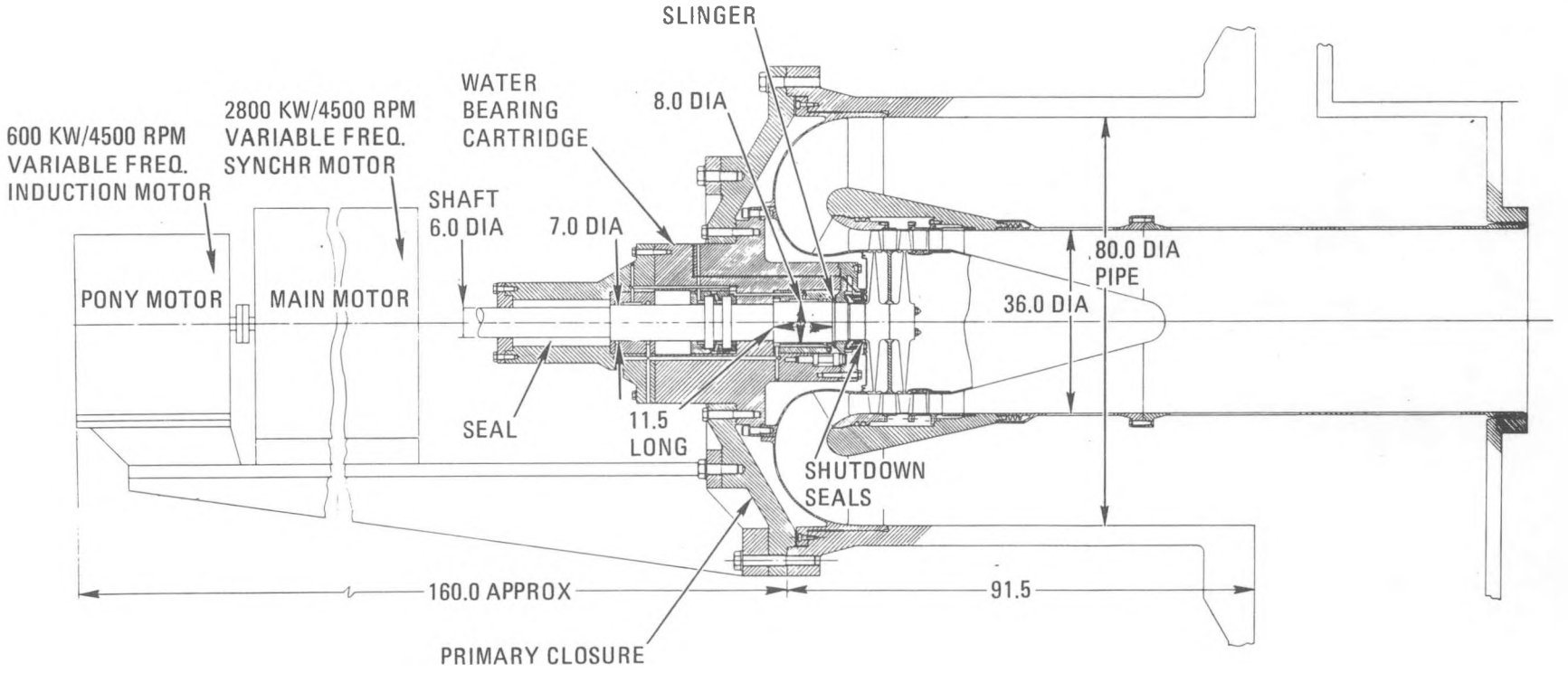

Fig. 4.3-1. Circulator arrangement for MRS-PH plant

TABLE 4.3-2
CONTROL ROD DRIVE DESIGN DETAILS FOR MRS PLANTS

CRD location	Below reactor vessel
CRD type	Offset drive arrangement
Number of CRD's	19 in-core 12 reflector rods
Capability for gravity assist rod insertion	Yes (counterbalance weight arrangement)
Capability for differing CRD's for diversity	Yes (electric, hydraulic, or pneumatic drives)
Access for CRD inspection and maintenance	Yes
CRD design status	Preconceptual
Technology base	Peach Bottom 1

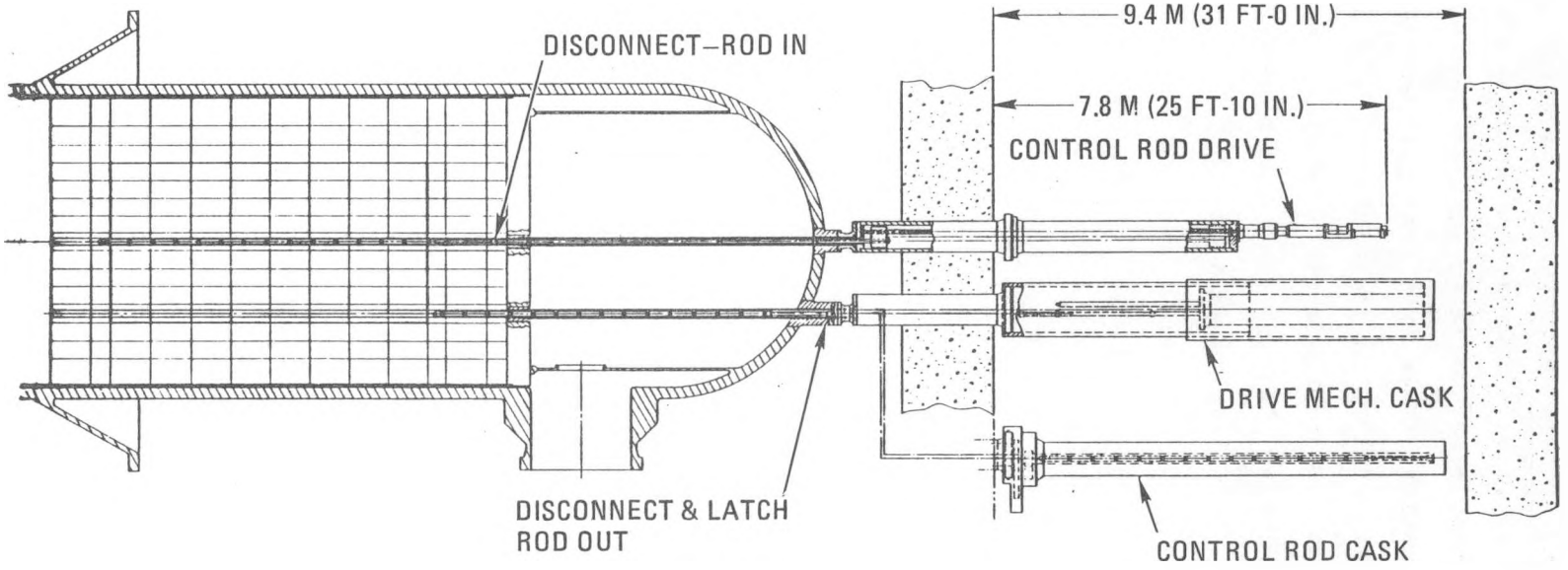

Fig. 4.3-2. Control rod drive concept for MRS plants

4.3.2.3. Fuel Handling System. For the in-line vessel MRS arrangement, with the heat exchangers (i.e., reformer and steam generator) installed above the prismatic core, a new refueling concept had to be established. Because of the long vertical reach from above, it was established early in the program that a horizontal refueling approach would offer the most viable solution. Accordingly, a concept was established with a horizontal refueling penetration in the upper plane of the lower reactor vessel. The design concept (shown in Fig. 4.3-3) embodies a twin telescoping arm arrangement capable of parallel operation. Grapple head vertical motivation is facilitated by means of a bi-stem arrangement. Major features of the fuel handling system are given in Table 4.3-3. The estimated refueling time is 15 days to replace the complete core every four years.

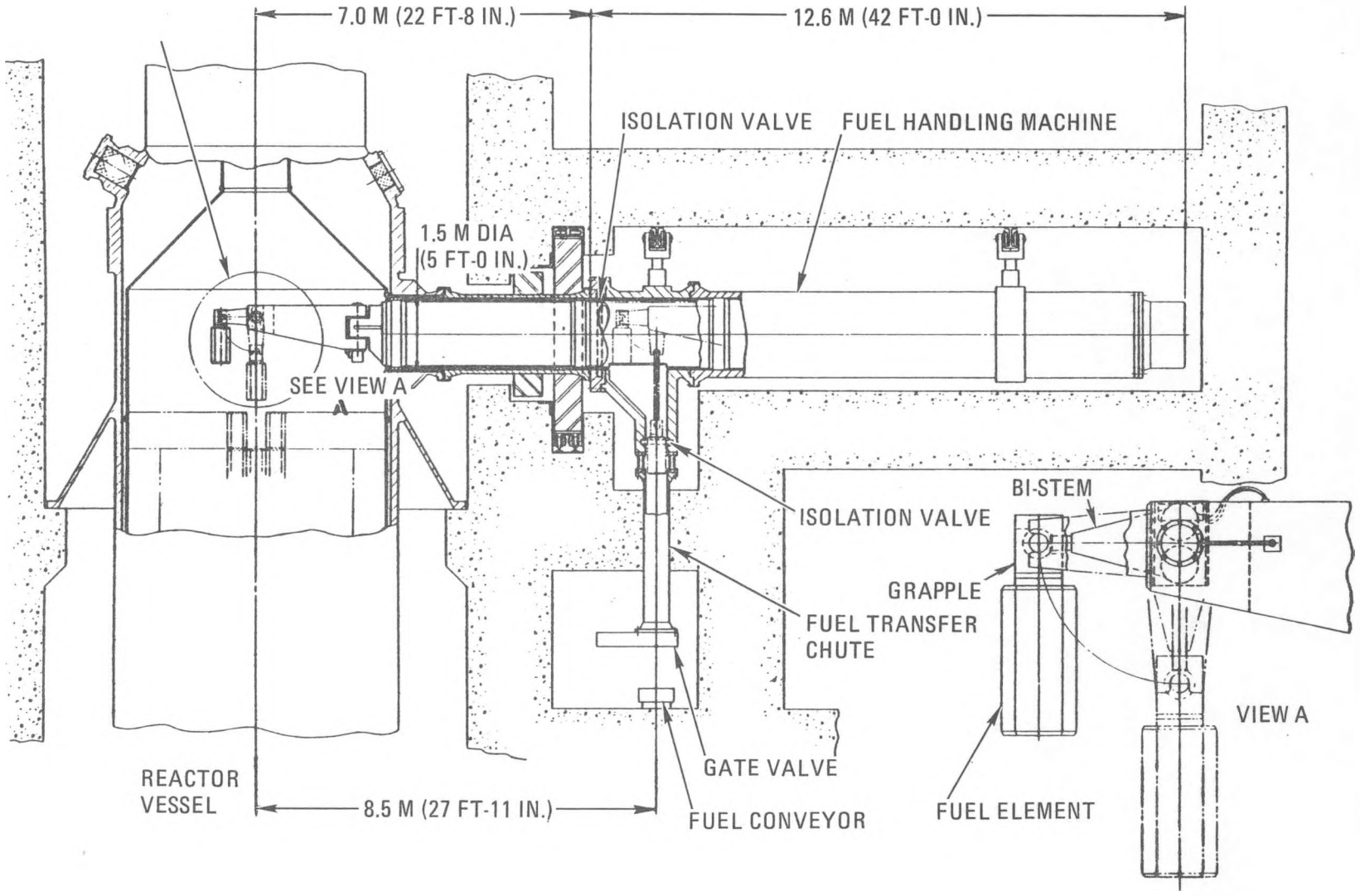

Fig. 4.3-3. Side refueling scheme for MRS plants

TABLE 4.3-3
FUEL HANDLING SYSTEM DETAILS FOR MRS PLANTS

Prismatic core refueling interval	4-yr batch (LEU/TH) 5-yr batch (HEU/TH)
Refueling location	Horizontal penetration in upper plane of lower reactor vessel
Fuel handling machine	New design for MRS
Major features	Twin telescoping arm arrangement capable of parallel operation
Grapple head motivation	Bi-stem arrangement for vertical motion of 6.7 m (22 ft)
Estimated refueling time	15 days to replace complete core (every 4 or 5 yr)
Fuel handling machine design status	Preconceptual
Technology base	Lead plant HTGR, with additional development needed for unique MRS requirements

4.4. MRS-SC/C CORE NUCLEAR DESIGN (6053030101 and 6053030200)

4.4.1. Scope

The scope of work reported here is to establish the basic parameters for an MRS-SC/C core and to perform necessary analysis to determine the maximum core power density and power level compatible with operation of an MRS-PH size of core at the lower-temperature SC/C conditions.

4.4.2. Discussion

Core physics calculations were performed toward determining a reference fuel cycle for the modular core with steam-cycle plant outlet helium temperatures. For commonality with the MRS-PH plant (particularly the vessel diameter), the core envelope was retained. Power limits due to fuel temperature and core pressure drop considerations are in the range of over 400 MW(t) and were not the determining factor for establishing the reactor thermal rating. With the given core envelope, the selected rating of 300 MW(t) was accomplished with a power density of 4.9 W/cm^3. Details of the salient core parameters and features are given in Table 4.1-1.

4.5. MRS-SC/C COMPONENT DESIGN STUDIES (6053050101 and 6053050201)

4.5.1. Scope

Tasks under this heading included establishing major parameters and the envelope for the MRS-SC/C helium circulator update CRD system concept and updating fuel handling concepts for the MRS-SC/C.

4.5.2. Discussion

4.5.2.1. Circulator Design. The location and orientation of the circulator are identical to those for the process heat plant. With the much lower system pressure loss for the MRS-SC/C (although with a higher thermal rating), the aerodynamic analysis indicated that optimum performance could be realized with a single-stage axial compressor. The power requirement for the circulator is 2131 kW (2857 hp). The major features of the circulators for both MRS variants are similar, and details are given in Table 4.3-1.

4.5.2.2. Control Rod Drives and Fuel Handling. In the areas of the CRDs and the fuel handling system, no additional work was performed. It was assumed that the configurations selected (as outlined in Section 4.3.2.2) would be nearly identical for both modular plant variants.

4.6. MRS-SC/C REACTOR INTERNALS DESIGN (6053030201)

4.6.1. Scope

The scope of work reported here was to identify differences between the reactor internals design of the MRS-SC/C and the MRS-PH.

4.6.2. Discussion

Design work on the reactor internals for the MRS-SC/C plant was limited and essentially only addressed the differences between the steam cycle and the process heat plant variants. The same configurations and materials were retained and the major features are the same as those outlined in Section 4.2.

4.7. MRS-SC/C PCRV CONCEPTS STUDY (6053030300)

4.7.1. Scope

The scope of this task was to establish a PCRV layout concept to meet the requirement for a 300-MW(t) HTGR-MRS-SC/C plant.

4.7.2. Discussion

Several PCRV concepts for a 300-MW(t) MRS-SC/C plant were evaluated. Six of these appeared to be technically viable. The study encompassed (1) single-cavity variants, (2) podded multicavity vessel concepts, (3) steam generator number and location, (4) circulator number and location, and (5) primary system gas flow path development for both normal operation and natural circulation in the decay heat removal mode.

The various PCRV concepts incorporate the following major features that are considered in the selection of an optimum plant:

1. Prismatic upflow core.

2. Uphill boiling, single or multiple steam generators.

3. Single-stage axial flow circulators (horizontal or vertical).

4. PCRV liner cooling water system for natural circulation cooling capability.

5. Side or top refueling.

6. Bottom head control rod operation.

7. Maximum cavity pressure of 4.86 MPa (850 psi) for vessel design.

8. 44.8-MPa (6500-psi) concrete at 60 days with forty-eight 12.7-mm (1/2-in.) diameter strand tendons for longitudinal prestressing and 12.7-mm (1/2-in.) diameter strands for circumferential prestressing.

All the concepts embodied natural circulation conducive to passive decay heat removal by the PCRV liner cooling system during an emergency condition as well as the inherent safety features of using a PCRV as a primary containment. In addition, the adoption of a PCRV for the smaller HTGR modular reactor systems offers the following advantages over a steel vessel:

1. Structural integrity, which is the result of redundant prestressing systems of multiple tendons and strands.

2. No exposure of the PCRV concrete to thermal cycling and no neutron embrittlement concern as in the case of a steel pressure vessel.

3. Vessel concrete designed to be in net compression throughout its life. In all the PCRV concepts studied, the concrete structure is the pressure-resisting primary containment, which also provides the required biological shielding. The PCRV liner cooling system is composed of cooling tubes welded to the concrete side of the liner, which limits the temperature exposure of the PCRV concrete to within design allowable values and permits removing decay heat during a loss of forced circulation event.

In the PCRV design and layout study, it soon became clear that for a small plant the single-cavity approach yielded a more cost-effective solution and provided a better natural circulation cool-down capability than the podded multicavity design, while allowing vessel diameters some 4.6 m (15 ft) smaller. These findings, which were postulated at the onset of the study, enabled maximum utilization of PCRV technology from the Fort St. Vrain plant.

With the selection of the single-cavity configuration, it was found that other major features of the nuclear heat source (NHS) were not strongly influenced by the number of steam generators and circulators. The design concept is shown isometrically in Fig. 4.7-1, with four steam generators positioned above the core and two horizontally mounted circulators near the bottom plane of the vessel. During normal operation, the primary coolant exits the core upper plenum, travels through a vertical duct, and enters the steam generator bundle. The gas exits the steam generator lower end to a shroud around the core and then flows to the main circulator before entering the core lower plenum. During emergency operation, the coolant exits the top of the steam generator into the PCRV main cavity through an emergency valve. The gas, which is cooled by the PCRV cooling system, induces the process of natural circulation.

The major features of the design shown in Fig. 4.7-1 are listed in Table 4.7-1. The PCRV diameter and height are 12.5 m (41.0 ft) and 30.5 m (100.0 ft), respectively. The prestressing system consists of linear and circumferential prestressing similar to that used for the large HTGR. The steam generators have concrete (or welded steel) closures through which a central superheat penetration passes. The main circulators are mounted horizontally at the elevation of the core inlet plenum, and access penetration for refueling is at the top of the vessel.

The PCRV embodies an emergency cooling system that establishes a natural convection flow pattern within the concrete pressure vessel sufficient to remove the decay heat generated in the core during an emergency shutdown. Core decay heat removal is accomplished by heat transfer to the liner cooling system that covers the entire interior surface of the concrete pressure vessel in which the core and associated heat exchangers are located. Redundancy in the liner cooling tube arrangement is used to improve the reliability of the system. The gas flow paths during normal operation and emergency conditions are indicated in Fig. 4.7-1.

In the event that an emergency occurs requiring shutdown of the reactor, and the primary gas coolant circulation system is for some reason

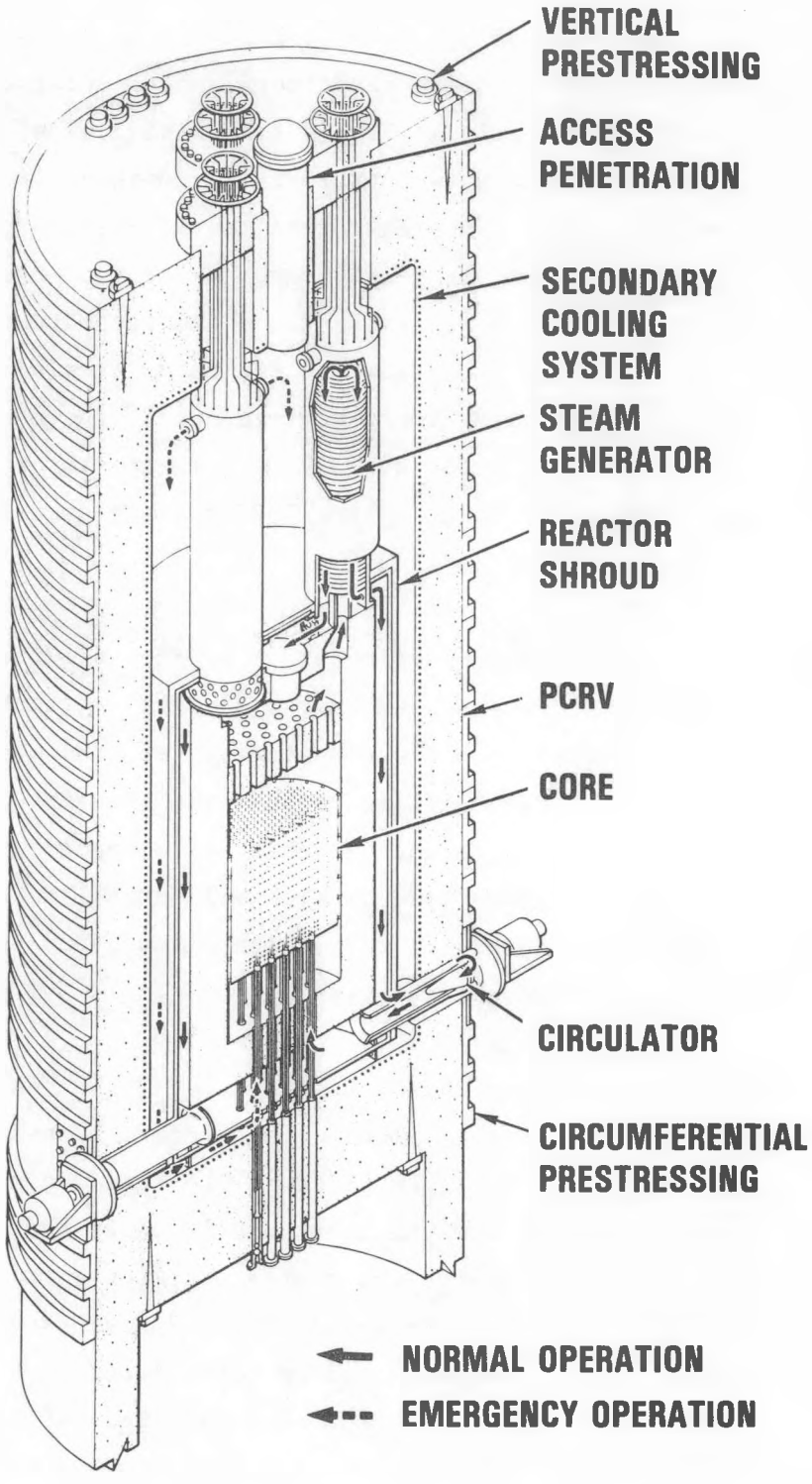

Fig. 4.7-1. PCRV design concept for HTGR-MRS-SC/C plant

TABLE 4.7-1
MAJOR FEATURES OF THE HTGR-MRS-SC/C PLANT

Rating and Performance	Reactor thermal rating, MW(t)	300
	Thermodynamic cycle	Variable steam cycle/ cogeneration
	Reactor outlet temp., °C (°F)	688 (1270)
	Max. system pressure, MPa (psia)	5.0 (725)
	Heat losses, MW(t)	5.0
	Nuclear steam supply system (NSSS) output, kg/sec (lb/hr)	121.6 (0.965×10^6)
	Electrical power output potential, MW(e)	112
Reactor core	Reactor core type	HTGR
	Fuel element	Prismatic element
	Helium flow configuration	Upflow
	Power density, W/cm^3	4.9
	Core layout	85 columns, 8 blocks high
	Core diameter/height, m (ft)	3.5 (11.5)/6.34 (20.8)
	Fuel cycle	LEU/Th or HEU/Th
	Refueling interval and type	4-yr batch loaded
	Core rods	In core and reflector
Plant design and layout features	Reactor vessel type	PCRV, single-cavity
	PCRV diameter/height, m (ft)	12.5 (41.0)/30.5 (100.0)
	NHS arrangement	Steam generator above core
	Steam generator type	Helical bundle with upflow boiling
	Circulator type	Horizontal machine - electric-motor-driven compressor
	Control rod drives	Bottom mounted
	Refueling concept	Top refueling arrangement
	Overall plant arrangement	Integrated configuration

rendered inoperative so that the circulators no longer draw coolant down the inner passageway, the emergency is automatically detected and the bypass valves located at the top of each of the steam generators are opened. These valves may be opened by gravity upon loss of primary coolant pressure differential across the circulator or by remote automatic control by the main reactor protective system. They may also have a backup control that will open them upon detection of an abnormal rise in temperature of the hot coolant gas at the top or the interior of the steam generators. Opening of the bypass valves during such an emergency allows the hot gas to divert radially outward into the region below the upper end wall and adjacent to the metal liner, from which point a natural convection flow is established within the NHS for the case where the system is pressurized.

In the case of a hypothesized system depressurization event, natural circulation is no longer induced, and the mode of heat rejection is by conduction in the core and radiation from the metallic reactor shroud to the water cooling coil system mounted on the PCRV side walls. Safety-related calculations have shown that, for the depressurized core heatup event, the temperature levels in small HTGR cores [up to 300 MW(t)] are such that essentially all the fission products are contained.

It should be recognized that the configuration shown in Fig. 4.7-1 is in a very early stage of design development, and efforts beyond the current preconceptual design status are necessary to yield an optimum, cost-effective solution. However, the approach selected satisfies the major design requirements and is based on proven PCRV practice. Recognizing that the vessel has a high aspect ratio, further investigation of seismic stresses in the PCRV and its supporting structure, in combination with the mechanical loads, is necessary.

A rough comparative engineering economic evaluation was made for all six PCRV concepts, which included relative costs of the PCRV, liners, penetrations, and cooling water systems. No technology development costs were considered in the estimates.

While the single-cavity, four-steam-generator configuration shown in Fig. 4.7-1 was shown to have a small economic penalty compared with the single steam generator arrangement, it offers improved plant availability features over the single steam generator concepts. This makes it the preferred concept of those studied.

4.8. MRS-SAFETY ASSESSMENTS (6053020001 and 6053020200)

4.8.1. Scope

The tasks under this heading included (1) performing core heatup consequences, (2) establishing decay heat removal, and (3) performing a preliminary mini-probabilistic risk assessment of an MRS-PH direct cycle plant.

4.8.2. Discussion

4.8.2.1. Safety Assessments. The safety assessments performed in this operating period covered essentially three major areas: (1) pressurized decay heat removal, (2) depressurized core heatup, and (3) preliminary risk assessment (PRA). In the decay heat removal studies, the following modes of operation were considered:

1. Main loop cooling system (MLCS), if the steam generator is operational. (For the MRS-PH variant, the process side of the reformer was assumed to be isolated at time zero.)

2. Pressurized decay heat removal by natural circulation using the vessel cooling system (VCS), facilitated by actuation of the bypass flow valve.

3. Depressurized decay heat removal by radial conduction and radiation from the lower vessel wall.

Studies performed for the two major modes of heat removal are briefly summarized below.

Pressurized Decay Heat Removal

An extensive effort was made in modeling the MRS-PH system to evaluate pressurized decay heat removal by natural circulation using the vessel cooling system. The basis for the model is shown in Fig. 4.8-1. For the in-line vessel arrangement with a core heat of 250 MW(t), natural circulation for the pressurized system (with radiation from the vessel walls as shown in Fig. 4.8-2) was proved feasible. Transients (as shown typically for the MRS-PH plant in Figs. 4.8-3 and 4.8-4) were developed in support of the reactor vessel and heat exchanger design. The analytical study for the MRS-PH plant indicated that natural circulation was feasible for the vessel limits of 450°C (800°F) and 6.2 MPa (900 psia) established by Combustion Engineering. These imposed limits allowed the utilization of a code-qualified alloy, SA-387.

Using the same analytical techniques developed for the MRS-PH plant, the models were updated for the MRS-SC/C concept. The analysis showed that the system energy balance (i.e., energies stored in the gas, core, steel vessel, etc.) to be very sensitive to the gap sizes of the pressure vessel annulus. For the 300-MW(t) thermal rating, the study indicated that natural circulation was feasible for the vessel limits of 346°C (665°F) and 9.3 MPa (1350 psia) established by Combustion Engineering. These limits allow the use of code-approved Alloy SA-533, which is used for LWR vessels.

A summary of the pressurized decay heat removal study is given in Table 4.8-1.

Depressurized Core Heatup Study

The safety-related studies for the MRS-PH plant essentially addressed the most severe postulated event, namely the unrestrained core heatup with

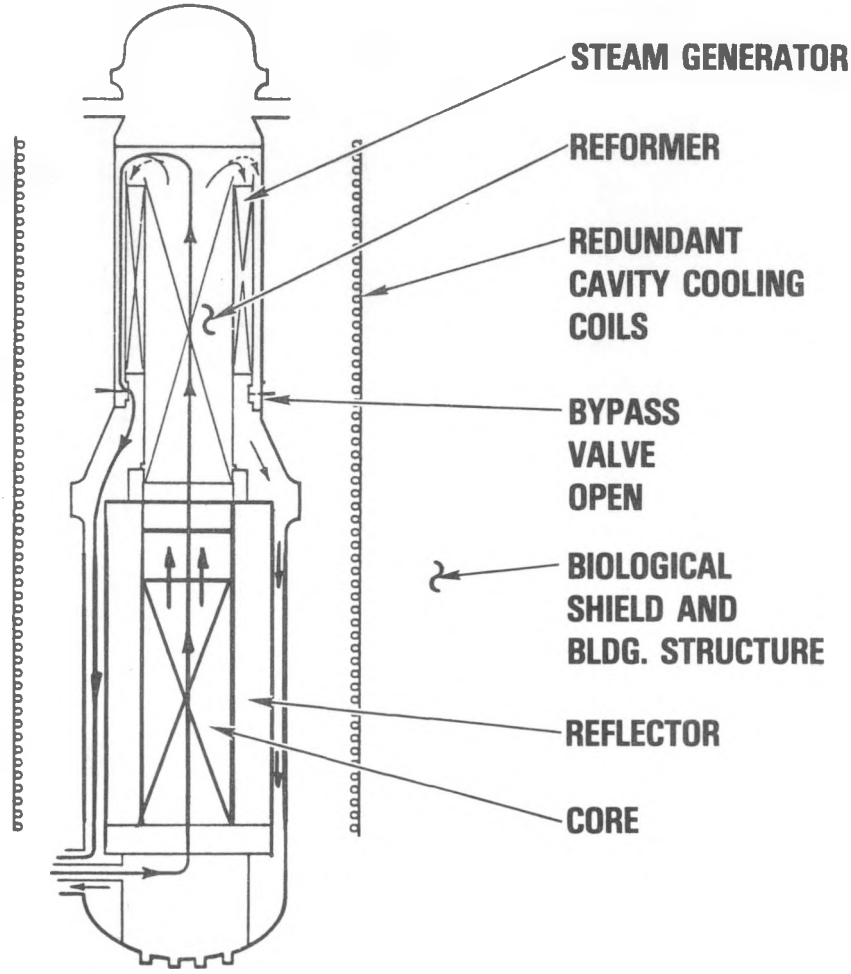

Fig. 4.8-1. Pressurized NHS natural circulation gas flow path with vessel cooling system operational for MRS-PH plant

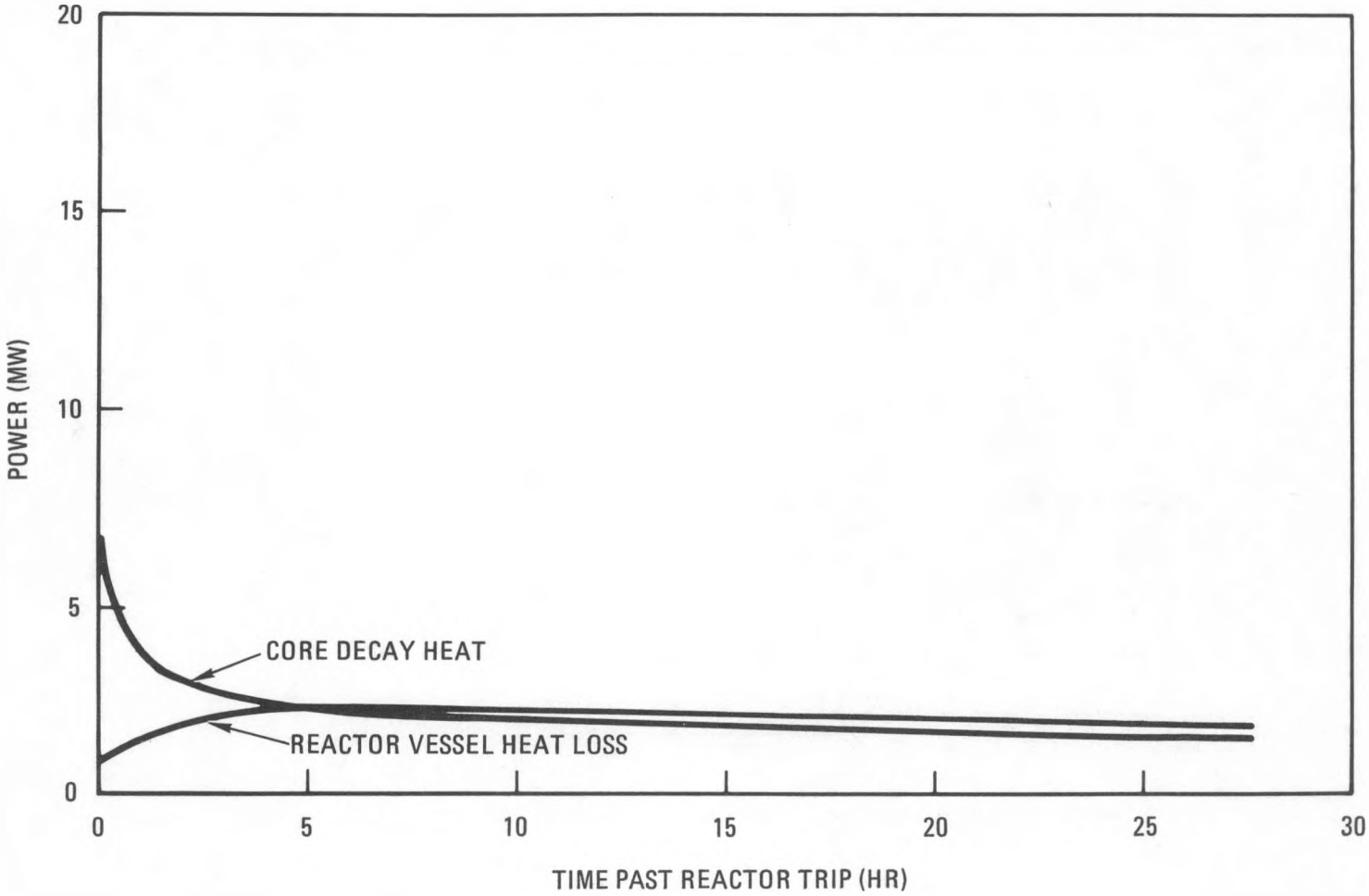

Fig. 4.8-2. MRS core decay heat passive vessel cooling characteristics

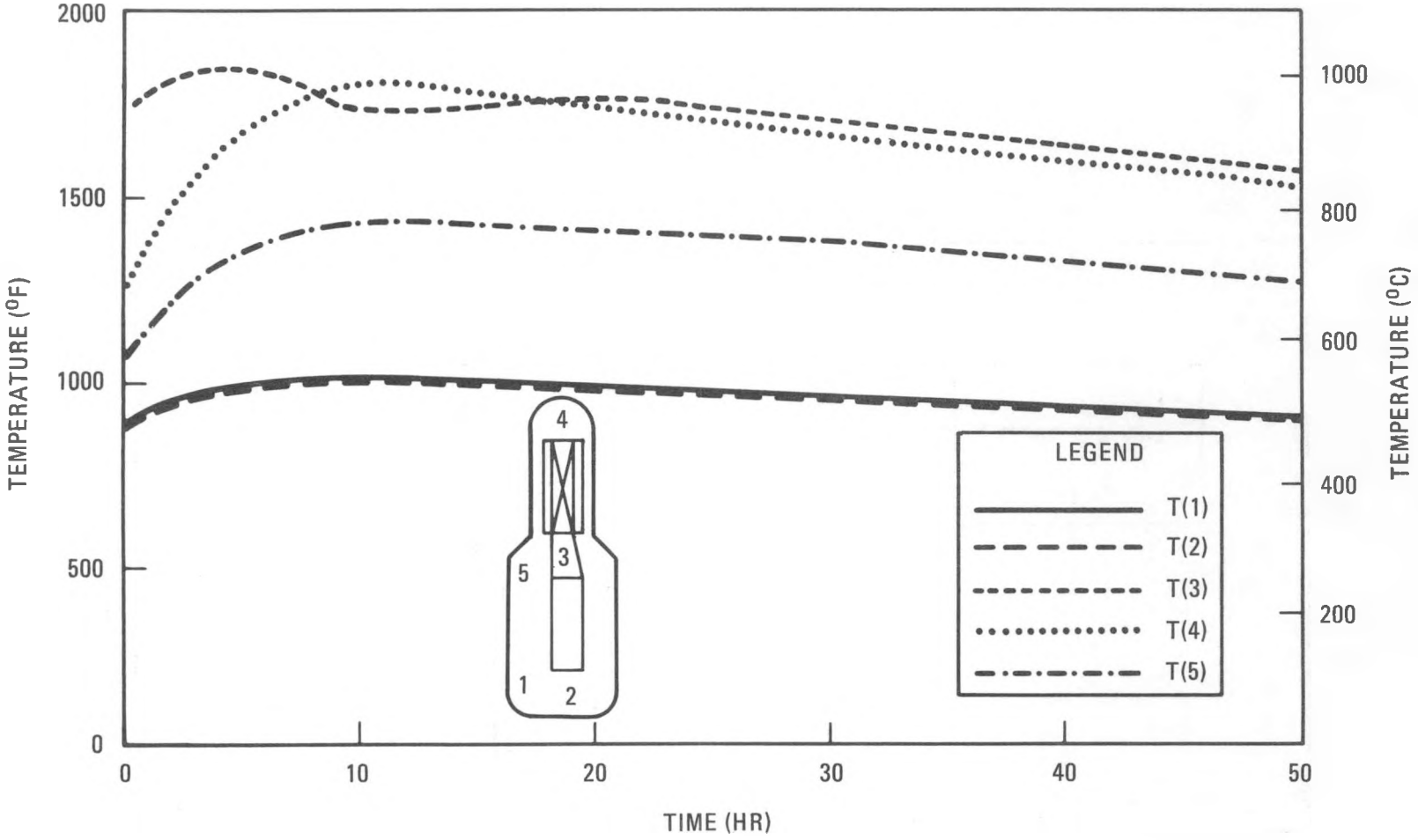

Fig. 4.8-3. Helium temperature transients during passive pressurized decay heat removal for MRS-PH plant

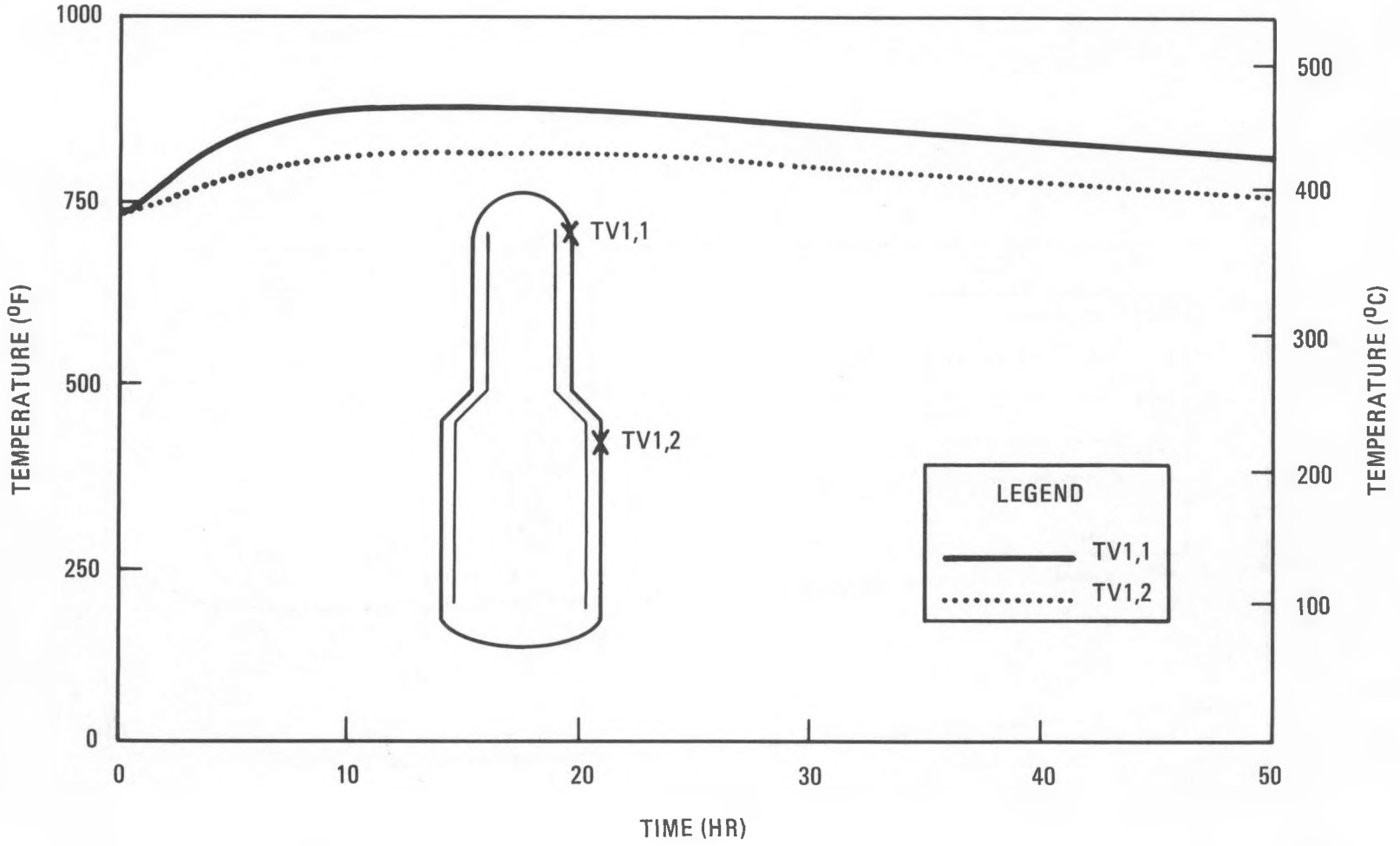

Fig. 4.8-4. Steel reactor vessel thermal transients during passive pressurized decay heat removal for MRS-PH plant

TABLE 4.8-1
SUMMARY OF MRS PRESSURIZED DECAY HEAT REMOVAL STUDIES

Natural circulation shown to be feasible for the selected configuration

- In-line vessel arrangement
- 250 MW(t) (4.1 W/cm^3) for MRS-PH
- 300 MW(t) (4.9 W/cm^3) for MRS-SC/C
- Prismatic core diameter of 3.5 m (11.5 ft)
- Gas flow path configuration
- Surface area of uninsulated reactor vessel

Study results indicate natural circulation feasible for the following vessel limits, allowing utilization of code-qualified materials:

- MRS-PH, 454°C (800°F) and 6.2 MPa (900 psia) - SA-387 MTL
- MRS-SC/C, 352°C (665°F) and 9.3 MPa (1350 psia) - SA-533 MTL

Analysis showed heat transfer from shroud to reactor vessel to be sensitive to annular dimension (optimization study required to determine how heat should be stored/dissipated in core, gas, and vessel wall)

Transient data developed were used in conceptual design of vessel and heat exchangers

the system depressurized. An extensive effort was made in analytical modeling and transient analyses for this task. In this mode of operation the heat rejection is primarily by radial conduction in the core and radiation from the lower part of the reactor vessel to the cooling coils on the biological shield. An array of transients was produced, and typical examples for the MRS-PH plant are shown in Figs. 4.8-5 and 4.8-6. Development of the isotherm map in Fig. 4.8-7 led to the generation of fission product release data as shown in Fig. 4.8-8. The studies for the MRS-PH showed significantly lower core temperatures than in the large monolithic HTGR, and the estimated volatile fission product release was on the order of 1% for the module rated at 250 MW(t).

Using analytical techniques developed for the MRS-PH plant, a study was performed for the MRS-SC/C variant. Again, depressurized core heatup was chosen as the basis for safety consideration, as it results in maximum fuel temperature and fission product release. While core physics and pressurized decay heat removal consideration indicated a core thermal rating of 400 MW(t) to be possible, this rating was not acceptable for the depressurized core heatup event, since it led to fuel failure on the order of 30%. A power level of 300 MW(t) was recommended for the MRS-SC/C module rating, and the results show the maximum fuel temperature to be 2093°C (3800°F) and the fission product release to be approximately 5% with vessel cooling.

The initial safety studies concluded that the modular reactor is benign and therefore has a negligible effect on public safety. A summary of the depressurized core heatup studies is given in Table 4.8-2.

Safety-Related Mini-Probabilistic Risk Analysis (PRA)

A mini-PRA was carried out and three initiating events studied: (1) loss of main loop cooling, (2) water ingress, and (3) system depressurization. Results were generated for the cases of a single-module plant and an arrangment embodying a multiplicity of modules. The results (summarized

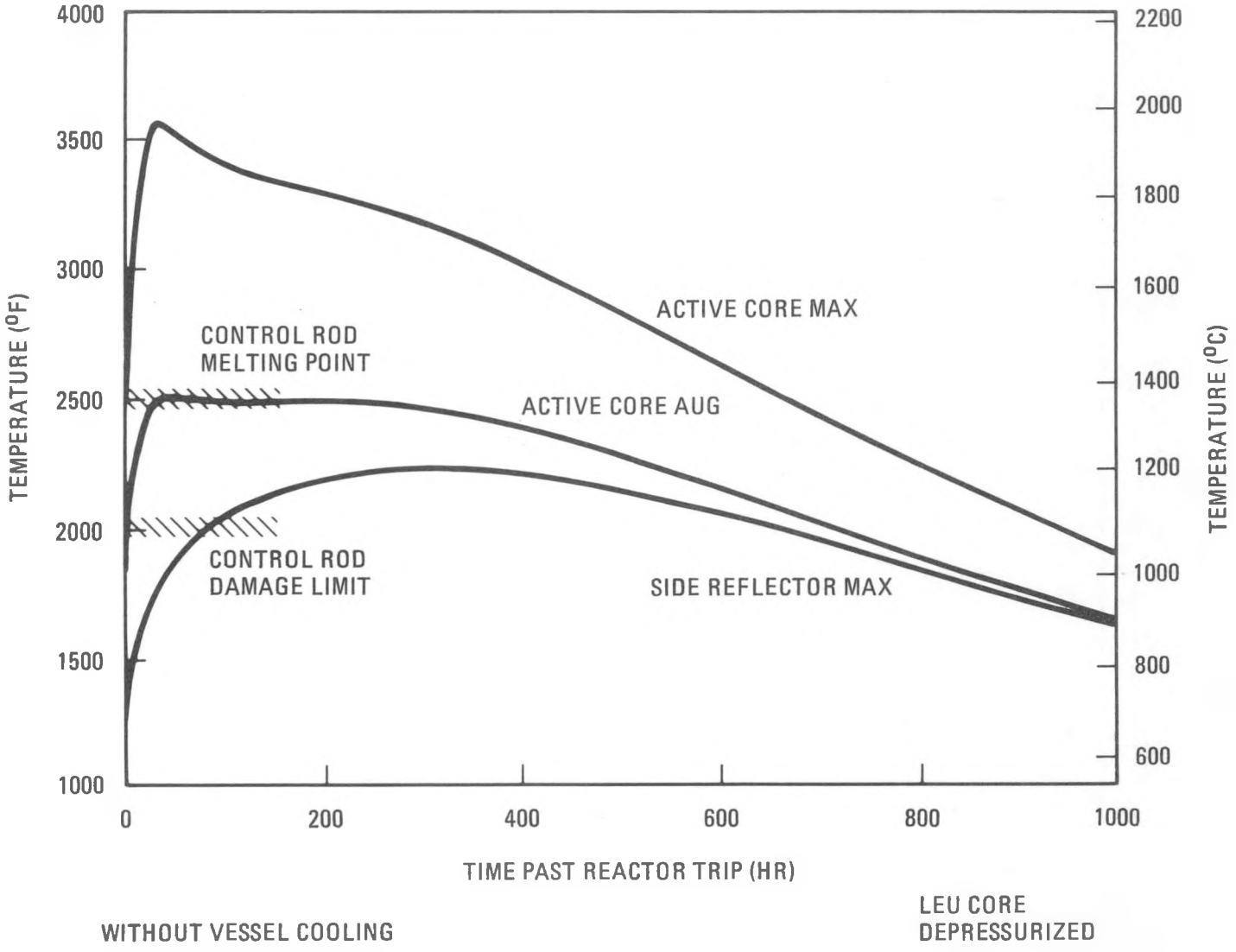

Fig. 4.8-5. Depressurized core heatup transients for MRS-PH plant

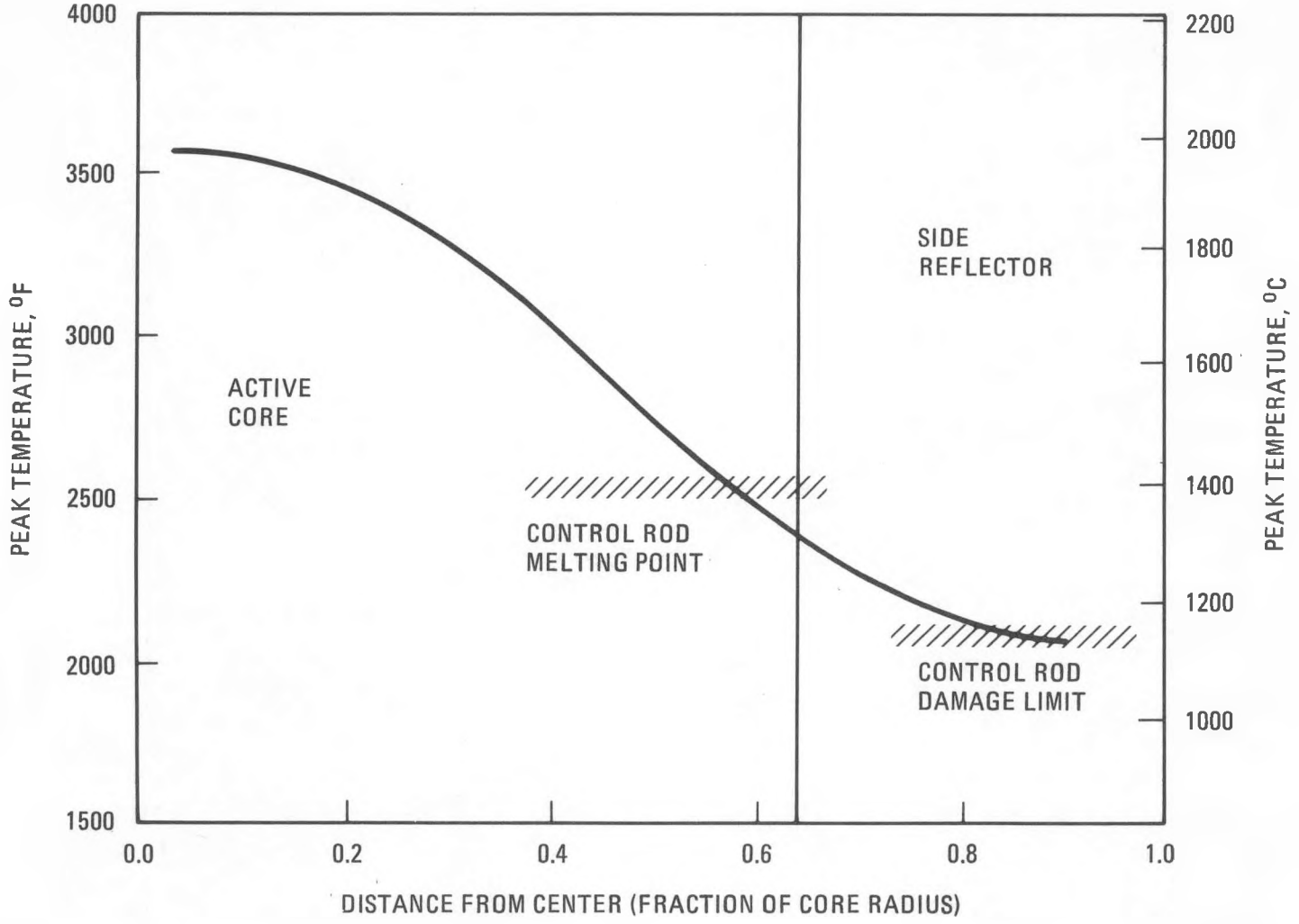

Fig. 4.8-6. Depressurized core heatup gradients for MRS-PH plant

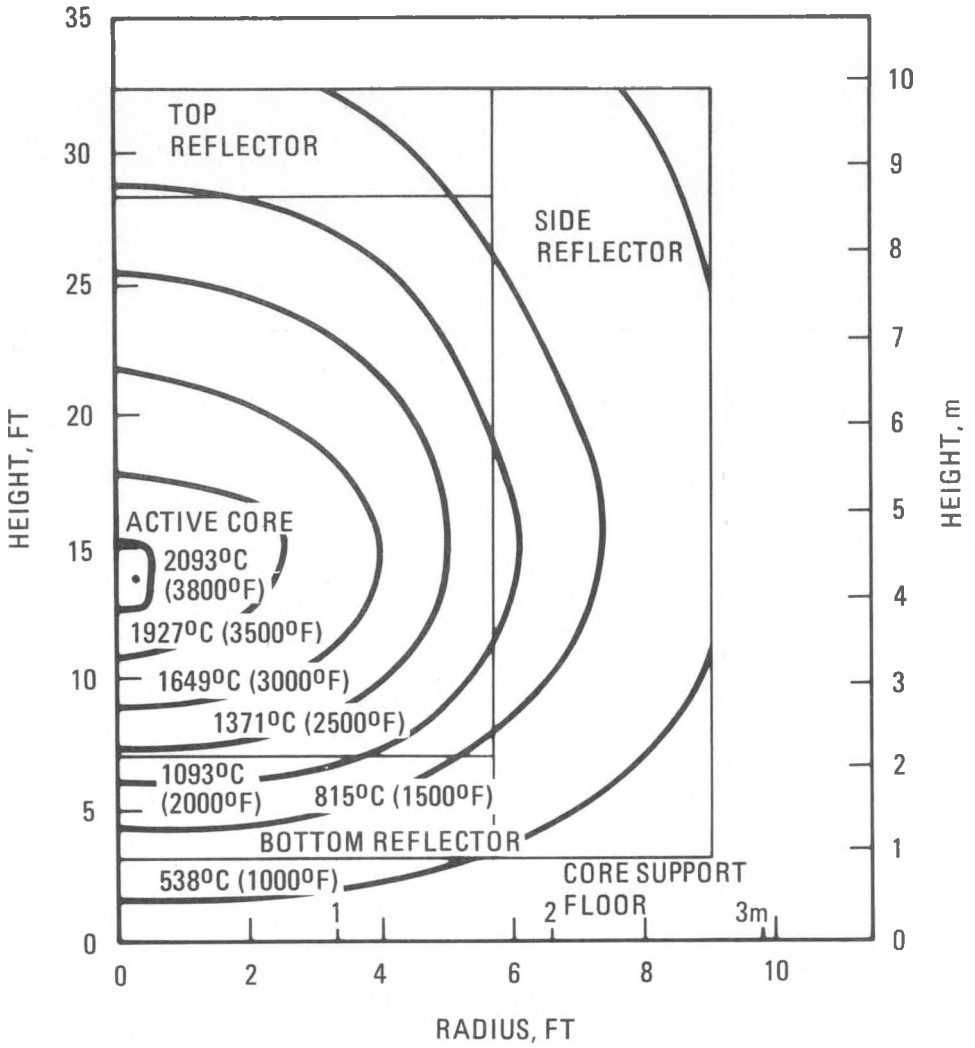

CONDITIONS:
4.1 W/CC CORE DIRECT CYCLE
REFORMING SYSTEM DEPRESSURIZED
WITHOUT VESSEL COOLING
TIME = 26 HR

Fig. 4.8-7. Depressurized isotherm map at time of peak core temperature for 250-MW(t) MRS-PH plant

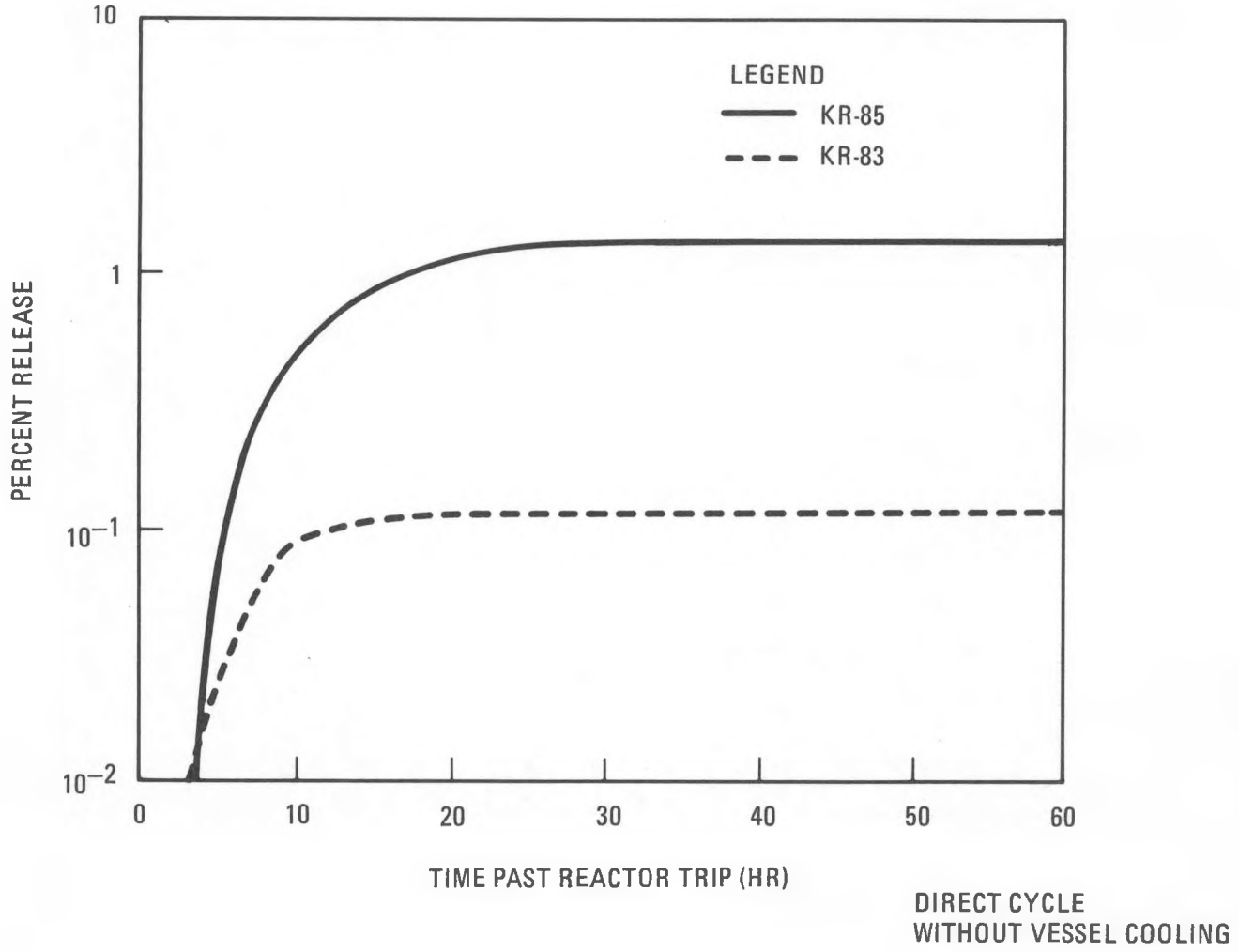

Fig. 4.8-8. Release of volatile isotopes during depressurized core heatup for 250-MW(t) MRS-PH plant

TABLE 4.8-2
SUMMARY OF MRS DEPRESSURIZED CORE HEATUP STUDIES

Modular reactor core heatup shows significantly lower core temperatures than in large monolithic HTGR

Maximum and average active core temperatures insensitive to active vessel cooling

Heat flow primarily in radial direction

Volatile fission product release estimate:

1% for 250 MW(t) MRS-PH core
5% for 300 MW(t) MRS-SC/C core

Modular reactor considered benign and therefore has a negligible effect on public safety

The small radionuclide inventory in each module, together with the small fraction of fuel failing under core heatup conditions [1% (for 250-MW(t) MRS-PH) and 5% (for 300-MW(t) MRS-SC/C)]. Release of long-lived KR-85 provides an in-depth defense to limit accident consequences.

Further analysis is required to assess the impact on reactor internals and NHS components during a core heatup

on Table 4.8-3) show the core heatup transients occur at relatively low frequencies and result in small radioactivity releases.

4.8.2.2. Fuel Cycle Cost for MRS-PH Plant. Fuel cycle cost data were generated for the 250-MW(t) MRS-PH plant based on GCRA guidelines. Costs were based on LEU/TH once-through fuel cycles with so-called equilibrium HTGR fuel handling costs and a 1995 start-up date. Costs assume 30-yr levelizing and a 0% inflation rate.

The reference design was based on a 4-yr cycle exposure with batch (whole core) refueling. It was recognized that changes to the MRS fuel cycle could improve the plant economics, particularly utilizing a 4-yr cycle exposure with graded refueling, based on refueling one-half of the core every two years (biennial). Efforts in FY-83 will concentrate on the biennial refueling approach. Fuel cycle cost data are summarized below for the 250-MW(t) MRS-PH Plant.

Cost Component	Reference LEU/Th Batch Loaded	Projected LEU/Th Biennial Refueling
Fuel depletion	13.6	8.43
Fabrication	2.79	2.94
Shipping	0.71	0.76
Waste	1.80	1.94
Total, mills/kWh(e)	18.90	14.07
$/GJ ($/MBTU)	2.01 (2.13)	1.49 (1.58)

4.8.2.3. Fuel Cycle Cost for MRS-SC/C Plant. Fuel cycle cost data were generated for the 300-MW(t) MRS-SC/C plant based on GCRA guidelines. Costs were based on LEU/Th once-through fuel cycles with so-called equilibrium HTGR fuel handling costs and a 1995 start-up date. Costs assume 30-yr levelizing and a 0% inflation rate.

TABLE 4.8-3
MRS-PH SAFETY RISK ASSESSMENT SUMMARY

Three initiating events investigated

- Loss of main loop cooling
- Water ingress
- Depressurization

	Median Frequency Per Site (8 Modules) yr
Consequences	
4 modules release (~1% fuel body inventory and circulating activity)	1.6×10^{-5}
1 module release (~1% fuel body inventory and circulating activity)	7.2×10^{-5}
1 module release (circulating activity only)	9.1×10^{-4}

Conclusions

- Core heatup transients occur at relatively low frequencies and result in small radioactivity releases
- Benign characteristics could provide siting flexibility for process heat applications
- Additional risk assessment work is needed
  - Evaluate other initiating events such as external explosions
  - Analyze investment risk

The reference design was based on a 4-yr cycle exposure with batch (whole core) refueling. It was recognized that changes to the MRS fuel cycle could improve the plant economics, particularly utilizing a 4-yr cycle exposure with graded refueling, based on refueling one-half of the core every two years (biennial). Efforts in FY-83 will concentrate on the biennial refueling approach. Fuel cycle cost data are summarized below for the 300-MW(t) MRS-SC/C plant.

Cost Component	Reference LEU/Th Batch Loaded	Projected LEU/Th Biennial Refueling
Fuel depletion	14.14	8.61
Fabrication	2.39	2.52
Shipping	0.61	0.66
Waste	1.54	1.67
Total, mills/kWh(e)	18.68	13.46
$/GJ ($/MBtu)	1.99 (2.10)	1.43 (1.51)

4.9. MRS SEISMIC SCOPING STUDY (6053050300)

4.9.1. Scope

The scope of the work reported here was to perform a seismic evaluation of an MRS concept embodying a single in-line vessel arrangement. Results are required to be generally applicable to process heat and the steam cycle variants.

4.9.2. Discussion

A report was prepared presenting a preliminary seismic analysis of the Reactor Confinement Building for a 250-MW(t) modular reactor system (MRS) plant design.

In-structure response spectra suitable for preliminary design are presented at each floor elevation of the Reactor Confinement Building for a 0.15-g operating earthquake satisfying for NRC requirements. The design response spectra represent an envelope for foundation conditions ranging from soft soil to competent rock. Interface loads at the reactor vessel, core, and tube bundle supports have been computed and tabulated. Maximum displacements and acceleration at various elevations of the reactor vessel/process heat module assembly were also obtained.

The Reactor Confinement Building was mathematically modeled as a system of lumped masses located at elevations of mass concentrations such as floors (see Fig. 4.9-1) interconnected by elastic members. The reactor vessel assembly/heat process module (see Fig. 4.9-2) has been modeled as three lumped masses as shown in Fig. 4.9-3). This simplified representation captures the fundamental response of the unit. Each mass point has six dynamic degrees of freedom, three displacements, and three rotations. The derivation of the stiffness matrices connecting the dynamic degrees of freedom is accomplished by modeling the connecting members as an assembly of elastic beam elements. The overall mathematical model, including the

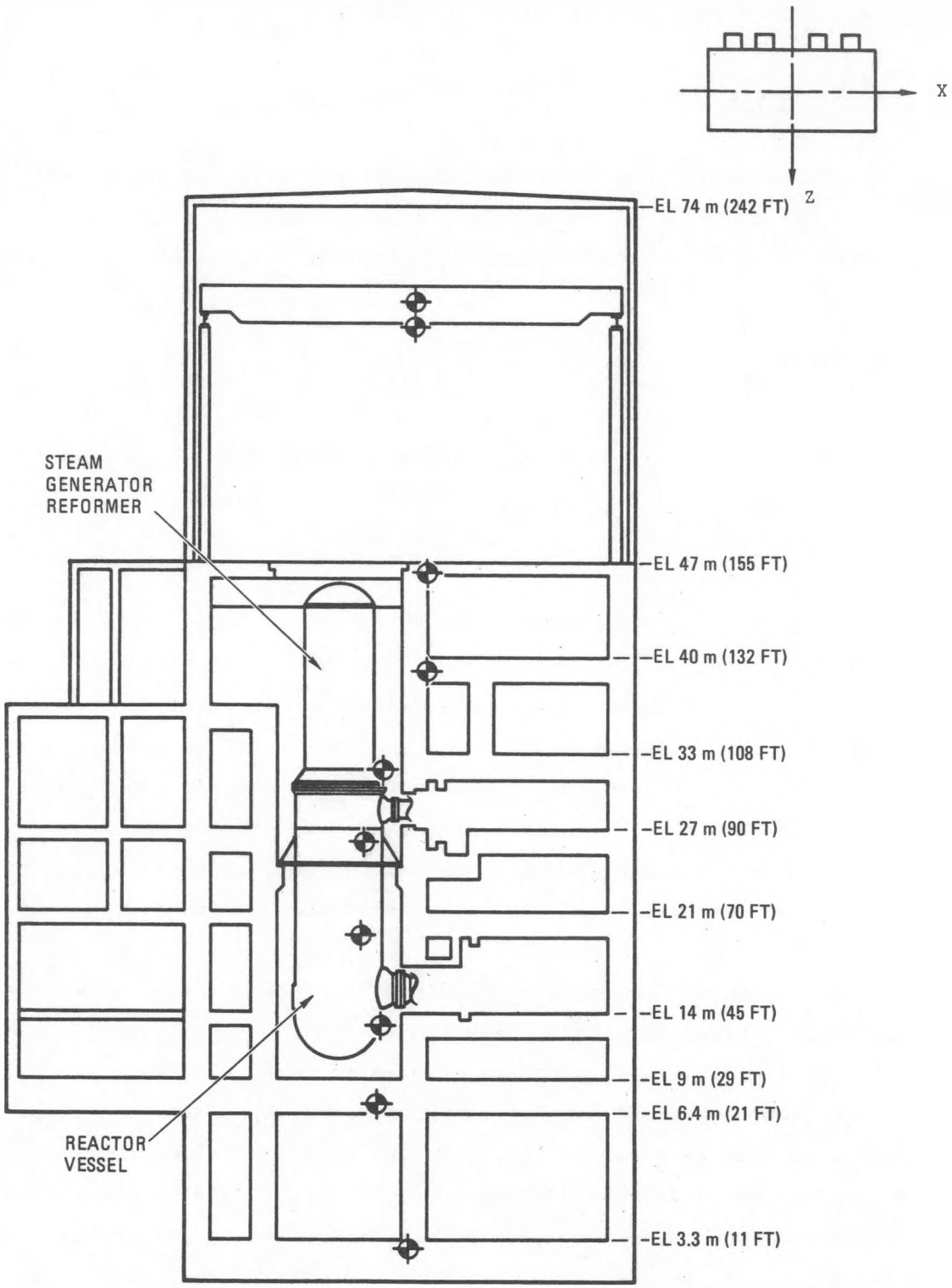

Fig. 4.9-1. Reactor containment building

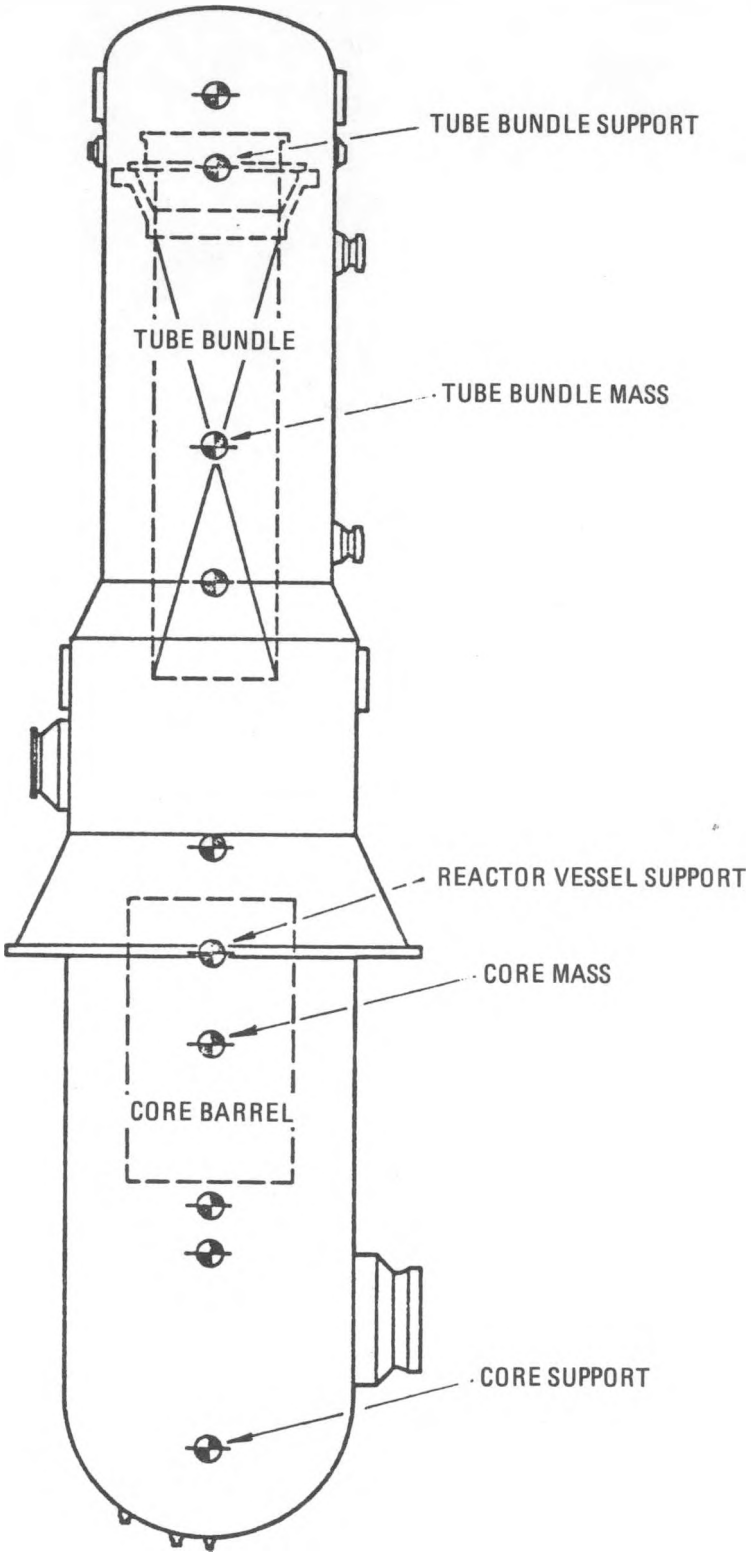

Fig. 4.9-2. Reactor vessel/process heat module assembly

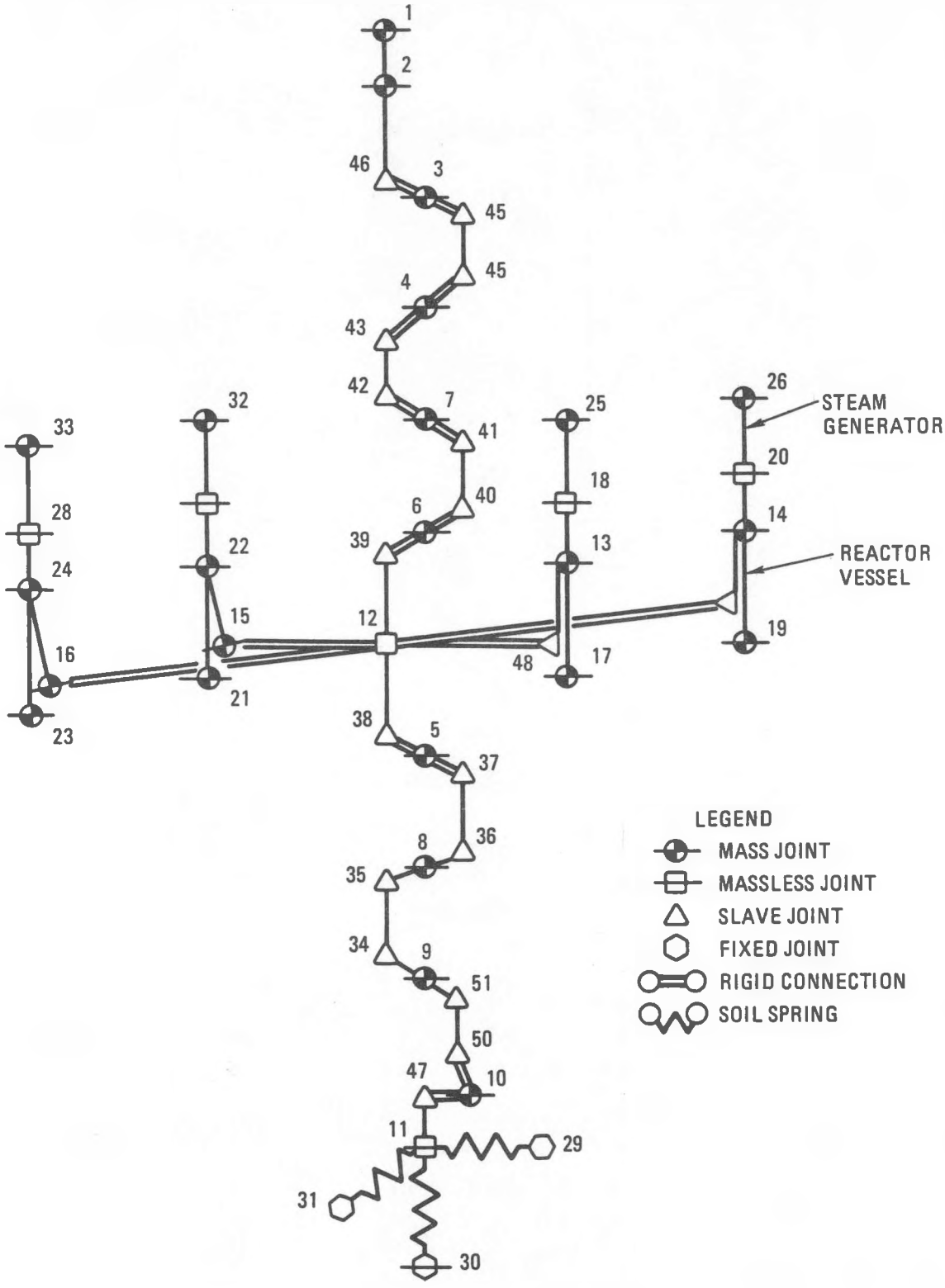

Fig. 4.9-3. Dynamic model of MRS

Reactor Confinement Building, the structure-foundation system, and the four reactor vessel/heat process modules, is shown in Fig. 4.9-3. The locations of the mass points, inertias, and elastic properties describing the mathematical model are given in Table 4.9-1 and Table 4.9-2 respectively.

The overall mathematical model was developed based on information drawings received from Bechtel, Combustion Engineering, and GA Technologies.

A wide range of soil conditions designed to encompass the site ranges were considered. For each soil condition analyzed, a set of six foundation springs and radiation dampers were computed.

A detailed mathematical model of the reactor vessel/process heat module was developed to determine interface loads. The model is made of an assembly of discrete mass points representing the reactor vessel, the core, the process heat module, the tube bundle, and their associated support structures (see Fig. 4.9-2). The mass points are connected by an assembly of elastic elements. Because of a limited knowledge of the reactor core dynamic behavior, the properties of the elastic members representing the core were approximate.

The in-structure response spectra at the reactor vessel support floor elevation shows that the current design configuration produces an amplification of the seismic excitation by a factor of 3.5 in the horizontal plane and by a factor of 2.6 in the vertical direction. Owing to the unsymmetrical configuration of the reactor confinement building, the in-structure response spectra in the "weak" Z-direction of the horizontal plane show consistently a higher amplification factor in both the rigid and elastic ranges.

TABLE 4.9-1
MRS - STRUCTURAL DYNAMIC MODEL NODE PROPERTIES

Node No.	Coordinates (in.) X	Y	Z	Inertia Properties ($lb/sec^2/in.$) Mass	Jx	Jy	Jz
1		2634		0.150+4			
2		2580		0.500+3			
3		1810	40	0.650+5	0.110+11	0.525+11	0.415+11
4		1550	40	0.105+6	0.180+11	0.850+11	0.675+11
5		795	-150	0.110+6	0.190+11	0.890+11	0.700+11
6	- 10	1040	-135	0.100+6	0.175+11	0.810+11	0.640+11
7	- 10	1250	- 90	0.110+6	0.190+11	0.890+11	0.700+11
8		520	- 90	0.100+6	0.175+11	0.810+11	0.640+11
9		230	-100	0.150+6	0.260+11	0.120+12	0.960+11
10		- 145	- 25	0.145+6	0.250+11	0.116+12	0.920+11
11		- 252					
12	- 10	972	-170				
13	336	1078	-204	0.130+4			
14	768	1078	-204	0.130+4			
15	-336	972	-204				
16	-768	972	-204				
17	336	678		0.130+4			
18	336	1217					
19	768	768		0.130+4			
20	768	1217	-204				
21	-336	678	-204	0.130+4			
22	-336	1078	-204	0.130+4			
23	-768	678	-204	0.130+4			
24	-768	1078	-204	0.130+4			
25	336	1667	-204				
26	768	1667	-204	0.660+3			
27	-336	1217	-204	0.660+3			
28	768	1217	-204				
29	1	- 252					
30		- 253					
31		- 252	1				
32	-336	1667	-204	0.660+3			
33	-768	1667	-204	0.660+3			
34		348	-220				
35		468	-220				
36		504	-220				
37		768	-220				
38	- 10	840	-170				
39	- 10	1008	-170				
40	- 50	-1080	-220				
41	- 50	1224	-220				
42		1296					
43		1512					

TABLE 4.9-1 (Continued)

Node No.	Coordinates (in.) X	Y	Z	Inertia Properties ($lb/sec^2/in.$) Mass	Jx	Jy	Jz
44		1584	10				
45		1812	10				
46		1860					
47		- 145					
48	336	972	-204				
49	768	972	-204				
50		- 132	- 80				
51		252	- 80				
52	- 50						
53	- 10						

TABLE 4.9-2
MRS - STRUCTURAL DYNAMIC MODEL MEMBER PROPERTIES

Member Number	Start Node	End Node	Material Number	Area A (in.^{2})	Shear Area Ay (in.^{2})	Shear Area Az (in.^{2})	Area Moment of Inertia (in.^{4}) Ix	Iy	Iz
1	11	47	1	0.326+7	0.275+7	0.275+7	0.124+13	0.173+12	0.457+12
2	50	51	1	0.100+7	0.430+6	0.430+6	0.400+12	0.690+12	0.186+12
3	34	35	1	0.125+7	0.540+6	0.540+6	0.400+12	0.787+12	0.309+12
4	36	37	1	0.125+7	0.540+6	0.540+6	0.900+12	0.787+12	0.309+12
5	38	12	1	0.140+7	0.600+6	0.600+6	0.400+12	0.770+12	0.305+12
6	12	39	1	0.140+7	0.600+6	0.600+6	0.400+12	0.770+12	0.305+12
7	40	41	1	0.125+7	0.540+6	0.540+6	0.400+12	0.693+12	0.205+12
8	42	43	1	0.110+7	0.470+6	0.470+6	0.400+12	0.670+12	0.204+12
9	44	45	1	0.113+7	0.490+6	0.490+6	0.400+12	0.670+12	0.220+12
10	46	2	2	0.180+4	0.700+3	0.700+3	0.170+10	0.102+10	0.680+9
11	2	1	2	0.100+1	0.0	0.0	0.100+8	0.140+5	0.450+4
12	17	13	3	0.654+4	0.346+4	0.346+4	0.925+8	0.463+8	0.463+8
13	13	18	3	0.654+4	0.346+4	0.346+4	0.925+8	0.463+8	0.463+8
14	19	14	3	0.654+4	0.346+4	0.346+4	0.925+8	0.463+8	0.463+8
15	14	20	3	0.654+4	0.346+4	0.346+4	0.925+8	0.463+8	0.463+8
16	21	22	3	0.654+4	0.346+4	0.346+4	0.925+8	0.463+8	0.463+8
17	22	27	3	0.654+4	0.346+4	0.346+4	0.925+8	0.463+8	0.463+8
18	23	24	3	0.654+4	0.346+4	0.346+4	0.925+8	0.463+8	0.463+8
19	24	28	3	0.654+4	0.346+4	0.346+4	0.925+8	0.463+8	0.463+8
20	48	13	2	0.376+4	0.199+4	0.199+4	0.847+8	0.420+8	0.420+8
21	49	14	2	0.376+4	0.199+4	0.199+4	0.847+8	0.420+8	0.420+8
22	15	22	2	0.376+4	0.199+4	0.199+4	0.847+8	0.420+8	0.420+8
23	16	24	2	0.376+4	0.199+4	0.199+4	0.397+8	0.420+8	0.420+8
24	18	25	4	0.444+4	0.235+4	0.235+4	0.420+8	0.210+8	0.210+8
25	20	26	4	0.444+4	0.235+4	0.235+4	0.420+8	0.210+8	0.210+8
26	27	32	4	0.444+4	0.235+4	0.235+4	0.420+8	0.210+8	0.210+8
27	28	33	4	0.444+4	0.235+4	0.235+4	0.420+8	0.210.8	0.210+8
28	12	15	7			Rigid			
29	12	16	7			Rigid			

In the actual configuration, the rigidity of the process heat module is such that its relative displacements are limited to less than 6.35 mm (1/4 in.), possibly making the use of any snubbers unnecessary.

Because of the complex configuration of the reactor vessel and the preliminary nature of the detailed information concerning the design, a better mathematical model is required to capture the dynamic behavior of various internal components.

A more detailed model of the reactor core should be included to capture more fully the core's dynamic behavior.

5. HTGR-GT/COGENERATION PLANT DESIGN

5.1. Scope (6052040301 and 6052050100)

The scope of work reported here was to establish the plant's potential and to make economic studies to identify the best thermodynamic cycle for a cogeneration plant.

5.1.1. Discussion

Since the HTGR-GT/C is regarded as a very long-term follow-on HTGR option, technological advancements projected for the next several decades were factored into the systems analysis. The major features considered were in the following three categories: (1) impact on performance, (2) effect on economics, and (3) change in plant design. The evaluation of advanced technology features were documented in the GA internal engineering data base.

In the systems analysis, the salient features of the gas turbine were studied for cogeneration application. The plant appears to have considerable inherent flexibility for accommodating different steam/electricity load splits through recuperator bypass. Overall plant optimization cannot be undertaken without first establishing the relative worths of steam and electricity. Cogeneration economics are very sensitive to the revenue worth of the excess electric power sold to the utility. Various performance arrays were developed and details of the study were documented during this period.

While not explored in the FY-82 effort, considerable engineering design and development will be required to verify the following:

1. Optimum plant layout for a single-loop gas turbine.

2. Advanced HTGR-GT/C features.

3. Steam generator/precooler mechanical arrangement.

4. Recuperator bypass (and other conceptual variants) for plant load adjustment and control.

6. HTGR APPLICATIONS AND APPLICATIONS PROCESS DEVELOPMENT

6.1. APPLICATION PROCESS DEVELOPMENT (6003010300)

6.1.1. Scope

The scope of work included (1) a study of HTGR-SC/C plant application to supply steam and electric power to selected shale surface retorting processes, and a comparative assessment with competing alternative sources of energy; (2) an assessment of HTGR application for modified in-situ (MIS) processes for shale retorting; and (3) the conceptual design of a reboiler for supplying steam at 80% quality (dry) for injection in a heavy oil/tar sands thermal recovery process.

6.1.2. Discussion

6.1.2.1. HTGR-SC/C Application to Shale Oil Retorting Processes. Under this subtask heading, two shale surface retorting processes were investigated for HTGR-SC/C application: (1) a modified Paraho process and (2) a direct steam (Marathon) retorting process.

Modified Paraho Shale Retorting Process Application.

In Ref. 6.1-1, Davy McKee originally studied the feasibility of integrating an 850°C (1562°F) (reactor coolant outlet temperature) HTGR process heat (HTGR-PH) plant with the Paraho process. The Davy McKee study compared the HTGR-PH with the conventional Paraho retorting process that uses product oil as its energy supply and showed that integrating an HTGR-PH reactor as the energy source conserved approximately one-third of the upgraded product oil produced [2,206 out of 7,160 m^3/day (13,876 out of 45,042 bpd)]. The HTGR-PH heats the recycle gas to about 705°C (1301°F) for retorting shale.

The present study focused on retorting shale with hot recycle gas at a lower temperature [510° (950°F)], and the gas heating is provided by primary steam from an 1170-MW(t) HTGR-SC/C plant that is an available technology.

Approximately 68,900 tonnes per day (76,000 tons per day) of mined shale are crushed and screened to produce approximately 65,300 tonnes per day (72,000 tons per day) of prepared shale [pieces nominally measuring 10 mm x 76 mm (3/8 in. x 3 in.)] for the Paraho retorts. About 3600 tonnes per day (4000 tons per day) of shale fines <10 mm (3/8 in.) are returned with spent shale for disposal. The sized shale is fed to twin batteries that have five Paraho retorts per battery. Each Paraho retort is a refractory-lined cylindrical vertical kiln having a capacity of approximately 6500 tonnes per day (7200 tons per day). Spent shale, along with shale fines, are disposed of in an environmentally acceptable manner.

Process Description. A process block flow diagram for the indirect heated retort with major process parameters is shown in Fig. 6.1-1. The heat of retorting is supplied by circulating part of the retort off-gas into the descending shale bed. Hot primary steam, supplied by the HTGR-SC/C plant at 538°C (1000°F), transfers 31.9 MW (1090 MM BTU/hr), about 27% of the total thermal HTGR-SC/C energy available, to the recycle gas and provides the necessary heat for retorting. The retort off-gas, containing entrained oil mist, flows from the top of the retort and passes through the oil recovery system. About 0.08 m^3/s (45,042 bpd) of hydrogenated shale oil and 474,000 m^3/day (16.74 MM SCFD) of fuel gas are produced by the process. A detailed description of the process is given in Ref. 6.1-2.

Process Energy Requirements from an HTGR-SC/C Plant. About 157 MW(e) electric power and 24.0 kg/s (192,000 lb/hr) of 1-MPa (150-psia) dry saturated steam are required for retorting 65,300 tonnes per day (72,000 tons per day) of shale. The largest portion of the plant energy is required for shale retorting, followed by hydrogen production and mining operations. The thermal energy requirement shown for shale retorting is exclusive of the heat recovered by retorted shale.

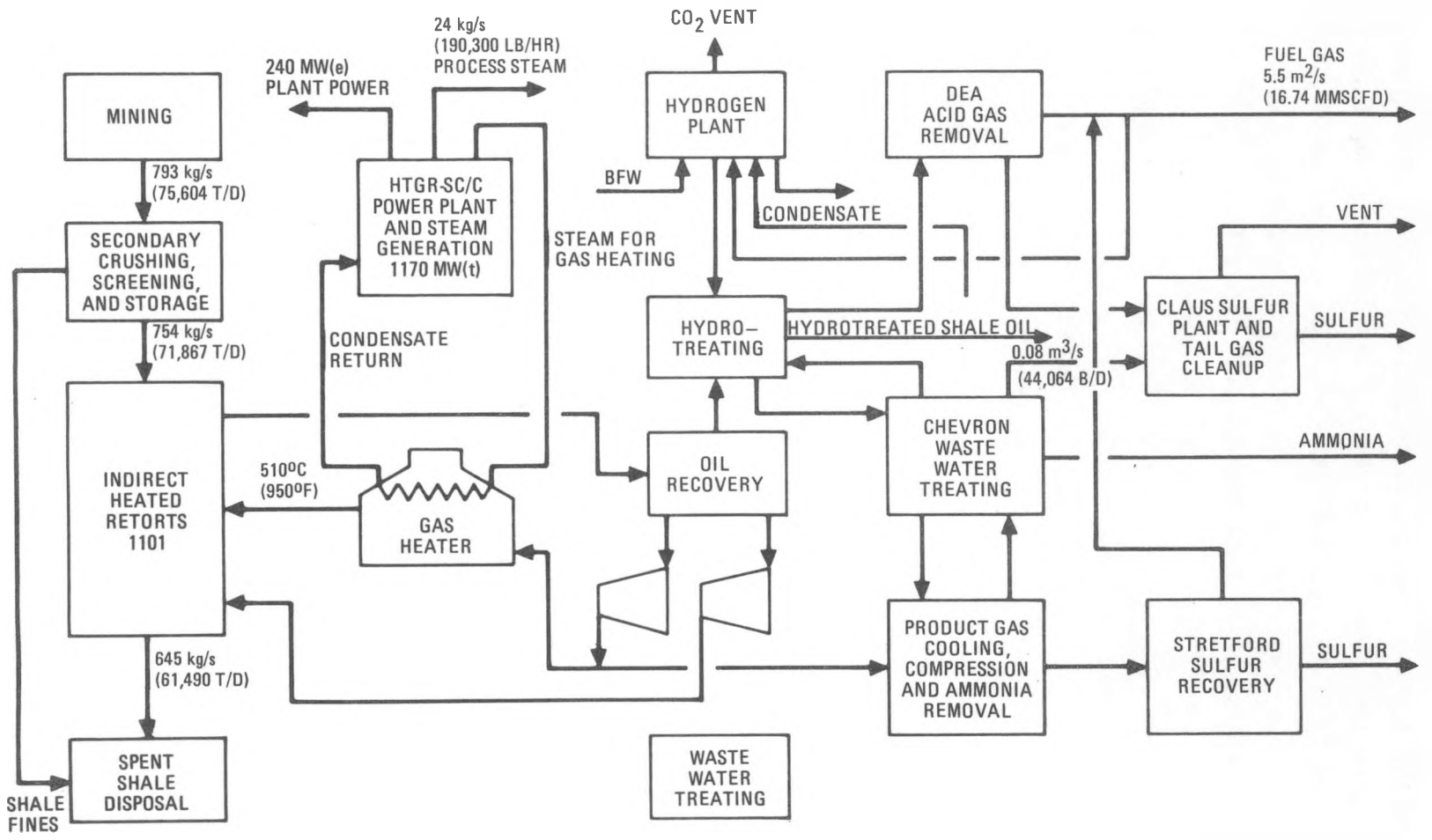

Fig. 6.1-1. Process block diagram for shale above-ground retorting with 510°C (950°F) recycle gas using an HTGR-SC/C plant

Figure 6.1-2 shows the process temperature-energy (T-Q) diagram, from which it can be seen that an 1170-MW(t) HTGR-SC/C plant can supply process thermal energy at or below 538°C (1000°F); this represents about 66% of the total thermal energy requirement. The HTGR-SC/C plant also provides 100% of the process electric power requirements [~157 MW(e)].

Plant/Process Heat Cycle. Figure 6.1-3 shows the HTGR-SC/C heat cycle for the modified Paraho process. This heat cycle uses split heat exchangers (HX's) to heat the recycle gas from 138° to 510°C (280° to 950°F). The gas is heated to 388°C (730°F) in HX 1 and from 388° to 510°C (730° to 950°F) in HX 2.

Approximately 24 kg/s (192,100 lb/hr) of steam at 14 MPa (160 psia) is extracted from turbogenerator T-G 2 for process use. Additionally, some steam from the HX 2 outlet is used in the hydrotreating process to heat fluid from 368° to 396°C (695° to 745°F). That heat load was specified to be 10.3 MW(t). The net electric power produced is 83,000 kW as summarized below:

	kW(e)
Gross generator output	275,000
Less: HTGR auxiliary power	- 35,000
Net electric power	240,000
Less: Shale plant electric power requirements	-157,000
Electric power for other uses or export	83,000

Cost/Economic Analysis. A preliminary cost estimate was made of the modified Paraho process to obtain a cost comparison with the Davy McKee study based on the use of an HTGR-PH (VHTR) reactor plant.

Table 6.1-1 shows process plant capital costs for the Paraho process using an 1170-MW(t) HTGR-PH plant, the standard Paraho retorting plant, and the modified Paraho process using an 1170-MW(t) HTGR-SC/C plant. A cost

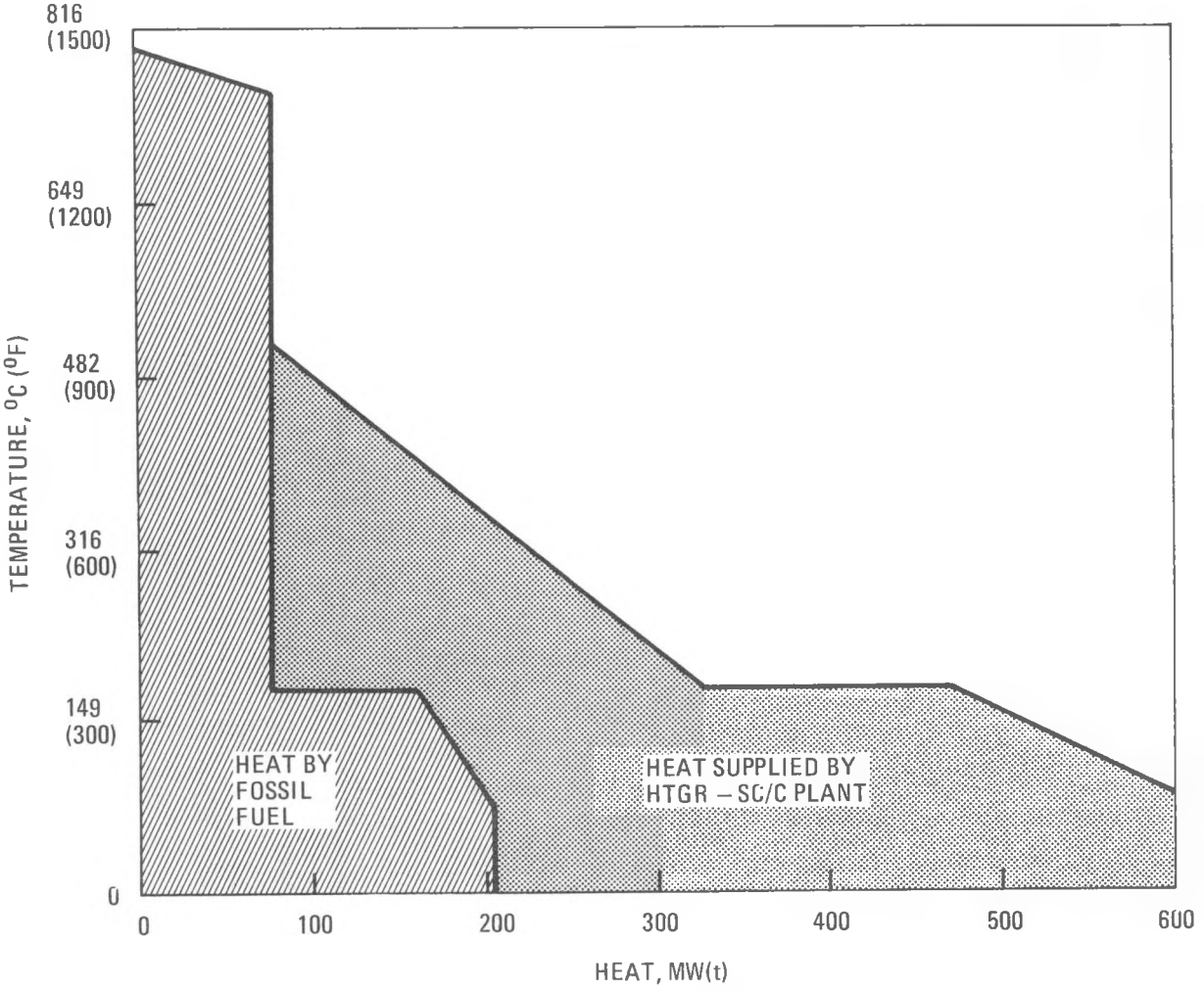

Fig. 6.1-2. Temperature-energy diagram for the modified Paraho process using an 1170-MW(t) HTGR-SC/C plant

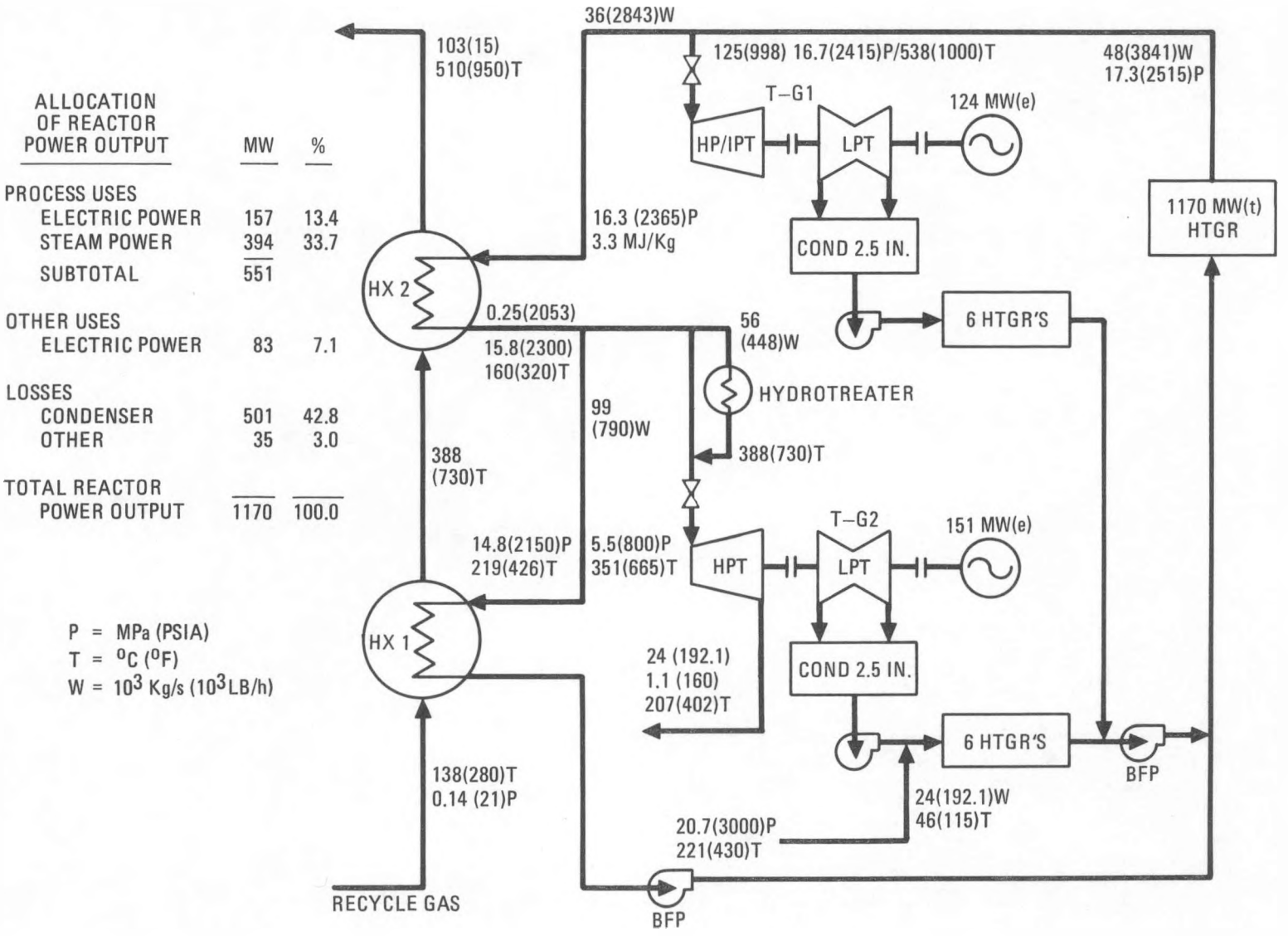

Fig. 6.1-3. 1170-MW(t) HTGR steam cycle for hot recycle gas [510°C (950°F)] retorting of oil shale

TABLE 6.1-1
PARAHO PROCESS PLANT/HTGR PLANT COST DATA

	Paraho HTGR-PH Plant	Modified Paraho HTGR-SC/C Plant	Standard Paraho Fossil-Fuel-Fired Plant
Plant specifications			
Thermal ratings, MW(t)	1170	1170	1311
Electrical ratings			
Gross, MW(e)	215	275	137
Net, MW(e)	130	240	137
Heat to process, MW(t)	532	598	600
Direct costs (M $, 1/80)	1205	1153	734
Construction service	241	231	147
Home office engineering service	174	167	106
Contingency	217	208	132
Total base cost (M $, 1/80)	1837	1759	1119

difference of approximately 78 million dollars (1/1980 dollars) [1837 M$ (HTGR-PH) versus 1759 M$ (HTGR-SC/C)] exists between the two nuclear plant cases, and this is mainly attributable to the HTGR-PH plant, which represents an advanced technology. The standard Paraho plant cost is about two-thirds that of a Paraho/HTGR plant capital cost, primarily because of the lower fossil-fuel-fired power plant cost.

Table 6.1-2 shows the economic results for the modified Paraho process using an 1170-MW(t) HTGR-SC/C plant along with the results of the Davy McKee economic study, which included an 1170-MW(t) HTGR-PH (VHTR) plant and the standard Paraho plant. The Davy McKee case with the HTGR-PH has only a marginal economic advantage over the modified Paraho process with the HTGR-SC/C plant. The fuel oil and gas used in the modified Paraho/HTGR-SC/C and standard Paraho processes were assumed purchased at the world market price.

Coal has not been considered as an alternative source of energy for shale operations in Colorado, since coal must be imported and transported to remotely located shale oil fields.

Environmental Considerations. Environmental considerations were primarily extended to four areas: (1) air, (2) water, (3) solid waste, and (4) thermal impact. Table 6.1-3 presents an overall emission summary for the modified Paraho process, which uses an HTGR-SC/C plant as its energy source, and shows a summary of air emissions from a standard Paraho retorting plant for comparison. The major source of sulfur dioxide (SO_2), nitrogen oxides (NO_X), and carbon monoxide (CO) will be fuel combustion for process heat, predominantly at the reforming furnace. As shown in Table 6.1-3, there is a considerable reduction in pollutant emission from a Paraho HTGR-SC/C plant as compared with a standard Paraho retorting plant. This reduction occurs primarily because of a substantial reduction in the use of the product oil as fuel.

Wastewater streams resulting from surface retorting facilities are treated for reuse as well as for dust control, spent shale moisturization, and shale disposal on site. The predominant source of solid waste will be

TABLE 6.1-2
ECONOMIC ANALYSIS OF MODIFIED PARAHO SHALE PROCESS WITH AN HTGR-SC/C PLANT IN COMPARISON WITH DAVY McKEE RESULTS USING AN HTGR-PH PLANT AND STANDARD PARAHO PLANT
(Basis: Private Industries Ownership, 30-yr Levelized)

	Paraho Process with HTGR-PH Plant	Modified Paraho Process with HTGR-SC/C Plant	Standard Paraho Fossil-Fuel-Fired Plant
Heat input to cycle, MW(t)	1,170	1,170	1,311
Shale feed, tonnes/day (tons/day)	59,490 (65,600)	65,180 (71,860)	59,490 (65,600)
Heat to process, MW(t) (tons/day)	532 (65,600)	598	600
Net electrical power output after process, MW(e)	0	83	0
Capital costs, M $			
Base capital cost, 1/80 $	1,837	1,759	1,119
Escalation through construction	250	240	154
Interest during construction	329	315	181
Total capital costs, M $	2,416	2,314	1,454
Annual costs, M $/yr[a]			
Fixed charges	314	301	189
Fuel costs			
Nuclear	22	22[b]	--
Oil	--	8	232[c]
Gas	--	35	32
O&M costs (power plant)	20	25	3
O&M costs (process)	144	157	143
Credit for electric power [d]	0	<29>	0
Total annual costs	500	519	599
Product			
Oil, m^3/s (bpd)	0.08 (45,042)	0.08 (45,042)	0.08 (45,042)[c]
Gas, mm SCFD (bpd, FOE)	13.6 (1713)	16.79 (2115)	14.43 (1817)
Total, m^3/s (bbd)	0.086 (46,755)	0.087 (47,157)	0.086 (46,859)

TABLE 6.1-2 (Continued)

	Paraho Process with HTGR-PH Plant	Modified Paraho Process with HTGR-SC/C Plant	Standard Paraho Fossil-Fuel-Fired Plant
Product Price			
Oil, $/m^3 ($/bbl)	263.51 (41.9)	272.25 (43.29)	314.64 (50.03)
Gas, $/GT ($/10^6 Btu)	6.63 (6.99)	6.84 (7.19)	7.92 (8.35)
Ratio of product price based on HTGR-SC/C plant	0.97	1.00	1.16

(a) 1995 projection in 1/1980 $, levelized over 30 yr.

(b) Includes nuclear fuel, 70 m^3/day (443 bpd) of fuel oil, and 5.5 m^3/day (16.79 MMSCFD) of fuel gas.

(c) Includes 2206 m^3/day (13,876 bpd) of fuel oil, 4.45 m^3/s (13.60 mmSCFD) of fuel gas.

(d) Power credit at $0.034/kW(e)-h, 1/80 $.

TABLE 6.1-3
AIR EMISSION SUMMARY
[kg/h (lb/day)]

	Particulates	SO_2	NO_x	CO
Paraho/HTGR-SC/C process [68,400 tonnes (75,400 tons) per day shale feed]	78 (4,128)	26 (1,398)	226 (11,971)	1,356 (71,757)
Standard Paraho process [60,000 tonnes (66,000 tons) per day shale feed]	102 (5,434)	38 (2,071)	424 (22,482)	1,346 (72,681)

shale-derived, including spent shale, raw shale fines, and mined raw shale. At present, no solid waste resulting from shale surface retorting facilities has been classified as hazardous by federal or state agencies.

The thermal pollution of Colorado waters under the aquatic life classification is limited, generally, to a maximum 3°C (5°F) increase over a minimum of a 4-hr period, lasting a 12-hr maximum.

Preliminary Conclusions. The modified Paraho shale surface retorting process integrating an 1170-MW(t) HTGR-SC/C plant has several advantages over the standard Paraho indirect retorting process, which uses a considerable amount of product oil as fuel. It also compares favorably with the indirect Paraho process that integrates an HTGR-PH plant (Ref. 6.1-1).

The Paraho/HTGR-SC/C process has also a finite advantage over the standard Paraho process, which burns approximately one-third of its gross upgraded oil produced as fuel. Other conclusions pertaining to the Paraho/HTGR-SC/C process are the following:

1. The HTGR-SC/C plant can supply approximately 67% of the process thermal energy and all of the on-site electrical power requirements and has a surplus of electric power [~83 MW(e)] for export or other uses.

2. The HTGR-SC/C plant reduces the environmental burden significantly in comparison with the oil-burning standard Paraho process.

3. The Paraho/HTGR-SC/C process retorts shale at a lower temperature compared with the Paraho/HTGR-PH process or the standard Paraho process; it thus requires more feedstock (approximately 10%) and a larger retort.

Direct Steam of Retorting of Shale (Marathon Process) Application.

The direct steam retorting process of shale, which was developed by the Marathon Oil Company of Denver, Colorado, and the application of an 1170-MW(t) HTGR-SC/C plant for supplying process heat, process steam, and electric power to 63,000 tonnes per day (70,000 tons per day) of shale was presented in Ref. 6.1-3. In that study, steam for retorting was assumed to be injected at 0.34 MPa (50 psia), and process/HTGR plant heat cycles were developed accordingly.

In the present study, a lower steam pressure for shale retorting was selected so that the critical pressure in the process, namely, the steam exhaust pressure from the evaporator side of the evaporator/condenser unit, is at least above atmospheric pressure. This resulted in a steam pressure of 0.17 MPa (25 psia) at injection into the retort.

The present study primarily updates the work reported in Ref. 6.1-3 by using the revised steam pressure value of 0.17 MPa (25 psia) and one 1170-MW(t) HTGR-SC/C plant to supply process steam and electric power. Other technical features of the process remain unchanged. A preliminary economic analysis was also performed to assess the Marathon/HTGR-SC/C process along with other surface retorting processes, such as the Paraho/HTGR-PH process, the Paraho/HTGR-SC/C process, and the standard Paraho process (which uses product oil as fuel).

Process Description and Heat Balances. Figure 6.1-4 shows the process arrangement for the direct steam retorting of 63,000 tonnes per day (70,000 tons per day) of shale with a steam injection pressure of 0.17 MPa (25 psia). The critical stage in this process is the condensation of steam, which is mixed with oil droplets and off-gas, exiting the retort. This condensation of steam is required for separating the raw shale oil. The heat of condensation is absorbed by secondary cooling water circulating in the evaporator side of the evaporator/condenser (E/C) unit. The secondary cooling water is evaporated to steam, which is compressed and further heated by HTGR primary steam to a level suitable for shale retorting.

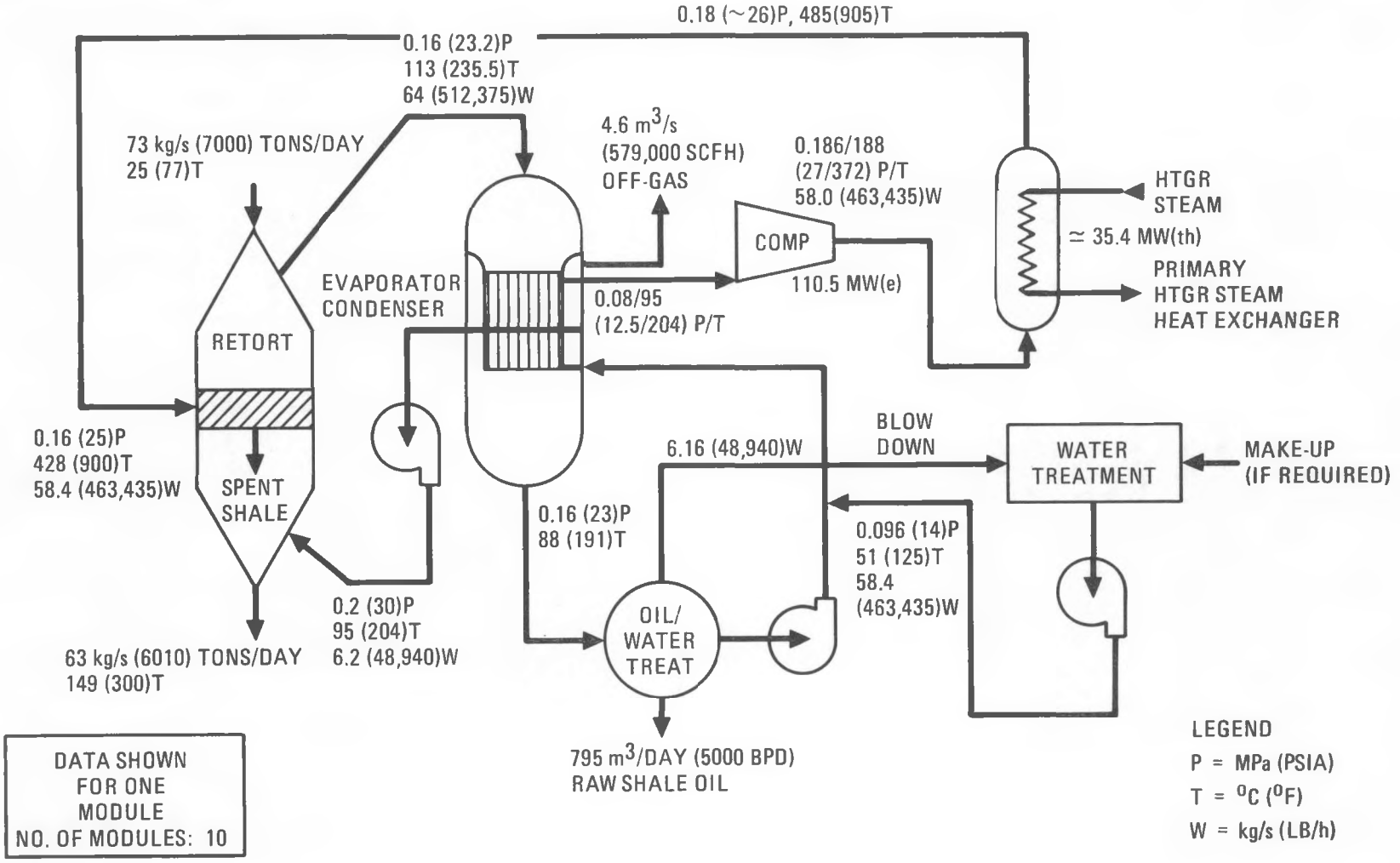

Fig. 6.1-4. Direct steam retorting of shale process arrangement

The performance requirements of the E/C unit are listed in Table 6.1-4. The exhaust fluid from the retort carries a sizable amount of particulate matter from the retorted shale. Separators will be installed at the retort outlet to remove as many particulates as possible, but many of the finer particles will remain in suspension and combine with the carried oil particles (especially the heavier and stickier ones) to create fouling accretions on the heat transfer surfaces. Cleaner conditions can be established in the evaporating side, within limits, as the oil/water treatment plant can provide medium-to-good feedwater treatment. Using the TEMA Standards (Ref. 6.1-4) as guidance, the following fouling resistances were adopted:

$$0.002 \frac{hr/ft^2-°F}{BTU} \text{ on the condensing side}$$

$$0.001 \frac{hr/ft^2-°F}{BTU} \text{ on the evaporating side}$$

The configuration of the E/C unit is illustrated in Fig. 6.1-5. It can be considered as the combination of a conventional shell-and-tube exchanger (the subcooled portion) with a conventional kettle-type reboiler (the boiling portion). The shell in the boiling portion is of a sufficiently large diameter to function as a surge tank and to house steam drying equipment in its upper part. Besides supplying steam, this unit also provides the injection water for cooling the spent shale portion of the retort, since the saturation temperature in the kettle is appropriate for retort injection.

The temperature-heat duty diagram for the E/C unit is illustrated in Fig. 6.1-6, with the heat duty defined as zero at the cold end and 100% at the hot end. The shell-side boiling temperature was determined by trial and error, based on a pinch-point temperature approach of 5.5°C (10°F). As Fig. 6.1-6 shows, the tube-side temperature droops as condensation proceeds, and the decline becomes steeper as the cold end is approached. This drooping creates a serious pinch-point problem, and is due to the presence of non-condensable gases. If there were no such gases, the tube-side temperature profile would be horizontal throughout, eliminating the pinch-point.

TABLE 6.1-4
EVAPORATOR/CONDENSER PERFORMANCE REQUIREMENTS

Shell side

Input: 64 kg/s (512,375 lb/hr) of treated feedwater at 52°C (125°F)

Outputs: 58.4 kg/s (463,435 lb/hr) of saturated dry steam

6.16 kg/s (48,940 lb/hr) of saturated water

Tube side

Inputs: 64 kg/s (512,375 lb/hr) of saturated steam at 111°C (233°F)

3.6 kg/s (28,291 lb/hr) of gas mixture at 111°C (233°F)

8.5 kg/s (67,630 lb/hr) of API 21 shale oil in the form of suspended droplets

Outputs: Condensate-oil mixture

Off-gas containing residual noncondensed steam

Minimum temperature approach

5.5°C (10°F) temperature difference at pinch point

Fouling resistances

$\frac{0.002 \text{ ft}^2/\text{hr}-°\text{F}}{\text{Btu}}$ tube-side fouling resistance

$\frac{0.001 \text{ ft}^2/\text{hr}-°\text{F}}{\text{Btu}}$ shell-side fouling resistance

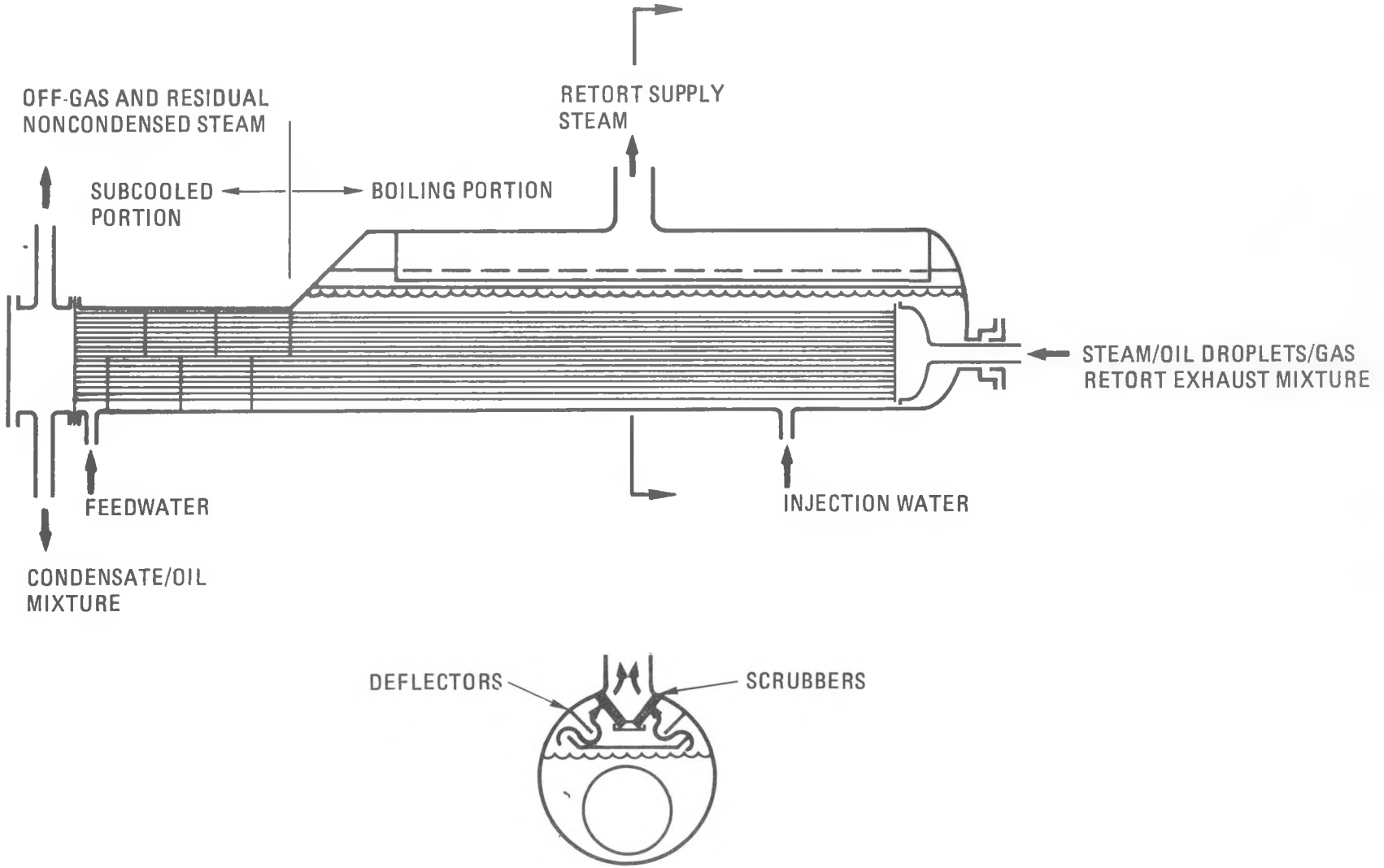

Fig. 6.1-5. Evaporator/condenser configuration

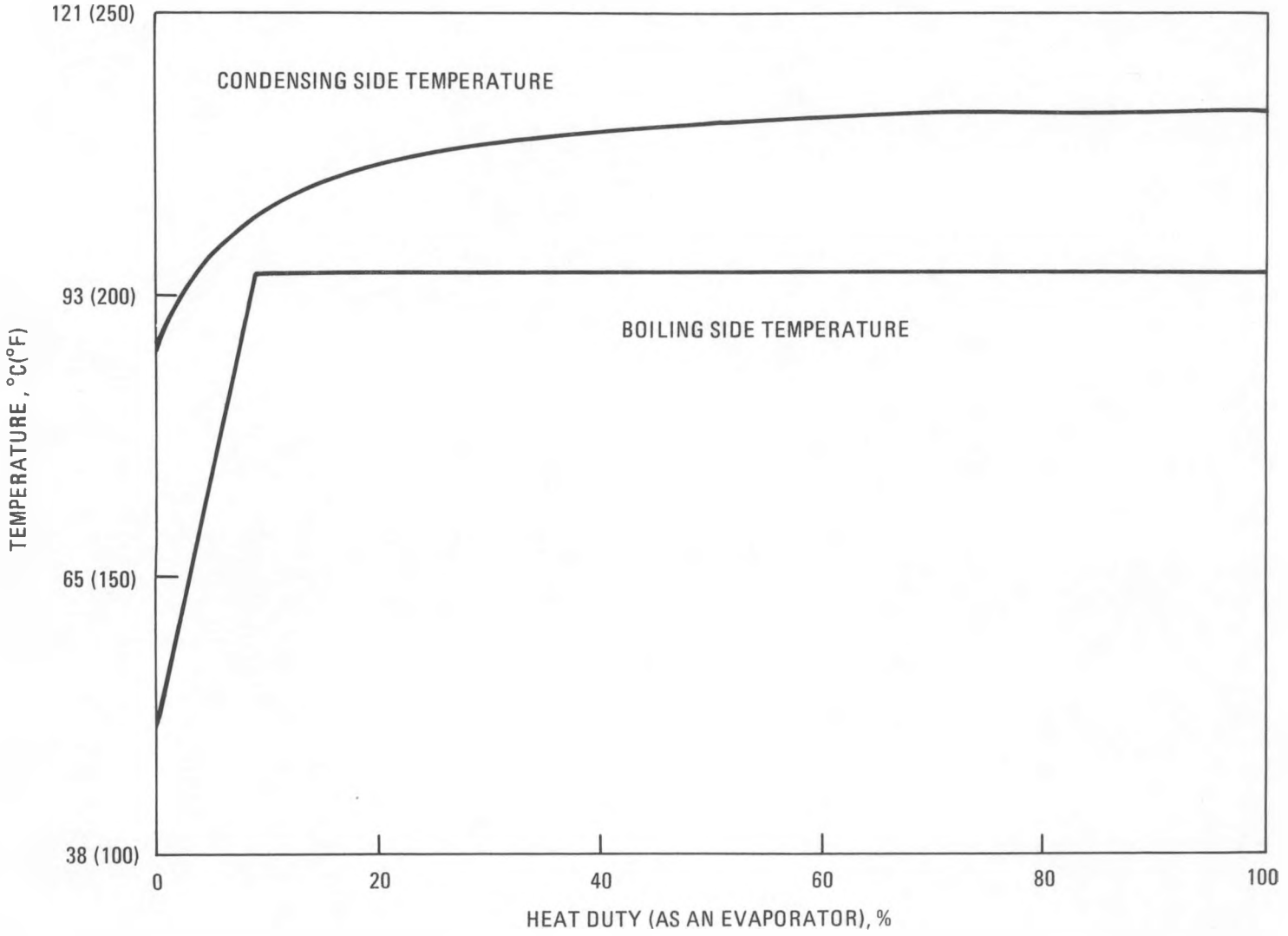

Fig. 6.1-6. Temperature-heat duty diagram for the evaporator/condenser

A major difference in the component arrangement exists between the Ref. 6.1-3 design arrangement and the present design arrangement (Fig. 6.1-4). The heater unit, used for heating the water from the oil/water separator unit prior to injection into the retorted shale heat recovery section, which was shown as a separate unit in Ref. 6.1-3, has been made an integral part of the E/C unit in the current arrangement. Water is heated to approximately 96°C (204°F) and the pressure is raised to 0.21 MPa (~30 psia) for injection into the retort vessel. It is preferred that the temperature of injection water be near its corresponding saturation temperature of 121°C (250°F) at 0.21 MPa (30 psia) as the water enters the retorted shale exit section. This accelerates the process of transforming water into vapor as the spent shale exits at 149°C (300°F) from the retort vessel. The present design, however, has a water entry temperature of 96°C (204°F) (limited by the E/C unit design), which is below the desired saturation temperature of 121°C (250°F).

Steam exits the evaporator at 0.09 MPa (12.5 psia) and is compressed to approximately 0.19 MPa (27 psia) and 189°C (372°F). The compressive power required is considerable and is estimated to be 105 MW(e) gross. The compressors are large, since they have to operate with a large volume of steam vapor at a low pressure. Steam exiting the compressor at 0.19 MPa/189°C (27 psia/372°F) is heated to a temperature of 485°C (905°F) at a pressure of 0.18 MPa (26 psia) by the primary steam from the HTGR plant.

Figure 6.1-7 shows the heat balance for the direct steam retorting process. Steam from the HTGR plant is supplied to heat the retorting steam, to the hydrotreater, and to the process [25 kg/s at 1 MPa (202,000 lb/hr at 150 psia, saturated)]. About 257 MW(e) (gross) electric power is cogenerated in the HTGR-SC/C plant and, after allowing 35 MW(e) for HTGR auxiliary power needs, a net of 222 MW(e) is available for process use. The process, however, requires 250 MW(e) of electric power for retorting 63,000 tonnes per day (70,000 tons per day) of shale, for upgrading raw shale oil, and for compressing steam. The resulting deficit of 28 MW(e) must be obtained from other sources.

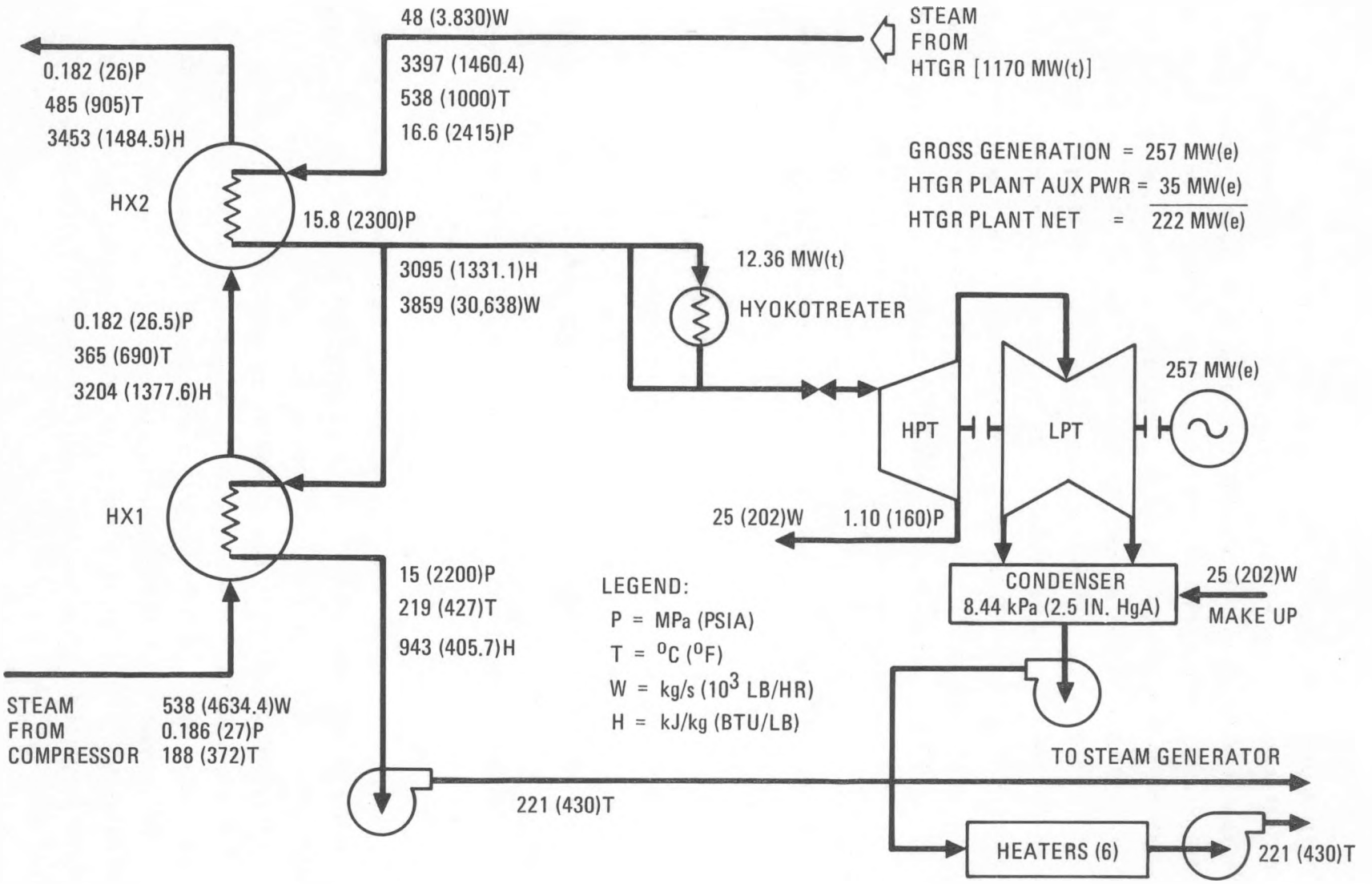

Fig. 6.1-7. Single 1170-MW(t) HTGR for shale retorting with steam

Conclusions and Future Work. The development of the direct steam retorting shale oil process to a commercial level rests upon the results of a large pilot plant operation. The key consideration in commercializing direct steam retorting of shale is the Fischer assay (>100%). At Fischer assays >100%, the direct steam retorting process may have a significant economic advantage over other surface retorting processes. The integration of an HTGR/SC/C plant as an energy source with the direct steam shale retorting process may accrue substantial product oil savings when compared with the standard Paraho process, which burns nearly one-third of its product oil as fuel.

Future work will consist of investigating direct steam shale retorting at near atmospheric pressure (a few inches of water). This will constitute the operation of the E/C unit at subatmospheric pressure. Low-pressure retorting is important in view of the practical difficulties anticipated in operating the retort vessel under pressure.

6.1.2.2. HTGR-SC/C Application to MIS Shale Retorting Process. The MIS process is in a developmental stage. Occidental Petroleum Corporation, the primary promoter of this process, plans to commercially retort shale deposits in Tract C-b of the Piceance Creek region in Colorado using the MIS process. Rio Blanco Corporation of Colorado has recently started investigating this process with two pilot plants in Colorado. Depending on the results of the pilot plants, commercialization efforts could ensue.

Process Description

The modified in-situ process involves the use of conventional mining techniques to remove a large volume of oil shale to create an underground cavern. Then, by drilling and blasting, the shale that overlies the open space is broken into small fragments. The blasting and breakage causes the mass of broken shale to expand into the void space created by the mining operation. This results in an underground rubble-filled chimney with sufficient permeability to be retorted in situ. The retorting method generally proposed consists of igniting the rubblized oil shale at the top of the

chimney, then passing the firefront downward through the bed of rubblized shale. When the shale is retorted, a small amount of supplemental outside fuel, such as shale oil, is used to heat the top of the rubble pile to the required temperature of 482°C (900°F). After a predetermined amount of rubblized shale has been heated, the supplemental fuel burners are removed. Combustion continues by injection of air into the retort to maintain the burn. The retorted shale oil flows down the retort by gravity, ahead of the burn, and is collected in a sump at the bottom of the retort. From there, pipelines carry the oil to storage at the surface.

With MIS, 20% to 40% of the shale is removed to form a void space into which the remaining shale is blasted to increase the permeability of the formation. The removed shale is then retorted above ground to increase the overall yield. Typically, a production of 7949 m^3/day (50,000 bpd) of shale oil will include 1590 m^3/day (10,000 bpd) produced above ground and 6559 m^3/day (40,000 bpd) produced from the MIS retort.

Energy Requirement for the MIS Process

In the original MIS process, air was continuously injected into the retort to maintain the combustion. However, a major problem in using 100% air is that the retort temperature becomes excessively high, with the maximum temperature exceeding 1000°C (1832°F). At such high temperatures, partial melting of the shale and possible interference with gas flow could result. Higher temperatures also result in a loss of oil yield because of oil combustion and coking.

The use of air and steam input is a promising alternative to the use of air and recycled gas. The resulting maximum temperature is within 1000°C (1832°F).

The MIS process uses about 658 kg (1450 lb) of steam per barrel of raw shale oil (Ref. 6.1-5). The net energy requirements estimated for the MIS process are shown below.

ESTIMATED ENERGY REQUIREMENTS FOR AN MIS FACILITY

Area	MW(e)	MW(th)
Mining	23.2	—
Crushing	2.2	—
Retorting	60.9	827
Hydrogen manufacturing	3.5	—
Hydrotroating	13.6	48
Total	103.4	875

HTGR Applicability

From the material balance data of a typical MIS pilot plant shown in Fig. 6.1-8, it is evident that a considerable amount of off-gas is produced from the MIS process. The heat content of the off-gas, based on 1.68 MJ/m^3 (45.3 BTU/SCF), is sufficient to provide all thermal and electric energy required for the processing retort, and in fact a surplus of energy is available from the off-gas produced. A commercial oil shale MIS operation will utilize the off-gas as the prime on-site energy source, since the key to developing a commercial MIS process lies in using the produced off-gas as fuel for MIS operation. There is no need for any external energy source, including an HTGR-SC/C plant, for the MIS process.

6.1.2.3. Reboiler Conceptual Design for Heavy Oil/Tar Sands Application. In Ref. 6.1-3, a reboiler conceptual design was developed to supply steam for enhanced oil recovery (heavy oil/tar sands) operations. The design assumed that the feedwater was treated to a level suitable for generating dry saturated steam (100% quality) at moderate and high pressures [4.8 and 13 MPa (700 and 1900 psia)].

The reboiler design developed during this reporting period was based on using conventional feedwater, as is now being done in the heavy oil fields. The conventional feedwaters contain a considerable amount of total dissolved solids (≥8000 to 9000 ppm), and the steam raised with this water is generally limited to 70% to 80% quality (dry) to hold the dissolved solids in

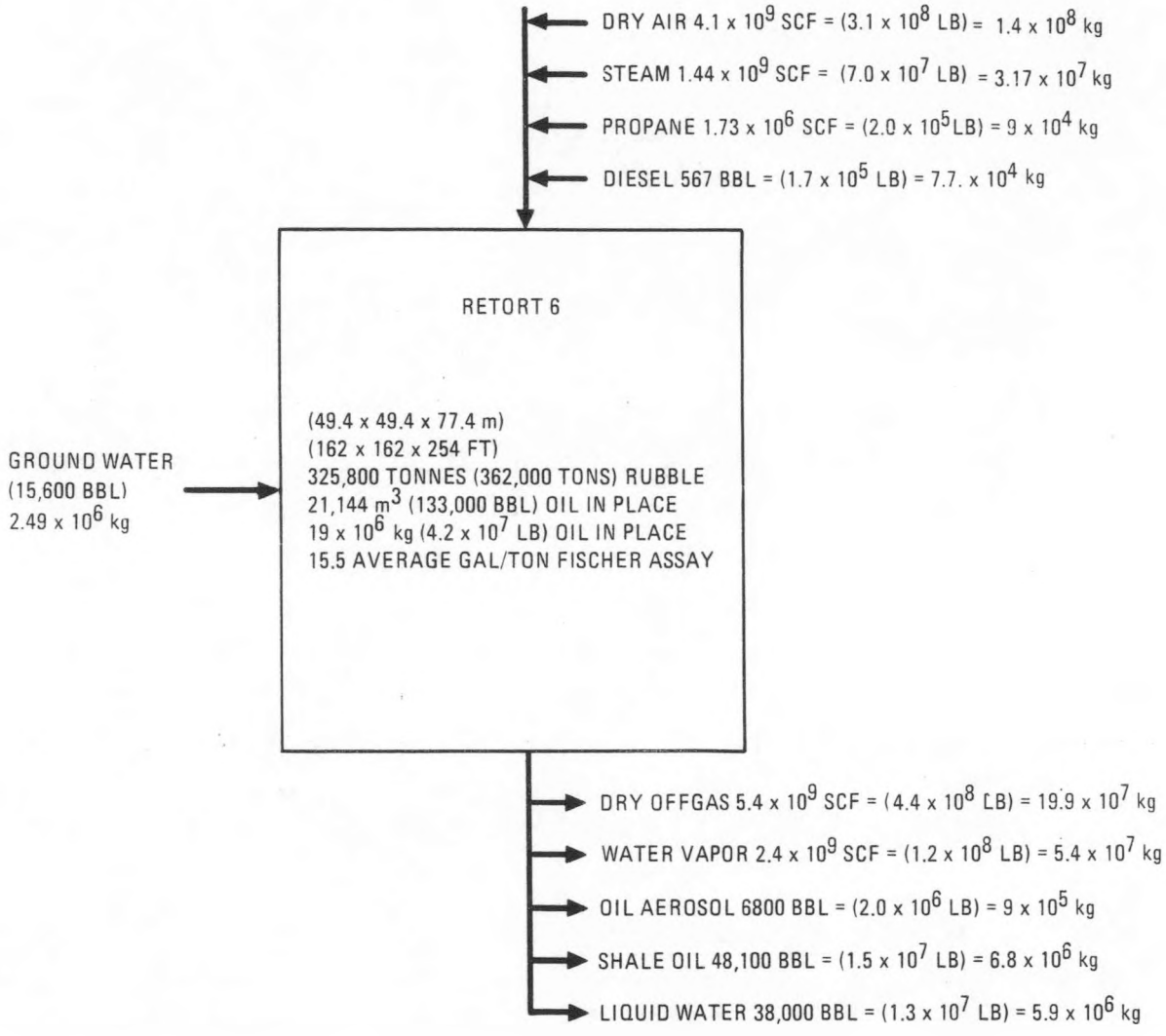

Fig. 6.1-8. Retort 6 material balance (from Ref. 6.1-5)

ESTIMATED ENERGY REQUIREMENTS FOR AN MIS FACILITY

Area	MW(e)	MW(th)
Mining	23.2	—
Crushing	2.2	—
Retorting	60.9	827
Hydrogen manufacturing	3.5	—
Hydrotroating	13.6	48
Total	103.4	875

HTGR Applicability

From the material balance data of a typical MIS pilot plant shown in Fig. 6.1-8, it is evident that a considerable amount of off-gas is produced from the MIS process. The heat content of the off-gas, based on 1.68 MJ/m^3 (45.3 BTU/SCF), is sufficient to provide all thermal and electric energy required for the processing retort, and in fact a surplus of energy is available from the off-gas produced. A commercial oil shale MIS operation will utilize the off-gas as the prime on-site energy source, since the key to developing a commercial MIS process lies in using the produced off-gas as fuel for MIS operation. There is no need for any external energy source, including an HTGR-SC/C plant, for the MIS process.

6.1.2.3. Reboiler Conceptual Design for Heavy Oil/Tar Sands Application. In Ref. 6.1-3, a reboiler conceptual design was developed to supply steam for enhanced oil recovery (heavy oil/tar sands) operations. The design assumed that the feedwater was treated to a level suitable for generating dry saturated steam (100% quality) at moderate and high pressures [4.8 and 13 MPa (700 and 1900 psia)].

The reboiler design developed during this reporting period was based on using conventional feedwater, as is now being done in the heavy oil fields. The conventional feedwaters contain a considerable amount of total dissolved solids ($\geq$8000 to 9000 ppm), and the steam raised with this water is generally limited to 70% to 80% quality (dry) to hold the dissolved solids in

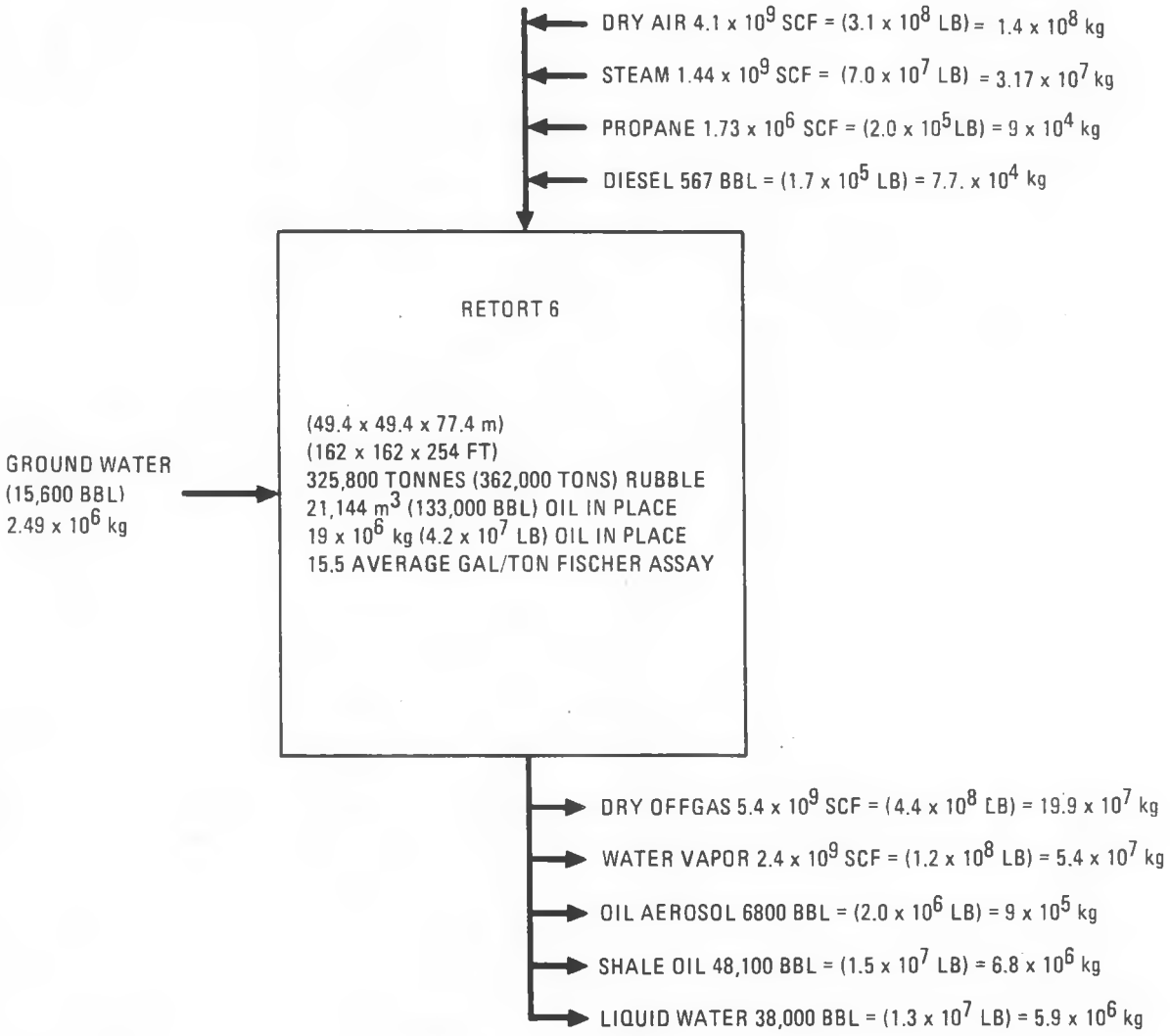

Fig. 6.1-8. Retort 6 material balance (from Ref. 6.1-5)

ESTIMATED ENERGY REQUIREMENTS FOR AN MIS FACILITY

Area	MW(e)	MW(th)
Mining	23.2	—
Crushing	2.2	—
Retorting	60.9	827
Hydrogen manufacturing	3.5	—
Hydrotroating	13.6	48
Total	103.4	875

HTGR Applicability

From the material balance data of a typical MIS pilot plant shown in Fig. 6.1-8, it is evident that a considerable amount of off-gas is produced from the MIS process. The heat content of the off-gas, based on 1.68 MJ/m^3 (45.3 BTU/SCF), is sufficient to provide all thermal and electric energy required for the processing retort, and in fact a surplus of energy is available from the off-gas produced. A commercial oil shale MIS operation will utilize the off-gas as the prime on-site energy source, since the key to developing a commercial MIS process lies in using the produced off-gas as fuel for MIS operation. There is no need for any external energy source, including an HTGR-SC/C plant, for the MIS process.

6.1.2.3. Reboiler Conceptual Design for Heavy Oil/Tar Sands Application. In Ref. 6.1-3, a reboiler conceptual design was developed to supply steam for enhanced oil recovery (heavy oil/tar sands) operations. The design assumed that the feedwater was treated to a level suitable for generating dry saturated steam (100% quality) at moderate and high pressures [4.8 and 13 MPa (700 and 1900 psia)].

The reboiler design developed during this reporting period was based on using conventional feedwater, as is now being done in the heavy oil fields. The conventional feedwaters contain a considerable amount of total dissolved solids ($\geq$8000 to 9000 ppm), and the steam raised with this water is generally limited to 70% to 80% quality (dry) to hold the dissolved solids in

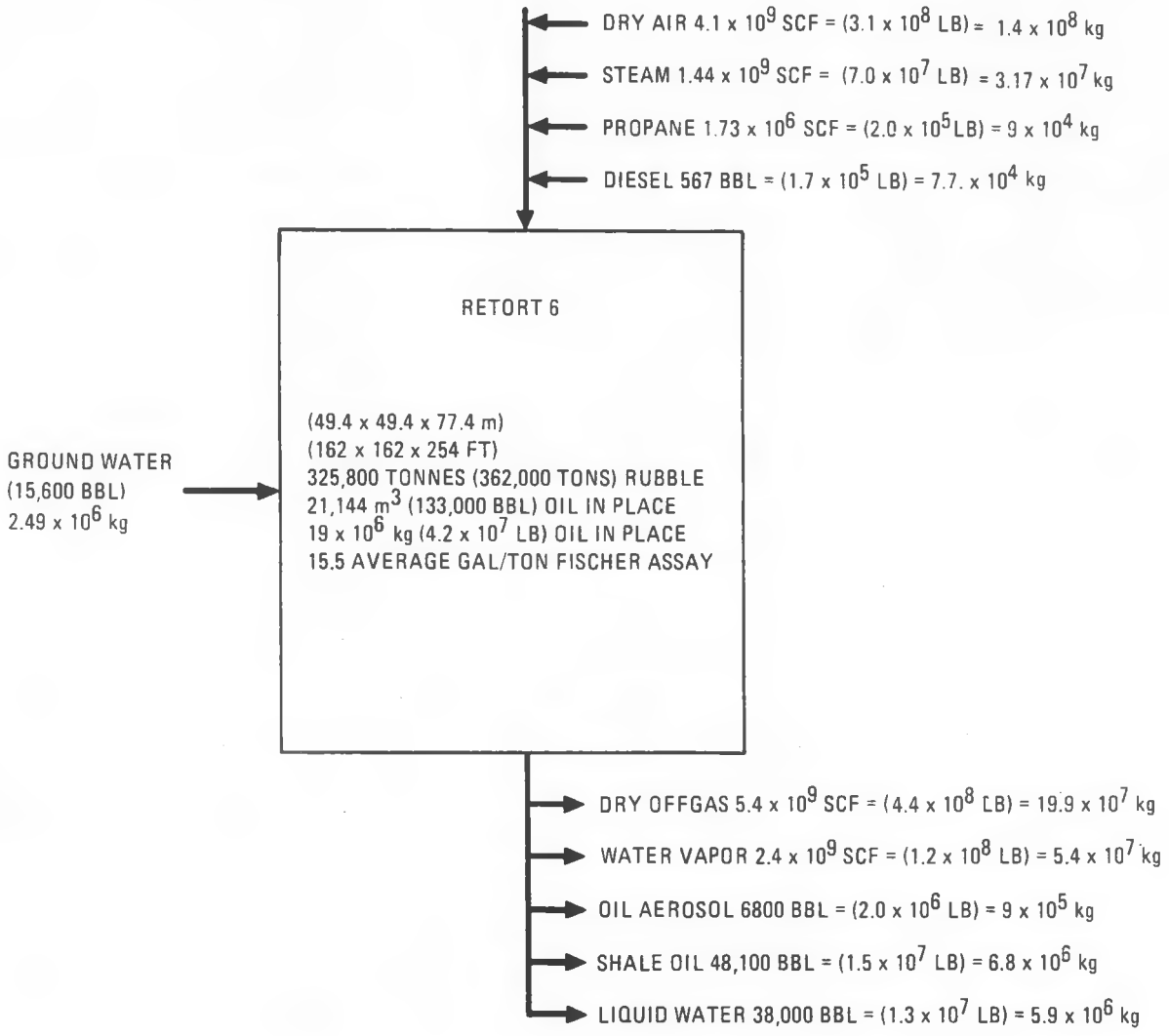

Fig. 6.1-8. Retort 6 material balance (from Ref. 6.1-5)

solution. A description of this conceptual reboiler design which receives heating steam from an 1100-MW(t) HTGR-SC/C plant is presented in this section. One 1170-MW(t) HTGR-SC/C plant can deliver about 378 kg/s (3×10^6 lb/hr) of injection steam/water via reboilers; thus, a large number of reboilers are required. The reboiler design must include features for assuring sufficient moisture in the secondary side steam passages to hold the dissolved solids in solution. Because of the number of reboiler units required, size compactness of the reboilers is also desired.

Configuration Selection

The once-through heat exchanger configuration was selected for this study based upon the conventional design used for fossil-fired units currently in use. In these conventional units, the potential for tube burnout is prevented by the use of a single large-diameter tube that eliminates flow maldistribution. The heat transfer surface area is limited by maintaining high velocity flow through the tubes having a high pressure loss and boiling out to only 80% quality. The high velocity and presence of moisture enables the flow to carry solids through the tubes without deposition. Because of the very large reboiler heat duty considered in the present study, the once-through heat exchangers could not be designed with a single tube. There is, therefore, a need to maintain uniform tube-side steam quality in a multitube reboiler configuration to prevent scaling of the inside tube walls. Tube burnout in fossil-fired units, which is the main reason for the use of a once-through design, should not be a problem in either the kettle type or the once-through type using HTGR steam for heating.

Design Requirements

The function of the once-through type of reboiler is to deliver steam of a quality not exceeding 80% dryness at the temperatures, pressures, and flow rates specified for the two cases in Table 6.1-5. Case 1 shows the conditions for oil recovery for a heavy oil field, and Case 2 shows the conditions for a tar sands field. This function is accomplished by passing primary steam from the HTGR through a series of shell and tube heat

TABLE 6.1-5
STEAM-TO-STEAM HEAT EXCHANGER DESIGN PARAMETERS

Case	Application	Reboiler					
		Primary Steam			Secondary Steam		
		Pressure [MPa (psia)] In/Out	Temperature [°C (°F)] In/Out	Flowrate [kg/s (lb/hr)] In/Out	Pressure [MPa (psia)] In/Out	Temperature [°C (°F)] In/Out	Flowrate [kg/s (lb/hr)] In/Out
1	Heavy oil recovery	7.3/6.9 (1065/1000)	413/65 (776/150)	356 x 10^6 (2.83 x 10^6)	6.7/4.6 (965/665)	26/258 80/497) Quality at exit = 80% (dry)	439 (3.49 x 10^6)
1	Tar-sands recovery	16.6/15.8 (2415/2300)	538/93 (1000/200)	244 (2.94 x 10^6)	15.2/13 (2200/1900)	38/331 (100/629) Quality at exit = 80% (dry)	484 (3.84 x 10^6)

exchangers. The steam is desuperheated, condensed, subcooled and recirculated to the steam generator of the HTGR after transferring its heat to the produced water.

The surface area is minimized in this study by splitting the evaporator into two 50% heat duty sections in series. The first stage has small-diameter thin wall U-tubes for compactness. The exit quality from the first stage is nominally 33% for the heavy oil case, and 23% for the tar sands case. this is well within the nucleate boiling range, and even with flow maldistribution no tube would approach the limit of 80% quality above which fouling is expected. The two-phase flow exiting the first stage then passes through a nozzle to produce homogeneous bubble flow prior to entering the second stage. It is attempted to obtain steam of uniform quality entering the second stage by arranging the two stages in direct alignment, with one first-stage unit for each second-stage unit. The tubes of the second-stage units are arranged so that each pass is in a horizontal plane to preclude steam/water separation at the 180 deg turns at the ends of the heat exchanger.

Conceptual Design

The evaporator units were sized using the Heat Transfer Research Institute (HTRI) computer code CST (Ref. 6.1-6). HTRI correlations for two-phase flow (Ref. 6.1-7) were also used to determine the acceptability of splitting the evaporator units into two 50% heat duty sections, in terms of having homogeneous flow centering the second stage.

The conceptual arrangement for both the heavy oil and tar sands cases are shown in Fig. 6.1-9. The economizers are Tubular Exchanger Manufacturers Association (TEMA) F-shells with axial counterflow; the first stage evaporators are TEMA X-shells with cross flow, and the second stage evaporators are TEMA E-shells with cross counterflow. The economizers were designed as separate units to obtain full counterflow heat exchange benefits. They are split into stages in series to limit shell diameter to 1.5 m (5 ft), and deaeration is interposed between stages.

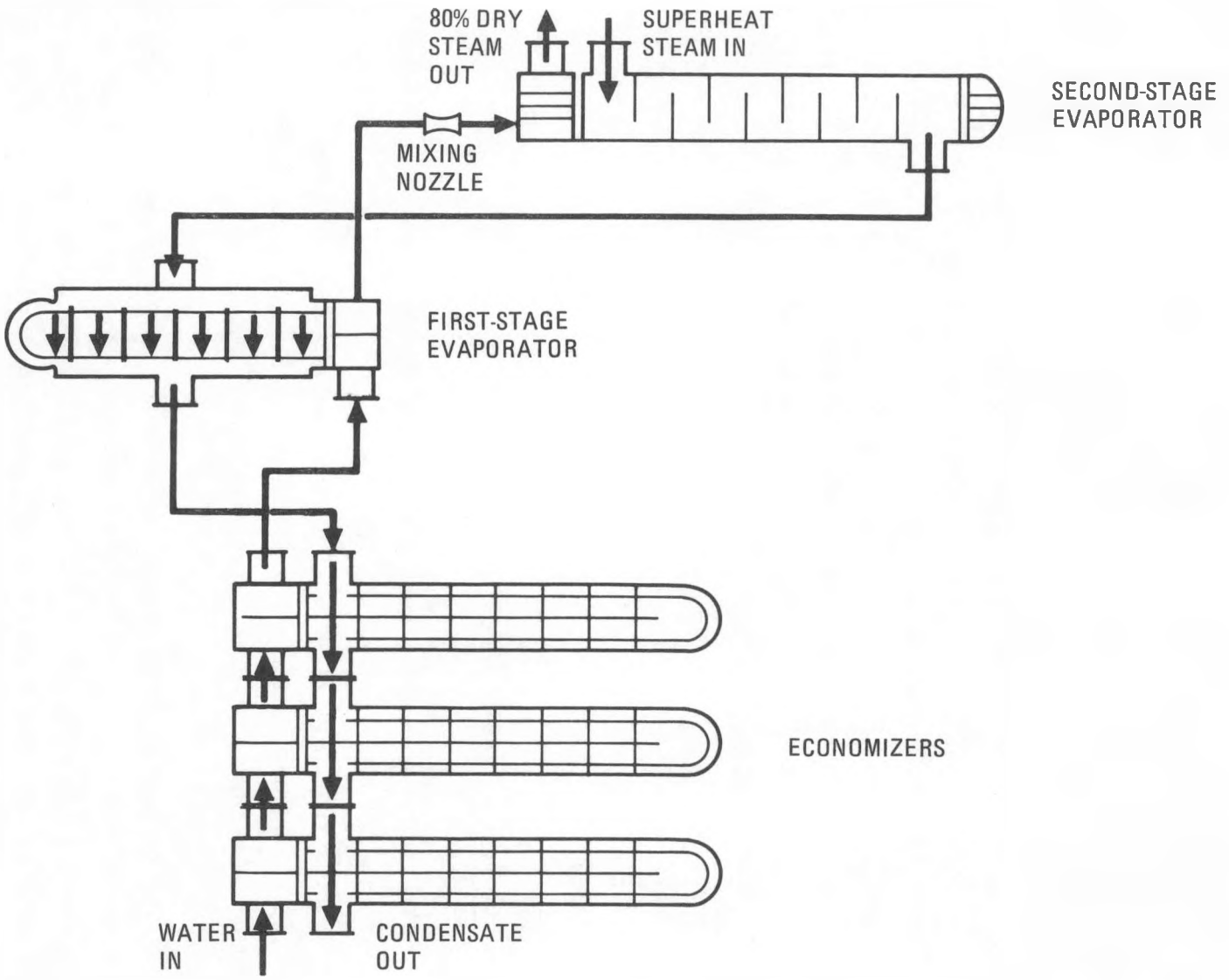

Fig. 6.1-9. Once-through reboiler conceptual arrangement (80% quality steam) for heavy oil and tar sands

A tube outside diameter of 19 mm (0.75 in.) was selected with a pitch/diameter ratio of 1.25 for compactness in the economizer and first stage evaporators. The second stage evaporators have 89 mm (3.5 in.) O.D. tubes with a 32 mm (1.25 in.) pitch/diameter ratio. This diameter is the same that is used by fossil-fired single-tube units and was considered maximum because of the influence of the tube wall thickness on the surface area. The pitch/diameter ratio is the minimum in accordance with TEMA standards.

The surface area calculations included fouling factors. The fouling factors on the tube side are dependent on the process water chemistry, which in turn is dependent on the specific site and process.

Results summarizing reboiler component surface areas, number of units, etc., are given in Table 6.1-6. The number of units was based on a maximum second-stage evaporator shell diameter of 1.5 m (5 ft) having 18 m (60 ft) -long tubes. The first-stage units then line up with the second-stage units so that a homogeneous two-phase mixture can be delivered through straight simplified piping. The number of economizer units, however, was based on a maximum shell diameter of 1.5 m (5 ft).

Material Selection

Materials selected for the major components are listed in Table 6.1-6. Carbon steel is specified throughout, except for tubing and for the shell of the Case 2 evaporator, since maximum metal temperatures should not exceed 371°C (700°F). Tube materials for all units is 2-1/4 Cr-1 Mo, which has satisfactory corrosion resistant properties. The shell of the Case 2 (tar sands) evaporator is 2-1/4 Cr-1 Mo, with an internal shield provided for protecting the shell from the initial steam temperature of 537°C (1000°F). A corrosion allowance of 0.125 in. is included on all internal supports and pressure parts, except on tubes as recommended by TEMA. A corrosion allowance of 1 mm (0.04 in.) or more, depending on the excess material of the standard gage selected, exists in the tubing material.

TABLE 6.1-6
SUMMARY OF RESULTS

	Heavy Oil Recovery			Tar Sands Recovery		
	Evaporator 1	Evaporator 2	Economizer	Evaporator 1	Evaporator 2	Economizer
No. units (series/parallel)	1/12	1/12	3/2	1/10	1/10	3/2
Total surface area, m^2 (ft^2)	11,665 (39,840)	29,101 (99,390)	13,392 (45,740)	26,642 (84,160)	36,886 (125,980)	15,070 (51,470)
Shell OD, mm (in.)	559 (22)	1600 (63)	838 (33)	1803 (71)	1067 (42)	914 (36)
Tube length, m (ft)	15.5 (51)[a]	18 (59)	13 (43)[a]	17 (55)	18.6 (61)	10.6 (35)[a]
Tube OD, mm (in.)	19 (0.75)	84 (3.5)	19 (0.75)	19 (0.75)	89 (3.5)	19 (0.75)
Shell thickness, mm (in.)	19 (0.75)	51 (2.0)	25.4 (1.0)	63 (2.5)	178 (7)	63 (2.5)
Tube wall gage	14 BWG	SCH.80	14 BWG	14 BWG	SCD.80	12 BWG
TEMA shell type	X	E	F	X	E	F
No. tube passes per shell	2	16	2	2	16	2
No. shell passes per shell	1	1	2	1	1	2
Tube material	Cr-Mo	Cr-Mo	Cr-Mo	Cr-Mo	Cr-Mo	Cr-Mo
Shell material	Carbon steel	Cr-Mo	Carbon steel	Carbon steel	Cr-Mo	Carbon steel

[a] To tangent of U-bend.

T-Q Plots

The temperature versus heat duty (T-Q) plots for each case are shown in Figs. 6.1-10 and 6.1-11. The heat duty for the Case 1 units is split nearly equally between the first stage, the second stage, and economizer because it was necessary to have a low steam quality between stage one and stage two. The pinch-point temperature difference is 28°C (50°F). The heat duty for the Case 2 units is split 42% in the stage-one evaporator, 31% in the stage-two evaporator, and 27% in the economizer. This unequal split was made to obtain 100% desuperheating in the first stage and 100% condensing in the second stage. The pinch-point temperature difference is 17°C (30°F).

Once-Through Reboiler Costs

Costs for Case 1 and Case 2 reboilers were estimated with the materials specified, and one spare was included. Costs were developed for the various carbon steel heat exchangers from data published in the Gulf Investment Estimating Manual, dated January 1, 1979, and escalated to present dollars. The data presented required extrapolation to satisfy the requirements of conceptual reboiler specifications.

Tube costs for 2-1/4 Cr-1 Mo were substituted for the carbon steel tube costs where required. There were no adjustments made in the labor costs due to the use of different types of tube materials, based on prior experience that the adjustment had little impact on the overall costs.

Table 6.1-7 shows cost estimates for the once-through type of reboiler in thousands of January 1982 dollars, FOB point of manufacture, and are for the total quantity, including a spare component each, indicated.

Conclusions and Recommendations

Findings from this preliminary study reveal that large heat duty and small log-mean-temperature differences associated with the reboiler design require large heat transfer areas and therefore compromise reboiler size

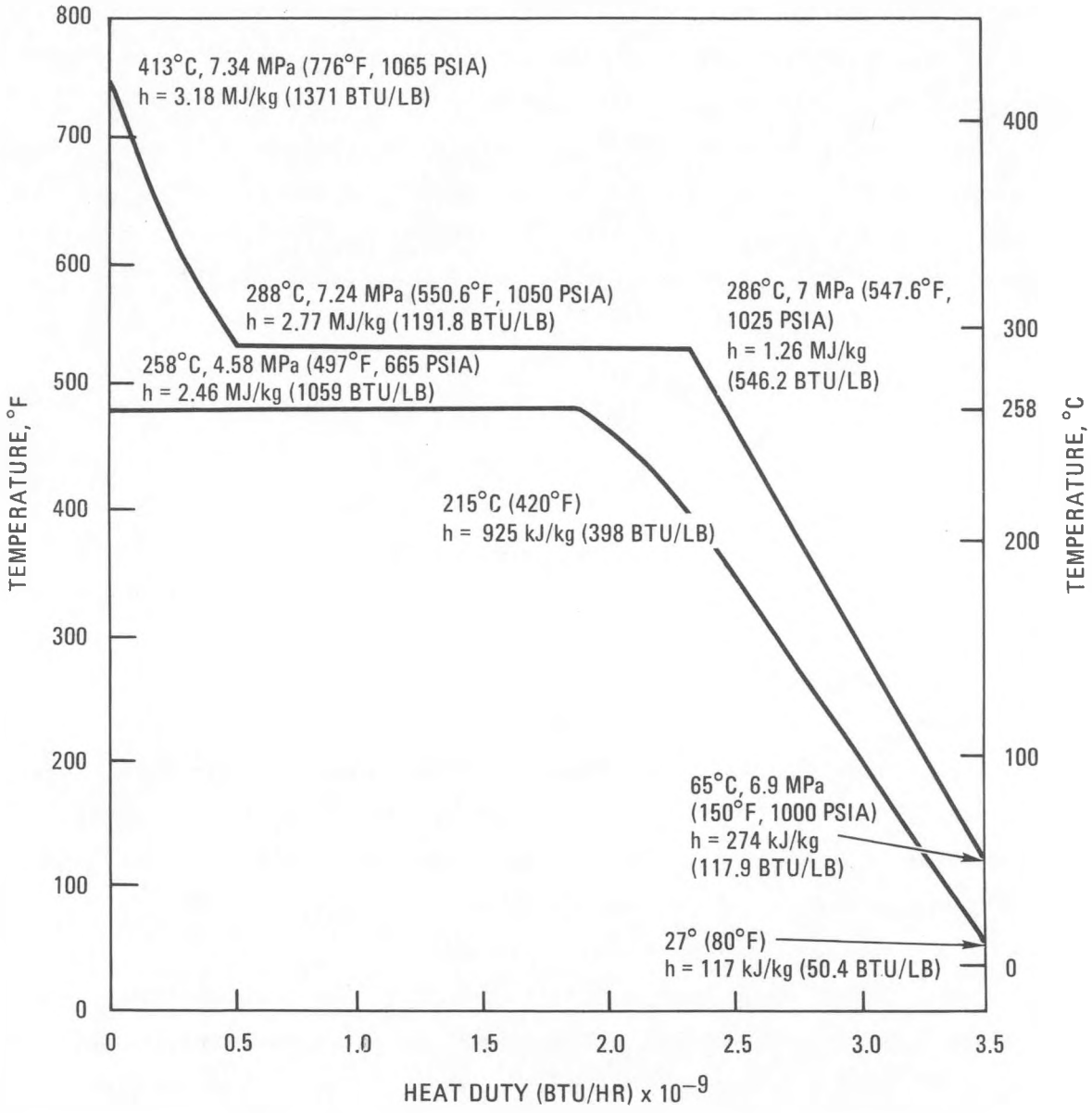

Fig. 6.1-10. Heavy oil recovery reboiler temperature versus heat duty

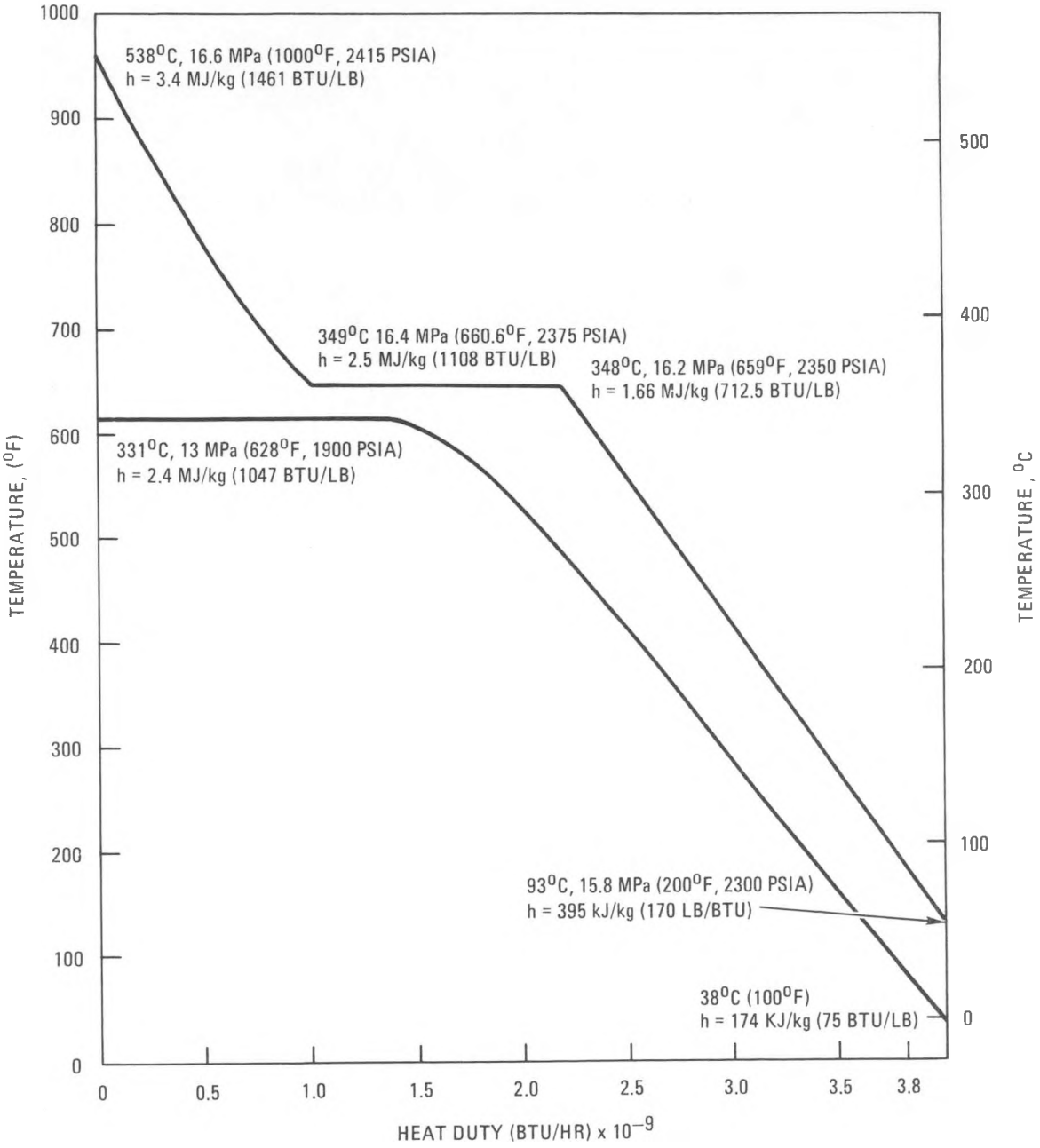

Fig. 6.1-11. Tar sands recovery reboiler temperature versus heat duty

TABLE 6.1-7
REBOILER COST ESTIMATE
(Thousands of January 1982 Dollars)

Case I heavy oil recovery	
12 each desuperheater + 1 spare	2,492.6
12 each condenser + 1 spare	972.4
2 each economizer + 1 spare	928.1
Case II tar sands recovery	
10 each desuperheater + 1 spare	5,490.3
10 each condenser + 1 spare	4,770.5
3 each economizer + 1 spare	2,283.3

selections. There is no known steam-heated reboiler designed for enhanced oil recovery applications using produced waters and, hence, reasonable assumptions have been made in developing the conceptual reboiler design. The key requirement in the present reboiler design is the assurance that the tubes not carry steam in excess of 80% quality (dry), which would otherwise result in scaling of tubes. While such a requirement can be met in the simplest way by adopting a single-tube configuration, as practiced in the small boilers of the heavy oil field, it is not considered practical for the large heat duty reboiler considered in the current study. Therefore, the transfer of homogenized steam/water mix from one stage to another, as included in the design, is a key design requirement. Any flow maldistribution or flow stratification should not be allowed to occur in the steam/water passages, and this leads to the need for experimental verification of the reboiler design and an in-depth survey of industrial operations of a similar kind or experience. Additionally, control and monitoring techniques of the quality of steam flowing through tubes of a reboiler operating continuously at steady state are not well known. It is believed that such techniques could be achieved with state-of-the-art technology.

While an overall conceptual design of the reboilers has been developed in the present study, further study is needed for a detailed evaluation and design of steam/water passages and of the subheadering of tubes that could implement the conceptual design assumptions made.

References

6.1-1. "Paraho Retorting of Oil Shale Using a Very High Temperature Reactor," Davy McKee Engineers and Constructors, prepared for GA under purchase order SC-771396.

6.1-2. "EPRI Technical Assessment Guide," Electric Power Research Institute Report EPRI PS-1201-SR, July 1979.

6.1-3. "HTGR Applications Program, Semiannual Report for the Period October 1, 1981 through March 31, 1982," DOE Report GA-A16831, 1983.

6.1-4. Standards of Tubular Exchanger Manufacturers Association, Fifth Edition, 1968.

6.1-5. "Occidental Vertical MIS Process for the Recovery of Oil from Oil Shale, Phase II, Quarterly Progress Report, December 1, 1980 - February 28, 1981," DOE/LC/10036-78 (DE81024981), May 1981.

6.1-6. "Computer Program CST," Heat Transfer Research Institute, April 1979.

6.1-7. "Design Manual," Heat Transfer Research Institute, March 1980.

6.2. APPLICATIONS SAFETY SITE SUITABILITY (6003010500)

6.2.1. Scope

The scope of the work reported here was to perform a preliminary siting study for a process steam 2240-MW(t) HTGR-SC/C plant at Port Arthur, Texas.

6.2.2. Discussion

6.2.2.1. Site Evaluation. NRC siting criteria (Refs. 6.2-1 and 6.2-2) have been applied to the results of SECPOP computer runs for locations at the Gulf Canal site and the Sabine Station site near Port Arthur, Texas. The SECPOP computer program, developed by the Office of Radiation Program, Environmental Protection Agency, uses the data from the U.S. Bureau of Census and prints out the population distribution around the specified location of the nuclear plant.

The sites listed below have been surveyed using the above population density criteria and the SECPOP code.

DEMOGRAPHIC ASSESSMENT OF CANDIDATE SITES

Site	Location Number	Latitude North	Longitude	Passed Criteria
Gulf Canal site	1	29°49'50"	93°58'27"	Yes
	2	29 49 32	93 58 29	Yes
Sabine Station site	5	30 1 47	93 52 52	Yes
	6	30 2 30	93 53 39	No

The census data input to the SECPOP code was from the 1970 census. In addition, for the Gulf Canal site at location number 1, preliminary 1980 census data for Jefferson County were used along with the estimated transient population. Again location number 1 passed both criteria.

It was concluded that the Gulf Canal site (location 1) is acceptable for reactor siting based on population density criteria, and that a possible

alternative site has been identified near the Sabine Station plant near Bridge City to the east.

6.2.2.2. Risk Assessment. External hazards from explosions on transportation routes, in tank farms, in major industries, and from pipeline releases were assessed for the Gulf Canal nuclear site. A deterministic evaluation of explosions at the site of release similar to that done in the Waterford-FSAR indicated that the Gulf Canal site essentially meets the present regulatory requirements. To analyze the risk from explosion hazards of traveling vapor clouds, a probabilistic risk assessment technique was adopted. The conclusion from this assessment was that the public risk from external explosions at the Gulf Canal site meets the quantitative safety targets, and hence the public risk is acceptable.

Methodology

The methodology starts with potential external hazards and the HTGR design. Potential hazards were obtained from maps and inspection of the site. From the potential hazards, initiating events were selected according to the relative likelihood that damage to the HTGR could occur.

After initiating event selection, accident progression analyses (APA) are performed. For a particular initiating event the APA addresses ways the event can result in a radiological release to the public.

The APA are translated into event trees that are then used to determine accident frequencies. An important consideration is vapor cloud phenomenology. Vapor release models were developed to describe the vapor escape to the atmosphere. From these models and from the size and composition of the release, models were developed describing the motion of the release through the air, its potential burning, and the blast produced in the event of detonation. From the explosion characteristics and plant design it was determined whether damage occurred to key HTGR components and structures. Damage thresholds for key components and structures are given in Table 6.2-1 as a function of blast overpressure.

TABLE 6.2-1
DAMAGE THRESHOLDS FOR KEY COMPONENTS AND STRUCTURES

Component or Structure	Damage Threshold kPa (psia)
Circulating water pump house	7 (1)
Main circulator controller building	7 (1)
Cooling tower switchgear building	7 (1)
Switchyard	7 (1)
Core auxiliary cooling water system (CACWS) air blast heat exchanger (ABHX) fans	14 (2)
Diesel cooling heat exchanger fans	14 (2)
Control and auxiliary diesel building (CADB)	414 (60)
Containment annulus building (CAB)	689 (100)
Containment dome	689 (100)
Ultimate heat sink (UHS) structures	758 (110)
Diesel cooling and fuel oil storage building (DCFSB)	827 (120)

Public risk assessments are then performed using the standard AIPA methodology (Ref. 6.2-3), although the specific model developed for vapor cloud detonations conservatively assume extensive containment damage.

In the final step, the event trees and consequences are combined into the external events risk assessment.

Initiating Event Selection

An initial external hazards evaluation focused upon:

1. Tanker explosions.
2. Truck explosions.
3. Storage tank explosions.
4. Pipeline releases.
5. Tank releases.
6. Toxic gas releases.

Tanker, truck, and storage tank explosions were found to produce less than 7 kPa overpressure at the plant site, and therefore cause no key component or structural damage. A deterministic evaluation of the overpressures, similar to that done in the Waterford FSAR at the reactor site from detonations at the site of release, for all the above-indicated hazard sources, indicates that the Gulf Canal site essentially meets the present regulatory requirements. The pipeline distances from the plant are very close to the deterministic criteria for distances proposed in NUREG-0625.

In addition to the above-indicated deterministic analysis, a probabilistic risk assessment technique was used to determine the safety risk from detonations of traveling vapor clouds from external hazard sources. An initial screening showed that releases from pipelines dominate the risk from external explosions. There are three types of pipelines, respectively carrying crude, natural gas, and refined products. Of these three types, the product pipelines were found to be the most likely to initiate accidents by

pipeline release. These releases could result in a vapor cloud traveling along the ground that could detonate at the vicinity of the plant.

Accident Progression Analysis

The APA for accidents initiated by combustible vapor cloud releases is illustrated in Fig. 6.2-1. The accident begins with an initial release of combustible vapor (event 1). Events 2 through 5 describe the type of vapor release. If there is no accompanying ignition, a single vapor cloud will form (event 2). If there is ignition, detonation might not occur, resulting in a torch that consumes all of the combustible vapor that is released. In this case there are no radiological consequences (event 4), since the plant is undamaged. Detonation may also result in a torch or, much like an explosion extinguishing an oil well fire, may allow the vapor to be expelled unburned (event 5). A second concern in the event of detonation is whether adjacent pipelines are damaged enough to contribute to the release. This is addressed by events 6 and 7.

Although the absence of significant damage to adjacent pipelines precludes a secondary release, sufficient damage to cause a secondary release does not necessarily contribute to the total unburned vapor release. This is because a torch can also accompany and consume the secondary release.

If at least one vapor cloud does form, its potential to damage the plant depends on wind direction (event 8). Even if the cloud moves toward the plant, it must still detonate with sufficient force to damage key components or structures (event 9). If the plant is damaged, a core heatup results only if reactor core temperatures are not maintained within acceptable limits (events 10 and 11).

Vapor Cloud Phenomenology

To determine the detonable mass and vapor cloud dispersion model, it is first necessary to estimate the pipeline inventory and the effective release rate.

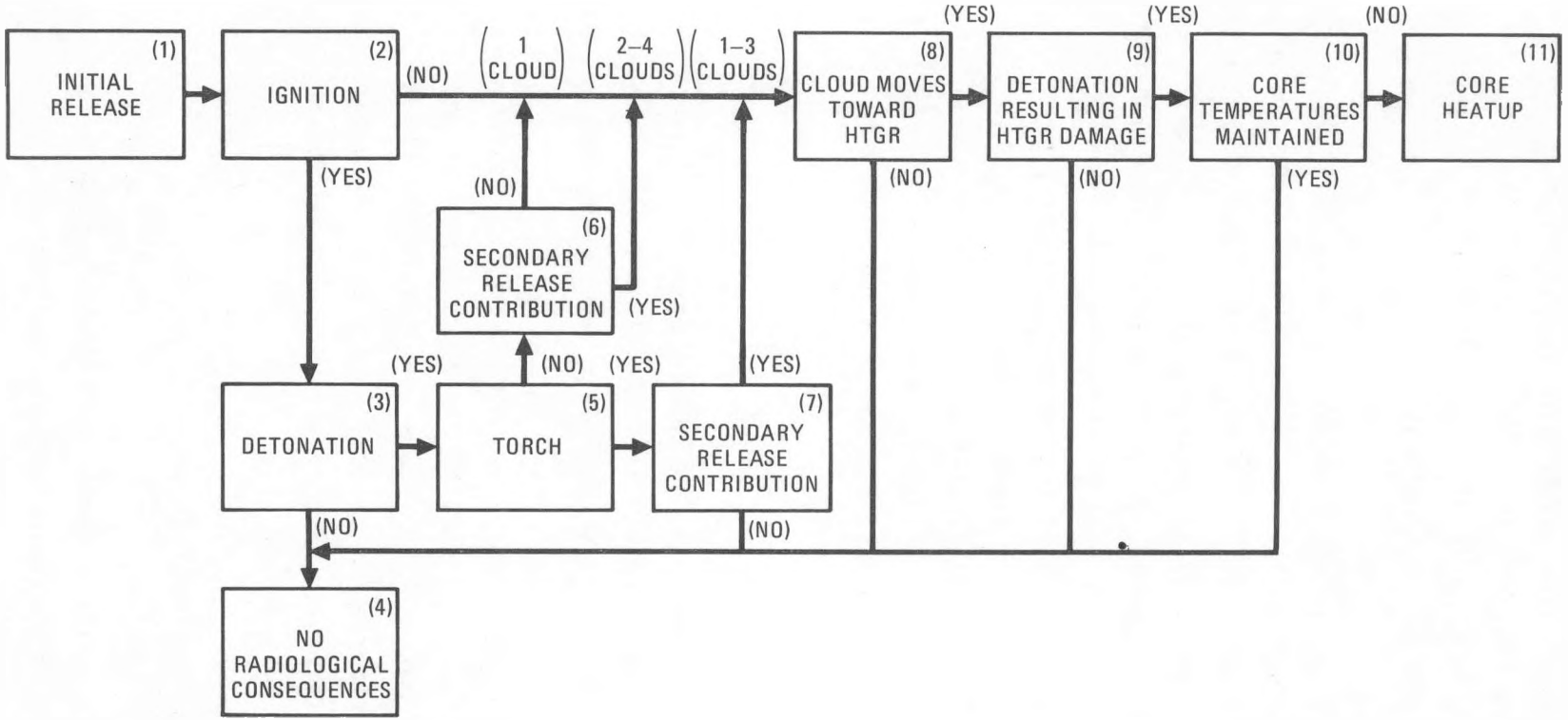

Fig. 6.2-1. Accident progression analysis

Port Arthur area maps show three product pipelines located relatively near to the Gulf Canal site. These near-field product pipelines are the 152-mm propylene and propane lines and the 101-mm butane line.

All three pipelines have a manual isolation valve at the refinery boundary. The propylene and butane pipelines also have manual isolation valves about every 18 km (11 mi). However, the next isolation valve (manual) on the propane pipeline is located at Fannett, which is ~33 km (20 mi) from the refinery. For this preliminary assessment it is assumed that, in the event of a pipeline leak, the release is comparable to the product mass normally contained in the pipeline between the refinery boundary isolation valve and the nearest downstream isolation valve. From the pipe lengths and the product densities, the table shown below was compiled.

PRODUCT MASSES ASSUMED AVAILABLE FOR RELEASE DUE TO PIPELINE BREAK

Product	Pipeline Designation	Density (g/cm^3)	Mass (Mg)
Propylene	I	0.5220	153.2
Butane	II	0.5844	76.25
Propane	III	0.5086	268.8
Ethylene	IV	0.3204	167.2

In addition to the three near-field product pipelines, the table above includes an ethylene line. This 203-mm (8-in.) -diameter line originates at an Arco polymers facility and intersects the route of the three near-field lines 7.7 km (4.8 mi) from the site. Beyond this junction all four pipelines run parallel. To simplify later analyses, the area within 7.7 km (4.8 mi) of the site will be referred to as the nearfield, and "farfield" will denote the region beyond 7.7 km (4.8 mi).

The mass release rate in the event of a leak was estimated by assuming choked flow conditions. This approximation assumes a direct proportionality between release rate and leak size. Although not rigorously correct, this

type of relationship resembles the results derived in Ref. 6.2-4 over much of the depressurization time.

If the depressurization time is relatively long, the vapor cloud will disperse as a plume that is characterized by clouds with large length-to-width ratios and short flammability range (i.e., the flammable region of the vapor cloud does not extend very far from the release source). The plume dispersion model used is documented in Ref. 6.2-5.

If the vapor cloud remains in the vicinity of the leak during the depressurization, most of the product is released into the flammable region. Relatively short depressurization times or low wind speeds are necessary. Under these conditions puff dispersion ensues. Puff dispersion is characterized by ellipsoidal clouds (i.e., length-to-width ratios approaching unity) and a long flammability range. The puff dispersion model used is documented in Refs. 6.2-5 and 6.2-6.

Event Tree Quantification

Figure 6.2-2 is the pipeline release event tree for near-field leaks. Notations appearing in Fig. 6.2-2 are defined in Table 6.2-2. The event tree morphology is based upon the accident progression analysis. For the initiating event, a linear leak frequency of 1.5×10^{-7}/m-yr is assumed, based on the occurrence of large leaks [crack lengths >0.3 m (11.8 in.)] in pipelines during the years 1978 and 1979 (the most recent data available). The total length of pipelines is 21.6 km (13.5 mi) in the near-field and 103 km (64 mi) in the far-field areas. The product of frequency per unit length is multiplied by the pipeline lengths to determine the initiating event frequencies in Fig. 6.2-2. Initiating event frequencies and nodal probabilities are derived in Ref. 6.2-7.

Figure 6.2-2 and a similar figure for the far field indicate that the N-BN branch is the only significant contributor to the risk in which a flammable cloud does reach the plant and detonates causing an immediate loss of core cooling, liner cooling, and containment integrity. The branches that

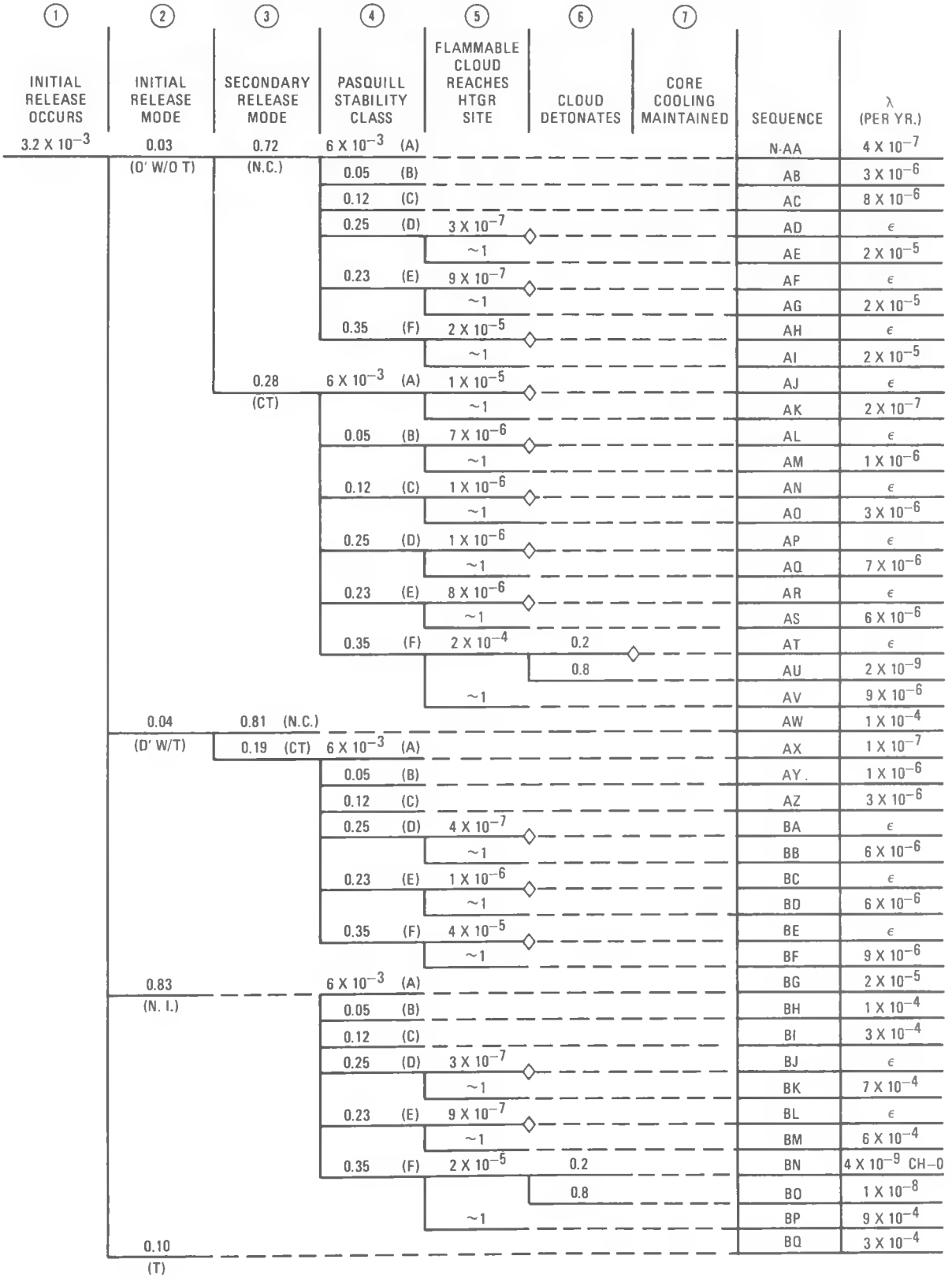

Fig. 6.2-2. Pipeline release event tree for near-field leaks

TABLE 6.2-2
EVENT TREE SYMBOLS

Notation	Definition
D' w/o T	The initial release mode involves detonation without a torch
D' w/ T	The initial release mode involves detonation with a torch
N.I.	There is no initial release ignition
T	The initial release burns with a torch
N.C.	The secondary release mode does not contribute to the vapor cloud
Ct.	The secondary release mode does contribute to the vapor cloud
A	Pasquill stability class A
B	Pasquill stability class B
C	Pasquill stability class C
D	Pasquill stability class D
E	Pasquill stability class E
F	Pasquill stability Class F
ε	Sequence frequencies $<10^{-9}$/yr
λ	Median event sequence frequency

end with a diamond symbol represent the cases in which the flammable cloud reaches the plant but the frequency is extremely low (less than 10% contribution to the total risk). Other branches in the event tree represent the cases in which the flammable cloud fails to reach the plant and therefore has little consequence. The N-BN sequence involves the following external events:

1. An initial product pipeline release occurs in the near field.

2. The initial release does not ignite.

3. Meteorological conditions correspond to Pasquill stability class F.

4. The flammable cloud reaches the plant site.

5. The cloud detonates.

6. It is conservatively assumed that the detonation causes an immediate loss of core cooling, liner cooling, and containment integrity.

Consequence Assessment

The initiating event, which is an external vapor cloud explosion, is assumed to simultaneously destroy all core cooling and damage the reactor containment building. Following reactor shutdown by control rod insertion, a slow core temperature rise due to residual decay heat results in the PCRV overpressurization PCRV relief valve opening. Circulating fission product activity is released to the failed containment and then to the environment. Core and PCRV temperatures continue to rise until fuel failure begins at ~2000°C (3632°F). Fission products (e.g., cesium or strontium) that are released from failed fuel diffuse through the graphite web to the coolant. The noble gases are not held up on the graphite and so are directly released to the coolant. Fission products released to the coolant may plate out on

cooler portions of the core or relatively cool PCRV surfaces, depending upon their volatility. Those fission products that escape the core and do not plate out are released to the failed containment in a slow, time-dependent fashion. After a period of ~2 days, the PCRV concrete begins to spall; its temperature reaches 899°C (1650°F). Concrete spalling produces the gases CO_2 and H_2O. This gas flow results in a higher radionuclide release rate to the containment and from the containment to the environment. Most of the concrete gas directly escapes the PCRV through the relief valve. However, a small fraction (~10%) can react with the core, producing CO and H_2, which are flammable. This has little significance for this event, which has a failed containment at time zero.

Fission products released to the environment through cracks and holes in the damaged containment structure are transported by the existing wind conditions over the surrounding area. In traveling from the containment out to the low population zone, the fission products in the radioactive cloud dilute with the air, decay, and fall out.

The radiological consequences associated with the N-BN core heatup sequence for a 2240-MW(t) SC/C plant at Port Arthur were calculated with the CRAC code. The CRAC code analyzes core heatup consequences including early and latent injuries and fatalities caused by exposure to and inhalation or ingestion of radioactive elements. The irradiation doses estimated by CRAC include external plume dose, inhalation dose commitment, dose from fallout on the ground, dose from ingestion of agricultural products, inhalation of resuspended fallout, milk dose from cows feeding on contaminated grass, etc. CRAC input includes site-specific data, such as population distribution surrounding the site out to 805 km (500 mi), site meteorological data, and site topography. Evacuation of the population surrounding the site was modeled assuming a 1-hr warning time and an evacuation speed of 1.8 km per hour (1.1 mi per hour). The results of the radiological consequence calculations for the Port Arthur site predict no acute fatalities or acute injuries. However, latent fatalities are predicted to occur in the population beginning at ~2 yr following exposure and continuing for about a 30-yr period.

The public risk associated with external explosion hazard is plotted in Fig. 6.2-3. It can be seen from this figure that the public risk from external explosions at the Port Arthur nuclear plant site is below the quantitative HTGR safety targets, and that hence the public risk is acceptable.

The large uncertainty in the accident frequency estimate is primarily attributable to the statistical variance in the vapor cloud dispersion parameters. Consequence uncertainties are dominated by the behavior of cesium during the accidents.

References

6.2-1. U.S. Nuclear Regulatory Commission, Regulatory Guide 4.7, Rev. 1, "General Site Suitability Criteria for Nuclear Power Stations," USNRC: Office of Standards Development, Washington, D.C., November 1975.

6.2-2. Patrick C. Higgins, letter to Steering Group, Committee on Reactor Licensing and Safety, dated May 15, 1981, Enclosure 1, Attachment B.

6.2-3. Fleming, K. N., et al., "HTGR Accident Initiation and Progression Analysis Status Report - Phase II Risk Assessment," DOE Report GA-A15000, April 1978.

6.2-4. Morrow, T. B., "When an LPG Line Breaks, How Does the Product Release/Disperse?," Pipeline and Gas Journal, June 1982.

6.2-5. Slade, D. H., "Meteorology and Atomic Energy 1968," AEC Report TDI-24190, National Technical Information Service, July 1968.

6.2-6. Landoni, J. A., "Hazards of Combustible Gases Accidentally Released from the Process Plant of HTGR Process Applications," DOE Report GA-A16365, September 1981.

6.2-7. Everline, C. J., "2240 MW(t) HTGR-SC/C External Events Risk Assessment for the Port Arthur Site," GA unpublished data, July 1982.

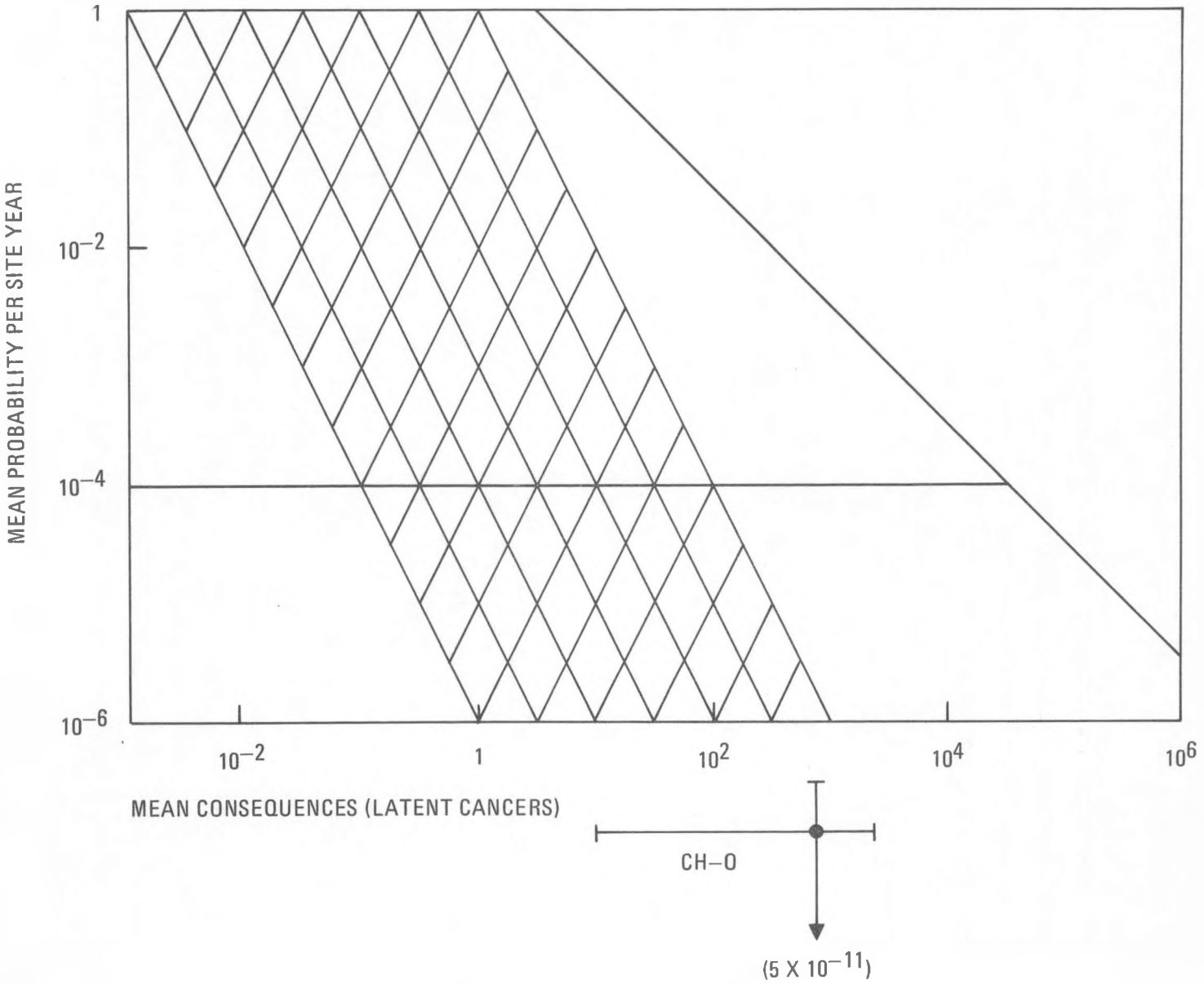

Fig. 6.2-3. Public risk estimate for externally initiated core heatups

6.3. HTGR-SC/C SITE SPECIFIC STUDY FOR REFINERY APPLICATION (6003050100)

6.3.1. Scope

The scope of the work reported here was to provide technical support for a study on the application of the HTGR-SC/C to supply steam and electric power for refineries at Port Arthur, Texas, and Alliance, Louisiana.

Specific work during this period included (1) support studies for use of reboilers at Port Arthur, and (2) review of HTGR applications for energy requirements, deployment scenarios, and a preliminary economic assessment of the Alliance refinery and other industries in the Alliance/St. Rosalie site area.

6.3.2. Discussion

6.3.2.1. Port Arthur Reboiler Study. The use of reboilers in industrial cogeneration applications of an HTGR have been proposed for two primary reasons:

1. Because of the less critical need for high-purity feedwater, reboilers would probably save considerable cost in water purification equipment.

2. Through the use of reboilers, tritium-containing steam is much less likely to reach the refinery. This has recently been classified as a nonproblem, leaving the choice purely in the realm of economics.

Ground rules that were adopted for this electrical power output comparison were the following:

1. The refinery steam need (rated conditions) is 378 kg/s (3,000,000 lb/hr) at about 4.48 MPa/357°C (650 psia/675°F). Steam will be generated at 4.8 MPa (700 psia) at the HTGR site.

2. Condensate (including make-up) is returned from the refinery at 38°C (100°F). This temperature is probably seasonally variable, but is thought to be an average value.

3. A single 2240-MW(t) plant reactor was used in the heat balances. Since that size of reactor can furnish all the steam needed, either with or without a reboiler, the addition of a second reactor plant would produce more electrical power but would not affect the comparison.

Cycles with Reboilers

Two variations in the arrangement of reboiler cycles were considered in this study. One (Scheme A) introduces the condensed high-pressure heating steam from the reboiler back into the condensate cycle at the first (low-pressure) feedwater heater inlet (Fig. 6.3-1). In this case, the condensate from the reboiler is subcooled to 49°C (120°F) and is then mixed with condensate from the condenser at 43°C (109°F) (2-1/2 in. HgA). In Scheme B, the condensed high-pressure heating steam from the reboiler is brought back into the condensate cycle at the No. 4 heater (deaerator) inlet (Fig. 6.3-2). It is subcooled in the reboiler to only 161°C (322°F), so that its temperature matches that of the condensate out of the No. 3 heater. The objective of Scheme B is to save some equipment costs by reducing the size (surface) of the reboilers. This is done by (1) increasing the temperature difference at the inlet and (2) reducing the size of the three low-pressure heaters by reducing the condensate flow to them and thereby reducing their heat duty.

Heat balance calculations (Figs. 6.3-1 and 6.3-2) show that Scheme A is thermodynamically more efficient than Scheme B to the extent that the electrical power generated is 35 MW(e) higher. It is judged that this additional power easily justifies the increased cost of equipment for Scheme A. A further advantage is that the condensate from the reboiler at 49°C (120°F) is cool enough to put through dimineralizers, whereas the 161°C (322°F)

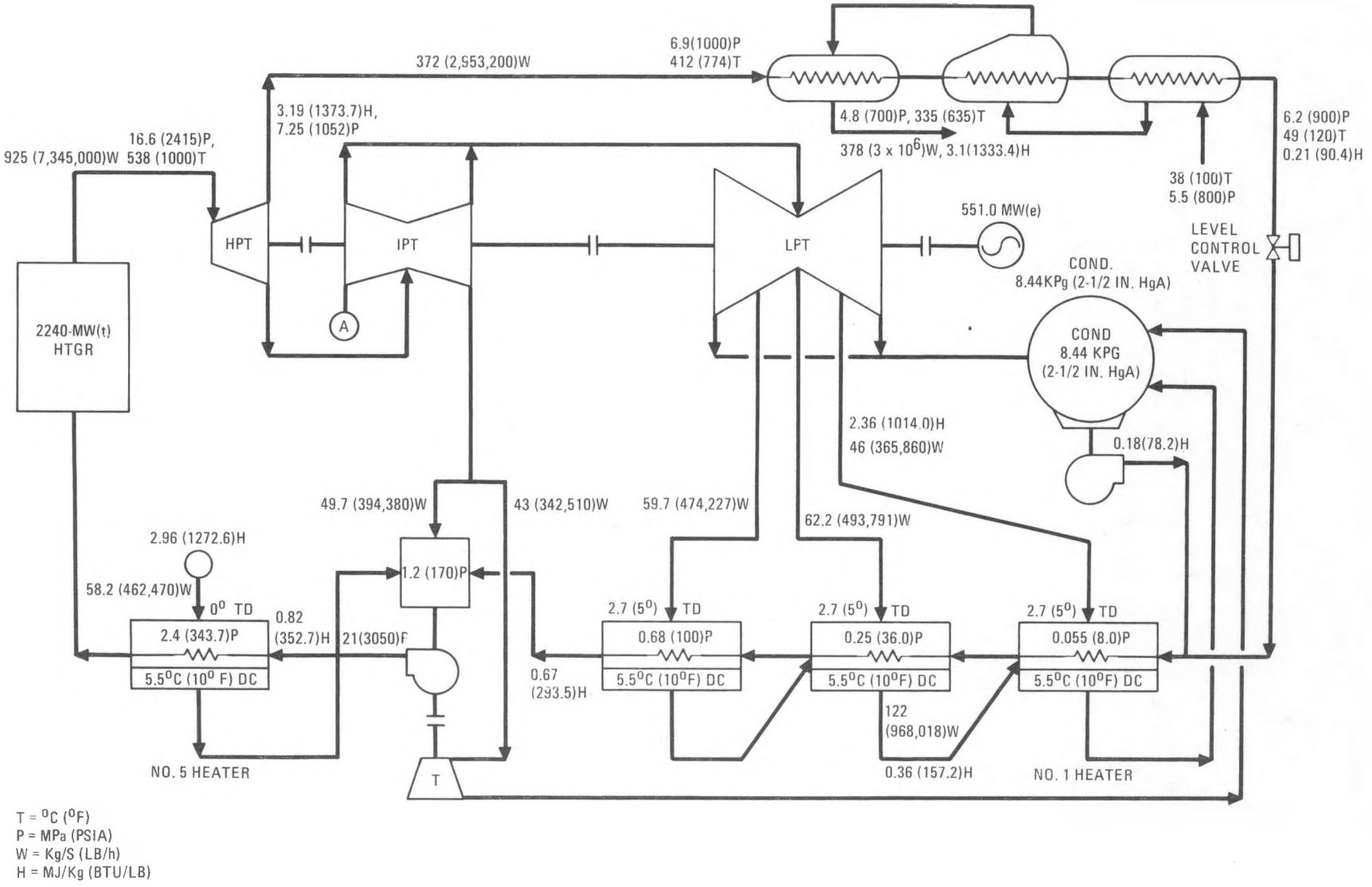

Fig. 6.3-1. Heat balance diagram for Port Arthur, Texas plant with reboiler, Scheme A

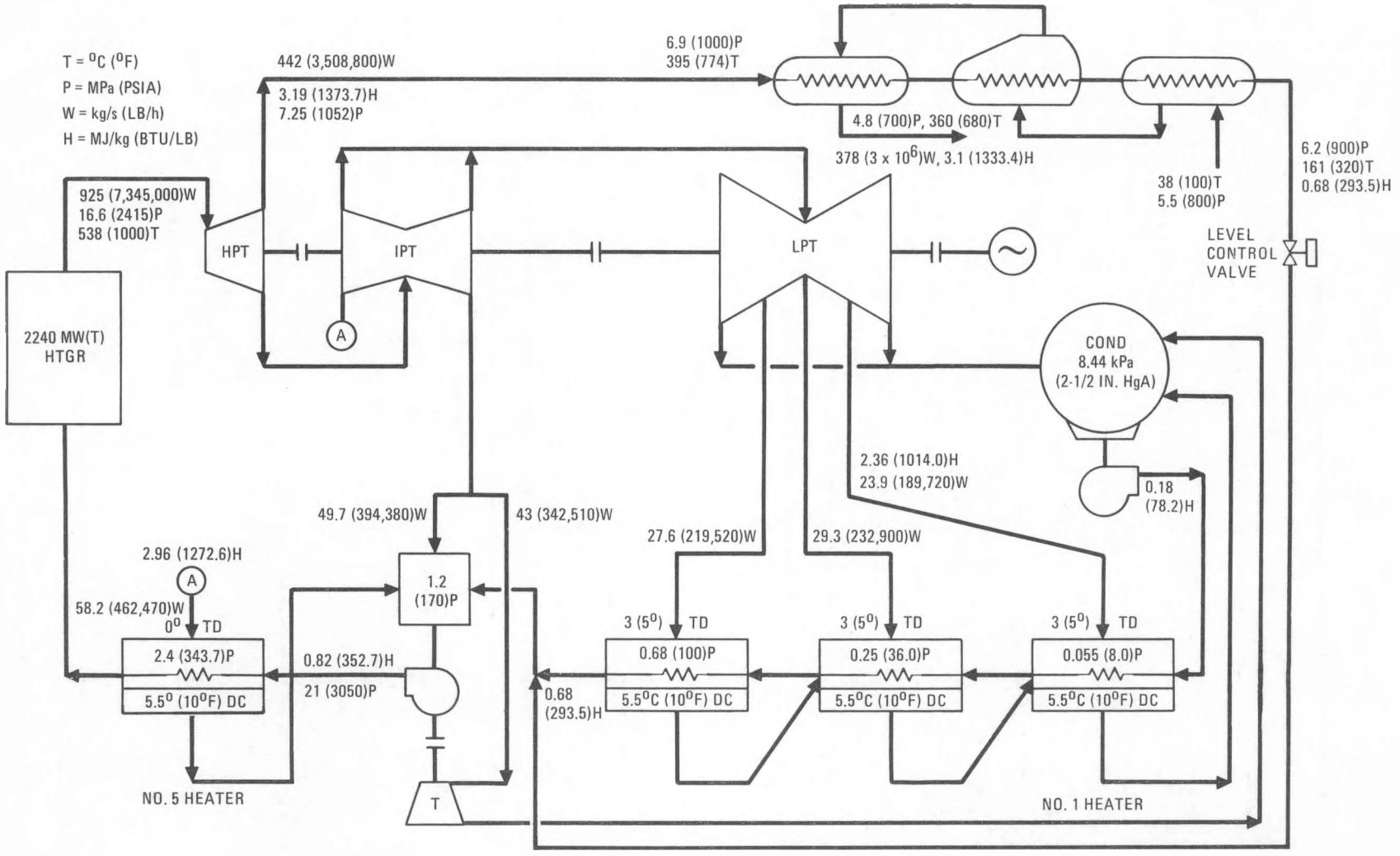

Fig. 6.3-2. Heat balance diagram for Port Arthur, Texas plant with reboiler, Scheme B

condensate in Scheme B is not. Therefore, Scheme A is the preferred reboiler alternate.

No-Reboiler Cycle

Figure 6.3-3 is a heat balance diagram for the no-reboiler case. The cycle arrangement is the same as the two reboiler cases. However, the high-pressure turbine exhausts at 5.1 MPa (736 psia), allowing a 5% piping pressure loss to convey the process extraction steam to the same point in the plant as the location of reboilers in Schemes A and B. Thus, in all three cases steam is available at 4.8 MPa (700 psia) at the transmission piping inlet. For reboilers, the design outlet steam temperature is 360°C (680°F). For the no-reboiler case, the expected temperature of the extraction steam is about 363°C (685°F). This small difference was considered inconsequential to the comparison.

Performance Comparison

As would be expected, the no-reboiler case provides greater electrical output. Generator terminal power for this case is 576.8 MW(e), as shown in Fig. 6.3-3. For the reboiler case of Scheme A, Fig. 6.3-1, generator terminal power is 551.0 MW(e). However, Scheme A uses 1.3 MW(e) more auxiliary power than the no-reboiler case because of a combination of less condensate pump power but additional power for a reboiler feedpump. Therefore, the net differential electric power generation is 27 MW(e) higher for the no-reboiler case.

Reboiler Design and Sizing

Figure 6.3-4 shows the reboiler concept arrangement for Scheme A of this study; the arrangement is similar to that for Case 3 in Ref. 6.3-1. It was concluded that the feedwater specified for the reboiler design would be at least as good as treated boiler feedwater and that the HTGR steam/condensate matches the purity of distilled water. For this reason, a combined fouling resistance of 0.0015 was used in the sizing calculations.

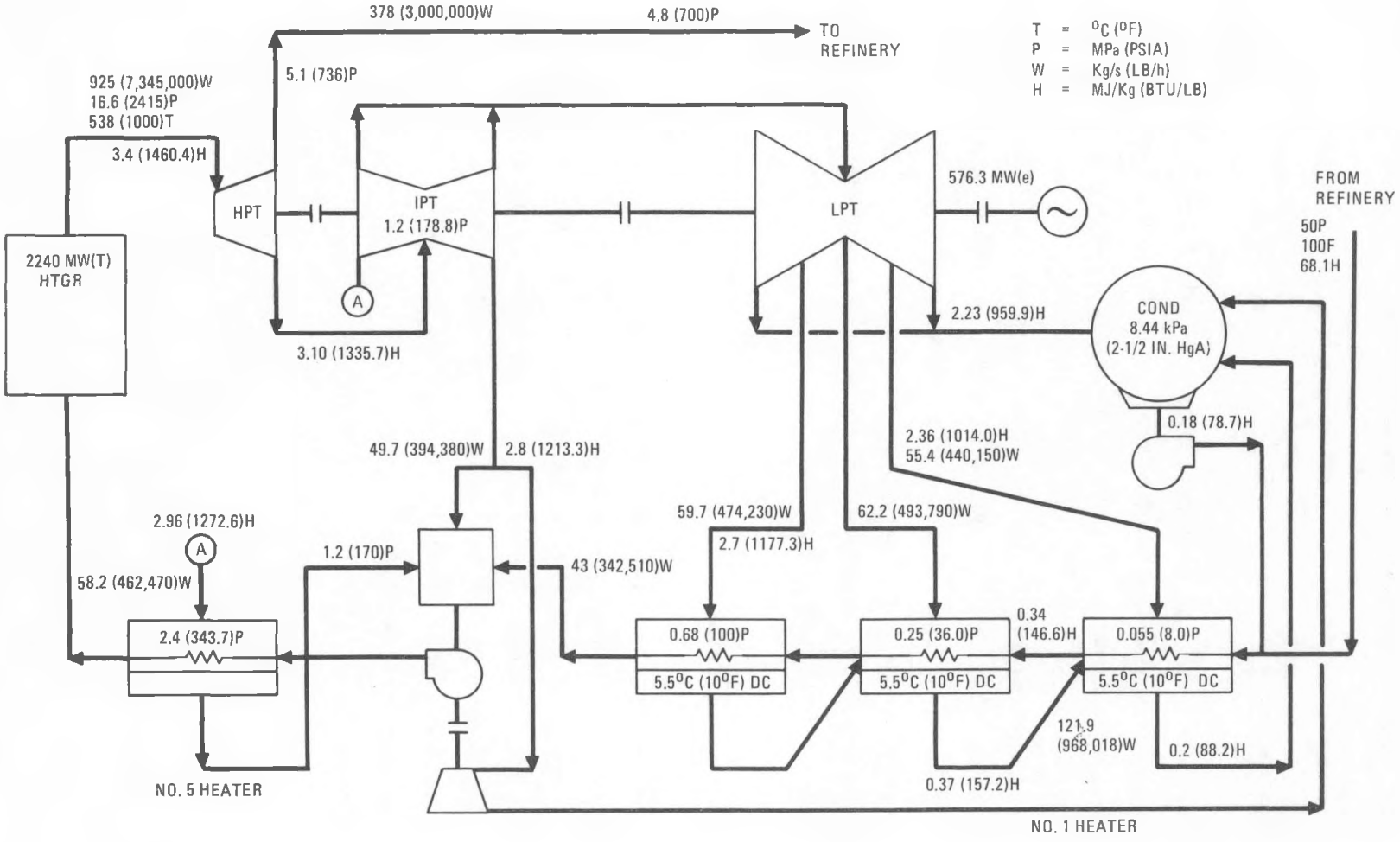

Fig. 6.3-3. Heat balance diagram for Port Arthur, Texas plant, no reboiler case

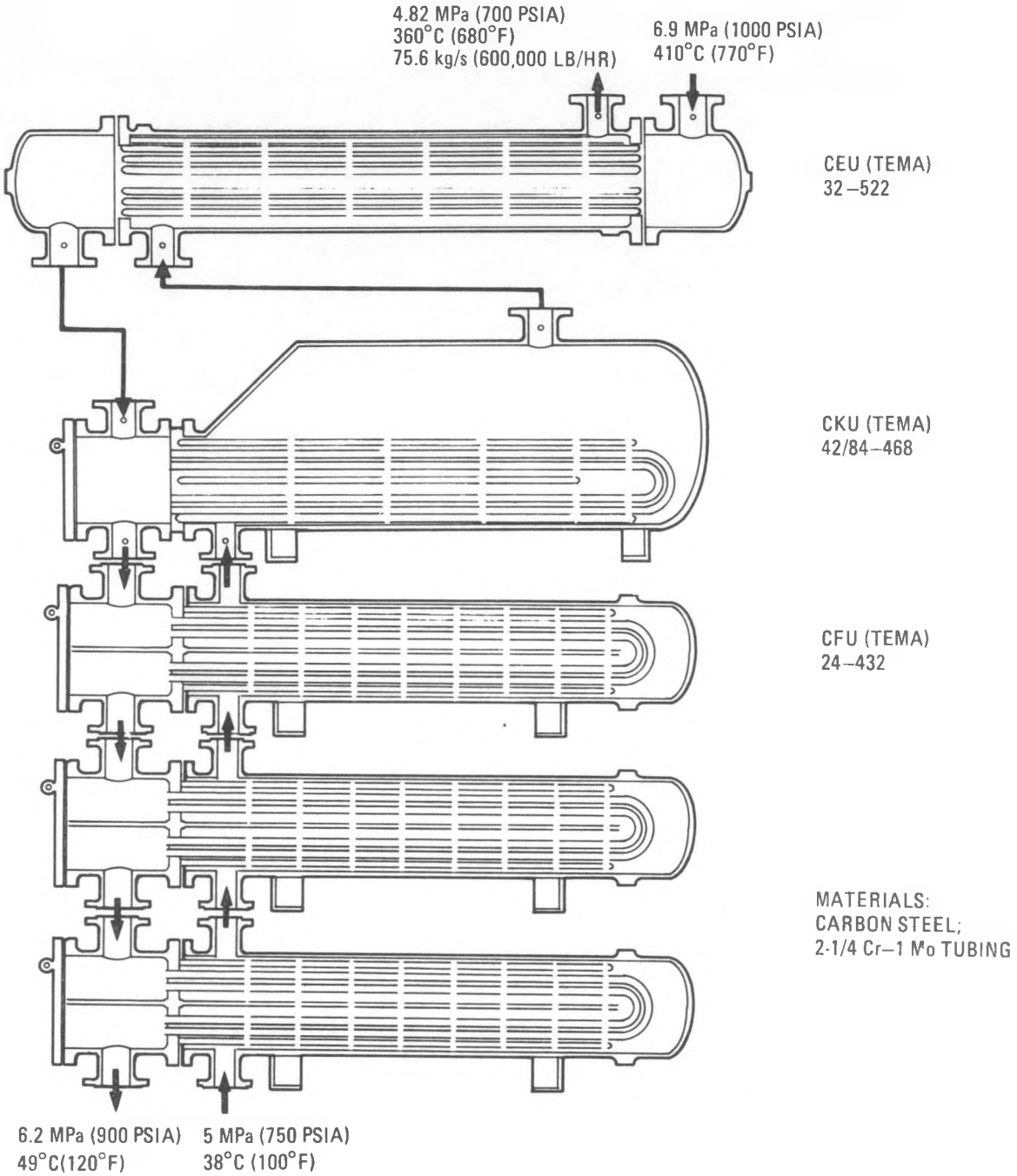

Fig. 6.3-4. Conceptual reboiler arrangement, Scheme A

It is recognized that the referenced reboiler design used 20°C (68°F) feedwater, while the heat balances of this study were based on 38°C (100°F) feedwater. It is believed the resulting differences in reboiler sizing and cost are negligible for the purposes of this study.

Five sets of modules with a steam capacity of 75.6 kg/s (600,000 lb/hr) can satisfy the 378 kg/s (3,000,000 lb/hr) demand. With the recommended nine modules for Port Arthur, there will be a margin of four to cover fouling and outages for cleaning. The estimated cost of the nine reboilers is ~$4,500,000.

Other Aspects of the Study

In addition to the factors of differential power generation and reboiler sizing that have been discussed here, there are a number of other economic aspects of the comparison of reboilers versus no reboilers. These include the differential capital cost of: (1) feedwater treatment systems, (2) control and instrumentation, (3) piping and valves, (4) the turbine-generator, (5) structures, and (6) pumps.

Consideration would also be given to maintenance and operating costs, since there may be an increase with reboilers.

6.3.2.2. HTGR-SC/C Applications at Alliance, Louisiana (St. Rosalie Site). The purpose of this study was to determine if the HTGR-SC/C concept was technically and economically viable for this application. The St. Rosalie site was selected because of its proximity to the Gulf Alliance refinery and particularly because the St. Rosalie site [owned by Louisiana Power and Light Company (LP&L)] had previously been selected as the potential location for two HTGR-SC electricity-producing power plants. Preliminary safety evaluation reports were in preparation when that particular project was terminated. The Alliance refinery is located less than 1.1 km (0.7 mi) from the St. Rosalie site boundary.

In the study recognition was given to the fact that the energy requirements for the Alliance refinery alone were insufficient to justify the use of a large HTGR plant. However, the existence of the St. Rosalie site close to the Alliance plant, the potential industrial growth in the area, and the availability of data on both site and users presented a good basis for the HTGR-SC/C application and evaluation.

Application Requirements

Table 6.3-1 lists the steam requirements assumed for each user (Alliance and new users). The required conditions, 4.65 MPa/371°C (675 psia/700°F), are met.

The steam demand varied between 0.95 and 5.9 MPa (125 and 850 psig). Several alternative possibilities were open by which the refinery could upgrade the steam for the relatively small amount of steam needed at higher pressure, and for operating reasons it was preferred to transmit steam at slightly lower pressure. For this reason, a maximum pressure of 4.57 MPa (650 psig) was selected. Additional capacity was included in the process HTGR plant to allow for modest steam demand fluctuation, and the electric variable cogeneration HTGR can accommodate more radical load changes (from 0 to 100% of steam demand) than the standard HTGR-SC. Steam at 16.6 MPa/538°C (2415 psia/1000°F) is available at the HTGR steam generator outlet.

HTGR and Coal-Fired Plant Process Coupling

Each of the two 2240-MW(t) HTGR-SC/C NHS plants is coupled to process steam and electric power users by identical variable cogeneration turbine plant arrangements. These permit the energy produced by each NHS to be used either for all-electric power generation or for varying degrees of electric power/process steam cogeneration at any time during the plant life, depending on the relative electric and steam demands. Such variable cogeneration flexibility provides greater protection for plant investment by permitting maximum use of the full reactor output capability.

TABLE 6.3-1
PEAK PROCESS STEAM REQUIREMENTS

Alliance refinery	
Steam temperature, °C (°F)	371 (700)
Steam pressure, MPa (psia)	4.14 (600)
Steam flow, kg/s (lb/hr)	21.4 (170,000)[a]
Electric power purchased, MW(e)	35
Average capacity factor, %	—
Availability required, %	100
New industrial capacity (each of two HTGR's)	
Steam temperature, °C (°F)	357 (675)
Steam pressure, MPa (psia)	4.65 (675)
Steam flow, kg/s (lb/hr)	304 (2,415,000)[a]
Electric power purchased, MW(e)	55
Average capacity factor, %	--
Availability required, %	100

[a] The total 629 kg/s (5,000,000 lb/hr) is the same as for the Port Arthur plant (Ref. 6.3-2).

Figure 6.3-5 shows the proposed variable cogeneration heat cycle to be used with each each 2240-MW(t) HTGR-SC/C.

For the sake of comparison, the coal plants were also treated as variable cogeneration plants. It should be noted that four 655-MW(t) coal-fired boilers, which are equivalent to one 2240-MW(t) HTGR-SC/C plant, constitute one variable cogeneration plant. The four units operate in parallel to supply steam to the process user and to the turbine generators.

Deployment Scenario and Schedule

The following characteristics were adopted as goals in the selection of the reference deployment sequence:

1. Flexibility. The ability to accept late modifications to process design conditions and/or project commitments, and to make appropriate changes to the plant designs with acceptable cost and schedule impacts.

2. Optimal Plant Configuration. The consistency of the deployment sequence with the final desired plant configuration. Equipment needed just for deployment and not for commercial operation should be minimized.

3. Opportunity for Demonstration. The ability to demonstrate the integrated operation of the central heat source and the process plant at minimum cost and risk, and the opportunity to feed results back to benefit the final plant configuration.

The energy demands and deployment schedules for the HTGR are shown in Figs. 6.3-6 and 6.3-7. Timing of process steam demand sets the pace for project construction. It is assumed that new industrial capacity would come on line in two stages, approximately 2 yr apart. Multiple stages would be appropriate and consistent, assuming two or more independent users or a phased expansion or startup of the process plants, and would satisfy a later

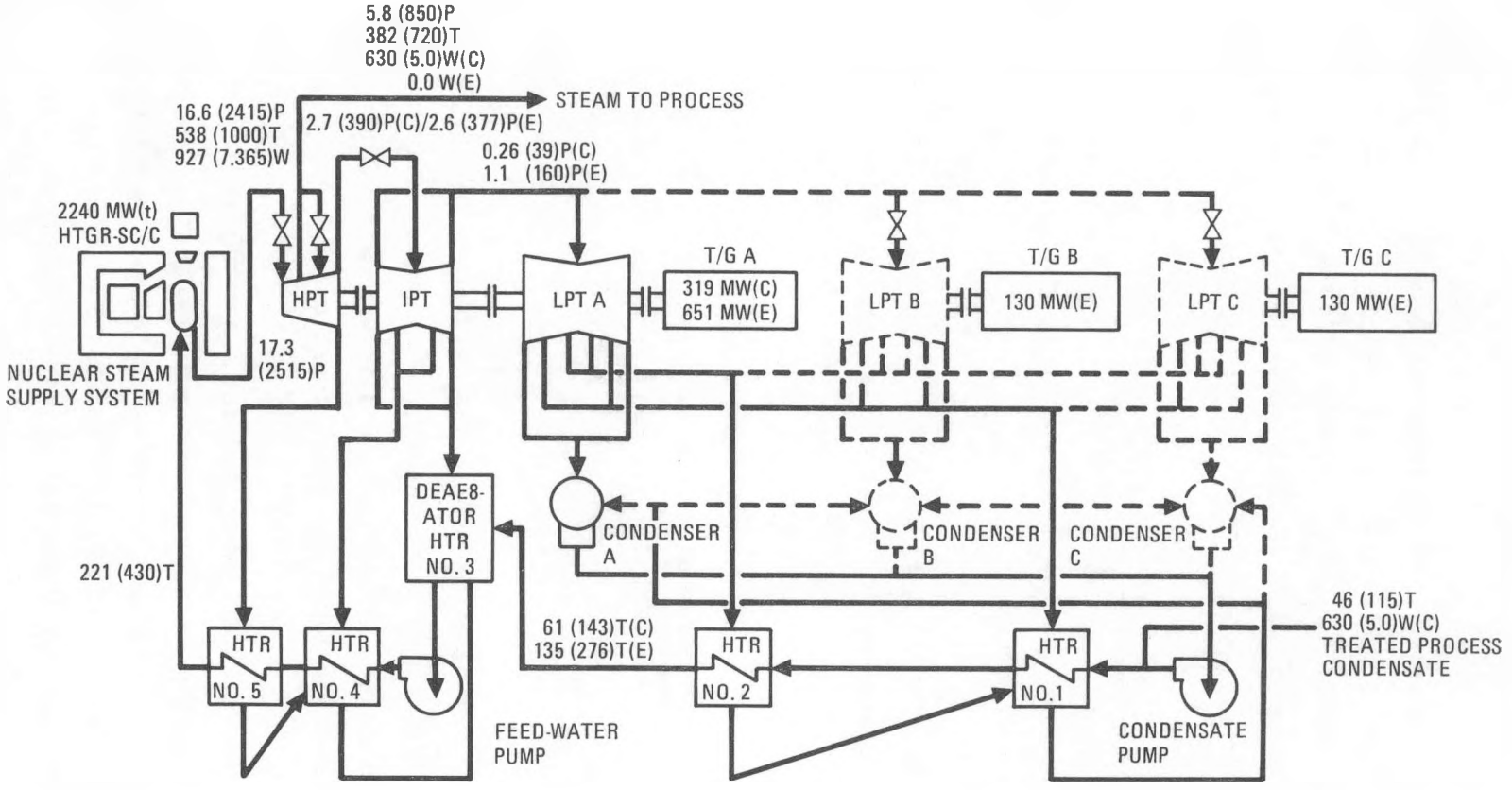

PERFORMANCE

	MAXIMUM COGENERATION	MAXIMUM ELECTRICITY GENERATION
GROSS OUTPUT	319 MW(e)	910 MW(e)
AUXILIARY POWER	88 MW(e)	90 MW(e)
NET OUTPUT	231 MW(e)	820 MW(e)
PROCESS HEAT	1852 MW(t)	0
NET EFF	93%	37%

LEGEND

P = PRESSURE, PSIA
T = °FAHRENHEIT
W = FLOW, Kg/S (10^6LB/HR)
(C) = MAXIMUM COGENERATION
(E) = MAXIMUM ELECTRICITY GENERATION
- - - = EQUIPMENT NOT IN USE DURING 100% COGENERATION MODE

Fig. 6.3-5. 2240-MW(t) HTGR-SC/C (variable cogenerator) plant

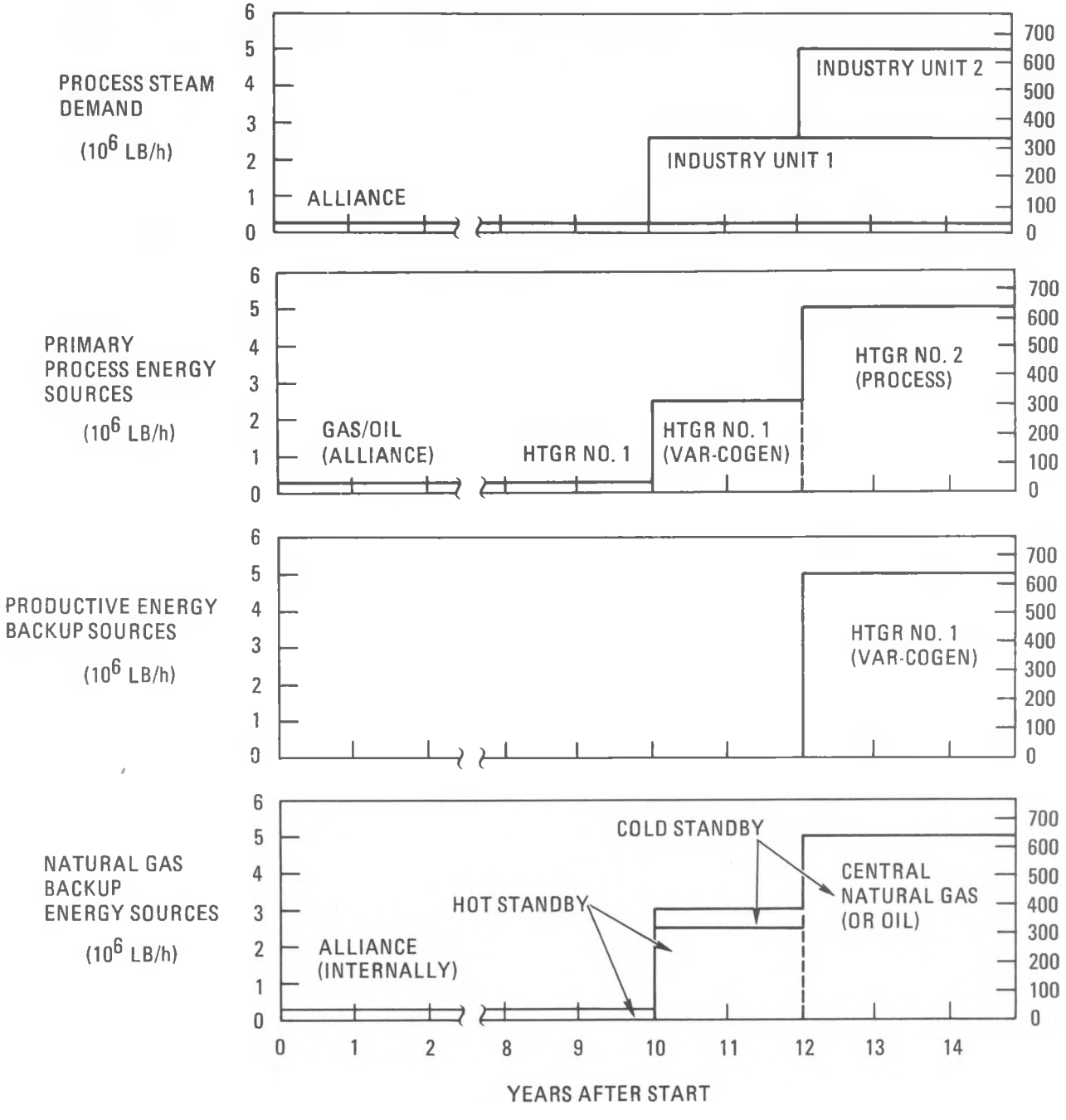

Fig. 6.3-6. Energy demand - HTGR

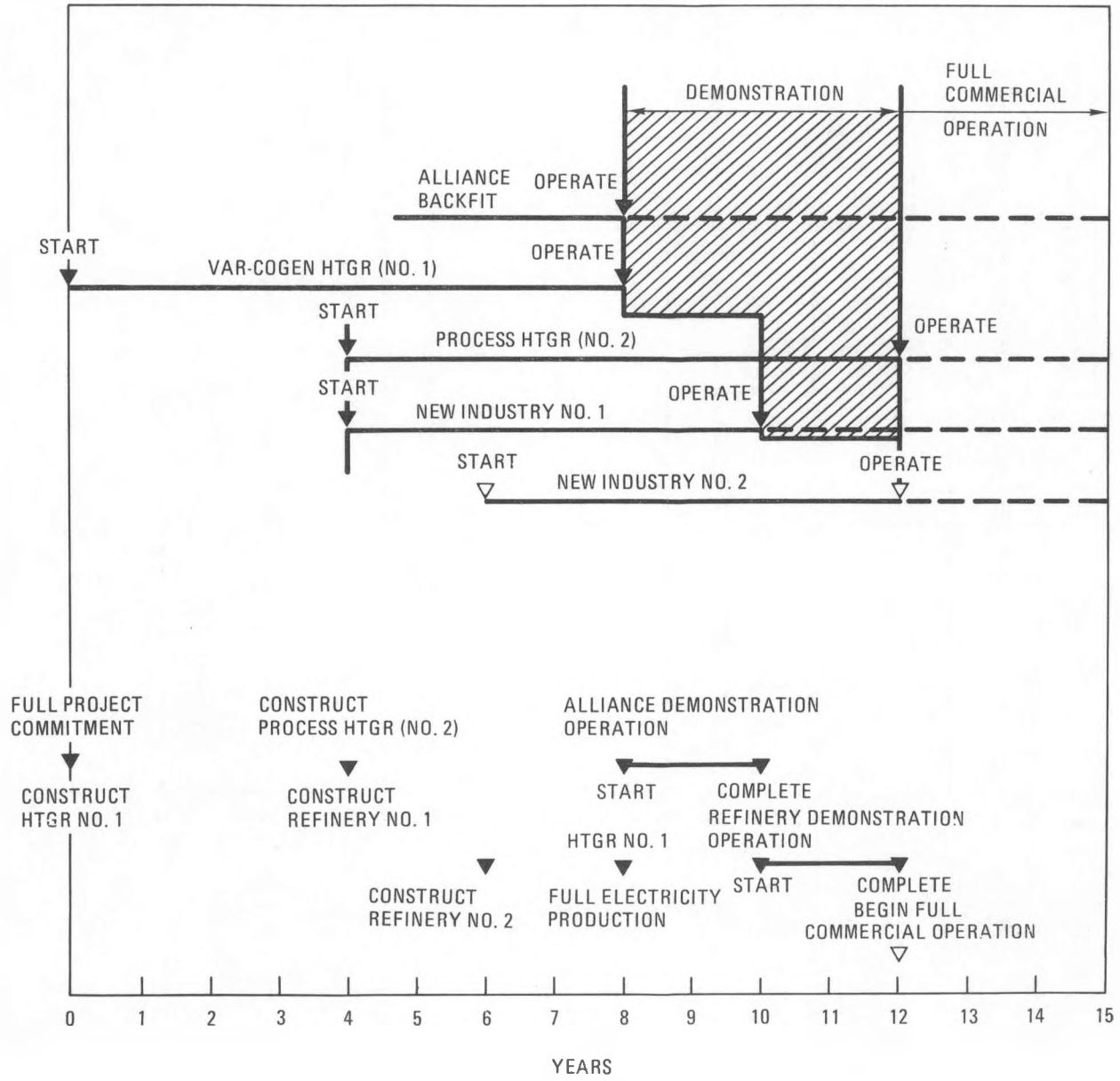

Fig. 6.3-7. Alliance HTGR-SC/C application, HTGR project construction schedule

desire on the part of some users to demonstrate operation before completing the last portion of the project. The same deployment sequence could also be used in the event both stages came on line closer together or even concurrently. However, the design assumed for the steam supply system and the construction schedules would need to be changed if the stages were far apart. For example, if the second stage were 10 years after the process HTGR, the process HTGR could not run at 100% as it is currently described.

It is assumed that firm commitments are obtained from all participants at the beginning of the project. There must also be assurance that the heat source will be available for startup of the process plants and that the initial operation will be smooth. This is accomplished in the reference sequence by constructing the variable cogeneration (basically electricity-producing) HTGR first and demonstrating its operation with process steam users.

HTGR Construction and Demonstration

Construction of the variable cogeneration HTGR minimizes the risks associated with design changes or schedule delays of the process steam users. This first plant can supply electricity economically for an indefinite time. Even assuming that the process plants are never completed, the first HTGR could continue as a viable electric plant, since the additional design modifications to permit diversion of process steam would be modest.

As presented, initial operation of the variable cogeneration HTGR includes demonstration of steam supply to Alliance. Two years are allowed for evaluation of operating characteristics. During this initial demonstration period, Alliance would maintain its internal steam supply capability as backup. For this reason, it is not critical that the HTGR come on line at any particular time, and some slippage to the HTGR schedule can be accommodated. The Alliance steam demand at this point in the schedule is small. Therefore, the interactive characteristics of the HTGR and the process steam user can be studied without major risk to Alliance or to the electricity-producing capability of the HTGR, and without large economic penalty.

The first new industrial capacity is scheduled to come on line after this small-scale demonstration but before the process HTGR is completed. The new industrial steam demand is also supplied by the variable cogeneration HTGR, demonstrating again the overall system characteristics, but in a larger and more realistic mode. Two years are also allowed for this demonstration. Because this refinery capacity is designed with full reliance on centrally generated process steam, backup to the single HTGR must be provided. Natural-gas-fired boilers are assumed, some maintained in hot standby so that reactor trips can be accommodated, and some in cold standby in case of unavailability of one of the hot standby units. Again, schedule is not critical, since the HTGR can continue producing electricity while waiting for the process plant to come on line.

The economic penalty of the second demonstration is not negligible. The variable cogeneration HTGR is precluded from producing 100% electric power for up to two years, which would require LP&L to make up capacity from presumably more expensive plants. Also, because the process HTGR is not yet available and the only backup is the natural-gas-fired boilers, higher fuel costs would be incurred to keep the boilers on hot standby and to operate them when the HTGR is being refueled or in an unscheduled shutdown. On the other hand, because steam will be provided reliably, the process user should pay commercial value for the steam, which will defray the aforementioned expenses.

The second HTGR plant is scheduled to begin operation when all planned refining capacity comes on line. For reference purposes, this was estimated at four years after the first HTGR and two years after the initial stage of the new refining capacity came on line. At this point, the intended commercial operation would begin, with the second HTGR providing all the steam, and the variable cogeneration HTGR basically providing electric power but also acting to back up the process reactor.

Coal-Fired Plant Deployment

The reference coal-fired plant [(four 655-MW(t) units], is basically a one-for-one substitute for a 2240-MW(t) HTGR. Accordingly, discussion of the deployment schedule concentrates on the unique differences of the coal plant. It is assumed that the refineries' needs for process steam will set the schedule and that therefore changes in schedule for the coal plant versus the HTGR centers around those dates. The proposed coal-fired plant energy demand and deployment schedules are shown in Figs. 6.3-8 and 6.3-9.

Construction and operation of the refinery capacity is unchanged from that presented for the HTGR scenario schedule. It is assumed that the Alliance demonstration can be reduced from two to one year, because the coal technology is better developed and needs less demonstration. The overall schedule required to construct coal plants and to place them in operation is taken as six years versus the HTGR's eight years. Because of these differences, the initial variable cogeneration coal-fired plant can be committed three years later than the HTGR, and the process steam supply plant can be started two years later than the HTGR.

Economic Evaluation

The results of the preliminary economic analysis are shown in Table 6.3-2. A review of the results shows that while the coal plant capital costs are lower than the HTGR plant capital costs, the levelized annual coal fuel cost is considerably higher than the nuclear fuel cycle cost. The overall net annual cost of the coal-fired plant is almost twice that of the HTGR annual cost. The annual steam production from the coal plant is only slightly higher than the steam production from the HTGR plant because of the assumed plant availability factors (85% for coal versus 80% for the HTGR). With the reference electric credit value of 0.035/kW(e)-h, the coal plant steam cost is approximately 83% higher than the HTGR steam cost on a 30-yr levelized basis. Figure 6.3-10 shows the relationship between the steam cost and electric credit for the Alliance/St. Rosalie scenario. As the

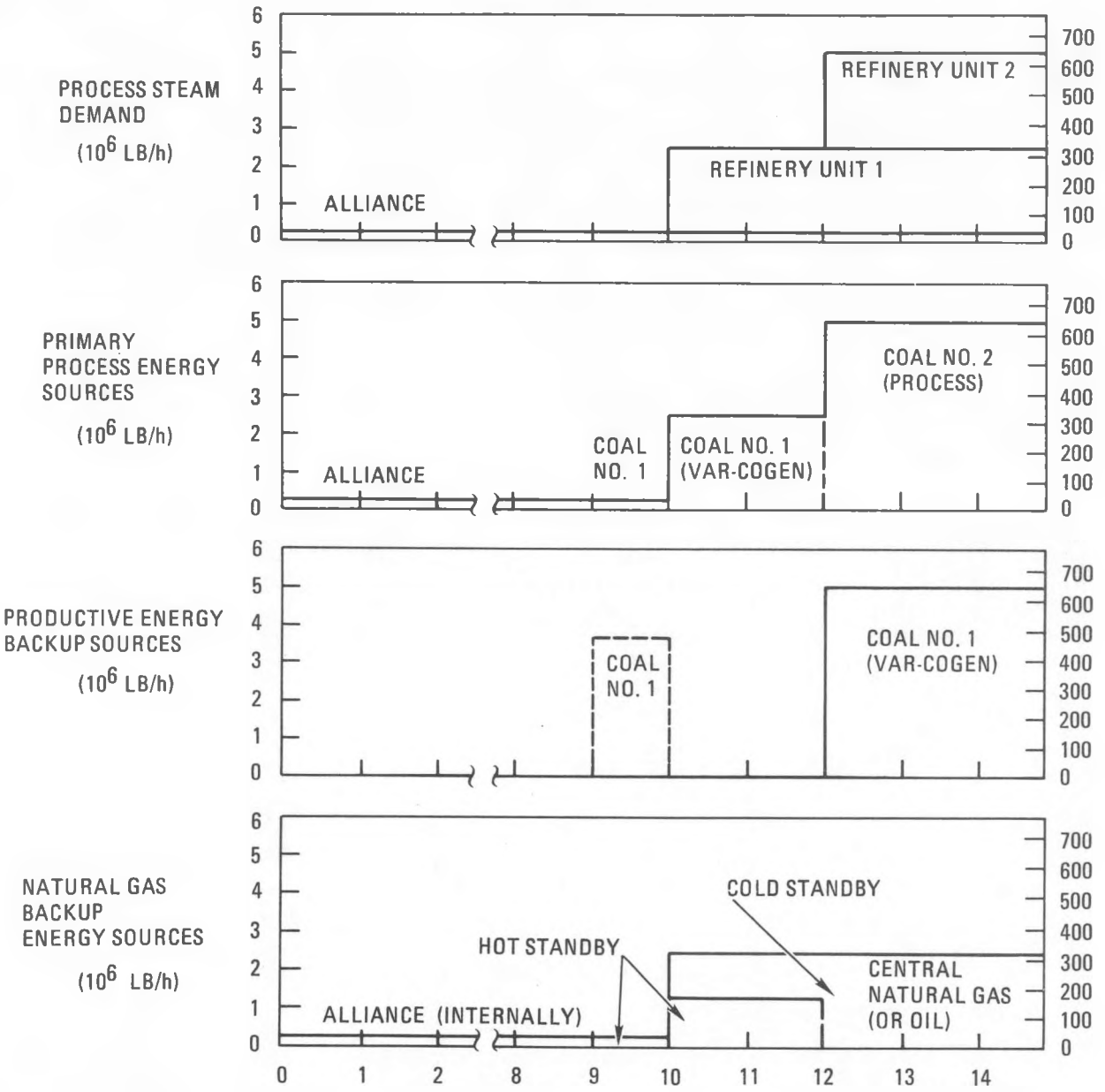

Fig. 6.3-8. Alliance/St. Rosalie application, energy demand versus coal

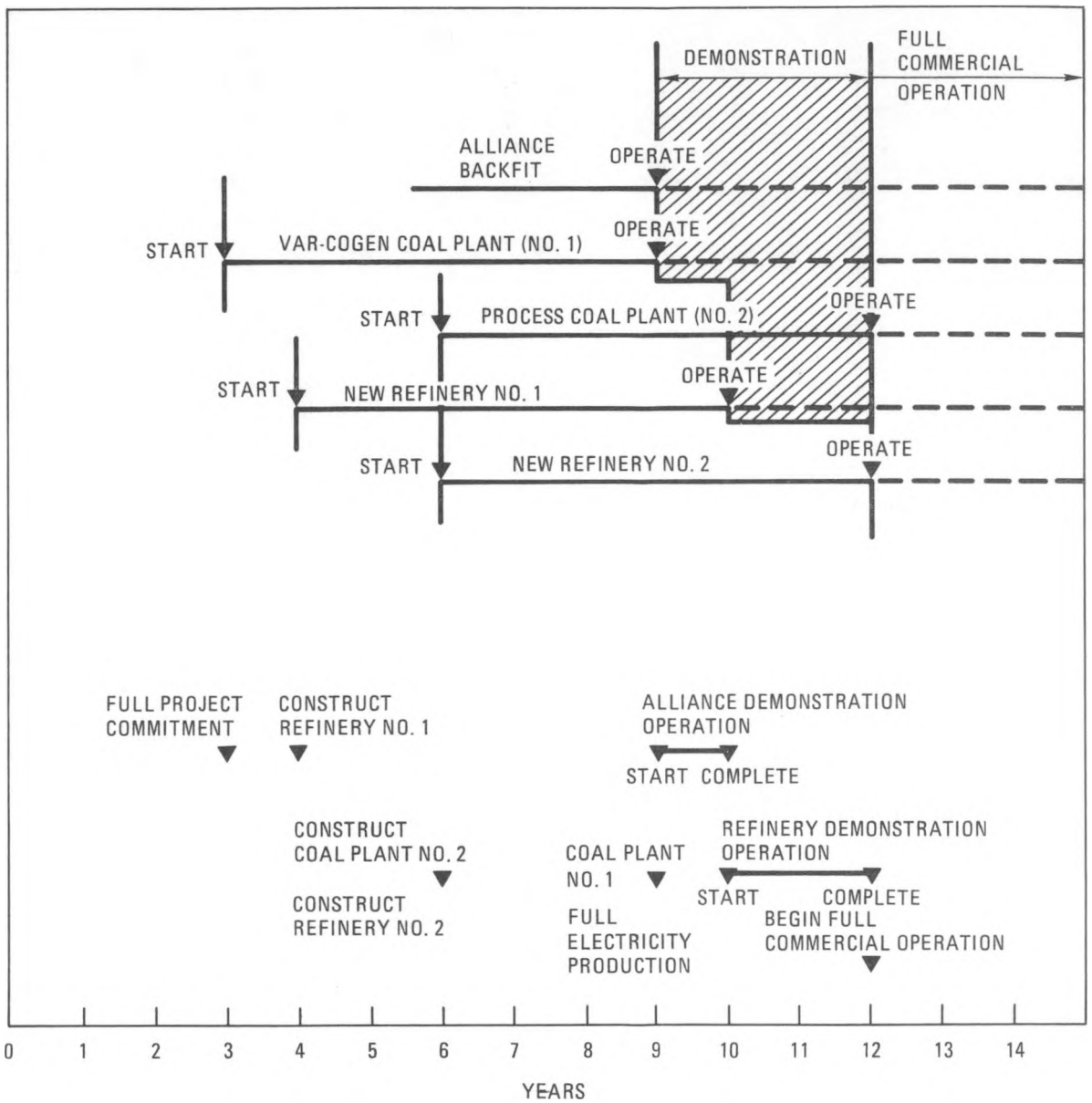

Fig. 6.3-9. Alliance/St. Rosalie application, coal-fired project construction schedule

TABLE 6.3-2
ECONOMIC ANALYSIS OF HTGR AND COAL PLANTS FOR ALLIANCE/ST. ROSALIE

Cost Categories	HTGR - 2240 MW(t)		Coal	
	Lead	Equivalent	Cogeneration [4 x 655 MW(t)]	Cogeneration [4 x 655 MW(t)]
Construction, manufacturing, and owners' costs, 1982 M$	1216	1001	863	863
Project indirect costs, 1982 M$	292(a)	220	177	177
Total capital costs, 1982 M$	1508	1221	1040	1040
Electric rating, MW(e)(b)	820	820	846	846
Construction period to commercial operation (months)	87	72	48	48
AFUDC	235	158	90	90
Total installed cost, 1982 M$	1743	1379	1130	1130
Annual revenue requirements, 1982 M$(c)				
Fixed	108	86	75	75
Fuel	71	89	179	202
O&M	31	33	46	48
Electric power credit	(187)	(59)	(220)	(71)
Total, 1982 M$	23	149	80	254
Annual process steam production, 10^6 GJ (10^6 Btu)	--	49.9 (47.3)	--	53.0 (50.26)
Process steam cost, $/GJ ($/MBTU)	3.45 (3.64)		6.30 (6.65)	

(a) Assumes $100 M support.

(b) Assumes the first cogeneration plant operated in all-electric mode. The second plant normally would generate 630 kg/s (5 x 10^6 lb/hr) of process steam and approximately 231 MW(e) (HTGR)/257 MW(e) (coal) electric power.

(c) Assumes COGENCO loan guarantee for debt (75%).

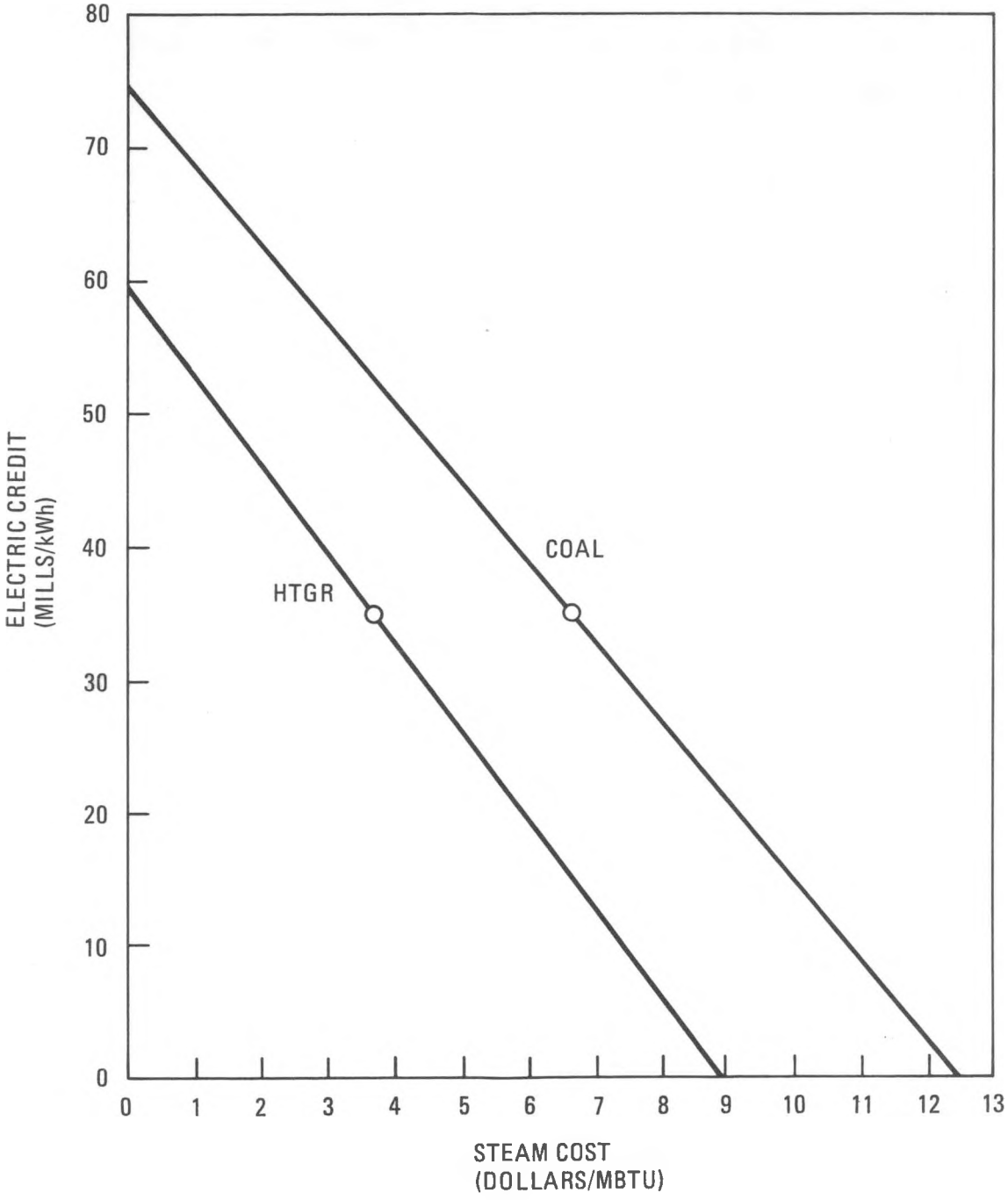

Fig. 6.3-10. Steam cost versus electric credit for Alliance refinery (1/1982 dollars, 1995/1997 delivery, 30-yr levelized)

electric credit increases in value, the steam cost is considerably lowered and vice-versa.

The key assumptions and ground rules used in the economic study may be summarized as follows:

1. The economic analysis was patterned after the UE&C economic analysis performed for the Port Arthur refinery (Ref. 6.3-1).

2. The capital costs of HTGR and coal plants were derived from UE&C's capital cost data prepared for the Port Arthur refinery (Ref. 6.3-1).

3. The financial assumptions for HTGR and coal plants were based on a COGENCO arrangement with a loan guarantee (COGENCO is a limited partnership that would construct, own, and operate the lead HTGR-SC/C plant; COGENCO would finance the lead plant with 25% equity and 75% debt).

4. The 30-yr levelized fuel cycle cost for the lead HTGR plant is $1.43/GJ ($1.51/MBTU) for 1995 startup and $1.47/GJ ($1.55/MBTU) for the equilibrium HTGR plant with 1997 startup. The corresponding coal fuel costs are $2.70/GJ ($2.85/MBTU) and $2.86/GJ ($3.02/MBTU), respectively.

5. The revenue requirement method was used to perform the economic analysis.

6. Other economic assumptions/ground rules employed in this study are shown in Table 6.3-3.

TABLE 6.3-3
ECONOMIC GROUND RULES

Unit Indirect Rates (%)

General Factors	Fossil Plant		Nuclear Plant	
	Single Unit	Twin Unit	Single Unit	Twin Unit
Construction services and field engineering[a]	20	15	25	20
Engineering and home office services and fees[b]	12	9	15	12
Contingency[c]	10	10	10	10
Owners' cost[d]	5	3	5	3

Fuel/Energy Cost Projections
(January 1982 $)

No. 6 fuel oil = natural gas ($/MBtu)	9.00
Coal ($/MBtu)	2.50
Uranium ($/lb)	40
Conversion ($/lb)	3
Separative work at 0.2% tails ($/separative work unit)	140
Electricity busbar sales value (mills/kWh)	35
Electricity replacement power cost (mills/kWh)	55

Fuel Energy Escalation Parameters
(Post-1995 real escalation rates, %)

	Constant Dollars	Inflated Dollars
Uranium	2.5	10.7
Coal	1.0	9.1
Gas and oil	2.0	10.2
Electric power	0.5	8.5
Labor, materials, construction, conversion, separative work units	0.0	8.0

Specific Plant Information

Plant Operation and Maintenance Costs (1982 $)

	Fixed (10^6 $/yr)	Variable [mills/kW(t)-h]
HTGR-SC/E	15.0	0.6
HTGR-SC/C	15.3	1.10
HTGR-SETS (draw salt)	15.5	0.65
HTGR-PH	15.3	0.65

TABLE 6.3-3 (Continued)

	Fixed (10^6 $/yr)	Variable [mills/kW(t)-h]
HTGR-TCP	(As-calculated increases for reformer plant pipeline and methanators)	
Modular	TBD	TBD
LWR	15.0	0.75
Coal electric	14.0	1.20
Coal cogeneration	14.3	1.70

Multiple Unit Fixed O&M Factors

Units on Site	Factor
1	1.0
2	1.75
3	2.50

Plant Schedules

	Time, Design to Operation (yr)	Time, Construction Period to Operation (yr)	Centroid of Expenditures as % of Construction Period
HTGR	10	6	50
LWR	10	6	50
Coal	8	4	50
Oil/gas	4	2	50

Fossil Boiler Efficiencies on High Heating Value of Fuel (all sizes)

Coal	
Standard	88%
Fluidized bed	86%
Oil	82%
Gas	82%

(a) On total direct costs.

(b) On total direct costs, construction services, and field engineering.

(c) On total field costs and home office engineering and fees.

(d) On total base costs and contingency.

Reference

6.3-1. "Feasibility of the High Temperature Gas-Cooled Reactor for Cogeneration of Process Steam and Electric Power for a Large Oil Refinery," DOE Report DOE/ET/34222-1, United Engineers & Constructors, Inc., July 1981.

6.4. AVAILABILITY COMPARISON STUDY (6003050200)

6.4.1. Scope

The work scope of this task was to (1) develop plant availability methodology, (2) evaluate the monolithic SC/C NHS availability, and (3) coordinate with GE and Bechtel and review the BOP designs to verify availability differences between the HTGR-MRS and monolithic plants.

6.4.2. Discussion

Information on this topic is discussed in Section 3.2 of this report, which was also completed under tasks 6053010100 and 6053010101.

6.5. SITE SPECIFIC STUDIES FOR HEAVY OIL RECOVERY (6003050300)

6.5.1. Scope

The scope of this task included studies to do the following:

1. Identify a large heavy oil field suitable for HTGR application to the steam flooding process for heavy oil recovery; collect geographical, reservoir, and recovery data; and establish energy requirements and steam parameters.

2. Perform preliminary assessment of seismic conditions, population density, water clean-up, and reboiler requirements.

6.5.2. Discussion

The site-specific heavy oil recovery study with an HTGR-SC/C plant included the following considerations:

1. The specific site should be amenable to the steam flooding process for heavy oil recovery, requiring steam pressures ≤17 MPa (2500 psia), which is the design limit of a standard HTGR plant.

2. The recoverable resource should justify the use of one or several HTGR-SC/C plants for supplying process steam and electric power for about 30 to 40 yr. The commercial operation of the HTGR-SC/C plant is assumed to start in 1995.

3. A reasonably acceptable site for locating the HTGR-SC/C plant should be available near the oil field. Such primary considerations as population density around the proposed HTGR site and proximity of other industries should be included in the preliminary HTGR site assessment.

4. Information should be obtained for assessing an HTGR-SC/C heavy oil process plant. This information, pertaining to the specific site, should include area field maps, geological maps, oil in place, reservoir characteristics, and major operators in the oil field (if the field is currently in operation); source, availability, and chemistry of water; the present method of steam generation; and environmental constraints.

5. Operating parameters for the specific heavy oil field, such as oil/steam ratio, steam injecton pressure and quality, rate of oil recovery, and process steam and electric power requirements should be procurable.

Application of the above guidelines qualified the Midway-Sunset heavy oil field of California (see Fig. 6.5-1) as a candidate site for a site-specific study for an HTGR-SC/C plant. The Midway-Sunset field, covering approximately 195 km^2 (75 mi^2) [(5 km x 40 km) (3 mi x 25 mi)], is in the southwest end of the San Joaquin Valley, Kern County, California. It is a proven heavy oil field, and the crude production is primarily through steam flooding. A description of the Midway-Sunset heavy oil field with geographical and geological maps is given in Ref. 6.5-1. The nearest city to the oil field is the city of Taft, which is located approximately 8 km (5 mi) from the Midway-Sunset oil field. The current population of Taft is estimated at <20,000.

The current oil recovery from the total field is about 0.21 m^3/s (113,000 bpd) and it is estimated to reach a rate of 0.22 m^3/s to 0.24 m^3/s (120,000 bpd to 130,000 bpd) in 1990. The major producers in the Midway-Sunset field are Santa Fe Energy Company, Shell Oil Company (U.S.), Standard Oil (California), and Mobil. The heavy oil in place is estimated at two to three billion barrels, which is locked up in several vertical zones. The present production is from two selected zones (Monarch and Potter), and as of December 1980 the recoverable crude from these two zones was estimated in excess of 600 million barrels. The steam pressure at the well injection head varies from reservoir to reservoir and averages ~3.50 MPa (500 psia).

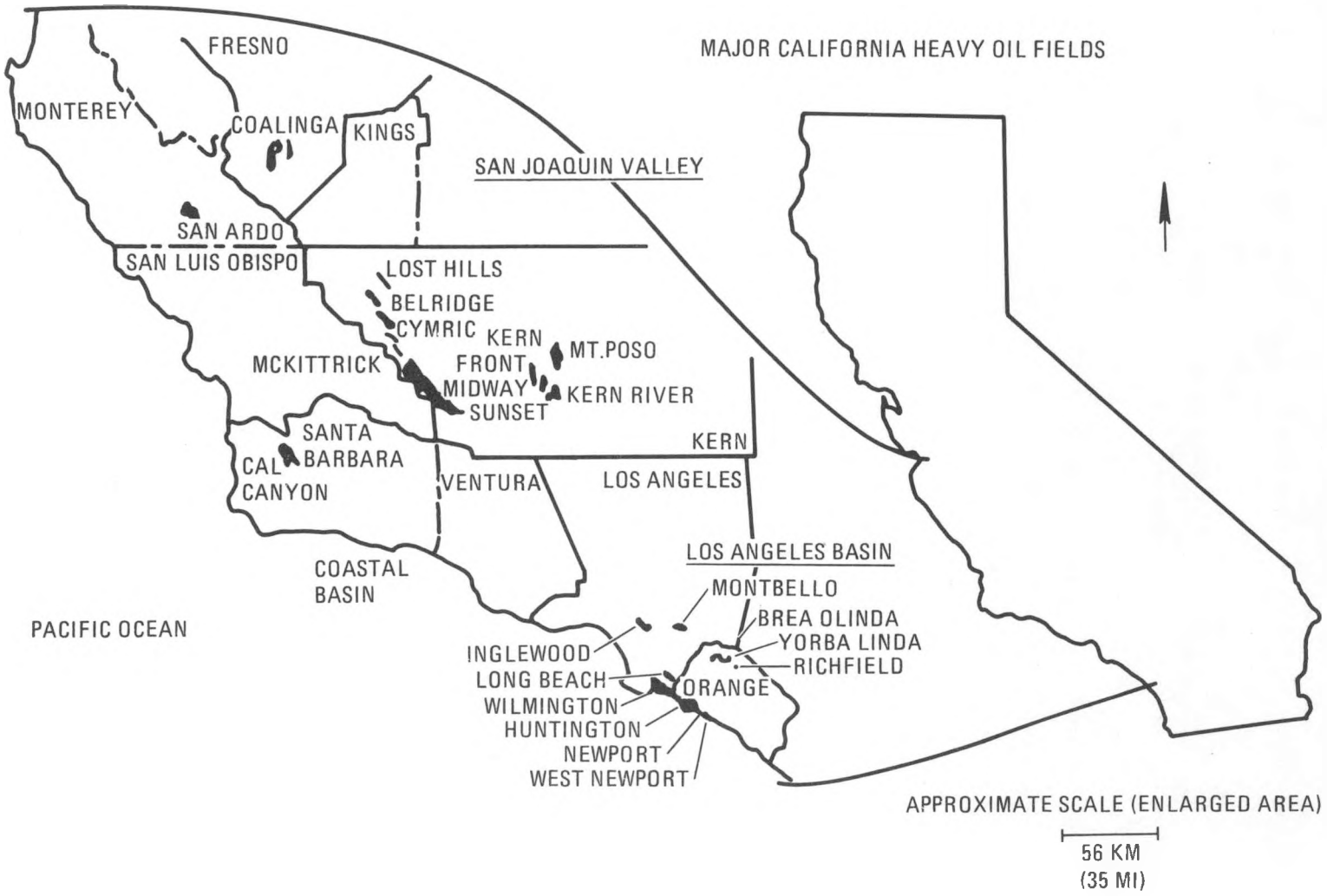

Fig. 6.5-1. Locations of the principal heavy oil fields in California

Steam is generated by oil-burning field boilers, and produced waters are used as feedwater after a nominal treatment. The steam is generated at about 70% quality to hold the dissolved solids in solution.

6.5.2.1. HTGR-SC/C Applicability Potential. Based on the projected heavy crude recovery rate at Midway-Sunset, using the conventional method, a recoverable crude will still be available that is sufficient to justify the process steam supply from one or two 2240-MW(t) HTGR-SC/C plants in 1995. Approximately one-third of the produced crude is burned as fuel in the field boilers for steam generation. Coal is not used by the producers as a source of energy in the California heavy oil fields because it would need to be imported from outside California (e.g., from New Mexico or Wyoming), and the cost of transportation is as high as the mining cost. In addition, the storage and burning of coal are a major environmental concern in the oil fields. Presently, the Midway-Sunset field is declared a non-attainment area, meaning that no new field boilers can be added without offsetting emissions from other operating boilers that are not equipped with the best available control technology (BACT). Thus, the HTGR plant is an excellent fit for heavy oil recovery operation on the basis of environmental advantage.

6.5.2.2. Cost/Economic Analysis. A preliminary cost/economic analysis was performed to estimate the cost of steam using three energy sources, namely, oil, coal, and the HTGR, for the heavy oil recovery operations in the Midway-Sunset field. Table 6.5-1 shows the results of the comparative economic study. The HTGR-SC/C plant has the lowest steam cost and has a substantial economic advantage over coal and oil. A preliminary cost study also indicated that the steam cost is the major portion of the cost of producing a barrel of heavy crude and constitutes approximately 50% to 60% of the cost of a barrel of heavy crude. Figure 6.5-2 shows steam cost as a function of credit for cogenerated electric power. Since a 2240-MW(t) HTGR-SC/C plant cogenerates substantial electric power [186 MW(e)], revenues accrued from electric power sale considerably decrease the steam cost (see Table 6.5-1).

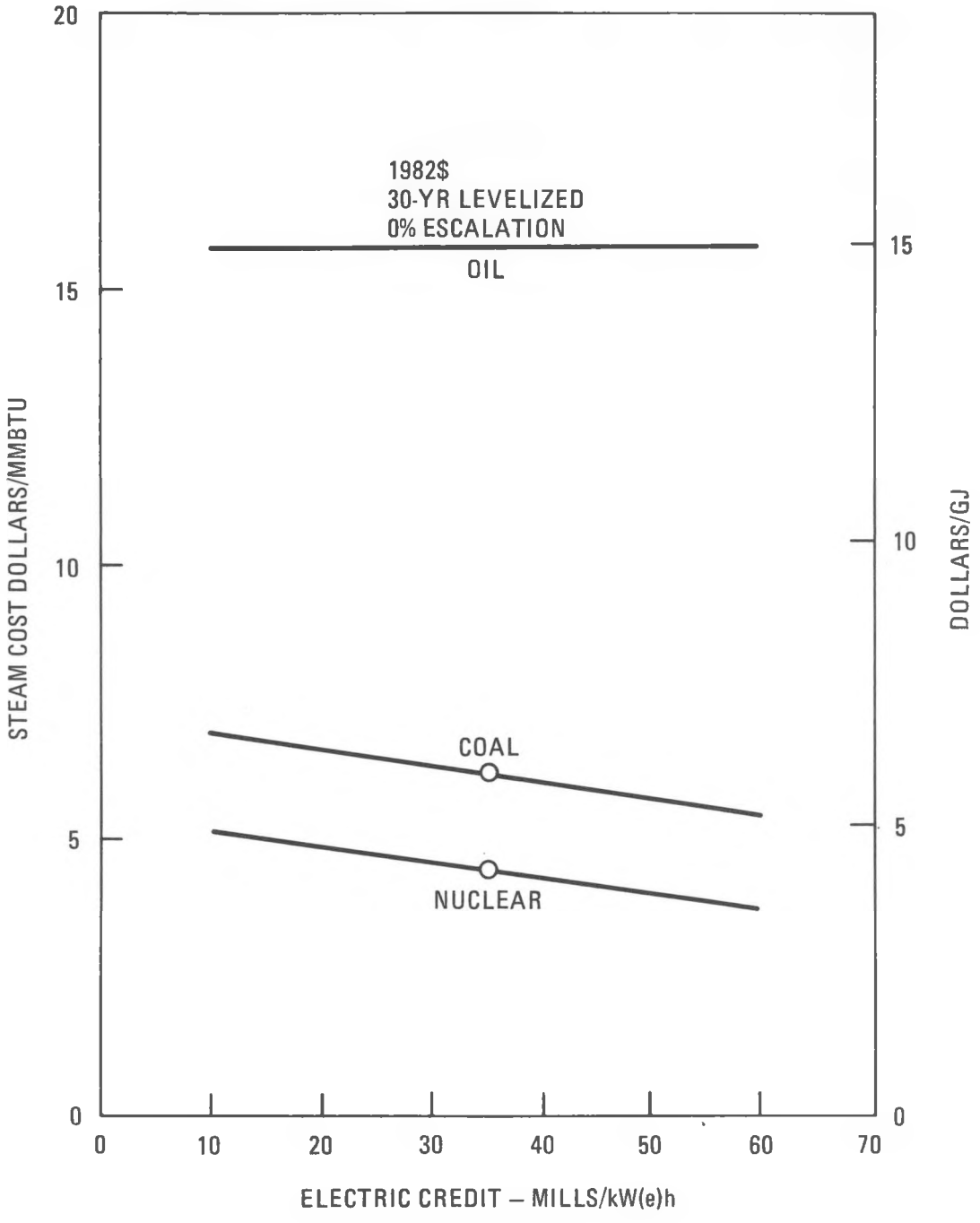

Fig. 6.5-2. Heavy oil recovery steam cost and electric power credit

TABLE 6.5-1
STEAM COST COMPARISON - HEAVY OIL RECOVERY

	HTGR Lead Plant[a]	Central Coal[a]	Field Boiler
Size	1 x 2240 MW(t)	4 x 655 MW(t)	127 x 50 MM Btu/hr
Fuel	LEU/Th once through	New Mexico coal	Lease crude
Energy to process (steam)	1852	1852	1860
Net electric product MW(e)	186	212	0
Availability			
Steam, %	75	85	90
Electricity, %	70	80	--
Total capital cost	1752	1307	--
AFUDC	246	102	--
Total installed cost, 1982 MM$	1998	1409	122
Annual revenue required, 1982 MM$/yr			
Fixed	134	93	8
Fuel	76	217	689
O&M	32	48	89
Electric power credit	(43)	(55)	0
Total	199	303	786
Steam cost, $/GJ in 1982 $ ($MMBtu in 1982 $)	4.54 (4.79)	6.10 (6.44)	14.90 (15.72)
Ratio: fossil/nuclear	1.0	1.34	3.28
Utility financing			
0% Escalation			

[a] Includes reboilers.

6.5.2.3. Special Considerations. A major consideration in siting an HTGR plant in the Midway-Sunset field is the seismic requirements. A preliminary investigation showed that seismic values of 0.25 g for the operating (OBE) condition and 0.5 g for the safe shutdown (SSE) condition may be required for siting a nuclear plant in the Midway-Sunset field. Therefore, the field may not qualify as a potential site for a lead HTGR-SC/C plant that has design seismic values of 0.15 g and 0.30 g for operating and safe shutdown conditions, respectively. However, with appropriate seismic provisions made in the HTGR-SC/C plant design, it can be sited in the Midway-Sunset field.

Reference

6.5-1. "Review of Midway-Sunset Field Oil Production," Case Engineering, Ventura, July 1982.

6.6. HTGR APPLICATION STUDIES (6003030001)

6.6.1. Scope

The work scope of this task was to (1) complete a study to extend the capabilities of the HTGR application to the SRC-II coal liquefaction process and (2) to review the German (BF) steam carbon process.

6.6.2. Discussion

6.6.2.1. Integration of an HTGR into an SRC-II Refinery. During this reporting period the report "Integration of an HTGR into an SRC-II Refinery" (Ref. 6.6-1) was completed and issued. The report presents in summary the results of work performed by GA together with that performed by Scientific Design, Inc., under subcontract to GA during 1980 to 1982. The work was to study the use of nuclear energy as the primary heat source in place of fossil energy consumed within a coal liquefaction process plant.

In these studies, the SRC-II coal liquefaction process was modified by the addition of an upgrading plant and flexicoking features to produce transportation fuels from the normal SRC-II product. This integrated plant is identified as a coal refinery because its products are analogous to those produced by an oil refinery. The products obtained from the plant are motor gasoline, jet fuel, liquefied petroleum gas (LPG), butanes, substitute natural gas, and in one case synthesis gas. By-products from the refinery are sulphur and ammonia.

The coal refinery requires considerable steam and electric power, consistent with that offered by the high-temperature gas-cooled reactor (HTGR). Descriptions of HTGR nuclear heat source options are presented. They include the sensible energy transmission and storage HTGR (HTGR-SETS), the steam cycle/cogeneration HTGR (HTGR-SC/C), and the process heat HTGR-PH concepts.

The process plant costs and economics were developed for the coal-fired, the HTGR-SC/C, and the HTGR-PH cases. Two cases were presented to provide the required steam for the process, one using a single 2240-MW(t) HTGR-SC/C, the other using two 1170MW(t) HTGR-SC/C's. The HTGR-PH heat source consisted of three 1170-MW(t) units.

Study Results

These studies showed that nuclear energy can replace essentially all of the fossil energy used in a representative coal liquefaction process plant, increasing the yield of the process plant by the amount of oil equivalent to the nuclear reactor used.

Based on a constant coal refinery feed of 352 kg/s (33,500 TSD), with the HTGR-SC/C the refinery product is increased by 8% and with the HTGR-PH by 13% above the conventional coal-fed process used in the studies. Product cost using the HTGR-SC/Ç is ~14% lower than for the coal process, while the HTGR-PH products costs are ~5% higher.

If coal prices reach $4.20/GJ ($4.34/10^6 BTu) or above, the HTGR-PH is shown to be a more economic energy source than coal.

It is also shown that the capital cost for the HTGR-SC/C integrated into the process system is ~15% higher than for the standard coal system studied. The HTGR-PH integrated capital cost is shown to be ~10% higher than for the coal system.

The use of an HTGR as a heat source increases the product per unit of coal consumed by 29% and extends the available coal resource significantly. In addition, because fossil fuels are reduced or eliminated, the release of carbon dioxide to the environment is reduced by a factor of 5; nitrogen oxides, carbon monoxide, and nonmethane hydrocarbons are almost completely eliminated; sulfur dioxide is reduced by 21%, and total suspended particulates by 36%.

Under the ground rules chosen for these studies, HTGR sizes of 1170 MW(t) and 2240 MW(t) were used. The reactor heat not needed for the process was used to produce electricity in the steam cycle cases. The production of by-product electricity accounted for 23% to 28% of the reactor power.

The economic ground rules were such that in the HTGR-PH case the price obtained for the by-product electricity was insufficient to pay for the added investment required to produce the by-product electricity. In the case of multiple reactor installations, however, better back-up energy for the refinery is obtained.

Because of the lack of current data on the potential advantages of improved availability using multiple HTGR-SC/C and HTGR-PH heat sources, it is recommended that additional studies be made in this area. It is also recommended that the HTGR-SETS plant concept with heat storage be included in these availability studies. In addition, it is proposed that studies be performed to consider changes in the process to reduce the capital cost and improve the economics of the refinery when integrated with an HTGR-PH plant. Summary comparison nuclear and non-nuclear data and an economic comparison of the three process cases (coal, HTGR-SC/C, and HTGR-PH) are shown in Tables 6.6-1 and 6.6.2, respectively.

6.6.2.2. Performance and Cost Comparison between the Bergbau-Forschung and the Exxon Catalytic Coal Gasification Processes, Using Nuclear Process Heat.

Depending on the subsequent treatment of the raw product gas, the final product of the Bergbau-Forschung (BF) coal gasification process is either synthetic natural gas (SNG), consisting almost exclusively of methane, or synthesis gas. For the Exxon catalytic coal gasification (ECCG) process, the final product is SNG. To gain some additional background information and also for comparison, several conventional coal gasification processes were briefly investigated. However, emphasis was on the final comparison between the process conditions, yields, and costs of the BF process (with catalyst) and the ECCG process. In both processes, the coal gasification reaction between the coal and steam takes place in a pressurized fluidized bed with a mixture of potassium salts acting as the catalyst.

TABLE 6.6-1
SUMMARY COMPARISON OF NUCLEAR AND NONNUCLEAR DATA

	Conventional	HTGR-SC/C	HTGR-PH
Process yields			
Feedstock coal	33,500	33,500	33,500
Fuel coal, tons/day	4,700	--	--
HTGR energy, MW(t)	--	1,800	2,530
Products, bbl/day			
Transportation fuels	75,750	75,750	96,910
Light ends	33,750	42,810	27,000
Total	109,500	118,560	123,910
Thermal efficiency, %	65	69	68
Product/feed, bbl/ton	2.9	3.5	3.7
Systems and costs			
Reactors installed	--	2 x 1170	3 x 1170
By-product electricity, MW(e)	0	161	381
Plant installed cost, 10^6(a)	2,550	3,227	5,794
Product cost, $/10^6$ Btu(b)	8.68	7.82	9.10
Product cost, $/barrel	50.34	45.36	52.78
Environmental impact			
CO_2 release, 10^6 tons/yr	9.8	6.4	1.8
NO_x, hydrocarbons, tons/yr	4.5	0	0
SO_x, tons/yr	2,290	1,900	1,810
Total suspended solids, ton/yr	1,060	790	680

(a) 1980 $ without escalation or AFUDC.

(b) No inflation, coal 1.88 $/GJ ($1.98/MMBtu), electric power credit 34 mills/ kWh.

TABLE 6.6-2
ECONOMIC COMPARISON OF THREE PROCESS CASES
(1995 PROJECTIONS, INDUSTRIAL OWNERSHIP)
(10^6 Dollars, January 1980)

	Coal	HTGR-SC/C 1-2240 MW	HTGR-SC/C 2-1170 MW	HTGR-PH 3-1170 MW
Coal feedstock [GW (109 Btu/stream hr)]	35.9	35.9	35.9	35.9
Coal fuel	5.0	--	--	--
Nuclear fuel to process	--	1800	1800	2531
(total installation), MW	--	(2240)	(2340)	(3510)
Process output	7.8	8.3	8.4	8.8
[GW (109 Btu/stream hr)]	(26.6)	(28.8)	(28.8)	(30.1)
By-product electricity, MW(e)	--	151	161	381
Stream factor	0.7	0.7	0.7	0.7
Capital cost (Base (1/80$)				
Energy plant	381	773	1075	2644
Process	2169	2152	2152	2650
Subtotal	2550	2925	3227	5794
ESC and IDC				
Energy plant	104	256	356	875
Process	593	607	607	747
Total	3247	3788	4190	7416
Annual cost				
Fixed	422	492	545	899
Energy plant fuel	85	41	44	67
Process feed	611	611	611	611
Energy plant O&M	205	33	47	59
Process O&M		189	190	176
Power purchased (credit)	--	(53)	(56)	(132)
Total	1323	1313	1381	1680
Product cost				
$/GJ	8.23	7.00	7.42	8.63
($/$10^6$ Btu)	(8.68)	(7.44)	(7.82)	(9.10)
($/bbl)[a]	(50.34)	(43.15)	(45.36)	(52.78)

[a] 1 bbl = 5.8 x 10^6 Btu
= 6.114 GJ.

There are two reasons that somewhat restrain a completely unbiased comparison betwen the two coal gasification processes. On the process side, there is a considerable difference in the analysis of the two coal feeds (Table 6.6-3). This not only affects the yield but also the gas treatment requirements. With regard to cost, there are variations in exchange rates. More importantly, because of differences in material and labor charges between the two countries, there may be considerable discrepancies in the cost of similar process equipment.

Before discussing the results of the comparison study, a brief summary of the two coal gasification processes is presented.

Bergbau-Forschung (BF) Process

The heart of BF's gasification process is the allotherm gas generator. In this horizontal pressure vessel, a fluidized bed is maintained along the vessel's horizontal axis by the injected process steam. Coal is fed at one end of the vessel and moves slowly as slug flow along the horizontal axis. The remaining ash is discharged at the other end. The raw product gas exits through a nozzle atop the vessel and is passed on for further processing, e.g., methanation to product SNG. Besides the process steam, hot secondary helium flowing through vertically inserted heat exchangers supplies additional process heat to the fluidized bed. The operating conditions are about 4 MPa (580 psia) and 810°C (1490°F) without catalyst and 754°C (1390°F) with catalyst.

Exxon Catalytic Coal Gasification (ECCG) Process

The ECCG gasification reactor is a vertical pressure vessel operating at 3.4 MPa (500 psia) and 690°C (1275°F). The fluidized bed is 6.7 m (22 ft) in diameter and 29.5 m (97 ft) high. The catalyzed coal feed preheated to 121°C (250°F) enters at the bottom head. The coal mixes and begins to react with the incoming 839°C (1543°F) steam and recycle gas stream. All reactions occur in the gasifier: steam gasification, water-gas shift, and methanation; the overall reaction within the gasifier is essentially

TABLE 6.6-3
COAL ANALYSIS
(Weight %)

	Germany, Westerholt		U.S.A., Illinois No. 6	
	As Received	Dry[a]	As Received	Dry[b]
C	78.01	79.1	59.81	69.67
H	4.99	5.06	4.33	5.05
N	1.30	1.32	1.58	1.84
S	1.23	1.25	3.60	4.19
Cl	0.17	0.17	0.07	0.08
O	8.09	8.2	8.11	9.45
Water	1.38	1.4	14.16	16.5
Ash	4.83	4.9	8.34	9.72
HHV[c]	13,880	14,070	10,930	12,730

[a] Reference 6.6-2, page 224.
[b] Reference 6.6-3, page 126.
[c] Higher heating value in Btu/lb.

thermoneutral. The raw product gas discharges through the top head and passes on to gas treatment facilities for ammonia and sulfur recovery. Ash buildup is regulated by controlled char solids discharge at the bottom head.

Comparison

Analyses of German Westerholt coal and U.S. Illinois No. 6 coal are shown in Table 6.6-3. The difference between the two, especially of the quality shown in the "As Received" column, is striking; data in this column are used in quantitative process calculations.

The carbon content of the Westerholt coal is about 30% higher than in the Ilinois No. 6 coal. The latter shows very high water, ash, and sulfur content.

Technical data from different coal gasification processes are summarized in Table 6.6-4. The data, taken from various references cited, were converted to U.S. customary system units where necessary. Besides the German and U.S. nuclear process heat applications, PNP and HTGR-PH, several conventional processes are also shown.

Part of the explanation for the apparent superior performance of the PNP application, when compared with the U.S. process, may lie in the difference in their coal feed compositions. The high water and ash content of the U.S. coal contributes to higher energy losses. Also, the higher sulfur and nitrogen content requires considerable extra energy for the sulfur and ammonia recovery. A probably better comparison between the German (BF) and U.S. (ECCG) nuclear process heat applications is made in Table 6.6-5.

In Table 6.6-5, the German and U.S. coal gasification processes using nuclear process heat are compared. The German BF process cases are shown with and without catalyst. The U.S. ECCG process uses a catalyst. On the basis of available literature, it appears tht the BF process consumes about

TABLE 6.6-4
PERFORMANCE COMPARISON OF COAL GASIFICATION PROCESSES[a]

	PNP 3000 Without Catalyst	PNP 3000 With Catalyst	Autotherm Lurgi	Industry Analage Ruhr	ECCG With Catalyst	ECCG With HTGR-PH 2340
Technical data						
Thermal rating, MW(t)	3000	3000	--	--	--	2340
Stream time, hr/yr	7500	7500	7500	7500	7884	7884
Thermal output, 10^{12} Btu/yr	76.8	76.8	--	--	--	63.0
Coal feed						
10^6 tons/yr	2.98	4.92	4.92[b]	4.01[b]	5.93[c]	4.76
10^{12} Btu/yr	82.7	136.6	136.6	111.3	129.6	104.1
Carbon conversion, %	95	95	~100	~100	90	90
Process energy						
MW(t)	1359	1467	2407	2395	1444	1446
10^{12} Btu/yr	34.8	37.5	61.6	61.3	38.9	38.9
Gas production						
10^9 SCF/yr	83.6	138.1	83.6	56.0	88.5	88.5
10^{12} Btu/yr	83.4	137.7	75.0	50.0	89.3	89.3
Electric power surplus, MW(e)	640[d]	598[d]	--	--	147[e]	330[d]
Heat ratios						
Btu process energy/lb carbon reacted	7879	5142	8447	10,314	7591	7591
Btu product gas/lb carbon reacted	18,880	18,883	10,285	8,413	17,426	17,426
Btu product gas/Btu process energy	2.40	3.67	1.22	0.82	2.30	2.30
Btu product gas/Btu thermal output (of HTGR)	1.09	1.79	--	--	--	1.42
Btu product gas/Btu (coal feed and process energy)	0.710	0.790	0.549	0.449	0.530	0.624
Btu product gas/Btu coal feed	1.01	1.01	0.549	0.449	0.689	0.858
Surplus electric power, MW(t)/ thermal rating	0.547	0.511	--	--	--	0.382

[a] Data base: Columns 1 through 4: Ref. 6.6-4, Appendix 3. Column 5: Ref. 6.6.3, pages 126, 133, and 151. Column 6: Ref. 6.6-5, Table 4-14.

[b] Quantity shown is probably gross coal feed, i.e., additional coal is included to cover all process energy requirements.

[c] Includes 1.17 x 10^6 tons/yr to cover off-site boiler and coal drying requirements.

[d] A nuclear power plant efficiency of n = 0.39 is assumed.

[e] A fossil power plant efficiency of y = 0.32 is assumed.

TABLE 6.6-5
PERFORMANCE COMPARISON OF NUCLEAR COAL GASIFICATION PROCESSES
(Normalized to U.S. Conditions)

	PNP 3000 Without Catalyst	PNP 3000 With Catalyst	ECCG With Catalyst 2340 HTGR-PH
Technical data			
Thermal rating, MW(t)	3000	3000	2340
Thermal output, 10^{12} Btu/yr	80.7	80.7	63.0
Coal feed			
10^6 tons/yr	3.13	5.17	4.76
10^{12} Btu/yr	68.4	113.0	104.1
Carbon conversion, %	95	95	90
Process energy			
MW(t)	1359	1467	1446
10^{12} Btu/yr	36.6	39.5	38.9
Gas production			
10^9 SCF/yr	67.4	111.3	88.5
10^{12} Btu/yr	67.2	111.0	89.3
Electric power surplus, MW(e)	640	598	330
Heat ratios			
Btu process energy/lb carbon reacted	10,290	6,723	7,591
Btu product gas/lb carbon reacted	18,893	18,893	17,426
Btu product gas/Btu process energy	1.84	2.81	2.30
Btu product gas/Btu thermal output	0.833	1.38	1.42
Btu product gas/Btu (coal feed and process energy)	0.640	0.728	0.624
Btu product gas/Btu coal feed	0.982	0.982	0.858
Surplus electric power [MW(t)] thermal rating	0.547	0.511	0.382

NOTES: 1. Streamtime = 7,884 hr/yr.
2. Coal feed = Illinois No. 6.

twice as much catalyst as the ECCG process; i.e., about 4.5. wt % versus 2.2, respectively.

To obtain a somewhat better comparison between the two coal gasification processes, the available data were normalized to U.S. conditions: A stream time of 7884 hr per year (90% load factor) was assumed and Illinois No. 6 coal was used as the process feed. With the introduction of Ilinois No. 6 coal as the BF process feed, BF's process energy requirement should have been increased to account for higher energy losses due to its higher water and ash content and also the increased energy need for the sulfur and ammonia recovery. Because these additional energy needs could not be ascertained, the process energy remained unchanged, as did the electric power surplus.

Nevertheless, as seen by the performance parameters (heat ratios), using the same data base (stream time and coal feed) brought the two catalytic coal gasification processes closer together. Yet there seems to be no reasonable explanation for the sudden jump in gas production with the introduction of a catalyst in the BF process, without any appreciable increase in the process energy requirement. The gas production increases 65%, but the process energy by only 7%.

It has been noted in Ref. 6.6-4 that with the addition of a catalyst, the process temperature decreases by about 38°C (100°F). And with this decreasing process temperature, the reaction heat demand is also somewhat lower but not to the extent indicated by BF's data. An interesting side note is that ECCG's process temperature at 690°C (1275°F) is 64°C (115°F) less than BF's process temperature with a catalyst. This indicates that, according to BF's data, the reaction heat requirement for the ECCG process should be less than BF's.

It appears that this sudden jump in BF's gas production with the addition of a catalyst cannot be explained without having access to some of BF's detailed process description and data.

Results of a cost comparison between the coal gasification processes using nuclear process heat (Table 6.6-5) are summarized in Table 6.6-6. The gas treatment facility cost (part of the process plant) for the PNP plant was left unchanged, despite a 20% reduction in the gas production when Illinois No. 6 coal is used. It was reasoned that the cost for increasing the facility for additional sulfur and ammonia recovery will offset this 20% production cut.

With data normalized for U.S. conditions, i.e., 90% load factor and Illinois No. 6 coal, the ECCG process with the HTGR-PH shows a distinct price advantage. However, it is important to recognize that these cost figures are very much subject to capital cost charges and the current exchange rate.

To assess the influence of capital cost and exchange rate on the product gas cost, Fig. 6.6-1 was developed for the PNP 3000 with catalyst plant. With the top abscissa, the total plant cost in deutsche marks can be converted into U.S. dollars by using the appropriate exchange rate. Or, in case an independent cost estimate of German process equipment or of the total plant is made in U.S. dollars, the lower abscissa will give the corresponding product gas cost.

References

6.6-1. Peterman, D. D., "Integration of an HTGR into an SRC-II Refinery," DOE Report GA-A16659, July 1982.

6.6-2. "Wasserdampfvergasung von Kohle," Bericht Zum Abschluss der Reference-phase, Bergbau-Forschung GmbH, et. al., April 1981.

6.6-3. "Exxon Catalytic Coal Gasification Process Development Program, Final Project Report," Report FE-2369-24, Exxon Research and Engineering Company, Baytown, Texas, December 1978.

6.6-4. "Wasserdampvurgasung von Kohle mit Hilfe von Prozesswaerme aus Hochtemperatur-Kernreaktoren," Praesentation der Bergbau-Forschung vor dem Gutachterausschuss des Bundesministenums fuer Forschung und Technologie am 16. September 1981 in Bonn.

TABLE 6.6-6
COST COMPARISON OF NUCLEAR COAL GASIFICATION PROCESSES
(Normalized to U.S. Conditions)

	PNP 3000 Without Catalyst		PNP 3000 With Catalyst		ECCG 2340-HTGR-PH	
	10^6(a)	$/$10^6$ Btu	10^6(a)	$/$10^6$ Btu	10^6(a)	$/$10^6$ Btu
Power plant cost, $	2023 x 10^6		2023 x 10^6		866 x 10^6	
Process plant cost, $	1188 x 10^6		1507 x 10^6		1196 x 10^6	
Total plant cost, $	3211 x 10^6		3530 x 10^6		2062 x 10^6	
Gas production, Btu/yr	67.2 x 10^{12}		111.0 x 10^{12}		89.3 x 10^{12}	
Capital cost charges	482	7.17	530	4.77	309	3.46
Coal cost	75	1.12	124	1.12	114	1.27
Catalyst	--	--	70	0.63	31	0.35
Nuclear fuel cost	64	0.95	64	0.58	52	0.58
O&M	127	1.89	176	1.58	166	1.86
Electric power credit	(202)	(3.01)	(189)	(1.70)	(104)	(1.16)
Total cost	546	8.12	775	6.98	568	6.36

NOTES:

1. Capital cost charges = 15% DCF on total plant cost.
   Note: Exchange rate (1/80): $1.00 = 1.725 deutsche marks.
2. Coal cost = $24/ton.
3. Catalyst cost = $300/ton. USA takes 2.2% of carbon feed; Germany takes 4.5% of carbon feed.
4. Nuclear fuel cost = $0.83/$10^6$ Btu.
5. O&M = $50 x 10^6 for power plant + $24.50/ton coal fuel.
6. Electric power credit = 40 mils/kWh.

(a) Annual cost.

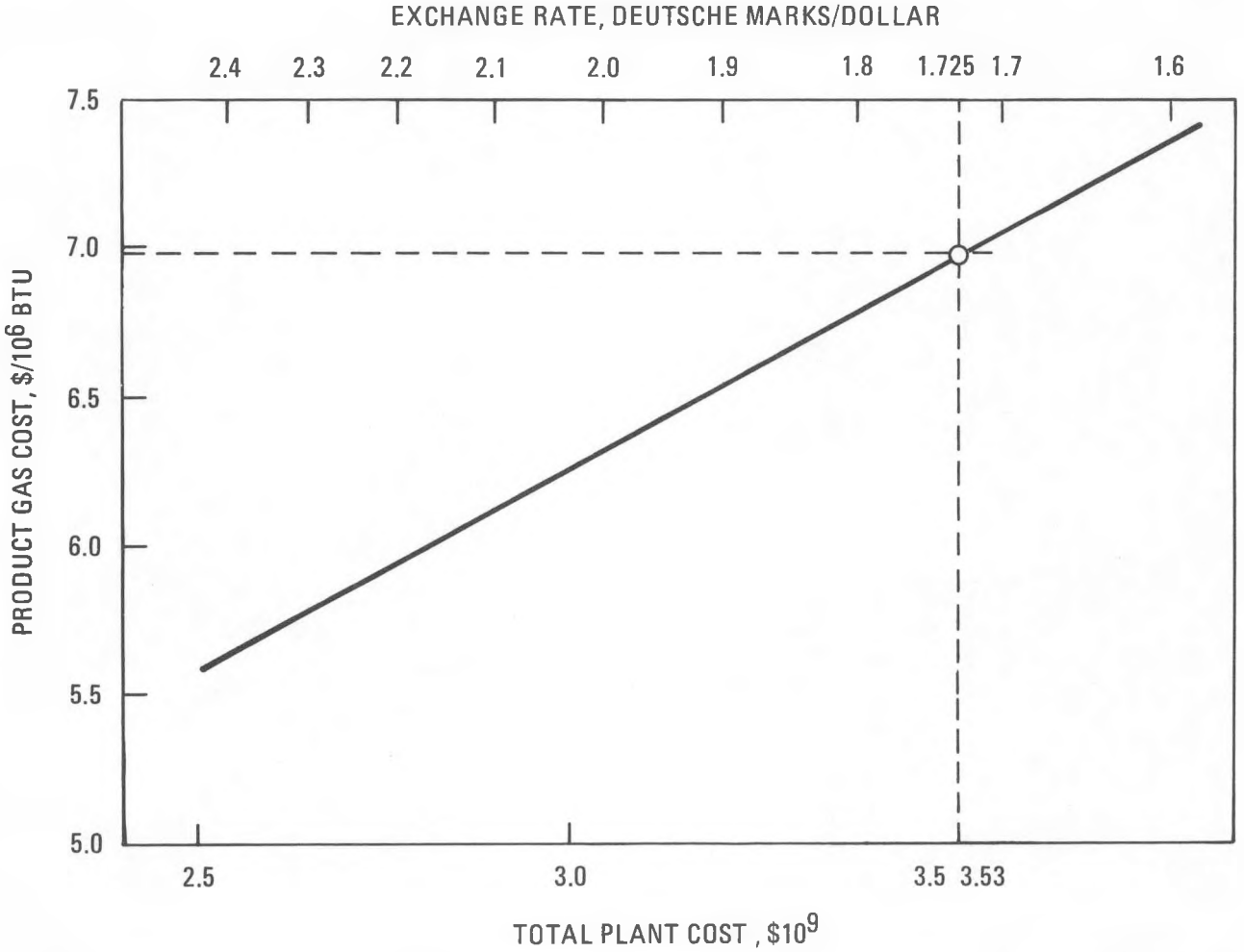

FROM REF. 6.6-4:	POWER PLANT COST	3490 x 10^6 DEUTSCHE MARKS
	PROCESS PLANT COST	2600 x 10^6 DEUTSCHE MARKS
	TOTAL PLANT COST	6090 x 10^6 DEUTSCHE MARKS

Fig. 6.6-1. Product gas cost from PNP 3000 with catalyst plant as a function of total plant cost or exchange rate

6.6-5. "HTGR Application Comparative Assessment Study," G. Hopwood, D. Peterman, R. Quade, R. Rao, B. Sibold and T. Van Hagen, Report GA-A16525, January 1982.

6.7. HTGR-SETS APPLICATIONS STUDY (6051020001 and 6003030001)

6.7.1. Scope

The scope of the work reported here includes the following:

1. To document recommended design changes for improving the cost and performance of long-distance energy transmission pipeline systems developed in FY-81.

2. To prepare plant performance for selected refinery applications.

3. To document appropriate draft input to the HTGR-SETS screening report.

Specific work under this heading for this reporting period was to complete and document costs and economic input for the HTGR-SETS screening report.

6.7.2. Discussion

This task concludes GA input to the screening phase for the HTGR-SETS applications screening report presently being coordinated by GCRA with GA and UE&C participation.

The SETS applications include (1) an on-site base load and peaking electric power plant, (2) a process steam cogeneration application (to be provided by GCRA), (3) an oil shale AGR application, and (4) three oil refinery repowering scenario applications.

Cost and economic analyses were performed on HTGR-SETS applications items (1), (3), and (4) based on technical input presented in Ref. 6.7-1. The oil shale AGR application work was performed under Task 6003030001 and is included here under the SETS heading for completeness.

6.7.2.1. SETS Base/Peak Electric Power Generating Plant Cost and Economics. The HTGR-SETS combined base/peak electrical-power generating plant uses the thermal energy developed in an HTGR to generate commercial electricity in base-loaded and peaking-system cycle power plants.

Table 6.7-1 presents the capital costs and power-generating economics of the HTGR-SETS combined base/peak electrical power plant and compares these results with corresponding projections for two conventional alternatives: (1) an HTGR-SC plant that operates in a cyclic mode to develop the required base/peak power characteristics and (2) a cycling coal-fired plant with the same power capacity. The table also includes data for an HTGR-SC that operates in a cyclic mode to serve as an economic benchmark against which the choices could be measured.

The economic data presented in Table 6.7-1 are based on the projected costs of energy production, following the GCRA ground rules. Work scope limitation precluded parametric sensitivity analysis, base/peak load split evaluation, and departures from ideal market conditions (i.e., peak to base load is constant all year). The table comparisons highlight two important results:

1. Both HTGR options are economically superior to the competing fossil alternative.

2. No economic advantage has been identified for the HTGR-SETS over the HTGR-SC operating in a load following or cyclic mode.

High fuel costs prevent the fossil alternatives from competing economically with the HTGR options for this application. The HTGR-SETS capital cost advantages accruing from its smaller reactor thermal capacity are overcome by its higher balance of plant (BOP) costs attributable to the indirect helium loop, the molten salt equipment, and the thermal storage provisions.

The implications of these economic projections need to be studied further. While the HTGR-SETS can be shown to have considerably lower

TABLE 6.7-1
ECONOMIC COMPARISON FOR COMBINED BASE/PEAK ELECTRIC POWER GENERATION[a,b]
(1995 Projections in 1/80 $ x 10^6, 30-yr Levelization, Utility Ownership)

	Indirect-Cycle 1170-MW(t) HTGR-SETS	2018-MW(t) HTGR-SC[c]	2124-MW(t) Coal-SC
Capital cost			
Base (1/80 $)	991	751	564
Escalation	124	94	78
AGFDC/IDC[d]	126	95	46
Total	1241	940	688
Annual cost			
Fixed	103	78	57
Fuel	25	29	112
Operation and maintenance	22	21	27
Total	150	128	196
Product Cost (mills/kWh)	54	41	63

(a) Load profile electric power cycle; 208 MW(e) for 16 hr/day, 773 MW(e) for 8 hr/day.

(b) Ground rules per Section 3, 80% capacity factor for HTGR-SETS plant, 46% capacity factor for 2018-MW(t) HTGR-SC and 2124-MW(t) coal-SC.

(c) Equivalent electrical capacity with cost data scaled from Ref. 6.7-1 on 2240-MW(t) HTGR-SC.

(d) Allowance for funds during construction/interest during construction.

power-generating costs than its fossil competition, in its current form it does not prevail economically over the cycling HTGR-SC plant. The cycling HTGR plant, however, requires a much larger reactor and must operate for two-thirds of the time at roughly one-third load. This unusual operation reduces the incentives for its deployment in the electric power market. A possible solution to this problem would be a reactor that has a better cost scaling relationship, where the smaller HTGR-SETS plant would not suffer as much of a unit cost penalty.

6.7.2.2. Oil Refinery Applications Cost and Economics. Three refinery applications were considered in the oil refinery applications studies. The first addressed the economic incentives for using a remotely sited HTGR-SETS facility to provide process steam electricity to a large oil refinery on the Texas Gulf Coast of the United States. The second application examined a smaller-capacity refinery that not only derived its electrical and process steam needs from a remotely sited HTGR-SETS facility, but also utilized the thermal energy in the molten salt to supply process heat directly, thereby replacing the fossil-fired heaters. The third application studied was the HTGR-SUPERSETS, which was an extension of the second. The SUPERSETS provided the refinery needs and additional user services through a large-capacity, multi-HTGR-SETS energy park.

Large Texas Refinery (Cogeneration)

Table 6.7-2 presents an economic comparison of these remotely sited concepts with three competing close-in plant options. The system steam capacities are approximately the same for all concepts, permitting direct economic comparisons to be made among all alternatives shown. An examination of the pipeline plant comparison reveals that the key difference lies in the lower net electric power generation for the SETS concept, due to substantial pumping penalties in the secondary helium and salt loops.

Close-in siting of a replacement energy supply plant at the refinery definitely favors the HTGR-SC/C relative to its assumed competition. The HTGR-SC/C maintains its advantage even at the 32.2-km (20-mi) separation

TABLE 6.7-2
ECONOMIC COMPARISON FOR LARGE OIL REFINERY APPLICATION
(1995 Projections with 1/80 $ x 10^6, 30-yr Levelization, Industrial Ownership)

	Close-in Plants			Pipeline Plants	
	Twin 1170-MW(t) HTGR-SC/C	2342-MW(t) Coal-SC/C	2250-MW(t) Existing Oil Plant	Twin 1170-MW(t) HTGR-SETS with Salt Pipeline	Twin 1170-MW(t) HTGR-SC/C with Steam Pipeline
Heat input, MW(t)	2340	2560	2250	2340	2340
Heat output, MW(t)	1926	1926	1926	1937	1937
Net electric power, MW(e)	322	232	120	103	272
Capital cost					
Base (1/80 $)	1225	844	--	1688	1767
Escalation	164	117	--	230	243
AFDC/IDC[a]	242	137	--	303	298
Total	1631	1098	--	2221	2308
Annual cost					
Fixed	212	143	--	289	300
Fuel	45	230	612	49	45
Operation and maintenance	49	49	18	38	38
Power credit	(99)	(65)	(34)	(29)	(76)
Total	207	357	596	343	307
Product cost					
[$/GJ ($/10^6 Btu) of steam]	4.87 (5.13)	8.41 (8.86)	14.04 (14.80)	8.03 (8.46)	7.18 (7.57)

[a] Allowance for funds during construction/interest during construction.

distance assumed for this study, although its competitive margin is reduced considerably. On the other hand, the HTGR-SETS does not appear to be economically attractive at the 32.2-km (20-mi) pipeline distance, owing to its unfavorable combination of higher pipeline cost, pumping penalties, and base-capital costs. The prospects for HTGR-SETS in this application could be improved if greater exclusion distances prevailed and/or additional refinery repowering needs required high-grade heat.

Refinery Repowering (Fixed Duties); Cost and Economics

This particular concept attempted to improve the HTGR-SETS role in a refinery complex beyond the cogeneration made by utilizing the high-temperature molten salt in the refinery heaters in addition to generating process steam and electricity.

To arrive at refinery plant equipment costs, a heat and material balance was developed for the molten salt based on refinery heat duty requirements and operating conditions, which were provided by Gas Cooled Reactor Associates (GCRA). Table 6.7-3 presents heat exchanger design and cost estimates and Table 6.7-4 summarizes total refinery plant equipment costs.

Tables 6.7-5 and 6.7-6 summarize base capital costs and economic projections for the HTGR-SETS refinery repowering application. The capital costs are derived from the HTGR-SETS application with appropriate adjustments to include the costs of the refinery heater complex and power station, the salt transmission pipeline, the revised secondary helium loop heat exchangers, and the doubling of the nuclear capacity by going to twin reactors.

The economic analysis generally followed the same FY-81 GCRA ground rules used in the other HTGR-SETS studies covered in this report. All HTGR cases are based on the high-enriched uranium (HEU)-recycle fuel cycle. Other exceptions include the consideration of 80% capacity factor as an alternative for all applications and the exclusion of 7% below-the-line

TABLE 6.7-3
HEAT EXCHANGER DESIGN SUMMARY FOR REFINERY APPLICATION
(Shell Side, Salt; Tube Side, Hydrocarbons)

Heat Exchanger Component[a]	No. of Units	Heat Duty (10 Btu/hr)	Surface Assumed[b] Area (ft^2)	HC[c] Material	Temperature (°F) HC Phase	HC In	HC Out	Salt In	Salt Out	Flow Rates (10^6 lb/hr) HC Liquid	HC Vapor	Salt	Pressure Drop (psi) HC	Salt	Approximate Nozzle to Nozzle Length (ft)	OD (in.)	Weight Full of H_2O (lb x 10^6)	Cost 1980 ($ x 10^6)
U-1 recycle gas	1	152	5,253	Nat. gas	Vapor	667	862	1050	926	--	0.978	3.29	3.3	35.8	29	36	0.039	0.2
F-1 ultrafiner	1	109	6,395	Nat. gas	Vapor	600	700	936	855	--	1.48	3.63	3.0	16.7	20	53	0.121	0.4
F-2 ultraformer	1	292	57,554	Nat. gas	Vapor	750	950	1050	784	--	1.79	2.96	12.7	7.5	44	77	0.353	1.1
F-3 No. 1 preheat	1	253	50,911	Nat. gas	Vapor	788	970	1050	828	--	1.68	3.08	11.1	6.7	40	77	0.328	1.1
F-4 No. 2 preheat	1	140	24,424	Nat. gas	Vapor	873	970	1050	917	--	1.73	2.84	5.3	6.3	34	73	0.226	0.6
F-5 No. 3 preheat	1	103	27,983	Nat. gas	Vapor	899	970	1050	917	--	1.74	2.08	5.6	3.8	36	75	0.241	0.6
F-6 No. 4 preheat	1	51	16,307	Nat. gas	Vapor	946	980	1050	962	--	1.80	1.55	3.8	1.3	23	76	0.197	0.5
F-7 regenerated gas	1	63	13,933	Nat. gas	Gas	460	1000	1050	520	--	0.152	0.32	0.6	2.5	46	44	0.087	0.3
U-2 recycle oil	1	36	2,747	Kerosene	Liquid	550	775	1050	600	0.267	--	0.216	0.4	16.2	38	22	0.025	0.1
D-1 distillate heater	1	106	15,259	Naphthalene	Mixed	450	700	795	530	0.332	0.110	1.08	4.7	15.7	46	46	0.093	0.3
G-1 feed heater	1	36	2,313	Kerosene	Liquid	570	630	1050	620	1.0	--	0.226	4.2	26.1	38	20	0.015	0.1
G-2 recycle oil heater	1	37	2,312	Kerosene	Liquid	550	660	1050	620	0.561	--	0.232	1.5	27.4	38	20	0.015	0.1
D-2 flexicoker unit feed heater	1	60	9,821	Naphthalene	Mixed	450	700	795	530	0.167	0.062	0.61	3.3	14.2	42	38	0.059	0.2
U-3 debutanizer reboiler	1	202	17,198	Naphthalene Butane	Mixed	508	631	926	600	0.950	0.315	1.68	5.0	22.8	43	50	0.115	0.3
U-4 sputter reboiler	1	194	17,804	Naphthalene Octane	Mixed	487	605	926	600	0.908	0.302	1.61	4.0	1.6	19	60	0.073	0.2
E-4 prefractionator reboiler	1	116	10,910	Naphthalene	Mixed	468	480	806	655	0.770	0.257	2.07	2.8	3.1	24	72	0.113	0.2
E-9 stripper reboiler	1	129	10,886	Naphthalene	Mixed	507	520	806	655	0.879	0.293	2.31	4.6	48.3	43	40	0.071	0.2
E-12 debutanizer reboiler	1	94	7,675	Naphthalene Butane	Mixed	405	450	806	655	0.603	0.201	1.68	5.3	47.3	53	34	0.049	0.2
H-1 atmosphere heater	1	550	46,162	Naphthalene	Mixed	450	660	807	640	1.88	0.627	8.9	3.9	20.3	50	92	0.363	0.8
H-2 vacuum heater	2	400	20,896	Naphthalene	Mixed	610	795	928	807	0.735	0.245	8.9	2.6	34.9	25	118	0.311	(0.7 each) 1.4
C-1 coking heater	1	160	19,843	Naphthalene	Mixed	680	930	1050	795	0.462	0.154	1.69	1.8	16.5	45	54	0.127	0.3
Total																		9.2

[a] See Fig. 6.7-4 for refinery heat balance.

[b] For determination of tube side transport properties.

[c] HC = hydrocarbons.

TABLE 6.7-4
REFINERY EQUIPMENT COST SUMMARY

Equipment	Cost (January 1980 $ x 10^6)
Heat exchangers (direct heating)	9.2
Piping	12.0
Isolation valves	0.1
Drainage tanks	0.3
Drainage tanks pumps	0.1
Heat exchangers (process steam)	3.3
Total refinery site cost	25.0

TABLE 6.7-5
COMPARISON OF TWIN 1170-MW(t) (REFINERY) WITH FOSSIL-FIRED COMPETITION, MIDDLETOWN FUEL COSTS AND SOIL CONDITIONS
($ x 10^6)

Fossil-Fired[a] Competition				Base Case Twin 1170-MW(t) HTGR-SETS	
Industrial Ownership[b]		Utility Ownership[b]		Industrial Ownership[b]	Utility Ownership[b]
			Capital		
Baseload electrical	91 (98)	(89)	Base (1/80 $)	1576 (1576)	(1576)
			Escalation	197 (197)	(197)
Refinery steam	378 (432)	(458)	IDC[c]	410 (410)	(200)
Total[d]	469 (530)	(547)		2183 (2183)	(1973)
			Annual		
			Fixed	284 (284)	(164)
			Fuel (HEU recycle)	45 (50)	(50)
			Operation and maintenance	38 (39)	(40)
			Total	367 (373)	(254)
Ratio to HTGR	1.28 (1.42)	(2.15)		1.00 (1.00)	(1.00)
Percent advantage over fossil-fired alternative	-- (--)	(--)		22 (30)	(54)

[a] Baseload electrical from 400-MW(e) industrial-owned coal-fired plant; refinery steam from existing natural-gas-fired boiler (includes fuel and operation and maintenance costs only).

[b] Numbers without parentheses represent 70% capacity factor; numbers in parentheses represent 80% capacity factor.

[c] Interest during construction.

[d] 1995 projection in 1/80 $ levelized over 30 yr; 1981 GCRA ground rules except as noted. Levelized coal cost $2.13/GJ ($2.25/Btu x 10^6), levelized gas cost $7.8/GJ ($8.25/Btu x 10^6).

TABLE 6.7-6
COMPARISON OF TWIN 1170-MW(t) (REFINERY) WITH FOSSIL-FIRED COMPETITION, GULF COAST FUEL COSTS AND SOIL CONDITIONS
($ x 10^6)

	Fossil-Fired[a] Competition				Base Case Twin 1170-MW(t) HTGR-SETS[b]		
	Industrial Ownership[c]		Utility Ownership[c]		Industrial Ownership[c]		Utility Ownership[c]
				Capital			
Baseload electrical	99	(108)	(99)	Base (1/80 $)	1636	(1636)	(1636)
				Escalation	205	(205)	(205)
Refinery steam	303	(346)	(367)	IDC[d]	425	(425)	(208)
Total[e]	402	(454)	(466)		2466	(2466)	(2049)
				Annual			
				Fixed	294	(294)	(170)
				Fuel (HEU recycle)	45	(50)	(50)
				Operation and maintenance	38	(39)	(40)
				Total	377	(383)	(266)
Ratio to HTGR	1.07	(1.19)	(1.79)		1.00	(1.00)	(1.00)
Percent advantage over fossil-fired alternative	--	(--)	(--)		6	(16)	(44)

[a] Baseload electrical from 400-MW(e) industrial-owned coal-fired plant; refinery steam from existing natural-gas-fired boilers (includes fuel and operation and maintenance costs only).

[b] Includes $60 million foundation allowance.

[c] Numbers without parentheses represent 70% capacity factor; numbers in parentheses represent 80% capacity factor.

[d] Interest during construction.

[e] 1995 projection in 1/80 $ levelized over 30 yr; Levelized coal cost $2.51/GJ ($2.65/Btu x 10^6), levelized gas cost $6.23/GJ ($6.58/Btu x 10^6).

owner's cost for all capital items. An allowance for the additional foundation work required to accommodate the poor soil load-bearing characteristics in the Gulf Coast area has been included where appropriate.

The economic study considered four types of comparisons: (1) HTGR-SETS versus fossil-fired alternatives, (2) 80% versus 70% capacity factor, (3) Gulf Coast, Texas versus Middletown, USA sites, and (4) private industry versus utility ownership.

Economic analyses of plants with more than one energy product frequently lead to results that are ambiguous or arbitrary and are subject to considerable interpretation. The problem arises when the results are presented in terms of "cost of energy produced" for each product, because this type of parameter cannot be developed without allocating a portion (or all) of the plant cost to the particular energy stream in question. Furthermore, determining these cost allocations tends to become more arbitrary as the number of by-products increases. Therefore, no attempt was made to derive individual energy stream costs for either the SETS refinery repowering study or the SUPERSETS energy park evaluation addressed in the following section. Instead, the HTGR-SETS application is measured against its fossil-fired competition by comparing the total annual cost for HTGR-SETS with the total annual cost of purchasing the equivalent fossil energy stream capacities (summarized in Table 6.7-7) separately on the open market.

Individual comparisons contain the assumptions underlying the on-the-market purchases. Tables 6.7-5 and 6.7-6 give the numerical results of these comparisons, which indicate the following:

1. HTGR versus fossil-fired alternatives. For industrial ownership, at 70% capacity, the HTGR shows a 6% and a 22% advantage over fossil-fired competition for the Gulf Coast and Middletown sites, respectively. These advantages are due to the cost of coal and natural gas, which more than offset the large HTGR plant fixed charges.

TABLE 6.7-7
FOSSIL-FIRED ALTERNATIVE ENERGY STREAMS FOR TWIN 1170-MW(t) HTGR-SETS
REFINERY REPOWERING APPLICATION

Baseload electrical, MW(e)	224
Refinery streams	
Heater duty, MW(t)	965
Balance of refinery stream, MW(t)	399
Total refinery stream, MW(t)	1364

2. 70% versus 80% capacity factor. Shifting from a 70% to an 80% capacity factor causes the HTGR advantage over fossil-fired alternatives to increase from 6% to 16% for the Gulf Coast site and from 22% to 30% for the Middletown site, assuming industrial ownership. These increased advantages are due to the higher variable component of fossil-fired energy costs as opposed to the higher fixed component of HTGR energy costs.

3. Gulf Coast, Texas versus Middletown, USA. At 70% capacity, the HTGR demonstrates 6% lower energy costs than its fossil-fired competition for the Gulf Coast site and 22% lower energy costs than its fossil-fired competition for the Middletown site. The greater advantage at the Middletown site is primarily due to higher natural gas costs at the Middletown site. These costs more than offset the less expensive coal and the lower-cost HTGR (as a result of better soil conditions).

4. Private industry versus utility ownership. At 80% capacity, the HTGR shows a 16% and a 44% advantage over fossil-fired energy for the Gulf Coast area for industrial and utility ownership, respectively. For the Middletown site, the HTGR at 80% capacity shows a 30% and a 54% advantage over fossil-fired energy for industrial and utility ownership, respectively. This advantage to the utility-owned HTGR is due to lower costs of capital, resulting in a lower fixed charge rate on capital cost.

For the twin 1170-MW(t) HTGR-SETS refinery repowering concept, the lowest-cost energy system of those examined, based on annual operating cost, is concluded to be the utility-owned twin 1170-MW(t) HTGR-SETS (refinery) operating at 70% capacity for the Middletown site at $245 million/yr, closely followed by the plant for the Gulf Coast site at $260 million/yr. However, the lowest product cost would occur with the same plant operating at 80% capacity.

SUPERSETS Cost and Economics

Table 6.7-8 gives the energy streams for four 1170-MW(t) slide-along HTGR-SETS nuclear heat sources and twin 2240-MW(t) HTGR-SUPERSETS plants. Tables 6.7-9 through 6.7-12 summarize the capital cost estimates and economic projections. These are based on the energy streams described in Table 6.7-8; comparisons are made with fossil-fired competition, including Gulf Coast and Middletown fuel cost, assuming utility ownership.

The large size and multiple-customer, multiple-service role of SUPERSETS suggest that private ownership may not be practical; therefore, utility ownership is assumed. In addition to making the types of economic comparisons described above, the SUPERSETS results also compare the economy of scale of a twin 2240-MW(t) NHS with the four-unit 1170-MW(t) NHS that served as the reference for this study. The statistics in Tables 6.7-9 through 6.7-12 reveal the following:

1. HTGR versus fossil-fired alternatives. For the twin 2240-MW(t) plant application, the HTGR shows a 47% and 48% advantage over the nearest fossil-fired competition for the Gulf Coast and Middletown sites, respectively. These advantages are due to higher coal and natural gas prices, which more than offset the large HTGR plant fixed charges, at both sites.

2. 70% versus 80% capacity factor. For the twin 2240-MW(t) plant, shifting from 70% to 80% capacity factor causes the HTGR advantage over fossil-fired alternatives to increase from 47% to 50% for the Gulf Coast site and from 48% to 51% for the Middletown site. These increased advantages are due to the higher variable component of fossil-fired energy costs as opposed to the higher fixed component of HTGR energy costs. Consequently, as capacity is increased for fossil-fired plants, proportionately more fuel is consumed. Conversely, for the HTGR (for which the costs are in comparison more fixed), the effect of an increase in capacity is a less proportionate increase in total costs. For the Gulf Coast

TABLE 6.7-8
FOSSIL-FIRED ALTERNATIVE ENERGY STREAMS SUPERSETS APPLICATION

	Four-Unit 1170-MW(t) HTGR-SUPERSETS	Twin 2240-MW(t) HTGR-SUPERSETS
Baseload electrical MW(e)	95	70
Process steam MW(t)	1774	1697
Peaking electrical MW(e)[a]	1100	1053
Refinery steam		
Heater duty MW(t)	965	965
Balance of refinery steam MW(t)	399	341
Total refinery steam MW(t)	1364	1306

[a] Availability 90%, load factor 33%, capacity factor 30%.

TABLE 6.7-9
COMPARISON OF FOUR-UNIT 1170-MW(t) HTGR-SUPERSETS WITH FOSSIL-FIRED COMPETITION, MIDDLETOWN FUEL COSTS AND SOIL CONDITIONS
($ x 10^6, Utility Ownership)

	Fossil-Fired Alternatives					Base Case Twin 2240-MW(t) HTGR-SUPERSETS[b]	
	Case I[a,b]		Case II[b,c]				
					Capital		
Baseload electrical	73	(83)	13	(14)	Base (1/80 $)	3171	(3171)
Process steam	521	(595)	241	(263)	Escalation	396	(396)
					AFDC[d]	403	(403)
Peaking electrical[e]	360	(360)	205	(205)	Total	3970	(3970)
Refinery steam	400	(458)	337	(383)	Annual		
Total[f]	1354	(1496)	796	(865)	Fixed	329	(329)
					Fuel (HEU recycle)	90	(100)
					Operation and maintenance	80	(83)
					Total[f]	499	(512)
Ratio to HTGR	2.71	(2.92)	1.60	(1.69)		1.00	(1.00)
Percent advantage over lowest-cost fossil-fired alternative						37	(41)

(a) Existing natural-gas-fired plants; includes fuel and operation and maintenance costs only.

(b) Numbers without parentheses represent 70% capacity factor; numbers in parentheses represent 80% capacity factor.

(c) Baseload electrical and process steam from coal cogeneration plant; peaking electrical from cycling coal plant; 965 MW(t) of refinery steam gas-fired (heater duty), fuel and operation and maintenance costs only; 399 MW(t) of refinery steam from coal cogeneration plant.

(d) Allowance for funds during construction.

(e) Peaking electrical power at 30% capacity factor.

(f) 1995 projection in 1/1980 $ levelized over 30 yr; 1981 GCRA ground rules except as noted. Levelized coal cost $2.13/GJ ($2.25/Btu x 10^6), levelized gas cost 7.82/GJ ($8.25/Btu x 10^6).

TABLE 6.7-10
COMPARISON OF FOUR-UNIT 1170-MW(t) HTGR-SUPERSETS WITH FOSSIL-FIRED COMPETITION, GULF COAST FUEL COSTS AND SOIL CONDITIONS
($ x 10^6, Utility Ownership)

	Fossil-Fired Alternatives					Base Case Twin 2240-MW(t) HTGR-SUPERSETS[b]	
	Case I[a,b]		Case II[b,c]				
					Capital		
Baseload electrical	59	(67)	14	(16)	Base (1/80 $)[d]	3291	(3291)
Process steam	418	(418)	267	(294)	Escalation	411	(411)
					AFDC[e]	418	(418)
Peaking electrical[f]	289	(289)	224	(224)	Total	4120	(4120)
Refinery steam	321	(367)	287	(326)	Annual		
Total[g]	1087	(1201)	792	(860)	Fixed	342	(342)
					Fuel (HEU recycle)	90	(100)
					Operation and maintenance	80	(83)
					Total[g]	512	(525)
Ratio to HTGR	2.12	(2.29)	1.55	(1.64)		1.00	(1.00)
Percent advantage over lowest-cost fossil-fired alternative						35	(39)

(a) Existing natural-gas-fired plants; includes fuel and operation and maintenance costs only.

(b) Numbers without parentheses represent 70% capacity factor; numbers in parentheses represent 80% capacity factor.

(c) Baseload electrical and process steam from coal cogeneration plant; peaking electrical from cycling coal plant; 965 MW(t) of refinery steam gas-fired (heater duty), fuel and operation and maintenance costs only; 399 MW(t) of refinery steam from coal cogeneration plant.

(d) Includes additional $120 million allowance for foundation.

(e) Allowance for funds during construction.

(f) Peaking electrical power at 30% capacity factor.

(g) 1995 projection in 1/1980 $ levelized over 30 yr; 1981 GCRA ground rules except as noted. Levelized coal cost $2.51/GJ ($2.65/Btu x 10^6), levelized gas cost $6.23/GJ ($6.58/Btu x 10^6).

TABLE 6.7-11
COMPARISON OF TWIN 2240-MW(t) HTGR-SUPERSETS WITH FOSSIL-FIRED COMPETITION, MIDDLETOWN FUEL COSTS AND SOIL CONDITIONS
($ x 10^6, Utility Ownership)

	Fossil-Fired Alternatives					Base Case Twin 2240-MW(t) HTGR-SUPERSETS	
	Case I[a,b]		Case II[b,c]				
					Capital		
Baseload electrical	54	(61)	10	(11)	Base (1/80 $)	2583	(2583)
Process steam	498	(569)	230	(251)	Escalation	323	(323)
					AFDC[d]	328	(328)
Peaking electrical[e]	345	(345)	196	(196)	Total	3234	(3234)
Refinery steam	383	(438)	330	(374)	Annual		
Total[f]	1280	(1413)	766	(832)	Fixed	268	(268)
					Fuel (HEU recycle)	83	(92)
					Operation and maintenance	48	(50)
					Total[f]	399	(410)
Ratio to SUPERSETS	3.21	(3.45)	1.92	(2.03)		1.00	(1.00)
Percent advantage over lowest-cost fossil-fired alternative						48	(51)

[a] Existing natural-gas-fired plants; includes fuel and operation and maintenance costs only.

[b] Numbers without parentheses represent 70% capacity factor; numbers in parentheses represent 80% capacity factor.

[c] Baseload electrical and process steam from coal cogeneration plant; peaking electrical from cycling coal plant; 965 MW(t) of refinery steam gas-fired (heater duty), fuel and operation and maintenance costs only; 341 MW(t) of refinery steam from coal cogeneration plant.

[d] Allowance for funds during construction.

[e] Peaking electrical power at 30% capacity factor.

[f] 1995 projection in 1/1980 $ levelized over 30 yr; 1981 GCRA ground rules except as noted. Levelized coal cost $2.13/GJ ($2.25/Btu x 10^6), levelized gas cost $7.82/GJ ($8.25/Btu x 10^6).

TABLE 6.7-12
COMPARISON OF TWIN 2240-MW(t) HTGR-SUPERSETS WITH FOSSIL-FIRED COMPETITION, GULF COAST FUEL COSTS AND SOIL CONDITIONS
($ x 10^6, Utility Ownership)

	Fossil-Fired Alternatives					Base Case Twin 2240-MW(t) HTGR-SUPERSETS[b]	
	Case I[a,b]		Case II[b,c]				
					Capital		
Baseload electrical	43	(49)	11	(12)	Base (1/80 $)[d]	2643	(2643)
Process steam	400	(457)	255	(282)	Escalation	330	(330)
					AFDC[e]	336	(336)
Peaking electrical[f]	277	(277)	214	(214)	Total	3309	(3309)
Refinery steam	307	(352)	278	(316)	Annual		
Total[g]	1027	(1135)	758	(824)	Fixed	274	(274)
					Fuel (HEU recycle)	93	(92)
					Operation and maintenance	48	(50)
					Total[g]	405	(416)
Ratio to HTGR	2.54	(2.73)	1.87	(1.98)		1.00	(1.00)
Percent advantage over lowest-cost fossil-fired alternative						47	(50)

[a] Existing natural-gas-fired plants; includes fuel and operation and maintenance costs only.

[b] Numbers without parentheses represent 70% capacity factor; numbers in parentheses represent 80% capacity factor.

[c] Baseload electrical and process steam from coal cogeneration plant; peaking electrical from cycling coal plant; 965 MW(t) of refinery steam gas-fired (heater duty), fuel and operation and maintenance costs only; 341 MW(t) of refinery steam from coal cogeneration plant.

[d] Includes additional $120 million allowance for foundation.

[e] Allowance for funds during construction.

[f] Peaking electrical power at 30% capacity factor.

[g] 1995 projection in 1/1980 $ levelized over 30 yr; 1981 GCRA ground rules except as noted. Levelized coal cost $2.25/Btu x 10^6, levelized gas cost $6.50/Btu x 10^6.

TABLE 6.7-13
HEAT BALANCE SUMMARY

	Fossil Case	HTGR-SETS High-Temperature Case	HTGR-SETS Low-Temperature Case
Process heat			
Retort absorbed, MW(t)	319	319	319
Hydrotreating absorbed, MW(t)	10	10	10
Process steam, MW(t)	50	51	52
Electricity generated, [MW(e)]	361 (139)	(317)	823 (317)
Process demand, MW(t) MW(t) [MW(e)]	361 (139)	(226)	(234)[a]
Excess	--	(91)	(83)

[a]Includes 195 MW(t) [75 MW(e)] for HTGR-SETS house load.

TABLE 6.7-14
PARAHO INDIRECT PRODUCT BALANCE SUMMARY

	Fossil Case	HTGR-SETS Low-Temperature Case	HTGR-SETS High-Temperature Case
Shale quality, m^3/Mg[a] (28 gal/ton)	0.117 (28)	0.117 (28)	0.117 (gas/ton)
Feed shale, kg/s (tons/stream day)	704 (66,871)	757 (71,867)	704 (66,871)
Yield % of quality	93.5	87.0	93.5
Raw shale oil, MW (bbl/stream day)	3053 (41,683)	3053 (41,683)	3053 (41,683)
Hydrotreated oil products, MW (bbl/stream day)	3300 (45,042)	3300 (45,042)	3300 (45,042)
Gross product gas,[b] MW (bbl/stream day)	149 (2,037)	174 (2,382)	149 (2,037)
Total gross products, MW (bbl/stream day)	3449 (47,079)	3474 (47,424)	3449 (47,079)
Purchased fuel, MW (bbl/stream day)	1156 (15,779)	204 (2,780)	204 (2,780)
Net product, MW (bbl/stream day)	2293 (31,300)	3270 (44,644)	3245 (44,299)
Ratio of net product to fossil-fired case	1.00	1.43	1.42

[a] m^3/Mg = cubic meters of oil per 10^6 g.

[b] Reformer feedstock deducted.

TABLE 6.7-15
PROCESS PLANT DIRECT CAPITAL COST COMPARISONS
PARAHO INDIRECT PROCESS

	Fossil Case	HTGR-SETS Low-Temperature Case	HTGR-SETS High-Temperature Case
Recycle gas temperature, °C (°F)	704 (1300)	510 (950)	538 (1000)
Retorting temperature, °C (°F)	510-538 (950-1000)	454 (850)	510 (950)
Oil yield Fischer assay, %	93.5	87	93.5
Feed shale amount without fines, kg/s (tons/day)	704 (66,871)	757 (71,867)	704 (66,871)
Process area capital costs (1/80 $ x 10^6)			
Mining	118	126	118
Secondary crushing and screening	65	70	65
Retorting and oil recovery	210	234	256
Spent shale disposal	23	25	23
Gas cooling, compression, and ammonia removal	3	3	3
Stretford plant	11	11	11
Wastewater treating	7	9	8
Hydrotreating	75	74	74
Hydrogen plant	44	44	44
DEA acid gas removal	2	2	2
Claus and Scot plants	4	4	4
Chevron wastewater treatment	13	14	14
Shale oil storage	8	10	10
Power plant and HTGR	73	545	545
Water supply	9	11	11
Off-site	73	70	71
Total direct cost	738	1252	1259

TABLE 6.7-16
PARAHO INDIRECT PROCESS
DIRECT + INDIRECT COST COMPARISON
(1/80 $ x 10^6)

	Fossil Case	HTGR-SETS Low-Temperature Case	HTGR-SETS High-Temperature Case
Total direct cost	738	1252	1259
Construction service	123	208	209
Home office engineering and service	110	186	187
Field office engineering and service	55	93	93
Total base cost	1026	1739	1748
Contingency	154	261	262
Total base cost including contingency	1180	2000	2010

TABLE 6.7-17
SUMMARY COST AND ECONOMIC COMPARISONS
PARAHO INDIRECT PROCESS
($ X 10^6)[a]

	Fossil Case	HTGR-SETS Low-Temperature Case	HTGR-SETS High-Temperature Case
Capital			
Base (1/80 $)	1180	2000	2010
Escalation	163	265	266
IDC[b]	191	409	411
Total capital	1534	2674	2687
Annual			
Fixed	199	348	349
Fuel (energy plant)	264[c]	22[d]	22[d]
Operation and maintenance (energy plant)	(Included in process)	19	19
Operation and maintenance (process)	149	157	149
Power credit	--	(18)[e]	(21)[e]
Total annual[f]	612	528	518
$/$m^3$ ($/bbl)[f]	321 (51.04)	291 (46.33)	289 (45.94)
Ratio to fossil fuel case	1.00	0.91	0.90

[a] GCRA FY-81 economic ground rules.

[b] Interest during construction.

[c] $5.01/MBtu (1/80 $) base value of product consumed in process.

[d] HEU recycle.

[e] 33.8 mills/kWh 1/80 $ power credit.

[f] 1995 projection in 1/80 $ levelized over 30 yr.